

GPO PRICE

\$____

CFSTI PRICE(S) \$

Hard copy (HC) # 4,00

Microfiche (MF) 2,00

ff 653 July 65

Edited by

ROBERT J. MACKIN, JR. and MARCIA NEUGEBAUER

Foreword by S. Chapman



Pergamon Press

RGT. 53

N 6 6. 3.8.9.4 6. 8 6. 3.8.9.74

(ACCESSION NUMBER)

(THRU)

(TAGES)

THE SOLAR WIND

Proceedings of a Conference

held at

The California Institute of Technology Pasadena, California, U.S.A.

April 1-4, 1964

and sponsored by

the Jet Propulsion Laboratory

Edited by

ROBERT J. MACKIN, Jr. MARCIA NEUGEBAUER

Foreword by

S. CHAPMAN

JET PROPULSION LABORATORY

CALIFORNIA INSTITUTE OF TECHNOLOGY

PASADENA, CALIFORNIA

THE SOLAR WIND

(JPL Technical Report No. 32-630)

Copyright © 1966 by the Jet Propulsion Laboratory, California Institute of Technology. All rights reserved. Printed in the United States of America.

Library of Congress Catalog Card No. 65-28056

This book, which describes one phase of the U.S. space research program, was prepared for the National Aeronautics and Space Administration by the Jet Propulsion Laboratory, California Institute of Technology, under Contract NAS 7-100.

CONTENTS

	ttendees									ix
E	ditors' Preface									xiii
F	oreword, by S.	CHAPN	MAN							XV
A	cknowledgmen	ts	***	***						xxix
				Ses	sion I					
		DITE	NIONI	ENTA	OBCE	DVEE	N INT			
					OBSE					
	-	INI	EKPI	LANI	ETARY	SPA	CE			
1				C	.1 0	1 337				
1.	Mariner-2 N									
	NEUGEBAU									3
4	Discussion								• • •	21
2.	The Relation									
1	by Conway								• • • •	25
	Discussion									32
3.	Interplanetary	_								
J.	JR., E. J. SM							ETT	• • •	35
	Discussion		• • •							50
4.	The Relations								and	
	the Solar Pla								• • •	53
1							···			66
5.	Satellite Obs		ns of	Me	v Phen	omena	Rela	ted to	the	
	Solar Wind:				D 4	ъ	T	I C		
	Explorer-12									
	U. D. DE									69
	IMP Obser				-					7.0
	CLINE, G									
	Discussion									80
6.	Interplanetary									0.2
	Satellite, by									83
1	Discussion					•••				103
7.	Radio Astron	omy O	bserva	ations	in Re	ation t	o the	Solar-V	vina	100
1	Problem, by								• • • •	109
					 Dan'4				···	120
8.	What We Kn									122
	Wind, by H.	S. BRI	DGE							123

Discussion

Session II

1	HEORIES OF THE IN						ANI)
1	FIELDS, AND OI	FEN	ERGE 7	LIC P	ARTI	CLES		
1								
9.	Models of the Interplane							
	LEVERETT DAVIS, JR.							147
1								157
10.	Evidence for a Collision-I	Free I	Hydrom	agneti	c Sho	ck in In	ter-	
	planetary Space, by C	. P. S	SONETT.	D. S	S. Coi	BURN,	and	
								165
/	Discussion							173
111	Magnetic Fields in the So							177
11.				_			OIN	
10	Discussion			• • •		1		182
V12.	The Penetration of Galacti		mic Ray	s into	the So	lar Syste	em,	
	by E. N. Parker							185
	Discussion		***					192
		Sessi	ion III					
	ORIGIN OF THE SO	LAR	WIND	ANI	тні	CORC) N A	
/	olden of the so	L/ III	WILL D	71111	, , , , , ,	2 COIC	J1 11	•
12	The Origin of the Solar Wi	nd by	FI	SCARE	•			199
15.								
111	Discussion							212
14.	Effects of Diffusion on the							
	and the Solar Wind, by J	. R. Jo	OKIPII					215
								218
15.	Reconnection and Ann	ihilati	on of	Magı	netic	Fields,	by	
	H. E. Petschek							221
		Sessi	on IV					
		50001						
	THE SOLAR WIND	AND	THE	MAG	NETO	SPHFI	RF	
	THE SOLITIC WITE	11112	1112		I L	JOI IIL		
V 16	Solar-Wind Interaction W	ith the	Magna	toenh	rot			
10.								221
N.=	Fluid Dynamic Aspects							231
17.	Solar-Wind Interaction W							
	Particle Aspects, by J. W. DUNGEY 243							
18.	18. The Mechanism for Reconnection of Geomagnetic and Inter							
	planetary Field Lines, by	y H. E	E. PETSC	HEK				257
. /	Discussion							263
19.	On the Occurrence of To							
1.	sphere, by B. U. Ö. Son							275
	spilete, of B. C. O. Solv	ILKU				•••		213

				CON	TENTS					vii
20.	The Motion by E. W. H			es Tra	pped i	in the	Magn	etosph	ere,	281
/	Discussion									294
21	Explorer-18									295
	Observation									275
	Interaction									315
23.	The Shape				_			ion of		
	Geomagne									337
	Discussion									347
				Sessio	on V					
	SOLAI							METS	5	
		Α	ND V	VITH	THE	MOON	1			
24.	The Interac								and	
	Artificial),									355
25.	Magnetohyo						ction of	f the So	olar	
	Wind With	Comet	ts, by L	UDWIC	BIER	MANN	• • •			365
/										369
	A Theory of							D		373
27.	The Magnet			Moon	, by T.	Gold			• • •	381
/	210000001011									389
/28.	A Probable	Obser	vation	of the	Wake	of the	Moon	, by N	. F.	-0-
	NESS									393
	Discussion					• • • •			• • •	400
										404
	ne index					***				401
Sub	ject index									404

Page intentionally left blank

ATTENDEES

ANDERSON, H. R., Jet Propulsion Laboratory, Pasadena, California.

ATHAY, R. G., University of Utah, Salt Lake City, Utah.

AXFORD, W. I., Cornell University, Ithaca, New York.

BACHER, R. F., California Institute of Technology, Pasadena, California.

BARDEEN, J. M., California Institute of Technology, Pasadena, California.

BARTH, C. A., Jet Propulsion Laboratory, Pasadena, California.

BEARD, D. B., University of California, Davis, California.

Bernstein, W., TRW-Space Technology Laboratories, Inc., Redondo Beach, California.

BIERMANN, L., Max-Planck-Institut für Physik und Astrophysik, Munich, Germany.

BLAKE, R., University of Alaska, College, Alaska.

BLOCK, L. P., Jet Propulsion Laboratory, Pasadena, California/Royal Institute of Technology, Stockholm, Sweden.

Brandt, J., Kitt Peak Observatory, Tucson, Arizona.

BRATENAHL, A., Jet Propulsion Laboratory, Pasadena, California.

BRIDGE, H. S., Massachusetts Institute of Technology, Cambridge, Massachusetts.

CHAMBERLAIN, J. W., Kitt Peak Observatory, Tucson, Arizona.

Снарман, S., University of Alaska, College, Alaska.

CHRISTY, R. F., California Institute of Technology, Pasadena, California.

CLADIS, J. B., Lockheed Missiles and Space Co., Research Laboratories, Palo Alto, California.

 ${\it CLINE}, T.\ L., Goddard\ Space\ Flight\ Center, NASA, Greenbelt, Maryland.$

COLBURN, D. S., Ames Research Center, NASA, Moffett Field, California.

COLEMAN, P. J., Jr., University of California, Los Angeles, California.

Davis, L., Jr., California Institute of Technology, Pasadena, California.

DEUTSCH, A., California Institute of Technology/Mt. Wilson and Palomar Observatories, Pasadena, California.

Drake, F., Jet Propulsion Laboratory, Pasadena, California.

DUNGEY, J. W., Imperial College of Science and Technology, London, England.

Edberg, J. R., Jet Propulsion Laboratory, Pasadena, California.

FREEMAN, J. W., National Aeronautics and Space Administration, Washington, D.C.

GOLD, T., Cornell University, Ithaca, New York.

HARRINGTON, J. V., Lincoln Laboratories, Massachusetts Institute of Technology, Lexington, Massachusetts.

Hess, W. N., Goddard Space Flight Center, NASA, Greenbelt, Maryland.

HINTON, F. L., California Institute of Technology, Pasadena, California. HIRSCH, W., Jet Propulsion Laboratory, Pasadena, California.

HONES, E. W., JR., Institute for Defense Analysis, Washington, D.C.

HOWARD, R. F., California Institute of Technology/Mt. Wilson and Palomar Observatories, Pasadena, California.

ISRAEL, M. H., California Institute of Technology, Pasadena, California. JEFFERIES, J. T., High Altitude Observatory, Boulder, Colorado.

JOKIPII, J. R., California Institute of Technology, Pasadena, California.

KALLMAN BIJL, H. K., University of California, Los Angeles, California.

KENNEL, C., Avco-Everett Research Laboratory, Everett, Massachusetts. KERN, J. W., RAND Corporation, Santa Monica, California.

LAZARUS, A. J., Massachusetts Institute of Technology, Cambridge, Massachusetts.

LEES, L., California Institute of Technology, Pasadena, California.

LEIGHTON, R. B., California Institute of Technology, Pasadena, California.

LIEBER, A. J., Ames Research Center, NASA, Moffett Field, California.

LIEPMANN, H. W., California Institute of Technology, Pasadena, California.

Lüst, R., Max-Planck-Institut für Physik und Astrophysik, Munich, Germany.

Lyon, E. F., Massachusetts Institute of Technology, Cambridge, Massachusetts.

MACK, L., Jet Propulsion Laboratory, Pasadena, California.

MACKIN, R. J., Jr., Jet Propulsion Laboratory, Pasadena, California.

McDonald, W. S., Jet Propulsion Laboratory, Pasadena, California.

MEAD, G. D., Goddard Space Flight Center, NASA, Greenbelt, Maryland.

MELZNER, F., Max-Planck-Institut für Physik und Astrophysik, Munich, Germany.

MÜNCH, G., California Institute of Technology, Pasadena, California.

NEHER, H. V., California Institute of Technology, Pasadena, California.

Ness, N. F., Goddard Space Flight Center, NASA, Greenbelt, Maryland.

Neugebauer, G., California Institute of Technology, Pasadena, California.

 $\label{eq:neugebound} \textbf{Neugebauer}, \textbf{M.}, \textbf{Jet Propulsion Laboratory}, \textbf{Pasadena}, \textbf{California}.$

Noble, L. M., TRW-Space Technology Laboratories, Inc., Redondo Beach, California.

OGILVIE, K., Goddard Space Flight Center, NASA, Greenbelt, Maryland. OLBERT, S., Massachusetts Institute of Technology, Cambridge, Massachusetts.

PALM, A., University of California, Berkeley, California.

PARKER, E. N., University of Chicago, Chicago, Illinois.

Petschek, H. E., Avco-Everett Research Laboratory, Everett, Massachusetts.

SCARF, F. L., TRW-Space Technology Laboratories, Inc., Redondo Beach, California.

SCHERB, F., Massachusetts Institute of Technology, Cambridge, Massachusetts.

Schweizer, F., Jet Propulsion Laboratory, Pasadena, California.

SERLEMITSOS, P., Goddard Space Flight Center, NASA, Greenbelt, Maryland.

Sheeley, N., Jr., California Institute of Technology, Pasadena, California. Siscoe, G., Massachusetts Institute of Technology, Cambridge, Massachusetts.

SLUTZ, R. J., National Bureau of Standards, Boulder, Colorado.

SMITH, E. J., Jet Propulsion Laboratory, Pasadena, California.

SNYDER, C. W., Jet Propulsion Laboratory, Pasadena, California.

Sonnerup, B. U Ö., Royal Institute of Technology, Stockholm, Sweden.

THOMAS, J., Ames Research Center, NASA, Moffett Field, Çalifornia.

VESTINE, E. H., RAND Corporation, Santa Monica, California.

Vogt, R. E., California Institute of Technology, Pasadena, California.

Watts, A. M., California Institute of Technology, Pasadena, California.

WEYMANN, R., University of Arizona, Tucson, Arizona.

WILCOX, J. M., University of California, Berkeley, California.

WILKERSON, T., University of Maryland, College Park, Maryland.

WOLFE, J. H., Ames Research Center, NASA, Moffett Field, California.

WYNDHAM, J. D., California Institute of Technology, Pasadena, California. ZIRIN, H., High Altitude Observatory, Boulder, Colorado.

Page intentionally left blank

EDITORS' PREFACE

THE Jet Propulsion Laboratory Conference on the Solar Wind, which was held on April 1-4, 1964, was first organized as an occasion to present the collected and analyzed results of the *Mariner-2* interplanetary experiments to scientists interested in the solar wind. The value of the Conference was increased enormously by the launching and successful operation of the *IMP* satellite (*Explorer 18*) and by the release of large quantities of preliminary data obtained from its experiments.

The ultimate aim of the Conference was to promote extensive discussions on one or another aspect of the solar wind by representatives of all the disciplines concerned with the subject. To accomplish this aim, it was necessary, first of all, to limit the attendance to a small fraction of the total number of scientists interested in the subject. Secondly, the number of formal papers was held to a minimum; each session included one or two invited review papers. The remaining papers, some of which were generated spontaneously at the Conference, were limited in time. As a result, informal and spontaneous discussions became a major feature of the Conference.

The participants represented 27 different scientific institutions in 4 countries. More important, they represented the fields of theoretical and experimental interplanetary physics, astrophysics, radio astronomy, solar physics, plasma physics, and aerodynamics. Perhaps one of the most impressive results of the Conference was the development of significant physical insights that arose from the exchange of views between scientists with quite different backgrounds.

This volume was prepared primarily from stenotype transcripts, although a few speakers submitted manuscripts. The illustrations were taken from the slides shown during the Conference, and from the blackboard diagrams drawn by the speakers during their presentations. Unfortunately it was necessary to omit from the book H. Zirin's excellent discussion and accompanying movie of solar surface phenomena. Also, some comments by mumbling speakers have been lost completely.

We have tried to retain much of the colloquial and conversational flavor of the verbal presentations, while making enough changes in the transcript to keep the text readable and unambiguous. In some cases, the material has been rearranged to promote clarity and logical order. References have been added wherever they seemed to be appropriate. The speakers were given an opportunity to review the manuscript at a late stage in the editorial process, and were encouraged to update the information presented; significant modifications to the original presentation

have been identified in footnotes. We hope that the number of technical errors is insignificant, but of course we accept full responsibility for those that exist.

That the Conference took place at all is primarily due to the energy and tenacity of Leverett Davis, Jr. The Conference owed much of its technical excellence to the planning activities of the Organizing Committee, to whom we are grateful. They are:

L. P. BLOCK	Royal Institute of Technology and Jet
	Propulsion Laboratory.
H. S. Bridge	Massachusetts Institute of
	Technology.
L. Davis, Jr.	California Institute of Technology.
R. Lüst	Max-Planck-Institut für Physik und
	Astrophysik.
D I 1/	T. D. I. T. I.

R. J. MACKIN, JR.	Jet Propulsion Laboratory.
E. N. PARKER	University of Chicago.
C. W. SNYDER	Jet Propulsion Laboratory.

Finally, we wish to express our gratitude to R. M. Van Buren who, in addition to supervising the technical aspects of preparing the manuscript for publication, played a major role in translating much convolute scientific prose into (it is hoped) readable, precise English.

The JPL sponsorship of the Conference represents one phase of the work carried out by JPL under NASA Contract NAS 7-100.

ROBERT J. MACKIN, JR. MARCIA NEUGEBAUER

Jet Propulsion Laboratory Pasadena, California July 1, 1964

FOREWORD

THE conference reported in this volume dealt, in terms of our present knowledge and understanding, with various aspects of events, originating mainly in the Sun, that occur in interplanetary space and in the neighborhood of the Earth. Two main kinds of data are described and discussed. One kind is the data relating to the *matter* that exists in those regions – the solar plasma, the Moon, cosmic rays, comets – and describing the properties of that matter such as (in the case of the solar plasma, for instance) density, speed, direction of motion, composition, and temperature. The other kind is the data relating to the magnetic field there present-its strength, direction, distribution (for instance, its degree of uniformity or non-uniformity), and its time changes. Facts and theories are described – the former according to observations (the best available, though still imperfect and incomplete) made by the most reliable and advanced instruments carried on such spacecraft as Mariner 2 and the Explorer series of satellites, especially IMP 1. Some comparisons are made between spacecraft data and data obtained from the surface of the Earth, such as auroral and magnetic data. The magnetic data appear in the form of either a description of the current system of polar magnetic substorms or the Bartels planetary 3-hr summarizing index, Kp, which is a measure of the activity of those geomagnetic changes that are caused by solar corpuscular action upon the Earth.

1. THE SOLAR WIND

The magnetic fields measured are those on the Sun (Paper 11 by Leighton), those carried away from the Sun by ionized gas (Paper 2 by Snyder and Neugebauer; Paper 3 by Davis, Smith, Coleman, and Sonett; and Paper 6 by Ness), or the field that comes up from the core of the Earth and is modified by wave and particle radiations from the Sun. The external and internal fields interact in the region around the Earth in ways by no means fully understood at present.

The solar magnetic fields reach toward the Earth with an appreciable intensity because they are transported by solar plasma. Hence the solar plasma is the primary feature to be considered. It is the subject of Paper 1 by Neugebauer and Snyder, and of Paper 8 by Bridge. The plasma comes from the Sun in three fairly distinct ways. The first is by perpetual general

outflow from the solar corona all over the Sun: I suggest that the term solar wind may be most appropriately reserved for this type of flow. It was first inferred by Biermann from his cometary researches (see Papers 24 by Biermann and Lüst, 25 by Biermann, and 26 by Beard). It may be called an escape flow. Although atmospheric escape was first envisaged by Johnstone Stoney, the solar wind appears to have a special character, elucidated theoretically by Parker. The Mariner-2 observations (Paper 1) confirm the existence of this continuing plasma flow. In Paper 13, Scarf discusses the solar-wind theories developed by Parker and Chamberlain, and indicates some of the difficult and complex questions still unsettled. The bearing of diffusion on the composition of the corona and of the solar wind is discussed in Paper 14 by Jokipii. The second and third kinds of solar plasma flow may be called ejected flows, although we do not know the mechanisms of the ejections.

2. SOLAR CORPUSCULAR STREAMS

The second mode of solar-plasma emission is in the form of laterally limited and intermittent jets, for which the term solar (corpuscular) stream has long been used. This mode of emission was postulated more than 50 years ago on the basis of the 27-day recurrence tendency in geomagnetic disturbances. Maunder and Chree were leaders in the investigation of this phenomenon, and Maunder gave the first cogent interpretation of it in terms of a solar stream. Though intermittent, the emission often continues for weeks or months, apparently from the same region on the Sun. The strength of the evidence for such streams has long been recognized, despite our inability to explain the emission (cf. the remark by Gold, relative to a different situation, in the discussion of Paper 9: "...in science one often has to proceed on the basis that a theoretical process is necessary to account for the observations, even if one cannot trace out the process in detail"). The areas of stream emission, called M regions by Bartels, still have not been identified with certainty. That such streams must have a spiral form as a result of the Sun's rotation was made clear about 35 years ago. The interest of this form, for streams that are carrying a magnetic field, and the possible influence of the streams on cosmic rays (see Paper 4 by Anderson, Paper 5 by Cline et al., and Paper 12 by Parker), were not recognized till later. These questions have been discussed by Alfvén, Gold, Meyer, Morrison, and Parker. In Paper 2, Snyder and Neugebauer raise interesting points concerning the nonradial emission of streams and concerning the interference between the solar wind and solar streams having different speeds.

3. SOLAR-FLARE EMISSIONS: PLASMA SHELLS

The third kind of solar-plasma emission is much more limited in time. since it occurs during solar flares, whose usual duration is about an hour or less. At least in some cases, the emission can be far from radial, because some flares produce terrestrial effects even though they appear quite close to the edge of the Sun. The short duration of emission implies that the outflow is radially limited, though a dispersion of the emission speeds will cause the radial extent to increase as the gas travels onward. The emission may be in the form of a cone, and the cone may sometimes have a wide angle; or the emission may possibly occur in a cluster of jets, forming a set of travelling clouds lying roughly on a spherical surface. Lateral expansion may cause the clouds to merge into a spherical shell (of less than hemispherical extent). In any case, plasma thus emitted may appropriately be called a plasma shell or solar shell. In this connection I may quote the following passage about the corona: "There is a growing suspicion among observational astronomers that the corona itself may be composed of fine dense streamers, unresolved in contemporary instruments to give the appearance of a more or less homogeneous coronal atmosphere." Paper 7 by Wyndham has some bearing on this question.

Although the action of the Sun is vital to the phenomena discussed at the conference, there was comparatively little discussion of the mechanism of the stream and shell emissions. Differences of view came to light concerning the level from which these emissions come. Parker seemed to regard at least the flare material as coming from the corona, like the wind. Gold remained ready to consider different levels of emission, at any rate down to the chromosphere (see the discussion of Paper 9). No decided stand was taken on this question by the solar experts present: Athay, Leighton, and Zirin.

4. SOLAR-PLASMA IMPACT ON THE GEOMAGNETIC FIELD

The impact of charged solar particles upon the Earth was first investigated experimentally by Birkeland (later by his followers in this field, Brüche and Bennett), and theoretically by Störmer, for streams of solar gas supposed to consist entirely of electrons. Schuster was prominent in

¹Parker, E. N., Interplanetary Dynamical Processes, Interscience Publishers, a division of John Wiley and Sons, Inc., New York (1963) p. 20 (footnote). Evershed indicated long ago that the *chromosphere* is by no means a uniform envelope: "... it consists of jets and miniature prominences..." See Evershed, J., *The Observatory* 48, 45 (1925)

criticizing such a hypothesis of solar action, because of the electrostatic repulsion and consequent dispersion of the particles. Lindemann (1919) proposed that the solar gas is neutral and ionized; namely, a plasma, in the terminology introduced (in a quite different connection) by Langmuir (1928). Lindemann's proposal, now generally accepted, was a constructive addition to a paper that demolished an ill-judged magnetic-storm theory that I proposed in 1918—itself an addendum to a useful morphological study of such storms.

5. THE CAVITY, MAGNETOPAUSE, AND MAGNETOSPHERE

Naturally when the first primitive attempt was made (1929) to infer the consequences of the impact of solar plasma upon the geomagnetic field, the simplest idealized conditions were considered. These conditions also corresponded with the state of knowledge at that time. Thus no account was taken of any matter in interplanetary space or in the space around the Earth, where the chief effects occur. The random motions in the plasma were assumed to correspond to a temperature of the order of 6,000 °K, but they were not taken into account to any extent in the theory. Nor was any magnetic field in the stream considered—the weak dipole field of the Sun was ignored, and the concept of the transport of magnetic fields by plasma had not yet appeared. Alfvén (1940) later proposed a very different solution to the problem, laying stress on the presence of the general solar field in the gas, and of an accompanying electric field.

Satellite exploration seems to have confirmed many of the results inferred by Ferraro and myself. Our main conclusions were that a cavity is formed in the plasma by the positively- and negatively-charged particles turning aside and back, and that the geomagnetic field is confined in this cavity—a region now known as the magnetosphere (the term was first proposed by Gold). Also, the compression of the field within this cavity is to be viewed as the result of the superposition of an additional field, which in turn is caused by electric current flow over the cavity surface. This flow results from the slightly different motions of oppositely charged particles at the surface of the cavity. The additional field annuls the geomagnetic field in the plasma outside the boundary of the cavity—that is, the plasma is shielded from the Earth's field, except in its surface layer. Within the cavity the field is increased above the surface of the Earth. This feature provides an explanation of the first phase of a typical magnetic storm, namely, the initial increase of the field, especially the horizontal component, over most of the Earth. Charged solar particles seem unable to enter the cavity, except possibly across small areas of its surface around two neutral points-one north and one south of the dipole equatorial plane — where a field line meets the cavity surface perpendicularly.

We determined the scale of the cavity, but not the form of its boundary surface; nor did we determine whether the cavity would be open or closed on the side of the Earth away from the Sun. These questions were dealt with much later by Zhigulev and Romishevskii, Hurley, Dungey, Beard, Spreiter and his colleagues, Johnson, and in this conference by Mead (Paper 23). Their results, which seem to be generally confirmed by satellite exploration, were based on the concept, introduced by Martyn, of a balance between the plasma pressure on the boundary and the magnetic-field pressure within the cavity.

All this work, however, is controverted by Alfvén in a recent article.² The great contributions he has made to magnionics—the branch of science dealing with the motions of charged particles in magnetic and electric fields³—entitle his views to serious attention. His depreciative comment on the calculations of the plasma-cavity form expresses perhaps more strongly an opinion voiced in Paper 16 by Axford. Dr. Alfvén and his colleagues have made and are making interesting experimental as well as theoretical researches on this general subject. Paper 19 by B.U.Ö. Sonnerup, from Dr. Alfvén's Institute, touches especially on the question of whether that part of the cavity behind the Earth is open or closed; he suggests that it is sometimes one, sometimes the other. Axford, in Paper 16, concludes that it is closed at a distance of more than 60 R_E; Slutz also has an interesting comment on this subject in the discussion of Papers 16–18.

6. THE SHOCK FRONT AND THE TRANSITION REGION

Satellite exploration has revealed an important feature that did not appear in the analysis by Ferraro and myself, because we did not consider any magnetic field transported by the plasma. This feature is a transition region outside the above-mentioned cavity boundary, lying between it and an outer shock-wave boundary. A shock wave was first suggested by Gold in 1955. In Paper 16, Axford gives an illuminating exposition of the conceptions *shock front*, *continuum*, and *supersonic* as applied to a plasma in a magnetic field. The influence of the magnetic field in the plasma has been investigated on aerodynamic principles by Kellogg (1962) and by Spreiter and Jones (1963). Paper 10 by Sonett, Colburn, and Briggs; Paper 21 by Lyon; and Paper 22 by Ness describe recent satellite observations of and in this transition region. In this branch of science, where so many mysteries confront us, it is pleasing to be told (Paper 22) of "remarkable agreement" between the observations and the results predicted by

²Alfvén, H., Space Science Reviews 2, 862 (1963)

³For an application, see Paper 20 (Hones) and its discussion

the aerodynamic treatments referred to. Scarf, in the discussion of Papers 16–18, indicated various complicating factors that must be considered in the theory of the transition region.

Gold's original suggestion of a shock wave made reference to the suddenness of the commencement of many magnetic storms. The behavior seems to have an adequate explanation in the analysis by Ferraro and myself, and it is not clear whether the shock front at the outer margin of the transition region bears on this suddenness. The cavity and the transition region must always be present, like the solar-plasma flow; but the sudden beginning of flare-produced magnetic storms implies a sharp enhancement of the plasma flow.

7. MAGNETIC STORMS WITH A MAIN PHASE: THE RING CURRENT

In many storms in which there is an initial increase of the surface field at the Earth, indicating increased flow, this first storm phase is followed by a larger decrease of the surface field. This decrease is often the main phase; it has a longer duration before the minimum field is attained, and a still longer period of recovery to normal. The main phase implies that there is a westward electric current, or an enhanced westward current, around the Earth. This is known as the ring current, first envisaged by Störmer in the form of an incomplete circuit of electron flow at a distance from the Earth beyond the orbit of the Moon. His suggestion of a ring current was made to remove a difficulty in his auroral theory. Schmidt, who later revived the idea on a more solid basis of geomagnetic evidence, did not speculate about how far from the Earth the ring current is located. Ferraro and I placed it within the plasma cavity, hence within a few R_E from the Earth. We tried hard, entirely without success, to infer its growth as a necessary consequence of the plasma flow upon and around the geomagnetic field. It was later recognized that there are many storms with a notable first phase that do not develop the typical main phase, which shows that the ring current does not inevitably accompany the plasma flow. But several satellites have confirmed that, in storms with a main phase, the kinetic energy stored in the Van Allen belts is enhanced; and magnionic theory, particularly as developed by Alfvén and Parker, shows that the main-phase decrease of the field at the Earth's equatorial surface is proportional to the kinetic energy stored in the belts. The current flow is not wholly westward; in that part of the ring current nearest to the Earth the electric flow is eastward-but farther away the westward flow is dominant. Akasofu and I have recently described geomagneticstorm evidence which we interpret as indicating that the ring current may at times flow in part through the ionosphere.

8. DOES THE SOLAR PLASMA CONTAIN A SIGNIFICANT NEUTRAL ATOMIC COMPONENT?

There has been much discussion as to whether solar particles can get into the cavity in the plasma. The particles that enter our atmosphere and produce the aurora come from the magnetosphere. Formerly no one doubted that these particles came from the Sun. Attempts have been made to show that some solar particles can diffuse across the cavity boundary, possibly helped by random variations of the plasma or of the magnetic field. Axford (Paper 16) considers that particles must bring into the magnetosphere from outside the extra energy present during magnetic storms. But the entry of particles from the Sun is doubted by many workers, who as an alternative propose that background particles belonging to the Earth's far-reaching atmosphere are in some way accelerated and energized. This problem was briefly discussed at the conference (see the remarks by Parker, Block and Axford in the discussion of Papers 16–18). Processes suggested by Kellogg, Alfvén, Parker, and Gold were mentioned.

Not very much attention was given at the conference to the question of why plasma flow leads to a main phase in some magnetic storms but not in others. One possibility, suggested by Akasofu and myself, is that the difference concerns the solar magnetic fields transported by the plasma; but no clear understanding has been reached as to how such differences could either govern or obviate the growth of the ring current. A quite different and perhaps more promising explanation of the differences in the development of storms has been proposed by Akasofu and McIlwain. Their explanation is that the ionized component of the solar plasma is sometimes accompanied by a small amount of neutral hydrogen atoms from the Sun, travelling with similar speed. If so, these atoms can without hindrance cross the cavity boundary, where their charged companions are turned away. Thus the neutral atoms can introduce kinetic energy far into the magnetosphere. There, by a transfer of their electrons to atmospheric particles with which they collide, the fast-moving hydrogen atoms become energetic protons, subject to the magnetic field, and members of the Van Allen belts. Thus they can contribute to the ring current and to the main phase of the storm. It is very desirable that future satellites investigate whether the solar plasma does contain neutral atoms, and if so, how many.

9. OPTICAL AND CORPUSCULAR SOLAR ECLIPSES OF THE IONOSPHERE

About thirty years ago I suggested that neutral atoms might play a significant part in the ionization of the ionosphere (on the sunlit hemis phere, of course), like the solar wave radiation that falls on the Earth.

xxii FOREWORD

Appleton suggested that solar eclipses might indicate whether or not this idea is valid. I showed that if the neutral particles have a speed similar to that of the plasma that causes magnetic storms—that is, of the order of 1,000 km/sec - then there would be a corpuscular eclipse at a place more than 1,000 miles away from the optical eclipse, and an hour or so earlier. Observations during eclipses showed conclusively that the E layer of the ionosphere is ionized by wave radiation from the Sun. Some people claimed to have observed corpuscular eclipses of the F layer, but these claims have remained doubtful. It is clear that particles with a speed of 1,000 km/ sec could not penetrate to the E layer; the fact that the particles that produce auroras do penetrate to the E layer, and even a little below it, is taken as an indication of accelerative processes affecting ionized particles in the region adjacent to the Earth. At the time, the possibility that charge exchange might affect the neutral particles was not considered; in those days the atmosphere was thought to extend not nearly so far out as it is now known to do. It now becomes of interest to examine whether the neutral particles suggested as contributing to the ring current, especially during the greatest magnetic storms, could appreciably affect the ionization of the F layer. Even if such an effect appears only above the F₂ peak. it may be observable now by top-level ionospheric sounders on satellites, such as those carried by Alouette and Ariel. The thermal motions of the neutral hydrogen atoms (which need not be the same as those of the plasma ions) would tend to blur the corpuscular eclipse. Even so, if there is a flux of neutral solar atoms, then a properly instrumented spacecraft would detect a corpuscular-eclipse track provided it passed through such a track not far from the Moon on the earthward side. Finally, it is possible that some of the kinetic energy introduced by the neutral atoms may be transformed into heat in (or conducted down to) the layers where Jacchia and his colleagues have found variations of atmospheric temperature and distribution closely associated with the Kp index.

10. SOLAR-EMISSION PROCESSES

The morphology of auroras and magnetic storms indicates that the particles causing them are subject to the geomagnetic field. In his original solar-plasma proposal, Lindemann tried to calculate how much of the gas, if it were originally partly neutral, would become ionized by the Sun's radiation on the way to the Earth. Kahn later investigated such ionizing effects more thoroughly—in connection with attempts to detect the plasma between the Earth and the Sun by Doppler change of absorption lines, such as those of singly ionized calcium. Akasofu has extended Kahn's

analysis to the ionization of neutral hydrogen atoms that are on their way from the Sun. The problem remains as to how neutral hydrogen atoms can escape from the Sun. If the plasma comes from high in the solar corona, like the solar wind, the absence of any hydrogen atoms there would preclude any neutral component in the solar corpuscular flow. It is possible to imagine the violent ejection of flare matter from much lower down, where there is neutral hydrogen, though we do not know any mechanism for such ejection. Another possibility is the Milne process (1926) for the acceleration of chromospheric particles such as ionized calcium and neutral hydrogen, which produce strong absorption lines in the Fraunhofer spectrum. Milne claimed that his process could give speeds of the order of 1,000 km/sec to a small fraction of the absorbing atoms, but we have no quantitative estimate of the flux that this process could provide under different solar conditions; the problem seems worthy of attention. Milne considered that Ca⁺ ions, which produce two of the principal absorption lines in the solar spectrum, would give the most plentiful component of the flow produced by his process. He did not consider the change of these ions to Ca⁺⁺ ions by further ionization on their way from the Sun; Kahn later inferred that a considerable fraction would be thus changed. This would modify the limiting speed of the Ca ions reaching the Earth. However, it is the neutral atoms ejected by the Milne process that are of chief

The nature of solar flares is still a great mystery. Parker, after careful investigation (1963), ruled out the mutual annihilation of magnetic fields as the source of the energy manifested in flares. In Paper 15, Petschek proposes a wave-propagation mechanism as a new and important element in the problem; this mechanism gives a much faster rate of reconnection than any heretofore estimated. It seems appropriate to call attention to the ideas, put forward over many years by Bruce, concerning the importance of electrical discharges in the cosmos, and in particular in the Sun's atmosphere. Bruce agrees that the Sun offers his ideas perhaps their greatest challenge, because of the very high electrical conductivity of the solar material at all levels. Any electrical discharge in the Sun's atmosphere demands an exceptionally rapid and strong means of generating differences in electric potential. For some years he made no suggestion as to how such potential differences could be built up in the Sun. Later he proposed as a possibility that small aggregations of the most refractory materials form at the level of the Sun's atmosphere where the temperature attains its minimum value of about 4,000 °K. An expert on electrical discharges, he asserts that wherever there is dust (particulate matter) and convection in a gas, separation of charge and the buildup of electric potentials will occur. He regards electrical discharges as a perennial feature all over the Sun, and as responsible for the emission of the solar

streams and shells that cause magnetic storms. At my invitation, he contributed a brief account of his ideas on this subject to the published version (de Witt, Hieblot, and Lebeau, 1963) of my 1962 lectures at the Les Houches summer school. At present it seems difficult to assess the merits of these ideas because of the lack of any quantitative estimates of some of the factors that, according to his views, must be involved. It is pertinent to note, in this connection, that there are still many unsettled questions concerning the lightning storms that occur only a few miles above our heads in our own atmosphere.

11. SOLAR-PLASMA FLOW AND COSMIC RAYS

The discovery of cosmic rays half a century ago revealed the presence in Nature of particles whose energy ranged up to values far beyond any previously contemplated. It gave a new stimulus to nuclear physics by leading to the discovery of new kinds of particles, and by prompting the invention of devices to produce high-energy particles for controlled research. Gradually it became evident that there were connections between cosmic rays and solar and geomagnetic phenomena, including the sunspot cycle and the 27-day recurrence tendency. These connections provoked in some laboratory physicists a novel interest in the long-continued recording of natural events, common in meteorology and geomagnetism, about which their attitude had often seemed supercilious. Thus the variations of cosmic rays came to be viewed in a new light – as indicators of conditions on and around the Sun, and out to great distances from it, that add to or influence the flow of the high-energy particles onto the Earth. The advent of satellites increased the value of cosmic rays as such indicators by enlarging the regions of space over which we can record their variations.

This subject is discussed in Papers 4, 5, and 12 by Anderson, Cline et al., and Parker, respectively. Many theories of the relations between cosmic rays and solar and geomagnetic phenomena have been proposed. These theories link cosmic rays with magnetic fields drawn out from the Sun by plasma in solar streams of spiral form, and also with disordered remnants of such fields well beyond the Earth's orbit. Paper 5 concludes that the cosmic-ray changes give evidence of long-continued, laterally limited solar streams and their magnetic configurations, quite independent of the powerful evidence for such streams afforded by statistics of geomagnetic disturbance.

Some uncertainty and difference of opinion appeared concerning the continuity or disconnection of field lines drawn out from the Sun's atmosphere, and concerning the rate of mutual annihilation of adjacent magnetic fields lying in opposed directions. This question, raised by Sweet and

Parker several years ago, bears on the cosmic-ray variations. The mechanism for magnetic-field reconnection proposed in Paper 15 by Petschek provides a means for much more rapid disconnection of field lines from the Sun than has previously been estimated.

The discussions of cosmic rays concern both those that were originally discovered (now called galactic) and those of less energy later found to be occasionally emitted by the Sun. The galactic cosmic rays bear on phenomena whose scale is far greater than that of the solar system, as indicated by Parker in Paper 12.

Perhaps I may be allowed this opportunity to comment on the nomenclature of the subject, which has long seemed to me to be needlessly cumbersome, somewhat antiquated, and almost reminiscent of popular ideas like death rays. I suggest the following substitute terms for the consideration of those concerned with the subject:

cosmic ray	cosmon
galactic cosmic ray	galacton
solar cosmic ray	helion
nebular cosmic ray	nephelon
alpha particle	alphon
beta particle	beton
gamma ray	gamon

The adoption of such terms would shorten discussion; for example, "the number density of galactic cosmic rays" would become "the number density of galactons" or "the galacton number density."

12. SOLAR PLASMA AND COMETS

Papers 24, 25, and 26 discuss the action of the solar plasma upon comets. Since comets have no magnetic field, the interaction involves considerations different from those concerning plasma impact upon the geomagnetosphere. Nevertheless, the production of ions around the nucleus and tail(s) of a comet, partly by charge exchange with solar plasma, creates a conducting region that affects the travel of the magnetic fields carried away from the Sun by the plasma. Some of the magnionic and hydromagnetic problems thus raised are discussed by Beard in Paper 26. Surfaces with some of the characteristics of shock fronts are formed on the sunward side of the comet nucleus, as inferred by Biermann in Paper 25.

Biermann and Lüst, in Paper 24, stress the value of comets as probes of the solar plasma and interplanetary space, especially in regions far from the Earth, and far from the near-ecliptic regions traversed by spacecraft engaged in planetary exploration. Such use as probes, however, is contingent on a fuller understanding of the nature of comets and their tails, and of the action of solar plasma upon them.

One present inference drawn in Paper 24 is that the interplanetary plasma does not rotate with the Sun at the distance of the Earth's orbit, nor beyond half this distance. This is not inconsistent with previous studies by Lüst and Schlüter, which had suggested that the rotation of the general heliomagnetic field would carry the plasma around with it up to distances of about $50\,R_8$ or $0.25\,AU$.

Paper 24 also suggests the use, as probes, of artificial comets in the form of ion clouds ejected from satellites.

13. SOLAR PLASMA AND THE MOON

The Moon offers an obstacle to the flow of solar plasma—a type of obstacle very different from either the Earth or comets. U.S.S.R. spacecraft observations suggest a low upper limit to the strength of any lunar magnetic field, and this is in accordance with the general view that the Moon is solid to the center—a hypothesis recently questioned by Runcorn (1963). In Paper 27, Gold considers the plasma action on the Moon on the basis of the usual view, neglecting any lunar magnetic field. He infers that the magnetic-field lines carried with the plasma will be forced some distance into the sunward face of the Moon; electric forces will be associated with their distortion. The crowded field lines on the sunward side will be bounded by a shock front. Variations of the solar-plasma flow and the field carried with it will produce considerable variations in the shock front. (Alfvén emphasized the great difference between the Moon's effects on a plasma entirely without a magnetic field, and its effects on one with even a very weak field; see footnote 2.)

One of the many original conclusions drawn in Paper 27 is that the magnetic measurements made by a satellite orbiting very close to the Moon may reveal the time history of long-past solar-plasma flow. Another is that the impact of solar electrons may produce X-rays dangerous to lunar explorers. Yet another is that the impact of the solar plasma will preclude any buildup of a lunar atmosphere from gaseous radioactive-decay products exhaled from within the solid body of the Moon.

Paper 28 by Ness reports remarkable observations that indicate the existence, on the dark side of the Moon, of a long, field-free tail. This tail may be called a magnetic corpuscular eclipse region, bordered by an irregular magnetic field. It is apparently not blurred out by random motions of the solar particles, a possibility mentioned in Section 9 in connection with another variety of corpuscular eclipse region. Figure 8, Paper 28, suggests that the magnetic eclipse region is of considerable extent, but it remains for future satellite exploration to reveal whether the

eclipse is able to affect the magnetosphere and to cause any observable magnetic change at the Earth's surface. If the effect occurs, it will be a corpuscular eclipse effect—perhaps more often observable than the optical eclipse effects, because the magnetic-eclipse region may be wider than the optical shadow region, and so may affect the Earth when the optical shadow may fail to reach us.

Paper 28 also mentions various views regarding the effects of the Moon on the Earth. The semidiurnal lunar atmospheric tide undoubtedly affects certain meteorological elements (especially pressure and wind), and also affects the geomagnetic field and cosmic rays. Many determinations of these lunar tidal effects have been made with suitably small probable errors. By contrast, few if any reports claiming to have identified lunar monthly changes in meteorological and other geophysical data have withstood critical examination. Bartels (1963) has given what seems to me an effective dismissal of one of the latest of such claims, affecting the statistics of geomagnetic disturbance (Bigg, 1963).

14. SOLAR PLASMA, THE AURORA, AND MAGNETIC STORMS

Perhaps the longest discussion, and one of great interest, deals with Papers 16 (Axford), 17 (Dungey), and 18 (Petschek). These papers discuss the phenomena that occur across, at, and within the cavity boundary of the magnetosphere. Paper 18 concerns the connection or reconnection of field lines of the interplanetary plasma with those of the magnetosphere. Paper 17 also deals with the interplanetary plasma field, and with neutral points from which proceed field lines that cover whole surfaces. The latter part of Paper 16 describes a system of magnetospheric circulation (cf. Axford and Hines, 1961) suggested by, and regarded as linked with, the polar electric current system. The configuration is shown in Fig. 1, Paper 16, in an idealized form (for which I am responsible -1935). Vestine and Obayashi and others have drawn somewhat similar diagrams based on better polar data than were available to me at the time. The current system usually has a rather different orientation, which is variable; but in general form the pattern has been thought to resemble the one shown in Fig. 1, Paper 16.

All this work bears on the aurora, the ring current, and on auroral and magnetic substorms, which are phenomena proceeding from the magnetosphere. Of all the regions discussed in this conference, the magnetosphere (above the ionosphere) is the one nearest to the Earth. It is a region much traversed by rockets and satellites. But the events occurring there are so complex and variable that, as may be considered natural, there is as yet no

accepted comprehensive theory of these events. Moreover, our recognition of important features of these events is still developing. For example, we are only now approaching a general conception (Fig. 2, Paper 17) of the morphology of so important a magnetospheric event as an auroral substorm (Akasofu, 1964). This morphology is closely connected with magnetic substorms and with their electric current system.

I confess with regret that I am often unable to follow arguments and speculations proposed on these subjects by my colleagues, including some of those given in the papers and discussions considered here. These arguments represent partly an *a priori* development of the kind attempted by Ferraro and myself, but going far beyond where we were able to penetrate. Such an approach is very desirable, but also very difficult: it must be combined with a comprehensive knowledge and study of the magnetic, auroral, and ionospheric phenomena observed from the Earth's surface and from satellites and space probes. The combined investigation is now occupying many very able minds, but the debate is likely to continue in lively fashion for at least some years longer.

S. CHAPMAN

Boulder, Colorado July, 1964

BIBLIOGRAPHICAL NOTES

Geomagnetism (Chapman, S. and J. Bartels, Oxford University Press, New York, 1940) gives references to the papers written before 1939 by Appleton, Bartels, Chree, Lindemann, Maunder, Milne, Schuster and others (including Ferraro and myself), mentioned especially in Sections 2, 4, and 5.

Geophysics, The Earth's Environment (ed. by C. de Witt, J. Hieblot, and A. Lebeau, Gordon and Breach, New York, 1963) gives references to several later papers by Akasofu, Alfvén, Beard, Bruce, Chamberlain, Dungey, Gold, Hurley, Kahn, Martyn, McIlwain, Parker, Spreiter and colleagues, Vestine, Zhigulev and Romishevskii, and others: see pp. 173, 174, 498–502, 549, 550.

The papers on lunar monthly effects, mentioned in Section 13, are:

Bigg, E. K., Journal of Geophysical Research 68, 1409 (1963).

Bartels, J., Nachrichten der Akademie der Wissenschaften in Göttingen, II Mathemmatisch-physikalische Klasse, Nr. 23 (1963).

Concerning the interior of the Moon, see:

Runcorn, S. K., Technical Report No. 32-529, Jet Propulsion Laboratory, Pasadena (1963).

For the magnetospheric circulation proposed by Axford and Hines, see:

Axford, W. I. and C. O. Hines, Canadian Journal of Physics 39, 1433 (1961).

ACKNOWLEDGMENTS

THE editors are grateful to the following organizations for their kind permission to reprint the material described below:

The American Geophysical Union, Journal of Geophysical Research:

Paper 6, Figures 1-16, Paper 22, Figures 1-16, Paper 28, Figures 1-3 and Figure 8 from N. F. Ness, C. S. Scearce, and J. B. Seek, 69, 3531 (1964)

Paper 8, Figure 7 from J. F. Steljes, H. Carmichael, and K. G. McCracken, 66, 1363 (1961)

Paper 19, Figures 1-4 from B. U. Ö. Sonnerup, 70, No. 5, 1051 (1965)

Paper 20, Figures 5 and 6 from J. M. Malville, 64, 1389 (1959)

Paper 20, Figures 7 and 8 from T. N. Davis, 67, 75 (1962)

Paper 23, Figures 1 and 2 from G. Mead and D. B. Beard, 69, 1169 (1964)

Paper 23, Figures 4–7 from G. Mead, 69, 1181 (1964)

The American Geophysical Union, Geomagnetism and Aeronomy:

Paper 20, Figure 4 from L. A. Yudovich, 3, 423 (1963)

The University of Chicago Press, Astrophysical Journal:

Paper 8, Figure 1 from W. I. Axford, A. J. Dessler, and B. Gottlieb, 137, 1268 (1963)

The American Association for the Advancement of Science, Science:

Paper 4, Figure 9 from H. R. Anderson, 139, 3548 (1963)

The Royal Astronomical Society, Monthly Notices:

Paper 7, Figures 1–5 and 7–11 from A. Hewish and J. D. Wyndham, **126**, No. 5, 469 (1963)

The American Institute of Physics, Physical Review Letters:

Paper 8, Figure 8 from D. A. Bryant, T. L. Cline, U. D. Desai, and F. B. McDonald, 11, 144 (1963)

Paper 10, Table 1 from C. P. Sonett et al., 13, 153 (1964)

D. Reidel Publishing Co., Space Science Reviews:

Paper 10, Figures 1 and 3 from C. P. Sonett, 2, 751 (1963)

Pergamon Press, Ltd., Planetary and Space Science:

Paper 16, Figures 1 and 2 from W. I. Axford, 12, 45 (1964)

Paper 17, Figure 2 and Paper 20, Figure 2 from S. -I. Akasofu, 12, 273 (1964)

U.S. Department of Commerce, National Bureau of Standards, Central Radio Propagation Laboratory, Boulder, Colorado:

Paper 2, Figure 2 from "Compilations of Solar-Geophysical Data" abstracted from CRPL-F, Part B (October, 1963)

North-Holland Publishing Co., Space Research II, ed. by H. C. Van de Hulst *et al.* (1961):

Paper 8, Figure 3 from K. I. Gringauz, p. 539

North-Holland Publishing Co., Space Research III, ed. by W. Priester (1963):

Paper 8, Figure 4 from K. I. Gringauz et al., p. 602

North-Holland Publishing Co., Space Research IV, ed. by P. Muller (1964):

Paper 8, Figure 9 from C. W. Snyder and Marcia Neugebauer, p. 89 The Mt. Wilson and Palomar Observatories:

Paper 11, Figures 1-4 and Paper 24, Figure 1

Interscience Publishers, a division of John Wiley & Sons, Inc., Interplanetary Dynamical Processes by E. N. Parker (1963):

Paper 12, Figures 1-3

John Wiley & Sons, Inc., Space Physics, ed. by Legalley and Rosen (1964):

Paper 13, Figures 1 and 2 from F. L. Scarf, p. 437

Plenum Press, Natural Electromagnetic Phenomena Below Thirty Kilocycles Per Second, ed. by D. F. Bleil (1964):

Paper 16, Figures 1 and 2 from W. I. Axford, p. 5

Papers 1 through 4 present work sponsored at the Jet Propulsion Laboratory by the National Aeronautics and Space Administration under Contract No. NAS 7-100.

Session I

PHENOMENA OBSERVED IN INTERPLANETARY SPACE

Page intentionally left blank

CHAPTER I

MARINER-2 MEASUREMENTS OF THE SOLAR WIND

MARCIA NEUGEBAUER AND CONWAY W. SNYDER

Jet Propulsion Laboratory, Pasadena, California (Presented by Marcia Neugebauer)

THE first publication concerning the *Mariner-2* plasma experiment was a rough preliminary account of the data presented by Neugebauer and Snyder (Ref. 1). The correlation between plasma velocity and geomagnetic activity was pointed out by Snyder, Neugebauer, and Rao (Ref. 2). I will quickly review a few points from these papers because they are pertinent to what I have to say.

Most of you know that *Mariner 2* carried a single curved-plate electrostatic spectrometer that always pointed at the center of the Sun. Figure 1 shows the analyzer's resolution function, which is defined as the fraction of particles that reaches the collector as a function of energy and angle of incidence. The aberration due to the spacecraft's motion was generally in the range of 2 to 6 deg. The area under the 6-deg curve is about one-third of the area under the 0-deg curve. The plasma was always in the range of angles that could be seen by the instrument, but sometimes we had to make large corrections to account for the aberration effect.

For each of the spectrometer's ten voltage settings (channels), the spacecraft transmitted a number proportional to the logarithm of the current measured for that particular range of energy per unit charge. The channels were scanned sequentially, with measurements spaced every 18.5 sec, so that from 37 to 111 sec were required to obtain a spectrum (depending on the width of the spectrum). Successive spectra were separated by 3.7 min, which was the basic time resolution for the measurement of plasma properties.

Method of Calculating Velocity and Temperature

Figure 2 is a sample spectrum. The logarithm of the measured current is given for each channel of energy per unit charge. The channels are equally spaced on a logarithmic scale. Many spectra have two peaks; when there is no obvious second peak, there is frequently a shoulder

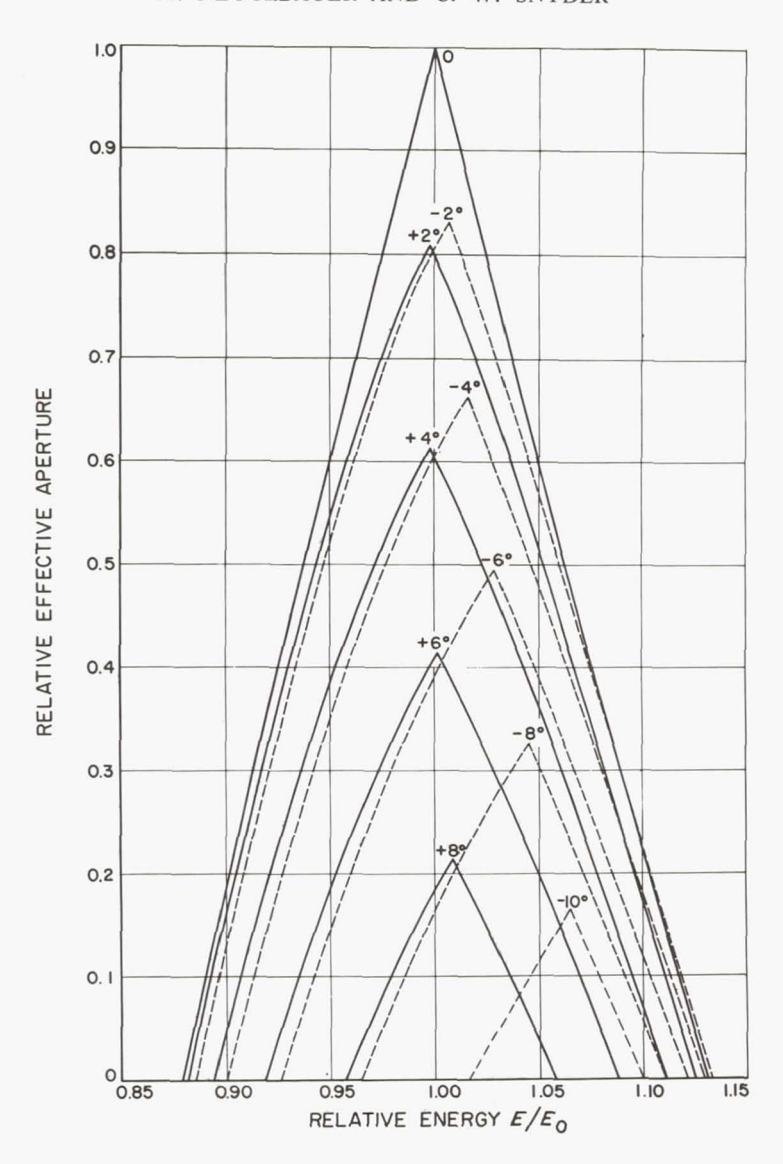


Fig. 1. Mariner electrostatic analyzer resolution function, or the fraction of a parallel beam of ions which reaches the collector as a function of energy and angle of incidence

where you can imagine a second peak. We have interpreted the left-hand peak as protons, and the right-hand peak we call alpha particles, although

heavier bare nuclei may be present. If the alpha particles were moving away from the Sun with the same velocity as the protons, they would have twice the energy per unit charge of the protons, which is what was observed. I will talk more about alpha particles later, but first I should like

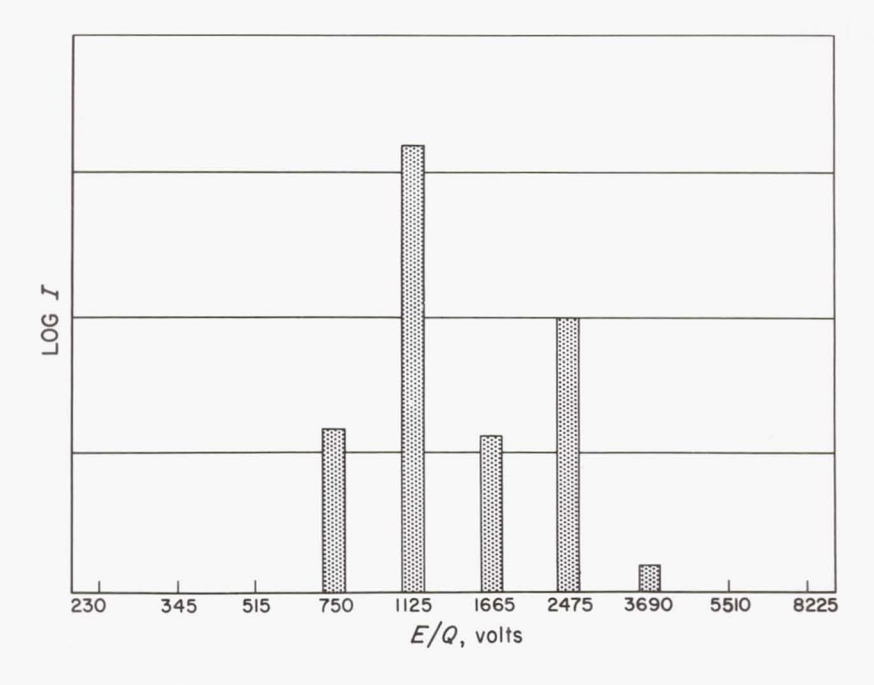


Fig. 2. Sample spectrum obtained by the Mariner plasma spectrometer

to outline the method we used for calculating velocity, temperature, and density from the data obtained.

For the first calculation, we assumed that the currents in the peak channel, and in the channels on each side of it, were due solely to protons with an isotropic Maxwell-Boltzmann distribution in the moving system. We defined the parameter ν as the ratio of the bulk velocity v to the velocity corresponding to the center of the peak channel v_m , and the parameter θ as the ratio of the thermal energy kT to the bulk energy $mv^2/2$. We defined I_{m-1} , I_m , and I_{m+1} as the currents in the channels just below the peak, at the peak, and just above the peak, respectively. For given values of the aberration angle (of a plasma arriving with velocity v_m) and the yaw angle (the angle between the spacecraft velocity vector and the analysis plane of the instrument), we integrated the proton distribution over the resolution function shown in Fig. 1. This integration

gave a unique relation between the pair of measured parameters (I_m/I_{m-1}) and I_m/I_{m+1}) and the pair of parameters $(\nu \text{ and } \theta)$ describing the plasma protons. Figure 3 illustrates this relation for a few specific values of ν and θ . The shaded areas are the envelopes of all different values of the aberra-

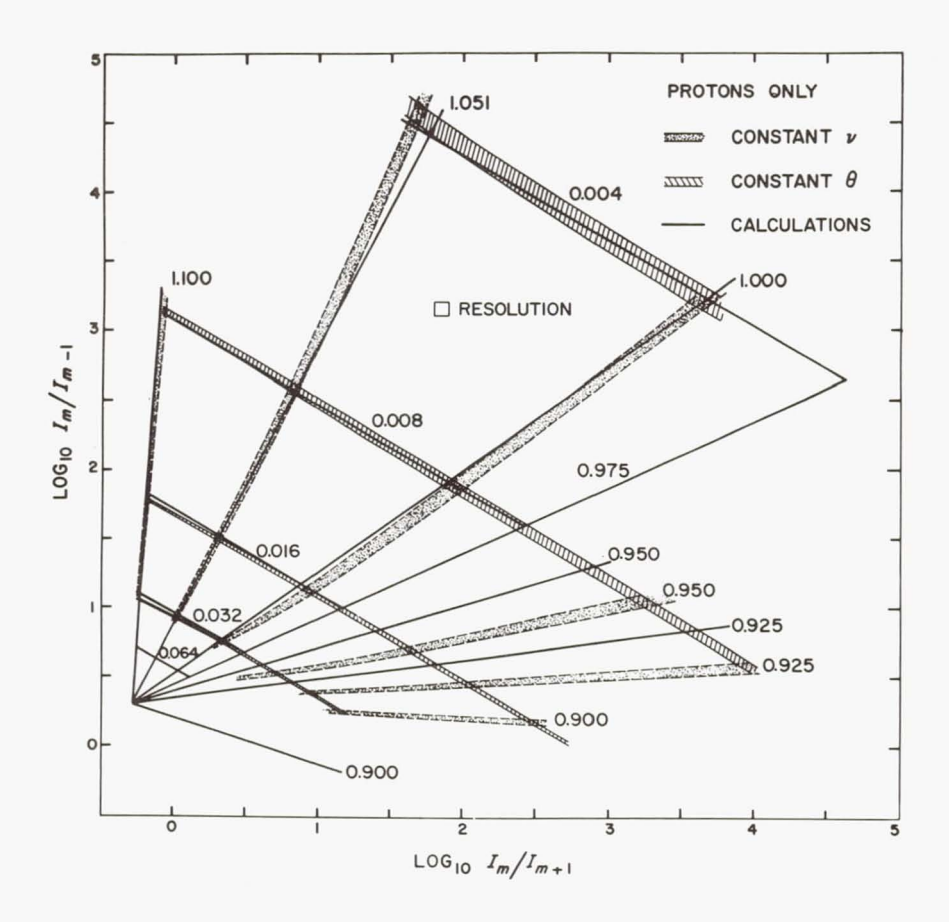


Fig. 3. Contours of constant ν and θ as a function of the currents in channels m-1, m, and m+1, assuming no contribution from alpha particles

tion and yaw angles for constant values of either ν or θ . The effect of the digitalization of the logarithm of the current is also indicated in Fig. 3 to show roughly the accuracy of the calculated parameters.

For the actual calculation of ν and θ from the observed ratios I_m/I_{m-1} and I_m/I_{m+1} , we used the straight lines which approximate the shaded envelopes. You may wonder why some lines, $\nu=0.925$ for example, aren't very close to the corresponding shaded areas. This displacement

was made in an attempt to correct for the effect of alpha particles. If it is assumed, say, that there are five alpha particles for every 100 protons, there is a considerable contribution of alpha particles to the current in channel m+1 when $\nu<1$, so that the curves of Fig. 3 are distorted to give those shown in Fig. 4.

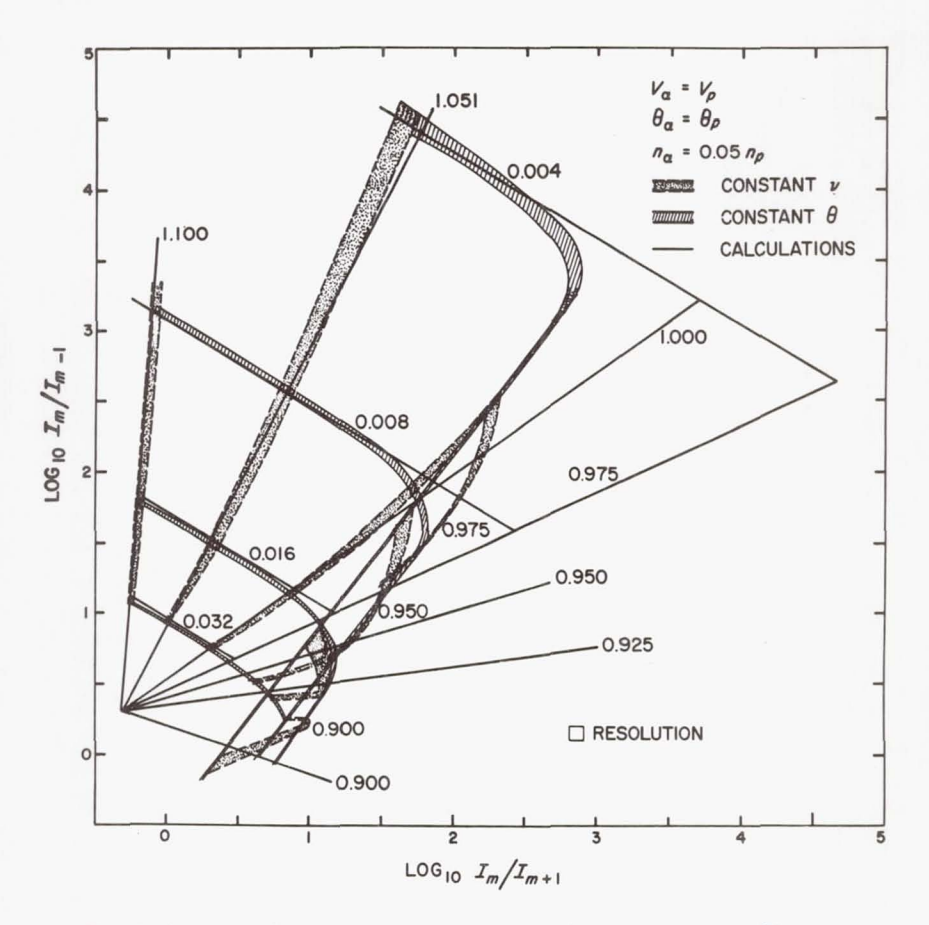


Fig. 4. Contours of constant ν and θ , assuming five alpha particles for every 100 protons

We used the straight lines shown in Fig. 3 or 4 to calculate all values of ν and to calculate θ when ν is greater than 1.000. The differences between the curves in Fig. 3 and those in Fig. 4 demonstrate that it is hopeless to calculate θ , and thus temperature, by this simple method when there is a considerable mixture of alpha particles in channel m+1.

Another point I want to make here is that, if the flow from the Sun is not radial, this nonradiality can be expressed as different effective aberration and yaw angles, which merely changes the values of ν and θ by amounts roughly indicated by the sizes of the shaded envelope areas. So in the determination of velocity and temperature, the fact that the solar wind may not be exactly radial is not very important. Nonradiality might affect the value of velocity by roughly 1%.

Time Dependence of Proton Velocity, Temperature, and Density

Figure 5 is a plot of velocity and temperature as a function of time. The time scale is based on January 1, 1962 as Day 1. In most cases the upper curve is velocity. Each point is a 3-hr average. The plot is on a 27-day scale so that you can see the recurrent peaks of hot, high-velocity plasma. The velocity varied from about 320 to 770 km/sec, the average for the entire mission being 505 km/sec. The temperature ranged from 3×10^4 to 6×10^5 °K. The average proton temperature was 1.5×10^5 °K. As you can see, the temperature more or less followed the velocity; when velocity increased, the temperature generally increased, too.

Temperature and velocity were calculated from the width of, and the energy per unit charge at, the peak of the proton spectrum respectively. Then we used the magnitude of the measured current, together with the aberration and yaw angles and the on-board electrometer calibration, to calculate proton density. In this calculation of density, the fact that we assumed the plasma flow to be radially outward from the Sun has a large effect on the values obtained.

In Fig. 6, the heavy line represents velocity and is the same as in Fig. 5. The lighter line represents density, its scale being on the right. You can see that density was generally highest between the high-velocity streams or at a leading edge. For example, on Day 280 we observe a high-velocity plasma catching up with a low-velocity plasma, and the density increased at this interface. We also see, over and over again, that in the middle of the streams the density was quite low when the plasma velocity was high. The range of the 3-hr averages in density was from about 0.2 to 70 protons/cm³.

Figure 7 shows a point-by-point plot of velocity, temperature, and density at the leading edge of the stream which corresponds to the magnetic storm of October 7, 1962 (Day 280). Conditions were very quiet until about 1547 UT, when there was a sudden jump in velocity. The velocity kept on increasing for about 2 days until it approached 800 km/sec. There are not as many temperature or density points as velocity points, because temperature and density were not calculated when alpha particles interfered with the calculation.

It is interesting to note that, on occasion, velocity and temperature

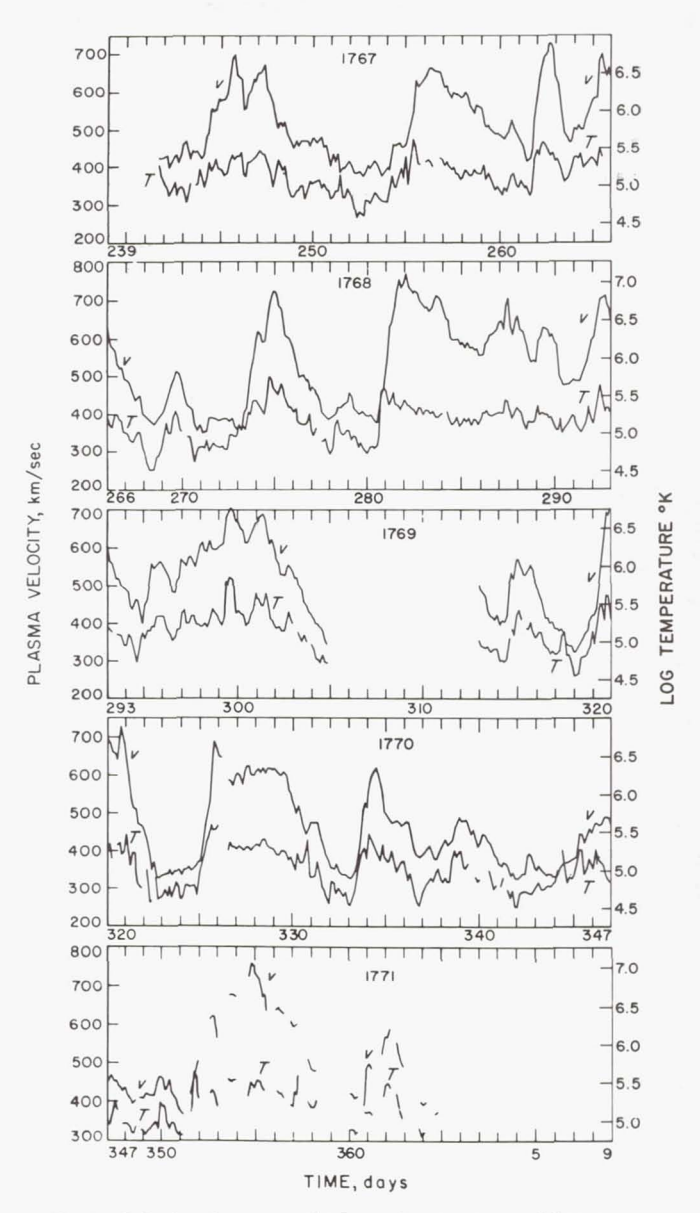


Fig. 5. Calculated proton velocity and temperature, 3-hr averages

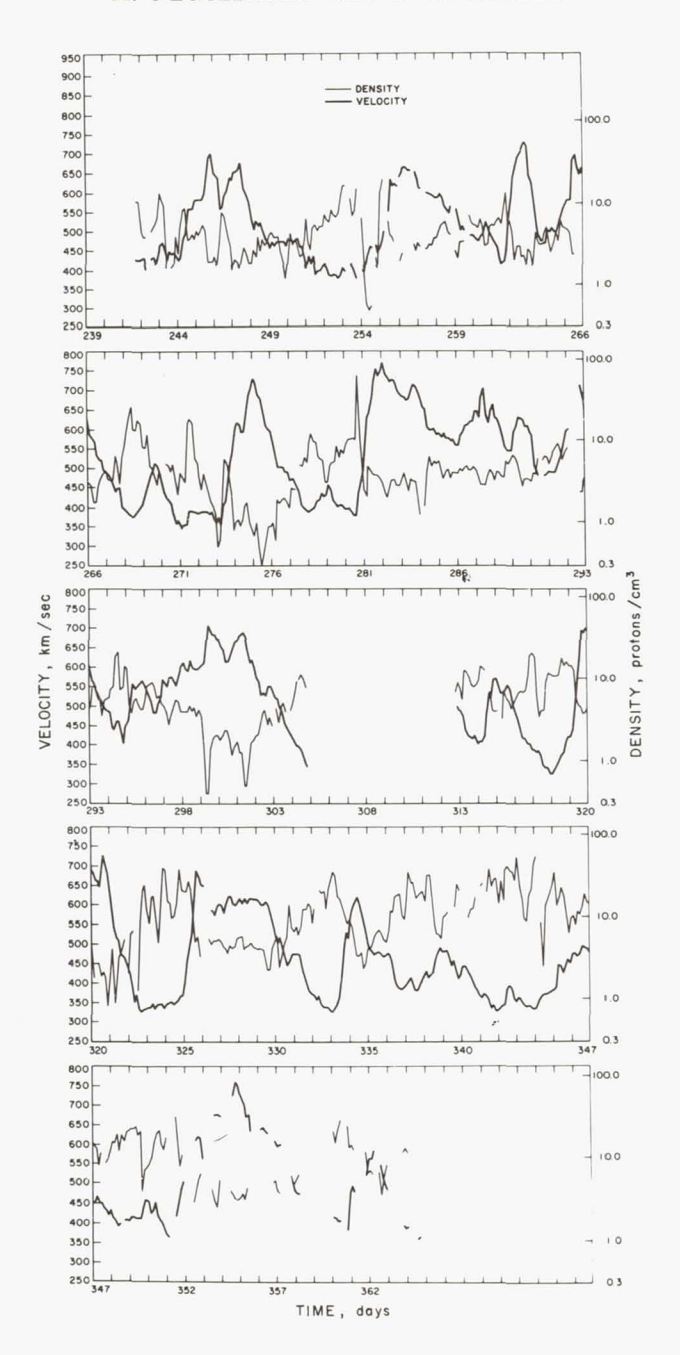


Fig. 6. Calculated proton velocity and density, 3-hr averages

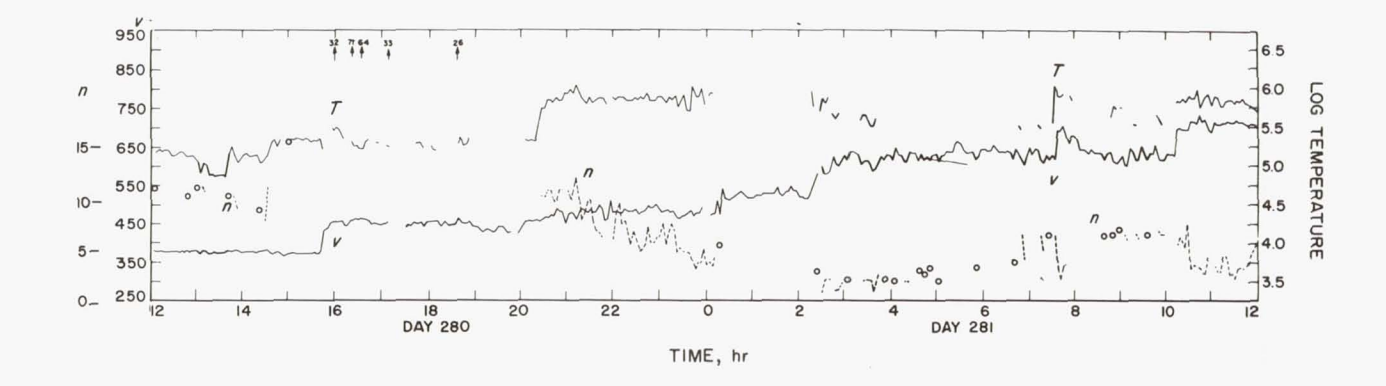


Fig. 7. Detailed plot of the proton velocity (v, km/sec), temperature $(T, ^{\circ}\text{K})$, and density $(n, \text{per cm}^3)$ for the 24-hr period beginning 1200 UT, October 7, 1962. The leading edge of a stream which later caused a geomagnetic storm is seen at 1547 UT, October 7, 1962 (Day 280)

had simultaneous, sudden jumps. By "sudden" I mean anything less than 3.7 min. There is an example of such behavior at 0737 UT on Day 281. At 1547 UT on Day 280, though, the temperature didn't change very much, although there was a large velocity jump. At about 2000 UT on Day 280, the jump in velocity preceded the jump in temperature by about 24 min.

Density appears to have started increasing about an hour before the shock front arrived, and eventually it got as high as 77 protons/cm³, which is the highest density we saw. The density than decreased and stayed low until the high-velocity stream had gone by completely.

Effect of Change in Distance From the Sun

You may have noticed in Fig. 6 that the density was higher at the end of the flight than at the beginning. Figure 8 shows roughly how the

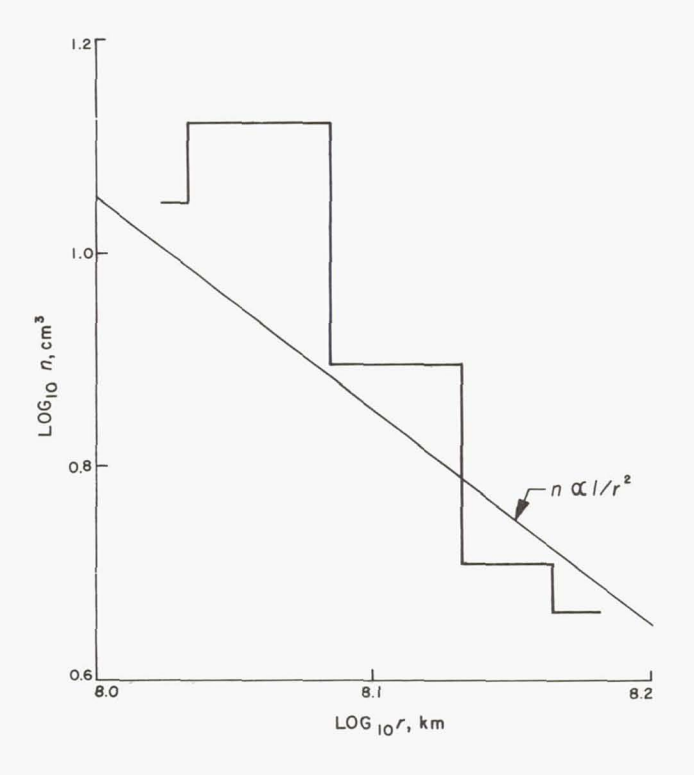


Fig. 8. Logarithmic plot of proton density vs. distance from the Sun. The density has been averaged over a solar rotation

density varied with distance from the Sun. The abscissa is the logarithm of the distance from the Sun. Each bar is an average over a whole solar rotation; the averaging was done in an attempt to take out the effect of solar activity. You can see that density decreased roughly as $1/r^2$, maybe a bit faster.

Similar computations were performed for the flux, J = nv. From Fig. 9 you can see that the flux showed a $1/r^2$ behavior a little better than did the

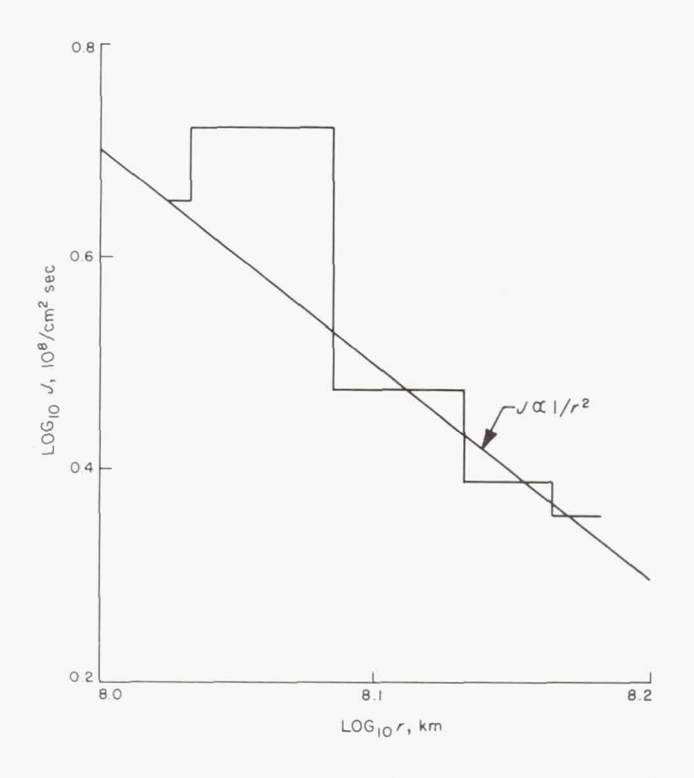


Fig. 9. Logarithmic plot of proton flux vs. distance from the Sun. The flux has been averaged over a solar rotation

density. However, when we plotted the similar velocity and temperature averages, we could find no obvious dependence on distance from the Sun.

Correlation with Kp

In Ref. 2 we concluded that there was a very good correlation between the Kp index, which we used as a measure of geomagnetic activity, and plasma velocity. The top rows of Fig. 10 and 11 show the daily average plasma velocity, while the middle rows are the sum of the Kp indices for a given day. These two quantities followed each other quite closely.

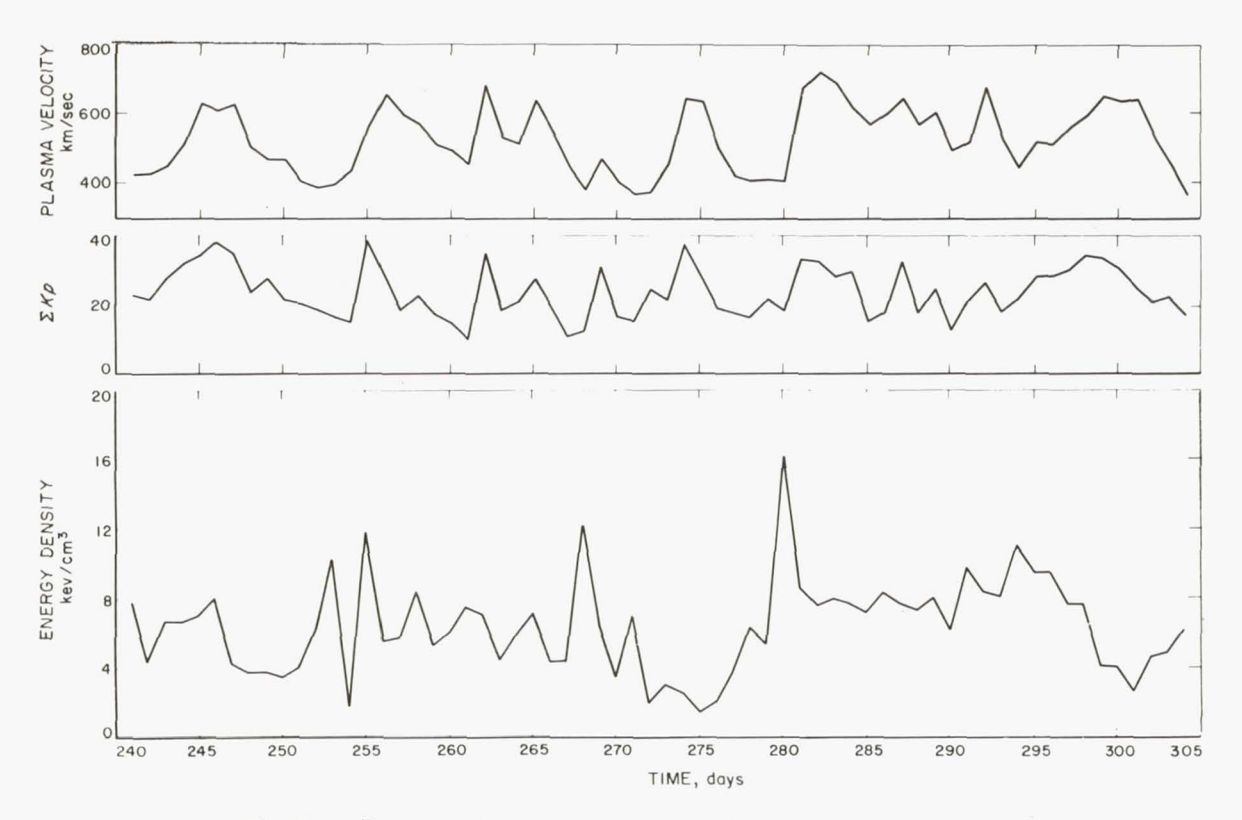


Fig. 10. Daily average plasma velocity, the sum of the eight Kp indices for each day, and the energy density of the protons' bulk motion, August 29 through October 31, 1962 (Days 241–304)

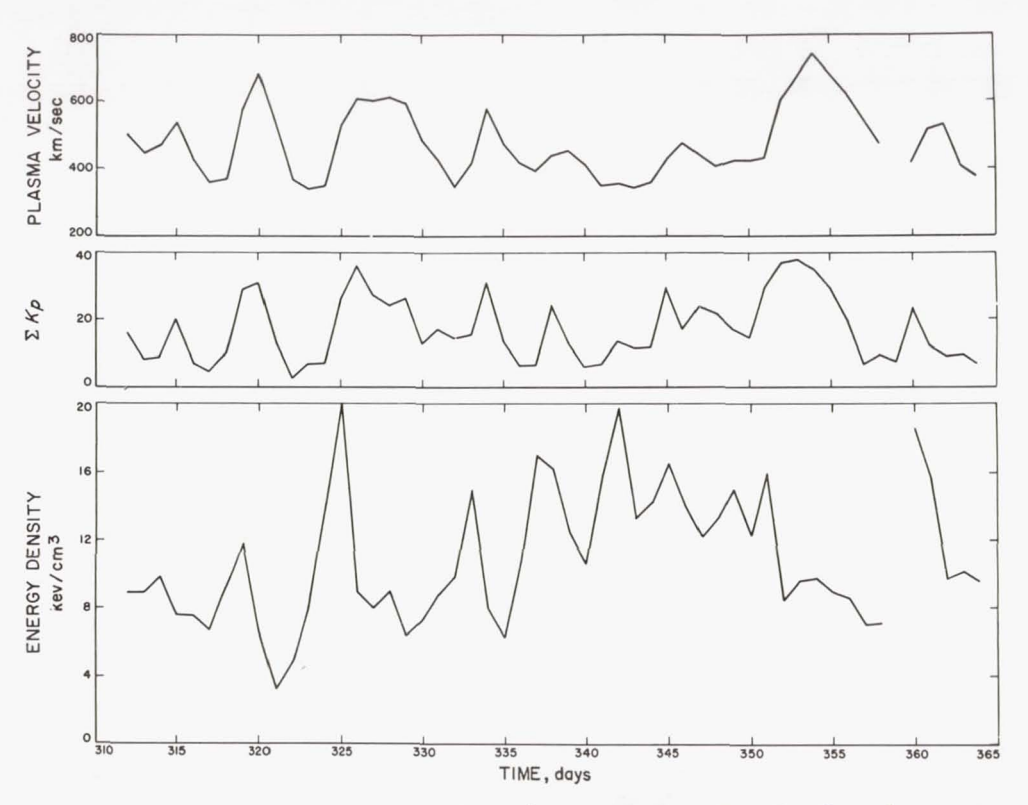


Fig. 11. Daily average plasma velocity, the sum of the eight Kp indices for each day, and the energy density of the protons' bulk motion, November 8 through December 30, 1962 (Days 312–364)

Earlier predictions of the dependence of geomagnetic activity on the solar wind generally were concerned with the plasma energy density or pressure. We have plotted the daily average of the energy density of the plasma bulk motion at the bottom of Fig. 10 and 11. You can see that the energy density was generally highest at the leading edge of a stream where the ion density was high.

Alpha-Particle Temperature

Let's return to the discussion of the alpha-particle part of the spectrum. What we have done so far is to take the current just below the peak (I_{m-1}) , the current at the peak (I_m) , and the current just above the peak (I_{m+1}) , and from these three numbers to calculate the density of protons, the bulk plasma velocity, and the proton temperature. Using these three parameters, plus the assumption that the alpha particles are moving away from the Sun with the same velocity and temperature as the protons, plus the value of the current in channel m+2, we calculated the ratio n_{α}/n_p , which is the relative alpha-particle density.

Next we tested the validity of these assumptions to see how good this model was. To do this, we used the value of the proton and alpha-particle

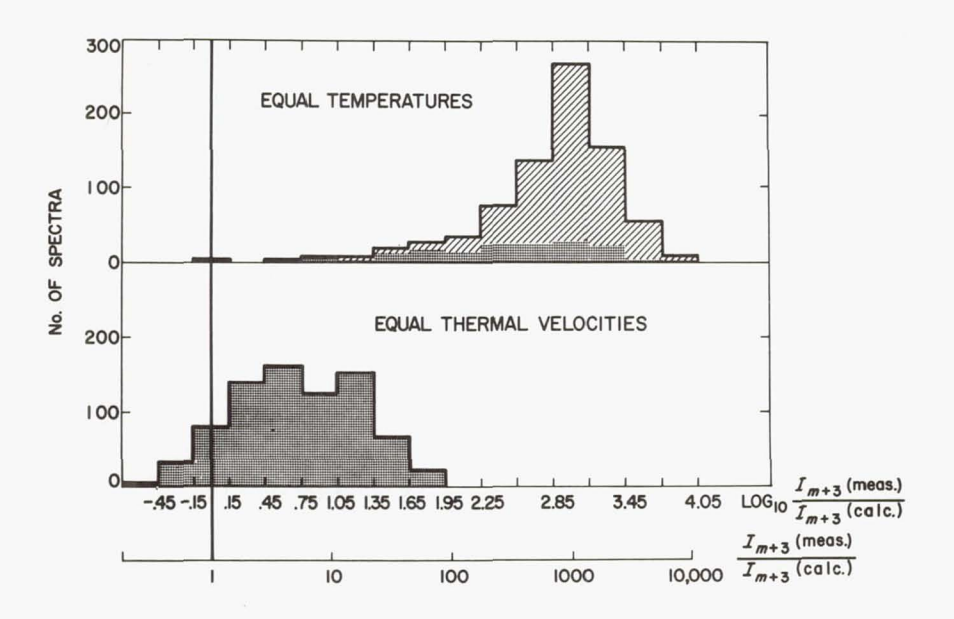


Fig. 12. Histograms of the ratio of the measured to the predicted currents in channel m+3, assuming that the protons and alpha particles had the same temperatures (upper histogram) and the same thermal velocities (lower histogram)

velocities, temperatures, and densities just calculated to predict the current in channel m+3, and then we compared the prediction with the measured value. In performing this calculation, we cheated a bit. We only considered the subclass of spectra for which ν was near 1.051. When ν equals this magic number 1.051, the alpha-particle peak should be centered on channel m+2 (the fourth point in the spectrum), thus permitting a more accurate determination of n_{α}/n_{p} than could be obtained if the alpha-particle spectrum were steep at this channel. Furthermore, when $\nu=1.051$, there was a negligible contribution of alpha-particles to the first three channels. Therefore, for the range of temperatures we observed, the assumption we used in finding n_{p} , ν , and T (that there were only protons in the first three channels) is valid.

Figure 12 contains two histograms of the ratio of the measured current in the fifth channel to the calculated current. If the model were acceptable, the upper histogram would be centered at a value of 1. The area shaded with lines represents spectra for which we couldn't really calculate the ratio; all we could get was a lower limit. Thus all the points represented by shaded lines should be even farther to the right. There is obviously too much current in channel m+3 by a factor of 10^3 or more. We conclude that the model isn't very good.

The calculation was repeated for the assumption that the alpha particles were four times hotter than the protons, which means that the two kinds of ions have equal thermal velocities instead of equal temperatures. The lower histogram in Fig. 12 shows the results of this calculation. The model is still not perfect, but is off by a factor of two or three instead of by a factor of 10³.

There are several models that might better fit the measured spectra. One model would be: $v_{\alpha} = v_p$ and $T_{\alpha} > 4T_p$. Since we couldn't see any physical basis for such a model, we didn't bother to calculate the amount that T_{α} must exceed $4T_p$. Another model would require equal thermal velocities, with the alpha particles moving away from the Sun slightly faster than the protons. We couldn't see any physical reason for this model either.

Professor Davis has suggested that perhaps we could move the histogram a little to the left by assuming that the spacecraft had a large positive charge. We could move the bottom histogram to the correct place by assuming the spacecraft was charged to something like 100 to 200 v. There is no hope of sufficiently shifting the upper histogram by any reasonable amount of charge.

We think probably the real weakness of our model lies in assuming that the ions have an isotropic Maxwell-Boltzmann distribution. However, we don't have enough points in our spectra to calculate a complex model in any detail.

Alpha-Proton Ratio

We took the points on the bottom histogram, for which $\log [I_{m+3}(\text{meas.})/I_{m+3}(\text{calc.})]$ was between -0.2 and +0.2, and determined the value of n_{α}/n_{p} for these spectra, which seemed to fit the equal-thermal-velocity model fairly well. Figure 13 shows the ratio n_{α}/n_{p} as a function of m (the peak channel number, which is proportional to the logarithm of the velocity).

The average ratio of alpha-particle density to proton density was about 0.046, which was lower than we had expected before we performed the calculation. There didn't seem to be any energy dependence of this ratio.

Dependence of Temperature Upon Magnetic Field

We have seen that the alpha-particle temperature seemed to be approximately four times the proton temperature, or that the two kinds of ions

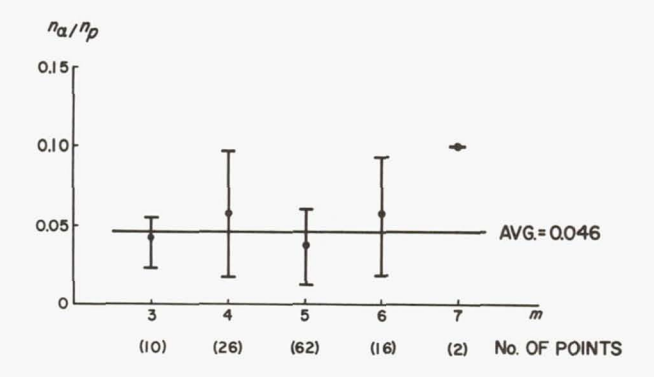


Fig. 13. Ratio of alpha particle to proton densities for those spectra which fit an equal-thermal-velocity model, plotted vs. *m*, the number of the peak channel. *m* is proportional to the logarithm of the plasma velocity

had equal thermal velocities. Also interesting is the fact that these thermal velocities were very closely equal to the Alfvén velocity. We took a representative sample of 212 spectra for which we knew both the density and the magnetic field, and found that the ratio of thermal velocity to Alfvén velocity was 1.2 ± 0.5 . This ratio is also the square root of the ratio of the kinetic-energy density of the thermal motions, nkT, to the magnetic-field energy density, $B^2/8\pi$. So, saying that the Alfvén velocity and the thermal velocity were approximately equal is the same as saying that there was equipartition of energy between thermal motions and the magnetic field, which some people might have predicted to start with.

I think this result suggests that the solar-wind particles have the random motions they do, not because they were heated to some temperature back near the Sun and have cooled since then due to adiabatic expansion, but because the ions are interacting with the magnetic-field disturbances.

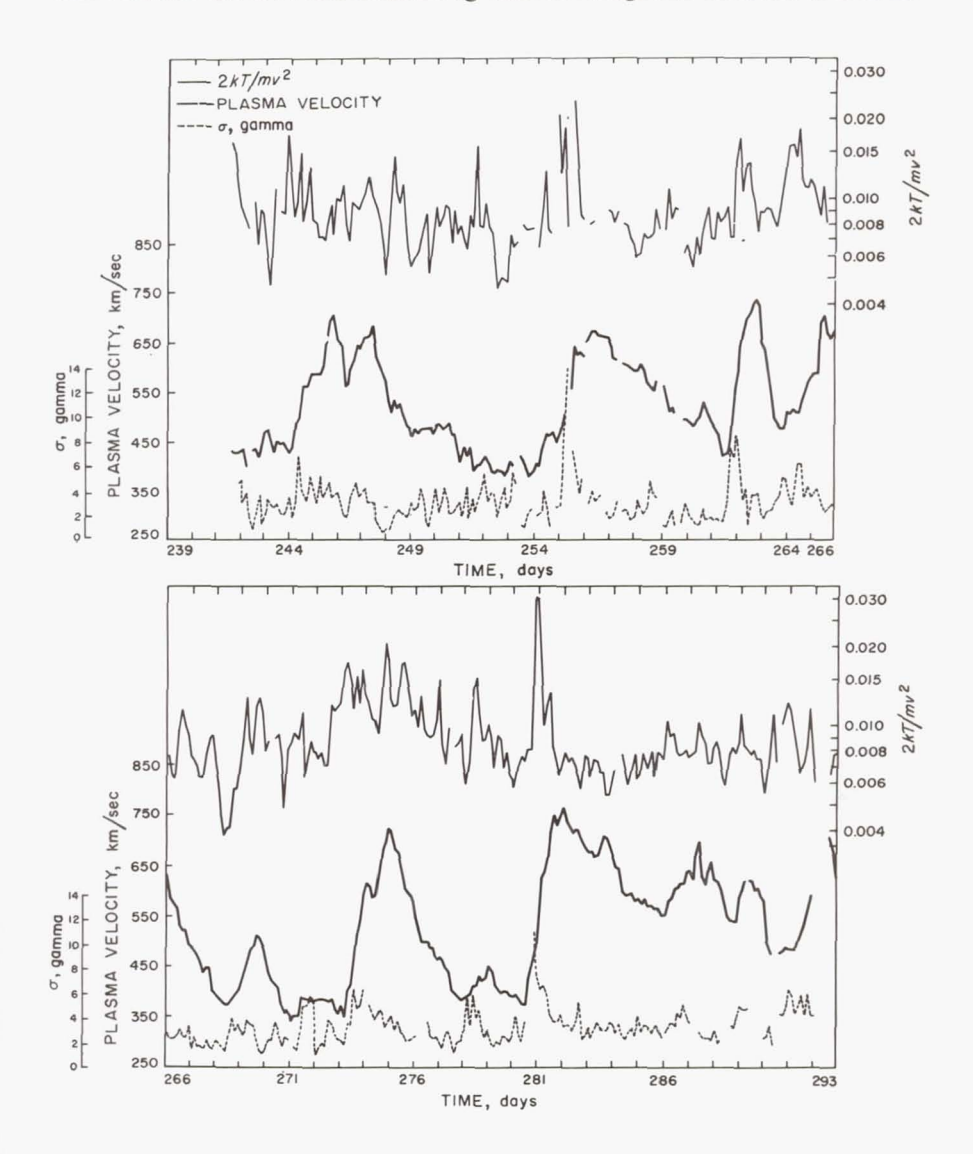


Fig. 14. Ratio of proton thermal energy to the energy of mass motion $(2kT/mv^2)$ plasma velocity, and the variance in the magnetic field, August 29 through October 19, 1962 (Days 241–292)

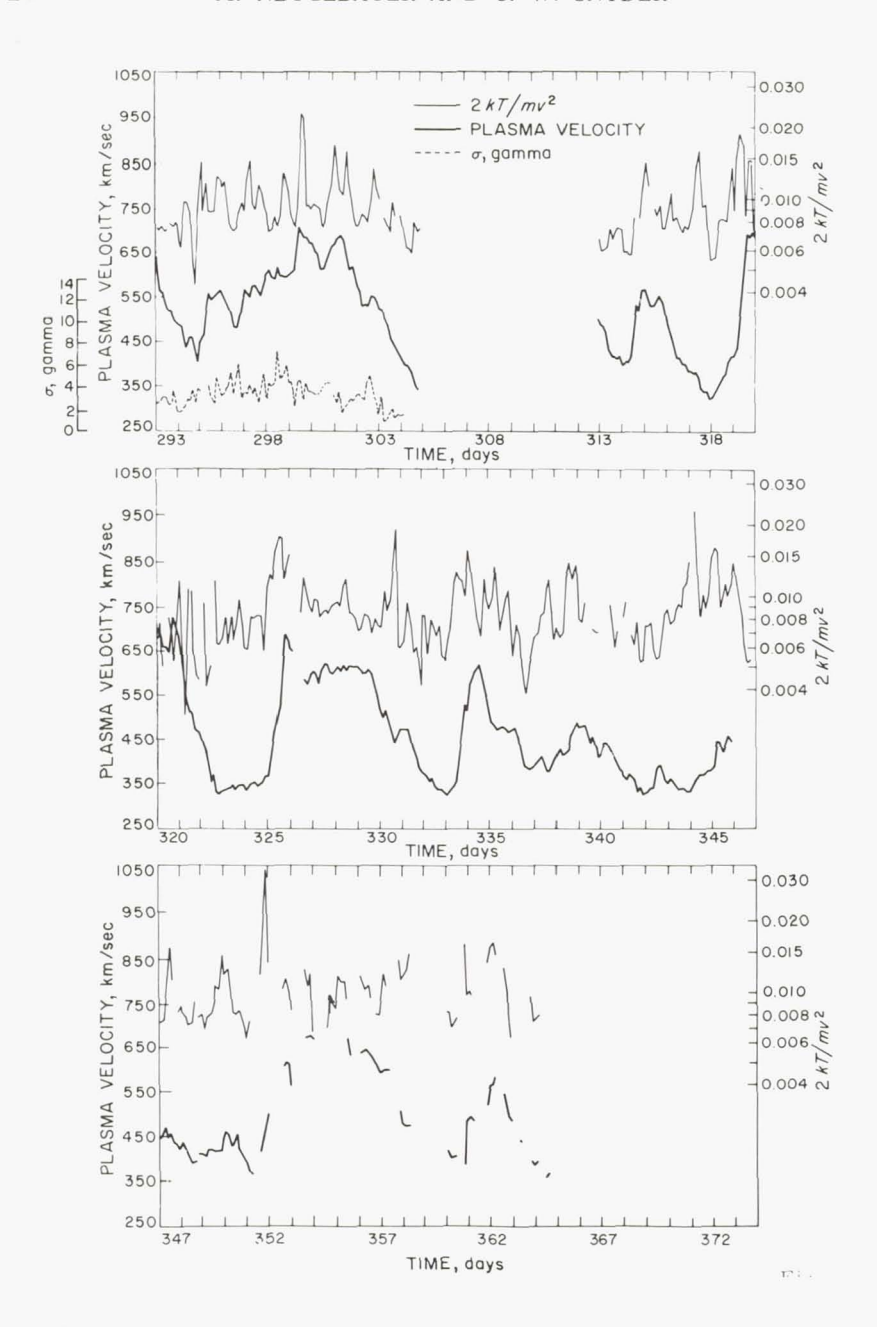


Fig. 15. Ratio of proton thermal energy to the energy of mass motion $(2kT/mv^2)$, plasma velocity, and the variance in the magnetic field, October 20 through December 30, 1962 (Days 293–364)

The plasma is turbulent and has magnetohydrodynamic shock waves moving through it. Ions are reflected from a shock with a velocity of the same order of magnitude as the velocity of the shock.

I think this speculation is somewhat verified by the plots in Fig. 14, in which the heavy lines are again the 3-hr averages of velocity. The dashed line is the variance in the magnetic field, or the standard deviation about each 3-hr average. The variance of the magnetic field was highest at the leading edges of the streams. There are good examples of this behavior on Days 255, 261, and 280. The field was a lot noisier where you might have expected turbulence; that is, where a high-velocity stream apparently overtook a slower moving plasma. The upper curve in Fig. 14 is the ratio of thermal energy to directed energy, which is the quantity θ discussed earlier.

Figure 14 shows that when there were many magnetic disturbances (shocks running around in the plasma), θ was high. In other words, as the spacecraft was overtaken by a hot, high-velocity stream, the temperature increased even faster than the velocity. There was generally a quite good correlation between θ and the variance in the magnetic field. Figure 15 shows the same type of data for the last three solar rotations sampled by *Mariner*. Here again you see that θ had increased and had then decreased again by the time the velocity reached its maximum value. Day 351 is a good example.

In conclusion, we think we have proved that the temperature of the solar-wind plasma is not simply related to the temperature at the base of the corona and that shock-wave heating may be an important process.

REFERENCES

- 1. NEUGEBAUER, M. and C. W. SNYDER, Science 138, 1095 (1962).
- 2. SNYDER, C. W., M. NEUGEBAUER, and U. R. RAO, Journal of Geophysical Research 68, 6361 (1963).

DISCUSSION OF NEUGEBAUER PAPER

BIERMANN: You have not discriminated between temperature and turbulence. Since the turbulence probably has a fairly high frequency, I think the proper conclusion is that you essentially have equipartition of energy between turbulence and magnetic-field fluctuations. I don't recall any convincing reason for relating these fluctuations to temperature.

NEUGEBAUER: It may be that purely thermal motions are very small, and that only turbulent motions are observable. I don't think we will be able to sort out these quantities until we get spectra with many more points in them.

PARKER: Over what period of time do you make the samples in the different channels?

NEUGEBAUER: It takes a second or slightly less. I don't think we are seeing the envelope of any hydromagnetic waves that may be present, because the cyclotron period is about 10 seconds for protons.

PARKER: If you are seeing turbulence, then it has a frequency of 1 cycle per second to get what you call the temperature. Do I understand you correctly? **NEUGEBAUER:** Yes.

NESS: With regard to Parker's statement, isn't the important time scale the time it takes to scan a spectrum, which is 3.7 minutes, rather than the time it takes to take each sample?

NEUGEBAUER: Not entirely. It takes 3.7 minutes to make a whole set of measurements. Each particular current measurement, however, takes less than 1 second. If there were eddies with periods lying between 1 second and 3.7 minutes, then the readings wouldn't repeat themselves from one measurement cycle to the next as well as they do. There was only one interval in the whole flight during which we got drastically different values of velocity and temperature from one 3.7-minute cycle to the next. Except for this one interval of a few hours, the plasma behaved reasonably well.

SNYDER: I think it is important to emphasize this point. It's very common to observe the same currents in all ten channels for 20 consecutive measurements. I think this does rule out the idea that we are seeing only turbulence.

BRIDGE: There is no reason to expect coherence between the phase of the fluctuations and your measurement period. In other words, I agree that if the plasma flow is steady, your time scale is moved down from 3.7 minutes to about 1 second, which is the time for one measurement.

PETSCHEK: Is the energy in the magnetic-field fluctuations comparable to the energy in the average magnetic field?

DAVIS: It depends on the frequency of the fluctuations. If you ask about fluctuations with a period of about 5 to 7 minutes, then most of the time the energy in the fluctuations is not nearly as large as the energy in the average field. If you ask about fluctuations with a period of a day, then the energy in the fluctuations is quite large.

PETSCHEK: But, if you make correlations on a short time basis, as was done, then apparently the thermal energy is higher than the fluctuating magnetic energy. Therefore, the observed particle velocity spread cannot be simply a reflection of hydromagnetic turbulence.

LÜST: How does the time response of the plasma instrument compare with that of the magnetometer?

NEUGEBAUER: The magnetometer makes six complete field readings for every complete plasma spectrum. Both instruments require about 1 second to make a single measurement.

NESS: Have you performed any spectral analysis of the magnetic fluctuations to determine the shape of the spectrum? I infer from your comments that there is a lot of energy at low frequencies and not very much at high frequencies. **DAVIS:** There is a lot more energy at low frequencies than at high frequencies. I think this will be clearer when Dr. Smith shows us his slides.¹

DEUTSCH: What about the possibility that an appreciable number of the particles now identified as alpha particles are really singly jonized helium atoms?

NEUGEBAUER: Since singly ionized helium would have an energy per unit charge four times that of a proton, it would not appear in the same place in the

¹See Paper 3

spectrum as the alphas. Since we did not see a peak at the appropriate value of energy per unit charge, there is probably at least an order of magnitude more doubly ionized than singly ionized helium.

Just a little singly ionized helium, however, would help shift the histogram (bottom of Fig. 12, Paper 1) slightly to the left and thus result in better agreement

between the measured spectra and the model.

CHAPMAN: Professor Parker, I was wondering if the ratio of protons to helium is a cause for concern, or if it could be explained by the way in which the solar wind develops.

PARKER: If you ask whether the expanding solar corona has a true solar abundance, of course you are confronted with the possibility that the heavier elements may have settled out. If you make a simple estimate of the rate at which the helium can be settling out and compare it with the rate at which the corona is expanding, then the two rates are about equal and you are left on the fence.

I think, in fact, that the corona probably does have a true solar abundance, but one can't be sure of that. The only real solution to the problem would be to measure the helium abundance in the solar wind day after day, and if you found it to be always the same, you could conclude that it was the true solar value.² **NEUGEBAUER:** Our ratios of alphas to protons did vary widely—from 0.01 to

0.30, roughly.

JOKIPII: I have recently carried out a fairly detailed investigation of the abundance of alpha particles, and it seems to me that there are two possibilities. Either the alpha particles don't fall out of the corona fast enough to keep a solar abundance, in which case their coronal abundance is increased; or else they do fall out fast enough to keep a solar abundance in the corona, in which case the solar-wind abundance is reduced. The actual situation is probably a mixture of the two. I would like to discuss this problem in detail tomorrow.³

²See Parker, E. N., The Solar Corona, ed. by J. W. Evans, Academic Press, New York (1963) p. 11

³See Paper 14

Page intentionally left blank

CHAPTER II

THE RELATION OF MARINER-2 PLASMA DATA TO SOLAR PHENOMENA

CONWAY W. SNYDER AND MARCIA NEUGEBAUER

Jet Propulsion Laboratory, Pasadena, California

(Presented by Conway W. Snyder)

We have seen a very good correlation between the velocity of the solar plasma, as measured by *Mariner 2*, and the amount of magnetic disturbance on the Earth. But what about the correlation between the velocity of the solar wind and things that are happening on the Sun? I have tried various ways to make some progress on this problem, and about all I can say is that the situation seems to be confused. I could perhaps sit down and leave it there, but I want to belabor the point just a little, if I may.

Extrapolation Procedure

On the assumption that the solar-wind velocity is constant from the Sun to wherever we observe it, we can calculate exactly where any given bit of plasma should have come from on the Sun. This is, of course, the assumption that underlies the Archimedes-spiral model. The spiral-field line connects the spacecraft to the source. The equation of the Archimedes spiral in its simplest form is $r = v(\phi_0 - \phi)/\Omega$, where Ω is the solar rotation rate at the solar latitude from which the particles are ejected. When the velocity increases, a spiral can catch up with the one ahead of it, but such a picture is rather hard to draw. Since the equation for the spiral is linear, let r = y and $\phi = x$; then these complicated spirals become straight lines and are a little easier to show.

Figure 1 shows these spiral-field lines in rectangular coordinates. The top line, E, represents the orbit of the Earth; the horizontal scale is in days and gives the Earth's position in a coordinate system that rotates with the Sun. The bottom line, S, represents the surface of the Sun, with the scale in days giving the time of passage beneath the Earth. The scales are adjusted so that the slanting lines, representing field lines, have the slope of the Archimedes spiral at the Earth, and the field lines shown represent the observations of velocity at 12-hr intervals.

The top section of Fig. 1 depicts a simple situation in which the region

between A and B on the Sun emits plasma having a velocity of 300 km/sec. Between B and C the velocity rises gradually (in 8 days) to 900 km/sec, and then falls back to 300 km/sec between D and E (again in 8

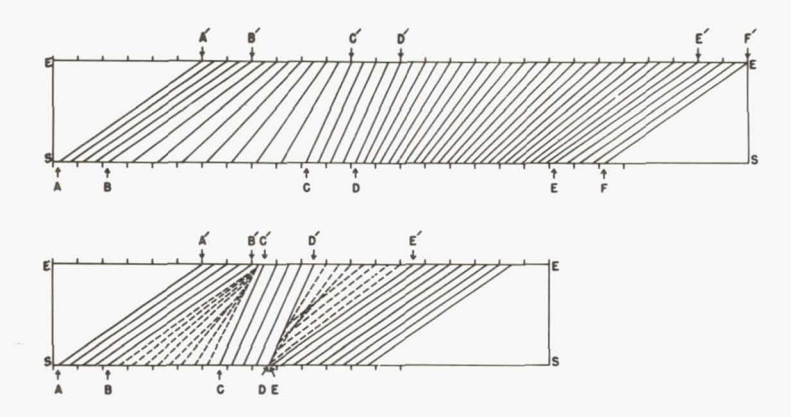


Fig. 1. Rectangular representation of r vs. ϕ plot for Archimedes-spiral field lines, showing the effects of changes in solar-wind velocity

days). If we look at the situation from the viewpoint of the Earth (where the corresponding letters are primed), the rise in velocity took only 4 days, and the subsequent drop took 12.

The lower half of the figure depicts a situation that was often seen by Mariner. The letters have the same meaning as before, but now the velocity rise takes place in a narrow region on the Sun (between B and C), corresponding to a difference of 4.5 days in central-meridian passage (CMP). The faster plasma sweeps the slower plasma ahead of it, so that the first line of high slope reaches the Earth less than 12 hr after the last line of low slope. The intermediate lines are shown dashed in this figure, but in the maps to be shown later they will be omitted, and a blank triangle, with its base at the bottom, will appear. The situation between D' and E' is even more confusing, for here the velocity decrease occurs in 4 days as seen at the Earth, and field lines observed during the decrease extrapolate back to points on the Sun to the left of the line D-D'. Omission of the dashed lines in this case will leave a blank triangle on the map with its base at the top. Such rapid drops in velocity, which appear more than a dozen times in the *Mariner* data, show that at these times, at least, the simple spiral model was not an accurate representation of the facts.

General Correlations

Figure 2 is the familiar picture showing one of the indices of magnetic disturbance, C9 (Ref. 1). From about the sixth through the tenth days of

R	Rot 1 st Nr. day	1 · U
665 532 122 477 643 112	19 J 2.	3 23 12 5, 1, 5 35 443 64, 2 432
465 33 2 2 13	62 M1	8 243 4 . 1 . 1 2 12 . 13 243 267 636 52 1 . 22 23 2
655 433 433	1762 A 1	
322 454 432	63 M1	
333 543 333	64 J 7	
222 222 211		543 23, 222 32, 343 224 476 52, 363 3, 2
111 124 332	66 /31	
, 35 544 422	67 A 27	
444 223 553	68 S 23	
333 22 , 224	69 0 20	
53, 2,3 43,	17 70 N 16	
2 13 2 1 1 23 1	71 0 13	
123 211 223	19 19	
321 112 211	62 F 5	
232 211 211	03 M4	., 265 753 2 21 31 1. 1. 3 156
22444431	1775 M3	1 .3. ,56 542 2 234 4 1 1 432 .32 2 566
122 454 553	76 A 27	2. 566 45 2 2 13 445 253 1 . 1 . 1 2 1 2 1 245
223 225 642	77 M24	. 2 . 245 323 3 47 32
122 221 112	78 J 20	32, ., 5 6 4 3 2 3 , 4 5 5 3 3 4 3 , , , 2 4 2 , , 6 3
122 144 421	79 1 17	· ·
, 23 422	1780 A 13	2 126 676 252 224 643 453 413 312 325

Symb	ol		,	2	3	4	5	6	7	8	
<i>R</i> =	0	1	16	31	46	61	81	101	131	171	
		15	16 30	31 45	46 60	61 80	100	130	131 170	*****	
C9	E	0	1	2	3	4	5	6	7	8	g
<i>Cp</i> =	_	all	a.2	246	ab	all	1.0	12	15	1.9	20
	o.1	a.3	a.5	0.7	a i	1.1	1.4	1.5 1.8	1.3	2.5	
Ap =	_	0	5		π	14	18	25	41	92	141
	4	7	10	11 13	14 17	24	40	91	140	400	

Fig. 2. Daily geomagnetic character figures C9 and sunspot numbers $\it R$ for solar rotation Nos. 1759–1780

the solar cycle, there was a persistent magnetic disturbance that appeared on every rotation for a year or so; it started back in solar cycle No. 1766, a month before *Mariner* was launched. Similarly, the most persistent stream of high-velocity plasma that we saw on *Mariner* was detected every time we were in position to see it, and it occurred on the sixth through the tenth days of the solar rotation cycle. Because of the uniqueness of that stream and the uniqueness of this particular recurrent series of magnetic storms, and because of the fact that at about the proper position on the Sun there is a series of calcium plages that start about this time and continue over the same period, it is extremely enticing to say there is some causal relationship between these phenomena.

When you try to determine the relationship in detail, however, about all you end up with is confusion.

Problems of Detailed Correlations

In the top third of Fig. 3 is plotted the 3-hr average plasma velocity shown in the previous paper for solar rotation No. 1767. The lines at the

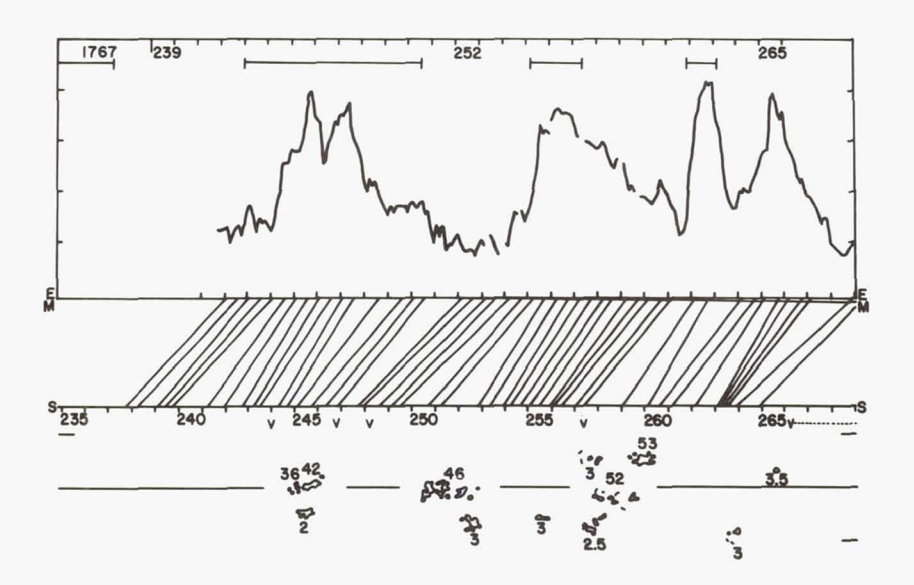


Fig. 3. Time plots of magnetic storms (bars), solar-wind velocity (3-hr average), extrapolation lines $(r - \phi \text{ plots})$ to the Sun's surface, counting-rate increases on *Mariner* GM counters (v), and features of the solar map. Solar rotation No. 1767

top indicate magnetic storms; these are the major magnetic storms of the year (Ref. 2). The numbers 239 through 268 are the days of observation, starting with January 1, 1962 as Day 1.

In the center of Fig. 3 are the straight lines representing the spiral magnetic-field lines. These are plotted exactly as those in Fig. 1 except for one thing—the slopes of the lines represent velocities measured not on the Earth but on *Mariner*. The spacecraft orbit is indicated by the line marked M, which is coincident with the Earth line E for the first few weeks.

The features in the solar map at the bottom of Fig. 3 are represented in terms of the time of their central-meridian passage (as seen from the Earth). This map of the Sun is drawn more or less to the proper scale and shape, and includes all of the plage regions that either had a magnitude of 3 or more, or had an area of 1000 millionths or more of the solar disk. Plages that belong to long-lived sequences are marked with the last two digits of their McMath number; plages that appeared on only one rotation are labeled with their intensity at CMP (2, 2.5, 3, or 3.5). The horizontal line represents the locus of points on the solar surface directly below the spacecraft.

If you ask: where did the high-velocity plasma observed on Day 245 come from?—by following the proper field line from *Mariner* to the Sun, you end up at a blank area on the map that had its CMP early on Day 243. The long-lived plage region that at first glance might be thought to be associated with the high-velocity plasma, is centered on Day 245, about 2 days to the right of the apparent origin of the field line. The plasma velocity would have had to be much greater than was observed to connect the central-meridian passage of the plage region with the observed velocity peak.

This was not universally the case, but there was a tendency in this direction: the source of the high-velocity streams seemed to be a day or so ahead of where you would like it to have been. I think the conclusion is simply that it is still true that the M regions are not visible on the surface of the Sun. There is really nothing new in this statement, but I think it is more direct than previous statements have been.

One other thing is indicated on Fig. 3. The little v's indicate the apparent sources of the increased fluxes observed by Van Allen's 213 Geiger counter, which was also on *Mariner*. The particles could have been either protons above 0.5 Mev or electrons above 40 kev. There were about 13 such peaks, and they also don't seem to fit too well with anything visible on the Sun.

In Fig. 4, which shows the next solar rotation, the magnetic-field line associated with the small velocity maximum early on Day 274 does appear to connect with the plage region labeled "?"; while the next peak, late on Day 274 and early on Day 275, appears to be connected with plage region 62. If these were the only cases we had, I think all you could say is, "Well, isn't that beautiful!" Immediately following these peaks,

however, on Days 281 and 282, there is a very large peak that doesn't connect clearly with any mapped feature, although plage region 66 lines up fairly well with the midpoint of the steep rise. The plage regions with central-meridian passages on Days 284 and 285 were of reasonably good

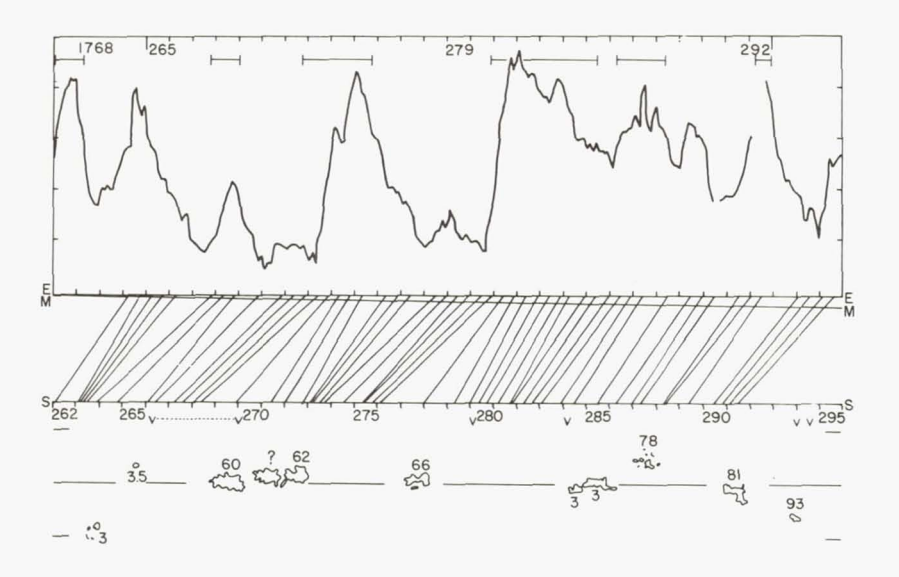


Fig. 4. Time plots of magnetic storms (bars), solar-wind velocity (3-hr average), extrapolation lines $(r-\phi \text{ plots})$ to the Sun's surface, counting-rate increases on *Mariner* GM counters (v), and features of the solar map. Solar rotation No. 1768

size and corresponded fairly well with the peaks on Days 287 and 288. The peak on Day 292, however, fell almost halfway between two plage regions.

The data for the next solar rotation, No. 1769, are displayed in Fig. 5 and show much the same behavior as that seen in the earlier rotations. It is interesting to note here that during the time that we had no data (because the spacecraft was turned off), there was no magnetic storm, even though there were magnetic storms at this same time both in the previous solar cycle and in the following solar cycle. Maybe we were lucky and didn't miss a stream in that particular region.

The data for solar rotation No. 1770 are given in Fig. 6. On Day 325 there was a very sharp rise in plasma velocity. If you follow back the field lines associated with this peak, you end up in a very clean region between visible plage regions that you might consider to be the source.

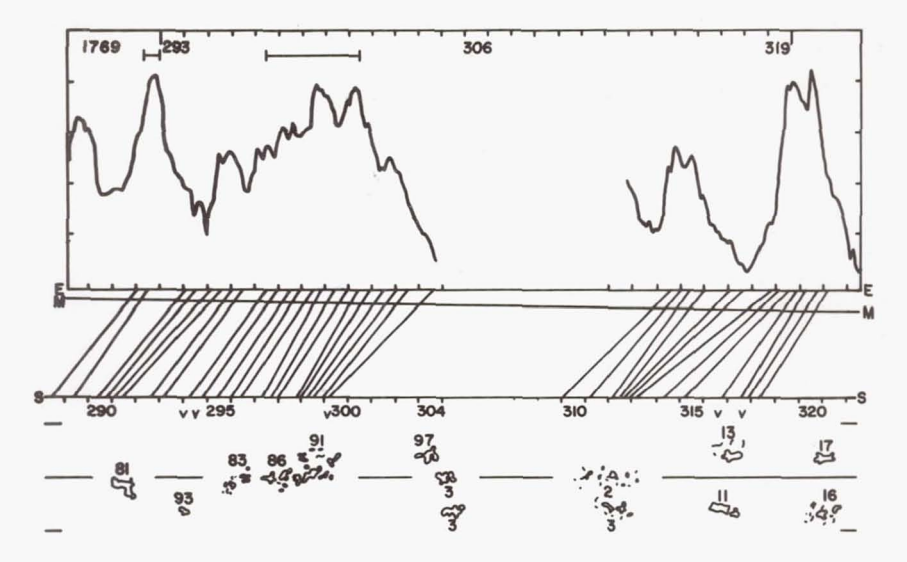


Fig. 5. Time plots of magnetic storms (bars), solar-wind velocity (3-hr average), extrapolation lines $(r-\phi \text{ plots})$ to the Sun's surface, counting-rate increases on *Mariner* GM counters (v), and features of the solar map. Solar rotation No. 1769

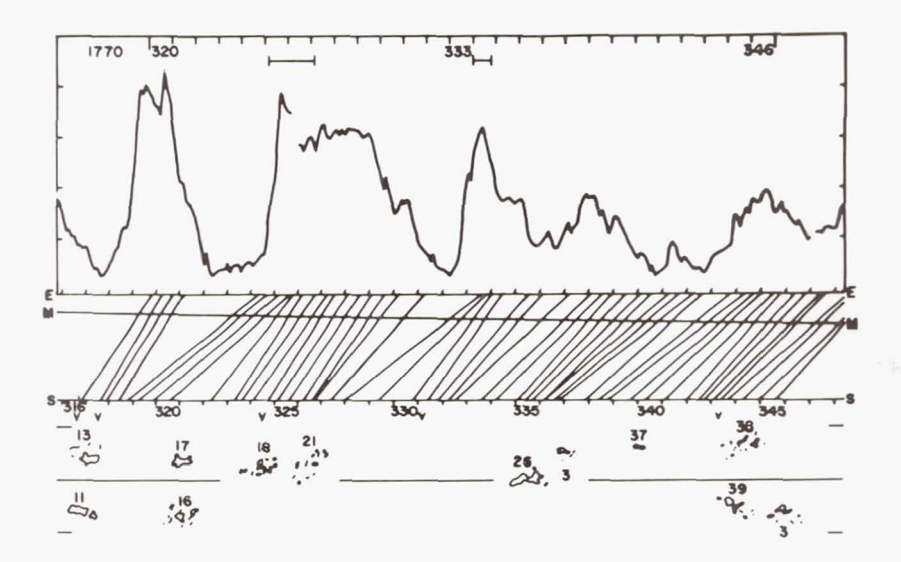


Fig. 6. Time plots of magnetic storms (bars), solar-wind velocity (3-hr average), extrapolation lines $(r-\phi \text{ plots})$ to the Sun's surface, counting-rate increases on *Mariner* GM counters (v), and features of the solar map. Solar rotation No. 1770

Figure 7 shows solar rotation No. 1771, the last one observed by *Mariner*. Again, the peak on Day 354 calculates back to a point on the Sun that is fairly clean, except for a little activity (not shown) well south of the spacecraft.

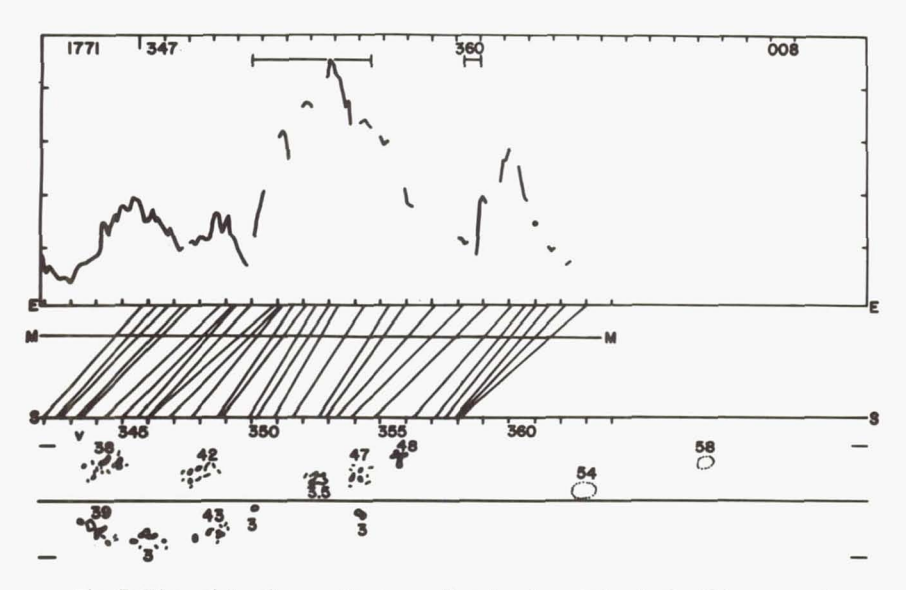


Fig. 7. Time plots of magnetic storms (bars), solar-wind velocity (3-hr average), extrapolation lines ($r - \phi$ plots) to the Sun's surface, counting-rate increases on *Mariner* GM counters (v), and features of the solar map. Solar rotation No. 1771

The data seem to indicate that there is no close correlation between the plage regions and the solar streams, unless either (1) the velocity is not constant, or (2) the high-velocity plasma is not shot out from the Sun in a radial direction, so that the simple Archimedes-spiral model is incorrect.

REFERENCES

- Central Radio Propagation Laboratory, Compilations of Solar Geophysical Data, abstracted from CRPL-F Part B, U.S. Department of Commerce, National Bureau of Standards, October (1963).
- 2. LINCOLN, J. VIRGINIA, Journal of Geophysical Research 68, various issues (1963).

DISCUSSION OF SNYDER PAPER

BRANDT: Have you tried correlating plasma velocity with coronal data? **SNYDER:** Not in enough detail to be sure of the answer. However, I think the answer will be the same as for the plage regions.

DAVIS: One thing I would like to emphasize at the moment is Dr. Snyder's concluding remark that perhaps the Archimedes-spiral model is not quite perfect. I think that the field strength is strong enough close to the Sun that it could

easily govern the motion of the wind. It doesn't seem at all surprising to me that the wind and the features on the Sun fail to correspond by a day or two, one way or the other.

ATHAY: A lot of work has been done in correlating M-region storms with surface features of the Sun. Mustel' finds that if you count all active regions within one or two days of central-meridian passage, then you can, in fact, correlate most of the M-region storms with an active region on the Sun. This does not prove, however, that the correlation has physical significance.

When you look at the surface of the Sun optically, very often the matter in a given active region will show high-speed motions that are preferentially in one quadrant rather than in all quadrants. Thus it is not unlikely that matter leaving the Sun will leave in a nonradial direction.

WILKERSON: Is there any correlation of the helium-hydrogen abundance ratio with solar rotation?

SNYDER: I don't think that we can see any. Our information on the heliumhydrogen abundance is really very sparse.

BLOCK: How compelling are the reasons for assuming that the velocity is constant all the way from the Sun to the Earth?

Let us assume that the magnetic-energy density is proportional to the inverse fourth power of the radius, and that the density, according to Neugebauer's data, goes as the inverse second power, so that the kinetic-energy density decreases as the inverse second power. This means that close to the Sun the magnetic-energy density is quite a bit stronger than the kinetic-energy density, and the plasma on the way out has to do some work against the magnetic field and is slowed down.

SNYDER: However, we need an acceleration to improve our correlations.

DEUTSCH: Let me ask Dr. Parker for an estimate of the transit time for a stream that, in the absence of a magnetic field, moves along one of his critical solutions and becomes a radial supersonic flow. Wouldn't this consideration be likely to change the transit time by just the day or two that is needed?

PARKER: That depends upon where you started counting time. If you started at a distance of about $2R_{\rm S}$ from the center of the Sun, you would have to add about a day. If you started from the top of the photosphere, you would have to add several months, because the gas takes so long to move from the photosphere to the corona.

DEUTSCH: So a simple gas pressure effect, even in the absence of magnetic fields, could conceivably account for the delays that the data seem to show? **PARKER:** Yes. In fact, I don't see that the magnetic fields play any significant role here. They have energy, but the energy is more or less stationary.

DEUTSCH: We have been told that the flow does not seem to be a simple adiabatic expansion. However, both the velocity profile and the temperature profile, I believe, correspond very well with such a model.

PARKER: One does not expect the flow to be adiabatic. But the temperature beyond 20 or 30 R_s is rather irrelevant to the final velocity of the wind, so for mathematical simplicity the flow is often considered adiabatic at large distances from the Sun. If you aren't interested in the temperature of the gas at 1 AU, then you may as well consider the flow to be adiabatic. If you do want to know the temperature, that is another problem.¹

¹See discussion in E. N. Parker, Interplanetary Dynamical Processes, Interscience Publishers, a division of John Wiley and Sons, Inc., New York (1963)

DEUTSCH: Does this mean it is coincidental that we observe temperatures corresponding to adiabatic flow?

PARKER: The temperatures that are observed seem to be way above the adiabatic values. If I remember the graphs that Mrs. Neugebauer showed, it seems that the temperature was sometimes close to a million degrees, which would be almost isothermal.

SLUTZ: Do the observations give information on the direction as well as the velocity of the flow? If they do, there may be some experimental evidence to support some of these conjectures.

SNYDER: There is absolutely no information about direction, because we were always looking directly at the center of the Sun.

It is clear that there are two major aspects of the plasma that are not very well determined: the alpha-particle abundance and the directional characteristics. Neither of these aspects has been well determined by more recent spacecraft either. I might add. This information will come along in the future.

NEUGEBAUER: Since we always saw a plasma flux, we do know that the flow was never more than 10 degrees from the radial direction.

SNYDER: Yes, I think this is a very important point. Although the flow may never have come directly from the Sun, it was never very far from radial.

ZIRIN: I have two remarks. First, with regard to the plage regions, I don't really see what is magic about CMP—although it is a very handy position on the Sun. These active regions really vary in their activity: on some days they are very active and on other days they are very quiet. CMP may not necessarily coincide with the day that the regions are most active.

Secondly, I think you have convinced me that in measuring the *Kp* index, one is measuring the velocity of the solar plasma. We therefore have 50 years of data to which we may now apply the same analysis.

SNYDER: The *Mariner* data represent the first time we have had an accurately known velocity with which to perform such an analysis. We should have been able to pinpoint the responsible solar regions within a degree or two, but we couldn't. The velocities that could be calculated from the *Kp* indices for the last 50 years would be a lot less accurately known.

INTERPLANETARY MAGNETIC MEASUREMENTS

LEVERETT DAVIS, JR.

California Institute of Technology, Pasadena, California

E. J. SMITH

Jet Propulsion Laboratory, Pasadena, California

P. J. COLEMAN, JR.

University of California, Los Angeles, California

C. P. SONETT

Ames Research Center, NASA, Moffett Field, California

(Presented by E. J. Smith)

The Mariner-2 Magnetometer Experiment

Among the instruments aboard Mariner 2 was a triaxial fluxgate magnetometer with three orthogonal sensors (Ref. 1), one along each of three axes (X, Y, Z) fixed in the spacecraft. The readings of each of three magnetic-field components were separated by 1.9 sec, and a complete set of readings was relayed to Earth every 36.96 sec. Although the accuracy of each reading was about 0.5γ ($1 \gamma = 10^{-5}$ gauss), the observed field was really the vector sum of the interplanetary magnetic field and a nearly constant spacecraft magnetic field; so this accuracy applies only to changes in the interplanetary field. The spacecraft field must be subtracted from the combined field in order to give the true interplanetary field; but determination of the spacecraft field, or "bias," depends on certain assumptions, and the bias may therefore be known significantly less accurately than to within 0.5 y. The data described in this paper were obtained in interplanetary space during late 1962 and far enough from the Earth to be unaffected by the Earth's presence. No magnetic measurements were obtained either inside the geomagnetic field or in the transition region.

The orientation of the spacecraft, and therefore of the magnetometer, was controlled so that the positive Z direction (roughly, the spacecraft axis-of-symmetry) pointed away from the Sun. The orientations of the other two axes, X and Y, depended upon the mode of operation of the spacecraft. From August 29 to September 3 the spacecraft was allowed to roll about the Z axis. On September 3 the spacecraft was stabilized

with the Y axis in a plane defined by the Sun, the Earth, and the spacecraft; at that time the X axis was nearly parallel to the direction of the north ecliptic pole.

The variation in the X- and Y- component readings during the period preceding the stabilization can be attributed principally to the roll of the spacecraft. The contribution of any quiet transverse interplanetary field, when averaged over many complete revolutions, should be zero. Thus, the averages of the observed field values represent the X and Y components of the spacecraft field. Fortunately, the interplanetary field was relatively undisturbed during this period, permitting a precise evaluation of these components. The center-to-peak amplitude of the variations in the X and Y components during roll represents the transverse component of the interplanetary field.

Preliminary analysis of the *Mariner-2* data revealed a large-scale interplanetary field with characteristics similar to those expected on the basis of theory. Specifically, the field tended (on the average) to lie in the ecliptic and to make the expected spiral angle. However, one could not just look at the data and derive such conclusions immediately, the problem being that the measurements were not absolutely accurate. The accuracy of the measurements was affected by the substantial spacecraft magnetic field, which changed both during and after launch. Immediately after launch, the spacecraft field was found to be much larger than had been indicated by measurements made prior to launch. We believe that all components also changed slightly during the flight.

Consequently, in order to derive the characteristics of the interplanetary field, it has been necessary to try to construct a reasonable model that is consistent with the observations. A preliminary look at the data indicated that the usual model of the interplanetary field was valid; so we decided to use this model, together with our data, to infer the spacecraft-field components to a reasonable degree of accuracy. This procedure obviously has important implications, not only for studying the large-scale field and its characteristics, but also for studying the smaller-scale field fluctuations.

Preliminary Results

I will begin by reviewing some of the preliminary results (Ref. 1). This will refresh the memory of those who have seen them before, and will, I hope, indicate that the techniques used to determine the spacecraft field were not completely arbitrary. In discussing the data, we shall use alternately the magnetometer coordinate system (X, Y, Z) and one (R, T, N) based approximately on the ecliptic; in the latter system, R is radially outward from the Sun, T is in the azimuthal direction (positive in the direction of planetary motion), and N points close to the north ecliptic pole (see Fig. 2, Paper 9).

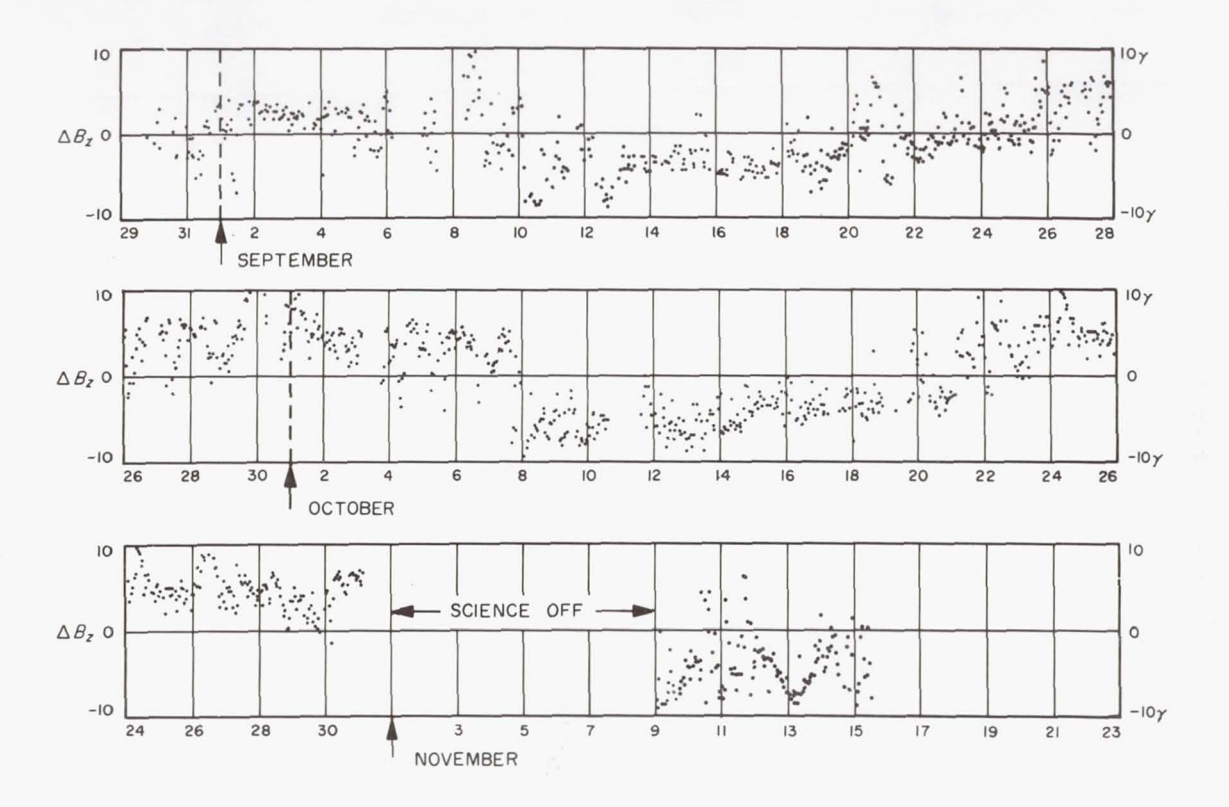


Fig. 1. Changes in the radial component of the magnetic field observed on $Mariner\ 2$ (not corrected for spacecraft field)

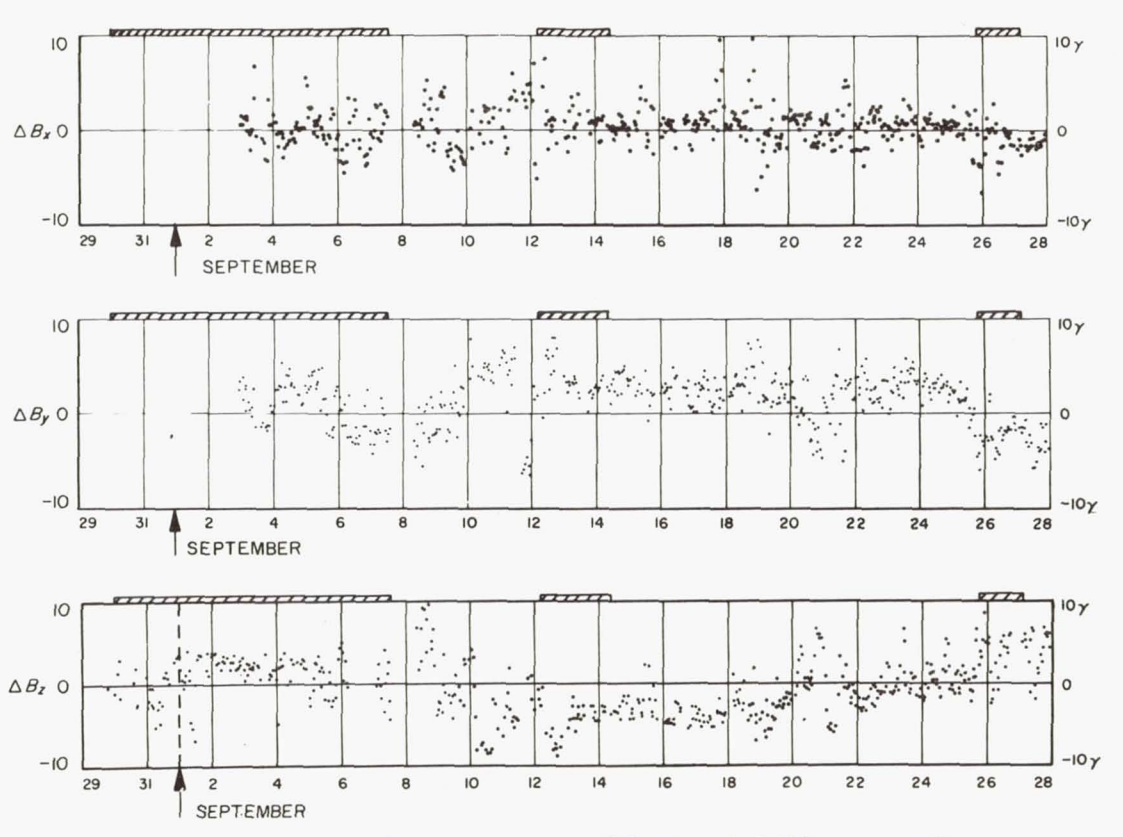


Fig. 2. Changes in the three components of the magnetic field (not corrected), given in spacecraft coordinates

Figure 1 shows the measured variation of the radial magnetic-field component ($\Delta B_R = \Delta B_Z$), not corrected for spacecraft field. Each point corresponds to an hourly average, and the data cover the period from the end of August to the middle of November. There are a couple of very interesting features in these data. The first is the extreme scatter in the data, which was due, it seems clear on further analysis, to the irregularities in the interplanetary field, that is, to the roughness of the field or to the disordering of the spiral structure. Another very marked feature is the periodic variation that coincided with the 27-day rotation of the Sun. This feature can be seen in two of the three components.

Figure 2 shows the data for only the first solar rotation (1767). The data for the period just prior to the start of Fig. 2 were obtained when the spacecraft was rolling. During this time it was possible, as described above, to determine the two spacecraft-field components that were perpendicular to the spacecraft-Sun direction; and averaging over the several days during which the spacecraft was rolling, we could obtain a fairly high degree of accuracy $(\pm 0.25\gamma)$.

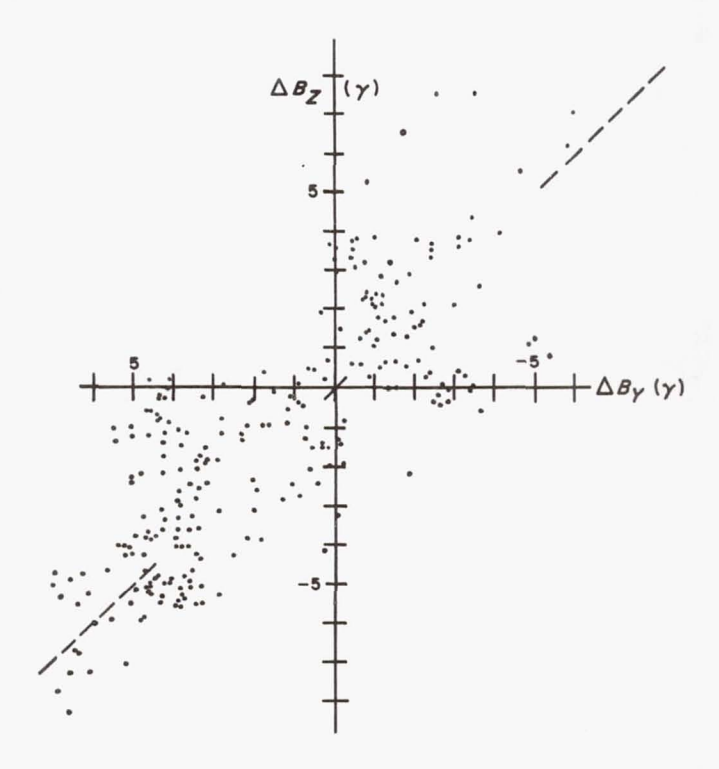


Fig. 3. Correlation between ΔB_z and ΔB_y (not corrected). The dashed line shows the expected average for theoretical spiral field lines from the Sun

The structure following September 9 is interesting, because as the radial component ΔB_Z changed, the transverse component ΔB_Y tended to change simultaneously in the opposite direction. This is just what you would have expected on the basis of the spiral model. You can see this correlation a little better by plotting the two components against each other, as shown in Fig. 3 in which the plane of the paper represents the ecliptic.

Each of the points represents a "smoothed" hourly average—the average value of five successive hourly averages. Despite this averaging, one can't help being impressed by the disorder and irregularity in these measurements.

We have drawn the coordinate-system origin so that the dashed line, which represents approximately the expected spiral-field direction, appears to fit the data points. The value of the Y component of the spacecraft field, consistent with this selection of the origin, is reasonably close—say within 5γ or so—to its value as determined during the roll period. Thus the data points represent the endpoints of the interplanetary-field vector only. Wherever the true origin may be, this figure shows the way the end of the vector moved, and one can say at the very least that there was a tendency to cluster in the first and third quadrants. There does seem to have been a preferred direction that was at an angle of approximately 45 deg to the radial direction from the Sun. Thus the results look very much like the expected spiral angle.

Correction for Spacecraft Fields and Zero Offset

I shall now describe briefly what can be called a second-order approximation to the interplanetary magnetic field-an attempt to infer and subtract all components of the spacecraft field throughout the flight. Since preliminary indications are that the average solar field does lie in the ecliptic and does make the expected spiral angle, one can derive the spacecraft components at all times on the basis of three assumptions. The first assumption is that the spacecraft fields in the X and Y directions were known at the start of the data interval. These data were obtained from the roll period. The second assumption is that the components in the ecliptic, averaged over several days, took the streaming angle that was based on the solar-wind velocity as measured by the plasma experiment. The third assumption is that the Z component of the spacecraft field remained constant throughout the period prior to the first solar-panel failure (October 31). A preliminary look at the data indicated that this last assumption is valid, and the results are consistent with this assumption. The Z component seemed to be much less susceptible to change than either of the other two components.

If for each day we compute the values that the *X* and *Y* components of the spacecraft field would have to have if the average interplanetary field

for that day were to fit the ideal spiral model, we get a rather irregular structure superimposed on some kind of slow drift. The irregular structure is presumably associated with the deviations of the interplanetary field from the spiral, but the slow changes, based on averages over several days, were taken to represent the spacecraft magnetic field itself.

Figure 4 shows the results of these calculations for the first 60 days of the flight. The solid curves represent the required corrections, that is, the negative of the inferred spacecraft fields. You can see not only that the spacecraft field was apparently changing, but that sometimes it changed very abruptly. It is important to note that these changes have little to do with, and are not responsible for, the correlation of the Y and Z (or T and R) components mentioned earlier. On the basis of our best evidence (although it is not completely conclusive) these changes seem to have been associated with some kind of currents flowing in the spacecraft—either ground-return currents associated with the spacecraft power system or some kind of thermoelectric current.

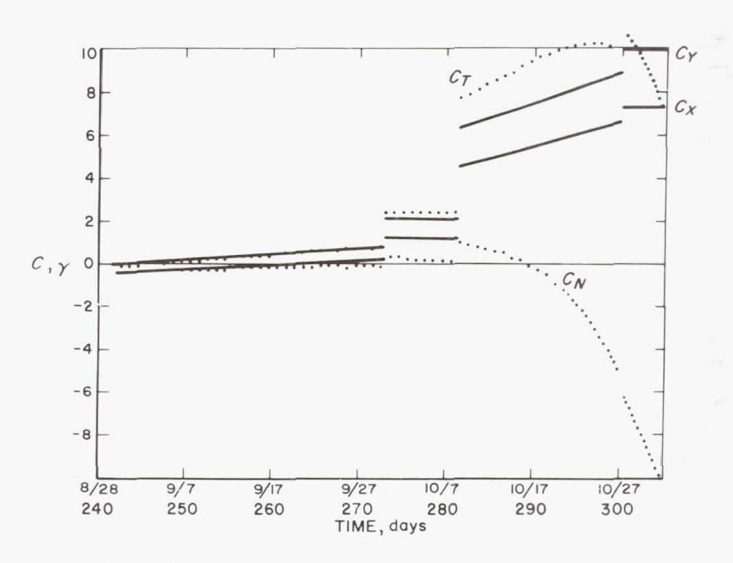


Fig. 4. Calculated corrections for Mariner-2 spacecraft fields

The C_T and C_N curves (dotted) show the corrections in solar-ecliptic coordinates. Notice that the spacecraft rolled through nearly 90 deg between Day 280 and Day 300 as it overtook the Earth in solar longitude. This roll helped in determining the spacecraft fields.

The main thing that one notices from the figure is that the spacecraft field was very stable for the first 6 weeks or so. The changes along both axes were apparently less than 1 γ . Then there were both abrupt changes

and periods of gradual change. The maximum corrections were about 10γ . It is difficult to know just how accurately one can do this sort of thing. If you consider the accuracy of the measurements and the accuracy associated with the digitalization of the data, and if you allow for the irregularities in the interplanetary field and so forth, then hopefully you can determine the spacecraft field to within perhaps 1γ but this may be

Corrected Data

a little optimistic.

The following figures show the corrected *Mariner-2* data over the same period of about 60 days. This period was prior to the time at which a rather catastrophic event occurred on the spacecraft: on October 31, one of the solar panels shorted. At the time the solar panel stopped providing power for the spacecraft, a very large but not-precisely-known change in the spacecraft field occurred. The spacecraft field was large enough that the magnetometer switched to the insensitive scale and gave less useful

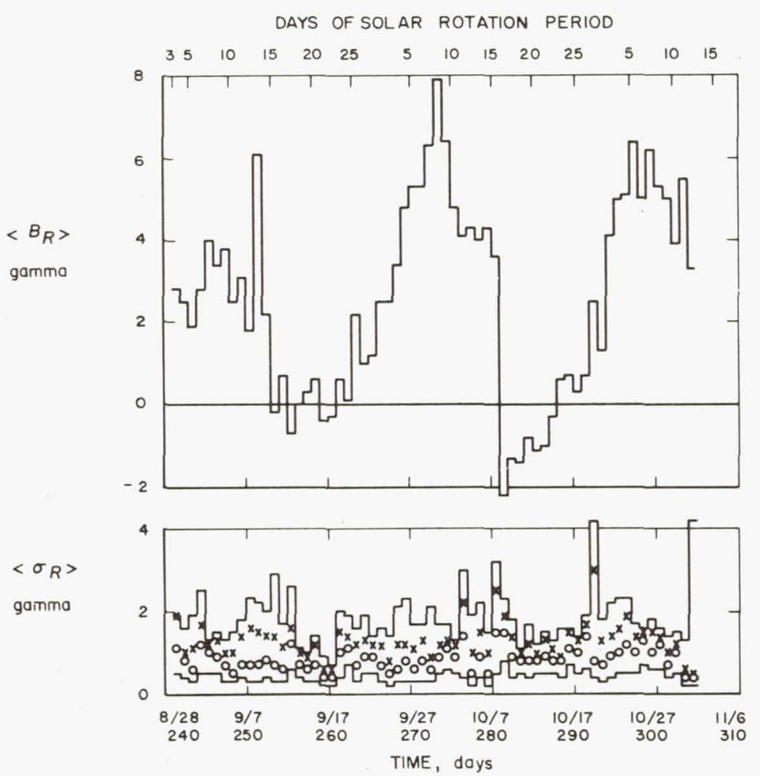


Fig. 5. Corrected interplanetary magnetic field, radial component, 1-day averages. The lower plot shows standard deviations for different time intervals: 3.7 min (bottom curve), 30 min (circles), 3 hr (crosses), 24 hr (top curve)

data. When the panel recovered, the field returned to normal and the magnetometer returned to its sensitive range—until a second failure occurred a week later.

The upper part of Fig. 5 shows the radial component of the interplanetary field. Each of the bars represents a daily average in the value of that field. The notable feature here is that the radial component did show a very strong periodic variation associated with the rotation of the Sun. (Solar rotation, in days, is shown at the top.)

One could conclude that the picture shown here suggests a solar magnetic-field configuration in which field lines come out of the Sun on one side, while the net outward flux is essentially zero on the other side. But since the values shown may well be uncertain to the extent of about 1γ , any such conclusion must be made very carefully.

WILCOX: This base line is different from the base line in the earlier figure, is it not?

SMITH: That is correct.

WILCOX: Is this one more accurate?

SMITH: This one is more accurate: this picture is the result of a careful analysis of the data. In the earlier figure, the zero base line was more or less arbitrarily placed through the middle of the pattern, which made the field look as though it were pointing outward on one side of the Sun and inward on the other. When Fig. 1 was first shown, we tried to explain that the result shown here (Fig. 5) would also be essentially consistent with the data, since there were uncertainties in the spacecraft field.

The lower part of Fig. 5 shows the standard deviations in the field; the different symbols represent standard deviations taken over different time increments. The lowest curve corresponds to a period of 3.7 min, during which time six measurements of the field were made. The circles correspond to a period of a half-hour. The difference between the circles and the lower curve gives you some idea of those fluctuations having periods between 3.7 min and a half-hour. The crosses correspond to a period of 3 hr, while the upper curve corresponds to a period of a whole day. The data indicate that there was a fairly wide distribution of frequencies.

Comparing the amplitude of the fluctuations with the amplitude of the field provides a quantitative measure of the scatter seen in Fig. 3. The field was very typically about 4γ ; the rms value of the fluctuations over a period of a day was perhaps 2γ or slightly more than 2γ .

NESS: What was the noise level associated with the digitalization?

SMITH: It corresponded to about $\frac{1}{4} \gamma$ rms. That was the electrical noise level in the instrument, and was about the same as the uncertainty in the digitalization. The step size between the binary-coded integers was about $\frac{1}{3} \gamma$. [The digitalization should not have significantly increased the mean of the standard deviations: it seems more likely to have reduced it.]¹

¹Added in manuscript

NESS: Is the lower curve consistent with the noise level in the sense of a digitalization error?

SMITH: Very close to it: some of the values are $\frac{1}{2}\gamma$. Presumably some of the low values could have occurred at times when the fluctuations in the interplanetary fields could not be distinguished from the noise in the instrument. There were periods (though not very many) lasting as long as several hours during which there were no changes—in any of the components—larger than just one digital number; thus there were times when the field was extremely quiet. Such periods were used in estimating the noise in the instrument, and the estimated value agreed with expectations based on working with the instruments on the ground.

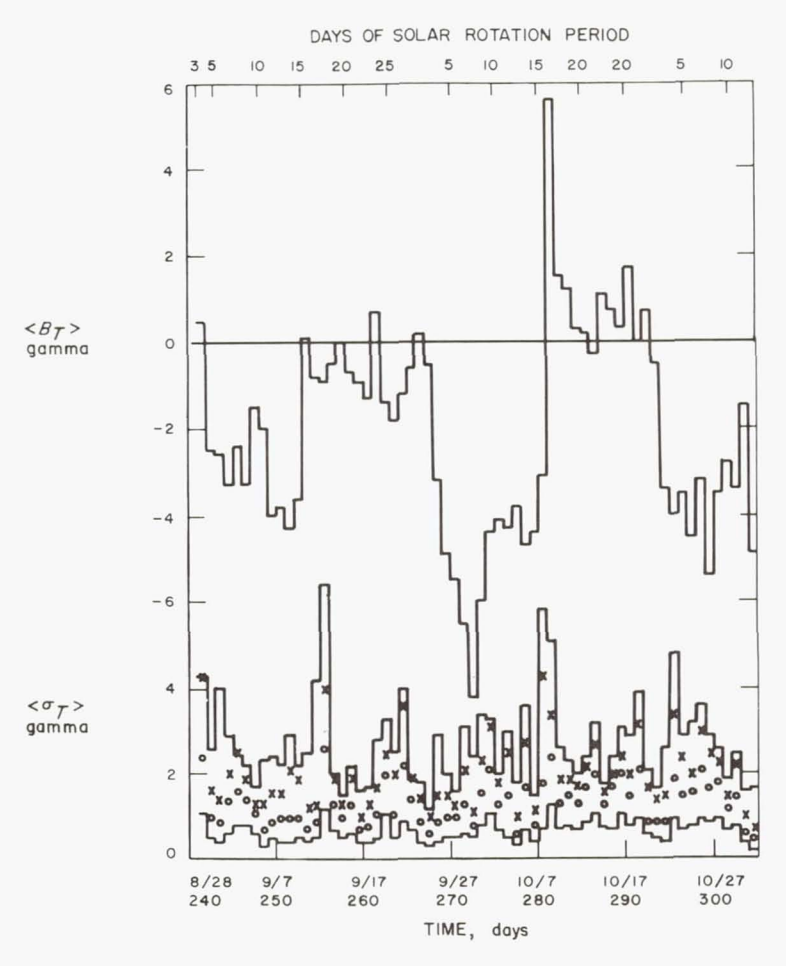


Fig. 6. Corrected interplanetary magnetic field, tangential component, 1-day averages. The lower plot shows standard deviations for different time intervals: 3.7 min (bottom curve), 30 min (circles), 3 hr (crosses), 24 hr (top curve)

Figure 6 shows the tangential component, which is positive in the direction of planetary motion. You can see again the presence of the 27-day pattern. The picture looks quite a bit different from that of ΔB_Y shown in Fig. 2, because not only has it been transformed to a different coordinate system, but significant spacecraft fields have been subtracted. In both this and the preceding figure, you can see that there was some kind of single, large source on the Sun that seemed to overshadow the other disturbed solar regions.

The lower half of the figure shows the standard deviations as before,

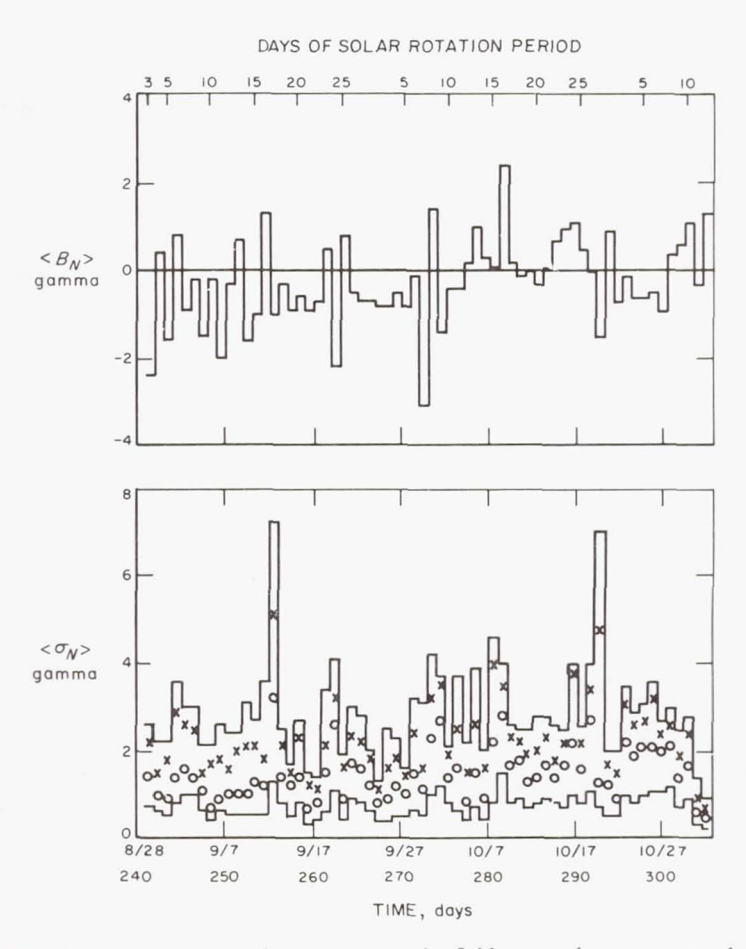


Fig. 7. Corrected interplanetary magnetic field, normal component, 1-day averages. The lower plot shows standard deviations for different time intervals: 3.7 min (bottom curve), 30 min (circles), 3 hr (crosses), 24 hr (top curve)

using the same symbols. Now, the interesting feature about these deviations is that they appear to be substantially larger. In Fig. 5, values of perhaps 2 γ were typical, and the standard deviations only twice exceeded 4 γ , even in the 1-day averages. The tangential component, as shown in Fig. 6, was apparently more disturbed than the radial component.

This aspect of the data is also seen in Fig. 7, which shows the normal component, B_N , perpendicular to the ecliptic. Here again you can see that the standard deviations were larger than those of the radial component by a factor of about 2. This figure has two other important features. First, this component shows no large effect associated with the rotation of the Sun. This fact tends to indicate that the calculated values of the space-craft fields were reasonably accurate. At least, we would expect that there would be no effect associated with the solar rotation remaining after the corrections for spacecraft fields were made.

Another interesting and somewhat troublesome feature is that while \mathbf{B}_N averaged near zero over this entire period of 60 days or so, there was a period, lasting just slightly over a month, in which there definitely appeared to be some average component that was out of the ecliptic—to the extent of about 1γ . Now, this component was negative, that is, opposite to the north ecliptic pole. The zero level for this period, which immediately followed the time that the spacecraft had been rolling, is believed to have been very accurately determined. During later periods, this southward-pointing component gradually vanished.

WILCOX: Did your corrections tend to make B_v average to zero?

DAVIS: Yes, the corrections could easily account for B_N going to zero in the last half of the diagram.

COLBURN: Does the part of your analysis involving the spacecraft rotation depend on the assumption that the spiral angle was in the ecliptic during the spacecraft roll period?

DAVIS: All you have to assume is that, over a period of 4 days, the interplanetary field did not have a variation that correlated with the rotation of the spacecraft. **SMITH:** It turned out that over this period of about 4 days, each of the half-day averages of the spacecraft field agreed to within $\frac{1}{4}\gamma$; the spacecraft field didn't change during this time.

GOLD: Can you tell us what the angle was between the spacecraft and the equatorial plane of the Sun during that period of time?

SNYDER: The solar latitude of the spacecraft was fairly constant during the first half of the mission, when the magnetometer data were most reliable. Starting at 7.1 deg north, it reached a maximum of 7.8 deg during the last half of September, and then decreased at an accelerating rate. It passed 6.0 deg on November 1 (Day 305), and 0.0 deg on December 7 (Day 341).

SMITH: Regardless of that, qualitatively, what you would expect at nonequatorial latitudes is inconsistent with the data. If the direction of the normal and radial components is determined by the general solar field, then there should be a positive normal component corresponding to a positive radial component. But the normal component was not positive, it was negative.

Figure 8 represents the interplanetary field in polar coordinates. In addition to the total magnitude B, the figure shows the angles β and Λ , defined by:

$$\langle B_N \rangle = \langle B \rangle \sin \beta$$

 $\langle B_R \rangle = \langle B \rangle \cos \beta \cos \Lambda$
 $\langle B_T \rangle = \langle B \rangle \cos \beta \sin \Lambda$

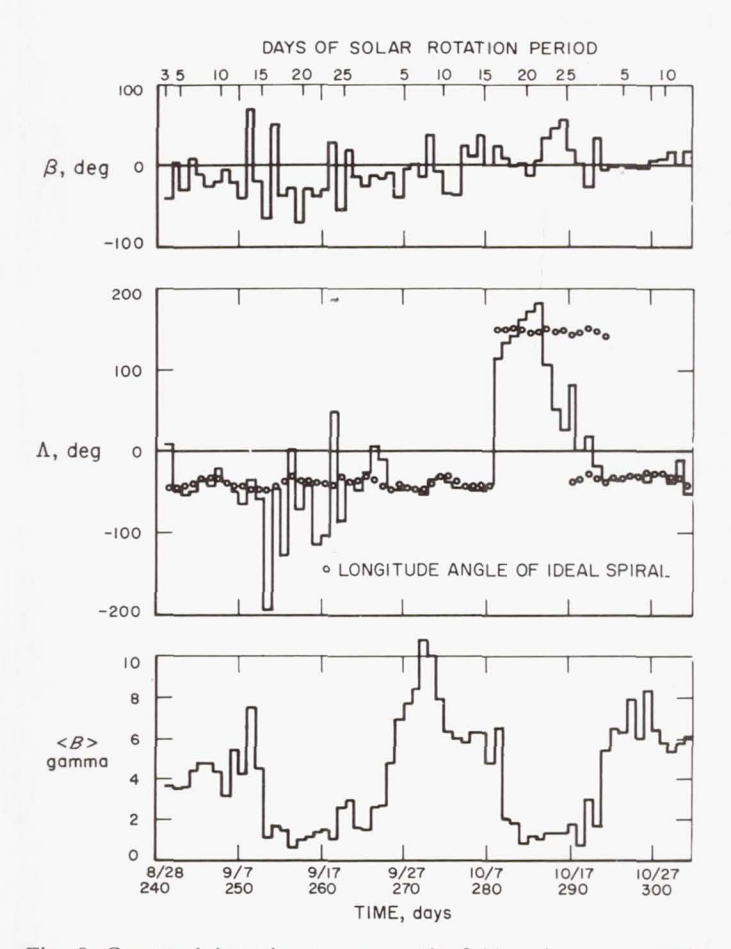


Fig. 8. Corrected interplanetary magnetic field, polar representation, 1-day averages. Λ is the azimuthal angle, measured from the radius vector; β is the polar angle, measured from the ecliptic: $\langle B \rangle$ is the total field strength

Thus Λ is the azimuthal angle of the projection of $\langle B \rangle$ in the ecliptic, and β is the ecliptic polar angle. The azimuthal angle Λ is compared with the theoretical streaming angle,

$$\Lambda_{\rm stream} = -\tan^{-1}(r\Omega_s/v)$$

This ideal streaming angle is shown by the circles on the Λ plot. You must remember that the good agreement is one of the assumptions used in eliminating the spacecraft field. However, you can see that there were periods during which the angle Λ deviated substantially from the expected spiral angle, even after a fair amount of smoothing.

The bottom of Fig. 8 gives a fairly clear picture of how the magnitude of the field varied over this period. The average value, about 4γ , seems

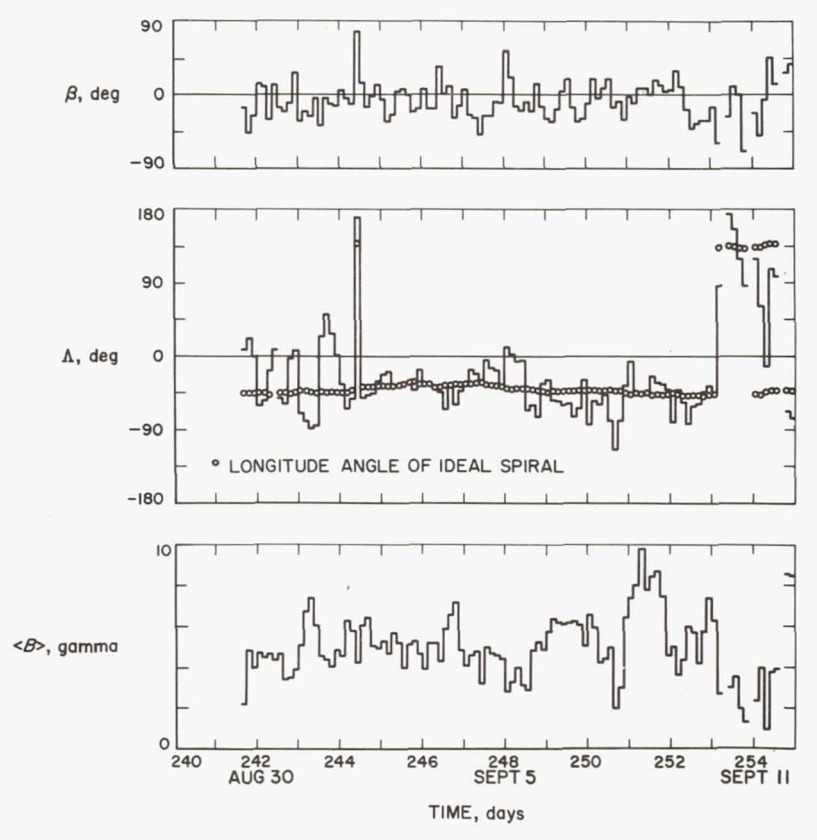


Fig. 9. Corrected interplanetary magnetic field, polar representation, 3-hr averages. Λ is the azimuthal angle, measured from the radius vector; β is the polar angle, measured from the ecliptic; Fig 8 $\langle B \rangle$ is the total field strength

quite reasonable, but variations extended all the way from about 1 to 10γ . There are no obvious nulls in the data, although the averaging time is too long for this fact to be significant.

Figure 9 shows 3-hr averages, plotted over a period of about 2 weeks. Here the average field magnitude was about 5 γ . There is no indication that the field really went to zero for any period as long as 3 hr. Now, when you compare the data with the calculated value of the spiral angle, you can see quite a bit of roughness of the field. Also, the field was out of the ecliptic for periods lasting several hours.

Figure 10 is a comparison between the fluctuations in the total field,

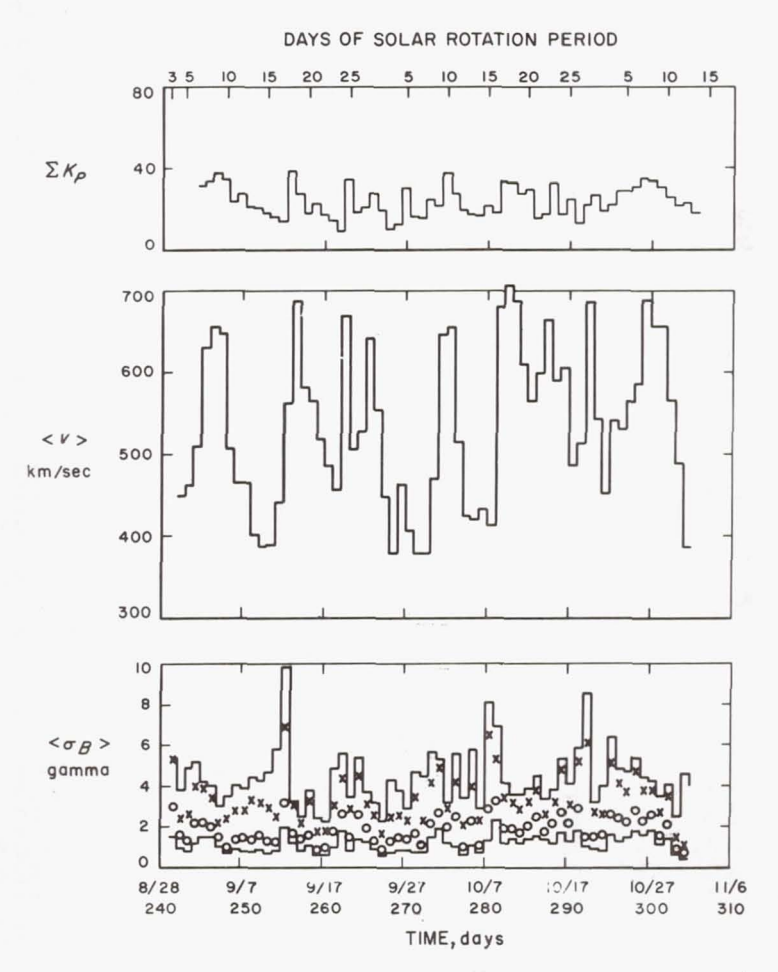


Fig. 10. Solar-wind and magnetic fluctuations. Top: the terrestrial magnetic-activity index ΣKp ; center: the daily mean solar-wind velocity; bottom: standard deviations of the total interplanetary magnetic field for various time intervals

the solar-wind velocity, and the Kp index of geomagnetic activity (see Papers 1 and 2). The standard deviation shown here is for the vector field (the square root of the sums of the squares of the standard deviations of the three components), and the symbols used are the same as those used in Fig. 5 through 7. The figure shows that there were fairly broad frequency spectra for these variations. Although there are some fairly pronounced peaks in both the daily and the 3-hr standard deviations, there is no direct correlation between these peaks and the peaks observed in the solar-wind velocity. Instead, the peaks in the fluctuations of the interplanetary field seem to correlate better with the periods of rapid increase in the solar-wind velocity. This is a fairly consistent result and seems at least physically plausible, because during this period of time one would expect fast-moving plasma to have been overtaking slower-moving plasma. It is not obvious that there should be any correlation with the Kp index, other than that implied by the correlation between the Kpindex and the velocity.

REFERENCES

 COLEMAN, P. J. JR., L. DAVIS, JR., E. J. SMITH, and C. P. SONETT, Science 138, 1099 (1962).

..... Science 139, 909 (1963).

DISCUSSION OF SMITH PAPER

NESS: I have a number of comments. Although I am very sympathetic to the problems of spacecraft contamination fields, I think that the assumptions you have made severely restrict your results. For instance, I think the assumption that the magnetic-field streaming angle is the one determined or deduced from the solar-wind velocity is a particularly bad assumption, because I think that all you get out of your polar diagrams, then, is essentially what you put into them: specifically, the data give you exactly the streaming angle, because that was the assumption that you made at the beginning.

I think you have made another bad assumption with regard to the radial component of the spacecraft field being constant. Finally, you have completely omitted the problem of whether the zero levels of the instruments have themselves shifted. I think the overall conclusions from the data are less significant because of the physics you build in to your attempt to solve the spacecraft contamination problem.

DAVIS: Well, I agree wholeheartedly that a substantial part of the agreement with the spiral-field model is a result of the initial assumptions, and it would certainly be much better if we didn't have to make any assumptions. But it is nevertheless true that the *Mariner* observations provide definite support for the presence of a spiral field in the Fall of 1962.

There is one slightly complicated point that Dr. Smith didn't emphasize particularly, namely, that we did not use three degrees of arbitrariness in our assumptions. Essentially only one degree of arbitrariness was used because of the

assumption that any changes in the spacecraft field would affect the Y and X axes in the ratio of 9 to 7, but would not affect the Z axis. The reasons for this assumption would take 10 minutes to discuss, and I am by no means completely confident that the assumption is correct. However, in several events it seemed clear that the changes were about in these proportions, and the assumption was made merely to be somewhat less arbitrary than we might have been. This means that if you want to juggle the tangential component around, you can do so perfectly freely; but then you are going to be stuck with some changes in the normal component. Or if you want to juggle the normal component around, you will have changes in the tangential component. By using this assumption, which has some merit, we were able to find a spacecraft field for which both components agreed fairly well with the spiral model.

The other comment that you made was that we can't tell whether these difficulties were due to the instrument or to the spacecraft field, and I agree with this too. But it doesn't really matter whether it is the zero of the instrument that shifts, or the zero of the spacecraft field—they both contaminate the measurement of the interplanetary field. We were trying to remove this contamination regardless of its source. As a member of the magnetometer team who hates to see the magnetometer blamed, I think (in spite of the fact that it doesn't make any difference) the indications are clear that the worst of these troubles were due to spacecraft fields rather than to trouble with the magnetometer.

I don't know if there is any moral for people who have different kinds of magnetometers on different kinds of spacecraft, but it is clear that the solar-panel troubles were part of the cause of this contamination. When the solar panel failed, we got an enormous shift in the field: when it repaired itself, the shift vanished. All I hope is that nobody else has solar panels that do the same things to them that these did to us.

ZIRIN: We were wondering if there may not be a reasonable connection between the predominantly plus sign of the radial component of the magnetic field and the fact that solar activity during this period (in fact, for the last couple of years)

was virtually limited to the northern hemisphere of the Sun.

DAVIS: I think there is a connection. But this brings us back to the model of how the gas rises from the surface of the Sun, fills up the corona, eventually decides it will become a solar wind, and blows out into space. I would argue that possibly the gas, as it wells up from the surface of the Sun, can't rise uniformly because of the magnetic fields in some regions. If you want to tell me that the solar wind comes predominantly from the northern hemisphere, I shall be very

happy.

WILCOX: As far as the polarity being right is concerned, the peaks came during the tenth day of the solar cycle and seemed to be related to a recurring active region that was shown to last over many cycles; and there was, on the Sun, a large unipolar region in the northern hemisphere (as you mentioned) whose CMP approximately coincided with these peaks. But here there is a disagreement of signs, because the unipolar region in the northern hemisphere is formed from the trailing half of the dipole region, which is negative—whereas you were finding positive field. The field could have been positive if the plasma velocity were caused by this unipolar region, but only if the magnetic field that was picked up by the solar wind came from some other region.

DAVIS: I am somewhat uncomfortable about this remark, but since the subject has been brought up, I think perhaps we should discuss it. I have talked with Dr. Howard, who has magnetograms from the Sun that should be very useful in discussing this point. The data are not so easy to interpret, however, because

he was in the Crimea at the time and the magnetograms didn't have his sympathetic attention while they were being taken.

Of course, we recognized this trouble with the sign. The prominent, negative, unipolar region on the Sun was, at this time, at approximately the correct location to explain the regions we saw, although it was off by about half a week.

Dr. Howard says that just before this period, earlier in the year, there was a large positive unipolar region on the Sun. Unfortunately, he didn't remember exactly where it was located. This large positive region had disappeared by September, but it had disappeared presumably by expanding and becoming weaker; so although the flux was not easily detectable, it hadn't necessarily vanished. Therefore this region may be the source of our positive flux.

GOLD: I don't really understand why there must be a straightforward correlation between the direction of the field observed in space and the sign of the unipolar region, or any kind of sunspot sign; because if the streaming occurs as the result of a rather small region on the Sun filling a large region of space (and I think that in many cases this is very likely), then of course it will bulge the lines of force that it takes with it and produce radial components that have both signs. It is just luck that determines which of these components the spacecraft happens to observe at any one time. I can't see that a unipolar region would fill all of space: any fast plasma that came out of the region would have to carry the lines of force from either side of it, so the lines of force would go out and come back again.

Therefore, it seems to me that you must not interpret as conflicting data the fact that the sign happens to be wrong. If you had been in the ecliptic, or a little above it, or a little below it, or in another place, you would have seen the other sign. I think that is all there is to it.

CHAPTER IV

THE RELATIONSHIP BETWEEN HIGH-ENERGY PARTICLES IN SPACE AND THE SOLAR PLASMA

HUGH R. ANDERSON

Jet Propulsion Laboratory, Pasadena, California

Introduction

Mariner 2 carried an ionization chamber and two Geiger-Müller counters. These instruments measured the total ionization in a volume of argon gas and the average omnidirectional flux of all the radiation able to penetrate 0.2 gm of shielding. This amount of shielding corresponds to a threshold of 10 Mev for protons or about 0.5 Mev for electrons, which have a somewhat less sharp cutoff. More extended accounts of the measurements made with these instruments are given in Ref. 1 and 2. Energetic particle measurements were also made on Mariner 2 by Van Allen and Frank (Ref. 3 and 4) whose instrument was a thin-window GM counter sensitive to electrons above 40 kev and protons above 0.5 Mev.

It is well known that the kinetic-energy density of galactic cosmic radiation is of the order of 1 ev/cm³, which is very small compared with the kinetic-energy density of the solar wind. It is also small compared with the energy density of the interplanetary magnetic field (except during certain increases of the radiation in interplanetary space resulting from the injection of particles by the Sun). Although these large differences in energy density do not always hold true, they prevailed throughout the time that we were making measurements with *Mariner*. We are therefore more or less justified in assuming that the motion of the energetic particles was wholly determined by the existing magnetic field, and that the presence of the energetic particles did not appreciably affect the field.

The effect of the magnetic field on the radiation measured by the *Mariner* instruments can be separated into two categories: (1) the modulation of galactic cosmic radiation, which we suppose amounts to the magnetic field allowing greater or lesser quantities of the radiation to reach a given position in the solar system, and (2) the determination by the field of the propagation and storage of charged particles injected into

the interplanetary medium by the Sun. I am going to discuss the *Mariner* data insofar as it illustrates these two types of modulation.

Modulation of Galactic Cosmic Radiation

During the 120 days of its operation, the *Mariner* spacecraft approached the Sun from 1 AU to approximately 0.72 AU, and in so doing it attained a maximum distance of about 81,000,000 km from the Earth. By comparing the radiation measured at the location of the spacecraft with that measured in space near the Earth at the same time, we can determine the so-called solar gradient, meaning any systematic change in the amount of radiation as the spacecraft approached the Sun. We can also observe the correlation of short-time variations in the radiation level (over periods of a few days) and see if the degree of correlation depends upon the separation of the two points of observation.

Ideally, we would like to have made the near-Earth measurements from an observation station outside the magnetosphere but near the Earth, using instruments with the same sensitivity to radiation as those on *Mariner*. Since this was not possible at the time, we have used two types of measurements made from Earth: (1) the pressure-corrected Deep River neutron monitor counting rate which, because it is very high, has a correspondingly high degree of statistical accuracy, and (2) the ionization-rate measurements made by Prof. Neher at Thule, at an atmospheric depth of 10 gm/cm² and at a magnetic latitude of 90 deg. These Thule balloon measurements were made only once a year; the ones made in July and August of 1962 and 1963 are the two sets I am going to mention here.

The idea is to determine the relationship between variations in the neutron counting rate and variations in the ionization rate in interplanetary space. This is done by comparing the neutron counting rate with the ionization rate measured by *Mariner* early in the mission, when it was close to the Earth, and then by comparing the neutron counting rate with the measurements made at Thule. Then we can use subsequent Deep River data to compute the ionization rate expected in interplanetary space near the Earth for comparison with the *Mariner* data taken during the latter part of the mission, when the spacecraft was far from the Earth. (I emphasize the ionization rate over the omnidirectional flux, because the ion chamber on *Mariner* was more stable and accurate than the GM tubes.)

Figure 1 (top) shows the hourly counting rate at Deep River, averaged over each day and plotted against time. The rate is scaled by a factor of 100. The standard solar rotation numbers and the interval during which measurements were made at Thule are indicated on the abscissa. Time is measured from January 1, 1962, which is taken as Day 1. Figure 1 (upper center) shows the daily averages of the ionization rate in the

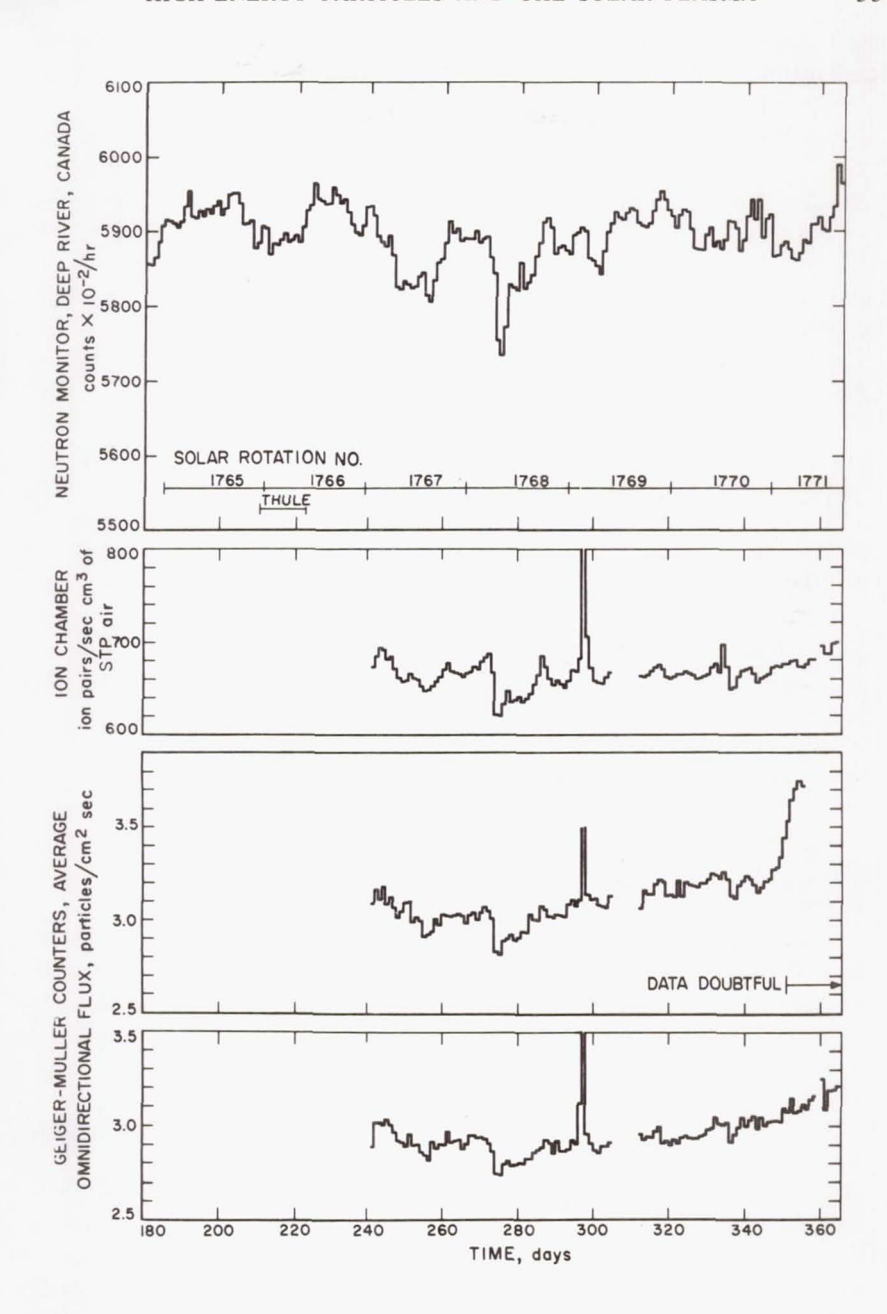


Fig. 1. Cosmic-ray activity during the *Mariner-2* flight, daily averages. Top: the Deep River neutron monitor; upper center: the ion chamber on *Mariner 2*; lower center and bottom: Geiger-Müller counters on *Mariner 2*

Mariner-2 instrument, referred to a standard atmosphere of air; below are shown the counting rates of the two GM tubes, divided by their omnidirectional geometric factor.

Except for the increase after Day 350 and the increase on Day 296, the average ionization rate appears to be quite constant. The fluxes increased gradually. I am of the opinion that the increase of the flux measured by the Be-shielded tube after Day 350 is an instrumental effect resulting from the increasing temperature associated with our approach to the Sun. The large increase on October 23, Day 296, will be discussed in the next section.

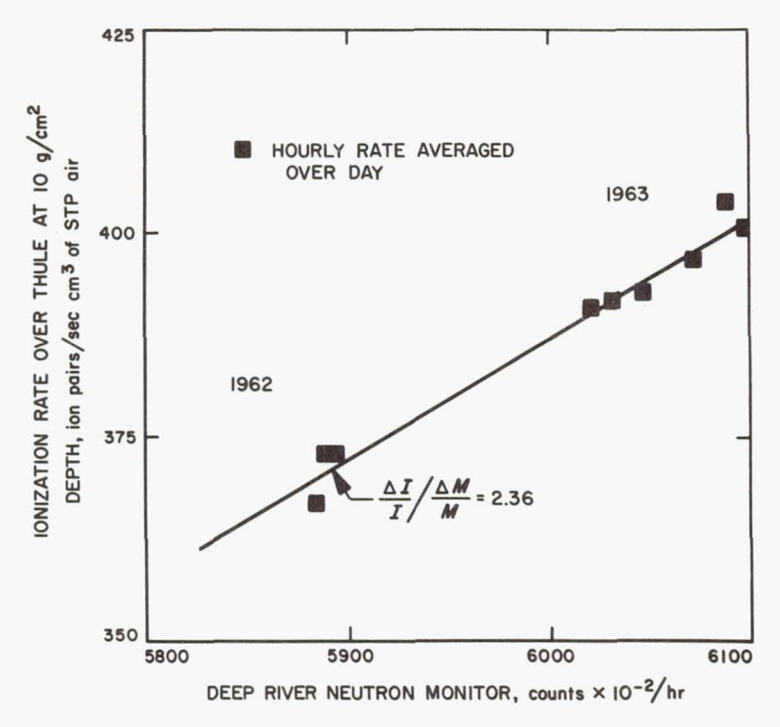


Fig. 2. Comparison of simultaneous recordings of the balloon-borne ion chamber at Thule, and the Deep River neutron monitor

A superficial look at the *Mariner* ionization rate indicates that it is reasonably well correlated with the neutron counting rate. I would like to show this result a little more quantitatively. Let us consider the relationship between the neutron counting rate and the measurements made at Thule; both are shown in Fig. 2. The Thule data are taken from a paper by Neher and Anderson (Ref. 2). The ratio of variations in the two rates is about 2.36 for this particular measurement time, which is somewhat less

than that found by Nerurkar and Webber (Ref. 5). I think the difference is probably due to the fact that we were looking at a different part of the solar cycle.

In Fig. 3, we show the rate measured by *Mariner* plotted against the neutron counting rate. The slope of the curve from the previous figure, normalized to the point indicated, is also shown. The least-squares fit

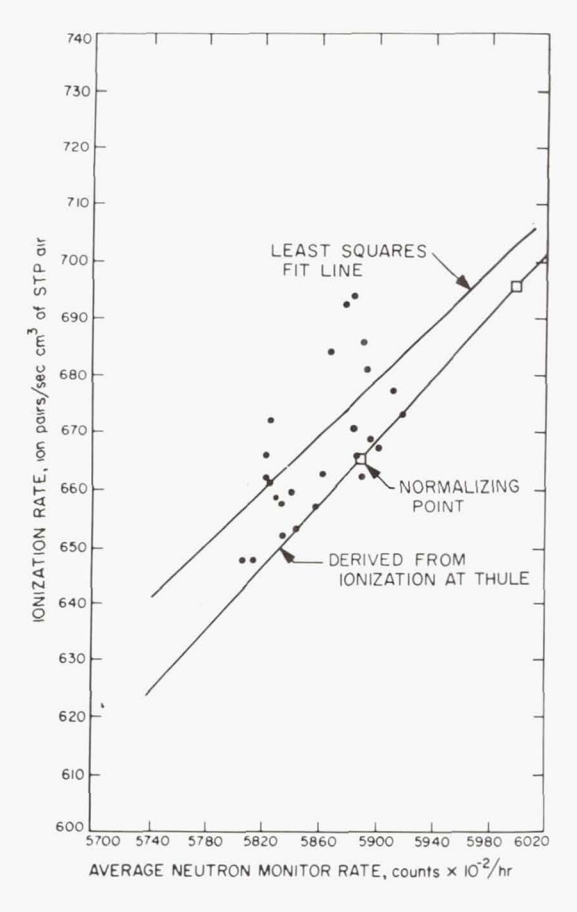


Fig. 3. Daily averages of the *Mariner-2* ionization rate vs. the Deep River neutron monitor rate: solar rotation No. 1767; Days 239 to 265; distance from Earth, 0 to 6.9×10^6 km

line has about the same slope as the line for the Thule measurements; indeed, the slope of the least-squares line is just a little more than 2, as opposed to about 2.4 for the Thule data. One tentative conclusion drawn from this figure is that the relationship between the Thule measurements

and the *Mariner* measurements is indeed a linear one, which is not too surprising.

Figure 4 is a similar plot for the subsequent solar rotation. Here the line is somewhat steeper. One reason the correlation looks so good in this

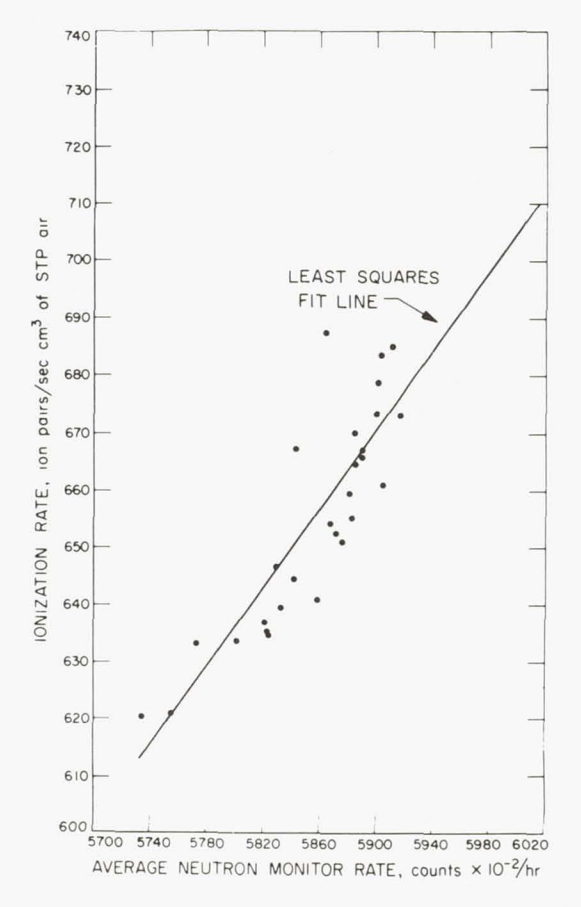


Fig. 4. Daily averages of the *Mariner-2* ionization rate vs. the Deep River neutron monitor rate: solar rotation No. 1768; Days 266 to 292; distance from Earth, 6.9 to 14.4×10^6 km

figure is that there was a Forbush decrease during this period, which gave a greater spread of intensities to work with.

Figures 5 and 6 show the third and fourth solar rotations during the *Mariner* flight. In these two periods, the slope decreased and the correlation deteriorated. 'The neutron counting rate increased 1% while, on the

average, the ionization rate remained fixed. In Fig. 6, the correlation is so bad that I don't think the slope is very meaningful. In the last rotation, shown in Fig. 7, the slope returned to approximately its value at the beginning, while the ionization rate rose about 2%.

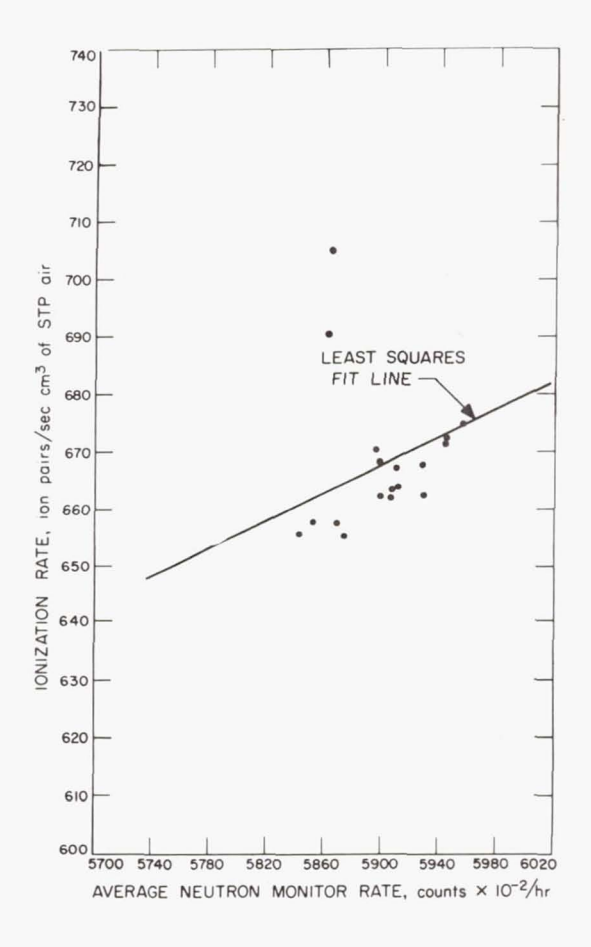


Fig. 5. Daily averages of the *Mariner-2* ionization rate vs. the Deep River neutron monitor rate: solar rotation No. 1769; Days 293 to 319; distance from Earth, 14.4 to 28.3×10^6 km

I had hoped to demonstrate, when I started out, that, as the spacecraft became more and more separated from the Earth, the degree of correlation between the measurements would decrease. The results we actually obtained are summarized in Table 1.

TABLE 1. Comparison of ionization rate in space with Deep River neutron counting rate

Solar rotation No.	Distance from Earth (10 ⁶ km)	Distance from Sun (AU)	Average neutron counting rate (counts × 10 ⁻² /hr)	Average ionization rate on <i>Mariner</i> (cm ⁻³ sec ⁻¹ atm ⁻¹)	ρ
1767	0.0- 6.9	1.0 -0.975	5861.7	666.9	0.639
1768	6.9-14.4	0.975-0.91	5857.5	655.4	0.849
1769	14.4-28.3	0.91 -0.81	5901.7	665.0	0.668
1770	28.3-55.4	0.81 - 0.73	5905.6	664.2	-0.022
1771	55.4-81.4	0.73 -0.71	5895.7	680.7	0.802

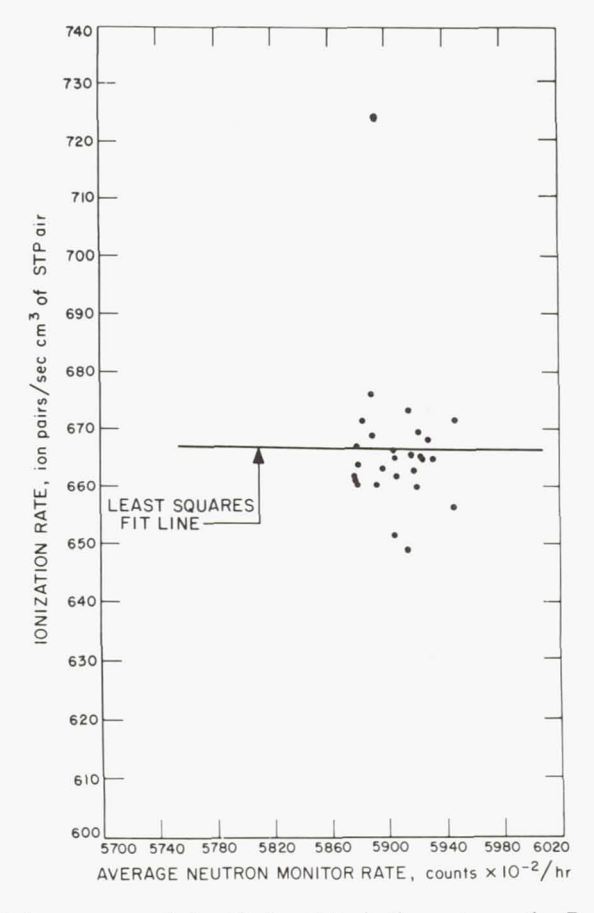


Fig. 6. Daily averages of the *Mariner-2* ionization rate vs. the Deep River neutron monitor rate: solar rotation No. 1770; Days 320 to 346; distance from Earth, 28.3 to 55.4×10^6 km

 ρ is the usual correlation coefficient given by

$$\rho = \frac{\sum\limits_{k=1}^{K} (\delta I_k \, \delta M_k)}{(K-1)\sigma_I \sigma_M}$$

where I = ionization rate and M = neutron counting rate. If there is no correlation, $\rho = 0$, and if there is perfect correlation, $\rho = \pm 1$.

It can be seen from Table 1 that ρ does more or less decrease through the first four rotations. Note, in particular, that the average ionization rate in space around *Mariner* appeared to be almost constant even though *Mariner* was approaching the Sun, while the average neutron counting

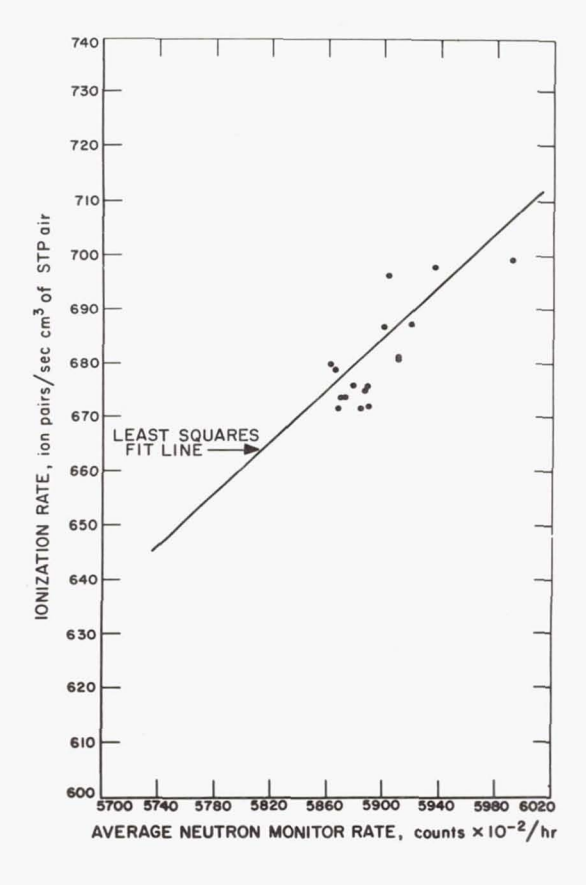


Fig. 7. Daily averages of the *Mariner-2* ionization rate vs. the Deep River neutron monitor rate: solar rotation No. 1771; Days 347 to 364; distance from Earth, 55.4 to 80.2×10^6 km

rate increased 0.75%. Hence, according to our assumptions, the ionization rate in space near Earth increased 1.7%. The difference in ionization rate between the two regions was 14.2 ion pairs/sec cm³ of STP air, corresponding to an apparent gradient of +9.3% per AU. This result was discussed by Prof. Neher at the Jaipur conference last Fall (Ref. 6).

What apparently happened during solar rotation No. 1771 was that the region of space around the spacecraft and the region around the Earth became magnetically connected again in some sense, so that the correlation increased. During this solar rotation, the radiation level rose, so that the apparent gradient was -2.6% per AU.

These results mean that, over this range of distances, the dependence of average flux on distance from the Sun and also the dependence of the degree of correlation on the separation of observation points are as much a function of time as they are of position in space. Presumably this isn't true if you go to a great enough separation, and it might not be true during other epochs of the solar activity cycle. I do think we have demonstrated that there can be a systematic dependence on distance from the Sun over about 0.3 AU during this part of the solar cycle.

Modulation of Energetic Particles from the Sun

I would like now to give an illustration of the second type of modulation which was observed by *Mariner*. Large increases in the ionization and counting rates were observed by the *Mariner* instruments on October 23 (Day 296, Fig. 1). The overall history of this event was rather characteristic of solar events. Figure 8 shows the excess flux (background subtracted), the excess ionization rate, and the inverse ratio of these two quantities, which is the average specific ionization of the particles observed during this event.

The initial increase occurred sometime between 18 and 30 min after a Class-2 flare on the western part of the Sun, which we will tentatively say was responsible for this increase. The rise time was about 142 min. The 1/e times of the decay, which changed from time to time, are also shown.

A particularly interesting feature of this flare event was the presence of a number of large oscillations shown in Fig. 9, which is a portion of the rising phase of this event. There were about 12 of these oscillations with an average period of approximately 18 min, so that the whole oscillation interval lasted a little over 220 min. The period covered in Fig. 9 shows the maximum amplitude, a factor of 2. The oscillations then gradually died out.

I think there are at least three possible ways that this type of variation could have been generated. The first possibility is that there were repeated impulsive injections at the Sun, so that we were seeing the resultant blasts as they went by our detector. The validity of this explanation is strengthened by the fact that the apparent propagation time from the flare was not much longer than the time required for a direct straight-line

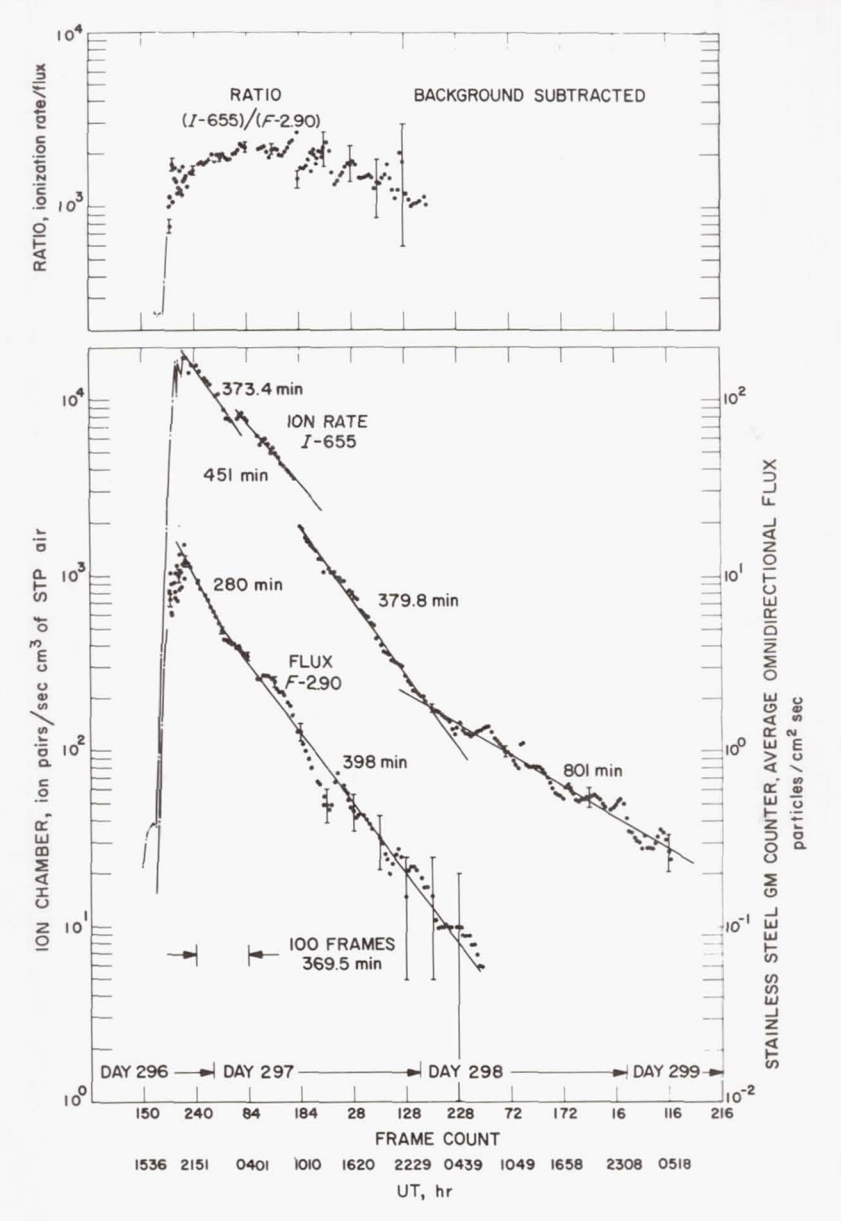
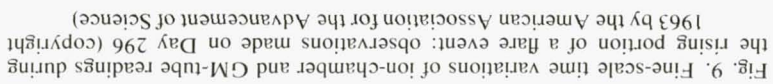
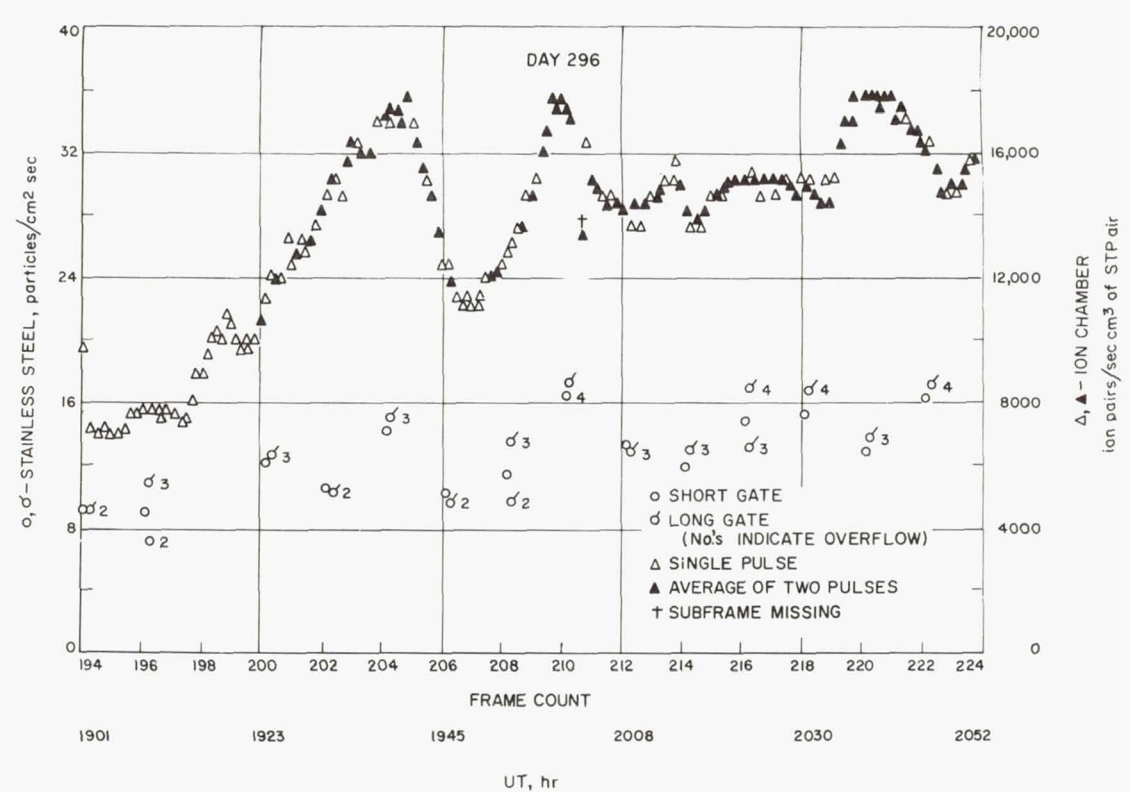


Fig. 8. Flare-associated activity observed on *Mariner* 2; Days 296 to 299, October 23–26, 1962

ANDERSON

HUGH R.





trajectory. However, in order to preserve the bunching of the impulsively injected particles, there is a maximum allowed spread in the energy or velocity of the particles and in the path lengths followed by the particles in reaching the spacecraft. The specific ionization we observed at the peak is consistent with the detection of protons of about 12 Mey, which have a velocity approximately 0.1 times the speed of light. Using this velocity, and the fact that Mariner was 0.9 AU from the Sun when the particles were observed, I calculate that, in order to keep the bunches from being completely washed out in the propagation from the Sun, the energy range of the particles at injection would have had to lie between 0.25 and 2.25 times the central energy. Taking into account the instrumental cutoff, we can say that the energies of the detected particles would have had to lie between 12.5 and 27 Mev to preserve any bunching originating at the Sun. Conversely, if the particles all had the same energy of 12.5 Mey, their distance of travel between the injection point and the spacecraft could vary by less than 0.18 AU out of a total distance of about 0.9 AU.

The second possibility is that we were seeing a single bunch of particles which oscillated in a kind of trap, and that we repeatedly saw the same particles as they went by. If the length of the trapping region were 0.34 AU or less, then in order to preserve bunching for 8 cycles after the maximum, the energy spread could not be more than ± 1.5 Mev about 12.5 Mev. It should be noted that the ion-chamber sensitivity peaks in the energy range between 12 and 20 Mev, so that a steep energy spectrum could produce a response similar to a nearly monoenergetic flux.

Both of these explanations implicitly assume that the magnetic-field configuration was static. A third possibility, of course, is that the field was not static, and the bunching was somehow the result of a wave-like phenomenon in the magnetic field. In view of the rather stringent requirements of the first two possibilities, I should like to inquire about the likelihood of such a dynamic bunching.

A similar type of oscillation, but with a longer period, can be seen in Fig. 8 during the decay phase of the event. The rate of ionization appears to be pumped up every 180 to 360 min and then to decay with a 380-min time constant. At least five such pumping actions can be seen in the data.

While the details of the physical processes are not clear, I believe we have shown that the magnetic field imbedded in the solar wind probably does modulate the galactic cosmic radiation inside the orbit of the Earth, and that it has an important effect on the propagation of particles from the Sun. I would like to thank Prof. Neher for the use of his facilities and time in making and calibrating this joint JPL-Caltech experiment. I am also indebted to Prof. Van Allen and Louis Frank for the use of their electron calibration facilities at the State University of Iowa.

REFERENCES

- 1. ANDERSON, H. R., Science 139, 42 (1963).
- 2. Neher, H. V. and H. R. Anderson, Journal of Geophysical Research 69, 807 (1964).
- 3. VAN ALLEN, J. A. and L. A. FRANK, Science 138, 1097 (1962).
- 4. Frank, L. A., J. A. Van Allen, and H. K. Hills, Science 139, 905 (1963).
- 5. Nerurkar, N. and W. R. Webber, Journal of Geophysical Research 69, 815 (1964).
- 6. Neher, H. V. and H. R. Anderson, Journal of Geophysical Research 69, 1911 (1964).

DISCUSSION OF ANDERSON PAPER

PARKER: There are two correlations that one might reasonably expect from a very simple model. First, when the spacecraft and the Earth are on the same radius from the Sun, then fields and plasma and so forth coming from the Sun must pass first the spacecraft and then the Earth. You might consequently expect a correlation between the *galactic* cosmic rays detected at the spacecraft and those detected near the Earth. Secondly, since the spacecraft moves more rapidly around the Sun than does the Earth, there comes a time when you might expect a correlation between *solar* particles detected at the spacecraft and those detected near the Earth. The latter case corresponds to both bodies lying on the same spiral flux tube.

Could you comment on how these ideas fit into your correlations, if at all?

ANDERSON: I think that, from the analysis I have presented here, you cannot distinguish an increase in the allowed number of galactic cosmic rays from an increase in particles from a small solar injection. If an increase occurred at both the spacecraft and the Earth during the time interval over which I averaged the data, which was a day, you would see a correlation for both of your cases.

By looking at the detailed time history of an event, you might be able to see, in some cases, a shorter rise time at the spacecraft than at the Earth, or some other distinguishing feature. However, since we don't get a very sensitive measure of the spectrum, I think it is going to be difficult to get definite results.

PARKER: Can you tell us when the vehicle crossed the spiral?

ANDERSON: I'm sorry, I haven't calculated that. It crossed in front of the Earth right at the beginning of solar rotation No. 1769.

SNYDER: I would guess it crossed the spiral many times, because the spiral changes.

NEUGEBAUER: In a recent publication¹ we plotted a function τ , the expected time delay between the spacecraft and the Earth. When $\tau = 0$, *Mariner* and the Earth would be on the same spiral. [τ passed through zero on Days 334, 335, and 345, and was very near zero throughout Days 338, 339, and 340.]²

BIERMANN: Were there any fluctuations in the magnetic field coinciding with those in the energetic radiation?

SMITH: Yes. The period was one in which the magnetic fields were extremely disturbed. This condition had existed for at least a day preceding this Class-2 flare, which also had Type-IV radio emission associated with it. It seems quite clear that these particles were coming through quite disturbed interplanetary fields and plasmas. However, we were unable to convince ourselves that there

¹Snyder, C. W., M. Neugebauer, and U. R. Rao, *Journal of Geophysical Research* 68, 6361 (1963)

²Added in manuscript

were any direct correlations between the particle flux and changes in the magnetic field.

We have attempted to do some power-spectral analyses of interplanetary field variations, but we don't have any results yet. For this particular time period, we performed a relatively crude analysis, searching for characteristic periods by measuring the time intervals between successive maxima. A histogram showing the preliminary results of this analysis indicated that the most common period in the magnetic field was about 2 to 3 minutes, which is different from the 18 minutes obtained by Dr. Anderson. We next looked at these fluctuations in terms of some kind of characteristic roughness scale, which corresponds to about 10⁵ km for a 3-minute fluctuation period.

BIERMANN: A period of 2 or 3 minutes is interesting, because the fluctuations may be directly related to turbulence and oscillations on the solar surface, which

have characteristic periods in this range.

BRIDGE: Wouldn't you expect the transmission of a shock across the vehicle to take a minute or so? This is the time observed for a shock at the Earth. It seems to me that the time scales for the arrival of particles at the spacecraft should be of the order of minutes, and it is therefore not clear that things go wild. We don't have enough time resolution on the spacecraft to see what is going on in detail.

SMITH: We don't see anything in the magnetic-field data which looks like a shock or a transition from a relatively quiet condition to a disturbed condition. The fields were large and very irregular throughout a whole day or so.

VOGT: My question concerns the cosmic-ray intensity gradient in the solar system. One would expect that, at the time of your observations, the time variations due to solar modulation would be most pronounced in the low-rigidity region. Your ion chamber is most sensitive to these low-energy particles, whereas neutron monitors are essentially insensitive to protons below about 1 Bev. Considering the fact that you used neutron monitor data to correct for time variations, and in view of a possibly inadequate procedure in correcting for time variations, how large an uncertainty do you assign to your result?

ANDERSON: It would depend on the energy spectrum that you assumed. I have not made a numerical estimate. Obviously what you say is true, but I doubt if one can really resolve the problem without another identical detector at the Earth. **CLINE:** With regard to the normalization of the low-energy particles detected on *Mariner*, I would suggest comparing the *Mariner* data with those of *Explorer 14*, which was up at the same time. *Explorer* carried a differential energy analyzer with the same energy coverage, and we could compare *Mariner* in deep space with

Explorer near the Earth. The data might then make more sense.

Page intentionally left blank

CHAPTER V

SATELLITE OBSERVATIONS OF MEV PHENOMENA RELATED TO THE SOLAR WIND

EXPLORER-12 OBSERVATIONS

D. A. BRYANT, T. L. CLINE, U. D. DESAI, and F. B. McDonald

Goddard Space Flight Center, NASA, Greenbelt, Maryland

(Presented by T. L. Cline)

THE topics I wish to discuss are relevant to a conference on the solar wind in that they concern observations of particles in the Mev range—particles that provide new information about the interplanetary medium. In this paper I shall present some new results and shall briefly review other *Explorer-12* results that have recently been published (Ref. 1 and 2).

Periodic Solar-Proton Fluctuations

Periodic modulations of solar-proton intensity were discussed by Dr. Anderson (Paper 4), in connection with observations made by *Mariner* far away from the Earth. *Explorer 12*, which had an apogee of 83,000 km, spent a lot of time outside the magnetosphere but inside the shock front. I must therefore qualify my remarks, because our detectors were not completely away from the Earth's influence.

Figure 1 shows a solar-proton event seen by Explorer 12 on September 10, 1961. The differential intensities of two components are plotted in the upper half of the figure on a linear scale. These plots show a modulation consisting of approximately periodic oscillations. If we replot these fluctuations by deriving the percentage deviations from the running means, we have the curves shown in the lower half of the figure. These differential energy components, from 5 Mev to about 100 Mev, cover a wide range of velocities. You will notice that there are uniformly-spaced minima that are in phase through all of the plots.

These fluctuations appear to be greater than statistical fluctuations. They are simultaneous over too wide a range of proton velocities to have been caused by direct solar influence: if they had originated at the Sun, the transit-time distribution would have destroyed the coherency. Therefore, either they are of local interplanetary origin, or they originate

specifically in the region between the magnetopause and the shock front. Such 1.5-hr variations have been seen near the Earth before (in balloon observations by Winckler, for example), but the range of proton velocities over which they were previously measured was not wide enough to show this lack of dispersion.

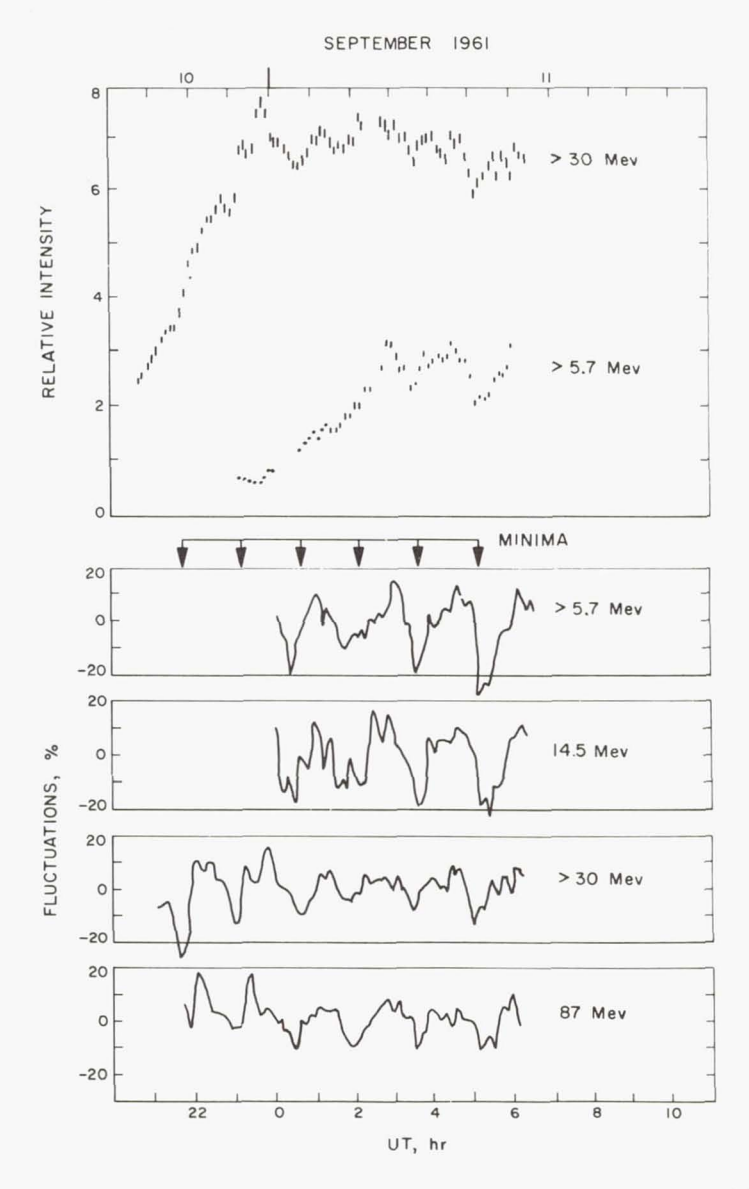


Fig. 1. Explorer-12 observation of the solar-proton event of September 10, 1961

We made measurements of three or four solar-proton events in 1961 and 1962. We find that the variations occur in all of the events; that they have periods ranging from 1.0 to 1.5 hr, depending on the event; and that they show up better during the rise period of the event than during the decay period. I would like to point out that the 1.5-hr period in Fig. 1 is different from the time periods quoted by Dr. Anderson in connection with the *Mariner* observations. This difference may be due to the fact that his detector was in deep space while ours was near the Earth. The fact that these intensity fluctuations are roughly periodic must be significant, although we do not yet have any theoretical explanation for the effect.

CLINE: No: the measurements were made between 60,000 and 80,000 km,

outside the magnetosphere but inside the shock front.

BRIDGE: At what local times were they observed? Was the measurement region close to the subsolar region?

CLINE: The satellite was on the sunward side of the Earth, toward noon.

Recurrent Particle Events

The second topic I should like to discuss is the 27-day variation in the intensity of very low-energy protons, as observed by *Explorer 12*. This effect was mentioned previously today, but I think it is worthwhile to elaborate on it, since it is relevant to another topic that I shall discuss later.

On September 28, 1961, there was a primary, velocity-ordered, solar-proton event. Figure 2 shows the integral intensity of protons with energies greater than 3 Mev. Two days later, during the decay of the primary proton event, the intensity increased to a new peak that was an order of magnitude above the previous one. We can trace the intensity decay of the primary event for about a week, before it gets into the noise. Then we see another increase on October 27, 27 days after the 2-day delayed increase. At the time of this new event, the solar region that caused the September-30 event was again near the central meridian. The recurrent event was about two orders of magnitude less intense than the event of September 30. Because the second delayed increase occurred at the time of a recurrent cosmic-ray decrease and between the two recurrent geomagnetic storms of October 26 and October 28, we considered it to be an M-region effect.

This recurrence pattern was also exhibited after the solar-proton event of November 10, 1961, which originated from a flare on the west limb. A delayed increase took place on December 1, 1961, and was very similar in character to the delayed increase of October 27. The fact that it occurred 3 weeks after the primary event, rather than 4 weeks, was due, we believe, to the fact that the Sun had to rotate only $\frac{3}{4}$ of a turn to bring the parent plage region to the central meridian.

There is, therefore, evidence for the existence of long-lived solar streams, plasma-magnetic-field configurations capable of either accelerating the protons locally, or of storing the protons from the original event for long periods of time-even for months. The other possibilities are

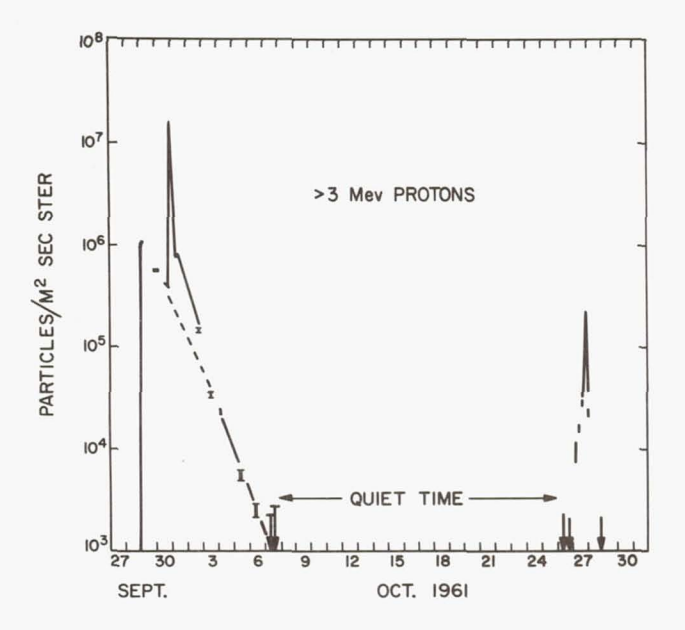


Fig. 2. Explorer-12 observation of the solar-proton events of September 28, September 30, and October 27, 1961

either continuous proton emission from the same plage region on the Sun, or a new emission of protons which are then guided from the solar atmosphere by this streamer configuration. I should call your attention to the fact that the energy spectra of the September-30 and October-27 events were very dissimilar. The differential energy spectrum of the 2-day delayed event was about E^{-3} to E^{-4} , whereas that of the later event was steeper than E^{-5} . Now, primary, velocity-ordered, solar-proton events show a transit-time dispersion; the low-energy protons arrive later than the high-energy protons, and thus the observed energy distribution of these events becomes steeper with the passage of time. Since the spectrum of the 27-day delayed event was steeper than the spectrum of the preceding one, one suspects that fresh emission from the Sun did not continue over a period of months, and that the observed protons were in fact "old" ones which had been trapped. In this case, it would be

necessary either that the trapping mechanism be more efficient at low energies or that the loss rate be an increasing function of energy.

The interesting facts are that this streamer can persist for months, and that it can continue to be narrowly confined. We are unable to tell whether there is another peak 27 days after October 27; at least, no such peak is obvious above our noise level. The intensity increase on October 27 is quite sharp, even after this long time delay; the width at half-maximum is only a day or so. Of course, the width increases as the sensitivity threshold decreases, and if our thresholds had been considerably lower, we might have observed another recurrence a month later.

IMP OBSERVATIONS OF PRIMARY 3-MEV ELECTRONS

T. L. CLINE, G. H. LUDWIG, and F. B. McDonald Goddard Space Flight Center, NASA, Greenbelt, Maryland

(Presented by T. L. Cline)

I SHOULD like now to present some new results from the *IMP* satellite, and to discuss the implications of these results in connection with the solar wind. I contend that we have detected, in interplanetary space, electrons of extraterrestrial origin, with energies of about 3 Mev.

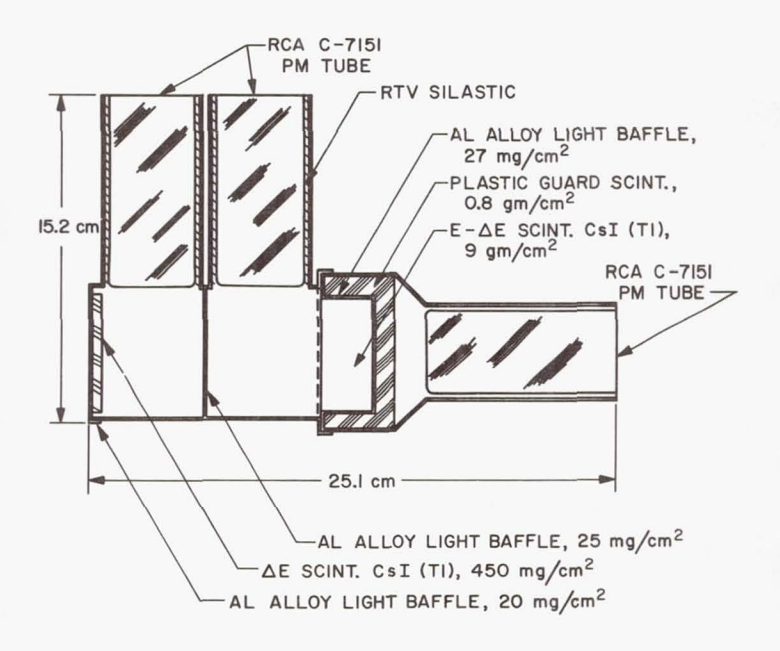


Fig. 3. dE/dx vs. E detector carried by IMP

Figure 3 shows a detector carried by IMP. It measures both the energy loss and the residual energy of a particle, which are indicated by a coincidence between the thin scintillator (ΔE) and the thicker one ($E-\Delta E$).

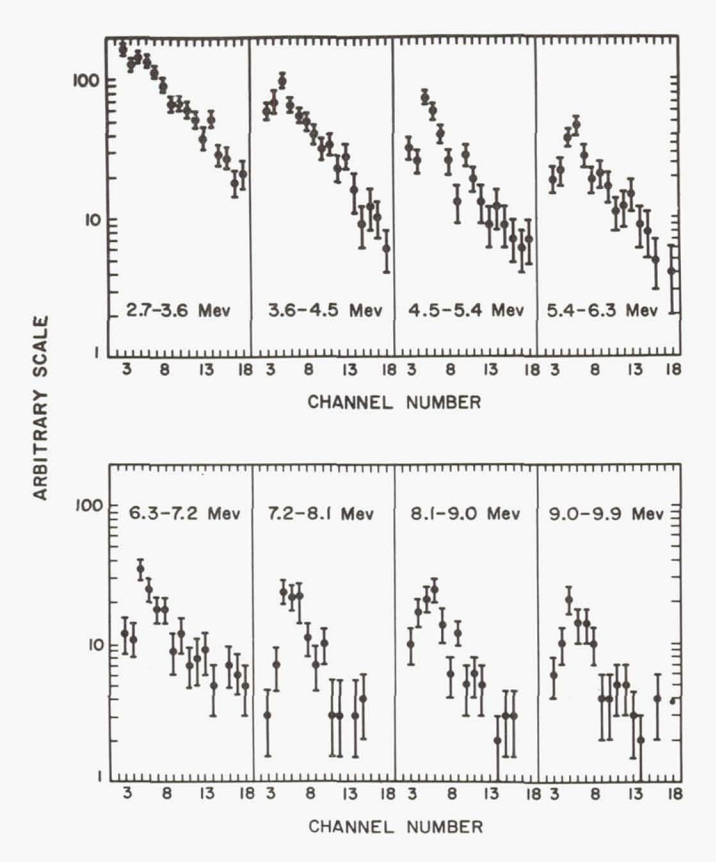


Fig. 4. ΔE distribution for November 27 to December 16, 1963; plotted for different energy ranges

Anticoincidence with a plastic scintillator at the back requires that incoming particles be fully stopped in the second crystal. When an event satisfies the coincidence-anticoincidence requirements, then both the ΔE and $E-\Delta E$ signals are fed to 256-channel pulse-height analyzers. Due to the low bit rate of the telemetry system, pulse-height analysis is possible only once per minute—the count rate is monitored independently. This instrument has good resolution, but it has one limitation. It is sensitive to some secondary emissions from the spacecraft: a neutral particle coming through the back can create a particle in the $E-\Delta E$ scintillator, and the

particle may then pass through the ΔE scintillator. We shall demonstrate that the effects of secondary emission have been eliminated in the data interpretation.

The data are studied by plotting a matrix of the number of events vs. ΔE pulse height vs. $E-\Delta E$ pulse height. If one takes constant-energy slices along the $E-\Delta E$ columns in the matrix of intensities, one sees (Fig. 4) a minimum-ionizing intensity peak that is prominent in each $E-\Delta E$ slice. This minimum-ionizing peak rides on a low-energy-loss background that is greatest at the lowest values of $E-\Delta E$. The background, we believe, is caused by the gamma rays that come from the spacecraft and that produce electrons in the cesium-iodide $(E-\Delta E)$ crystal.

We shall tentatively assume that the low-energy component of this minimum-ionizing contribution to the counting rate represents electrons. This component is plotted as a function of time for November, December, January, and February (Fig. 5, top curve). To demonstrate that these particles must be primary electrons, we investigate their time variations and compare these time variations with those of the primary protons. The graph AB shows telescoped galactic cosmic-ray protons, and the graph AB \hat{C} shows those particles, both low-energy protons and electrons, that stop in the counter.

The relevant fact shown by this figure is that there are three increases in the electron counting rate, with about a 28-day separation between them, and there are no such increases in the medium-energy or high-energy protons. We have normalized the top three counting rates, so that the same increase could be compared from one graph to another. For example, when there is an increase on the ABC graph from about 12 to 13 counts/readout, that entire contribution (1 count/readout) to the increase in intensity is accounted for by the electron increase from 3.5 to 4.5; the proton increase was essentially zero.

We cannot claim that these are primary electrons merely because their modulations are unlike those of medium-energy or high-energy protons. For example, if low-energy protons to which our instrument is not sensitive were incident on the spacecraft, they could produce gamma rays which in turn could produce electrons in the detector. However, if there were 27-day recurrent increases of such low-energy protons, they should occur at the same times as the recurrent cosmic-ray decreases (on December 4, for example). Fortunately, *IMP* carried a detector that indicated no increases in the low-energy (>1-Mev) protons on these days (Ref. 3). Such proton increases were observed, but they were displaced by about 2 weeks from the observed electron peaks, and they produced no discernible effect in our electron rates. These arguments seem to provide conclusive evidence that we detected primary electrons.

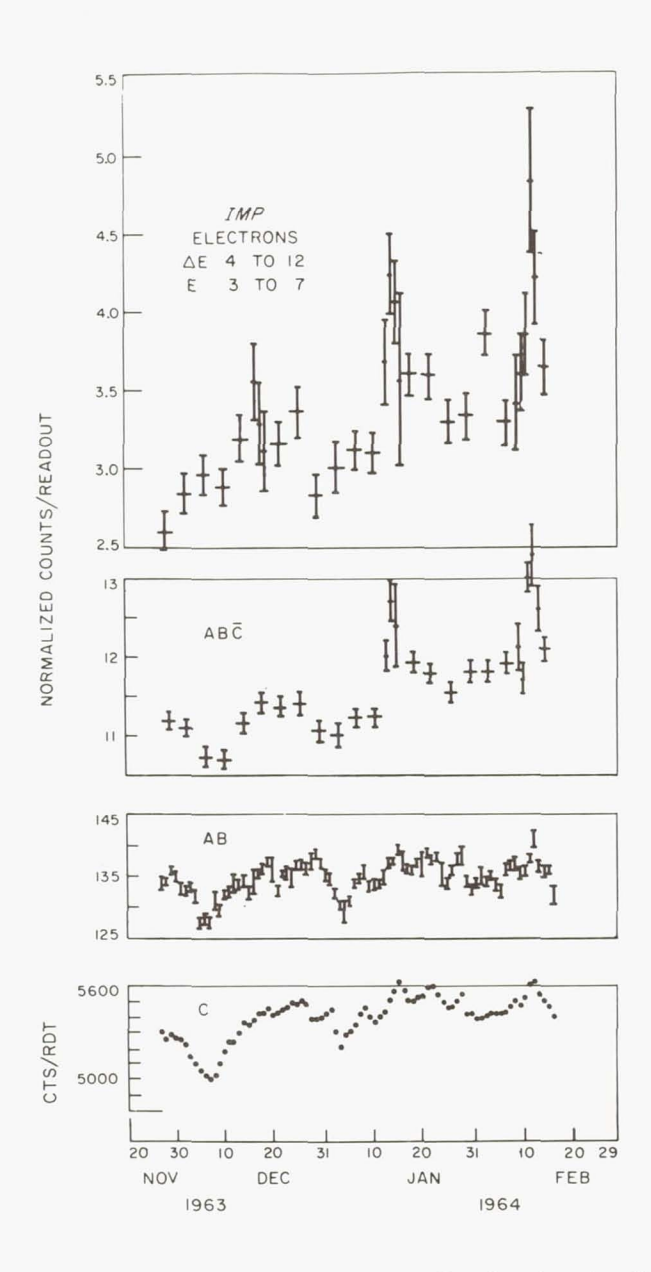


Fig. 5. IMP observations of various counter recordings from launch to February 15, 1964. Counter A records ΔE , counter B records $E - \Delta E$, and C is the guard counter. The top graph shows selected AB $\bar{\rm C}$ counts believed to correspond to primary electrons

Figure 6 shows the ΔE distribution for the January 14–15 increase. Here we see that even at the very low energies, there is a very distinct minimum-ionizing peak: that is, the quiet-time gamma-ray background is not seen. This indicates that the observed increase was not even partly

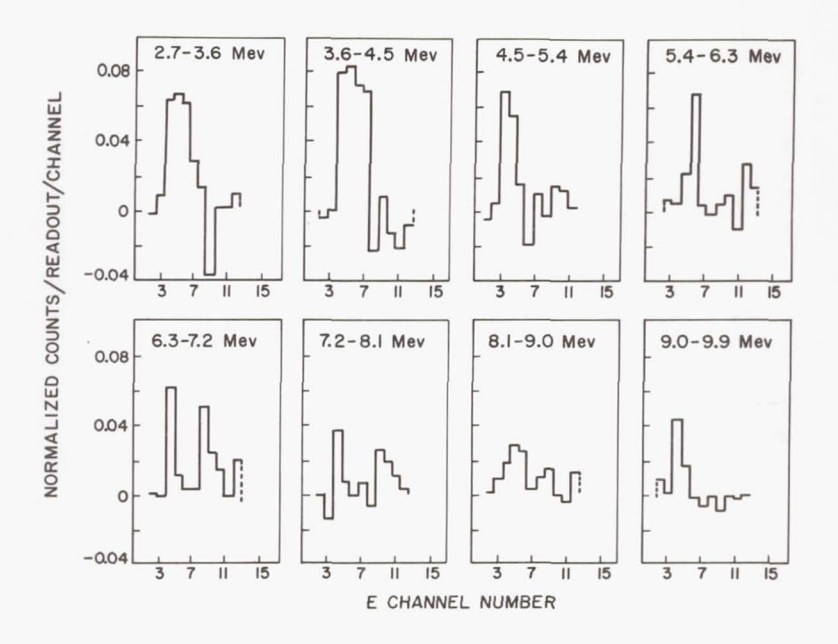


Fig. 6. ΔE distribution for the increase of January 14–15, 1964; plotted for different energy ranges

caused by gamma rays from the spacecraft. The top half of Fig. 7 shows a pulse-height distribution of the integrated minimum-ionizing counts/ readout for the January 14–15 intensity increase. The distribution has been converted (in a relatively uncorrected way) to an approximate intensity in electrons/cm² sec ster Mev. The quiet-time distribution is shown on the bottom half of the figure: there is a steep slope, followed by a departure that we can attribute to protons if we claim that there is a power-law distribution of electrons. The proton component has a pulse-height distribution which is peaked at about 13 Mev; the protons do not fire the guard counter—either because the counter is inefficient or because the protons turn into neutral particles when they interact in the detector. The protons that cause these counts are secondaries; if we disregard them, we are left with an electron excess.

The January 14–15 increase gives us a counting-rate distribution without any secondary effects: there are no protons at the high-energy end,

and there are no spacecraft gamma rays at the low-energy end. So we believe that the intensity increase is caused solely by primary electrons. The intensity is very low indeed.

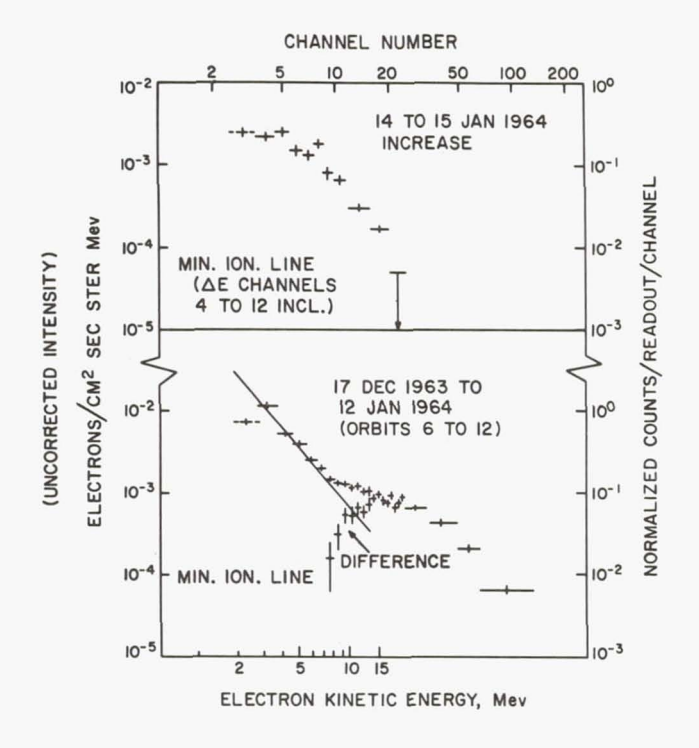


Fig. 7. Pulse-height distribution of electrons. Top: during the increase; bottom: during the quiet time

The three increases of electron counts are plotted in Fig. 8 for comparison with the Kp index. The three sections of the plot are at 27-day intervals. The three increases correlate roughly with very quiet solar times; in fact, they occur when the Kp index is near zero. However, the three quiet solar times indicated by the Kp index are 27 days apart, while the electron increases show some phase slippage because they are about 28 days apart. The first two increases occurred at quiet times, but the third increase seems to come after a quiet time—it occurs at the same time as a sudden commencement. One is tempted to believe that the electrons in these increases are galactic, because the intensity increases when the interplanetary region becomes quiet; but I admit we are not convinced. If they are galactic, then the solar modulation is such as to let particles of 3-Mv rigidity diffuse to 1 AU.

If these electrons are from the Sun, and we suspect that they really are, then they have an unexpectedly high intensity. Unlike solar protons, which are present only during certain events, the electrons are present

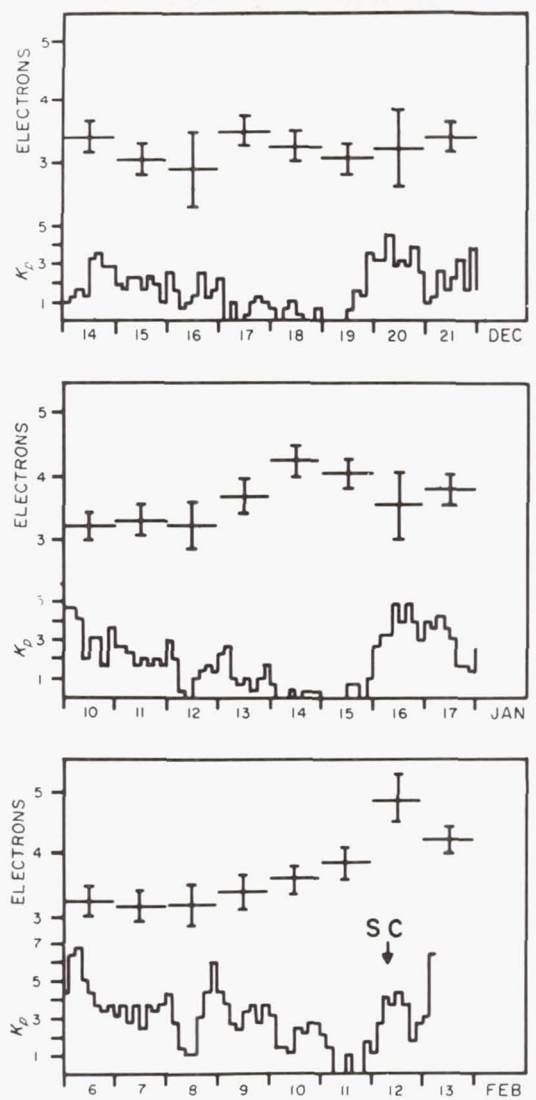


Fig. 8. Plots of electron counting rates during increases. The *Kp* index is plotted for comparison

every day—and this fact is significant. In any case, the electrons and protons exhibit qualitatively different modulation effects. Further study should be very promising.

REFERENCES

- 1. Bryant, D. A., T. L. CLINE, U. D. DESAI, and F. B. McDonald, Proceedings of the IUPAP International Conference on Cosmic Rays, Jaipur, India (to be published).
- BRYANT, D. A., T. L. CLINE, U. D. DESAI, and F. B. McDonald, Physical Review Letters 11, 144 (1963).
- 3. FAN, C. Y., G. GLOECKLER, and J. A. SIMPSON, *Explorer-18* Symposium, Goddard Space Flight Center (to be published).

DISCUSSION OF CLINE PAPER

VOGT: I have two questions. My first question concerns your interpretation of the partial anticorrelation of electron intensity and solar activity, which leads you to conclude that these electrons may be of galactic origin. Isn't it possible that originally a certain electron intensity (galactic or solar) existed in the solar system, and that this intensity was periodically depressed as a result of solar activity; while on the third passage of the active region the modulation was completely wiped out by the injection of solar electrons?

CLINE: Any increase by itself is not too significant statistically, but the fact that these three events occurred with a 28-day period lends credence to a relation between them.

VOGT: It may be the same active region, which modulates on the first two passages then produces only on the third.

CLINE: I think I can answer that only by saying that one should not invoke as many causes as there are effects.

VOGT: My second question concerns your discussion of the recurrent proton events. You suggested that the change in the spectrum of the recurrent events argues against continued production of solar particles. I think that this idea is quite tempting. However, we actually do not yet have a satisfactory understanding of solar-particle acceleration and injection. It seems possible to me that upon the return of an active region, some of its physical characteristics may have changed; consequently, particle emission of different spectral character would occur. This still could be continued production.

AXFORD: In the October event, are you associating the 27-day peak with the September-30 event or with the original flare? Also, at the time of the September-30 event there was a lot of fluctuation on the peak, and I think that at one time you interpreted this fluctuation differently. Are you changing your mind on that now?

CLINE: I was speaking today of the fluctuations of the primary solar-proton events such as that of September 28, not of the delayed events such as that of September 30. The intensity of the recurrent event of October 27 was too low to follow the details of the event statistically, whereas the intensity was high on September 30.

Returning to your first question, possibly two completely different phenomena are taking place. It is possible that the September-30 event is not phenomenologically identical to the October-27 event, but differs from it only in that the Sun has to rotate once more. The former is probably a delayed shock front coming from the September-28 solar-proton event. I would like to point out that the November-10 solar-proton event, which occurred on the west limb, was followed 3 weeks later by a recurrent event; but it was not followed in 2 days by a sudden plasma event.

BRIDGE: Isn't it perfectly reasonable to imagine that the September-28 event essentially produced particles by the diffusion process; that 2 days later, when the plasma arrived, you saw the particles trapped in that flare; and that 28 days later, you then saw the flare come around again?

CLINE: Yes.

BRIDGE: It is really stretching things to give it any other interpretation, isn't it?

CLINE: This is the simplest approach.

MEAD: What was the position of the Moon during the electron peaks?

CLINE: The Moon? I don't know.

SNYDER: There are too many things with 28-day periods—that's our problem.

Page intentionally left blank

CHAPTER VI

INTERPLANETARY MAGNETIC-FIELD MEASUREMENTS BY THE IMP-1 SATELLITE

N. F. NESS

Goddard Space Flight Center, NASA, Greenbelt, Maryland

I WANT to discuss today the results of the interplanetary magnetic-field measurements taken by the *IMP-1* satellite. This particular experiment involved the joint effort of myself, C. S. Scearce, and J. B. Seek of the Goddard Space Flight Center, NASA.

The IMP-1 Satellite

Figure 1 is an artist's conception of the Interplanetary Monitoring Platform and shows certain salient features that are directly related to the experiments carried out on board. The basic spacecraft structure is octagonal, 8 in. high, and $27\frac{1}{4}$ in. between the flat surfaces of the octagon. Four antennas, which transmit at 136 Mc, and four solar paddles are arranged symetrically around the octagon. The other appendages, one along the axis of the octagon (spacecraft spin axis) and the two long, diametrically opposed booms perpendicular to this axis, support magnetometer sensors. The 13-in, sphere on top contains the absorption cell of a rubidium-vapor self-oscillating-type magnetometer. The two bottom appendages support fluxgate magnetometers. All of the magnetometer supports are twice as long as conceived in the original payload design because, as the spacecraft hardware was developed and its magnetic properties determined, it became obvious that the magnetic-field experiment would be severely compromised if the sensors were not placed at a more remote distance from the basic structure.

Certain instruments are mounted around the octagon faces of the spacecraft body. The device that looks like a smokestack performs the same function as a conventional smokestack, except that it removes heat from the prime converter by radiation rather than by convection.

The satellite was launched on November 27, 1963, in a highly elliptical orbit (period = 93.5 hr) with an apogee of approximately 31.7 R_E. The orbit had an apogee–Earth–Sun angle of 25.6 deg, so that the initial

apogee was on the sunlit side of the Earth. Indeed, on the first inbound pass on November 30, 1963, the satellite came very close to passing through the subsolar point of the magnetosphere.

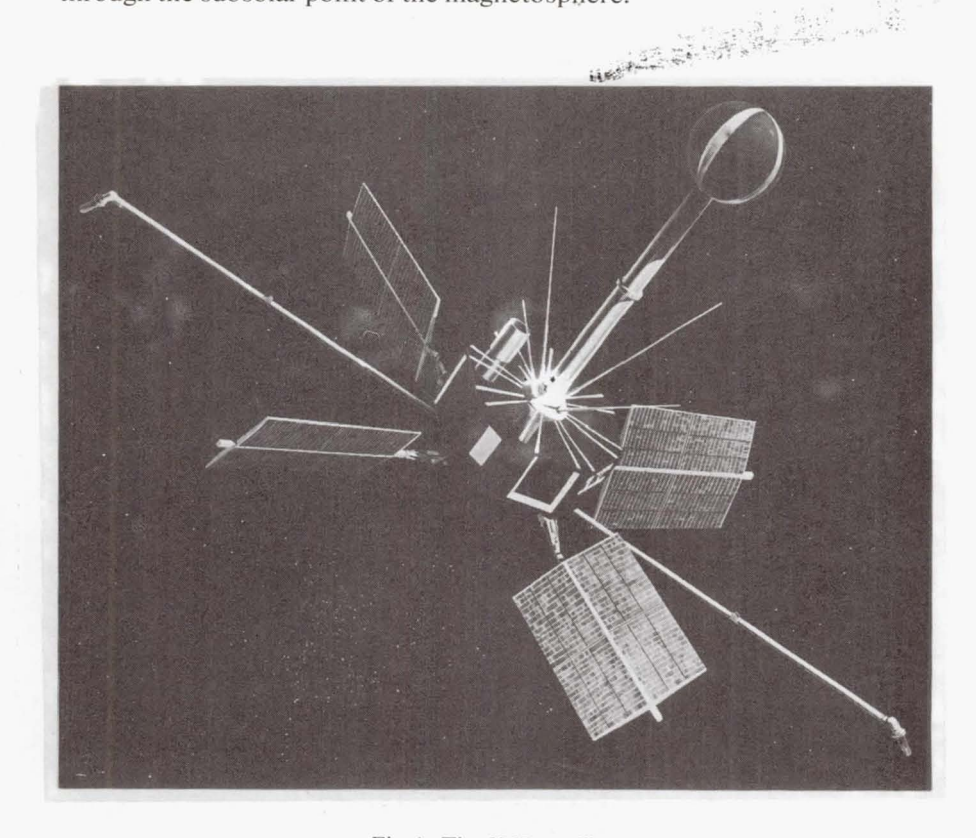


Fig. 1. The IMP satellite

The Magnetic-Field Experiment

The purpose of the magnetic-field experiment was to investigate four principal phenomena in space: (1) interplanetary magnetic fields—solar origin; (2) solar—terrestrial "transients" (magnetic storms); (3) collisionless shock wave (solar-wind interaction with the geomagnetic field); (4) geomagnetic cavity boundary (magnetopause).

Today I will discuss items 1 and 2; discussion of items 3 and 4 will be deferred to a later session (see Paper 22).

Figure 2 is a schematic cross-section of the satellite, showing the location of sensing elements relative to the main body of the spacecraft. Each of the fluxgate magnetometers is located approximately 7 ft from the

center of the 138-lb spacecraft, and the rubidium-vapor magnetometer is mounted at a distance of 65 in. Extreme efforts were made in the development of the spacecraft instrumentation to avoid spacecraft magnetic-field contamination due to two principal sources: (1) ferromagnetic materials and (2) fields generated by circulating currents. We participated in the solution of these difficult problems with the technical staff at GSFC, and with the co-experimenters on board the spacecraft.

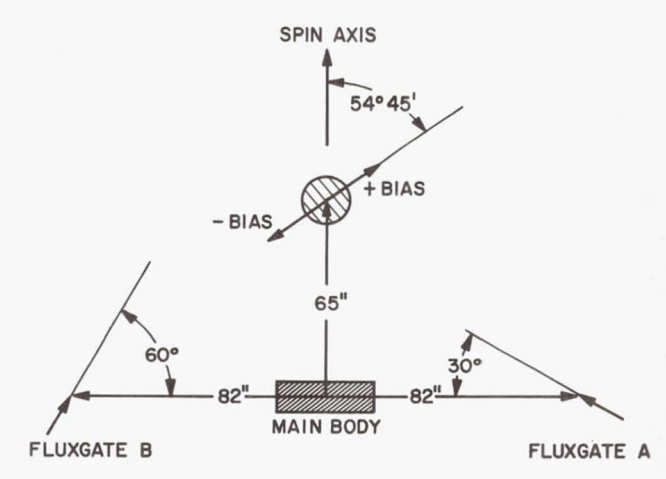


Fig. 2. Schematic cross section of *IMP*, showing instrument locations and orientations

Other aspects of the instrumentation are illustrated in Fig. 2. The flux-gate elements are not both mounted at the same angle to the spin axis. As the satellite spins, the magnetic field detected by each mono-axial sensor is spin modulated. The ability to detect vector magnetic fields in space at various inclinations to the spin axis depends upon the orientation of the sensor to the spin axis. Fluxgate A, mounted at 30 deg to the equatorial plane, is more sensitive to magnetic fields that are perpendicular to the spin axis, since a larger component is projected along its axis. On the other hand, fluxgate B is more sensitive to magnetic fields that are oriented parallel to the spin axis of the satellite.

The rubidium-vapor magnetometer measures only the magnitude of the magnetic field. On the sphere atop the spacecraft, there is a set of bias coils that creates a known vector magnetic field. The response of the instrument depends on the magnitude of the vector sum of the known field and the unknown field. By proper analysis, one can uniquely determine the magnitude and direction of the unknown ambient field. A similar bias-coil arrangement was used on the *Explorer-10* satellite. It also

was used on the instruments carried by Ranger 1 and Ranger 2, although in different configurations because the Ranger satellites were not spin-stabilized but were laboratory platforms oriented in space.

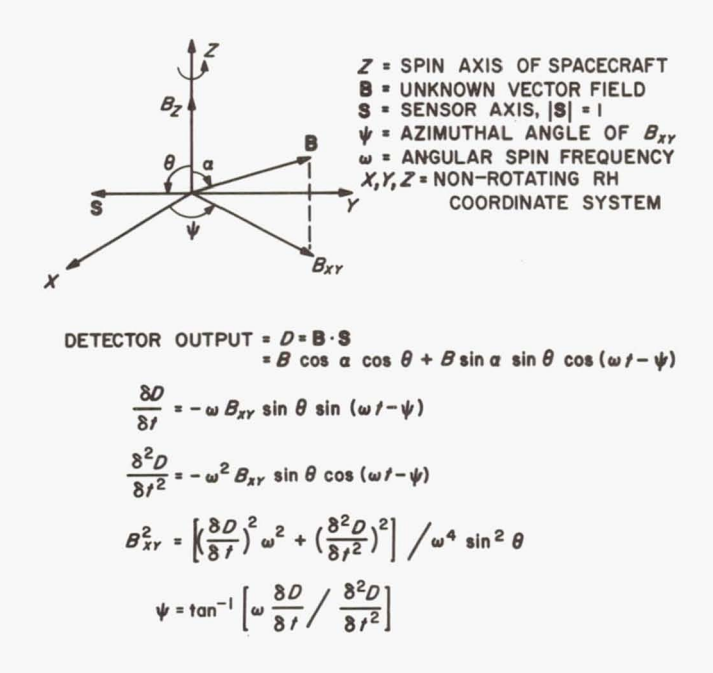


Fig. 3. Spacecraft coordinate system and detector outputs

Figure 3 presents the coordinate system which is most appropriate for interpreting anisotropic phenomena with a spin-stabilized spacecraft. We define the spin axis of the spacecraft to be the Z axis, and the XZ plane to be the plane containing the satellite–Sun vector. The magnetic-field vector \mathbf{B} is then described in terms of its magnitude and two angles, the polar angle α and the azimuthal angle ψ .

The detected output is the dot product of the sensor axis with the magnetic field, and consists of a dc component and an ac component (at the spin frequency). The dc component of the detected output measures $B\cos\alpha$, which is the component of the field parallel to the spin axis. The ac component of the detected output is dependent upon the component of the field perpendicular to the spin axis. Thus $B\sin\alpha=B_{xy}$.

In the analysis, we use linear numerical operators to determine the first and second time derivatives of the spin-modulated signal. From these two time derivatives and the spin frequency, we can determine the angle ψ and the component of the magnetic field perpendicular to the spacecraft spin

axis. Substituting B_{xy} and ψ back into the equation for the detected output, the parallel component of the magnetic field can then be determined. A similar analysis procedure applies to the rubidium-vapor-magnetometer data, although the modulation of the detected output is no longer linear. The rubidium-vapor magnetometer is not a particularly sensitive device for vector measurements when compared with the fluxgate magnetometers, which are direct vector devices. We therefore instrumented the spacecraft and scheduled the telemetry transmission to favor the data from the fluxgate magnetometers, in order to provide definitive vector measurements of the interplanetary field.

Fluxgate magnetometers, however, are only relative devices, and their zero levels are not absolutely known. They may be calibrated in the laboratory, although one has no assurance that the zero level will be stable over an extended period of time. The variation is associated with properties of the core material used in the basic sensor itself. The use of a rubidium-vapor magnetometer, which is an absolute device, has allowed us to calibrate the zero levels of the fluxgate magnetometers in flight. In addition, the rubidium-vapor magnetometer has a much more extended dynamic range and permits measurements up to $300 \, \gamma$.

Figure 4 represents a sample of the telemetry format and provides an indication of the schedule used for sampling the outputs of the three magnetometer sensors. A telemetry sequence is defined to be 81.9144 sec long. Following a sample of fluxgate A, there is a sample of fluxgate B, with a total of four samples uniformly spaced in time at approximately 20-sec intervals. Each sample is 4.80 sec in length. The peaks and valleys do not line up as time progresses from Sequence I to Sequence III, because the telemetry format period is not the same as the spin period of the satellite. The spin rate of the satellite has varied between 22.1 and 25.2 rpm, or a period of a little less than 3 sec. In one transmission of the fluxgate magnetometer, about $1\frac{1}{2}$ rolls of the satellite take place.

Every fourth sequence, the rubidium-vapor magnetometer data occupy the entire telemetry transmission, and no other scientific data are communicated to the ground. The data accumulated by the other sensors on board are interlaced in the gaps shown in Sequences I, II, and III. Sequence IV was included in the format primarily because of the manner in which the information was transmitted from the rubidium-vapor magnetometer. The output frequency was applied directly to phase modulate the carrier. Subsequent digitalization of the rubidium-vapor magnetometer data was done with ground equipment.

In addition, Fig. 4 illustrates the programming of the bias-coil system which adds the known vector field of 20γ to the unknown field. During the second and third quarters of Sequence IV, the bias coil is turned off, and we measure only the magnitude of the unknown magnetic field. The

88 N. F. NESS

particular data sample in Fig. 4 was made at a distance of approximately 100,000 km, far beyond the magnetopause boundary and the shock wave, and shows the magnetic-field strength in interplanetary space to be about 5γ . There is, however, another feature of these data which explains why

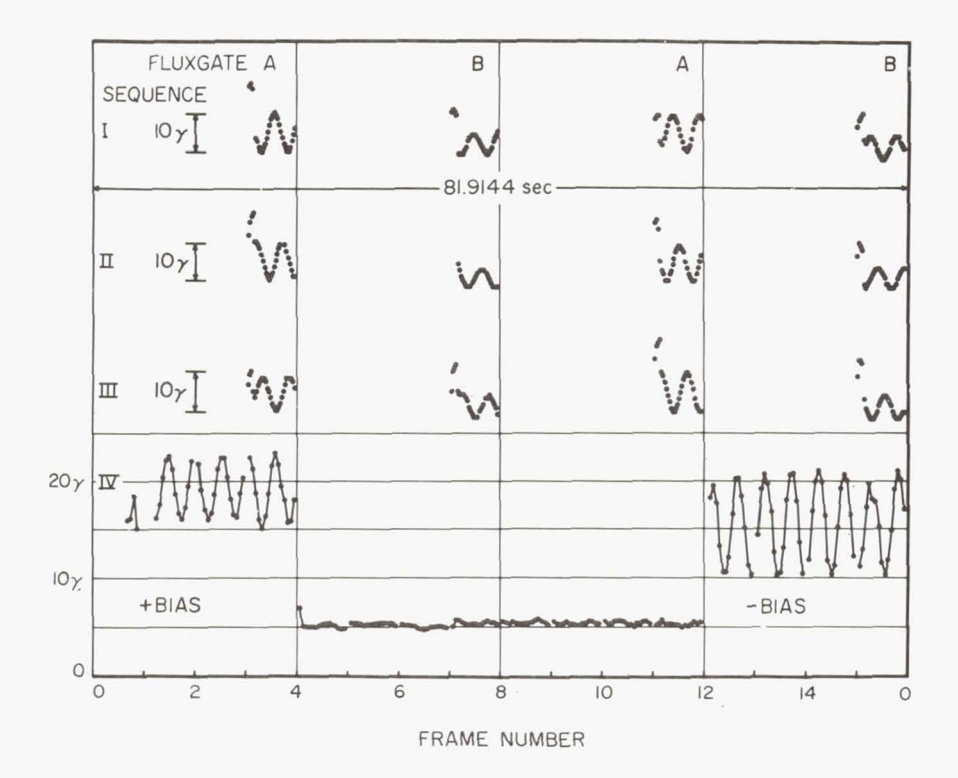


Fig. 4. Typical data sequence. Sequences I–III contain alternating intervals of data from the two fluxgates. Sequence IV records the rubidium-vapor magnetometer with positive, negative, and zero bias

we have selected this period for illustration. If there were spacecraft magnetic fields present, then when the bias coil was off, a spin-modulated component associated with the contamination field would be seen. From a number of samples of data, we have estimated this spin-modulated component to be less than 0.5 γ , peak-to-peak. We feel that, on an absolute scale, the uncertainty is $\pm 0.25 \gamma$. This is an inflight determination of spacecraft magnetic fields with an absolute magnetometer.

During the last quarter of Sequence IV, the current through the coil system is reversed and the bias is called negative. The spin modulation has a visually different appearance. The motivation for the reversal is to

distribute our sampling so that we do not preferentially detect certain fields because of a sensitivity that depends upon orientation. If the spin modulation is significant in the first quarter, it may well not be significant in the fourth quarter. The converse may also be true. The particular sample in Fig. 4 indicates good spin modulation over both positive and negative biases, indicating a relatively significant perpendicular component of the magnetic field relative to the spin axis.

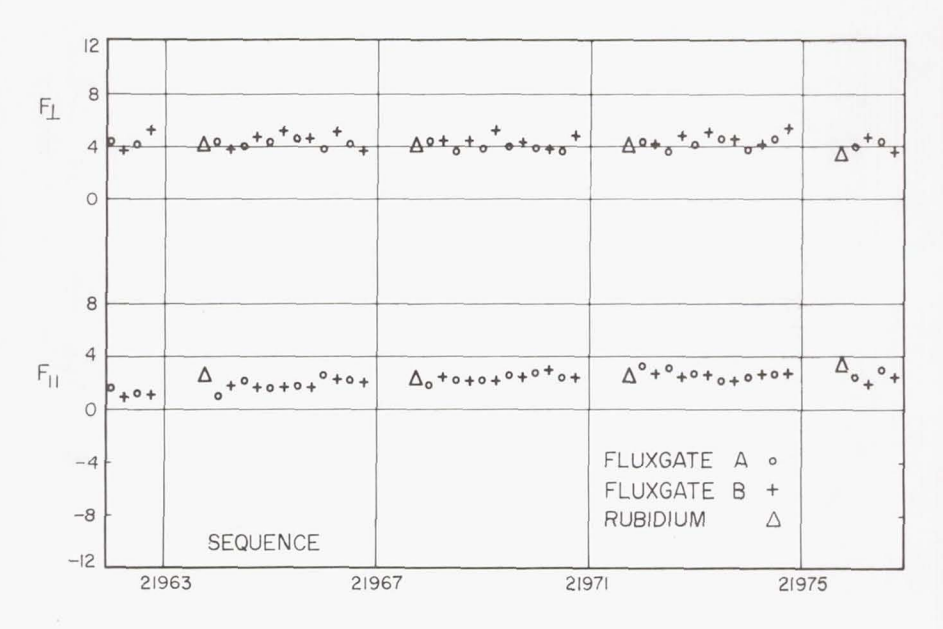


Fig. 5. Comparison of data from the three magnetometers

Figure 5 illustrates the results of comparing the zero level of the fluxgate magnetometers with the rubidium-vapor magnetometer. In this case our telemetry sequences are uniquely identified by a serial number, 21963; four sequences later, the serial number is 21967; and so on. The triangles represent the rubidium-vapor-magnetometer data, the circles represent fluxgate A, and the crosses represent fluxgate B. F_{\parallel} and F_{\perp} are the components of the magnetic field parallel and perpendicular to the spin axis.

In this presentation of the data, the results from fluxgate A have not been adjusted. The data associated with fluxgate B, however, have been adjusted for the parallel component by -2.1γ . Over the time interval that we have analyzed these data, which is approximately 70 days, this zero offset on fluxgate B has changed from -2.1 to -2.5γ . We are confident

that our calculation of the fluxgate zero levels is also consistent with the noise level on the spacecraft ($\pm 0.25 \gamma$).

Figure 6 presents the coordinate system in which the data will be presented. The origin is located at the center of the Earth, but the axes

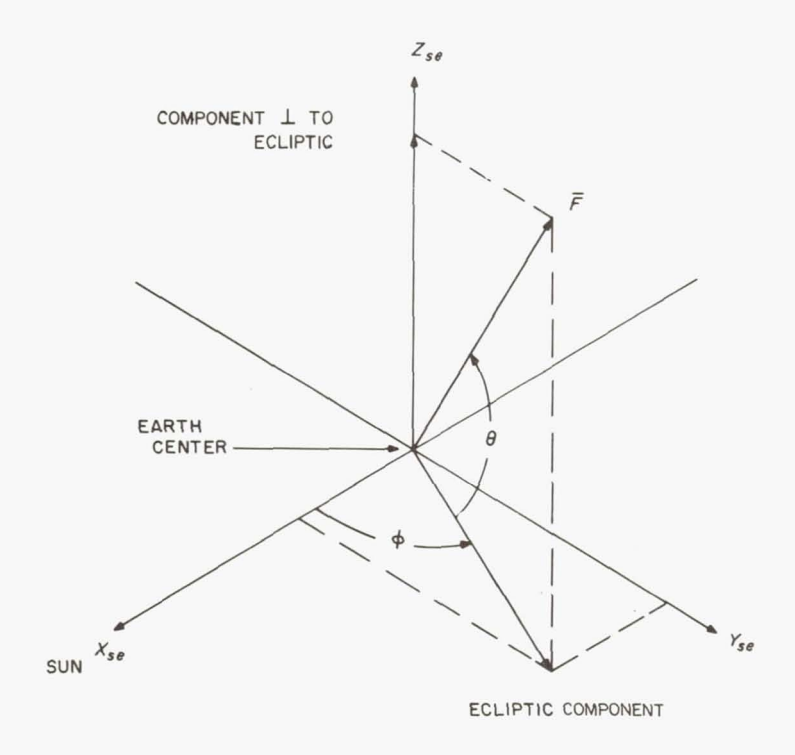


Fig. 6. Solar ecliptic coordinate system

are chosen to reflect the fact that the phenomena under investigation are associated with the Sun. X_{se} is directed from the center of the Earth to the Sun. The Z_{se} axis is defined to be perpendicular to the ecliptic, and the Y_{se} axis is chosen to make a right-handed coordinate system. The data are actually presented not in component form, but in magnitude and two angles. It is unfortunate that the symbolism and the characters we have chosen are not consistent with those chosen for the *Mariner* data previously discussed (Paper 3). θ is the latitude angle of the field vector above or below the ecliptic; ϕ is the azimuthal angle which is zero for a field vector pointed toward the Sun, and 180 deg for one pointed away from the Sun.

The IMP-1 Orbit

The characteristics of the orbit are particularly important with respect to sampling interplanetary magnetic fields and the solar wind, undisturbed and undistorted by the presence of the Earth and its magnetic field. In Fig. 7, the plane of the paper represents the ecliptic; the Sun is off to the

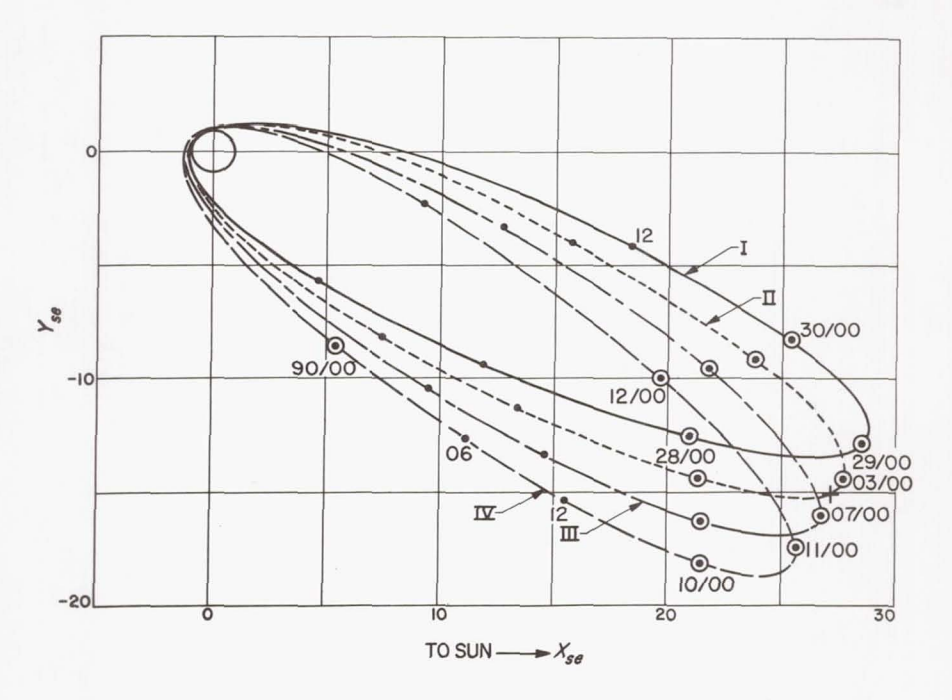


Fig. 7. First four *IMP* orbits, projected on the ecliptic. Distance is in R_E

right. The first four orbits of the *IMP-1* satellite are plotted, and the points on the trajectory indicate universal time. A double zero means zero hours on a particular day: for example, the first labelled point is zero hours on November 28.

One of the unique aspects of a highly elliptical orbit is that the satellite spends most of its time near apogee. Thus our sampling of the interplanetary medium is very long compared to the sampling time in the vicinity of the Earth, where the data would be prejudiced and compromised by the effects of solar wind–geomagnetic field interactions.

It can be seen from Fig. 7 that the line of apsides, or apogee–Earth line, starts out at about noon minus 25 deg and steps around about 4 deg per orbit, since each orbit takes about 4 days. The data to be discussed are taken from the first through the nineteenth orbits.

Figure 8 illustrates the orbital characteristics projected on a plane perpendicular to the ecliptic, the $X_{se}Z_{se}$ plane. The satellite, on the outbound pass, is some 5 or 6 $R_{\rm E}$ below the ecliptic. At apogee, the satellite is below the ecliptic, and on the inbound pass, the satellite rises above the ecliptic. As the orbit progresses, the projection of the trajectory on the $X_{se}Z_{se}$ plane in Fig. 8 becomes foreshortened. At the present time, the projection of apogee onto this plane is at a negative value of X_{se} .

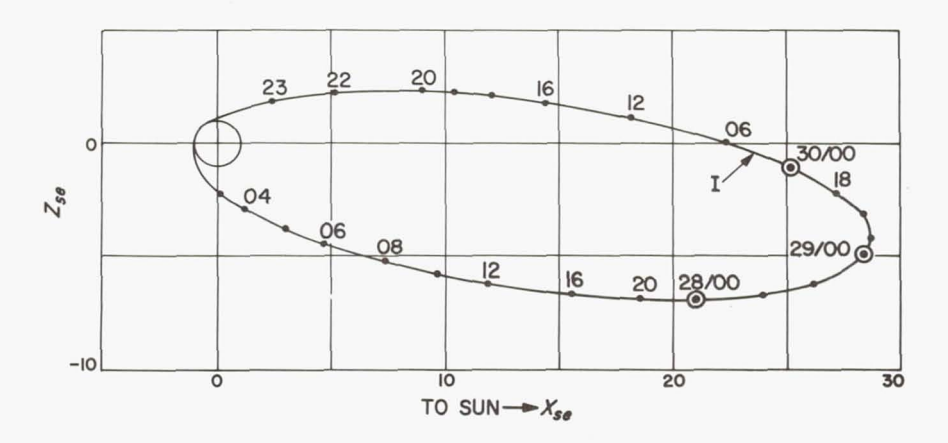


Fig. 8. Projections of IMP trajectory on a plane perpendicular to the ecliptic.

Distance is in R_E

Features of the Interplanetary Magnetic Field

Orbit 11. In Fig. 9, \bar{F} is the average of 12 measurements of the magnetic field made by the fluxgate magnetometers over a time interval of approximately 5 min. Each point represents the 5-min average thus obtained, \bar{F} is plotted from 0 to 20 γ , and θ from -90 to +90 deg, the center line being the ecliptic. ϕ is 0 and 360 deg toward the Sun, and 180 deg in the antisolar direction.

For the time being, I will not discuss the bottom half of Fig. 9, but will concentrate on the magnetic-field data on January 6, 1964. Although the magnitude of the magnetic field (which was about 4 γ in this case) does vary, in general it is quite stable. When we look at the angular information, we see that the magnetic field, at least at this particular time, was directed below the ecliptic, at angles ranging from 10 deg to 40 deg, but the angle appears to be more variable than the magnitude on the time scales that are displayed.

The azimuthal angle ϕ started out at approximately the theoretical streaming angle associated with solar-wind velocities of 400 km/sec. It

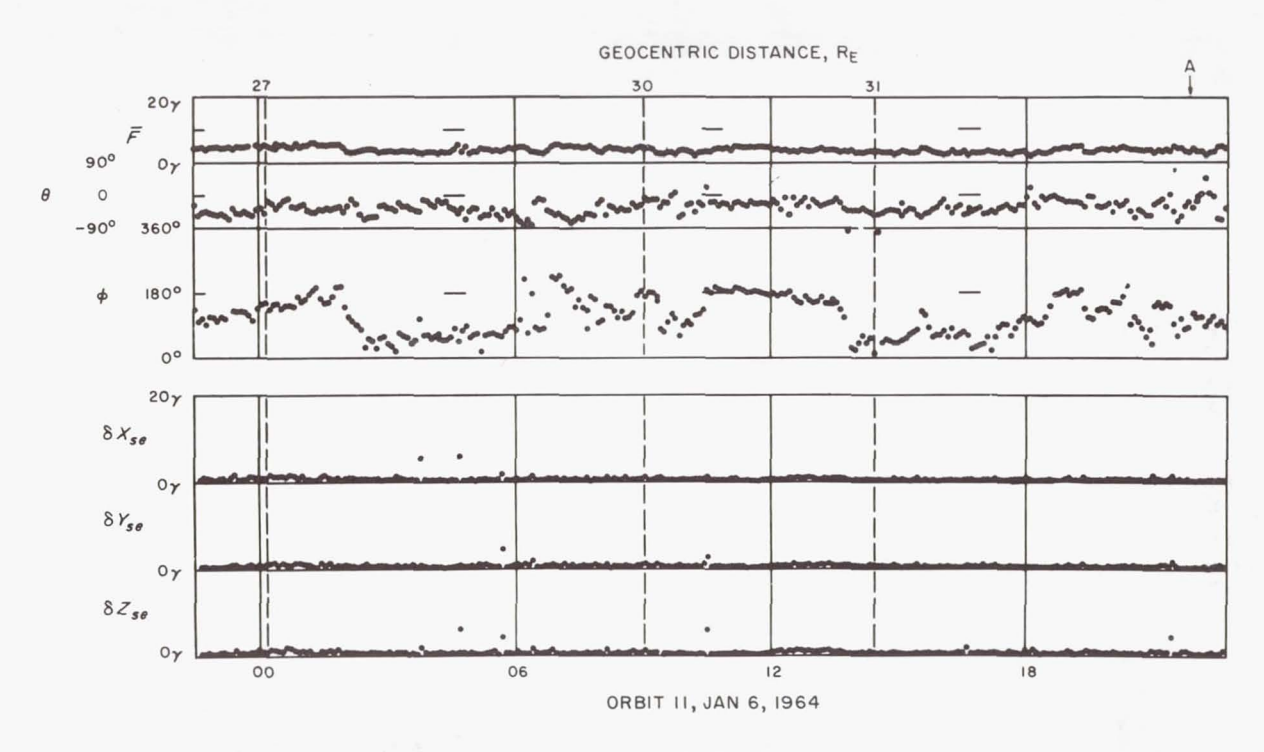


Fig. 9. Magnetic-field data from Orbit 11: each point is a 5-min average

then changed to point back toward the Sun, then varied a bit, then pointed away from the Sun, then back toward the Sun, and so on. But in general, the magnetic field was as impressive in the local coherency of its direction as of its magnitude. It did not vary randomly back and forth, but seemed to present a very sensible picture of a relatively stable topology of field lines.

In an attempt to investigate the stability of the magnetic field in interplanetary space and in the transition region, we have also included a computation of the 5-min rms variance of the solar-ecliptic components of the magnetic field. These variances are plotted in the bottom half of Fig. 9. The magnitude of the variance was very low—slightly larger than the 0.25 γ associated with the basic sensitivity of the instrumentation in the spacecraft. In general, it lay between 0.25 and 0.40 γ .

There are occasional samples in interplanetary space in which the variance appeared quite large. The data that are plotted in Fig. 9 have not been culled for wild shots or noise (spurious samples associated either with the telemetry system or the ground digitalization equipment) except where the ground digitalization equipment was able to specify unambiguously that a sample was in error. We have not omitted a point simply because it doesn't lie close to all the other points in its immediate neighborhood. However, I feel that, at least for the particular data shown here, these large-variance samples are wild shots, because there is indication in other samples of our data that coherent variations of the field do exist. When such coherent variations are found, they generally exist for more than the 5-min interval that each point in Fig. 9 represents.

Orbit 11 is continued in Fig. 10. Early in the day, the field was still about 4 or 5 γ . It then increased to 6 or 7 γ and subsequently decreased slightly. First the field was directed 70 or 80 deg below the ecliptic, then it came up to 10, 20, or 40 deg. The angle ϕ originally was pointed toward the Sun, then moved away from the Sun, and later took the very characteristic angle, predicted by Parker (Ref. 1), associated with a solar-wind velocity of approximately 400 km/sec.

In Fig. 10, the variance was again quite low, although in this case we note that there appeared to be some coherency on the time scale in which large variances were observed. We also note that at approximately 1100 UT, for example, the field didn't change in magnitude when the variance was large.

Let us now inspect the particular sample at approximately 2230 UT, when the field was at the streaming angle and then suddenly changed to approximately the antistreaming angle. The antistreaming angle is the angle at which the field line is in the ecliptic and at the proper inclination to the solar direction, but points toward, rather than away from, the Sun. We have seen this behavior repeatedly in our data and interpret it to be

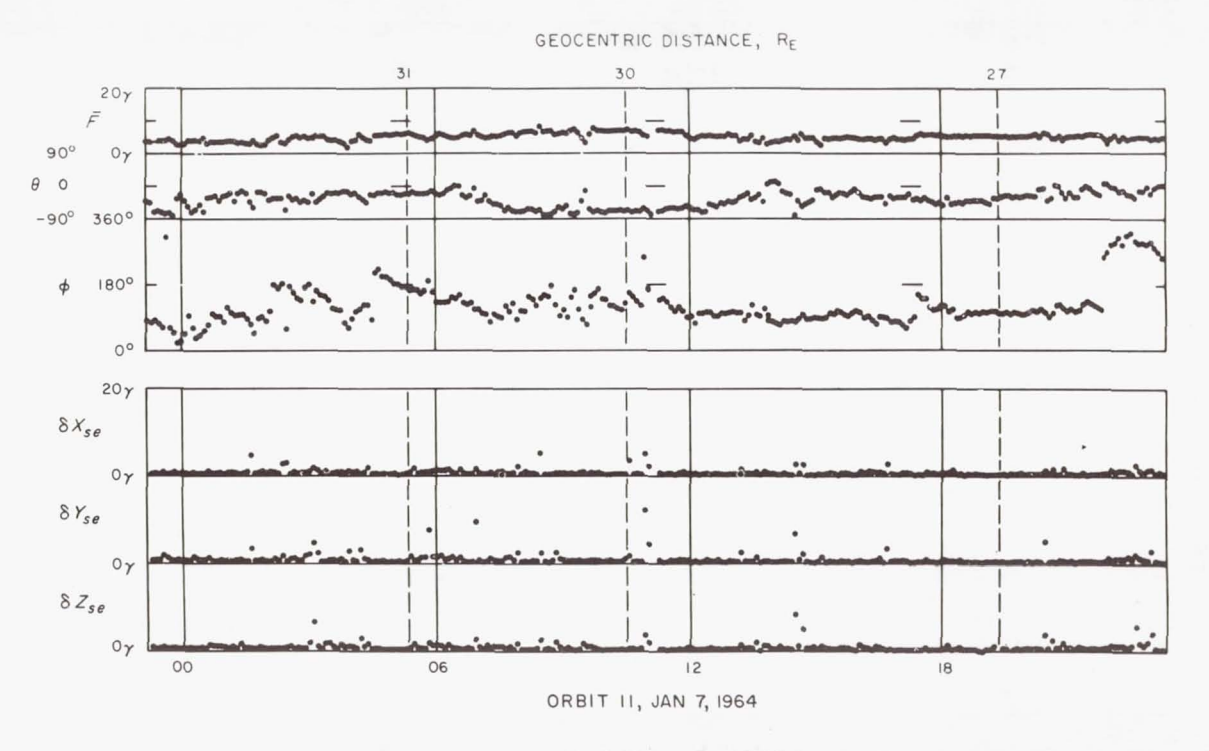


Fig. 10. Magnetic-field data from Orbit 11, (cont'd)

representative of filamentary structures of the interplanetary magnetic field. At the same time that the field changed direction abruptly, you will notice that the magnitude seemed to decrease.

We have looked at these 5-min time averages in detail, and indeed in certain cases the strength of the magnetic field became as small as about 0.5 γ . We interpret these periods to be associated with neutral surfaces at which the magnetic field went to zero.

Figure 11 indicates the theoretical angle ϕ and its associated angle ϕ' , which would be predicted from an axially symmetrical, uniformly streaming wind. The important point of Fig. 11 is that, in general, the angles ϕ

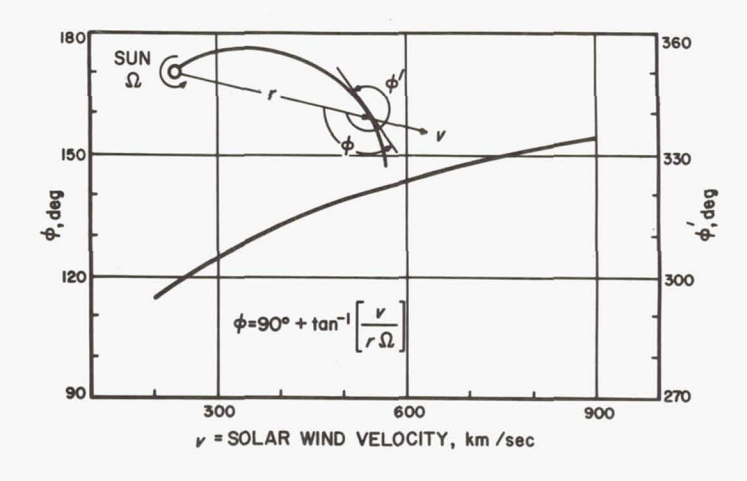


Fig. 11. Theoretical interplanetary magnetic-field streaming angle as a function of solar-wind velocity

and ϕ' are fairly insensitive to velocity—insensitive in the sense that ϕ changes from 125 deg at a velocity of 300 km/sec to about 140 deg at 600 km/sec.

Figure 12 illustrates data from Orbit 15. Again, the field was stable in magnitude at 4 or 5 γ and then increased to 6 γ . In this case, the field lay in the ecliptic for an extended period of time and then started to move below it. At the same time, the field was directed radially away from the Sun and then was close to the theoretical streaming angle for an extended period of time, although it was below the ecliptic. The variance again was small. There are no obvious examples, in Fig. 12, in which the filamentary structure of the field is indicated.

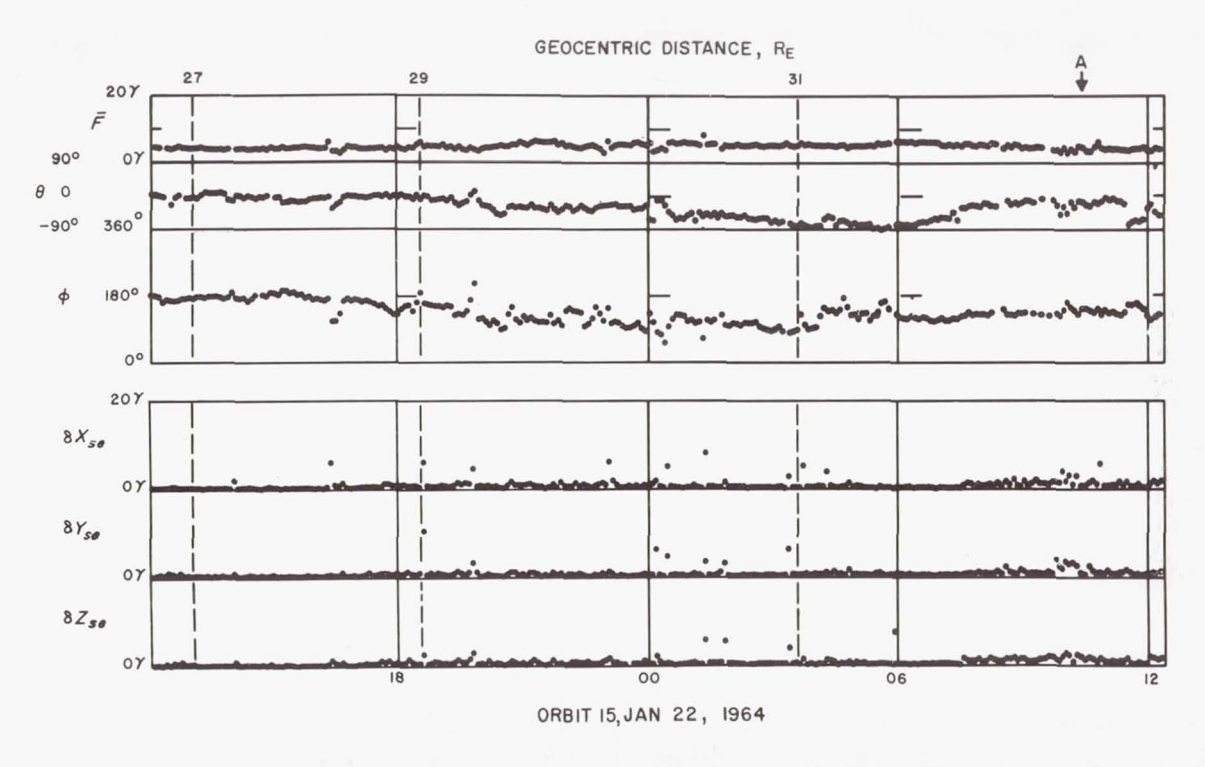


Fig. 12. IMP magnetic-field data from Orbit 15: each point is a 5-min average

I have presented the data we have only briefly. I would like to summarize the interplanetary-field data by saying that it suggests the combination of the ideas of a uniformly expanding solar corona (Ref. 1) with the ideas that the magnetic-field sources must indeed be individual and discrete sources, either in the photosphere or at greater heights in the solar corona (Ref. 2). What we have seen is evidence that the general filamentary structure very strongly reflects the continuous expansion of the solar corona, remarkably in agreement with the theoretical models. We have not yet had an opportunity to investigate the details of the neutral surfaces to determine exactly what the ramifications of this phenomenon are or what the other sensors on board may be observing.

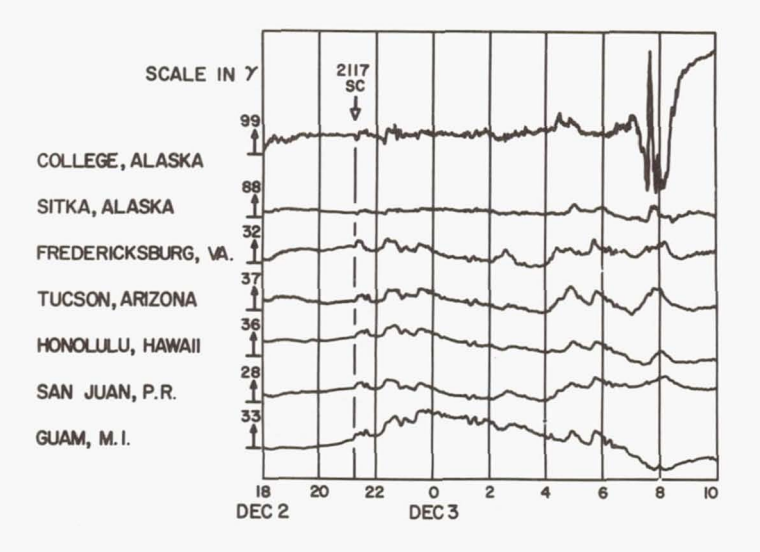


Fig. 13. Regular-run magnetograms near the beginning of the storm of December 2, 1963

Magnetic Disturbances

I would now like to go to the portion of our data which deals with solar-terrestrial transients. The cross near the apogee of Orbit 2 in Fig. 7 marks the location of the satellite at the time of the sudden commencement of a magnetic storm on December 2, 1963. I am certain most of you are well aware that the past few months have been a very quiet time in the solar cycle, and we were very fortunate to observe this one magnetic storm just as the satellite approached apogee. Except for the Earth's heliocentric orbital motion of approximately 30 km/sec, the satellite was essentially stationary in space when the storm occurred.

Figure 13 shows the regular-run magnetograms obtained on the surface of the Earth on December 2. This collection of standard-type magnetograms indicates the characteristics of this particular storm. One unusual aspect of the storm is the fact that its onset time and its onset characteristics were amazingly identical from station to station. The important point here is that the onset time can be established at 2117 UT, not only by this data from around the world in latitude and longitude, but also by the data in Fig. 14, which is a selected set of rapid-run magnetograms.

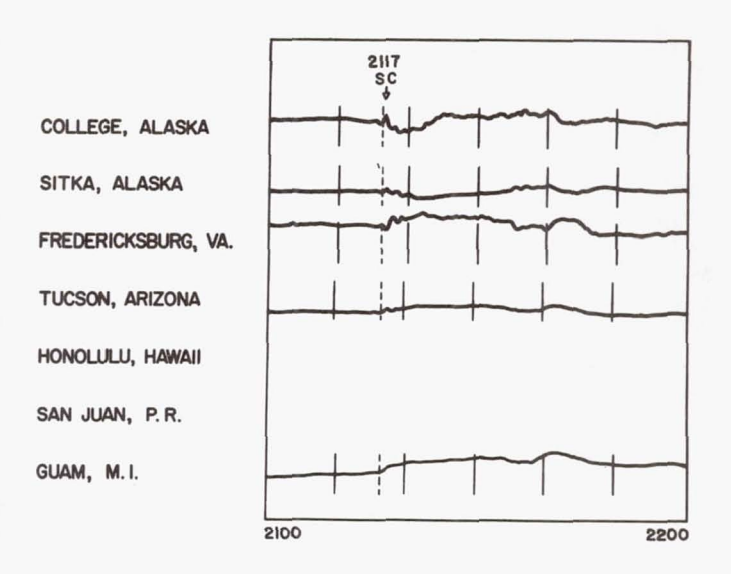


Fig. 14. Rapid-run magnetograms of December 2, 1963

Figure 15 illustrates the data, in our normal 5-min averages, of the interplanetary magnetic field preceding and slightly after the sudden commencement of the geomagnetic storm indicated by the line SC. Early on December 2, the field was approximately 7 or 8 γ , and it then increased in magnitude to 10 γ . You will notice that, at the sudden commencement, the magnitude took an abrupt drop to 2 or 3 γ , a slight increase back up to about 10 γ , and then another abrupt decrease to 2 or 3 γ . From then on, the field generally increased in magnitude and resumed its earlier characteristics, not unlike the interplanetary fields we had seen either previous to or subsequent to these data.

Continuing on December 2, the field appeared to be pointed back toward the Sun but showed considerable variation. The variance was also noticeably higher as we approached the storm time, rising to 1, 2, or 3 γ in each of the components.

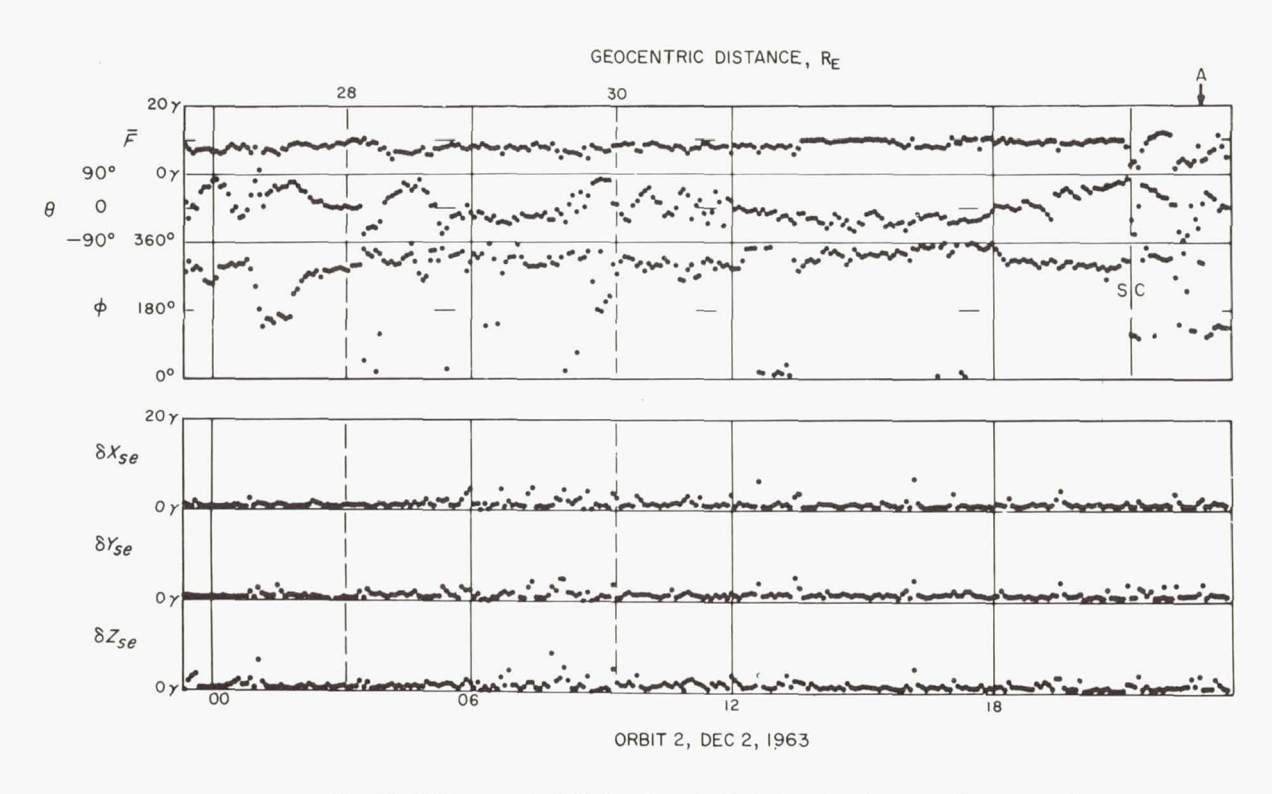


Fig. 15. *IMP* magnetic-field data from Orbit 2, showing the onset of the magnetic storm of December 2, 1963

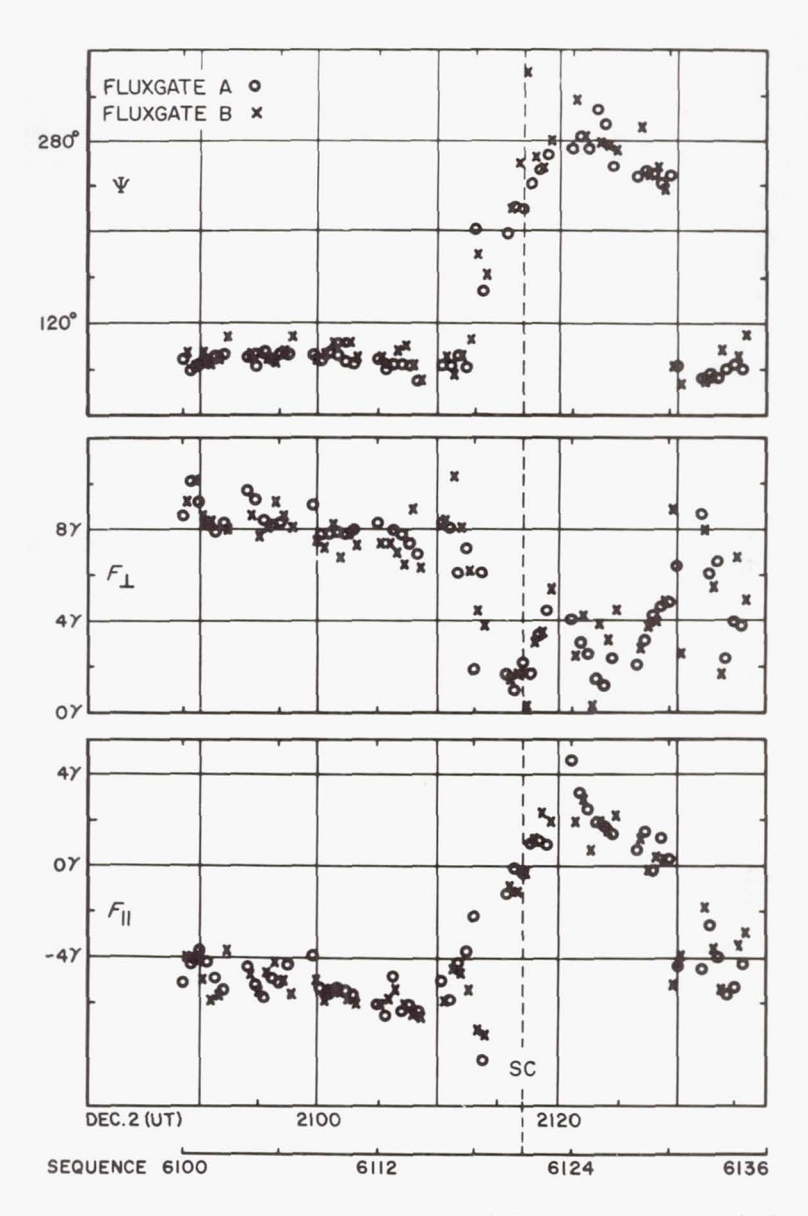


Fig. 16. *IMP* magnetic-field data at the time of the storm onset, shown in the spacecraft coordinate system on an expanded time scale: the points are distinct samples of the magnetic field, 20 sec apart

Figure 16 shows the magnetic-field data in the payload coordinate system. ψ is the azimuthal angle, and F_{\perp} and F_{\parallel} are as defined previously. To determine the onset time of the magnetic storm as observed at the satellite, Fig. 16 presents the data on an expanded time scale. The circles and crosses mean exactly the same as before; they represent distinct samples of the magnetic field, 4.8 sec in length. Each of the points is separated by 20 sec from the adjacent measurement. The gaps are associated with the rubidium-vapor magnetometer transmission whose data have not yet been folded into this particular representation.

The magnetic field angle ψ showed a very stable configuration until about 2114 UT. The magnitude F_{\perp} decreased slowly while F_{\parallel} became more negative up to this same time. The break in the character of the magnetic field is very clear in ψ , less clear in F_{\perp} , and even less clear in F_{\parallel} . Nonetheless, the identification of the onset time is clearly unique.

The other point to note about the data is that—and I do not consider this only coincidental—the magnetic field changed in such a way that at the same time that F_{\parallel} goes through zero, F_{\perp} also goes to zero. Thus we have another neutral surface. Following this period, the field strength increased somewhat, returned to zero (although not as distinctly as before), and then recovered.

If we identify 2114 UT as the time at which the spacecraft sampled the storm front, we have a 3-min propagation time between the satellite and the Earth. If we assume that the motion was radial from the Sun to the surface of the Earth, and if we neglect any variation in the velocity of the disturbance through the transition region and the magnetosphere, we arrive at a propagation velocity for the first disturbance of approximately 700 km/sec. This velocity is in reasonable agreement with energies of plasma associated with magnetic storms as measured in the past by other satellites. It is also consistent with the general transit time of magnetic disturbances which are uniquely associated with identifiable solar-flare activity. The assumption we have to make is that transit-time measurements really make only an estimate of the velocity of propagation.

Another important point is that there were neutral surfaces associated with the storm front. Finally, the magnitude of the field was not large. It increased to only about 10γ . No large increases were detected, at least on the time scale on which we sampled our data.

REFERENCES

- 1. PARKER, E. N., Astrophysical Journal 128, 664 (1958).
- 2. GOLD, T., Nuovo Cimento Suppl. 13, Series 10, 318 (1959).

DISCUSSION OF NESS PAPER

PARKER: Did I understand you to say that the December-2 storm was associated with a solar flare and was not one of the recurring type?

NESS: No: the storm appeared to be the fifth in a recurrent series. Its identification with a solar flare is not clear.

BIERMANN: I didn't quite understand what you said about the filamentary structure of the magnetic fields as determined by your measurements.

NESS: A full explanation requires statistics that we have not as yet accumulated. However, the data suggest that we have seen fields that are oppositely directed. The time required for the polarity to change from one sense to the other, and back again, is sometimes as short as one or two hours. At other times, a polarity reversal takes 12 or even 22 hours. The time scale is quite variable. The only dimension that we can say anything about, at the present time, is what we interpret to be the thickness of the December-2 storm front. If we take a propagation velocity of 700 km/sec and the interval of time between the onset of the storm and the recovery of the angle ψ , we arrive at a thickness of about 0.005 AU for the storm front. Unfortunately, this estimate was made independently of the plasma data. Clearly we are going to have to investigate the detailed correlation of these phenomena before we can establish the thickness of such storm fronts in space.

MEAD: In considering whether the field is predominently in the ecliptic or not, if you use any spherical coordinate system and look at the latitude distribution, I think you will find that a random series of directions will tend to be concentrated, by a factor of $\cos \theta$, around the equator. There is zero probability for θ to be 90 deg. The distribution in your data appeared to be somewhat concentrated in this manner, even though the field appeared to be predominently below the ecliptic. I would like to see, sometime, a latitude distribution compensated by the factor of $\cos \theta$.

NESS: I think the problem here, which we are working on, is one of statistics. We want to work with a real physical field rather than with a field constructed from the time averages of the field's components. We also want to do a histogram analysis to determine the preferred orientation. For instance, we might divide the sphere into 10-deg or 20-deg "buckets" and count over, say, 1 to 3 hours.

I admit that the data we have illustrated here indicate the field to be directed preferentially below the ecliptic. I think this is a reasonable statement. We do not yet know what the association is between the field direction relative to the ecliptic and the angle ϕ relative to the solar direction. We will be working on that.

DUNGEY: I think you said you haven't had time to compare data, but I wonder if you have anything to say about any association of your data with Dr. Cline's data, which was discussed this morning. What happened to the magnetic field at the time he observed these electrons?

NESS: I don't know.

COLEMAN: You suggested that quiet, steady fields were relatively unique when considered in terms of previous results. I would like to point out that steady fields have been observed on numerous occasions by both *Mariner* and *Pioneer 5*. Quite frequently the fields observed by *Mariner* remained steady within about 1 γ . and with *Pioneer*, we had many transmission periods when the field didn't change by more than a small fraction of this value.

NESS: It is my impression that, of all magnetic-field data that have been collected,

our result is the first to show steady conditions lasting from 6 hours to several days.

SMITH: I think it would be fun to try to make some comparisons between the *Mariner* and *IMP* results. Such comparisons may be a bit premature, but I hope that we would at least approach a condition where the picture would become consistent, so that we could see what the interplanetary fields look like. Part of the problem, I think, is that we have an optical illusion. We have plotted data in very different ways and to different scales, which makes comparison a little difficult.

NESS: I think the field configurations seen by *IMP* are amazingly stable relative to the configurations from *Mariner* that you have published and presented today. Eventually, we will have longer term statistics so that we can compare data; but there appears to me to be a considerable difference in the interplanetary medium between then and now.

SMITH: That may well be true, because I think conditions were generally more disturbed during the *Mariner* flight than they have been during the *IMP* flight. During the *Mariner* flight, for example, we had a dozen magnetic storms over a period of about 4 months. How many magnetic storms have you seen on *IMP* so far?

NESS: We have sampled only one. There have been a total of three magnetic storms over the 4-month period since launch.

SMITH: Also, we saw several fairly large storms as well as several small ones. The Kp indices during the IMP magnetic storms indicate they were fairly small. So conditions were, I think, much more variable during the *Mariner* flight. On *Mariner*, we saw several storms during which the interplanetary magnetic field increased by an order of magnitude. The strength rose from a typical value like 5γ to something closer to 50γ .

NESS: Then we are in complete agreement. Either the interplanetary medium has drastically changed, or the results are not comparable for other reasons. **SMITH:** But I think the change is quantitative. In your data, when you look over a 1-day period, you don't see the spiral angle. The same is true of the *Mariner* data. It is only when we average over a period of several days that we can begin to see a persistent direction in space which corresponds reasonably well to the streaming angle.

Can you say, from your results, that the interplanetary magnetic fields appear to have some preferred orientation in space? How would you characterize the direction of interplanetary magnetic fields based on just the *IMP* results?

NESS: The first feature is the filamentary structure at the streaming and antistreaming angle. Another feature is that the field is pointed away from the Sun for extended periods of time, which is compatible only with an infinite solar-wind velocity.

SMITH: We saw this too. If you averaged your data over a period of 15 orbits, or something like that, wouldn't you find that the interplanetary field tends to lie in the ecliptic?

NESS: No, I don't think so. Since we are being qualitative, I have the impression that we have so far seen in our data a preferential value of θ .

GOLD: I don't agree with the point of view that it is possible to deduce the field configuration from the streaming. Mr. Ness said that the field configuration is not compatible with anything other than infinite velocity. That is a very naive interpretation of what is going on and an interpretation that cannot be right in any case. The outstreaming from the surface of the Sun of any kind of messy

field that is occurring there, will carry into space a field with all kinds of directions. The interplanetary field will depend on the field that existed in the vicinity of the Sun in the first place. If the field near the Sun had noise, it is going to march through space possessing that noise. Such a field configuration is compatible with any kind of solar-wind speed.

I agree, of course, that there would be a statistical tendency for the field to be aligned along the garden-hose angle. But one cannot deduce the speed uniquely from the magnetic data. Perhaps, from heavy statistics, one could determine the average speed; but this is a very doubtful procedure, because if the average speed varied widely was wouldn't get a very good result.

varied widely, you wouldn't get a very good result.

NESS: I am not certain I understand our disagreement.

GOLD: My disagreement with you only concerns the phrase about an infinite

velocity.

NESS: That was a facetious statement. I thought I made the general remark in the formal presentation that the direction of the streaming angle really doesn't measure the velocity very well at all. I agree with you that what we are seeing is structure in the medium, rather than waves.

GOLD: Your observation that the strength of the field stays very constant while the directions are very variable is surely indicative of a flow pattern in which the magnetic pressures dominate over gas pressures, turbulent pressures, and everything else in the reference frame of the gas.

HESS: Such a model doesn't really work though, does it, if you consider the

measured temperatures and the measured fields?

NEUGEBAUER: The thermal and magnetic pressures are comparable, but there is a question as to how much those data are contaminated by the alpha particles, and how accurately the thermal broadening of the plasma spectrum is known. It is not very clear what the thermal situation is – how the temperature of the gas compares with the turbulent pressure.

BRIDGE: I would like to ask Prof. Gold if he would elaborate a bit. If you stretch out fields of opposite sign from limited regions, and this goes on for a long-enough time, then I don't understand how the result essentially differs from Parker's stationary models.

GOLD: In Parker's model the velocity vector is radially outward from the Sun, and there is a pre-existing field which is being moved in a phonograph-groove

manner by the outflow of the gas.

Now, in my model, there is some complex field, of whatever shape you like, in the vicinity of the Sun. The outflow takes that field into space with whatever configurations the flow pattern will produce. This model is not capable of leading to a steady-state situation, because new field lines are being dragged out from the Sun. In Parker's model no new field lines are drawn out from the Sun, therefore no cutting-off of field lines is required, and a steady configuration is allowed to exist.

In my model it is apparent that the pole strength of the Sun is being increased every time there is an outburst, so it is necessary to have a way of cutting such things off. This means there must be dissipation in the interplanetary gas, and I have supposed this to be associated with the neutral planes that necessarily are formed in such a situation. The lines get themselves cut off and leave individual clouds that fly away, with the lines jumping back in order not to increase the pole strength of the Sun indefinitely.

I regard it as very significant that one sees all directions present and a great tendency toward neutral sheets, which I think is exactly what this model demands. **PARKER:** In his attempt to propagate his interplanetary Cyrano de Bergerac.

whose nose (magnetic tongue) marches on before by a quarter of an hour, Tommy (Gold) has stated the correct properties of the configuration according to my model, but he has overlooked the fact that you will find most of those same characteristics in his configuration, too. My model, in which the magnetic lines of force have an underlying Archimedes spiral, makes no attempt to put arrows on the lines of force; the lines generally point both in and out. Filaments with reversing senses are just as intimate a part of this picture as they are of his—with one difference: in my model one is not playing with the problem of continually severing rather massive fields.

GOLD: How would your model have any field component normal to the ecliptic? **PARKER:** Your picture of my model was drawn from the idealized case of a perfectly uniform radial wind, which was known to be a fiction at the time it was first pointed out. As soon as you have any variations whatever in the wind (and these were anticipated and have now been measured), you get fields which fluctuate in any direction you like.

I would also like to comment on your remarks about the relative magnitudes of the magnetic and gas pressures. I don't think they have any theoretical grounds. You ought to work out the dynamics of this model sometime.

DAVIS: I think there is one thing that shouldn't be overlooked in this discussion. Regardless of how one wants to shift the zero levels in our *Mariner* magnetometer data, one cannot avoid observing a structure in the magnetic field which reappears every 27 days. You can change the character of this recurrence, but you can't get rid of it. I think this means there is something imbedded in the Sun that lasts for at least a month. I think this recurrence has nothing to do with what Prof. Gold has suggested, unless it is the remnant of something that started a year ago and has persisted all this time without being cut off.

BRIDGE: I want to ask one question of the *Mariner* plasma people. You said you have seen several magnetic storms for which the energy increased gradually over a long period of time after the beginning of the storm. Was this same effect present for all magnetic storms?

NEUGEBAUER: Yes: in every case, it took one or two days for the velocity to reach its maximum value. However, we weren't observing these streams head-on; they were overtaking us, because their motion about the solar axis was much greater than the spacecraft's. I am not sure we ever saw any plasma connected with a sudden outburst or solar flare.

BRIDGE: I think it is significant that the observed plasma energy increases so slowly across the boundary of a stream that gives you a sudden commencement. It seems to me that, in moderate events like these, you wouldn't expect such a great azimuthal extent of Gold's magnetic bottle regions, even though his model may be correct for higher-energy events. I think that, for most events, it is quite possible to get the filamentary structure from the model that Parker proposed.

NESS: You are quite right in that the directional characteristics of the field structure are dominated by the Sun's rotation, and all we are seeing here is a reflection of this fact.

LÜST: Since during the *Mariner* flight there was apparently a 27-day structure in the magnetic field, which may be in contradiction to the *IMP* measurements, I don't think that one can exclude either Parker's or Gold's model right away.

SMITH: I don't think there is any question about the existence of real structure in the interplanetary field. As I understand it, you will get the spiral configuration provided the field lines attach to a rotating Sun. If one allows for the fact that sometimes the field sticks out from the Sun more strongly than at other times,

then in spite of its limitations, the 110 days of *Mariner* magnetic-field data are consistent with a wiggly spiral structure—that is, spiral lines with smaller-scale irregularities superimposed.

GOLD: So far as the *Mariner* data are concerned, was the field always pointed outward from the Sun and never in toward the Sun?

SMITH: No, that is not true, but the sign seemed to be persistent for a solar rotation on the large scale. On the smaller scale, there are possibly null points in the field and reversals in the direction associated with the irregularities.

Page intentionally left blank

CHAPTER VII

RADIO ASTRONOMY OBSERVATIONS IN RELATION TO THE SOLAR-WIND PROBLEM

J. D. WYNDHAM

California Institute of Technology, Pasadena, California

THIS paper is concerned with the application of the techniques of radio astronomy to the study of the interplanetary medium, and is largely based on a recently published paper by A. Hewish and J. D. Wyndham (Ref. 1). At present, these techniques permit an investigation of the broad features of the solar corona and interplanetary space. We can say something about the radial variation of electron density; we can put limits to the size of the coronal irregularities (the fluctuations in electron density); and we can say something about the mean direction of the coronal magnetic field.

Observational Procedure

The method used is to look at radio sources through the corona. Radio waves from these sources undergo a process of irregular refraction due to the existing non-uniformities of electron density, which results in an apparent increase in the angular diameter of the source. The angular size of the "scattered distribution" ("scattered distribution" is defined as the brightness distribution produced when a point source is viewed through the corona) can be measured for various relative positions of Sun and source using a radio interferometer. The effect is most pronounced at meter wavelengths, and in this wavelength range, interferometer spacings of several kilometers are needed to detect the small scattered distributions (angular size \sim minutes of arc) which occur at large radial distances from the Sun. Using this method, we have now detected scattering out to distances of the order of 100 $\rm R_{\rm S}$, so that we are in effect investigating the interplanetary medium. Slee (Ref. 2) has also detected radio scattering at similar distances.

Figure 1 shows the paths, relative to the Sun, of two radio sources that have been used in making observations. One is a well-known radio source, the Crab Nebula, whose path lies almost entirely in the equatorial regions of the Sun. The other, 3C 123, provides a scan across the polar regions

of the Sun at a distance of about 30 R_s. The following discussion will concern mainly the results obtained using the Crab Nebula, and will therefore apply to the Sun's equatorial regions.

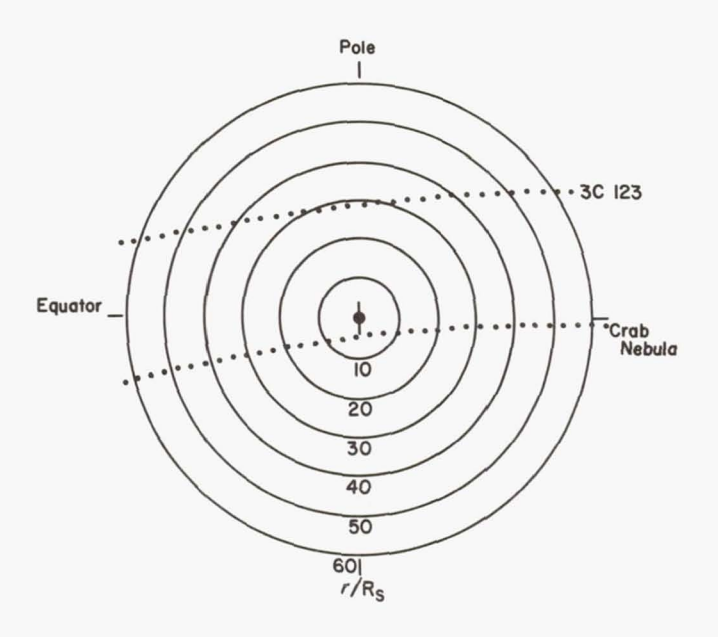


Fig. 1. Positions of the Crab Nebula and 3C 123 relative to the Sun in 1962

Radial Variation of Scattering

Figure 2 shows the variation with radial distance from the Sun of the angular size of the scattered distribution in 1959. ϕ_0 is the angular halfwidth (to 1/c) of the scattered distribution in a direction perpendicular to the radius vector from the Sun. As shown later, this is the direction in which maximum scattering occurs. These observations were made at frequencies of 38 and 178 Mc using the Crab Nebula, and the 178-Mc points have been scaled to 38 Mc according to the law $\phi_0 \propto$ (wavelength)² as shown by Hewish (Ref. 3). If ϕ_0 is assumed to vary as the x^{th} power of the radial distance, then the best straight line fitted to these points reveals a value for x of -2.24.

Similar observations made during an intermediate phase of the solar cycle, 1960–62, are presented in Fig. 3, 4, and 5. The 26.3-Mc points in Fig. 4 have been scaled to 38 Mc, while in Fig. 5, ϕ_0 denotes scattering in an east-west direction. These observations indicate a less steep radial variation of scattering, with a mean value for x of about -1.4.

Magnetic Fields

The radio scattering is anisotropic, and observations using interferometers with three different axes enable us to define the scattered distribution in the form of an ellipse. Such scattering indicates the

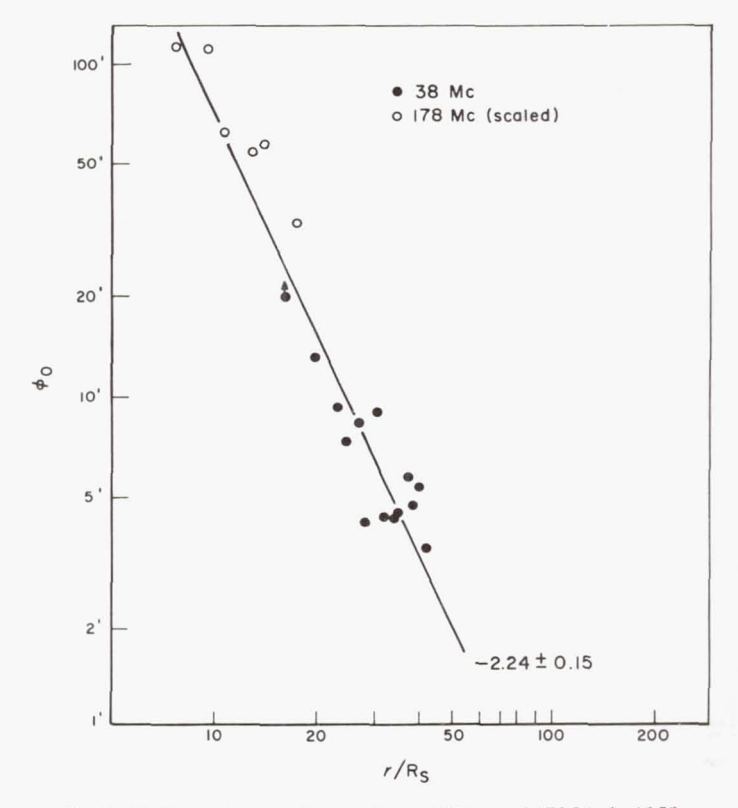


Fig. 2. Radial variation of scattering at 38 Mc and 178 Mc in 1959

existence of irregularities in the shape of elongated filaments, which scatter preferentially in a direction perpendicular to their length. By observing a source as it moves relative to the Sun, a series of ellipses is obtained whose minor axes trace out the mean direction of the filaments.

Figure 6 shows the mean directions of the filaments in 1958, 1959, and 1960 from observations of the Crab Nebula. The 1958 measurements are due to Högbom (Ref. 4) and those in 1959 to Gorgolewski and Hewish (Ref. 5). The directions are largely radial from the Sun, especially close to the equatorial plane.

The filamentary irregularities are maintained by magnetic forces, and their direction is also the mean direction of the coronal magnetic field.

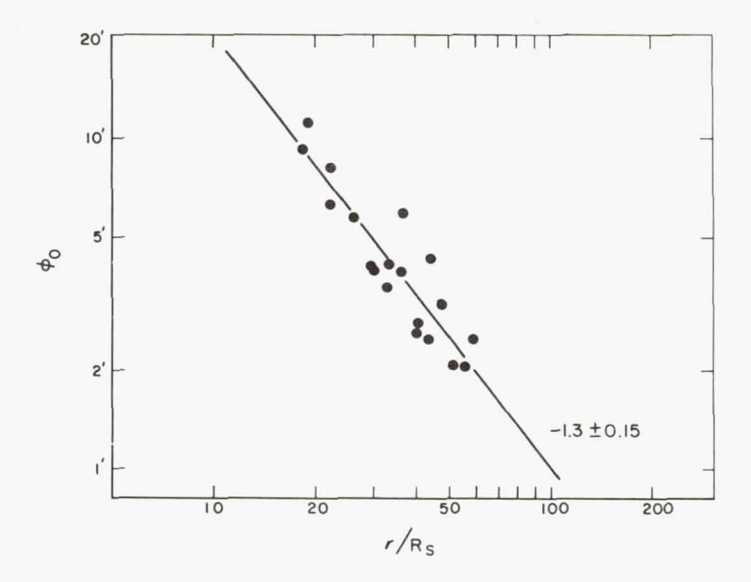


Fig. 3. Radial variation of scattering observed at 38 Mc in 1960

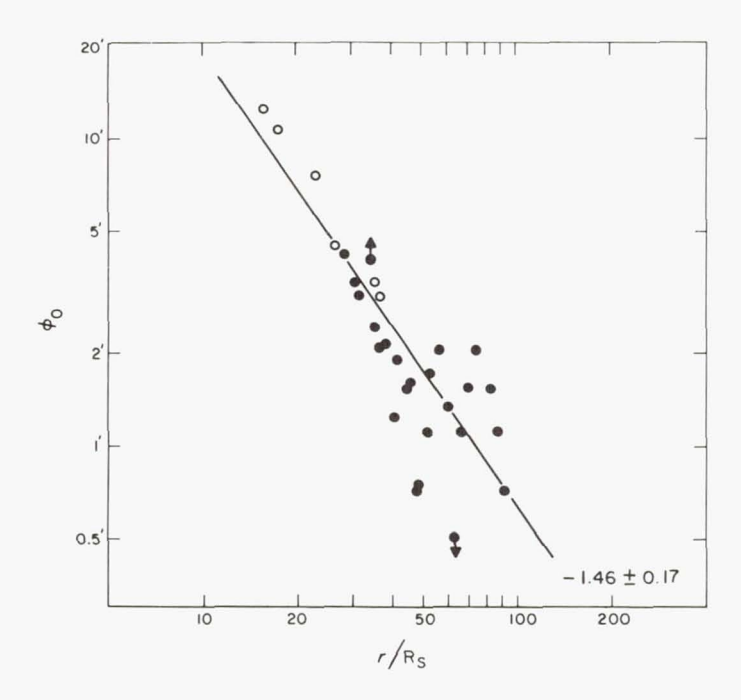


Fig. 4. Radial variation of scattering observed at 38 Mc (o) and 26.3 Mc (\bullet) in 1961

This provides independent evidence for a radial magnetic field, though the lines of force could be curved in the equatorial plane.

Latitude Effects

The two sources, 3C 123 and the Crab Nebula, provide scans across

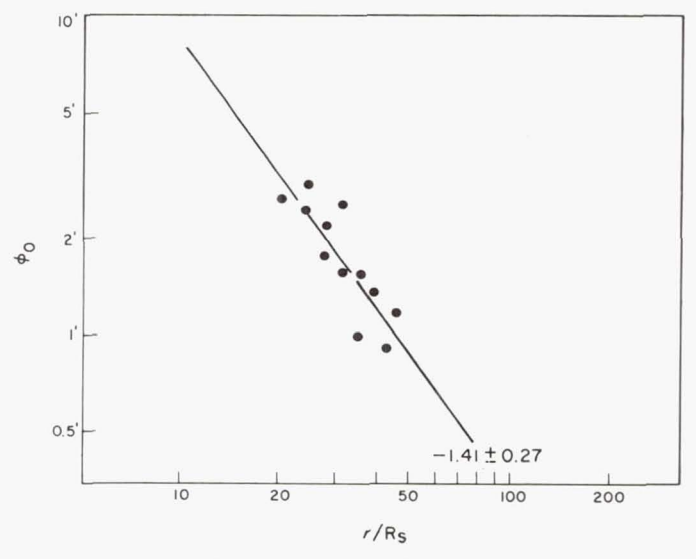


Fig. 5. Radial variation of scattering observed at 38 Mc in 1962

different regions of the corona and allow a comparison to be made of the polar and equatorial regions. The variation of the scattering angle ϕ_0 with heliographic latitude is shown in Fig. 7. The scattering is plotted as a polar diagram for three different radial distances in Fig. 7a, while Fig. 7b is a contour of constant scattering ($\phi_0 = 1.8$ min). The scattering becomes more pronounced towards the equator, indicating a greater concentration of filaments and/or higher electron densities.

Solar Cycle Effects

In common with most other solar phenomena, the magnitude of the radio scattering varies markedly with the phase of the solar cycle. This variation is illustrated in Fig. 8, where the scattering at several radial distances has been plotted vs. year. The effect is observable out to a distance of 40 $R_{\rm S}$, with the scattering peaking around sunspot maximum and decreasing toward sunspot minimum.

Upper Limit to the Scale of the Irregularities

It can be shown, using a ray theory due to Chandrasekhar (Ref. 6),

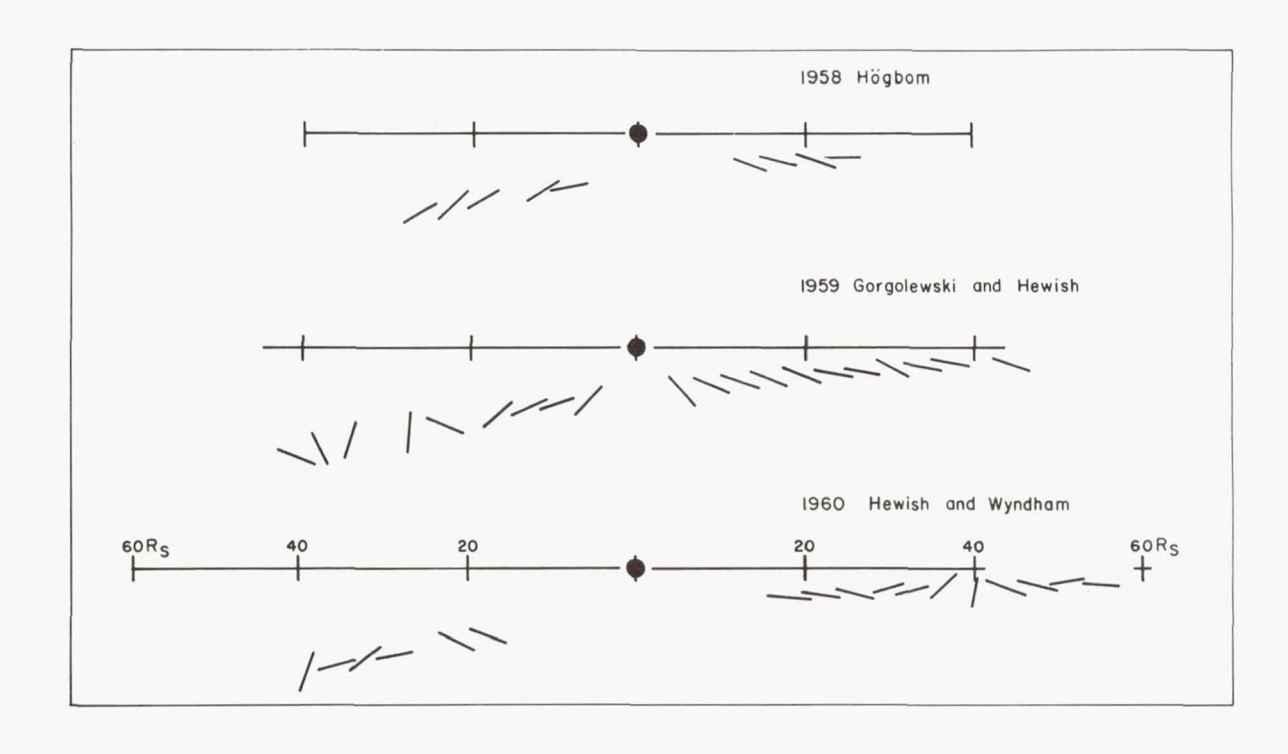


Fig. 6. Mean directions of coronal filaments

that when a point source is viewed through the corona, the scattered distribution of radiation is not smooth. It contains fluctuations in intensity on a scale comparable to that of the coronal irregularities themselves. In this case, a multiple-scattering mechanism is operative, for which $\phi_0 \propto (\text{wavelength})^2$, and any observed value of ϕ_0 sets an immediate upper limit to the angular size of the irregularities.

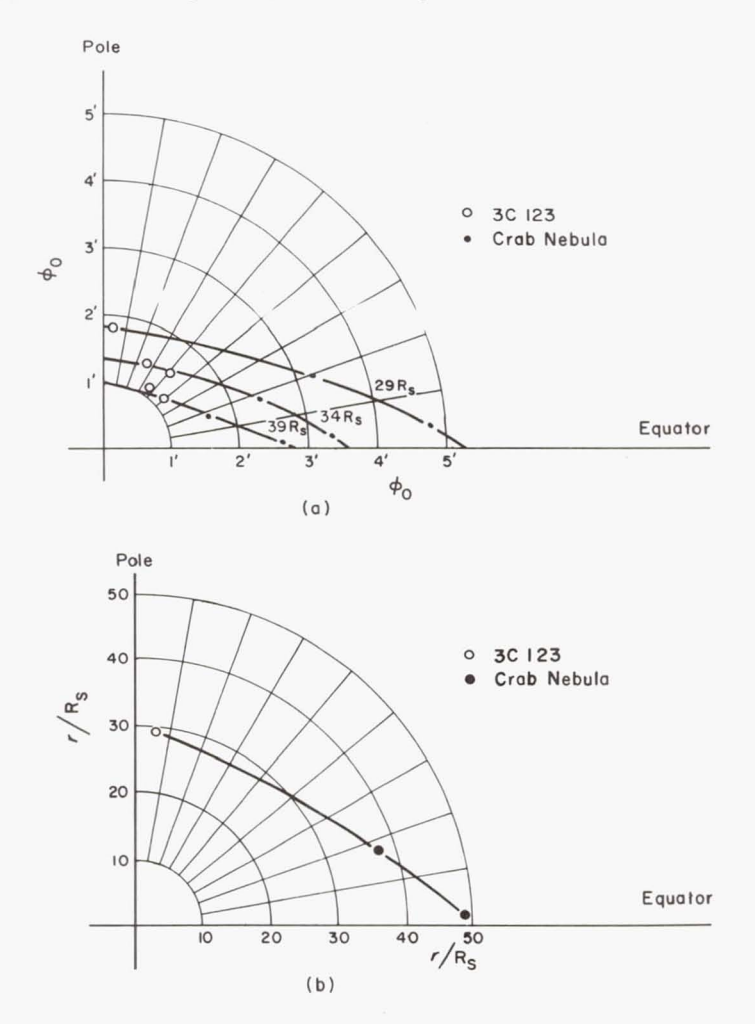


Fig. 7. (a) Values of the scattering at three radial distances, plotted as a polar diagram, and (b) a contour of constant scattering, for $\phi_0 = 1.8 \text{ min}$

The smallest scattering angle yet observed was measured by Slee (Ref. 2), who used an east-west interferometer with a 10-km spacing and

a frequency of 85.5 Mc. Using the source 3C 273, he measured a value of ϕ_0 of 6 sec at a distance of 65 R_s. A comparison of this value with our own results for the same period at a frequency of 38 Mc shows that the scattering angle ϕ_0 did indeed depend on the square of the wavelength.

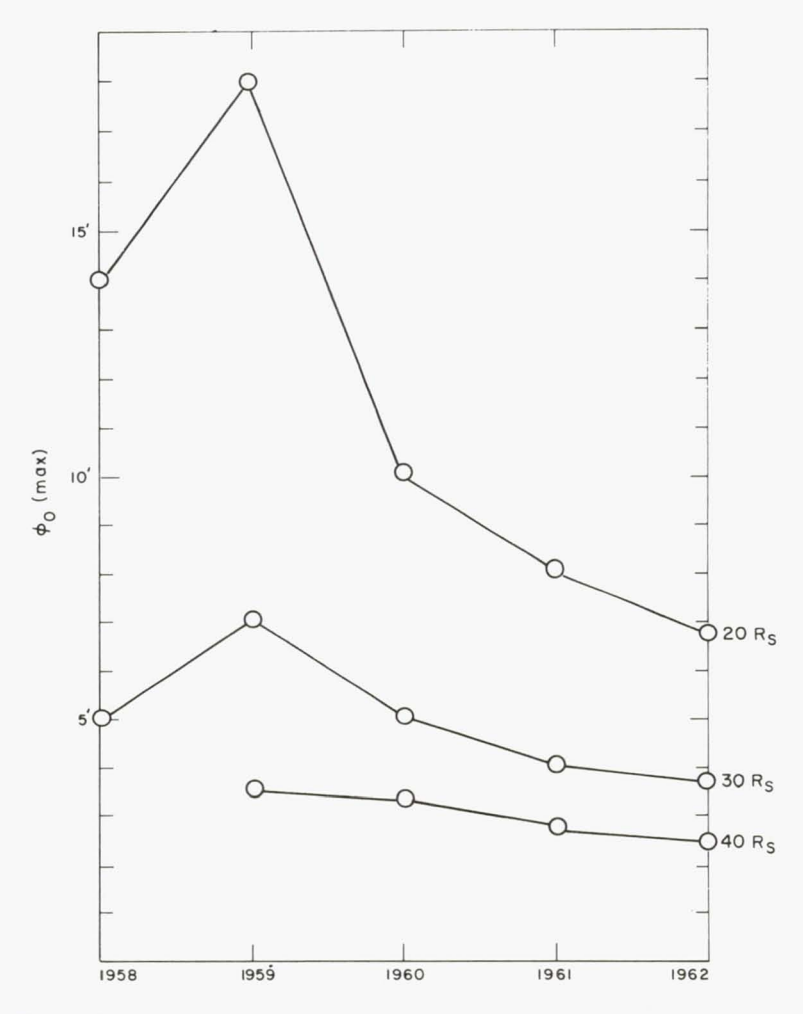


Fig. 8. Variation of scattering with the phase of the solar cycle at 20, 30 and 40 R_S

Hence the angular size of the irregularities is less than 6 sec. At the distance of the Sun, this angle corresponds to a physical size of less than 5×10^3 km, which is an upper limit for the lateral scale of the filamentary irregularities. If we extrapolate back to the surface of the Sun, assuming

the lateral scale to be proportional to radial distance, we find that these filaments would have a size of about 100 km, which is of the same order as the scale of the photospheric granules and chromospheric spicules. Our observations would indicate, therefore, that the fine structure we see on the Sun extends far out into the corona.

The value of 5×10^3 km is to be regarded as a definite upper limit for the width, at 65 R_s, of the filamentary irregularities responsible for the radio scattering.

A Model of the Solar Corona

A simple model of the extended corona, consistent with the radio

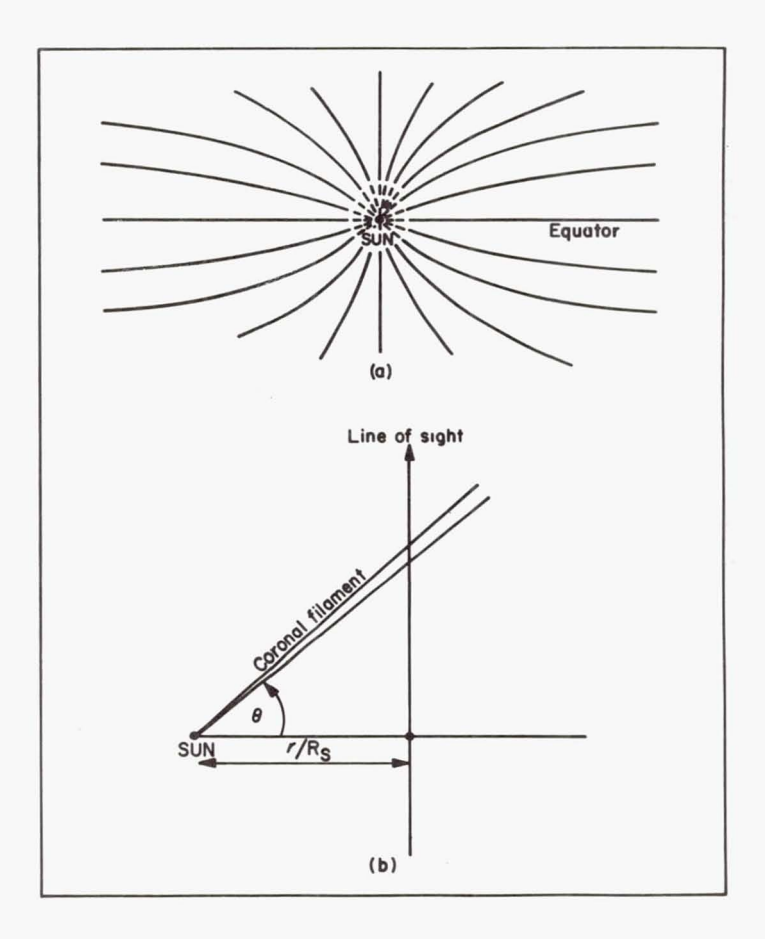


Fig. 9. (a) The model adopted for a restricted outflow, as seen from the equatorial plane, and (b) the geometry of the scattering model, as seen from above the North Pole

data, has been constructed in the following manner. The corona is regarded as a collection of filaments. In the equatorial plane (Fig. 9b) the filaments are radial from the Sun, with a lateral scale proportional to the radial distance. It can be shown that over the range of distance covered by the observations (20 to $80~R_{\rm s}$), the conclusions reached are not affected by curvature of the filaments in the equatorial plane. In a perpendicular plane (Fig. 9a), we have allowed the possibility of curved flow lines, the

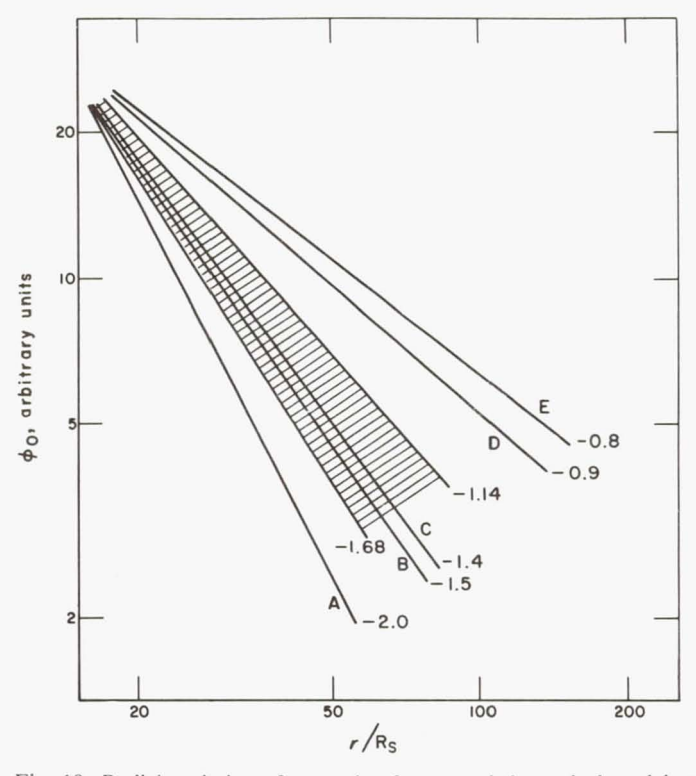


Fig. 10. Radial variation of scattering for several theoretical models compared with the observations:

A.	Parker	$\alpha = 1$
B.	Chamberlain	$\alpha = 1$
C.	Parker	$\alpha = 0.7$
D.	Chamberlain	$\alpha = 0.7$
E.	Parker	$\alpha = 0.4$

lateral scale of the filaments varying as distance to the power α , where $0 \le \alpha \le 1$. For $\alpha = 1$, the corona is spherically symmetric; while for $\alpha = 0$, it is disk-like in the equatorial plane.

Assuming the equation of continuity to hold for flow along a filament, we have calculated the radial law of scattering for a series of models. In

these models the velocity of outflow varies between a rapid solar wind, as proposed by Parker (Ref. 7), and a gentle expansion in which the material just escapes from the Sun, as proposed by Chamberlain (Ref. 8). For the case of the solar wind, the velocity is assumed to be constant beyond $20~R_{\rm S}$, the point at which our observations begin.

Figure 10 shows some results. The shaded region gives the range of slopes (values of x) in which a model must lie to be consistent with the observations made during the period 1960-62 (Fig. 3, 4, and 5). Some

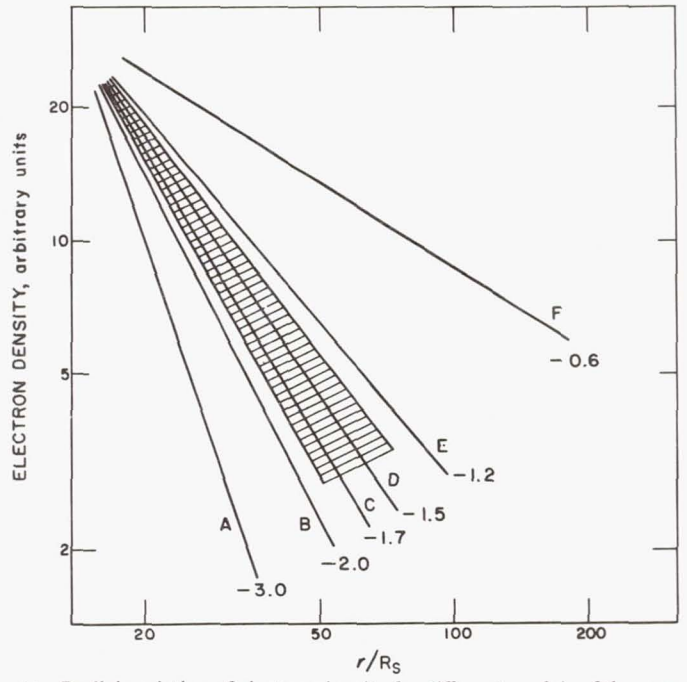


Fig. 11. Radial variation of electron density for different models of the corona:

A. Ingham (Ref. 9)

B. Parker $\alpha = 1$ C. Parker $\alpha = 0.7$ D. Chamberlain $\alpha = 1$ E. Chamberlain $\alpha = 0.7$ F. Chapman (Ref. 10) $T_0 = 10^{6}$ °K

theoretical models are also shown. It is apparent that a spherically symmetric outflow, according to Chamberlain ($\alpha=1$, model B), and a restricted solar wind ($\alpha=0.7$, model C) are both in accord with observation. A spherically symmetric solar wind (model A) is not in agreement with our results for this intermediate phase of the solar cycle. The steeper slope obtained in 1959 (Fig. 2) would, however, point to a solar wind with spherical symmetry close to sunspot maximum.

Using our model and the 1960–62 results of the variation of scattering with radial distance, we have calculated the limits within which the radial law of electron density must lie. These are illustrated by the shaded region of Fig. 11, together with some other models for the electron density variation. As a steady solar wind is now well supported by space-vehicle measurements, these results indicate that density depends on radial distance as $r^{-1.7}$ for distances from 20 to 80 $R_{\rm S}$ and probably beyond (model C).

REFERENCES

- 1. HEWISH, A. and J. D. WYNDHAM, Monthly Notices of the Royal Astronomical Society 126, 469 (1963).
- 2. SLEE, O. B., Monthly Notices of the Royal Astronomical Society 123, 223 (1961).
- 3. HEWISH, A., Monthly Notices of the Royal Astronomical Society 118, 534 (1958).
- 4. HÖGBOM, J. A., Monthly Notices of the Royal Astronomical Society 120, 530 (1960).
- 5. GORGOLEWSKI, S. and A. HEWISH, The Observatory 80, 99 (1960).
- CHANDRASEKHAR, S., Monthly Notices of the Royal Astronomical Society 112, 475 (1952).
- 7. PARKER, E. N., Astrophysical Journal 132, 821 (1960).
- 8. Chamberlain, J. W., Astrophysical Journal 133, 675 (1961).
- 9. INGHAM, M. F., Monthly Notices of the Royal Astronomical Society 122, 157 (1961).
- CHAPMAN, S. and H. ZIRIN, Smithsonian Contributions to Astrophysics 2, No. 1, 1 (1957).

DISCUSSION OF WYNDHAM PAPER

LÜST: I have one question concerning the electron densities. Your results are concerned only with slope, but if you assume the scale of the irregularities which you have given, 5×10^3 km, would it not be possible to determine the absolute variance of the density?

WYNDHAM: No, because you have to know the number of irregularities through which the radiation passes.

LÜST: What if you put in your scale and make some assumptions about the number of irregularities?

WYNDHAM: There are two possibilities: you could have closely-packed filaments, or you could have just a few widely-spaced filaments. These two cases give widely different figures for the variation in electron density, and for the mean density.

In order to obtain limits between which the electron density must lie, we have made some calculations in which we assumed either closely-packed filaments or just a few filaments in the line of sight. At a distance of $20~R_{\rm S}$, assuming a scale of 5×10^3 km, the density in a filament lies between 7.5×10^3 /cm³ and 300/cm³, and the mean density lies between 10/cm³ and 300/cm³.

DEUTSCH: Did you not tell me in private conversation that the density irregularities could correspond to a deficiency of electrons?

WYNDHAM: This is true. The irregularities could be holes in a continuous corona. We don't know what the mean density is. The filaments could be all there

is of the corona, or the filaments could be small fluctuations of a much larger mean density.

DAVIS: You speak of the curved-flow pattern out to distances of 20 or 30 R_s or more. This pattern would seem to require, with a high-velocity wind, very substantial forces to produce the resulting acceleration.

WYNDHAM: Yes.

DAVIS: There is another interpretation possible. Could you get away with another structure that has the curvature of the filaments without having to have the velocity follow the same pattern?

WYNDHAM: I am unable to answer that question.

GOLD: Why can we not measure the mean refractive index, at the nearest approach, for a source that is crossing somewhat above the Sun? Why can we not find the source displacement as it goes across?

WYNDHAM: These observations relate to distances greater than $20R_S$. Only at distances of the order of $5R_S$ does refraction become large enough to be measured by our techniques.

GOLD: Even with widely-spaced antennas?

WYNDHAM: At large radial distances, the scattering effect would mask any refractive effect.

At distances of closest approach, you have a complicated situation in which refraction and scattering can occur together; furthermore, a complicated scattered distribution results because the lines of force are radial rather than parallel. It is difficult to disentangle all these effects.

BIERMANN: You mentioned that your filaments have, at most, a diameter of 5,000 km. I think we see about the same size in the plasma tails of comets. I wonder whether the evidence from the *IMP* included anything that could be compared or related to this.

NESS: The length scales implied by the *IMP* magnetometer data are strongly prejudiced by the local solar-wind velocity, since the instrument only observes the structure streaming past it. 5,000 km is about the smallest scale one could take as being indicated by our data.

PETSCHEK: I thought the data from *IMP* showed variations on much longer time scales (implying larger distances), while your statement is that you have no fluctuations over larger distances. Is there some disagreement here?

WYNDHAM: We fancy a model in which the filaments responsible for the radio scattering tend to have a structure no greater than 5,000 km at a distance of 65 R_s. They can be as long as you like, but this is the lateral scale.

PARKER: Would larger structures actually interfere with your interpretation? **WYNDHAM:** Yes. We could not explain our observations by scattering from coronal filaments whose scale was greater than 5,000 km.

PARKER: Suppose you had a scale of a million kilometers, would you see it at all?

WYNDHAM: If we had a scale that large, all we would see, I should think, is a displacement of the source without any increase in diameter, depending upon the density.

PARKER: But you wouldn't see displacement because it would be less than your resolution?

WYNDHAM: Probably.

PARKER: It would not interfere with your interpretation, is that correct?

WYNDHAM: This is true.

GOLD: I think all you really meant to say is that you cannot interpret your

observations with large structures. However, your observations have nothing to say about whether large structures are present or not. You can only say that there is a sufficient number of small structures present.

WYNDHAM: That is correct.

WILKERSON: You mentioned that the scattering was checked at two wavelengths at least. Was it checked at more than two?

WYNDHAM: This particular observation was only checked at two wavelengths. WILKERSON: To what extent can you justify looking at only two wavelengths? WYNDHAM: In previous observations made at several different frequencies, it has been shown in all cases that the scattering depended on the square of the wavelength. This same dependence on wavelength was found to hold in the present instance, to within our experimental error.

HESS: How long does it take to make one measurement? What kind of time variations might one try to look for?

WYNDHAM: We look at the amplitude of the source once each day for a period of a few minutes to a half-hour, depending on the resolution of the antennas. We have observed no time variations with periods less than a day, although other workers have published accounts of rapid events with time scales of the order of minutes.

BRATENAHL: I was curious about the map of the orientation of filaments. These things probably are changing with time, although different filaments are mapped on different days, of course.

WYNDHAM: Each line is a single day's observation. A line represents the mean direction of the field on that particular day.

LÜST: Has this filamentary structure been detected so far using only the Crab Nebula, or are there data available from the other source?

WYNDHAM: The observation of radio scattering, using any source, points to an irregular structure. Whether this structure is filamentary can only be determined by making observations with resolution in different directions. So far, only the Crab Nebula has been used for this purpose, so observations with other sources say nothing about the shape of the irregularities.

LÜST: Or about the size?

WYNDHAM: Simultaneous observations at different frequencies with any radio source will enable us to say something about the size. Observations of the source 3C 123 were made at one frequency only.

CHAPTER VIII

WHAT WE KNOW AND WHAT WE DON'T KNOW ABOUT THE SOLAR WIND

H. S. BRIDGE

Massachusetts Institute of Technology, Cambridge, Massachusetts

Theoretical Setting

In order to have a basis for discussing what we know (or don't know) about the solar wind, I should like to cast these remarks in the framework of Parker's theory. I don't mean to imply that Parker's theory is the correct one, or that there is any feature about it that is correct; but I think that it does provide a frame of reference in which we can examine both the experimental results and the theory.

Figure 1, from Axford, Dessler, and Gottlieb (Ref. 1), shows an extension of Parker's ideas. It is a solution to the hydrodynamic equation giving a flat velocity profile from near the Sun out to some boundary. The flow pattern produces spiral magnetic-field lines that co-rotate with the Sun. In this model the termination of the spiral structure at the outer boundary of Region I is supposed to result from the balance of some dynamic pressure that the wind is running into. In Region II, the field presumably gets wound up; this region is some sort of turbulent region. Ultimately the field becomes detached by dissipative processes and wanders off into the stellar system, thus preventing the turbulent fields in Region II from increasing their intensity without limit.

The interesting feature of this picture, of course, is that there must be some sort of turbulent structure in Region II. A situation of this kind provides a possible explanation of the 11-yr modulation cycle of galactic cosmic rays. The idea is that the general radial motion of the plasma pumps out magnetic-field irregularities, and that the cosmic rays diffuse into the solar system against the flow velocity. Furthermore, the transit time of the gas up to this point is of the order of a year or so, so that, if the plasma velocity changes, there is a relaxation time involved that may help to explain some observed details of the cosmic-ray cycle.

What We Would Like to Know

Let me summarize briefly the plasma properties that we would like to measure experimentally. We would like to measure: the bulk velocity of

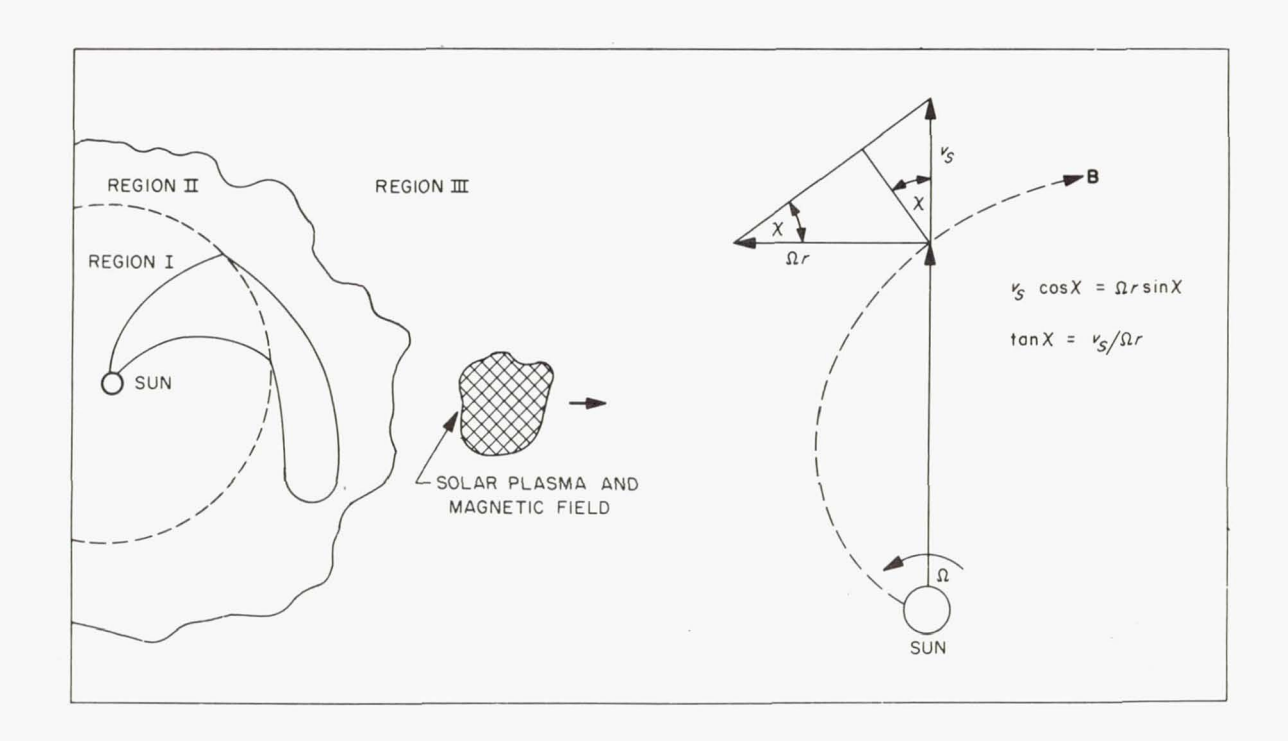


Fig. 1. Model of the solar wind with imbedded magnetic fields. (From Ref. 1)

the plasma motion; the direction of the flow; the longitudinal spread in velocity, which gives us some idea of the temperature; and the transverse velocity spread, which tells us whether the distribution in the rest system is isotropic. We would like to know the electron energy distribution; we would like to know the magnetic-field directions and magnitudes; we would like to know something about the correlation between the magnetic-field fluctuations and the motions of the electrons, a subject about which we know very little at the present time. Then, of course, we are concerned with the general spatial features of all these properties, say in azimuth and in radial distance; and we would like to know how these features vary with time.

Now let me make just a few comments about these quantities—about how we measure them and why. The energy of the bulk motion is mostly contained in the positive-ion component; in fact, for reasonable plasma velocity, the kinetic energy of the free electrons is so small compared to that of the positive ions that it can be neglected. Consequently, most of the experimenters have devoted their attention to the positive ions. According to various theoretical models and experimental evidence, one wants to measure protons in the energy range from about 10 ev to perhaps 20 kev. Most of the energy measurements at present cover only a fraction of this range. Later I shall explain my reason for thinking that these limits are important.

Various schemes have been used for measuring the proton energy; all of these schemes involve electrostatic analysis, and so they measure the kinetic energy per unit charge. When we try to identify the composition of the particles, however, we need in addition some sort of velocity analysis, which so far has not been made. But even with a velocity analysis, one cannot determine the mass uniquely: one can determine only the mass per unit charge. So the identification of particle composition has barely begun; much additional work still needs to be done.

I should like to point out, too, that the energy resolution and coverage of present instruments are really not sufficient to do the job, particularly in respect to the overlapping of energy ranges by samples whose spacing is comparable to the energy window. One would really like to determine the energies to within about 1%, and one would like to have energy windows that overlap so that they lead to a good measurment of the total plasma flux. If you then consider an energy range that extends over more than three decades, you have an impossible problem in technique. Inherently, then, the plasma measurements require a long time and are difficult measurements to make.

Good energy resolution is important, because the temperatures and velocities of the plasma can vary widely, depending on where the plasma is. If the plasma goes through a shock transition from a region of highly supersonic flow, you expect the angular distribution to become isotropic; so you want to measure a rather high temperature, which is concurrent with perhaps a rather low mean drift energy.

I think these problems are being attacked at the present time, but the fact is that our present instruments are far from ideal.

What We Have Learned from Early Experiments

To summarize the solar-wind experiments is quite a job, and the really relevant experiments have been explained in a detail that I could not possibly give them. Nevertheless, I should like to reiterate some of the main features of these experiments.

Table 1 (Ref. 2) summarizes solar-wind measurements up to and including the recent *IMP* satellite (*Explorer 18*), with emphasis on the properties of the particles rather than on the properties of the magnetic field. I have omitted the Russian Mars shot from this table, because I didn't have much information about it.

Figure 2 summarizes graphically the various measurements that have been made by spacecraft. Some of the orbits have been rotated about the Earth–Sun line into the ecliptic—the aim was to get an appropriate representation of the orbits relative to the position of the Sun, which controls what goes on around the Earth. The procedure would be valid if the flow were axially symmetric about the Earth–Sun line.

Pioneer 1 carried a magnetometer, and from about 12 R_E to perhaps 14 R_E it recorded a magnetic field with rather large fluctuations. Beyond 14 R_E , the field dropped off to quiet values. There was a lack of transmission at distances less than 12 R_E , so that the fluctuations probably extend farther back toward the Earth than shown.

The same behavior was observed by *Pioneer 5*, whose orbit was toward the evening side. Here again the magnetic field showed large fluctuations from $10 R_E$ to about $15 R_E$.

A number of relevant particle measurements have been made, such as the Russian measurements made by Lunik 2 on the night side of the Earth. During the Lunik-2 flight, data concerning positive- and negative-ion fluxes were transmitted until the spacecraft hit the Moon, although between 30 and 40 $R_{\rm E}$ there was unfortunately no transmission of data because the spacecraft was not within range of the receiving stations. An interesting feature of this flight is that, in the region between 12 and 30 $R_{\rm E}$, no values of positive flux were recorded. Since the absolute sensitivity of the Russian instruments appears to be about $10^8/{\rm cm}^2$ sec, it is not surprising that the Russian workers didn't observe anything in this region. Lunik 2 did observe an electron flux at a distance of about $10~R_{\rm E}$, and a flux of positive ions beyond $40~R_{\rm E}$. It is important to remember that the Russian experiments really measured the flux of positive ions

TABLE 1. SUMMARY OF SOLAR-WIND MEASUREMENTS¹

Vehicle	Date	Direction				
		Az (hr)	Incl (deg)	Apogee R _E	Principal results, plasma and fields	Remarks
Pioneer I	Oct 11 1958	12.2	+5	18.6	Large $\Delta B/B$, ?-13.5 R _E B _{int} < 6 γ if nonradial	$A_{\mu} \sim 5$ measurements from 12.3–14.8 R _E
Pioneer 4	Mar 3 1959	8.5	-18			
Lunik 2	Sept 12 1959	21	-7		7.9-11.8 R _E , $\phi^- = (1.5-4)10^8$ 11.8-30 R _E , $\phi^{\pm} \sim 0$	200 ev < E < 20 kev Roll modulated
Lunik 3	Oct 4 1959	16.2	-8		Many cases $\phi^+ < 10^8$ 19.8 R _E , $\phi^+ = 4 \times 10^8$	Roll modulated
Pioneer 5	Mar 11 1960	16.5	+25		Large $\Delta B/B$, 9.4–15.7 R _E $B_{\perp} \sim 3\gamma$ quiet, 5–60 γ disturbed	Launched during recovery phase of storm First satellite detection of Forbush decrease
Venus probe	Feb 12 1961	17.5	+ 10		26 R _E , $\phi^+ \sim 2 \times 10^8$ 297 R _E , $\phi^+ \sim 1 \times 10^9$	Plasma probe Sun oriented E > 50 ev
Explorer 10	Mar 25 1961	20.8	-35	46.6	$v \sim 300 \text{ km/sec}$ $\phi^{+} \sim 2 \times 10^{8}/\text{cm}^{2} \text{ sec}$ $T \sim 5 \times 10^{5} \text{ 'K}$	Detailed observation of B in magnetosphere boundary region
Explorer 12	Aug 15 1961	(13→8)	-33	13.1		Detailed observation of magnetosphere boundary
Mariner 2	Aug 27 1962				Typical values: v = 360-700 km/sec $n = 0.3-10/\text{cm}^3$ $T = 6 \times 10^4-5 \times 10^5 \text{ °K}$	Plasma detector solar oriented, 104 days of data
Explorer 14	Oct 2 1962	(8.5→18)	-33	16.4		Detailed observation of magnetosphere boundary
Explorer 18	Nov 27 1963	(12→6)	-33	31	$v \sim 250-440 \text{ km/sec}$ $\phi^+ \sim 3-8 \times 10^8/\text{cm}^2 \text{ sec}$	Detailed observation of magnetosphere boundary, transition region, and inter- planetary space

'See Ref. 2

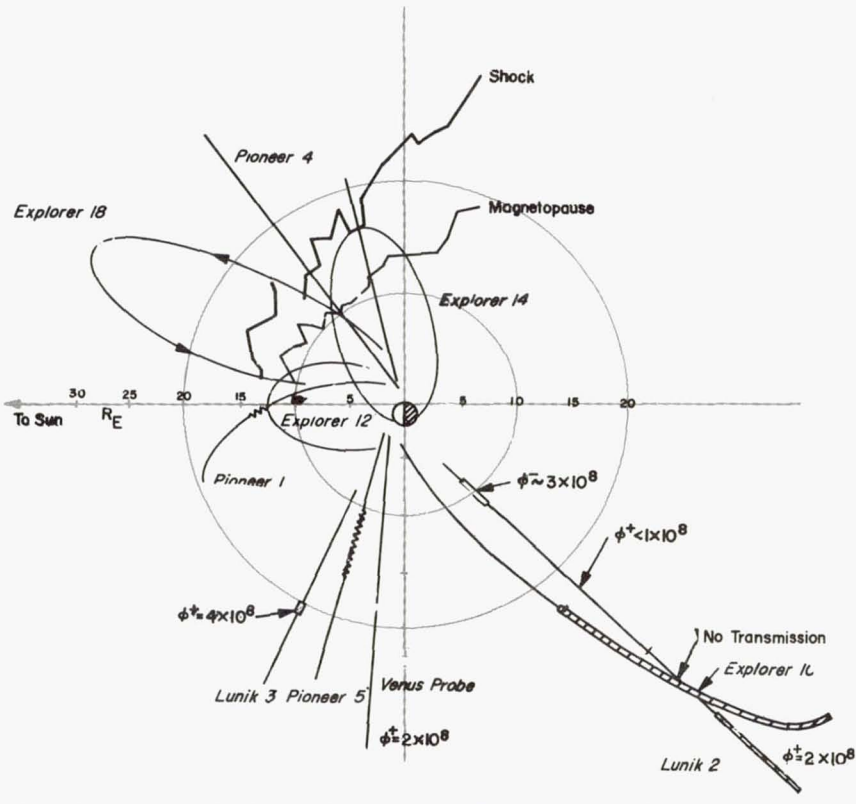


Fig. 2. Graphic summary of solar-wind experiments, showing spacecraft trajectories in Earth-Sun coordinates

above about 15 ev. From that flux you must subtract any flux of electrons with energies high enough to pass the negatively-biased outer grid. The kind of trap that was used (Fig. 3) really measured the difference between the electron flux above a certain energy and the proton flux above a certain energy.

The *Lunik-2* result for positive ions is, of course, consistent with the results obtained by *Explorer 10*. Figure 2 doesn't show the fluctuations in

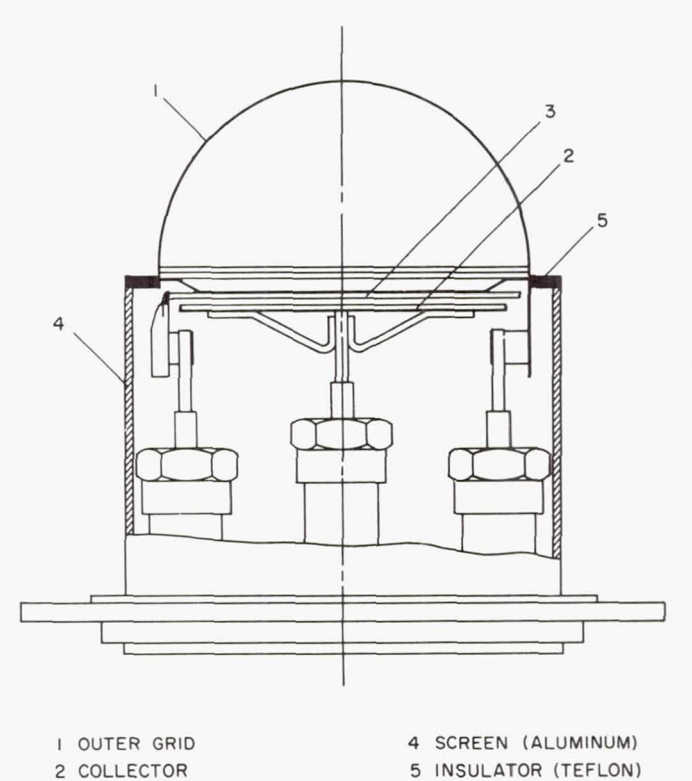


Fig. 3. Russian ion trap

3 INNER GRID (TUNGSTEN)

plasma properties observed by Explorer~10; but starting at 22 R_E and continuing throughout the rest of its useful life, Explorer~10 observed alternate periods of "plasma" and "no plasma."

Lunik 3 also encountered positive-ion fluxes, this time amounting to about $4 \times 10^8 / \mathrm{cm}^2$ sec. Unfortunately, these measurements were not continuous, so the plasma flow cannot be mapped as a function of the position of the probe. Again in this measurement, the ion energies were not well determined.

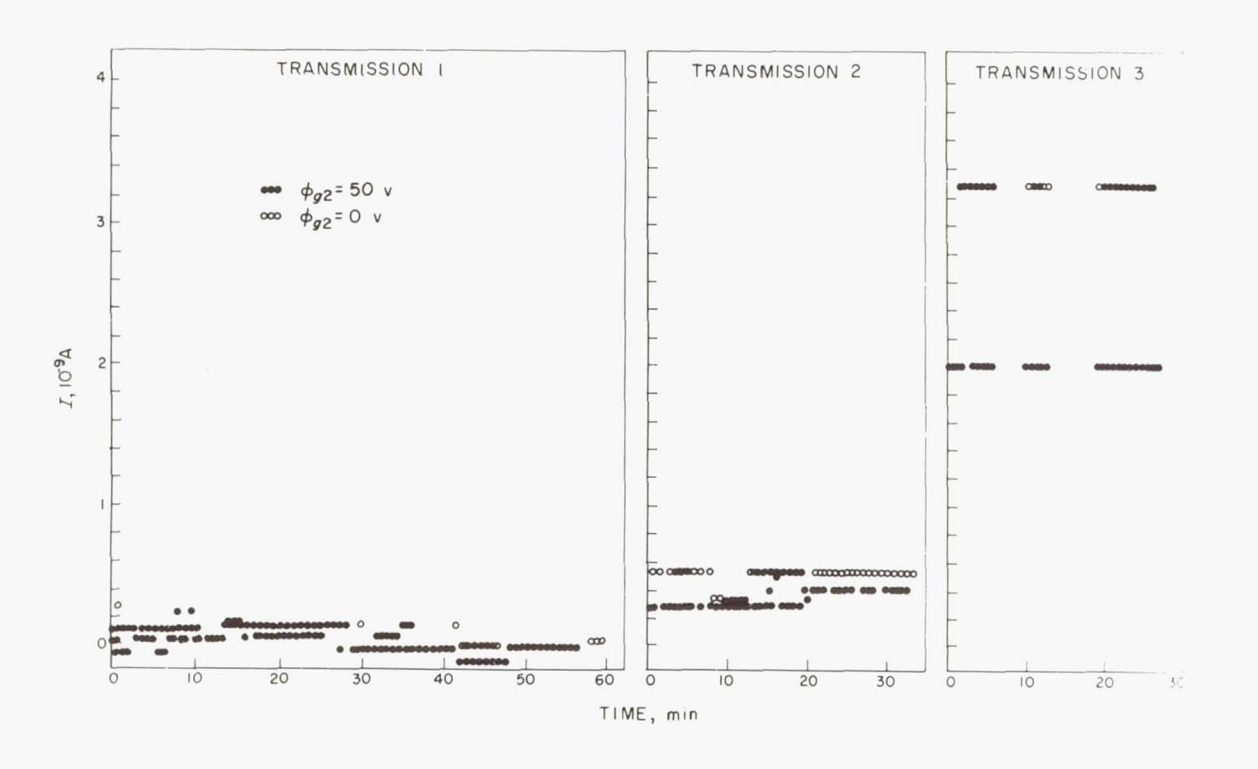


Fig. 4. Sample of results from the Russian Venus probe of 1961. Transmission 1 is from inside the magnetosphere, transmission 2 from slightly outside, and transmission 3 from still farther out

The same sort of results were obtained on the Russian Venus shot. The left section of Fig. 4 is a "transmission" of the observed currents inside the magnetosphere, which were very low; the center section shows the currents observed outside the magnetosphere; and the right-hand section shows the currents observed at an even greater distance. The fluxes shown in the right-hand section correspond to something like $4\times10^8/\mathrm{cm}^2$ sec, and the two currents are the readings of two different traps with different bias conditions.

Extensive measurements were obtained on *Explorer 12* regarding the magnetic conditions at the boundary of the magnetosphere. Since these measurements do not pertain to conditions in interplanetary space, however, they will not be discussed further.

Explorer 14 certainly penetrated the magnetopause and may have penetrated the shock transition upon occasion, although the results that have been reported so far for the transition region are not very definitive. The lifetime of Explorer 12 extended from 13 hr (with respect to the Sun at 12 hr) around to about 8 hr: Explorer 14 has gone essentially all the way around, I believe.

The main point to be drawn from this résumé is that all of these results are consistent with our present picture, namely: a shock created on the sunward side of the magnetosphere by the plasma flow; inside the shock, a transition region a few $R_{\rm E}$ thick; and inside the transition region, the magnetosphere. This picture tends to be confirmed by the IMP plasma results. Rough positions for the shock front and magnetopause, according to these results, are shown in Fig. 2 by the appropriately labelled solid lines. These lines connect the points where changes in plasma properties were observed. If you look at the positions at which the various earlier results were obtained, I think you will see that everything agrees moderately well.

What We Have Learned From IMP

Now I should like to talk about the results that were obtained by the MIT plasma probe on the *IMP* satellite and that pertain to the interplanetary region of space. The *IMP* results that pertain to the magnetosphere and to the transition region will be discussed later (Paper 21). I shall summarize only the main features of the data—there is little more I can do until more work has been done in the way of analysis. For a detailed description, we need to know the continuous time history of the flux and of the energy values; up to now we simply have not considered this kind of data.

Figure 5 shows the character of the roll modulation observed outside the magnetosphere (the satellite rotated at $\sim \frac{1}{3}$ rps). The probe is mounted so that the direction of view is perpendicular to the spin axis. As the

satellite rotates, the plasma flow in the azimuthal plane is sampled about every 20 deg, and the directional character of the flow can be seen by examining the current as a function of time (that is, as a function of rotation angle). The graphs correspond to different energy windows, and the arrows indicate the position of the Sun. You will notice that in a particular energy region the flux peaks at a particular angle: it is apparent that in

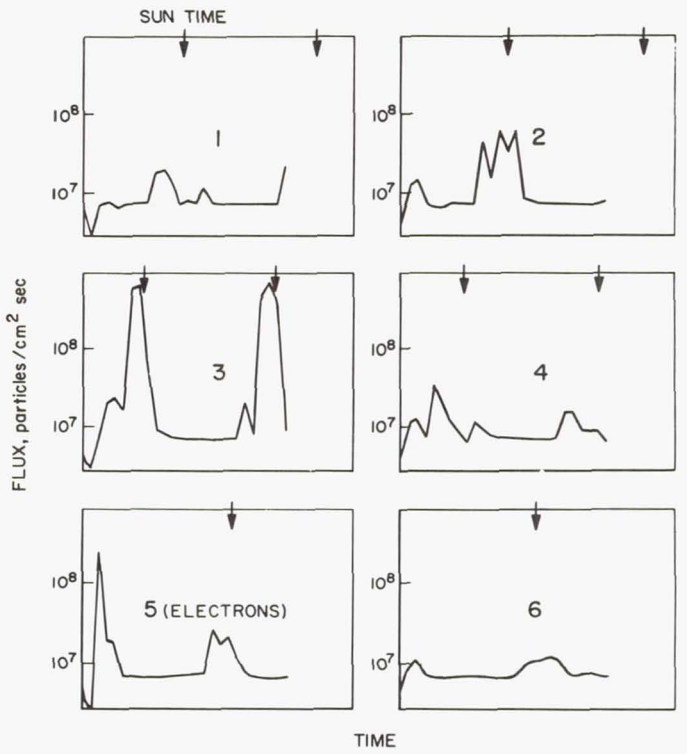


Fig. 5. *IMP* solar-plasma measurements for different energy windows. Data are from Orbit 10, outbound, taken at 17.8 R_E, a normal–Sun angle of 36 deg. an ecliptic latitude of –20.8 deg. and a solar ecliptic longitude of 286.3 deg.

the azimuthal plane the direction of plasma flow is within 20 deg of being radially outward from the Sun, just as we assumed it would be on the basis of previous results.

Figure 6 shows a section of the "summary" data from the inbound pass of a later orbit. On the first (top) line, an average value of the energy in ev is plotted as a function of time. The next (lower) section shows the plasma flux observed when the probe is pointed toward the Sun, compared with the minimum flux observed during the rotation. The values have been summed over the measured range of energies, so these lines represent the maximum and minimum total flux observed. You will notice that in

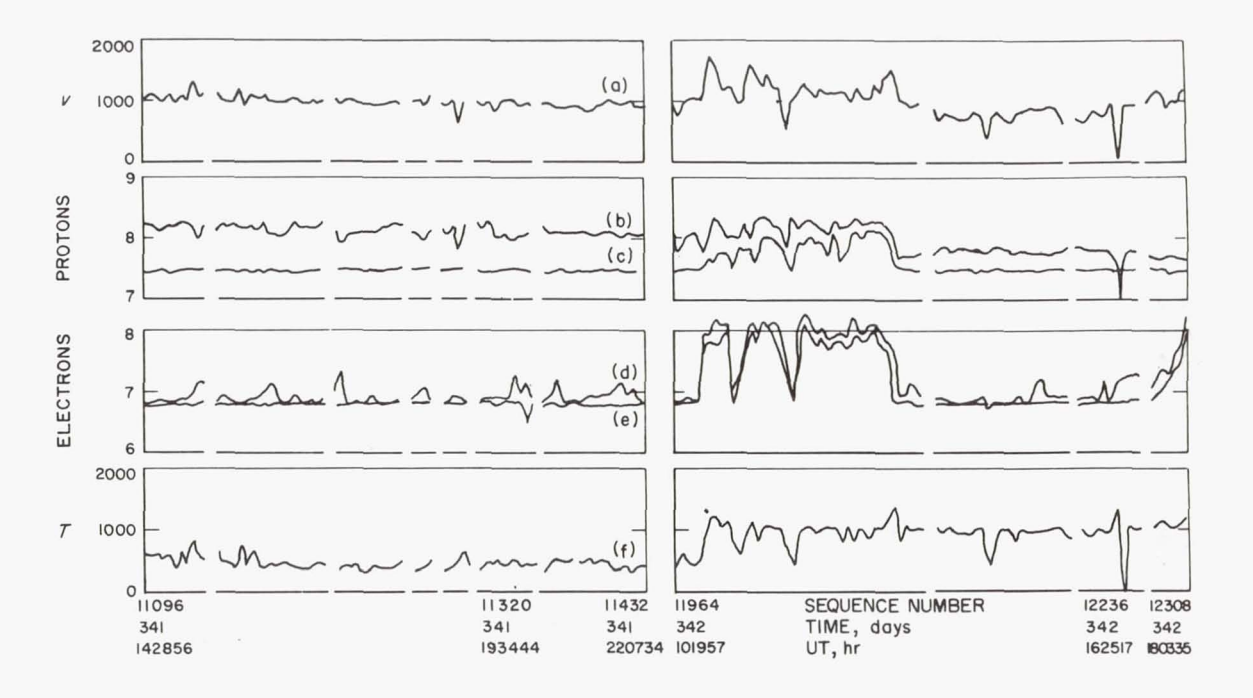


Fig. 6. Summary solar-plasma data from the inbound portion of the IMP orbit. V is mean energy; the next two lines are proton and electron fluxes on a logarithmic scale; and T is the second moment of proton energy distribution, believed to be suggestive of temperature

this particular section of data, conditions are quiet indeed; the energy and the flux are both fairly constant. In the next line we have plotted some electron data, which I don't want to discuss. (There is one electron energy window on the plasma-probe bias schedule. We hope it will give us some significant information, but we don't know what the data mean yet.) Finally, on the bottom line we have plotted something that is supposed to represent the plasma temperature. What you see on the right half of the figure is the transition into the magnetosphere. The initial jump in electron flux, for instance, would be called the shock. The next discontinuity would be the magnetopause, which will be discussed in more detail in Paper 21.

So this is the kind of summary data that we are getting, and it will, of course, be correlated with other satellite data as they come along.

NEUGEBAUER: What is the temperature? Does the figure say that the random energy is 20 or 30 percent of the flow energy? If so, it is much higher than that detected by *Mariner*.

LYON: You shouldn't associate the "temperature" plot with the thermal energy. The "temperature" is simply the second moment of the distribution, and includes noise.

BRIDGE: That is a problem. We plotted this quantity to get some indication of the change in the width of the energy distribution function as the satellite went through the shock front, but I don't know what it means quantitatively. It does seem to give one a nice measure of what happens, and it provides a way of looking at the data and of recognizing the large changes that occur in the plasma energy distribution.

WILKERSON: The left-hand electron curve indicates that the electrons are much more nearly isotropic than the protons.

BRIDGE: Yes, it does, except for the occasional little bumps between the shock and the magnetopause. The bottom line, which is the noise level, is about one-tenth of the electron signal. The noise in the proton channel is a little higher, because it is the sum of the noise in all five energy windows. We are essentially seeing energies that vary from a few hundred ev in the interplanetary region to a mean energy of something like a couple of kev in the transition region.

My discussion so far has concentrated on the direct plasma measurements. Let me just summarize what I think are the important features of those measurements. Most of what we really know about the behavior of the plasma in the interplanetary region comes from the *Mariner-2* results. The most important feature, which is now confirmed by the *IMP* results, is that the plasma really is there all the time. Its energy or velocity goes up and down; in fact, the *IMP* measurements, so far, show that the velocity varies from maybe 250 km/sec to maybe 400 km/sec. In spite of this variation, the velocity is generally very steady. However, I don't think one can really make general statements at this time about the properties of the plasma, other than the one statement that the plasma is always there. This is a fairly important statement. though, considering

the various theories of how the plasma is emitted from the Sun: it means that there are no large regions on the Sun that don't emit plasma.

What We Have Learned from Energetic-Particle Experiments

According to Parker's model, the properties of the plasma essentially determine the magnetic-field configuration that exists between us and the Sun. One way of studying the plasma properties is to study the motion of solar protons, which have been observed under a variety of conditions. So I would like to spend a few minutes talking about the present state of our knowledge concerning the propagation of particles from the Sun. Here I am in something of a predicament. People often remark that it is nice to have these interdisciplinary activities. But if you want to know something about the properties of plasma, for instance, you have to become involved in about three or four other disciplines about which you know nothing; this can be a bit of a handicap. So if I can't do anything else in this particle area, maybe by some erroneous remarks I can provoke comments from experts who know all about particles.

I think that our knowledge of how solar protons reach the Earth has recently been advanced by systematic consideration of the ways in which the particles can propagate. The Goddard group has been particularly active in this field, and these authors have emphasized that solar protons can reach the Earth in essentially four ways (Ref. 3).

First, there are high-energy flare particles that come almost directly from the flare to the Earth. In this case the rise time of the particle intensity is essentially comparable to the transit time; the intensity rises in a matter of, say, 20 or 30 min to full value.

The second mode of propagation is one in which a considerably longer time interval is involved, and which appears to be characteristic of a diffusion process; in this mode the rise time to maximum intensity takes hours. The types of flares that are likely to exhibit either of these first two types of behavior are now becoming pretty well understood, I think.

The third type of propagation is one in which particles emitted from the flare are trapped in the plasma that is emitted at the same time; the particles reach the Earth simultaneously with the arrival of the trapping region of the plasma.

The fourth type of propagation involves a class of particles whose presence apparently depends on solar rotation, and it is somewhat different from the third or trapping mode.

The first three types of propagation can be illustrated by the phenomena observed in connection with a single solar flare. Let me remind you of the sequence of events that occur during a solar flare. Normally the flare on the Sun is visible for a period of a few hours. The particle emission, however, apparently coincides very closely with the characteristic brightening

and broadening of the $H\alpha$ line. This brightening lasts for only a few minutes and essentially provides a time reference for the emission of the solar particles from the flare. A few minutes later, the solar cosmic rays begin to be observed at the Earth, and the delay corresponds to a time roughly equal to the transit time, assuming rectilinear propagation. As I have said, the characteristic rise time of the particle intensity depends on whether some sort of direct path exists between the flare and the Earth, or whether the particles have to diffuse to reach us.

Now, 1 to 2 days after this series of events, one observes marked effects on the Earth. In general, there is a sudden commencement, and shortly afterward there is a Forbush decrease. One explanation of these phenomena, which was advocated chiefly by Prof. Gold, is shown in Fig. 7 in connection with one of the more famous flare events. The right half of this figure illustrates what is called the magnetic-tongue or bottle concept. This concept explains the propagation of particles from the Sun to the Earth along magnetic lines of force that have been pulled out of the flare (b); it also explains the Forbush decrease in the galactic cosmic radiation (c). The point is that if this configuration exists at the time of the flare, then the particles propagate directly; if it doesn't exist at the time of the flare, the particles have to diffuse. Both of these types of propagation are illustrated by the flare of November 12, 1960.

The left half of Fig. 7 is an artist's representation of the supposed configuration, taken from Steljes, Carmichael, and McCracken (Ref. 4). The magnetic-field configuration was supposedly produced by the flare outbursts on November 10 and November 11. Its effect was observed on November 12 as a gradual rise in particle flux, which was followed by another increase in intensity when the Earth entered the trapping region. Had the November-12 flare occurred at a time when the Earth was already in the fields produced by the earlier flares, there would have been a rapid rise in intensity.

An interesting fact is that approximately 2 days after the November-12 event there was a sudden commencement, which corresponded presumably to the arrival of the plasma ejected at the time of the November-12 flare. The delay times for the onset of the magnetic activity at the Earth correspond to the direct transit time of protons with energies of the order of a few kev—say from 2 to 3 kev up to 20 kev. Thus, I think that one of the questions to be answered is: what is it that arrives at the Earth at this time? We know that whatever it is, it passes over the Earth very rapidly—in a matter of minutes. Presumably, it is the shock front that is emitted simultaneously with the plasma, but what does the plasma look like behind this shock front? How do these shocks propagate through the interplanetary medium?

I don't think that at this point we have any experimental evidence

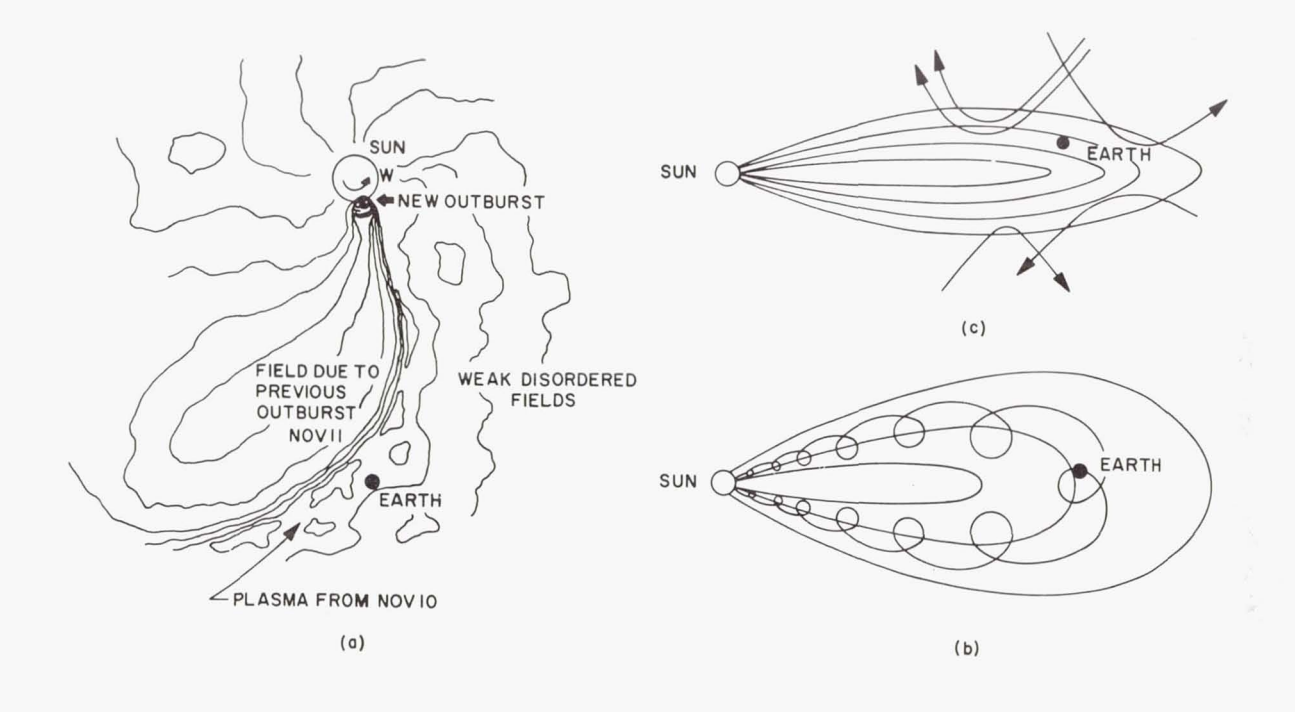


Fig. 7. (a) Model of the interplanetary field-plasma configuration during the solar flare of November 12, 1960. (From Ref. 4) (b) Action of solar magnetic fields to trap solar cosmic rays (c) Deflection of galactic cosmic rays by a magnetic field carried with the solar plasma

concerning these questions, or concerning the plasma conditions that exist in events of this magnitude. But we must plan to provide, during the next solar cycle, instrumentation that is capable of measuring these quantities, and it is important that the theorists tell us just how to design this equipment. Providing equipment that can measure up to 20 kev is a very different matter from designing equipment measuring to only 3 kev.

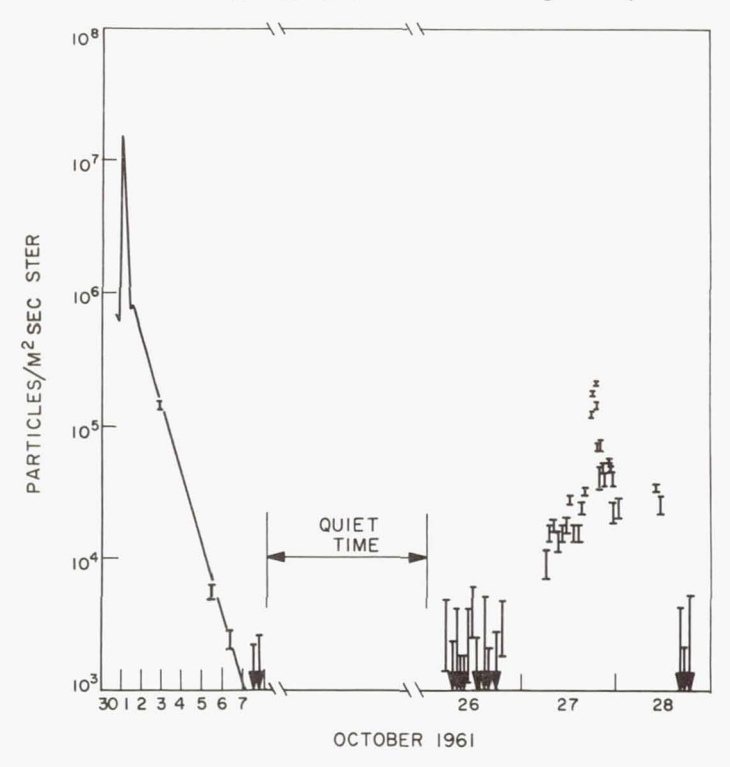


Fig. 8. Protons observed on *Explorer 12* presumably associated with the flare event of September 28, 1961. (See Paper 5)

Figure 8 is similar to one that Cline presented earlier (Paper 5) and illustrates the fourth type of particle propagation, the type that depends on solar rotation. It seems possible to me that in the flux rise of October 27, we see the Earth enter a trapping region that contains flare particles emitted back on, I think, September 28. These particles reached us originally by the diffusion process. Then 27 days later, we see the same protons again, with energies above a few Mev. On the basis of this evidence, I don't believe that these particles are continuously emitted from the Sun.

It must follow that in the plasma flow pattern there is a magnetic trapping region that contains these particles. Whether that trapping region is destroyed in the next 27 days, or whether all the particles leak out, I don't know. However, it seems perfectly clear that on the Sun there is a region that was previously the site of a flare; that the region emits particles that are somehow then contained in a field; and that the field envelops the Earth and must have some sort of boundaries separating it from the rest of the plasma. Now, what does the field region look like? How is it set up? Does it stay there? I think that the existence of this stream must mean that the lines of force are still connected to the Sun. They are rooted in the Sun, because if they became detached from the Sun, they would have had to live for 27 days, at least, within a distance of 1 AU.

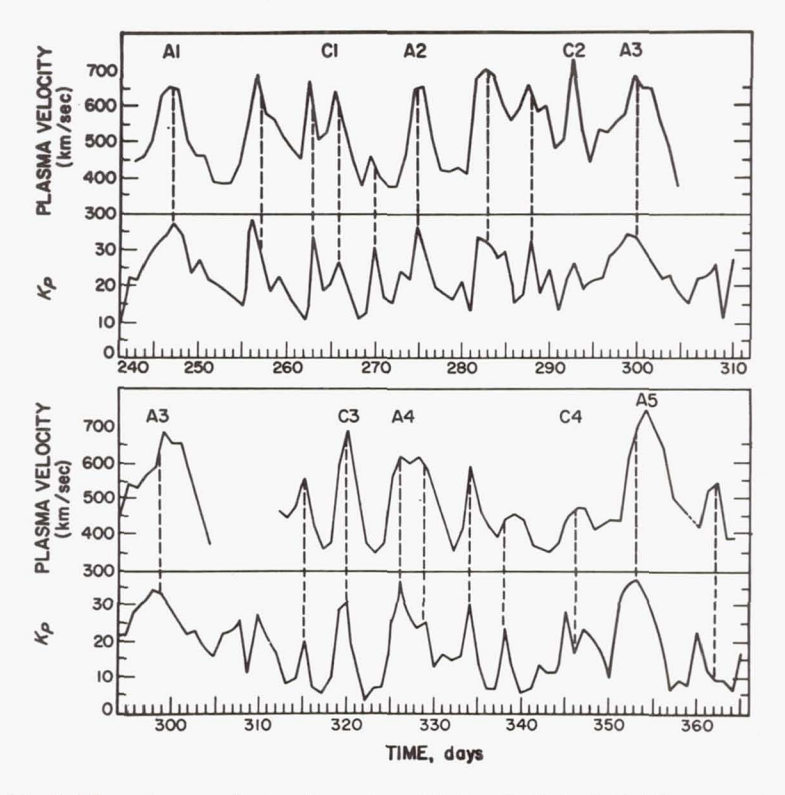


Fig. 9. Mean plasma velocity observed on *Mariner 2*; *Kp* is plotted for comparison. (From Ref. 5)

There is one other point that should be emphasized, namely: when the Earth entered this trapping region, there was a sudden commencement. Presumably this sudden commencement was associated with the boundary between the stream and the rest of the plasma. What did that boundary look like? It probably looked something like the boundary that exists after a large solar flare, when you see a magnetic storm and a Forbush

decrease; but perhaps it was quantitatively different. I think one reason it may have been different is that this trapping region was one that was overtaking the Earth as a result of solar rotation, rather than one that was overtaking the Earth as a result of plasma motion outward from the Sun. Yet we saw a sudden commencement at this point—so we must have run through some sort of a transition region or shock in the plasma flow.

The other evidence concerning the 27-day periodicities is the evidence mentioned by Dr. Snyder. In Fig. 9 we see the preliminary results from $Mariner\ 2$ (Ref. 5), showing the 27-day periodicity and the plasma velocity both correlated with the Kp index. Again we have a situation where the plasma properties appear to change with the azimuth angle in the ecliptic. Now, is this behavior close to the steady-state behavior of the flow, or are there discontinuities between the various velocity regions that are defined by this flow pattern?

In summary, then, it seems that there is a continuous gradation in the phenomena: we have everything from a plasma containing trapped protons to essentially free particles. Is the emission from the Sun really qualitatively different in all these cases, or is it basically always the same? What do the boundaries between these situations look like—in terms of magnetic field and in terms of particles? The evidence we have suggests that the properties of the plasma particles are not quite what we would ordinarily expect. For instance, we presumably have a situation where a shock propagates through the medium at a speed several times the speed of the positive ions. If this is true, to what extent and in what way does the plasma-proton energy depend on the distance of the protons behind the shock front?

Our greatest need at this point is a theory that can explain all of these phenomena, and even a few predictions would be of great value to the experimenters. The satellite results should provide us with new information concerning the magnetic-field and plasma configurations, and this new information may enable us to put the pieces together.

REFERENCES

1. AXFORD, W. I., A. J. DESSLER, and B. GOTTLIEB, Astrophysical Journal 137, 1268 (1963).
2. Pioneer 1

SONETT, C. P., D. L. JUDGE, A. R. SIMS, and J. M. KELSO, *Journal of Geophysical Research* 65, 55 (1960).

SONETT, C. P., E. J. SMITH, and A. R. SIMS, Space Research, ed. by H. KALLMAN BIJL, North-Holland Publishing Co., Amsterdam (1960) p. 921.

Pioneer 4

VAN ALLEN, J. A. and L. A. FRANK, Nature 184, 219 (1959).

Lunik 2

GRINGAUZ, K. I., Space Research II, ed. by H. C. van de Hulst, C. de Jager, and A. F. Moore, Interscience Publishers, Inc., New York (1961) p. 539.

GRINGAUZ, K. I. et al., Space Research III, ed. by W. PRIESTER, Interscience Publishers, a division of John Wiley and Sons, Inc., New York (1963) p. 602.

Lunik 3

Ibid.

Pioneer 5

COLEMAN, P. J. JR., L. DAVIS, JR., and C. P. SONETT, *Physical Review Letters* 5, 43 (1960).

COLEMAN, P. J. JR., C. P. SONETT, D. J. JUDGE, and E. J. SMITH, *Journal of Geophysical Research* **65**, 1856 (1960).

Venus Probe

Op. cit. Lunik 2

Explorer 10

BONETTI, A., H. S. BRIDGE, A. J. LAZARUS, B. ROSSI, and F. SCHERB, *Journal of Geophysical Research* **68**, 4017 (1963).

Explorer 12

BRYANT, D. A., U. D. DESAI, and F. B. McDonald, *Journal of Geophysical Research* 67, 4983 (1962).

Mariner 2

See Paper 1

Explorer 14

Frank, L. A., J. A. Van Allen, and E. Macagno, *Journal of Geophysical Research* 68, 3543 (1963).

CAHILL, L. J. and P. G. AMAZEEN, Journal of Geophysical Research 68, 1835 (1963). Explorer 18 (IMP)

See Paper 21

- 3. BRYANT, D. A., T. L. CLINE, U. D. DESAI, and F. B. McDonald. AAS-NASA Symposium on the Physics of Solar Flares, SP-50, ed. by W. N. Hess, National Aeronautics and Space Administration, Washington, D.C. (1964) p. 289.
- 4. STELLES, J. F., H. CARMICHAEL, and K. G. McCracken, Journal of Geophysical Research 66, 1363 (1961).
- 5. SNYDER, C. W. and M. NEUGEBAUER, Space Research IV, ed. by P. MULLER, Interscience Publishers, a division of John Wiley and Sons, Inc., New York (1964) p. 89.

DISCUSSION OF BRIDGE PAPER

AXFORD: I should like to question the suggested interpretation of Dr. Cline's data, namely, that the recurrent proton emission on October 27, 1961 was not a burst of new protons, and that protons are not produced continuously in this active region. In fact, there are no good reasons for saying that the emission of new protons does not occur all the time.

On September 28 there was a burst of protons associated with a flare. There was a sudden commencement on September 30, and a new burst of particles somehow associated with the shock wave was observed. Some time later, on October 27, there was another burst associated with another sudden commencement. Now, the October event has been associated with the September-30 event because it occurred 27 days later.

It is important to note, however, that the September-28 flare was 30 deg east of the central meridian. The active region took 2 more days to get around to the central meridian, so that it is equally reasonable to associate the October-27 event with the central-meridian passage of the region that caused the September-28 event.

BRIDGE: What you are saying is that the events are not associated. You are not saying that there is continuous emission.

AXFORD: I think there is no evidence to justify saying that there is *not* continuous emission.

BRIDGE: Of course, if there were continuous emission, it wouldn't alter the argument. What really alters the argument is to say that the two events were not caused by the same flare. It is a question of whether the lines of force are characteristic features that essentially maintain their configuration for long periods of time.

DAVIS: I am very happy to see you supporting the concept of permanent magnetic features that come around time after time and that possibly guide particles out to us from the Sun; such features possibly mark the location of interesting regions on the Sun, where particles may be emitted when there are flares or other changes there. But for the experimentalists to put on the theorists the burden of making a trapping mechanism that will confine particles for a month, when one has all the drifts and loss mechanisms to contend with, seems absolutely hopeless.

GOLD: I was going to make that same point, as usual with even greater vigor. Such long-period trapping is absolutely inconceivable—when we talk of such low-energy particles, when we know that the field is not smooth, when we do see these particles that are imbedded in that crinkly field, and when all that stuff is shooting out at a speed such that it has gone a long way past the Earth. It is inconceivable to have any trapping mechanism without having an extremely smooth field to prevent any outflow.

The diffusion mechanisms that have been discussed will normally determine the location of the low-energy particles. These particles will travel very much with the plasma at the plasma's rate of outflow. The high-energy particles, on the other hand, will not see the small crinkles; they may see a field that looks to them essentially like a smooth field.

BRIDGE: I quite understand your point. I simply wanted forcibly to point out the consequences of Cline's conclusion. This is not the only event.

GOLD: I would also remind you that when people plotted the flare-produced magnetic storms many years ago, they were led into believing just the same story. There was a 27-day recurrence in the flares, and it was difficult to distinguish what they called M-region storms from the flare storms, because there was also a statistical tendency for the flare storms to occur in the regions that came around every 27 days.

BRIDGE: Are you saying that you can explain these observations simply by the statement that you saw a flare and that 27 days later you looked and you happened to see something?

GOLD: I would say it more strongly than that. I would say that the probability of comparatively low-energy particles existing in a magnetic region that is connected to a disturbed region is very high. Small flares occur all the time in the disturbed regions, and particles normally cannot get to the Earth except when the configuration is suitable.

BRIDGE: But you don't argue, then, that the magnetic configuration is essentially preserved over a period of 27 days?

GOLD: No: but I would think that the location of the source of the outstreaming is preserved over much longer periods; so it is from that place that a magnetic configuration stretches out at any one time. They need not be the same lines of force. Whether it is a steady process is not at all indicated by the observations.

PARKER: You agree that a spiral is formed quite independently?

GOLD: Absolutely: anything pushed out from a region on the Sun will lead to

the formation of a spiral, and the spiral will be formed by either the same lines of force forever or by a succession of puffs.

CLINE: There is one interesting piece of evidence about the event of September 28, 1961. During the previous solar rotation, there was a flare on the west limb on September 10. The plasma stream from that flare could have been seen sometime between September 28 and September 30, but it was obscured by this new event that occurred, of course, in the same plage region. The September-10 solar flare produced a burst of low-energy particles, and a sudden commencement 2 days later. But since the emission was from a region that was 90 degrees west of the central meridian rather than near the central meridian, the orientation was not right for setting up a streamer: the configuration of the 2-day-delayed events must have another geometry.

Page intentionally left blank

Session II

THEORIES OF THE INTERPLANETARY PLASMA AND FIELDS, AND OF ENERGETIC PARTICLES

Page intentionally left blank

MODELS OF THE INTERPLANETARY FIELDS AND PLASMA FLOW

LEVERETT DAVIS, JR.

California Institute of Technology, Pasadena, California

ALTHOUGH I cannot devise a model that will explain all of the data we saw yesterday, I should like to discuss various models based on that data and to indicate some of the important considerations necessary for the construction of a satisfactory model.

Our present knowledge of the solar wind includes two very striking facts which I think deserve to be emphasized: first, long-lived jets of high-velocity gas are ejected from the Sun; and secondly, the interplanetary magnetic-field component perpendicular to the ecliptic seems to be predominantly directed toward the south. Let me begin by discussing each of these facts.

High-Velocity Jets

A jet of high-velocity gas may be continuously ejected from about the same region of the Sun for a period of at least four or five solar rotations. At least one of the jets observed by *Mariner* always had a relatively strong outward field. This field presumably had the classic spiral pattern, although the *Mariner* data do not definitely prove that it did.

Figure 1 combines two of the figures shown by Dr. Smith yesterday (Paper 3). The lower curve shows the radial component of the magnetic field; the upper curve shows the component in the direction of the planet's motion. Each point is the average over 1 day. No reasonable assumption about the zeroes of the magnetometer will allow any significant change in the tangential component for the first 10 days or so. In the case of the radial component, the zero may be shifted up or down, but the character of the successive humps that show up at 27-day intervals cannot be changed. It is very plausible to place the zero of B_R as indicated in the figure, because this produces the expected spiral field from Day 3 to Day 12 of the solar rotation period. During this interval, the field has a strong outward radial component that reappears in successive rotation periods.

The Southward Component of the Field

I am greatly puzzled by the fact that the data from both *Mariner* and *IMP* indicate a tendency for the field component perpendicular to the ecliptic to be predominantly toward the south. Figure 2 shows, in perspective, the coordinate systems used by the *Mariner* and *IMP* experimenters. In each case, the ecliptic is the plane of the paper. The only line

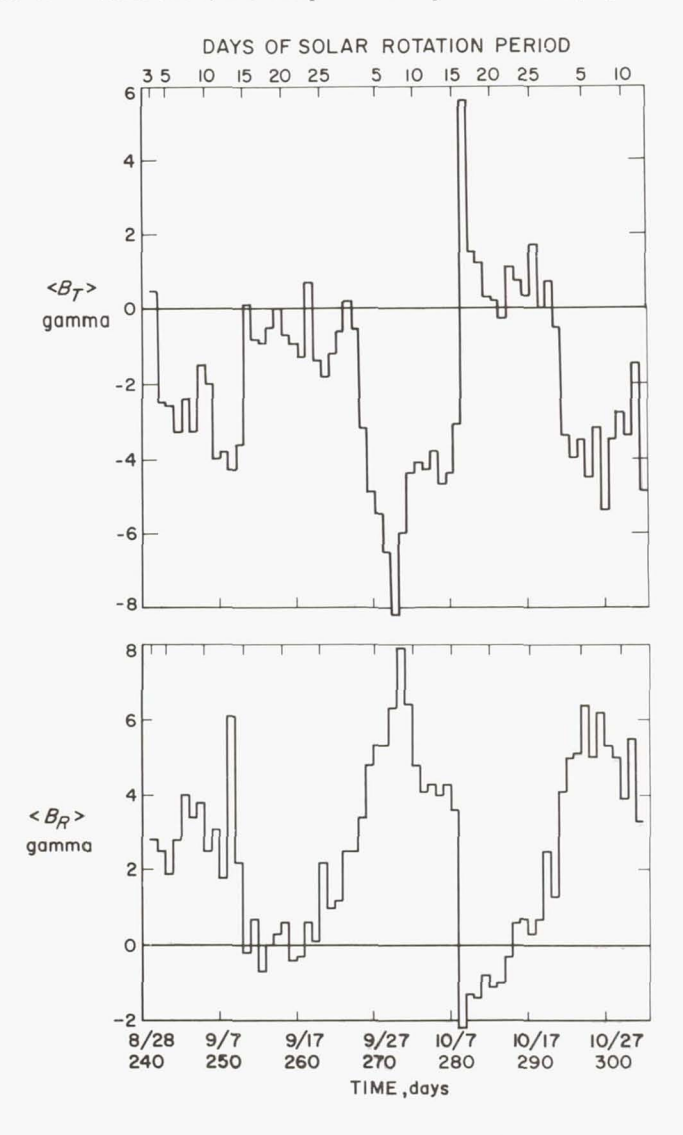


Fig. 1. Radial and tangential components of the interplanetary magnetic field; daily averages from August 30 to November 1, 1962

out of this plane is the north polar axis of the ecliptic: the N (normal) axis for Mariner, the Z axis for IMP. The planets move along the T (tangential) and -Y axes. For Mariner, the R (radial) axis is radially outward from the Sun; for IMP, the X axis is radially inward. The traditional spiral-field directions in the ecliptic are indicated by the longitude angles Λ and ϕ .

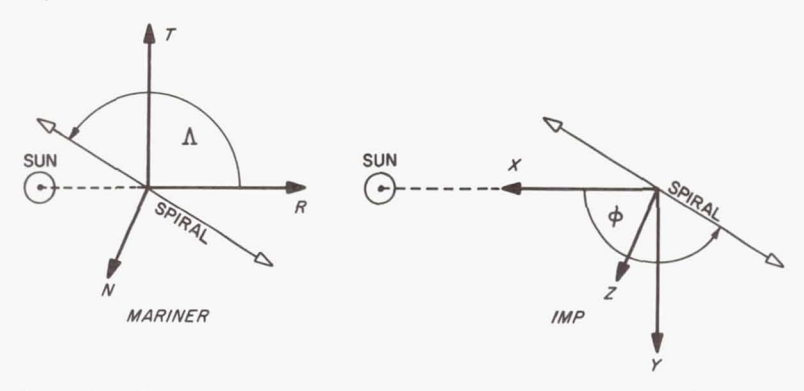


Fig. 2. Coordinate systems used by the *Mariner* and by the *IMP* experimenters. All lines except N and Z are in the plane of the paper, which is the ecliptic. The latitude is denoted by β by the *Mariner* experimenters and by θ by the *IMP* experimenters

The tendency for the average value of the component normal to the ecliptic to be southward is evident, in the *Mariner* data, from the negative values of B_N or of β ; in the *IMP* data, it is evident from the tendency of θ to be negative. B_N is very often as much as 1γ negative in both sets of data; it is hard to imagine that it averages less than 0.1γ . If the magnetic field is convected outward, and if B_N averages even 0.1γ , then the outwardly convected flux in this component alone will be 10^{23} Maxwells/yr. This amount of flux, it seems to me, would be very difficult to explain: it is the flux of 100 typical sunspots.

The direction of the field is as puzzling as its size. The polar field of the Sun has the same sign as that of the Earth at the present time in the 22-yr sunspot cycle. Thus an approximately dipole field blown out in the solar equatorial plane has a B_N of the wrong sign. If you say that the spiral pattern should be parallel to the Sun's equatorial plane rather than in the ecliptic, then you find that, in December, the equatorial plane is tipped by 7 deg and runs from north of west to south of east. A correlation then exists between B_N and B_T , with $B_N = B_T/8$. I don't think this configuration can explain the observations at all, because the most dependable *Mariner* observations were made in September, and no such correlation was detected. However, we should keep this configuration in mind for future observations.

One way to explain the negative sign is to consider Babcock's model (Ref. 1), in which the solar wind carries field lines away from the Sun, thereby leading to the necessary reconnection of field lines in the corona. Babcock's model will give you the right sign, but a grossly insufficient quantity of flux. [However, if the phase lag between the change of polarity at the poles and the end of spot activity near the equator is taken properly into account, this model also yields the wrong sign.]¹

Plasma Motion and Field Geometry

Now I should like to talk about some effects of plasma motion on the field geometry. This is a very simple-minded, naive kind of discussion. Suppose that a field pattern has been established somewhere in the corona. The gas comes out and arrives near the orbit of the Earth. What happens to the field pattern? Well, a lot of things may happen. As the gas comes out, a lot of twisting around may occur, on a not-too-big scale. We can call this twisting around "stirring." If such stirring were dominant, then the field patterns near the Earth would show very little relation to those in the corona. Any systematic structures in the interplanetary field would be difficult to find; the normal component would not show a predominantly negative sign; and the field would not show an outward radial component that stays approximately the same for 7 or 8 days. Such regularities, however, are observed, and convince me that stirring is not important.

Another possibility is just the opposite behavior. Consider a rectangular block that comes out radially from the Sun, with neither rotation nor shear, but with different expansions along the three axes. It is not necessary to assume a uniform spherical expansion all around the Sun; assume only that this block moves radially in a small cone. Let L_R be its length in the radial direction, L_T its length in the tangential direction, and L_N its length in the normal direction. How do these lengths vary with r—the distance from the Sun? The lengths normal to the radius, L_N and L_T , are proportional to r. If the velocity v of the solar wind were constant, L_R would not change. But if v varies with r independently of time, the front of the block speeds up before the rear does, and L_R is proportional to v. If this fact is not obvious, let n(r) be particle density and note that both $nL_RL_TL_N$ (the number of particles in the block) and nvL_TL_N (the flux out of the cone) remain constant.

Since the material of the solar wind is a very good conductor, the magnetic flux through each side of the block remains constant, and it is easy to see what happens to the field strengths. The radial component B_R is proportional to r^{-2} ; and B_N and B_T are each proportional to $(nv)^{-1}$. To

¹Added in manuscript

find how the field patterns change, consider B_T/B_R and B_N/B_R . Both of these ratios are proportional to r/v or, since nvr^2 is constant, to nr^3 . Thus if nr^3 increases, the field patterns are flattened so that they contain mostly tangential and normal components. If nr^3 decreases, the patterns are stretched out radially and contain mostly radial components.

Any reasonable model of the solar wind can supply an estimate of n(r) adequate for our purposes. Without implying that the calculations of Noble and Scarf (Ref. 2) are necessarily more than plausible approximations, I have used their values of the solar-wind density and velocity for Fig. 3. This figure shows the ratio $nr^3/n_1r_1^3$, where the subscript refers to

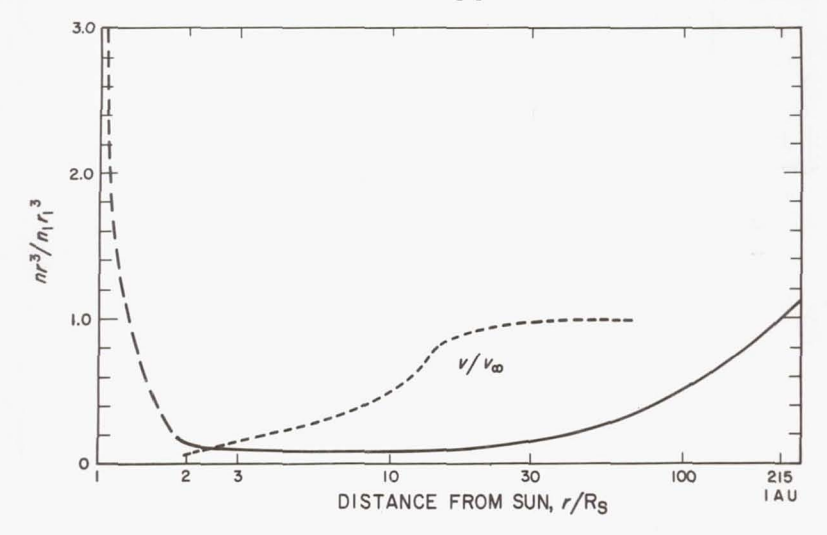


Fig. 3. Distortion function for a uniform expansion in the solar wind, and the solar-wind velocity

conditions at 1 AU. As you go toward the Sun from the orbit of the Earth, nr^3 decreases substantially, dropping to less than one-tenth of its value near the Earth. It returns to this latter value at about 1.3 R_s , and below this point in the corona it rises very rapidly. Thus if a structure is formed by stirring up lines of force below 1.3 R_s in the corona, and if it then comes out in a pure expansion with no further stirring, it will arrive at 1 AU with its pattern stretched out radially. The pattern will be shortened in the radial direction compared to the starting configuration only if the structure was formed at a level above 1.3 R_s .

The third feature that we should discuss is the shear. The Sun does not merely sit still and emit clouds of gas: it rotates with angular velocity Ω . We have been considering a block that comes out from the Sun. Let's follow the motion of the two faces that are normal to the radius. Suppose that the motions are a function of the radial distance only, and that at any

instant the inner surface is moving in the same way that the outer surface did a short while previously—when it was at this radius. The inner surface shares the rotation of the Sun a bit longer than the outer surface, and the block is sheared through the classic garden-hose angle. This angle is:

$$\psi = \tan^{-1} \left[\frac{(\Omega - \omega) r}{v} \right]$$

where $\omega(r)$ is the angular velocity of the solar wind resulting from the conservation of angular momentum and from magnetic stresses. Close to the Sun, where v is small and magnetic stresses dominate the motion, corotation occurs; that is, ω is very nearly equal to Ω . Therefore, there is very little spiraling close to the Sun.

Now, combine the effect of the shear and the pure expansion to see what happens to patterns embedded in the gas as it comes out from the Sun. We find that

$$\frac{B_T}{B_R} = \left(\frac{B_T}{B_R}\right)_0 \frac{nr^3}{(nr^3)_0} - \frac{(\Omega - \omega)r}{v} \tag{1}$$

If the field pattern near the Earth resembles closely the ideal spiral much of the time, the last term of Eq. 1 is dominant. We must then conclude that if the flow starts in a region well outside 1.3 $R_{\rm S}$, then the field is very nearly radial there. If the flow starts well inside 1.3 $R_{\rm S}$, then the large value of $(nr^3)_0$ in that region suppresses the first term; that is, the field becomes radial near 1.3 $R_{\rm S}$ by radial stretching. On the other hand, if there are times when the field pattern near the Earth does not resemble an ideal spiral, stirring does not have to be involved; it may be that the first term is significant and that the pattern is the result of some field in the tangential direction embedded at the start.

Possible Models

What kind of models can we construct from all this? I shall mention three possibilities. First, let's consider a model in which little irregular structures are formed somewhere in the corona and then blow out more or less as separate units. I should like them to start somewhere above 1.3 R_s , because it takes too long for a cloud to come out if it starts at a lower level. Pictures of prominences and solar motions suggest that there is too much stirring below this level for structures to remain undistorted until they leave the Sun. But clouds that come out as a unit from 1.3 R_s (without further stirring) will be distorted in such a way that B_r/B_R and B_N/B_R will increase by the time the clouds reach 1 AU. I don't think we observe this phenomenon; hence, I don't expect such clouds to be an important part of the model.

Next, consider a model in which many short loops of field lines rise

above the photosphere. The tops of the loops are blown outward every day or two; the bottoms are left connected to the Sun. This is Gold's model (Ref. 3), except that I may have been unduly specific about the time scale. The model produces fields in essentially the classic spiral pattern, except during infrequent intervals when the top of a loop is seen as it passes by the observer. It would be hard to distinguish these loops from those in Parker's model (Ref. 4). However, the radial field component in this model could be expected to change sign with a frequency determined by the scale of the original small loops; I certainly don't see how there would be a large structure showing the same sign month after month

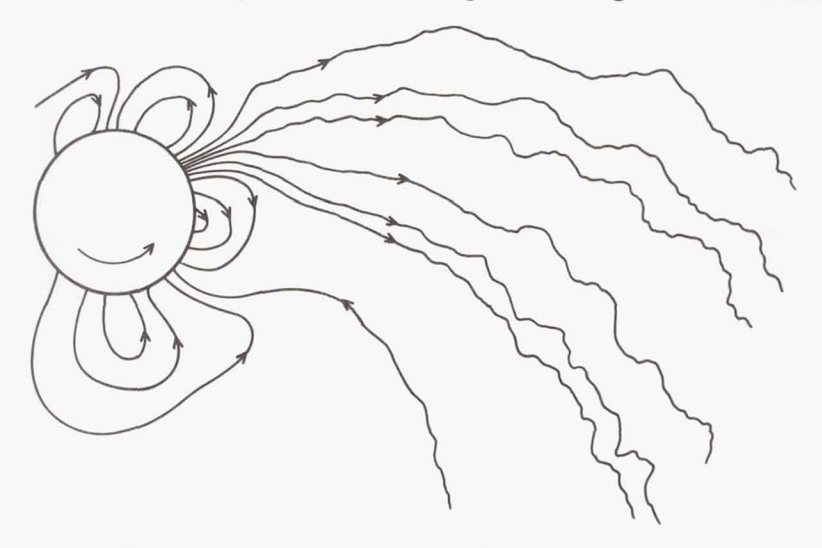


Fig. 4. Suggested model of a plasma and field configuration extending outward through the solar corona

as the Sun rotates. Perhaps during the other half of the solar rotation period—when small shifts in the zero of the *Mariner* magnetometer would greatly change the interpretation of the data—this model might fit the observations. Even so, I am not very sympathetic toward this model.

The model that I prefer is based on Fig. 4. Near 1 AU (215 $R_{\rm S}$), the ratio of $B^2/8\pi$ (the magnetic stress) to ρv^2 (the momentum flux of the solar wind) is very small and the wind dominates—it blows the field lines wherever it wants to go. But as one goes toward the Sun, the magnetic forces increase more rapidly than does the momentum flux; and within 10 to 20 $R_{\rm S}$ the magnetic field dominates the situation, and there is a lot of magnetic structure. Thus it does not seem plausible for the gas to start at the photosphere, well-up uniformly over the entire Sun, rise into the corona, and accelerate outward to form the solar wind. A magnetic field of a gauss or so, if it has the right configuration, should be able to suppress

such motion. I prefer to think that the gas finds places where the field lines are smooth and nearly radial, and that *there* is where it wells up. When it reaches a high enough level in the corona, where the local magnetic structures should become much weaker and more regular, the gas rising from each source can spread out and fill a substantial part of the upper corona. Here the heated gas begins to pick up velocity and to become the solar wind. Hence the wind that comes from an extended region of the upper corona may really originate in a small region of the photosphere, where the magnetic field is regular—and the polarity of the field would thus naturally be the same throughout the entire volume of the gas.

Features of the Preferred Model

The figure shows a few other features, which I shall mention but shall not discuss in detail. There appears to be no reason that the magnetic nozzle from which the solar wind flows should point precisely in a radial direction. If it is inclined slightly forward, the gas that comes directly toward the Earth will leave the Sun when the source is slightly east of the central meridian. This may explain the discrepancy which Dr. Snyder found (Paper 2) between (1) the velocity of the solar-wind jets and (2) the elapsed time between the central-meridian passage of the apparent sources of the jets and the arrival at *Mariner* of the high-velocity gas.

I see no reason for the solar wind to flow perfectly smoothly and to sweep the field out in an ideal spiral pattern. Observations indicate a large variety of irregularities in the field at 1 AU, with characteristic times that range from a few seconds, on rare occasions, up to minutes or hours or days. If these characteristic times are multiplied by velocities of the order of 500 km/sec, the presumed dimensions of the irregularities will be anything from a few thousand kilometers to a substantial part of an astronomical unit. The irregularities should not only be convected outward at the solar-wind velocity; they should also propagate as magnetoacoustic waves. It is attractive to suppose that in many cases they are Alfvén-type waves, which fluctuate more in direction than in magnitude, but there may be cases in which compression is more important. The irregularities may be caused by a number of factors: the gas, as it flows out of the magnetic nozzle, may already contain some embedded magnetic structures; the flow may be somewhat irregular and unstable; or streams of different velocity and density may interact somewhere between the corona and the spacecraft.

This mechanism for the origin of the solar wind allows for the production of all kinds of structures in the interplanetary field. It is certainly possible to have filaments in which high field strengths and low plasma pressures alternate with low field strengths and high plasma pressures. To say more before the observations are studied will only lead to erroneous speculation.

BIERMANN: Excuse me, may I ask a question? Where would you put the boundary that defines the limit of approximate co-rotation?

DAVIS: Presumably the solar wind gets started somewhere between 1 and 10 $R_{\rm S}$, and by the time it reaches 10 $R_{\rm S}$ it has most of its velocity. If one extrapolates inward the conditions observed near the Earth, then a balance between magnetic forces and momentum flux—or equality between the wind velocity and the Alfvén velocity—is reached somewhere between 10 and 20 $R_{\rm S}$. Inside this boundary the magnetic field dominates, and it is plausible to think that co-rotation occurs all the way out to this point of balance.

One way to attack such questions is to look for a steady-state solution to the angular motion of the gas as it flows outward in a region where the radial component of the field has spherical symmetry. The radial motion of the uniform outflow is assumed to be known, and the angular motion is deduced by balancing the rate of change of angular momentum against the magnetic forces. The modification of the magnetic field by the angular motion is included in the model. One might expect that the tendency of the gas to conserve angular momentum would tilt the field lines backward, in a direction opposite to the rotation direction. This would indeed be the case if the field were relatively weak; but where the field is strong, the steady-state solution shows the field lines leaning forward. The solution is really impossible, because it has a bad singularity at the radius where the Alfvén velocity equals the wind velocity. This singularity may possibly be eliminated by including viscosity and a finite conductivity; but I would guess that the resulting steady-state solution, in which the field lines would still lean forward near the Sun, would not be stable. It may be that no steady-state solution is possible, and in the strong-field region there may be some kind of flapping of the field lines that produces the irregularities seen farther out. Until this model is explored more carefully, however, any such suggestion must be regarded as a

WILCOX: Do you expect the field lines to spread out to the same extent in the direction perpendicular to the ecliptic that they do in the ecliptic?

I have assumed that the field lines diverge radially in both directions, as though coming from the center of the Sun. If you want to introduce suitable forces to make the wind flow nonradially, you can make the spreading in the direction normal to the ecliptic either greater or less than the spreading in the ecliptic.

One other appealing feature of the model shown in Fig. 4 is that the magnetic nozzles may easily have a variety of profiles. In fact, until better observations can be made near the Sun, the theorist can suggest any reasonable profile he likes without fear of contradiction; thus he can produce streams with almost any desired combination of velocity and density. Trying to fit the Neugebauer and Snyder data (Paper 1) to the purely radial nozzle of Parker's model (Ref. 4) is rather awkward. Parker's most easily varied free parameter is either the energy supply or the temperature, but when either of these parameters is changed to increase the solar-wind velocity, it must also considerably increase the density. The magnetic nozzle provides at least one more degree of freedom, which makes it easier to explain the observations.

Effects in Overtaking Streams

Finally, let me mention one more feature that should be included in these models. We learn from the Neugebauer and Snyder results that there are places on the Sun where the gas comes out with high velocities and other places where it comes out with low velocities. This structure persists for several solar rotations. We see these streams only when they go by the spacecraft, but it is hard to believe that they do not just rotate with the Sun. Now consider what happens when, due to the rotation of the Sun, a fast stream overtakes a previously emitted slow stream. Consider this phenomenon in a frame of reference that moves radially outward at an intermediate velocity. The fast and slow streams will appear to flow together and collide. The gas from both streams will pile up in a growing intermediate region of higher density, temperature, pressure, and field strength. In any case, two shock waves will be generated. If the difference in velocity between the two streams is very small, the shocks will be very weak, and the effects will be hard to detect; if the difference in velocity is of the order of twice the magneto-acoustic velocity for the region, the shocks will be strong, and the effects should be quite noticeable. Figure 5 is based on an illustration of Dessler and Fejer (Ref. 5) and shows a possible structure that could be formed under such

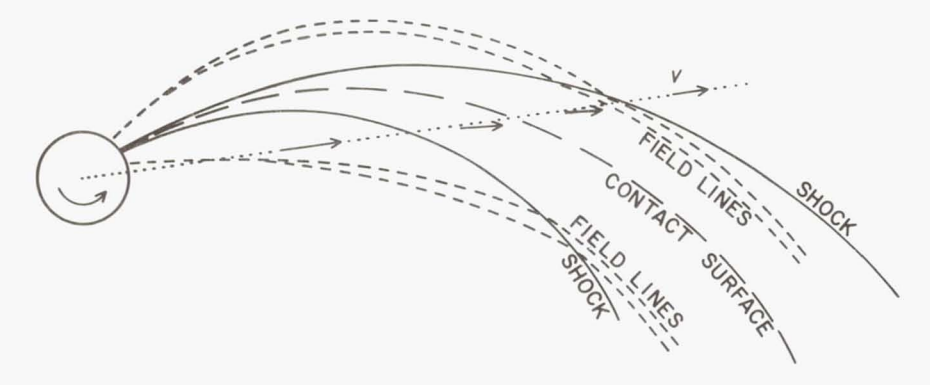


Fig. 5. Double shock due to a fast wind overtaking a slow wind

circumstances. The arrows along the dotted line show the velocity of the solar wind in the various regions. In the high-velocity region inside the spirals, and in the low-velocity region outside the spirals, the velocity is assumed to be precisely radial. Since the shocks are oblique, the flow is refracted, and between the two shocks the velocity has a small component in the -T direction. The gas that was originally part of the fast stream (decelerated as it passed through the inner shock) and the gas that was originally part of the slow stream (accelerated as the outer shock overtook it) may have different temperatures and densities, but they have the same pressure. They are separated by a contact surface as indicated. I

suspect that the velocity on each side of, and tangent to, the contact surface may be different, leading to the possibility of wave generation and instabilities. In the two undisturbed regions, the magnetic-field lines are shown making the usual ideal spirals appropriate to the wind velocities. The field lines are refracted as shown in the figure when they cross the shock fronts; they must run parallel to the contact surface, since they cannot cross it. I suspect that some elements of this double shock should be included in the model of the interplanetary field, but I have not explored the matter in detail.

REFERENCES

1. BABCOCK, H. W., Astrophysical Journal 133, 572 (1961).

2. Noble, L. M. and F. L. Scarf, Astrophysical Journal 138, 1169 (1963).

3. Gold, T., Astrophysical Journal Suppl. 4, 406 (1960).

4. PARKER, E. N., Interplanetary Dynamical Processes, Interscience Publishers, a division of John Wiley and Sons, Inc., New York (1963).

5. Dessler, A. J. and J. A. Fejer, Planetary and Space Science 11, 505 (1963).

DISCUSSION OF DAVIS PAPER

AXFORD: I think these ideas are pretty sensible, but I would like to know whether the field lines close anywhere.

DAVIS: Well, the divergence of **B** is certainly zero. I think it is very sensible to assume that the field lines close somewhere inside the Sun and that any line that enters must also leave. But if, as indicated in Fig. 5, Paper 9, the field has been blown out for several months in one of these spirals, then I think it is more profitable to suppose that all the lines of force connect onto the interstellar lines and wander off to the far ends of our galaxy. Worrying about whether these lines close is pointless, as long as the net flux out of the solar system is zero.

The Origin of High-Velocity Streams

LÜST: This picture is very interesting, but it comes back to a question that was not, I think, really discussed yesterday. I would like to hear your opinion.

You interpret the *Mariner-2* data as indicating that there are, on the Sun, localized places where the outflow will have emphasis, and I think that at one stage Snyder was even entertaining the idea that all of the plasma comes from a limited number of sources on the Sun. The *IMP* results are very important in this connection, because they indicate that the solar wind is blowing all the time, even with no solar activity. My question is: how do you reconcile the idea of a solar wind blowing from everyplace with the idea of a persistent, high-intensity wind blowing from only certain places on the Sun?

DAVIS: Well, different people view the solar wind in different ways, and I am probably not speaking for Snyder and Neugebauer at all. My view is this: there are many magnetic structures close to the Sun; farther away, the magnetic structures have all been combed out, for one reason or another, so that the field lines are more or less radial and have different polarities: The magnetic field forms various kinds of nozzles. In some places the nozzles produce a high-velocity stream of one density; in other places they produce a low-velocity stream of another density. The solar wind comes out from everywhere on the Sun, but it

has different properties in different places, and this pattern is relatively steady. As the magnetic fields evolve over a period that is sometimes a few hours and sometimes a few months, the pattern changes. This evolution can probably explain the differences between the *IMP* data and the *Mariner* data.

GOLD: I agree very much with the general outlook that you have presented. In addition, I think you have clarified what I said yesterday.

Concerning the question of permanent, long-lived structures, I would say that the rate at which field lines are cut off depends greatly on the density and flow velocity in the entire region in which cutoff occurs. If the density and flow velocity are high, then a magnetic structure will not readily cut itself off. If there is a place on the Sun that keeps pumping out gas at a reasonably steady rate, then I think it is perfectly reasonable to assume that the field lines will have a very long life. On the other hand, I have seen pictures of sudden outbursts in which gas comes out from chromospheric levels where the fields are tangled. These outbursts must drag out new field lines, and unless cutoff occurs, the total pole strength of the Sun will be increased. Fortunately, cutoff readily occurs when an outburst produces a plug of high-velocity gas which is connected to the Sun only by lines of force on which there is little or no gas.

There is a typical coronal shape that is very important (Fig. 1). I want to emphasize again that while you often see the plain, strung-out things, you often see

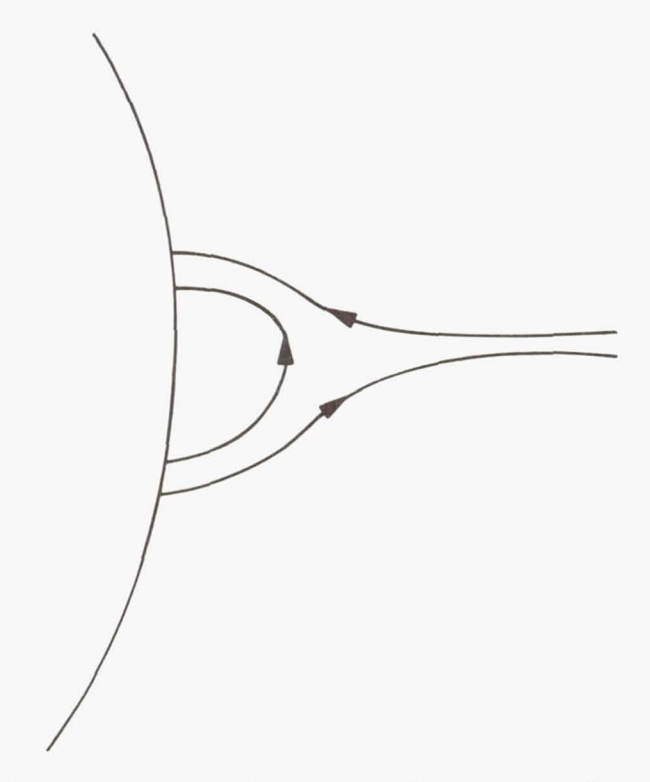


Fig. 1. Coronal cusp believed to be associated with the "necking-off" of magnetic-field lines. Arrows indicate the assumed magnetic-field direction

cusped features also. In fact, on about half the solar-eclipse pictures that you look at, you can see at least one such structure on the limb. A structure of this kind must mean that lines of force have been drawn out and are being cut off. The shape clearly implies emerging lines of force on one side and entering lines of force on the other side.

DAVIS: I don't think there is much disagreement. One thing that is implicit in this discussion and that probably should have been said explicitly, is that conditions are very different throughout the solar cycle. When *Mariner* was flown, I think there were very few bursts that carried matter out from the Sun; thus, it is not surprising that we saw no strong evidence of such bursts. At other times in the solar cycle, however, conditions are probably very different.

DUNGEY: I would like to ask Dr. Davis how he thinks plages fit into this picture. I am a bit confused about whether he thinks the high-speed streams come from plages or from between plages. Plage regions have both a high temperature and a high value of vertical field. On the other hand, I think that people have found, for

the most part, a negative correlation between plages and M regions.

DAVIS: It is easy and natural to invent models in which there is a close connection between the plages and the sources of the high-speed jets, but it is just as easy to invent models in which there is no connection. The smartest thing I could do would be to say I don't know whether there is any connection, but I am not that smart. I think that plages are involved in the photospheric fields and in supplying energy to heat the corona. In my picture, you may think of a plage region being somewhere down in the roots of the tangled fields (Fig. 4, Paper 9), which may not be so arranged that the wind comes out easily. You may happen to get a little extra energy into the corona by waves coming up from the plage region. The field configuration could set up a nice nozzle a short distance away, and then the solar wind would blow out strongly through the nozzle instead of at the place where it receives most of its energy. When the wind reaches the Earth, it affects the magnetosphere and causes the M-region storm.

DUNGEY: Did Conway Snyder (Paper 2) find his sources between the plages? **DAVIS:** Yes, but I can also account for this by tilting the magnetic nozzle. I don't think that I know just where to put my nozzles, but I think they fit in somewhere. [We now need better observations and a carefully developed theory for the gas flow in a magnetic nozzle; this theory should include the effect of the angular momentum of the gas and the effect of inclined field lines.]¹

DEUTSCH: If I understand you, the energy would come up from the plage in the form of waves, since waves can penetrate the transverse field somewhat more

easily than matter can.

DAVIS: Yes, I agree with that. I have not considered conduction along the field

lines, although this process is also important.

BRATENAHL: I would like to comment on Dr. Gold's picture (Fig. 1), which indicates where the necking-off process takes place. I think that if one takes the Babcock model fairly seriously and does his thinking in that context, one can perhaps recognize structures of the same form as Dr. Gold's, but of a much smaller scale. One can imagine a whole hierarchy of such structures, depending on the previous history of the magnetic arrangement. One can make a rather nice quiescent-prominence model out of a configuration like that. I think one can begin to recognize how the smaller-scale members of the "necking off" family are related to the quiescent prominences. If indeed these smaller members possess the same

¹Added in manuscript

topology, they must necessarily be arranged at the edges and intersections of bipolar regions. This would suggest, it seems to me, that the nozzles are associated with prominence-like structures. The nozzles may sometimes line up with the tops of quiescent prominences; but most of the time they line up with larger-scale members of this family farther out in the corona, where the density is so low that they are no longer visible except in the highest-quality eclipse pictures.

ATHAY: I don't really understand all the concern about trying to trace features observed in space back to specific locations in the lower elevations of the Sun's atmosphere. In most photographs of the corona, many of the features in equatorial regions show rather strong curvature somewhere in their structure. If you select one of these far out in space and trace it back to the surface of the Sun, then you frequently find enough curvature to shift the base by at least one or two days' rotation of the Sun. So I really don't think you can expect to use any simple theory to trace a given line from space to a lower elevation in the Sun's atmosphere and find a one-to-one correspondence of features.

Neutral Points and the Necking-Off Process

PETSCHEK: According to Dr. Gold's picture, there should be a region where the wind is blowing toward the Sun rather than away from it. Should we be able to see that?

GOLD: Yes. The return of arched lines of force back to the Sun does imply an inward-blowing wind, doesn't it? If we ever make solar probes that go close to the Sun, we will be interested in looking for this phenomenon.

Of course, it is very unlikely that this necking-off process occurs on any substantial scale beyond 1 AU, because at about that distance the scale of the disturbance has become so large that the process for drawing the stuff together takes a very long time.

PARKER: I would like to direct a question to Dr. Gold. He has discussed for some time the idea of cutting off lines of force on this rather large scale. I wonder if he would be kind enough to step to the board and calculate for us how he proposes to carry out this cutting-off of lines of force?

GOLD: In the first place, let me say that in science one often has to proceed on the basis that a theoretical process is necessary to account for the observations, even if one cannot trace out the process in detail. The fact that we are not in a position to calculate a certain process in detail doesn't mean that it is right for us to ignore its possibility or to rule it out altogether.

In the second place, I would like to refer the question to Dr. Petschek, who has stronger and clearer views than I have on the methods of computing this cutting-off process.

PETSCHEK: I was going to discuss this problem tomorrow in connection with the magnetosphere boundary (Paper 18). I have made a calculation that indicates that the rate at which oppositely-directed field lines approach each other is of the order of the Alfvén speed divided by the logarithm of the magnetic Reynolds number. Since logarithms can be only so large, the velocity at which the field lines approach each other can be only as small as about one-tenth of the Alfvén speed. (A fuller discussion of this basic process will be given in Paper 15.)

If a neutral region is blown out with the wind, which is traveling at ten times the Alfvén speed, the region would travel a distance of about a hundred times its own dimension before being cut off. Ness observed (Paper 6) that a reversal of field direction can occur within a period of about 1 hour, which at solar-wind

velocities corresponds to a distance of 0.01 AU. So it is possible for the field lines to be cut off at a distance from the Sun of the order of 1 AU.

I am somewhat bothered by Gold's picture, in which a stream traveling at a velocity much higher than the Alfvén speed is cut off at a stationary place, rather than at a place that is carried along by the wind. The cutting-off necessarily occurs at a velocity less than the Alfvén speed, while the flow has a velocity higher than the Alfvén speed.

PARKER: That is the point that Davis made, and the one I had in the back of my mind when I asked Gold to make a calculation of his process. I would point out to him that the necessity for this cutting-off to occur at the rate he implies is not at all obvious. Perhaps I misunderstood how much of this cutting-off he thinks is necessary. At first I thought he required a lot, but later I decided he didn't

require quite so much.

GOLD: I think that, at a time of high solar disturbance, gas is blown up from regions where the field strengths are of the order of a thousand, or at least a few hundred, gauss. On that basis alone, if the gas comes indeed from the chromosphere and from regions of a thousand gauss, then the cutting-off process is required in order to retain the average pole strength for the Sun. Otherwise the amount of gas blown out from one disturbed region could easily produce all of the magnetic field found in interplanetary space. A cloud of gas and its magnetic field would therefore need to be cut off in roughly the time it takes to be replaced by the next one, in order not to increase the total flux extending into space. PARKER: If I understand you correctly, you believe that the cutting-off is associated principally with flare outbursts, because fresh lines of force must be carried away with each outburst. Why do you feel that fresh lines of force must be carried away with each outburst?

GOLD: I can't see that this big explosion in the chromosphere concentrates its force on only the few places where the lines of force are already sticking out.

PARKER: Why not?

GOLD: Because on limb cinematographic pictures you see a brightening at levels that are generally below 10^4 km.

PARKER: The average height of a flare is 3×10^4 km.

GOLD: But the brightening occurs at levels much below that, although great velocities are produced, I agree, up to 3×10^4 or 4×10^4 km. I am not going to worry about the precise levels, but the outbursts occur in the regions where the magnetic fields are strong and very localized. These are regions where most of the lines of force make a sharp loop and return to the vicinity from which they left. I cannot see why a big explosion would contrive to push out gas at only those places where the lines of force were already sticking out.

PARKER: Are you assuming that the gas in the outburst actually comes from the visible flare and does not come from, say, a higher level in the corona?

GOLD: Yes, I would assume that. I should think the observers would generally agree with this point of view.

PARKER: The arches in a flare are remarkably steady.

GOLD: When you see a phenomenon that may be a limb flare, you often see the highest velocities occurring at the lower levels.

DEUTSCH: Isn't it true that you are referring to a surge phenomenon, and that the material in a surge often reverses direction?

GOLD: I think cinematographic pictures show velocities quite as high as those we have seen in the solar wind. The highest velocity we have seen is 1,000 km/sec, and we often see a velocity of 400 km/sec. Of course, you have to understand that

the velocity is seen in projection, and although you don't know the angle, you do know that, on an average, the apparent speed is less than the actual speed. I think these observations are compatible with the theory that gas is ejected from the Sun into interplanetary space.

DEUTSCH: My point is: isn't material then usually observed to turn around and

go back to the Sun?

GOLD: Yes, in most surges, but one sees limb flares very rarely. Only a small fraction of all flares can be successful in ejecting gas; otherwise there would be too much gas and magnetic-field strength in space. [Furthermore, one does see high-velocity surges with no suggestion of any return motion.]²

MEAD: I would like to ask Dr. Davis to clarify a point concerning Fig. 5, Paper 9. To what extent can the velocity vector of the solar wind be other than radially outward? Can the velocity vector differ from the radial direction by, say, 20

degrees, or is the difference pretty much limited to a few degrees?

DAVIS: To answer your question I would have to spend a couple of hours calculating the flow from the Navier–Stokes relations. Some refraction of the velocity vector occurs when the solar wind goes through an oblique shock, but I don't know how much. From discussions that I have heard, I would guess the change in direction to be more like a few degrees than like 20 degrees. This is a wild guess, although the actual change shouldn't be hard to calculate.

Let me mention one other thing that is relevant to some of our discussion. In the relations that I discussed earlier, the Mach number is given by:

$$M = \frac{v}{V_{\perp}} \propto v \, \frac{\sqrt{n}}{B}.$$

If the magnetic field has only a radial component and obeys a $1/r^2$ law, then the Mach number is proportional to $1/\sqrt{n}$ regardless of the velocity of the solar wind as it is getting started down near the Sun. The density of the particles near 1 AU is something like $10/\text{cm}^3$. The wind starts down in the corona where the density is many powers of 10 larger, and the Mach number there is less than 1. This cutting-off process we have been talking about can occur very efficiently at the elevations mentioned by Dr. Gold: so efficiently, in fact, that I should think it would be difficult for any gas to blow out. The nozzle would be cut off before anything happened, unless this were prevented by certain properties of the field structure.

WILKERSON: I have a question for Dr. Gold. Would you indicate how your pattern (Fig. 1) looks in three dimensions?



Fig. 2. Plasma and magnetic-field structure believed to correspond to the coronal cusp shown in Fig. 1

²Added in manuscript

GOLD: In one plane, the pattern is like the one shown in Fig. 2, which shows the connection of the two regions as the magnetic field cuts itself off. There is also a returning flow and a central, neutral sheet, which, in the idealized case, stretches out to infinity in the plane perpendicular to the paper. In the actual case, this neutral sheet is probably crinkly rather than flat, and it ends in adjacent magnetic structures. This tendency to make a neutral sheet is interesting, because a neutral sheet is such a particular configuration. Every outburst that ejects gas far into space has a great tendency to make elongated fields. For this reason alone, such outbursts have a tendency to produce a very close approximation to a general zero-field sheet.

BIERMANN: I have a question for Dr. Gold or Dr. Davis. Do the cutting-off process and magnetized-cloud formation in your pictures have any relation to the similar processes demanded by Babcock in his theory of the solar cycle? Listening to the discussion, I have the feeling that the extent of these processes may perhaps be greater than you originally stated.

DAVIS: My comment on that is that on Mondays, Wednesdays, and Fridays, I believe in the drawing-out of lines of force, and on Tuesdays, Thursdays, and Saturdays, or perhaps only once a year when I think of Babcock's model, I am willing to draw pictures showing a lot of reconnection above the sunspots. But the reconnection is not at equatorial latitudes. I don't know whether this dodge will keep me out of trouble, but we may very well know nothing about the latitude dependence of these processes.

BRATENAHL: The Babcock model does have important reconnections between sunspots, but it also has an equally important one across the equator. Unfortunately, there is no observational evidence for this equatorial reconnection, at least at the lower levels. It may be visible at higher coronal levels, if you know what to

look for in high-quality eclipse pictures.

So I don't see why the reconnections could not always be related to the one that Babcock refers to, even though only a small fraction of the reconnections lead to the new pole. Most of the reconnections are random and don't lead to a new dipole moment on the Sun; thus, you may draw as many reconnections as you want to, as long as you allow a few percent of them to produce the new polar field.

GOLD: In fact, I think that, Babcock model or no, the solar-surface phenomena indicate that no connection pattern can be permanent. One certainly has to understand the physics of the reconnection process in order to comprehend the necessary reshuffling of sunspots. If one calculates a field decay that occurs by diffusion, one finds that the time constants are much too large; obviously then, we are concerned with a physical process other than ohmic decay. I vote strongly for the theory that the changes arise from the cutting-off process which follows the juxtaposition of opposing field lines. We have seen this process close to the Sun in connection with changes of field in the sunspot-disturbed region: we see it, on a larger scale, in connection with the requirements for filling space with field without drawing out too much field afresh. I think that cutting off opposing lines of force is the dominant method of reconnecting solar field lines.

BIERMANN: Of course, in laboratory experiments the constancy of magnetic flux is often apparently violated and, for reasons we don't clearly understand, reconnection generally proceeds much faster than we would like to think. It seems that we have to check the effect on all scales.

I also want to comment on a question that came up several times concerning the flow direction. For distances larger than, say, 0.5 AU, the evidence from

comets shows that the flow should be radial to within a very few degrees, except at times of very large disturbances. However, if there are storms, the deviations from the radial direction may be much larger.

LÜST: It is important to know the time scale for the disconnection of field lines in the solar wind in order to know where the disconnection takes place—inside the solar atmosphere, in the outer part of the solar atmosphere, or at some distance from the Sun. If the disconnection time scale is about equal to or shorter than the time required for the solar wind to move through the inner solar system, then Gold's picture of disconnecting field lines in the solar wind is relevant. If the disconnection time scale is long—on the order of a year—then no disconnection can occur in the inner solar system. Nevertheless, such a picture can still be used in Babcock's theory for explaining the change of sign in the solar magnetic field.

SMITH: I would like Dr. Davis to clarify a point for me. Since the fields in your pictures (Fig. 4, Paper 9) are really three dimensional, we come back to the question of how the field lines are connected out in space. Your model, as I understand it, makes it possible for the field lines to return to perhaps a different latitude. However, if you are restricted to observations in the ecliptic, for example, then you may not see the lines returning. It seems to me that the possibility of field lines returning to a different latitude is consistent with the *Mariner* observations, yet it satisfies the requirements of those who like to see arrows on all the lines of force.

DAVIS: I think that the field lines could certainly come back out of the ecliptic. If you take Prof. Gold's model seriously and assume that you have lots of loops coming out, you would be surprised if you didn't see the same amounts of pluses and minuses. They may not be connected, but they should be somewhat equal in quantity.

When we see, as we did in the *Mariner* data, periods of 10 or 12 days during which one sign strongly predominates, then we argue that the roots of this field are peculiar. We can also argue that the Sun had a large, temporary, unipolar region on it, and we may not see the effect again until another such unipolar region occurs.

THE FLOOR: I would like to make one comment concerning the reconnection of field lines and the question of the reconnection rate. Suppose that reconnection actually occurs sufficiently far from the Sun that it can be seen by a space probe. The thing we would like to measure, of course, is the electric field, which is simply a measure of the cutting-off rate. This would be a very difficult measurement; but if there is such an electric field, then particles are accelerated. An adequate measurement of the accelerated particles may provide you with a measurement of the electric field and, hence, a measurement of the reconnection rate.

GOLD: When cutting-off processes occur, they provide a certain amount of kinetic energy to the particles in the medium. This energy is comparable to the magnetic energy that was initially present in the gas in the region involved: it is by no means a trivial amount, for it is about 10 percent of the flow energy. A fraction of the turbulence of the solar wind may derive from this energy source. In fact, it seems to be otherwise difficult to account for observed small-scale turbulence in a gas that is continuously emitted from a source that subtends a very small angle.

EVIDENCE FOR A COLLISION-FREE HYDROMAGNETIC SHOCK IN INTERPLANETARY SPACE

C. P. SONETT, D. S. COLBURN, AND B. R. BRIGGS

Ames Research Center, NASA, Moffett Field, California (Presented by D. S. Colburn)

THE collision-free hydromagnetic shock has been the subject of several investigations (Ref. 1), both theoretical and experimental. The phenomenon is not completely understood, and most models have been one-dimensional. For the present, our analysis of the phenomenon must rely upon observations, and this paper will describe some of these observations and will present some of the implications involved.

The Observations

The particular event considered here was observed almost simultaneously at three places: on Mariner, which was 10.7×10^6 km from the Earth and about 33 deg east of the Earth–Sun line; on the Earth, using ground-based magnetometers; and on $Explorer\ 14$, which was in orbit at the time.

Figure 1 is a photograph of a model of the event. It shows the proton flux and the magnetic field as observed at *Mariner* during a 2-hr period on October 7, 1962. The time base runs from left to right. There are five strips representing the currents observed by Neugebauer and Snyder in various energy channels of the proton flux analyzer (channels 3 through 7). A comparatively uniform flux was observed until 1547 UT, when the predominance of the current jumped from channel 4 to channel 5. The current in the lowest-energy channel, number 3, decreased, while a measurable current simultaneously appeared in channel 7. This jump has been interpreted as an increase in bulk velocity from 380 km/sec to 460 km/sec (see Paper 1). At the same time, the particle density more than doubled, from 15 protons/cm³ to 32 protons/cm³, and a substantial increase in proton temperature (from 1.2×10^5 to 1.7×10^5 °K) occurred. The temperature is defined by the spread of velocities observed by the plasma detector.

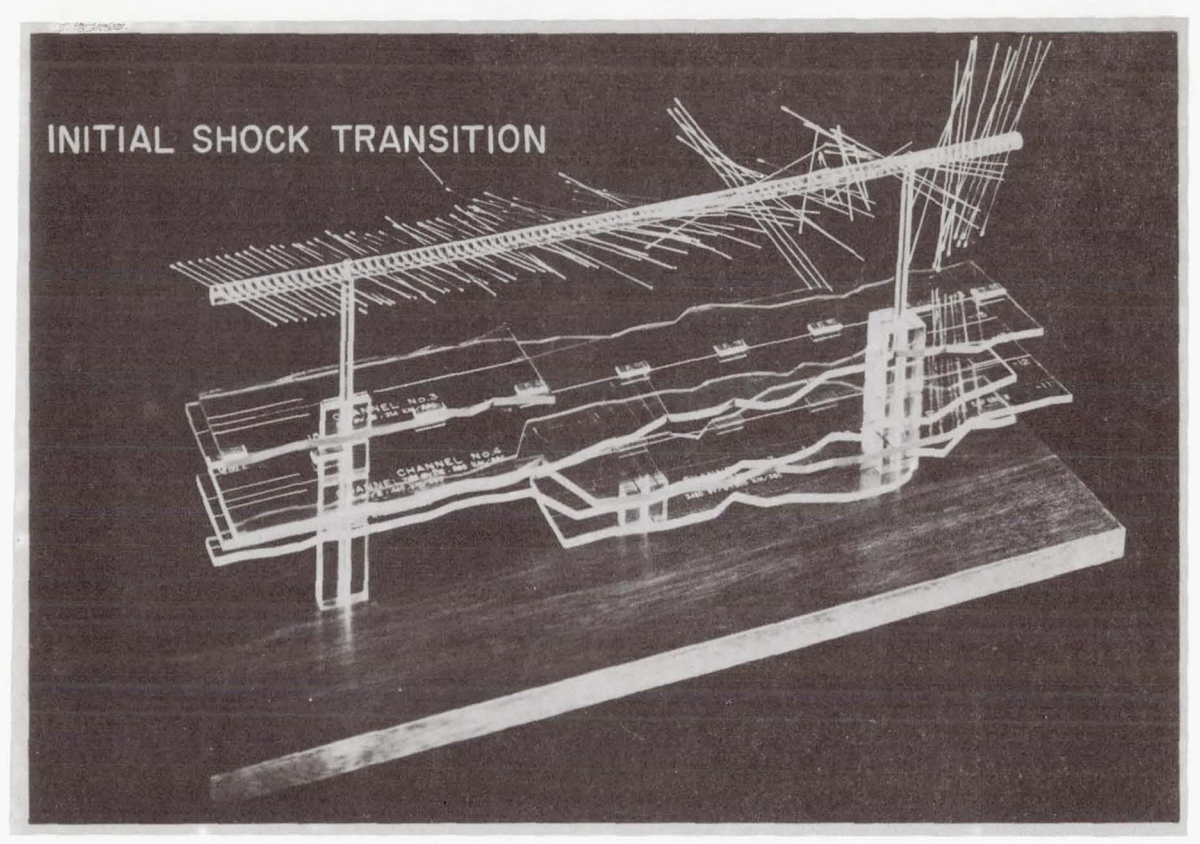


Fig. 1. Representation of magnetic field (above) and proton flux (below) observed by *Mariner 2* during the event of October 7, 1962

At the top of Fig. 1 are shown the magnetic-field vectors for the period under consideration. The values shown are subject to a correction based on the better knowledge that we now have of the magnetometer bias; however, the correction would not change the fact that until 1547 UT there was a uniform, steady field. A spike was observed at the moment of the shift in plasma velocity; and the spike was followed by a different average field with oscillatory behavior, and by increasing disorder as time progressed. This disorder lasted for hours.

Figure 2 shows the magnetometer data plotted in the spacecraft coordinate system (defined in Paper 3). Both the jump and the spike are characteristic of many of the theoretical analyses which have been made for collision-free shocks. There also seems to be structure present, with a

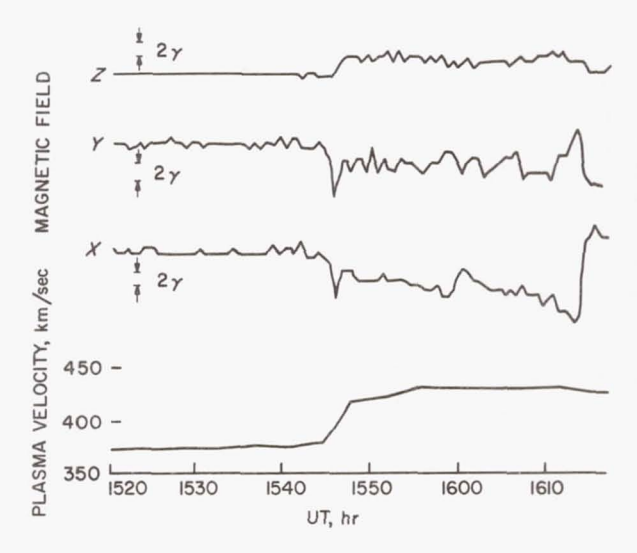


Fig. 2. Plot of magnetic-field and plasma velocity observed by *Mariner 2* during the event of October 7, 1962

period roughly twice the 37-sec interval between magnetometer readings. The corresponding wavelength of the structure would be 35,000 km, corresponding to about 100 proton gyro radii. The shock width is somewhat larger than a gyro radius, but is of course much smaller than the mean free path.

Figure 3 shows ground-based magnetometer records for this period. Fifty-one stations reported a sudden commencement at 2026 UT, 4.7 hr after the shock was seen at *Mariner*. This elapsed time was used to establish a shock speed.

Figure 4 shows the proton flux for the same period, measured by John Wolfe's *Explorer-14* plasma probe. The plasma detector had been measuring no plasma flux; this condition was consistent with the evidence that the probe was inside the Earth's magnetosphere. Within 2 min of the time that the sudden impulse was observed on the ground, however,

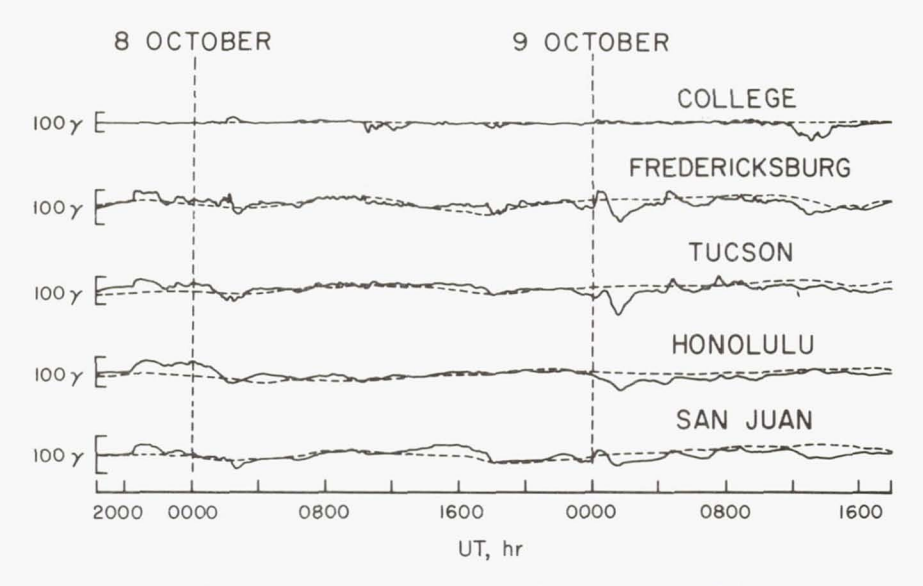


Fig. 3. Geomagnetic observations at several stations, October 7-9, 1962

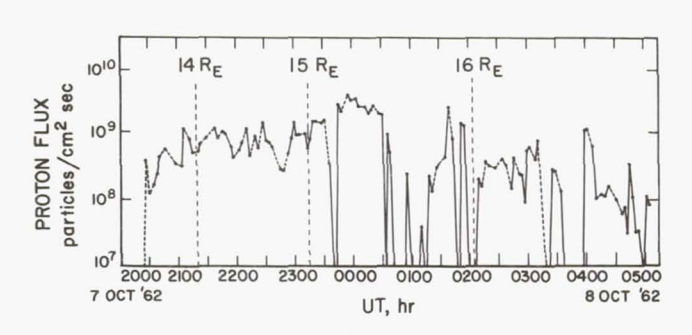


Fig. 4. Explorer-14 plasma observations on October 7, 1962. (From John Wolfe)

the plasma detector began to detect an appreciable proton flux. Furthermore, the proton flux was in a direction primarily 30 deg away from the Earth-Sun line and from the subsolar point, which is consistent with a

flow of protons around the magnetosphere. Our interpretation is that the event created a sudden pressure change sufficient to cause the magnetosphere to contract—thereby suddenly putting the *Explorer* vehicle outside of the magnetosphere, where it could detect the protons streaming past.

Properties of the Shock

The position of the *Mariner* spacecraft is illustrated in Fig. 5. The Earth–Sun line defines the **R** direction; **T** is in the ecliptic in the direction of planetary motion; and **N** is in a northerly direction. The spacecraft was offset from the Earth–Sun line by the distances shown in the figure. The velocities of the spacecraft and the Earth were approximately equal ($\sim 30 \text{ km/sec}$). The shock-normal direction, obtained from the magnetic field in a manner to be described, is slightly oblique. If a shock plane is constructed at the location of the spacecraft, the point at which this

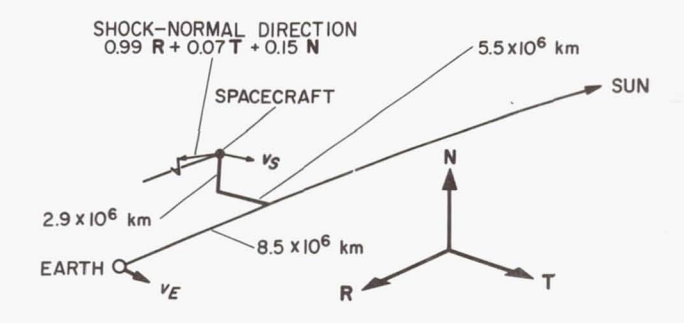


Fig. 5. Location of Mariner-2 spacecraft in heliocentric coordinates

plane intersects the Earth–Sun line can be determined. For the elapsed time (4.7 hr) and the distance from the point of intersection to the Earth, the shock speed is calculated to be slightly greater than the speed of the plasma: the shock has a Mach number of about 4.5.

By knowing the magnetic field before and after the event, we may establish the orientation of the shock plane as follows: the shock plane must contain the vector $\mathbf{B}_2 - \mathbf{B}_1$, where \mathbf{B}_1 and \mathbf{B}_2 are the magnetic-field vectors before and after the shock, respectively. It can also be shown that the plane containing \mathbf{B}_1 and \mathbf{B}_2 (and their difference) must be at right angles to the shock plane. Figure 6 shows the velocities and magnetic fields in the shock-plane coordinate system.

Let us now examine the properties of this event in the shock-plane coordinate system. The input parameters are: the magnetic field on both sides of the shock; the measured particle density ahead of the shock, taken as 15 protons/cm³; and the velocity ahead of the shock—380

km/sec. The velocity is assumed to have been entirely in the radial direction. The Rankine-Hugoniot equations of momentum and flux conservation (Ref. 2) are applied to obtain values for velocity and density behind the shock. The calculated values are then compared with those measured

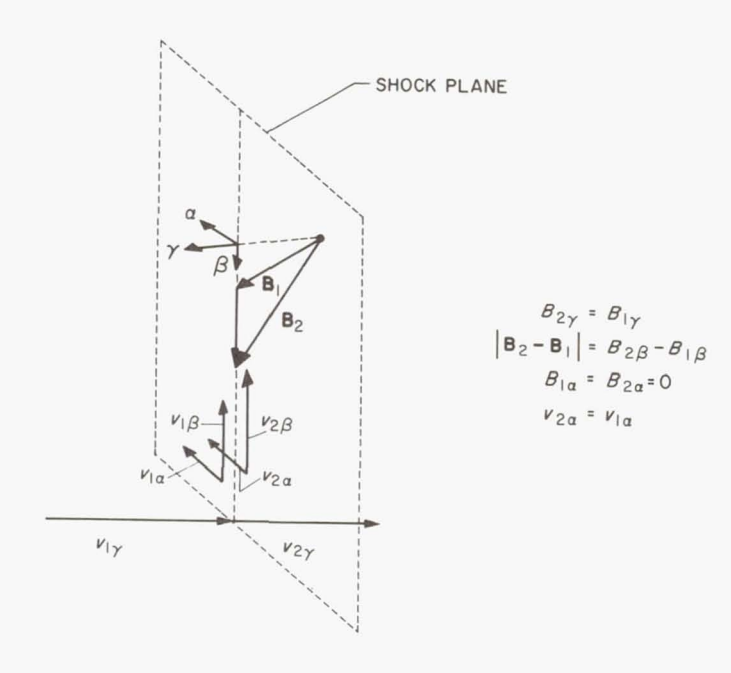


Fig. 6. Velocities and magnetic fields in shock-plane coordinates

by *Mariner*. If this was an oblique hydromagnetic shock, there must have been a change in velocity parallel to the change in the magnetic field. The velocity behind the shock must therefore have had substantial *T* and *N* components. The velocity direction cannot be obtained from the *Mariner* data, but the magnitudes can be compared.

The results of this computation are given in Table 1. The magnetometer zero correction that was used was not very different from the one discussed by Dr. Smith (Paper 3). The post-shock plasma velocity is about 2 deg from the radial direction. The density obtained is consistent with the density measured by *Mariner*, allowing for experimental error introduced by digitalization. In calculating density we considered the aberration due to the spacecraft's motion about the Sun. The correction to the density indicates the effect of the 2-deg nonradial flow, and this effect turned out to be unimportant. [While the Alfvén Mach number of the post-shock gas is found to be 1.3, the relevant wave velocity for computing

a Mach number would appear to be the fast magnetosonic velocity for the given magnetic-field orientation, and the post-shock gas travels at a speed that is only 0.8 of this velocity. The similarly-defined magnetosonic Mach number for the pre-shock gas is 2.3.]¹

The Problem of the Temperature

The treatment of the energy equation required additional considerations. An equation of state had to be assumed and, for want of anything better at this time, we took the γ of the gas to be 5/3. Both the input and output temperatures were then computed, and compared with the measured values. It can be seen from Table 1 that the computed temperature difference across the shock is much larger than that which was measured. We have assumed that the electrons went through the same temperature change as the protons.

Table 1. Measured and computed gas parameters, pre- and post-shock values for $\gamma = 5/3$

Parameter	Pre-Shock Measured	Post-Shock	
		Computed	Measured
B (10 ⁻⁵ gauss)	5R - 3.7T - 2.2N	_	5.9R-9.3T-6.1N
v (km/sec)	380R	450R+10T+14N	458 R
n(cm ⁻³)	15±2	34	32±4
T (°K)	1.2×10^{5} (measured) 1.1×10^{5} (computed)	2.4×10 ⁵	1.7×10^{5}
Mach No.	4.2	1.3	1.3

NOTE: Shock velocity is 509R based upon transit time and computed shock-normal direction.

Figure 7 indicates the sensitivity to the assumed value of γ ; if a low value of γ is chosen, a higher average computed temperature—but a smaller temperature difference—is obtained; for a large value of γ , the converse is true. Some theoretical studies propose that $\gamma=2$, because the magnetic field constrains only two degrees of freedom of the gas. It has also been proposed that energy is dissipated in the form of waves, and that there are increased degrees of freedom associated with the wave structure, which would suggest that $\gamma=\frac{4}{3}$. This is the area that is least well

Added in manuscript

determined by our calculations, and it would be very interesting to have other shock evidence and other calculations in order to ascertain more closely the appropriate value of γ .

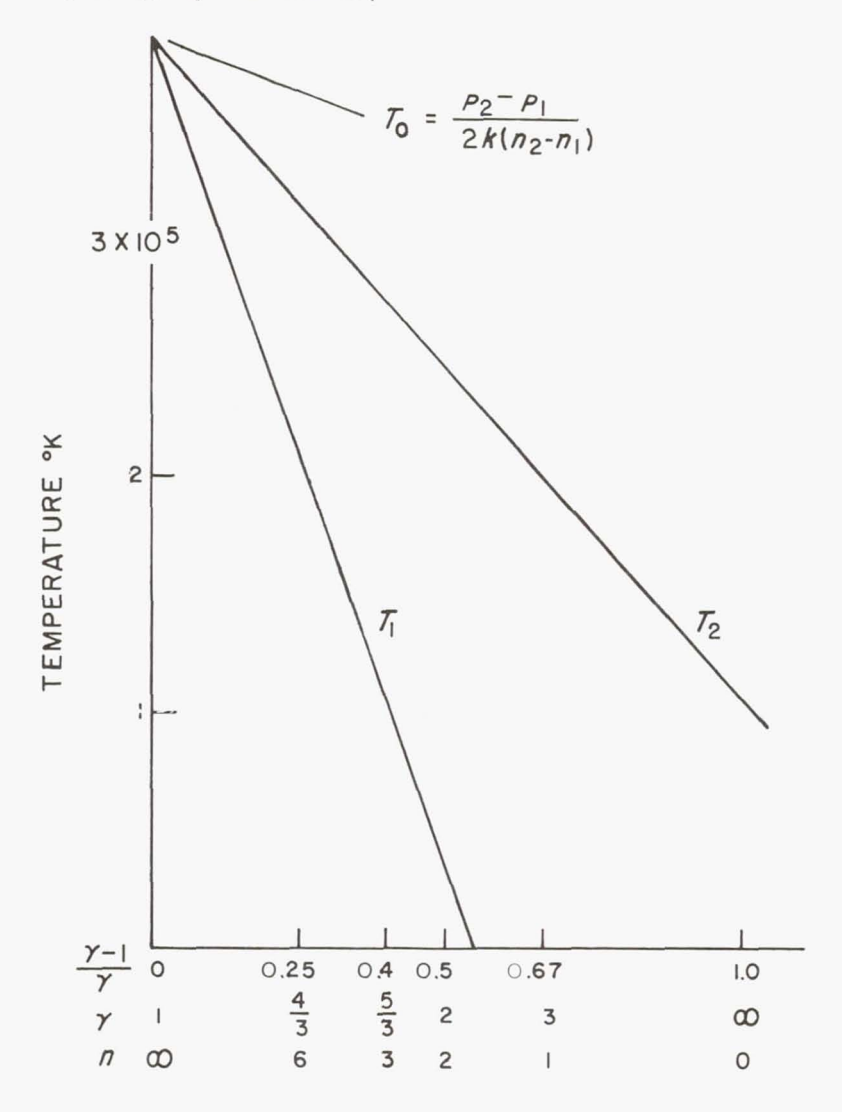


Fig. 7. Variation of temperatures with γ (ratio of specific heats)

In spite of all these difficulties, it is interesting to note that there has been definite evidence of a steep, collision-free shock front, across which there were sudden changes in the velocity, particle density, and magnetic field. This shock front maintained its steep character during the 4.7 hr

it took to reach the Earth, and over a distance of something like 0.05 AU, while going at a super-Alfvén speed relative to the gas in which it was traveling. Furthermore, the Rankine-Hugoniot relations seem to apply for describing the changes across such a shock front.

The authors acknowledge the assistance of Leverett Davis, Jr., E. J. Smith, and P. J. Coleman, Jr., who, with C. P. Sonett, carried out the *Mariner* magnetometer experiment; and of Conway W. Snyder and Marcia Neugebauer, *Mariner* plasma experimenters. They also appreciate suggestions from P. A. Sturrock, J. W. Dungey, and J. R. Spreiter.

REFERENCES

1. ADLAM, J. H. and J. E. ALLEN, *Philosophical Magazine* 3, 448 (1958).

AUER, P. L., H. HURWITZ, and R. W. KILB, *The Physics of Fluids* 4, 1105 (1961).

Davis, L. Jr., R. Lüst, and A. S. Schlüter. Zeitschrift für Naturforschung 13a, 916 (1958).

DUNGEY, J. W., Philosophical Magazine 4, 585 (1959).

SONETT, C. P., D. S. COLBURN, L. DAVIS, JR., E. J. SMITH, and P. J. COLEMAN, JR., *Physical Review Letters* 13, 153 (1964).

The potential importance of such shocks in interplanetary space has been pointed out by: Gold, T., Gas Dynamics of Cosmic Clouds, ed. by H. C. van de Hulst and J. M. Burgers, North-Holland Publishing Co., Amsterdam (1955) p. 103.

Parker, E. N., Interplanetary Dynamical Processes, Interscience Publishers, a division of John Wiley and Sons, Inc., New York (1963).

2. THOMPSON, W. B., An Introduction to Plasma Physics, Pergamon Press, London (1962) p. 92.

DISCUSSION OF COLBURN PAPER

BIERMANN: What do you mean when you say the Mach number was equal to about 4?

COLBURN: If we consider an observer to be at rest in this gas, the shock front advanced toward the observer with a velocity four times the Alfvén speed. Relative to the gas behind the shock, the Mach number should have been less than 1, although actually our calculations show it was a little greater than 1. Some of the assumptions that we have made may have been off by that amount. DAVIS: Was 509 km/sec the velocity at which the shock front moved along the radius vector from the Sun, or was it the velocity with which the shock front moved normal to itself?

COLBURN: It was the radial velocity and was about 4 percent greater than the normal velocity because the shock was slightly oblique.

DAVIS: I would also like to ask about any additional equations that you used with the shock equations. Did you use some of Maxwell's equations?

COLBURN: Yes. Besides conservation of flux, momentum, and energy, we also used conservation of tangential electric field.

OLBERT: You used $E = -v \times B$ for the electric field on both sides of the shock? **COLBURN:** Yes.

DAVIS: I have still another remark, which is important to some of the things that we were involved in yesterday (discussion of Paper 3). The calculations just presented depend upon knowing what the field strengths were before and after the shock, which, in turn, depend upon knowing what the bias fields were in the spacecraft. At the time that Drs. Sonett, Colburn, and Briggs embarked on this

study, we did not have the estimates that were presented to you yesterday (Paper 3). They made a very admirable and very extensive calculation using a variety of biases, and they found that, for most spacecraft biases, the results did not seem to be consistent. About the time they were ready to say what biases were consistent, we were about ready to say what we thought the spacecraft biases should be. These values agreed as closely, I think, as you could expect from either type of analysis, and this agreement gives me a little greater faith in the biases that Dr. Smith used as a basis for discussion yesterday, at least for October 7.

NESS: Again, I think that if you make this sort of zero correction and argue only on the basis of internal consistency, you get out exactly the physics you put in at the beginning. It seems to me that if you got widely different characteristics of the shock by assuming different biases in the zero level of the *Mariner* fluxgates, it means that the results are very critically dependent upon the values of the bias fields and that you have to know the exact values before you can really understand the physics. You should be very careful to consider the possibility that the physics really isn't what you think it should be.

DAVIS: When you have data that is not as complete as you would like, you have two choices. You either throw it away and say, "Well, forget about that part of the solar cycle for another eleven years," or you say, "We will learn what we can." One way to learn what we can is to see if our data fit a consistent model. I think it is very pretty that the data we are discussing do fit a shock and do agree with most of the things that we think should happen in a shock. The discrepancies are really not worth arguing about.

WILKERSON: I don't see how you can have it both ways. On the one hand, you say that, you get agreement, except for little differences that aren't worth talking about, but on the other hand there is this factor of 2 in the temperature. Since temperature information (that is, agreement or disagreement with the Rankine–Hugoniot relations) has been very useful in studying laboratory shock waves in the past, I don't see how you can use both of these arguments simultaneously.

I grant that we should try to find out everything we can, but since we don't know very much about this kind of shock wave yet, I think it is a little risky to use self-consistency arguments as a test of both experimental validity and theory. **DAVIS:** I think temperature is a convenient tool for describing the amount of energy in the random motions of the gas. The measured temperatures may disagree somewhat with the predicted temperatures, but not greatly.

NESS: I have a question about the flow of protons around the Earth. At the time the protons were detected on *Explorer 14*, was the probe inside the Earth's bow shock?

COLBURN: Yes. The data are consistent with a picture in which *Explorer 14* was outside the magnetosphere but inside the shock boundary, since if it had been outside the shock boundary, one would expect the flow to have been from the direction of the Sun. Later, *Explorer 14* did observe a flow that was coming directly from the Sun, which implies that at that time the satellite was beyond the shock.

WILKERSON: If you even believe in an equation of state, it seems to me that you have to allow for the variability of γ in order to account for additional degrees of freedom (that is, turbulence) created by the shock wave. It might be worth looking at the influence of a change of γ .

SMITH: It wasn't clear to me from the discussion whether or not γ had a single

value that was consistent with the temperatures observed before and behind the shock.

COLBURN: No, it did not.

PETSCHEK: Can't one solve the problem by saying that some of the energy went into the electrons? All you know from the conservation-of-energy equation is the sum of the electron and ion temperatures.

COLBURN: If we say that equal amounts of energy went into the electrons and the protons, we have the results I have given. If we could say that a larger proportion of energy went into the electrons, then we would have a calculated temperature more consistent with the experiment. I understand that one of the probes, in going through the shock around the magnetosphere, sensed primarily electrons rather than protons, which may suggest that the electrons received the major portion of the available energy.

DAVIS: If you recall Marcia Neugebauer's discussion (Paper 1) of the difference in temperature between the alpha particles and the protons, you realize that you must have a very non-Maxwellian distribution on both sides of the shock and that

the situation is very complicated.

It is intriguing to consider that the gas starts with relatively little random energy and that, as it goes through the shock, it converts some of its bulk motion into a motion that is more or less random. If, in this process, the excess energy goes into the circular motion of particles around the field lines, then the alphas will have four times the temperature of the protons, which is a very nice coincidence.

OLBERT: I would like to know if the temperatures defined by Snyder and Neugebauer and the temperatures used in this present paper, with $\gamma = 5/3$, are identical. I was under the impression that the temperatures calculated by Snyder and Neugebauer were based solely on a one-dimensional random motion.

NEUGEBAUER: We calculated temperature from the spread in the radial direction, which is the width of the velocity peak. In our recent work, we assumed that the random motion was isotropic, even though we could only observe the one dimension. Thus, the two temperature definitions are identical.

NESS: I think we have additional information from the interaction of the solar wind with the Earth's magnetosphere, which indicates that γ must lie between

5/3 and 2. I intend to discuss this tomorrow (Paper 22).

COLBURN: I would like to add that, despite the possible uncertainties in some of our calculations, the purpose of considering a single case like this is not so much to prove a point in physics as to suggest a possible area for future investigation and a method by which such events can be systematically explored.

Page intentionally left blank

MAGNETIC FIELDS IN THE SOLAR PHOTOSPHERE

R. B. LEIGHTON

California Institute of Technology, Pasadena, California

THERE was considerable discussion following Dr. Davis' paper (Paper 9) concerning how the lines of force that start in the photosphere of the Sun are connected, and how they may become reconnected as a result of various phases of solar activity. I can't pretend to say anything about the reconnection of lines of force, but people here at Caltech, at Mt. Wilson, and elsewhere have been measuring the magnetic fields at the solar photosphere for some time, and a pretty good picture is available of what the fields are like at that level. It was not always clear to me that the people who were trying to follow lines of force into space were adequately taking into account what we now think this magnetic pattern is, so it might be worthwhile to try to describe briefly how the lines of force are thought to look.

Figure 1 is a pictorial record of the magnetic fields in the regions near sunspot groups. If you ignore the large-scale imperfections (the streaks and so on, which are not magnetic fields), and the very tiny scale things (which are noise and some dust specks), then you are left with some rather patchy dark and light areas. The dark areas, let's say, indicate north polarity and the light areas indicate south polarity. You can see that there are a number of bipolar regions, with the polarities reversed in the two hemispheres (the equator is roughly across the middle of the picture). Figure 1 indicates that the magnetic field is patchy, but has the same polarity over fairly large regions. The individual north and south regions are fairly large, after having grown out of smaller north and south regions which came from sunspots.

The right-hand side of Fig. 2 again shows a magnetic pattern with, let's say, bright south-polarity regions and dark north-polarity regions. This figure illustrates that one can, in a way, see the magnetic field by observing the chromospheric network, which is represented in the left half of Fig. 2. If you look carefully, you will see that wherever there is a region of

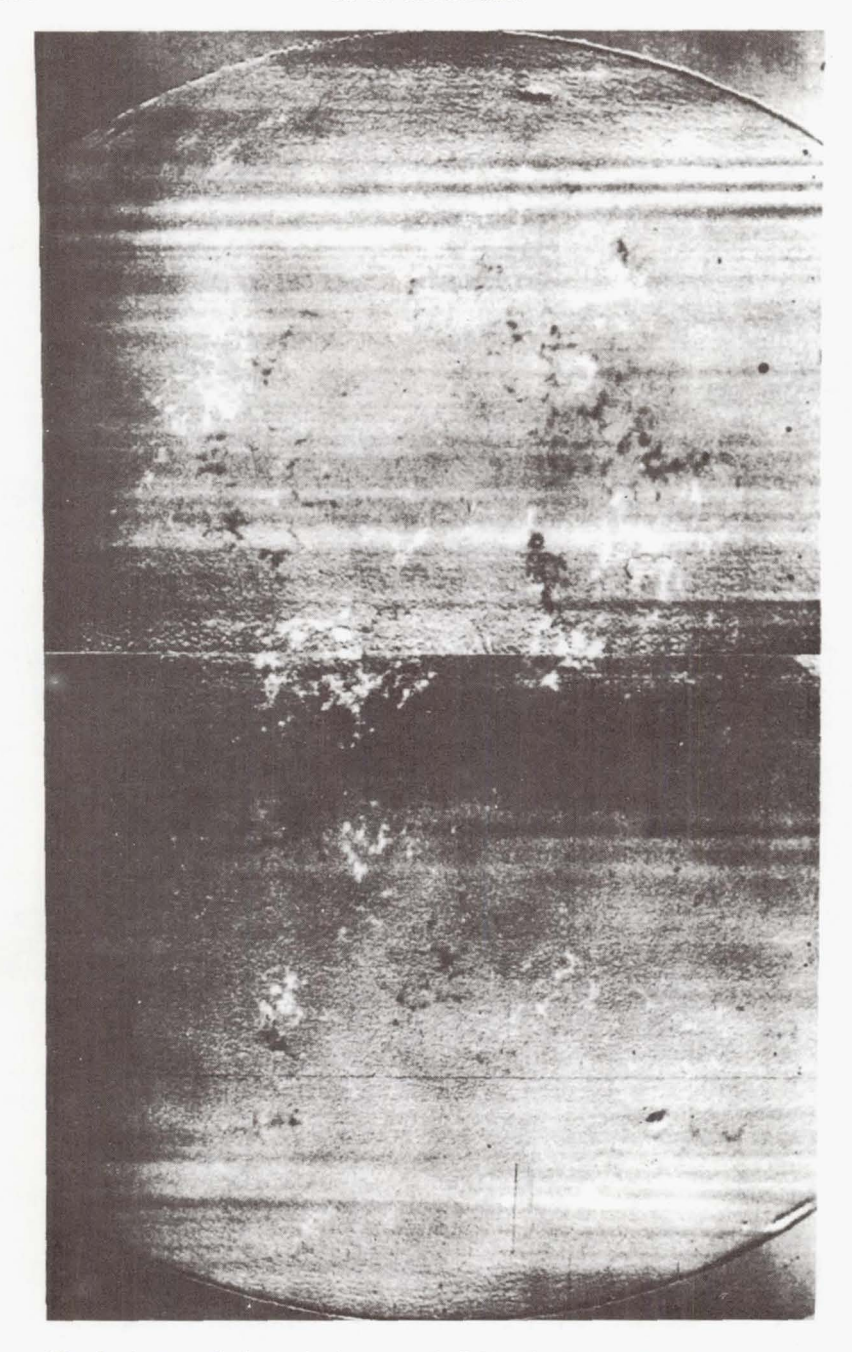


Fig. 1. A map of photospheric magnetic fields: the light and dark areas have opposite polarities

concentrated magnetic field, there is a corresponding region of emission in the chromosphere. I point out this correspondence so that if you look at a spectroheliogram, you can guess where the magnetic field is entering or leaving the Sun. Of course, this means there is a high magnetic-field strength in the plage regions surrounding sunspot groups.

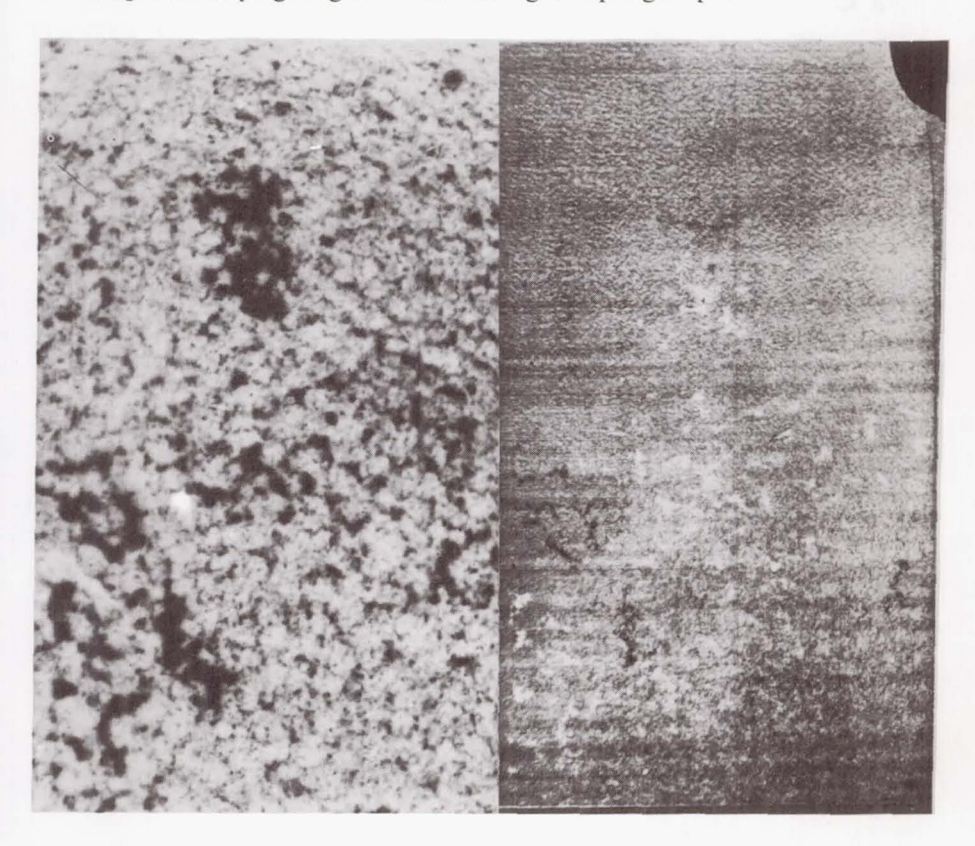


Fig. 2. Magnetic map (right) and a spectroheliogram of chromospheric emission (left) of an active region on the Sun

Figure 3 shows an $H\alpha$ spectroheliogram, illustrating another case in which the bright regions are concentrations of the magnetic field. But in this figure, there are also some dark filaments, so-called disk filaments, which seem consistently to separate areas of opposite polarity. So one can say with some certainty that lines of force coming out of a bright region close to one side of this boundary of zero magnetic field, which is what we think it is, must end somewhere close by on the other side of the filament.

You can imagine, then, lines of force starting close to one side of these

boundaries and looping over to the other side, and somehow supporting or having a quiescent prominence as the line of demarcation between the polarities. It is interesting that these boundaries show a remarkable stability over several rotations of the Sun. The prominence, having gone around the Sun as the Sun rotates, will reappear in very much the same

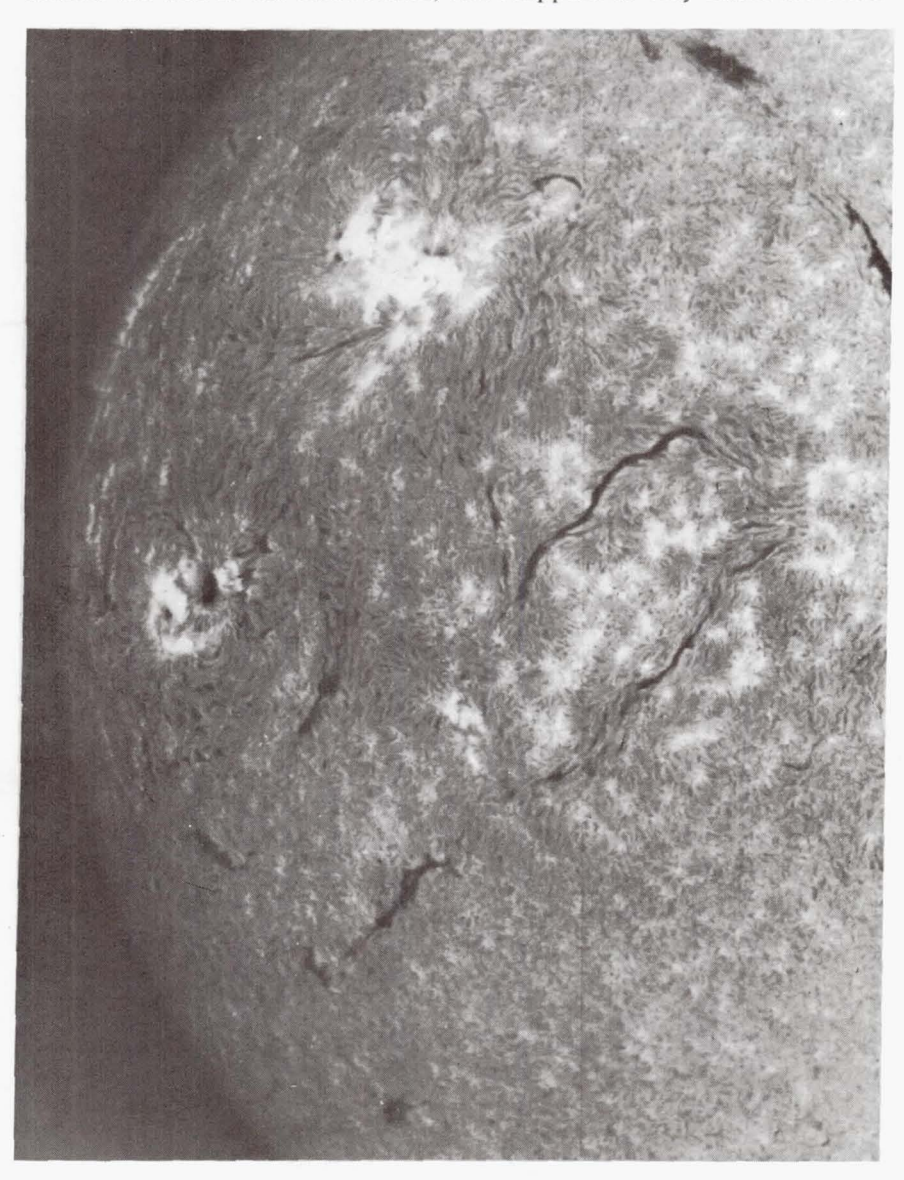


Fig. 3. An Hα spectroheliogram of an active region with disk filaments

place as before, having been somewhat elongated and changed by the differential rotation of the Sun.

I am trying to establish some principles by which you can determine for yourself, on other occasions, where the lines of force might go. You can, of course, see in Fig. 3 the iron-filing effect of the lines of force near the sunspot groups.

Figure 4 shows a rather early version of the magnetograph representation of the magnetic field on the Sun. With the aid of this figure, we can

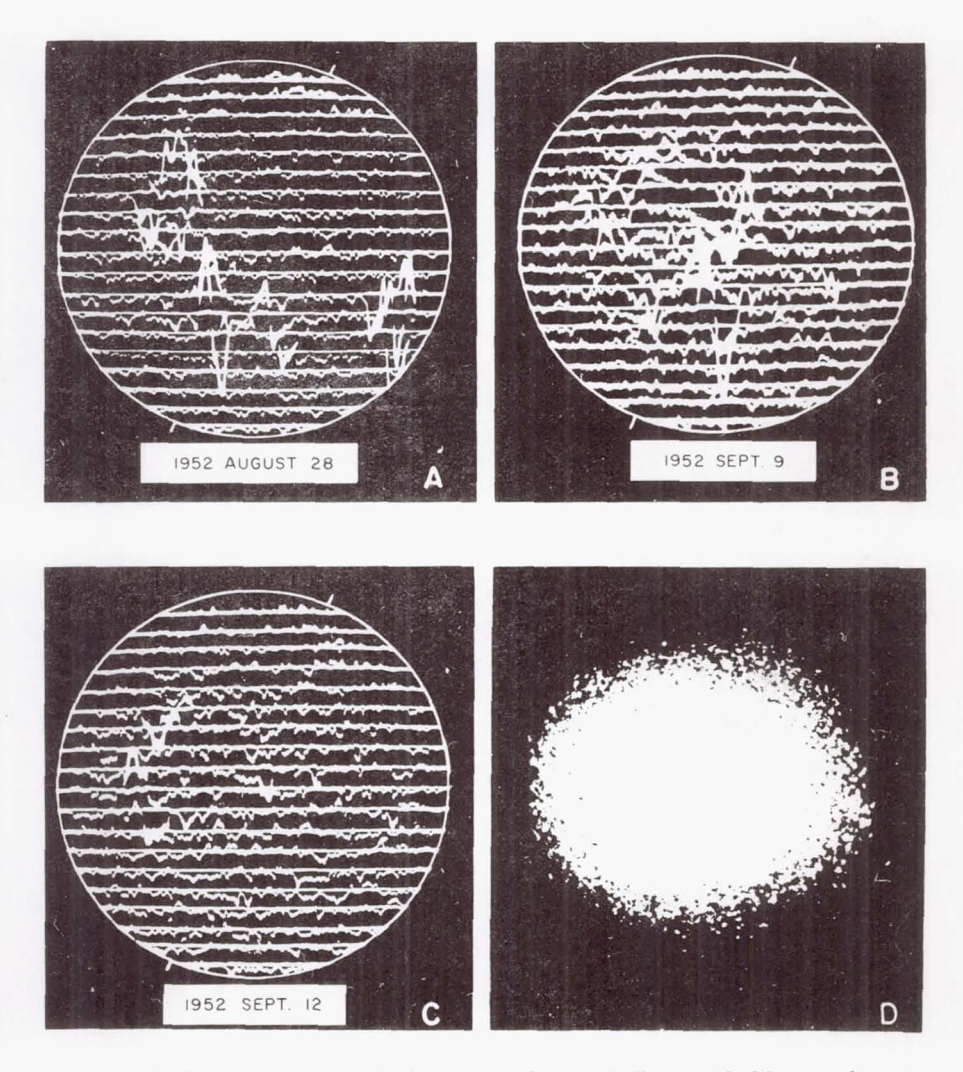


Fig. 4. Solar magnetograms (a, b, and c) and spectroheliogram (d). Photographs from the Mt. Wilson and Palomar observatories

now perhaps understand the small-scale fields with a variation of strength over regions of 10,000 to 20,000 km or so, which represent those concentrations of magnetic field that we saw in the previous figures. However, we note also that the field retains a single polarity over a considerable region of the Sun; it does not flip back and forth over small areas. There are places, of course, where the field is much stronger, corresponding to regions where recently there were sunspot groups. We also note that, in the polar regions, the field tends to have some non-zero average value, which gives rise to the idea of a general dipole moment for the entire Sun.

So, if I had to draw a picture of the lines of force on the Sun, by using the one equation that I am sure we all agree with, $7 \cdot \mathbf{B} = 0$, I might draw some bipolar regions of field, which might sometimes be embedded in larger but very much weaker regions. Near the poles of the Sun there might be fairly large regions of opposite polarities.

The lines of force, then, might be concentrated into little narrow channels, but with the same polarity over fairly large regions. At some other place on the Sun, there would be similar concentrations of lines of force, with the arrows going the other way. Presumably you could draw small loops connecting the parts of a bipolar region, but since this region might be embedded in a larger region, some of the lines of force might extend outward for a very large distance before they reconnect—just where they reconnect is beyond my direct knowledge. However, I think it has to be said that every time you draw a line of force that goes off into space, you had better draw one somewhere that comes back to a similar kind of region. I would think that if we have a large unipolar region, the lines of force leaving this region would automatically return to another unipolar region of nearly similar size.

How the field lines are modified by the ejection of material at the beginning of explosive events that are down close to the photosphere, is a very proper subject for speculation.

DISCUSSION OF LEIGHTON PAPER

SMITH: Do you anticipate that some of the field lines joining large unipolar field regions cross the equator?

LEIGHTON: Yes. The lines of force have to come back to the Sun.

SMITH: I noticed that the filaments were turned at an angle; are the field lines at right angles to these filaments?

LEIGHTON: The filament is a boundary between two regions of opposite polarity. The lines of force probably go across the filament nearly at right angles to it.

SMITH: One could then find field lines that were going from one solar latitude to another solar latitude?

LEIGHTON: Yes.

SMITH: Then, perhaps some of the field lines could, after all, be directed out of the ecliptic. I think we have all been, to a certain extent, victims of the fact that we are forced to draw figures in planes, so that we either look into the

ecliptic or at a plane perpendicular to it.

If we follow Dr. Leighton's model, then as the Sun rotates under us, it is certainly conceivable that we would observe fields of predominantly one polarity. Since we make observations only in the ecliptic, we would not see the oppositely directed field lines which return to the Sun at some different latitude. It seems to me that this argument makes it at least plausible that a result of the kind seen on Mariner 2 could occur. Whether you accept it or not, of course, as Dr. Ness likes to point out, depends largely on what the spacecraft biases are. The fact that the field seems to be directed predominantly outward from the Sun for an entire solar rotation is really not the fundamental problem and doesn't contradict any basic physics. You cannot establish the conservation of magnetic flux by making observations only in the ecliptic.

I would also like to comment on some of the differences between various models of the interplanetary field. I think some of these differences are actually more apparent than real. Professor Gold and others like to talk about drawn-out loops of field lines. They clearly want to assign directions to the field lines, and they like to think of a region in interplanetary space where the field lines curve

back and return to the Sun.

units away.

Once the field lines have left the Sun, they can presumably extend outward for a great distance. The dimensions of the interplanetary cavity are not really known, but Dr. Davis has estimated a radius of 50 or maybe even 100 AU. The *Mariner* data indicate there were several long-lived regions on the Sun. The plasma from such a region continues to go out into space, so that the distance at which the field lines turn around is soon past the orbit of the Earth and far beyond the observations of the spacecraft, perhaps many tens of astronomical

Because the Sun rotates, you would expect a spiral structure and some kind of a "wrapping around" of the field lines from the long-lived region. I am thinking of a model which Piddington described, and on which Dessler has also made comments. You might expect the spiral to cross the Earth's orbit at an angle of about 45 deg. As the plasma emission continues, these field lines form very large spiral angles, approaching 90 deg at a distance far beyond 1 AU. If the lines originated from some small, bipolar region on the Sun (a sunspot group, for example), then you would have oppositely directed spiral lines close together. If you had several of these long-lived disturbed regions, then during a 27-day period you would see several such reversals of the magnetic field. Then if you looked at a region of space within 1 AU, you would see a picture very similar to Parker's model, except that Dr. Parker has not concerned himself with just how the lines return.

However, as Dr. Leighton has shown, there is no reason to assume that the situation is this simple. Dr. Davis made a similar comment concerning his study of solar magnetographs, which showed a sunspot field spreading out to become very weak. Field lines that start at one place near the ecliptic may return to another place very far from the ecliptic, so that the return of the line of force

may not be seen from a spacecraft.

WILCOX: It appears that the base line for the *Mariner* magnetometer was finally chosen so that the radial field component was almost always positive during several solar rotations. However, if you look at the solar magnetograms for any latitude during several solar rotations, you nearly always find approximate equality between positive and negative polarities: you almost never find two rotations during which the polarity is all positive. Even giving full consideration to

your comments about magnetic-field lines running out of the ecliptic, it may be that a constantly positive polarity during two rotations is an unlikely event.

COLEMAN: We¹ have studied the orientations of the magnetic-field component that is perpendicular to the solar radius. If you assume any sort of crude spiraling at all, then you would expect this component to point one way for a field line leaving the Sun, and to point in the opposite direction for a field line returning to the Sun. In the first 60 days, we saw such reversals in this transverse component. We know the zeroes of the two pertinent magnetometers pretty well for this period. We haven't yet looked for any sort of correlation between the directions and the magnitudes to see if the flux roughly averaged out to zero. But we do know that for a small fraction of the time during the first two rotations, the observed field reversed itself.

WILCOX: Then don't you think that there is something to be explained when you look at the magnetograms?

COLEMAN: I would think, from looking at Dr. Leighton's pictures, that there can be conditions on the Sun that cause you to see more of one polarity than the other during any given rotation. I don't think such conditions can last for very long, but I think they existed during the time of the *Mariner* observations.

LEIGHTON: Such conditions may last a *very* long time. The north and south poles of the Sun by no means have the same strength, or total flux. If you believe that the lines of force that come from one pole must return somewhere else than to the other pole—where better than to the equator? It is very difficult to measure the net flux coming out of any region, because the calibration of the magnetogram is never good enough. However, I see absolutely nothing wrong with the idea that there may be, for years at a time, an average south polarity, say, distributed around the equator in a very irregular fashion.

THE PENETRATION OF GALACTIC COSMIC RAYS INTO THE SOLAR SYSTEM

E. N. PARKER

University of Chicago, Chicago, Illinois

The Interplanetary Magnetic Fields

The lines of force of the interplanetary magnetic fields originate on the Sun and are extended through space by the solar wind. The fields move outward with the solar wind, sweeping all charged particles along with them. The galactic cosmic rays, which fill interstellar space outside the solar system, penetrate into the solar system against these outward-sweeping fields, so that the cosmic-ray intensity is considerably reduced here deep in the solar system (Ref. 1 and 2). Variations in solar conditions, affecting both the solar wind and the magnetic fields, lead to varying reduction of the cosmic-ray intensity.

The basic, underlying pattern of the interplanetary magnetic field has a unique form based on the assumptions that:

- a. There is an approximately radial outflow of ionized gas from the Sun,
- b. The magnetic lines of force carried in the gas generally remain connected to the Sun for at least a few days after leaving the Sun, and
- c. The Sun rotates with an angular velocity Ω .

It follows that the lines of force in interplanetary space have the general form of an Archimedes spiral (Ref. 2 and 3)

$$r = \frac{v(\phi - \phi_0)}{\Omega} \tag{1}$$

The components of the field are given by

$$B_r \propto \left(\frac{R_s}{r}\right)^2$$

$$B_\theta = 0$$

$$185$$
(2)

and

$$B_{\phi} \propto \frac{R_{\rm S} \Omega}{v} \frac{R_{\rm S}}{r} \sin \theta$$

along any given spiral line of force. Here r is the radial distance, θ is the polar angle, and ϕ is the azimuth measured around the Sun. The general appearance of this type of field pattern is illustrated in Fig. 1.

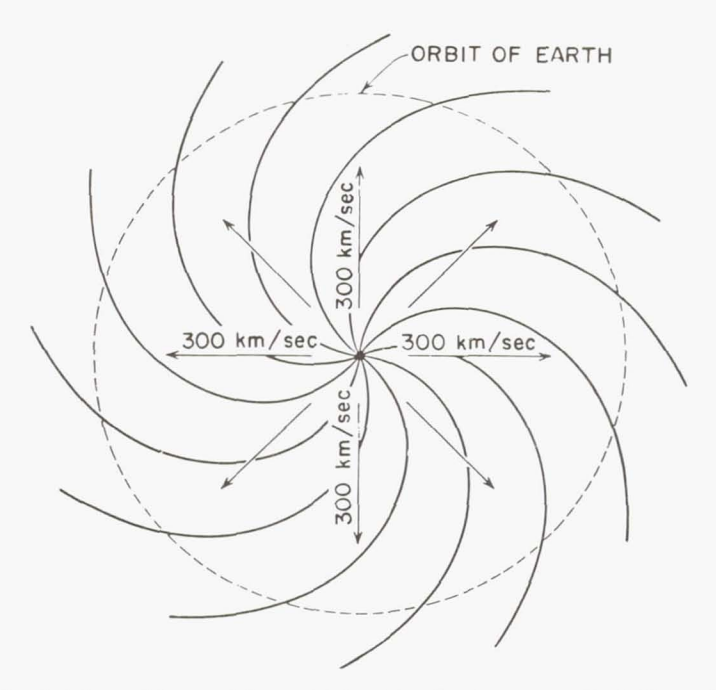


Fig. 1. Lines of force of the quiet-day interplanetary magnetic field, resulting from the extension of the general solar field by an idealized, uniform 300-km/sec quiet-day solar wind

This general spiral pattern presumably extends as far into space as the solar wind does—some 10 to 100 AU (Ref. 2 and 4). On this underlying pattern are superposed a variety of both small and large magnetic irregularities, caused by variations of v with θ , ϕ , and t, by variations of $B(\theta,\phi)$ with t, by instabilities in the wind, etc. (Ref. 2 and 5).

Forbush Decreases

The basic, smooth field by itself would not greatly impede the penetration of cosmic-ray particles into the solar system. The distortions in the field may be an extremely effective impedance, however. For instance, a sudden outburst in the solar corona leads to a blast wave that propagates outward through the solar system. Figure 2 shows the distortion of the

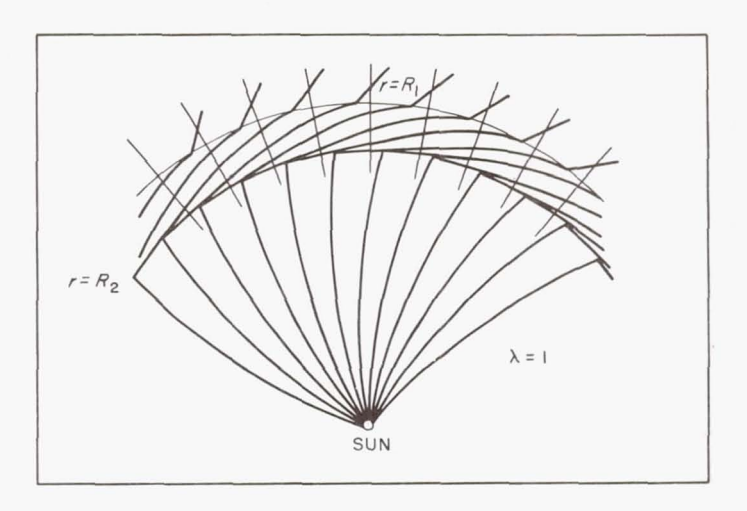


Fig. 2. Distortion of the quiet-day interplanetary field by a blast wave. The shock radius R_1 at the head of the blast wave is taken to be v/Ω , and equals 1 AU for a quiet-day wind velocity of 440 km/sec

basic field pattern by an idealized blast wave (infinite Mach number, spherical symmetry, etc.); the blast wave is driven with constant velocity by the enhanced corona. One essential feature of the wave is that it compresses the magnetic field, which then becomes a reflector of cosmic rays. Compression of the field by a factor f produces a reflectivity of 1-1/f, which may be 90% or more. The high reflectivity tends to isolate the region between the wave and the Sun, so that individual cosmic-ray particles in that region tend to remain there for several hours. During their confinement the particles undergo adiabatic expansion, leading to a reduction of the cosmic-ray energy density by as much as 50%.

Figure 3 shows the energy spectrum of this reduction $(\Delta\mu/\mu_0)$ computed from the idealized blast wave of Fig. 2. The extent of the flat portion of this energy spectrum depends on the thickness (R_1-R_2) of the compressed-field region. The flat part of the spectrum may initially extend to energies as high as 10^{11} ev. Full reduction sets in during the time that the blast wave sweeps past the observer—this time period may range from a few hours in the case of a single blast wave to as long as several days in the case of successive blast waves. During the recovery phase, the $\Delta\mu/\mu_0$

curve becomes progressively steeper, as indicated in Fig. 3. The rapid onset and flat energy spectrum are characteristic of a Forbush decrease (Ref. 2 and 6).¹

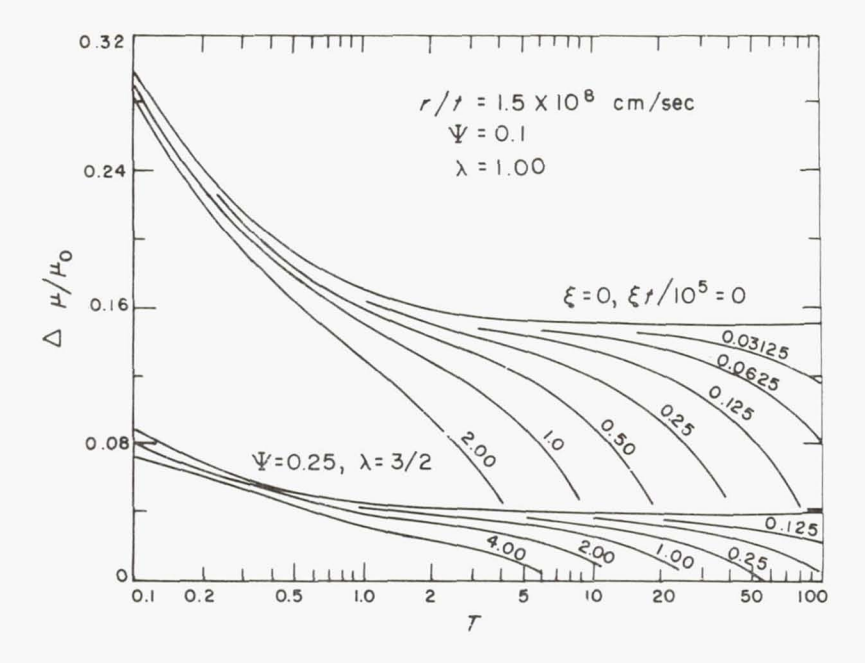


Fig. 3. Relative cosmic-ray decreases $\Delta\mu/\mu_0$ for the two cases of a strongly driven blast wave ($\lambda=1.0, \psi=0.1$) and a freely coasting wave ($\lambda=1.5, \psi=0.25$) with various amounts of particle drift into the region behind (represented by the parameter ξ). (Here, the blast-wave radius is proportional to $t^{1/\lambda}$, defining λ ; and ψ is the transmission coefficient of the blast wave.) The curves apply to protons, so that T represents energy measured in units of the rest mass -931 Mev. The mean blast-wave velocity r/t in transit from the Sun to the Earth is taken to be 1.5×10^8 cm/sec. For the case $\lambda=1$, the curves represent the subsequent time dependence of $\Delta\mu/\mu_0$ if ξ is replaced by $\xi t/10^5$. Otherwise the curves correspond to the decrease following the passage of the wave at time $t=10^5$ sec

11-Year Variation

The outward convection of small-scale irregularities (from 10⁵ to 10⁷ km) in the underlying magnetic pattern produces a continuous reduction of the cosmic-ray intensity throughout the inner solar system. To illustrate some of the general physical properties of this reduction, we use the idealization introduced many years ago by Morrison (Ref. 7) when he was discussing the passage of cosmic rays in clouds of disordered field.

¹The Forbush decrease, which follows a flare on the Sun, should not be confused with the recurring 27-day cosmic-ray storm, which usually has a gentler onset and a softer spectrum

He took the particle motion to be an isotropic random walk with a length of step comparable to the scale of the irregularities. The field is probably not so disordered that this treatment of the particle motion can be considered to be rigorous. The effective diffusion coefficient is probably greater parallel to the field than it is perpendicular to the field. But this analysis is adequate to illustrate the physical consequences of the field disorder. The diffusion coefficient K is taken to be one-third the step length times the particle velocity. The net particle flux in the frame of reference that is moving with the magnetic irregularities is $-K\nabla N$, where N is the number of cosmic-ray particles per unit volume. The irregularities are, of course, moving with approximately the solar-wind velocity v, so that in treating the present problem, the transport Nv must be included too. The total transport flux is then $\mathbf{F} = N\mathbf{v} - \mathbf{K} \nabla N$. For steady conditions, conservation of particles yields $\nabla \cdot \mathbf{F} = 0$. The idealized case of spherical symmetry about the Sun yields F = 0. This expression integrates to $N(r) = N_0 e^{-n}$, where n is the integral of v/K from r to interstellar space, and N_0 is the cosmic-ray density in interstellar space. Typical step lengths of 10^{11} to 10^{12} cm give $K = 10^{21}$ to 10^{22} cm²/sec, with a reduction of intensity ranging from $e^{6.0}$ to $e^{0.6}$, respectively, in a 400-km/sec wind and over a distance of 10 AU. Thus the reduction of the galactic cosmic-ray intensity in the solar system is both large and uncertain. The expected variations of v and K with solar activity should produce the observed 11-year cosmicray variation (Ref. 1 and 2). Recent analysis by Simpson (Ref. 8) shows the interesting fact that the variation in the cosmic-ray intensity lags behind the level of solar activity. The lag is different on the rising and falling sides of the solar cycle and is different for different particle energies, but the general lag suggests that the diffusion of cosmic rays through the interplanetary fields may begin as far out as 30 AU, where the wind arrives some 4 months after passing the orbit of the Earth.

The spectrum of the cosmic-ray reduction resulting from the irregularities in the field depends in some detail upon the form and scale of the irregularities (Ref. 2 and 9). Suffice it to say that the reduction diminishes with increasing particle energy and is not flat, as the Forbush-decrease spectrum can be. Simple models (Ref. 1 and 2) predict an energy dependence proportional to $E^{-\gamma}$, where γ ranges from 0.5 to 2 or more. Analysis of the observations has produced a variety of results, all in this general range.

27-Day Variation

The 27-day recurring cosmic-ray decreases presumably result from the enhanced solar-wind velocity and increased field disorder associated with active regions on the Sun. Sarabhai (Ref. 10) has suggested that the fast wind from a hot coronal region crowds into the slower wind from

elsewhere around the Sun, and that this crowding may be responsible for much of the recurrent variations.

Diurnal Variation

The well-known diurnal variation in the cosmic-ray intensity (Ref. 11 and 12) represents a net streaming of the cosmic rays at 400 km/sec in the direction of the Earth's orbital motion. The streaming results from a combination of two effects: the interplanetary field is semi-regular in the vicinity of the Earth's orbit (Ref. 13 and 14), so that particles tend more to move along the lines of force than to diffuse across them; and the magnetic irregularities beyond the Earth's orbit (Ref. 1 and 15' permit sufficient diffusion to neutralize any θ or ϕ gradients of the cosmic-ray intensity that might have been introduced by the polarization field $\mathbf{E} = -\mathbf{v} \times \mathbf{B}/c$ as the particles entered the solar system (Ref. 16). The result is that the principal streaming of the cosmic-ray particles in the vicinity of the Earth is limited to the electric drift $\mathbf{u} = \mathbf{E} \times \mathbf{B} = \mathbf{v}_{\perp}$ and to an arbitrary velocity \mathbf{v}_{\parallel} along the magnetic lines of force. The fact that there is no net radial streaming under steady conditions determines v_{II}. The net streaming $V_{\perp} + v_{\parallel}$ is readily shown to be $\Omega \times r$, which is the velocity of rigid rotation with the Sun and which agrees with observation.

Outstanding Problems

This discussion has summarized the physics of the penetration of interstellar cosmic rays into the solar system. The development of a more quantitative model must await additional and more quantitative observations of the interplanetary fields, both near and far from the Earth's orbit. The theory, illustrated by the idealized examples given here, shows that the variation in the cosmic-ray intensity at 1 AU depends principally upon the irregularities introduced into the basic spiral magnetic form (Eq. 1 and 2). Observations must concentrate upon the nature of these irregularities in order to make possible a more detailed picture of cosmic-ray variation. The observational studies that are presently developing (Ref. 17, 18, and 19, and Papers 1, 4, 6, and 8) promise to further our understanding of conditions during low solar activity; future observations will tell us more about conditions during periods of increased solar activity.

Several outstanding theoretical problems are worth mentioning. First there is the matter of improving the simple, isotropic-random-walk treatment used in the discussion so far. The isotropic random walk is a language sufficient for discussing cosmic-ray propagation, but it does not yield a really quantitative model. The effective diffusion coefficient K_{\parallel} (along the field) should exceed the coefficient K_{\perp} (Ref. 2 and 9). Another treatment has been given recently by Axford (Ref. 20), in which

he suggests that the net cosmic-ray streaming \mathbf{u} is determined by the condition:

$$0 = e(\mathbf{E} + \mathbf{u} \times \mathbf{B}/c) + m\kappa (\mathbf{v} - \mathbf{u})$$
(3)

where κ is the frequency with which individual cosmic-ray particles collide with the magnetic irregularities. He derived the right-hand term by considering the analogous situation of diffusion in a partially-ionized gas, in which \mathbf{u} is the velocity of the ions, \mathbf{v} is the velocity of the neutral atoms, and κ is the ion-neutral collision rate.

Another problem is: how much higher is the interstellar cosmic-ray density than the cosmic-ray density observed near the Earth at sunspot minimum? For lack of any contrary evidence, we often consider the two densities to be equal, taking this as the most conservative estimate of the galactic cosmic-ray intensity. But there is now some evidence that the interstellar cosmic-ray density may perhaps be much higher than that observed near the Earth at sunspot minimum. There is no evidence from space observations that the solar wind is much weaker during the present solar minimum than it was a few years before the minimum. Thus one might expect that the fractional change $-\triangle n/n$ in n ($n = \int \frac{v}{K} dr$) has been small, say less than 0.1. But the cosmic-ray density near the Earth, $e^{-n(1-\triangle n/n)}$ has increased about 40%. If $\triangle n/n$ is to be significantly less than 1 while e^{-n} changes by 40%, then n must be somewhat greater than 1. Furthermore, the diurnal variation continues essentially undiminished through sunspot minimum, suggesting again that n is generally at least of the order of unity. So perhaps the cosmic-ray density in interstellar space is considerably greater than that observed in the vicinity of Earth at sunspot minimum.

Consider how the energies of cosmic-ray particles near the Earth compare with the energies of the particles in interstellar space. We have recently calculated the time that a cosmic-ray particle from interstellar space may spend in the interplanetary fields before being observed at the Earth (Ref. 21). Using the simple model of complete magnetic-field disorder beyond the Earth's orbit (this model should be correct in order of magnitude), we find that the typical cosmic-ray particle observed at the Earth has spent days in the solar system. During this time it has been undergoing adiabatic deceleration in the expanding magnetic fields that are carried by the solar wind; and when observed at the Earth, its energy may be less than half the energy it had when it first entered the solar system.

Altogether then, we suspect that the *energy density* of cosmic rays in interstellar space may be much greater than that observed near the

Earth at sunspot minimum. This point is of interest not only to discussions of cosmic-ray penetration into the solar system, but to discussions of galactic dynamics as well. Even if the cosmic-ray pressure in interstellar space were only 10^{-12} dyne/cm², as observed at the Earth, the cosmic-ray pressure would still be the dominant gas pressure there (Ref. 1). Thus the consequences of a higher interstellar cosmic-ray energy density, say 10^{-11} erg/cm³, would be profound. The arguments for the higher density are by no means hard and fast, and we have given them here more to suggest the present dilemma than to settle anything. We feel that the interstellar cosmic-ray density is really not known, and that it is very important for us to determine it.

REFERENCES

- 1. PARKER, E. N., The Physical Review 110, 1445 (1958).
- PARKER, E. N., Interplanetary Dynamical Processes, Interscience Publishers, a division of John Wiley and Sons, Inc., New York (1963).
- 3. PARKER, E. N., Astrophysical Journal 128, 664 (1958). The Physical Review 109, 1328 (1958).
- 4. PARKER, E. N., Astrophysical Journal 134, 20 (1961).
- 5. PARKER, E. N., The Physical Review 109, 1874 (1958).
- 6. PARKER, E. N., Astrophysical Journal 133, 1014 (1961).
- 7. Morrison, P., *The Physical Review* **101**, 1397 (1956).
- 8. SIMPSON, J. A., Proceedings of the Study Week on the Problem of Cosmic Rays in Interplanetary Space, Pontifical Academy of Science, Vatican City (1962) p. 323.
- 9. Parker, E. N., Journal of Geophysical Research 69, 1755 (1964).
- 10. SARABHAI, V., Journal of Geophysical Research 68, 1555 (1963).
- RAO, U. R., K. G. McCracken, and D. Venkatesan, Journal of Geophysical Research 68, 345 (1963).
- 12. Bercovitch, M., Journal of Geophysical Research 68, 4366 (1963).
- 13. STELJES, J. F., H. CARMICHAEL, and K. G. McCracken, Journal of Geophysical Research 66, 1363 (1961).
- 14. McCracken, K. G., Journal of Geophysical Research 67, 447 (1962).
- 15. MEYER, P., E. N. PARKER, and J. A. SIMPSON, The Physical Review 104, 768 (1956).
- 16. PARKER, E. N., Planetary and Space Science (submitted for publication).
- COLEMAN, P. J. JR., L. DAVIS, JR., E. J. SMITH, and C. P. SONETT, Science 138, 1099 (1962).
- 18. NEUGEBAUER, M. and C. SNYDER, Science 138, 1095 (1962).
- Bonetti, A., H. S. Bridge, A. J. Lazarus, B. Rossi, and F. Scherb, *Journal of Geophysical Research* 68, 4017 (1963).
- 20. AXFORD, W. I. (to be published).
- 21. PARKER, E. N. (in preparation).

DISCUSSION OF PARKER PAPER

AXFORD: As Prof. Parker mentioned, he and I are basically in agreement over the diurnal variation, although there are slight differences between his results and mine. I find that the streaming velocity of the cosmic rays parallel to the Earth's orbit is

$$\frac{\Omega r}{1 + (1/\omega \tau \sin \chi)^2}$$

where ω is the gyro frequency, τ is the collision time, and χ is the garden-hose angle. This expression permits a certain amount of freedom, because it is possible to vary ω , τ , and χ . I adopted a slightly different approach in that I allowed the diffusion to be anisotropic, so that it's easier for particles to run along the field lines than to diffuse across the field. Also, I have assumed that diffusion occurs everywhere in the interplanetary medium.

The remark about the cosmic-ray density in the interstellar medium is quite an interesting speculation, although of course one doesn't know quite what numbers to use for K or for the size of the solar-wind cavity. If the gradient near the Earth is 10%/AU, and if it is maintained out to 100 AU, then the cosmic-ray density could be 10 times the value observed near the Earth, although this is perhaps a little extreme. As Prof. Parker said, this means that the cosmic-ray density in the universe may be somewhat higher than we would expect

from local measurements.

This raises difficulties concerning the magnetic-field strength of the galaxy. With suitable assumptions about the electron component in the cosmic radiation, one interpretation of cosmic radio-noise data gives a high value for the galactic magnetic field of 3γ . Direct observations suggest that the field is at most about 0.5γ . The maximum cosmic-ray intensity observed at sunspot minimum is such that the energy density of cosmic rays is already equal to the energy density of a magnetic field of 0.5γ ; so if the cosmic-ray intensity is greater than the intensity we observe, and if 0.5γ is the actual field strength, then the cosmic rays will either blow up the galaxy (since they cannot be contained in the magnetic field) or else they exist throughout the universe at this density.

Another interesting feature is that if the cosmic-ray density is indeed high outside the solar system, then the solar wind may not necessarily be contained by the galactic magnetic field, as usually thought, but by the cosmic rays. We should write the momentum equation for the solar wind as

$$\rho v \frac{\partial v}{\partial r} = -g\rho - \frac{\partial p}{\partial r} - \frac{\partial p_c}{\partial r}$$

where the last term, which isn't normally included, is the pressure gradient of the cosmic rays. Although the local cosmic-ray gradient is quite small, the integrated effect could be large.

BIERMANN: Can the diurnal variation be regarded as independent evidence of the spiral pattern of the interplanetary magnetic field—or is that going too far? **PARKER:** My impression is that, since the angle of the spiral cancels out in the algebra, almost any ordered field connected with the Sun would give the same result.

BIERMANN: Can we conclude, from the *Mariner-2* or the *IMP* data, that the lines may be connected to the Sun 50 percent of the time, but no more than that? **PARKER:** The diurnal variation does not rule out such a conclusion. I would rule it out on other grounds.

BIERMANN: I mention this only because there seems to be rather general agreement that the lines are connected.

PARKER: Well, I made that assumption in front of this audience, expecting that if anyone disagreed, he would rise to his feet.

BIERMANN: I wish to put in the record that I favor the "50-percent-of-the-time" conclusion.

COLEMAN: In your model of the Forbush decrease, if one blast wave is followed by another that is moving faster than the first, then the particles trapped between the two blast waves would be adiabatically compressed by the reverse of the

mechanism that you used for deceleration. Wouldn't you expect, then, that the recovery from the first Forbush decrease would be faster than usual? Has such an effect ever been observed?

PARKER: I am sure you can find examples of such a phenomenon.

LÜST: I think your point—that one might expect the cosmic-ray energy density in interstellar space to be about 10 times larger than we thought—is very interesting, although somewhat uncomfortable. Therefore, I would like to ask: how sure can we be that the density is this great?

PARKER: I think the basis for this large cosmic-ray density in interstellar space is somewhat shaky, yet it is not so much an apparition that it will readily go away. Looking at the work done by others on the diurnal variation, I get the impression that, when the acceptance cones of high-latitude cosmic-ray stations are properly folded into the observations, one no longer has a great wandering of the cosmic-ray anisotropy in space. As I say, this was not my work, although it seems to me to be correct; so that I feel somewhat trapped by the circumstances and have to say that maybe the cosmic-ray energy density is 10^{-11} erg/cm³ in interstellar space. However, I certainly wouldn't urge this density upon anyone else, and I don't even like the idea myself.

SNYDER: We used to be very uncomfortable with the idea that even the observed cosmic-ray intensity near the Earth could prevail throughout the galaxy. However, the recent discovery of the enormous amounts of energy available from radio sources seems to have removed the difficulty. I suspect that it is only our parochial viewpoint that makes us uncomfortable.

CLINE: With respect to the suggestion that the cosmic-ray density in interstellar space may be very high, I would like to add a remark concerning the *Explorer-11* gamma-ray measurements. The gamma rays measured on this mission can be attributed to nuclear collisions between cosmic rays and interstellar material. If half or more of the gamma rays seen by *Explorer 11* were truly primary gamma rays, then either the interstellar cosmic-ray density is indeed higher, by a factor of 10, than that measured here in the solar system, or else the interstellar material is 10 times denser than previously believed. This factor of 10 may be pure coincidence and may or may not be meaningful, but it does fit with Dr. Parker's comments.

ANDERSON: I would like to ask Dr. Parker what cosmic-ray energies he's talking about in discussing this factor of 10.

PARKER: I was talking about particles of the order of 2 Bev, because most of the cosmic-ray energy density seems to be at this energy.

BIERMANN: I believe 10^{-31} gm/cm³ is the most recent figure for the density of matter in the universe. If this were completely converted from hydrogen to helium, with the released energy of $10^{18.8}$ ergs/gm going mainly into cosmic rays, the energy density of cosmic rays would be something less than 10^{-12} erg/cm³. I am extremely hesitant to accept the idea that the whole universe is filled with cosmic rays having an energy density of even 10^{-12} erg/cm³.

AXFORD: Your figure of 10^{-31} gm/cm³ is debatable within a factor of 10^3 . If the universe were dominated by cosmic rays in this manner, I do not see that the problem of where the energy is derived would be a greater mystery than the problem of where mass is derived in a cold universe.

LEIGHTON: We all agree upon the outflow of gas as far as the ecliptic is concerned, but what about the flow in polar directions? I am wondering if the numbers we are talking about might be greatly affected by dropping the spherical symmetry from your model.

PARKER: We have no direct observations of the symmetry of the solar gas outflow, so I would appeal to Prof. Biermann's analysis of comet tails. It should be easier for the gas to escape from the poles because there are no magnetic fields that impede the flow. On the other hand, the outflow might well be somewhat slower there, because the polar corona at sunspot minimum seems to be somewhat cooler than at the equator. I have considered oblate rather than spherical models, and I don't think lack of spherical symmetry changes any of the numbers in any interesting way. I have tried to get interesting effects this way and failed.

SLUTZ: The spiral patterns evident in the flow of the solar wind seem to imply a rather interesting effect of the magnetic field on the direction of flow. Of course, at 1 AU, the magnetic pressure is too small to have any effect on the wind. But nearer the Sun, where the two pressures are approximately equal, the distortion of the magnetic field is such that both the tangential and the radial velocities of the wind are increased, thus introducing a mechanism to produce a cylindrical expansion.

PARKER: There are several effects that contribute to what you call a cylindrical expansion rather than to a spherical expansion. For example, I have already mentioned that the polar fields on the Sun would like to close. I think the point here is that none of these effects changes the order of magnitude of any of the velocities or fields. The observations are hard to get, because one must separate small effects from the main effect.

SLUTZ: I certainly agree with that. The effect of the magnetic field on the flow direction is mentioned merely as a mechanism for emphasizing the cylindrical over the spherical expansion. We need more observations in this region.

DAVIS: Presumably the galactic cosmic-ray electrons would be affected more than the protons by this diffusion mechanism, and would take longer to diffuse into the solar system. Thus it might be difficult for any galactic electrons to reach the Earth, which would be too bad because they seem to be observed.

PARKER: Before we can discuss the ability of the electrons to penetrate into the solar system, we have to determine a little better the nature of the irregularities between here and infinity. In general, the ability of a particle to get into the solar system depends neither entirely upon its velocity nor entirely upon its rigidity. Now, the electrons have one slight advantage over protons, in that they always have a velocity of c, whereas 100-Mev protons have a velocity of c/2.

I agree that 100-Mev electrons would have a more difficult time getting into the solar system than would protons of the same energy. If you extrapolate the electron density observed here, you get very extraordinary interstellar electron fluxes. However, I don't think that the electrons we see are necessarily galactic particles; they may be of solar origin.

AXFORD: Since there are neutral sheets in the interplanetary field, there is also a way of producing fast electrons in the local interplanetary gas, rather than at the Sun. Perhaps the electrons observed by Dr. Cline and others come from such a source.

VOGT: Meyer and I observed an increase in the number of high-energy (several hundred Mev) electrons in connection with the July, 1961 flare group. These particles were probably accelerated at the Sun. Otherwise, the available experimental evidence concerning high-energy electrons does not tell us whether they are of galactic or solar origin.

CLINE: I have a comment about solar-flare electrons. On *IMP* we detected a solar-proton event on March 16 of this year, following Type-IV radiation. The electron content of the particle flux was very low, with an upper limit of perhaps

2 or 3 percent. However, we think that at least 50 percent of these electrons were caused by locally-produced gammas, and the rest may or may not have also been secondary particles.

ANDERSON: Your argument for the large cosmic-ray flux in interstellar space depends partly on the statement that the fractional variation of the cosmic-ray flux observed on Earth is large compared to the fractional variation in the solar-wind flow. Does any experimental evidence demonstrate that the change in the solar wind between solar maximum and solar minimum is really that small? Would you care to make any predictions?

PARKER: I agree that the variation in the solar wind isn't really known. But when I compare the *Mariner* data with the *IMP* data, I am surprised that the differences in wind velocity are not larger, because the cosmic-ray intensity really changed quite a bit between the time of *Mariner* and the time of *IMP*.

BRATENAHL: What about the Kp index as an indication of plasma velocity? **PARKER:** Well, Kp is another one of these funny things that we don't understand. The wind can vary only a little bit while Kp varies enormously. *Mariner* hasn't calibrated Kp above a velocity of 750 km/sec, so I don't know how reliable the Kp index is as an indication of velocity.

CHAMBERLAIN: On the question of how far the solar wind extends out from the Sun, I understand that your figure of 40 AU was based on the lag between the cosmic-ray maximum and sunspot maximum. As I recall, however, auroras and geomagnetic storms have about a 2-year lag behind sunspot maximum.

In addition, how valid is the estimate that the interplanetary shock front lies where the pressures balance? In front of the Earth, there seem to be both a magnetosphere boundary and a shock front. Might not two boundaries also exist between the interplanetary and the interstellar gases?

PARKER: The pressure balance theory agrees very nicely with the measurements of the magnetosphere boundary. Formal solution of the hydrodynamic equations puts the shock about where the stagnation pressure of the wind becomes equal to the interstellar pressure.

CHAMBERLAIN: But then isn't there a turbulent region to be considered beyond the boundary?

PARKER: Undoubtedly.

CHAMBERLAIN: I wonder to which boundary the pressure balance theory

should apply.

PARKER: For the boundary between the solar wind and the interstellar gases, the shock lies near the pressure balance. For the solar wind and the geomagnetic field, which is a rather different situation, the boundary of the magnetosphere (at about $10~R_{\rm E}$) lies at about the distance where the pressures balance. I think the point is that it makes a difference of less than a factor of two, whatever one assumes. And 40~AU is far more uncertain, because no one knows the interstellar pressure. For this reason, I usually quote 10~to~100~AU as the probable distance to which the solar wind blows.

Session III ORIGIN OF THE SOLAR WIND AND THE CORONA

Page intentionally left blank

THE ORIGIN OF THE SOLAR WIND

F. L. SCARF

TRW-Space Technology Laboratories, Redondo Beach, California

Coronal Models and the Solar Wind

Hydrodynamic or continuum equations are naturally used to describe the circulation, temperature distribution, pressure distribution, etc, in a dense planetary atmosphere where the state of the gas is dominated by collisional effects. In the last few years, it has become apparent that similar conditions prevail in the lower corona of the Sun, and various solutions to the fluid equations have been discussed in great detail. The most significant result of the hydrodynamic approach was Parker's prediction (Ref. 1) that steady-state outward streaming of the entire corona should occur. Parker showed, in particular, that pressure gradients can accelerate the fluid to supersonic speeds, producing a continuous plasma wind in interplanetary space. This solar wind was identified with the stream suggested by Biermann's comet-tail studies (Ref. 2); and subsequent measurements and calculations strongly support the original theory, in the sense that the interplanetary wind can be regarded as a hydrodynamic extension of the luminous corona.

The quantitative models are based on the moment equations for conservation of mass, momentum, and energy. These equations are valid in the region where the velocity distributions for the coronal plasma particles do not deviate greatly from local equilibrium functions. This restriction implies that all mean free paths are small compared to scale heights, and it ensures that local temperatures and pressures are meaningful. In addition, energy transfer by conduction and viscous dissipation is significant. If the velocity gradients are sufficiently small, coefficients of thermal conductivity and viscosity can be defined as follows:

$$\mathbf{Q} = -\mathbf{K}(T) \, \nabla T$$

$$\tau_{ij} = \eta(T) \left[\frac{\partial v_j}{\partial x_j} + \frac{\partial v_i}{\partial x_i} - \frac{2}{3} \, \delta_{ij} \, \nabla \cdot \mathbf{v} \right] \tag{1}$$

and the Navier-Stokes continuum equations result (Ref. 3).

Most theoretical investigations have been based on idealized models that contain the assumptions that steady, spherically-symmetric flow is set up, and that the effects of solar rotation, magnetic fields, and viscosity need not be explicitly included. The last of these assumptions is customarily made because the dimensionless Prandtl number $(\eta C_p/mK)$ which should be a measure of the viscous effect, is very small: for a fully-ionized hydrogen gas, Chapman has estimated (Ref. 4) that¹

$$K(T) \simeq 10^{-6} T^{5/2} \text{erg/cm sec}^{\circ} K \tag{2}$$

$$\eta(T) \simeq 10^{-16} \, T^{5/2} \, \text{gm/cm sec}$$
(3)

The first quantitative fluid model of the corona was proposed by Chapman and Zirin in 1957 (Ref. 5). No streaming was considered, so that

$$\nabla \cdot \mathbf{Q} = -\nabla \cdot \{ \mathbf{K} (T(r)) \nabla T(r) \} = 0 \tag{4}$$

Equations 2 and 4 readily lead to a specific distribution, $T(r) \simeq T(a)(r/a)^{-2/7}$, and when this distribution is inserted into the hydrostatic equilibrium equation, surprisingly high coronal densities ($n_e \simeq 300/{\rm cm}^3$) are predicted near the Earth for $a \simeq R_{\rm S}$ and $T(a) \simeq 2 \times 10^6\,{\rm ^\circ K}$.

In the subsequent Parker model (Ref. 1), the possibility of finite streaming was introduced, and the flow patterns were investigated using an ad hoc temperature distribution. It was assumed that the lower corona is nearly isothermal, with $T_0 \approx 1$ to 2×10^6 °K out to 10 to 20 R_s, and that in the outer region the temperature decreases according to an adiabatic law. Figure 1 shows some typical solutions to the momentum and continuity equations (with $\eta = 0$). Near the coronal base, the particles are strongly accelerated outward by the pressure gradients and retarded by solar gravity. The streaming is formally analogous to the flow pattern through a Laval nozzle, and for most boundary conditions the streaming speed remains subsonic, with a rapid decline after passing through the effective nozzle in the region around r_0 . All of these subsonic solutions have been extensively studied by now, and before the existence of a continuous wind was verified, Chamberlain (Ref. 6) proposed that the corona might be described by the lowest unbound or breeze solution, which is a form of evaporation. However, even before good measurements were available. Parker emphasized the possibility that the corona

 1 The evaluation of these coefficients is somewhat arbitrary, since the Debye shielding modifying the Coulomb potential is generally inserted in an *ad hoc* manner; all numerical work discussed below uses K $T^{-5/2}=7.4\times10^{-7}$ and $\eta T^{-5/2}=1.2\times10^{-16}$

can be described by the critical solution, which attains supersonic speed. He showed that the plasma would then flow past the Earth with a speed of 300 to 600 km/sec, in accordance with present observations (Paper 1).

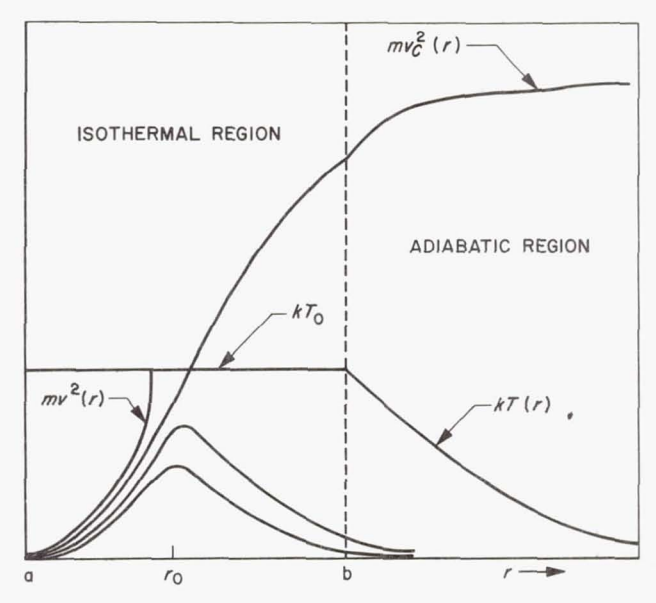


Fig. 1. Solutions to the momentum and continuity equations for a model solar corona with an isothermal-adiabatic temperature distribution

In his original paper, Parker also examined the effects of rotation and of the general solar magnetic field, and he pointed out that a particular configuration for a rotating magnetic field gives no net electromagnetic force on a nearly radial plasma stream. Figure 2 shows explicitly how this comes about. In the frame of the Sun (primed variables) there is no electric field, and \mathbf{v}' is parallel to \mathbf{B}' ; both vectors have the garden-hose form, because at large distances the corona should not rotate with the Sun. In an inertial frame, E_{θ} no longer vanishes, and \mathbf{v} is nearly radial (past some co-rotation radius), but \mathbf{B} is essentially unchanged. The recent measurements of field magnitude and field direction near the Earth confirm the general validity of this model (Papers 3 and 6).

Our main concern now is the question of the origin of the solar wind, and one may ask at first just why the solar corona chooses to flow continuously in this supersonic mode rather than in any of the subsonic ones. Although a completely rigorous answer to this question has not

been given (it requires formulation and analysis of an exceedingly complex initial- and boundary-value problem), many interesting speculations based on the equivalent steady-state patterns (and in particular on the long-range behavior of the pressure terms) have appeared. However, all of these arguments depend on the detailed evaluations of the flow

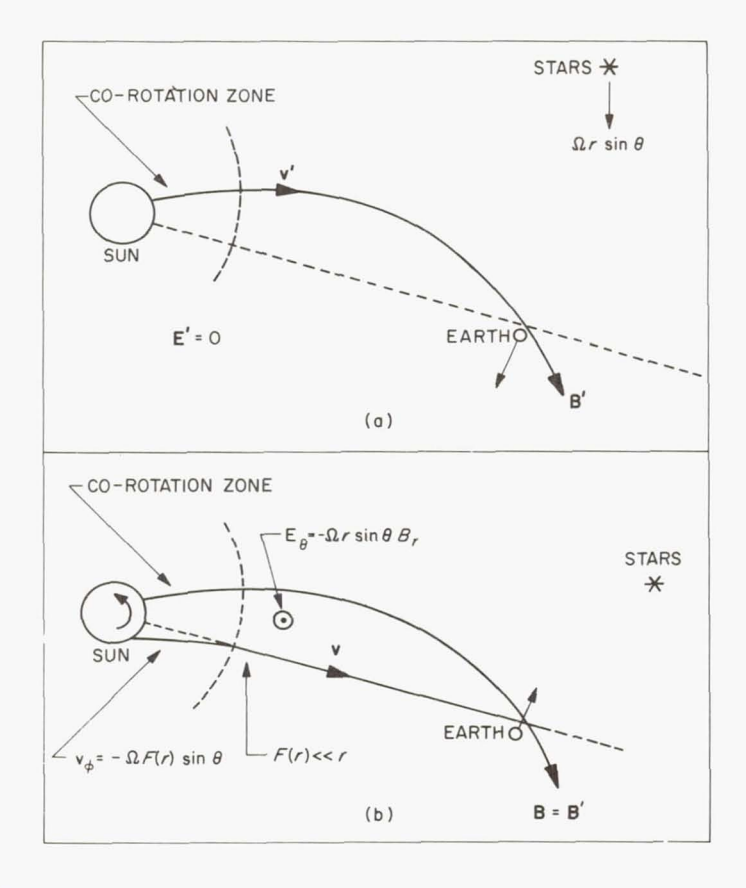


Fig. 2. Illustration of the argument for no electromagnetic interaction between a spiral magnetic field and a nearly radial plasma stream. (a) Sun frame (b) inertial frame

patterns. Since considerable progress in understanding the steady-state energy and momentum balance has been made in recent years, we turn first to this aspect of the problem of the wind's origin.

The Problem of Coronal Heating

One apparent difficulty with the Parker model was related to the need for a large, approximately isothermal region in the corona; it has never seemed likely that any solar heat source external to the corona could, by itself, maintain a nearly uniform temperature out to 10 or 20 $R_{\rm s}$ (Ref. 7). However, in one of Chamberlain's investigations of the evaporative solutions (Ref. 8), an interesting and suggestive discussion of the dynamic energy balance was given. Chamberlain postulated that the solar heat source only extends over a thin shell near the base of the corona. He studied the velocity and temperature distributions that are determined by solving the complete energy and momentum equations in the absence of both viscosity and an external heat source. For radial flow, the equations are (in standard notation):

$$nmv\frac{dv}{dr} + \frac{dp}{dr} + \frac{GnmM_S}{r^2} = 0 ag{5}$$

$$\frac{mv^2}{2} - \frac{GmM_S}{r} + \frac{5}{2}kT - \frac{Kr^2}{c}\frac{dT}{dr} = constant$$
 (6)

where p = nkT and the constant $c = nvr^2$. In essence, the conductive heat transport of the Chapman model is combined with Parker's concept of finite streaming in order to obtain the dynamic temperature distribution.

Inspection of these thin-shell equations suggests that, in the lower corona, sufficient heat may be transferred by conduction to maintain a nearly uniform temperature out to 10 or 20 $R_{\rm S}$, even in the presence of fast streaming. De Jager (Ref. 9) and Parker (Ref. 10) tried to confirm this conjecture using analytic techniques, and Noble and Scarf (Ref. 11) investigated it numerically. In our original numerical treatment, viscous effects were again ignored; reasonable values for the density, temperature, and velocity at 1 AU were chosen; and the equations were integrated inward toward the Sun. The temperature gradient at 1 AU was varied until the value was found that leads smoothly through the transition into a subsonic lower corona.

The theoretical electron-density profile shown in Fig. 3 is the result of one of the early integrations of Eq. 5 and 6 for a 10% helium content and a 2×10^6 °K temperature at the base of the corona. The speed at 1.25 R_s is 9.14 km/sec, the sonic transition occurs near 5 R_s, and the speed and density at the Earth are 352 km/sec and 3.4 ions/cm³, respectively. The parameter A is $2 \text{K}(T_0) GM_S m/k^2 T_0 (nvv^2)$.

Reference 11 lists the articles from which the experimental curves of Fig. 3 were taken. Our first numerical prediction obviously differs from the experimental $n_e(r)$ curves by at least a constant factor, but the general agreement in shape already strongly supports the thin-shell conductive-heating model. Since $A \sim K(T_0)/n$, the profile shown in Fig. 3 clearly suggested the need for further integrations with smaller values of A,

and these have now been carried out. Before the results are presented, however, some comments on the curve labeled "subsonic solution" are in order. Here n_e , T, and dT/dr at $r=1.25~\rm R_S$ have been fixed at values appropriate for the solar-wind expansion, but v (1.25 $\rm R_S$) has been reduced

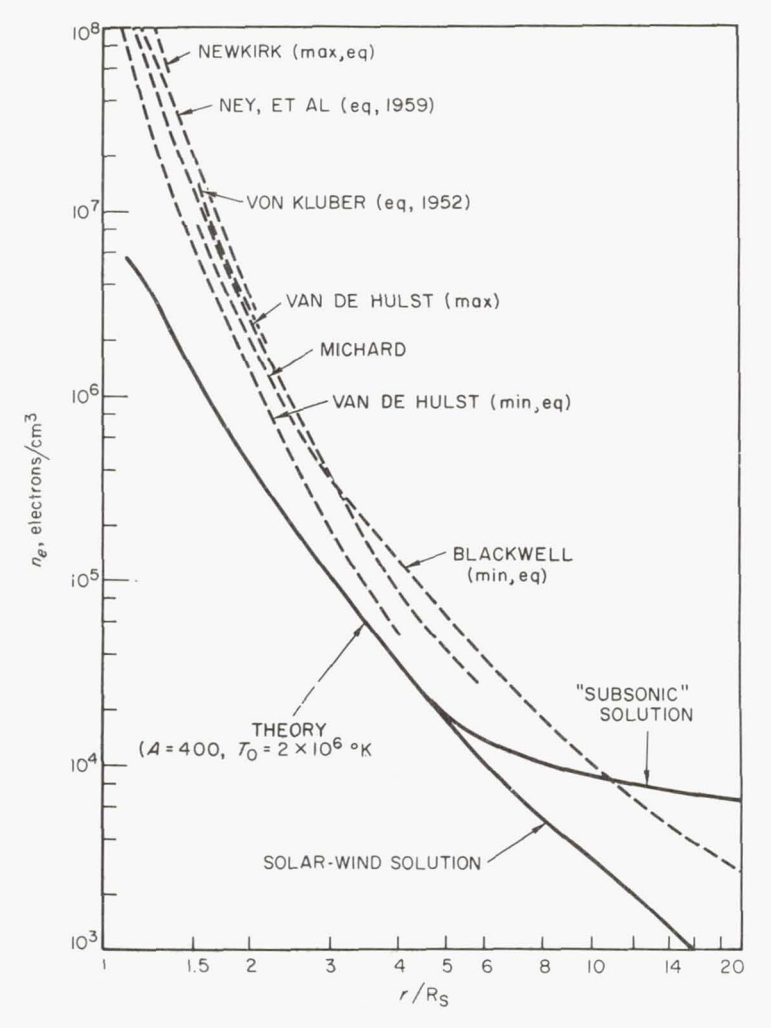


Fig. 3. Experimental and theoretical electron-density profiles; no viscous terms are included

from 9.14 km/sec to 9.04 km/sec. In this case, the speed stays very close to the critical value up to the crossover ($r = 5~R_{\rm S}$), then it drops rapidly, causing the density to increase. At 20 R_S the subsonic density is about

50 times the supersonic one, so that the lack of a sharp knee in the observed coronal-density curve already indicates very strongly that the actual expansion is supersonic. The temperature distributions are essentially the same in the two cases, so that the subsonic pressure is also about

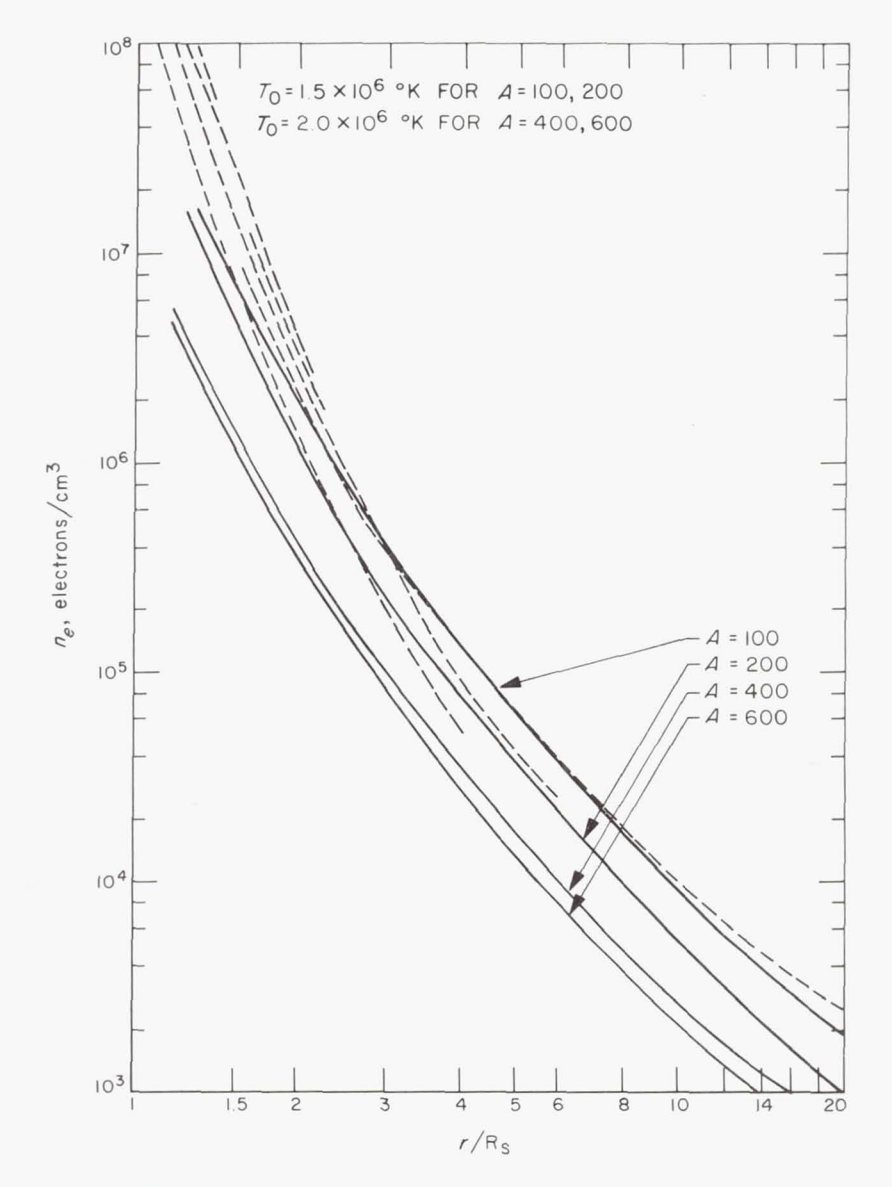


Fig. 4. Experimental and theoretical electron-density profiles. The theoretical curves are for different values of the parameter A; viscosity is again neglected

50 times greater than the supersonic one at 20 $R_{\rm s}$. We shall return to this point later.

Figure 4 shows the results of additional numerical integrations of the conductive heating equation (Ref. 12). The $\mathcal{A}=100$ curve agrees fairly well with the observations beyond 2 $R_{\rm S}$, but it is clear that below 2 $R_{\rm S}$ the predicted densities are much too low. This immediately suggests that an external heat source penetrates the corona to 1.5 to 2.5 $R_{\rm S}$, but other explanations for this discrepancy are possible (the helium concentration may be considerably higher near the chromosphere; the solar gravity field may be weakened below 2 $R_{\rm S}$ by co-rotation effects; and deviations from spherical symmetry may be extremely important in this region). Thus it is premature to assign a specific boundary to the heating region at this time.

[In the supersonic region (r > 5 R_s), the computed density curve is consistently slightly less than the Blackwell curve. The theoretical curve is lowered even more when viscous effects are taken into account. However, in the discussion it was pointed out by Brandt and others that Blackwell now believes that his results should be revised downward, and the final theoretical distribution agrees well with recent radio astronomy density determinations beyond about 6 R_s (Ref. 13).]²

Effects of Viscosity

For radial flow, the full Navier-Stokes equations have the form

$$nmv\frac{dv}{dr} + \frac{dp}{dr} + \frac{GnmM_s}{r^2} = \frac{4}{3}\frac{d\eta}{dr}r\frac{d}{dr}\left(\frac{v}{r}\right) + \frac{4}{3}\eta\frac{d}{dr}\left[\frac{1}{r^2}\frac{d}{dr}(r^2v)\right]$$
 (7)

and

$$\frac{mv^{2}}{2} - \frac{GmM_{S}}{r} + \frac{5}{2}kT - \frac{Kr^{2}}{(mvr^{2})dr} - \frac{4}{3}\frac{\eta r^{2}}{(rvr^{2})}\left(v\frac{dv}{dr} - \frac{v^{2}}{r}\right) = constant \quad (8)$$

The viscous corrections were originally examined because Eq. 5 and 6 have anomalous solutions $[T(\infty)>0 \text{ or } T(r<\infty)=0]$, and it was hoped that the steady-state viscosity terms would eliminate these. In fact, it soon became evident that, even for extremely small values of η/K , the η -dependent terms ultimately overwhelm the conductive one if the flow is supersonic (as $r\to\infty$, $\eta v^2>>KT$). A possible physical explanation for such a large effect is that, even though viscous dissipation vanishes for a completely uniform dilation, radial streaming does not generally produce a uniform expansion of the volume element; thus viscous stresses are finite.

²Added in manuscript

Figure 5 illustrates just how the viscous term modifies the streaming speed near the Sun. The parameter B is equal to $(2\eta \ kA/3\text{K}m)$, and the curve labeled $B \equiv 0$ is the A = 200 profile associated with Eq. 5 and 6. The heavy curve (B = 2.46) is a solution to Eq. 7 and 8, with a viscous coefficient appropriate for a 10% helium corona (B/A = 0.0178), for pure

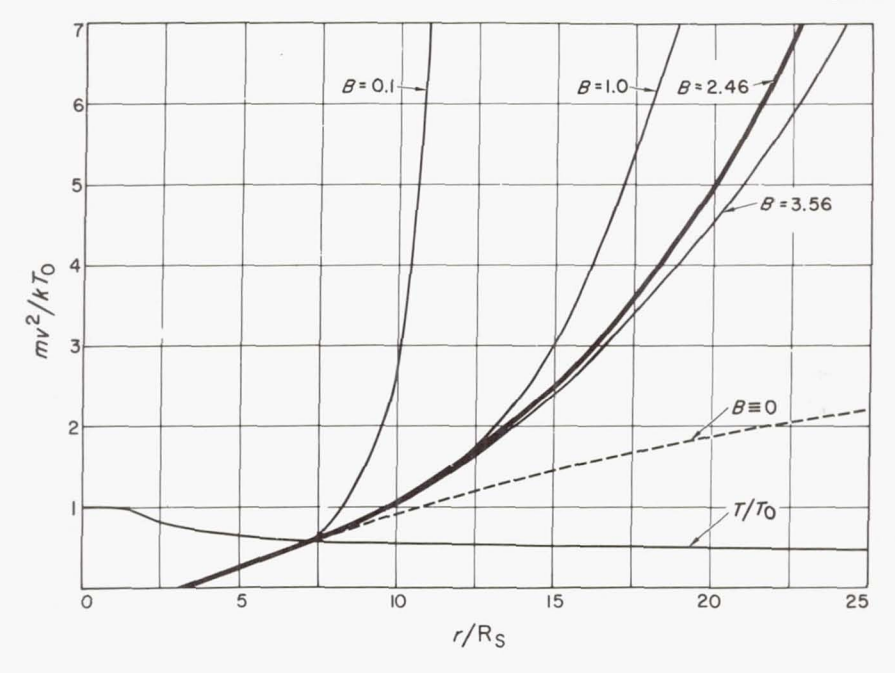


Fig. 5. Effects of the viscous term on the streaming speed of the solar wind near the Sun. Here A = 200, and B = 2.46 is the appropriate viscous coefficient for a 10% helium corona

hydrogen, and for 10% helium, B must be reduced by a factor of 0.69); the T(r) curves are essentially independent of B in this region. If only the $B \equiv 0$ and B = 2.46 curves are examined, Fig. 5 seems to be nonsensical, because the viscosity has the apparent effect of speeding up the flow. Solutions were computed for other values of B, and they show that if the $B \equiv 0$ curve is ignored, then the viscous terms do produce a sensible decrease in the flow. The $B \equiv 0$ conductive heating case is clearly singular, and Fig. 5 illustrates a fact well known to aerodynamicists: there is a great difference between fluid flow with an arbitrarily small amount of viscosity and fluid flow with no viscosity at all.

Treatment of the Region Beyond 15 R_S

The viscous energy redistribution has two important effects. First, as mentioned above, it brings the computed $n_e(r)$ curve into excellent

agreement (see footnote 1) with observations beyond 2 R_s (for A = 100, $T_0 = 1.5 \times 10^6$ °K and $m = 0.62 m_p$, or 10% helium). Secondly, it produces very steep velocity gradients in the region past 15 R_s, and $\eta(T)$ is not well defined in the presence of such steep velocity gradients. The complete expression for the viscous tensor τ_{ij} is (Ref. 3):

$$\tau_{ij} = \tau_{ij}^{0} + \frac{\eta(T)}{nkT} \left[\tau^{ij} \left(\nabla \cdot \mathbf{v} \right) - \left(\mathbf{v} \cdot \nabla \right) \tau^{ij} - \tau^{ki} \frac{\partial v^{i}}{\partial x^{k}} - \tau^{kj} \frac{\partial v^{i}}{\partial x^{k}} + \frac{2}{3} \partial^{ij} \tau^{ki} \frac{\partial v^{i}}{\partial x^{k}} \right]$$
(9)

+ diffusion terms + higher moments,

where τ_{ij}^0 is given by Eq. 1. Clearly the conventional relation between stress and strain is only established if the bracketed terms in Eq. 9 can be neglected. Thus, the Navier-Stokes equations cannot be justified when $\eta(T)$ ($\nabla \cdot \mathbf{v}$) becomes comparable to nkT. Fig. 5 suggests that this onset of "slip flow" occurs somewhere between 15 and 20 R_s.

Various formal corrections to the Navier-Stokes equations yield the very complex Burnett or 13-moment equations, which are supposed to apply in the slip-flow region; but in practice aerodynamicists have little confidence in their utility (Ref. 14). It is frequently asserted that the Navier-Stokes equations are valid well beyond their established limits of applicability. We observe that the quantity (λ/T) (dT/dr), where λ is the electron mean free path, is very small long past 15 or 20 R_s, so that some kind of fluid flow is maintained even when the transport coefficients become ill-defined. Moreover, it can be shown that the velocitydependent corrections tend to decrease both η and K. For these reasons we tentatively "cut off" both Q and τ at a breakdown radius $r_{\tau} \approx 15$ to 20 R_s, and we attach an adiabatic solution to the flow beyond r_1 . Since Eq. 7 and 8 do have other solutions that exhibit adiabatic behavior at large distances, it is possible to think of the variations in K and η as causing a shift from one branch of the Navier-Stokes solutions to another. (However, we have no real justification for abruptly attaching an adiabatic curve, and this technique should be considered as a way of obtaining the minimum flow speeds.)

Some velocity and temperature distributions constructed in this way are shown in Fig. 6. The best fit to the Blackwell and Erickson data requires $T(2 \text{ R}_{\text{S}}) \approx 1.5 \times 10^6 \,^{\circ}\text{K}$, $v(2 \text{ R}_{\text{S}}) \approx 18 \,\text{km/sec}$, with $r_1 \approx 18 \,\text{to} \, 20 \,$ R_s. For this 10% helium case, where A = 100 and B = 1.26, $v(1 \text{ AU}) \approx 300 \,\text{to} \, 400 \,\text{km/sec}$, and $n(1 \text{ AU}) \approx 5 \,\text{to} \, 6 \,\text{ions/cm}^3$.

These calculations indicate that the detailed structure of the corona and of the wind is well understood in the region 2 $R_S < r < 20 R_S$, and we have a fair degree of confidence in the predictions of outer coronal densities and streaming velocities. On the other hand, it is very difficult

to anticipate how the thermal or velocity distributions will vary with distance from the Sun.

Velocity Distributions and Field Effects

For the velocity distributions shown in Fig. 6, the mean free paths become comparable to the scale heights in the region between 0.25 and

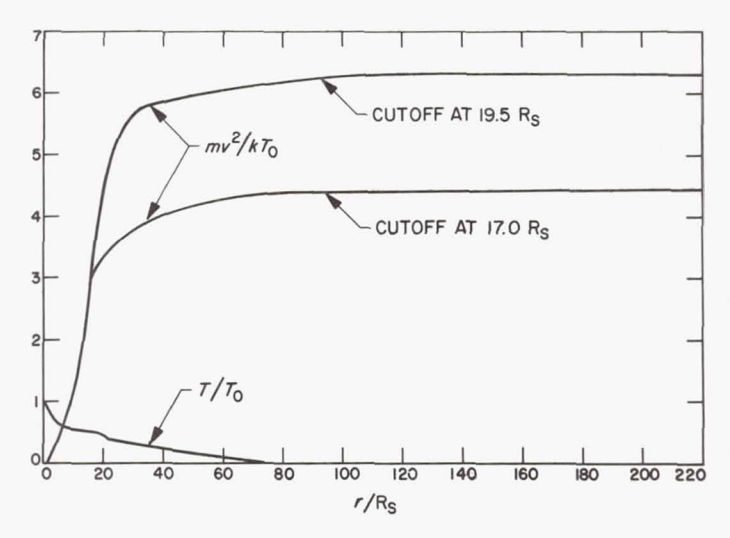


Fig. 6. Effect of cutting off thermal conductivity and viscosity (and attaching an adiabatic solution) at 17 R_s and 19.5 R_s

0.5 AU. This would normally mean the onset of free molecular flow, for which the concept of temperature is no longer defined—because when collisions become too infrequent to restore a statistical velocity distribution, anisotropies associated with the spherical geometry immediately become important.

The true situation is much more complex, and probably much closer to a fluid picture, because of the weak magnetic field that is embedded in the collisionless plasma. If the anisotropy that develops is such that $nk(T_{||}-T_{\perp}) > B^2/4\pi$ or $nkT_{\perp}^{-2}/T_{||} > B^2/8\pi$ (the subscripts refer to motions parallel and perpendicular to **B**), then various magnetohydrodynamic instabilities are triggered. The magnetic field becomes disordered, and particle scattering from the field irregularities then plays the same role with respect to the restoration of local equilibrium and thermal isotropy as particle-particle scattering normally does. Parker has argued that this mechanism causes the fluid model to be valid very far beyond the limit set by the condition $\lambda dT/dr \simeq T$.

210 F. L. SCARF

Analysis of solar cosmic-ray trapping (Ref. 15 and 16) does suggest that a thick, highly-disordered magnetic shell may "start" near 1.5 or 2.5 AU, and the *IMP* and *Mariner-2* magnetic-fluctuation data (Papers 3 and 6) show that a moderate amount of disorder exists between 0.7 and 1 AU. The approximate equality of nkT and $B^2/8\pi$ seen by *Mariner* (Paper 1) also strongly supports the magnetic-binding concept. However, the degree to which the field disorder produces local equilibrium is not well known, and a residual anisotropy is certainly possible. If it is true that $T_{\alpha} \simeq 4$ T_p , then it is clear that the magnetic thermalization is not equivalent to collisional thermalization.

Termination of the Solar Wind

It seems unlikely that moderate field-induced changes in the distribution functions could extract a significant amount of streaming energy in the outer region, and it is usually assumed that the solar wind continues to coast outward until it is stopped by some external force such as that produced by interstellar particles and fields.

It is formally possible for the wind to "stop itself" by undergoing a discontinuous, collisionless shock and becoming a hot plasma with v on the order of $V_A = \sqrt{B^2/4\pi nm} \approx 50$ to 100 km/sec at $r \ge 1$ to 2 AU. A weak disturbance could possibly trigger such a shock. Although this possibility has some very interesting consequences, we feel that it is not likely to occur in the idealized de Hoffman–Teller form. The collisionless shock is a questionable phenomenon even in an ordered field, and a field that is so highly disordered that it binds the collisionless plasma into a fluid should play no other major role in the energy–momentum balance.

Some weak evidence supports the contention that the solar wind flows out at least as far as 5 AU; radio-noise emission from Jupiter (Ref. 17) and activity of comet Schwassmann–Wachmann (Ref. 18) display correlations with solar activity, with time delays consistent with the solar-wind velocity. This distance is not unreasonable, because the interstellar medium is so dilute ($n \sim 1 \text{ atom/cm}^3$, T = 100 °K, $p = 10^{-14} \text{ dyne/cm}^3$) that a dynamic pressure balance gives a minimum stopping distance on the order of 50 AU. The most likely stopping mechanism would then involve fast proton charge exchange with interstellar hydrogen (Ref. 19), or as Parker noted, interaction with cosmic rays (Paper 12).

Subsonic or Supersonic?

The concept of a dynamic pressure balance again brings up the question of the origin and stabilization of the solar wind. Although p (interstellar) $\approx n(mv^2 + kT)$ can only be satisfied by the solar-wind solution for $r \ge 50$ AU, the corresponding pressure balance for any of the subsonic solutions requires a much greater radius because of the much greater

density (see Fig. 3). Parker (Ref. 1) noted this disparity and proposed that, since the corona expands into a near vacuum, the streaming that yields the lowest pressure at any given radius (the solar-wind solution) must ultimately be obtained. This implies that any star that possesses a suitable atmosphere (thermal and streaming speeds at the base less than the escape velocity, density high enough to ensure continuum flow, temperature high enough to produce significant conduction) and a general magnetic field (to allow magnetic coupling to take over when the mean free paths become long) will ultimately develop a solar wind.

It is very difficult to comment on the strength of this pressure argument. since certain assumptions about the "initial" conditions surrounding the Sun must be made. All steady-state solutions, both subsonic and supersonic, satisfy the requirements of energy and momentum conservation, and in every case the pressure ultimately decreases enough to produce a steady-state balance. Very severe self-consistency difficulties are already encountered when one tries to construct the subsonic analogue of Parker's spiral field: the spiral wraps up, $7 \times B$ becomes large, the nonradial currents become significant, and Ohm's law is not trivially satisfied. This appears to preclude any steady, subsonic flow (Ref. 20) for a rotating magnetic star such as the Sun. I believe that pressure arguments are less important, since at the onset of a possible disordered magnetic shell (say $\triangle B/B \approx 1$ near 2.5 AU), the dynamic wind pressure is still at least three to four orders of magnitude greater than the interstellar hydrostatic pressure; during the course of the wind's remaining journey of at least 45 AU to the hypothetical stopping region, complex non-equilibrium phenomena may develop and obscure the flow and the interaction. It is difficult to conceive a magnetic disordering that binds such a dilute plasma ($n \approx 10^{-3}$ particle/cm³ at 50 AU) into a genuine fluid over such a huge range ($\triangle r \approx 50 \text{ AU}$). Nevertheless, it does seem likely that even if magnetic forces were unimportant, a "minimum pressure" principle could operate in a stochastic sense. That is, the conditions at the coronal base are constantly changing, and after a very long time, one would expect that the effect of all large-scale and small-scale fluctuations in n, T, v, and **B** would be to establish the mean flow that corresponds to the lowest asymptotic pressure. From another point of view, the range of possible flow patterns is limited, because any strong blast wave could trigger the wind (Ref. 11).

Stability of Flow

A related question concerns the stability of the fast expansion once it has been set up. As we have seen, if T, dT/dr, and n at 2 R_S are fixed at the critical values and $v(2 R_S)$ is lowered by 1%, then the fluid remains on the subsonic branch, and just beyond 5 R_S the steady-state streaming

speed becomes very small compared to wind speeds. It takes about a day for the front to reach 5 R_s and learn that it is supposed to be subsonic, and it is inconceivable that 1% fluctuations in $v(2\ R_s)$ are rare during such time scales. It is clear that some stabilizing force must continuously be effective; the strong viscous and electromagnetic forces probably account completely for this local stabilization by accelerating any lower-velocity front up to the ambient value in the region of the supersonic crossover (Ref. 11). However, further study of the time-dependent problem is needed before these questions of the origin, stability, and termination of the wind are completely settled to the satisfaction of all.

REFERENCES

- 1. PARKER, E. N., Astrophysical Journal 128, 664 (1958).
- 2. BIERMANN, L., The Observatory 77, 109 (1957).
- 3. Burgers, J., Plasma Dynamics, ed. by F. Clauser, Addison-Wesley Publishing Co., Inc., Reading, Mass. (1960) p. 119.
- 4. Chapman, S., Astrophysical Journal 120, 151 (1954).
- CHAPMAN, S. and H. ZIRIN, Smithsonian Contributions to Astrophysics 2, No. 1, 1 (1957).
- 6. CHAMBERLAIN, J. W., Astrophysical Journal 131, 47 (1961).
- 7. Noble, L. M. and F. L. Scarf, Journal of Geophysical Research 67, 4577 (1962).
- 8. Chamberlain, J. W., Astrophysical Journal 133, 675 (1961).
- DE JAGER, C., Space Research III, ed. by W. PRIESTER, Interscience Publishers, a division of John Wiley and Sons, Inc., New York (1963) p. 491.
- 10. PARKER, E. N., Astrophysical Journal 139, 72 and 93 (1964).
- 11. Noble, L. M. and F. L. Scarf, Astrophysical Journal 138, 1169 (1963).
- 12. SCARF, F. L. and L. M. NOBLE, AIAA Journal (submitted for publication).
- 13. ERICKSON, W. C., Astrophysical Journal 139, 1290 (1964).
- SCHAAF, S. A. and P. L. CHAMBRÉ, Flow of Rarefield Gases, Princeton University Press, Princeton, N. J. (1961).
- 15. MEYER, P., E. N. PARKER, and J. A. SIMPSON, The Physical Review 104, 768 (1956).
- 16. McCracken, K. G., Journal of Geophysical Research 67, 447 (1962).
- 17. CARR, T. D., A. G. SMITH, H. BOLLHAGEN, N. F. SIX, and N. E. CHATTERTON, Astrophysical Journal 134, 105 (1961).
- 18. RICHTER, N., Astronomische Nachrichten 277, 12 (1949).
- AXFORD, W. I., A. J. DESSLER, and B. GOTTLIEB, Astrophysical Journal 137, 1268 (1963).
- SCARF, F. L., Space Physics, ed. by D. P. Le Galley and A. Rosen, John Wiley and Sons, Inc., New York (1964) p. 437.

DISCUSSION OF SCARF PAPER

LÜST: In his calculation of electron densities from the observed zodiacal-light intensity, shouldn't Blackwell have taken the streaming of the plasma into account? I was wondering whether his density distributions might be in error.

ATHAY: I don't believe that is the case. The question of streaming vs. hydrostatic equilibrium does not enter into the calculation. The scattering brightness alone implies a density.

ZIRIN: The method used for the reduction is to take the observed brightness distribution in the corona, and relate it to density by using an integral equation. The equation involves an assumed density model in the Baumbach form, in which

the density equals something times r^3 , plus a term times r^7 , and so forth. But as Dr. Athay said, I don't believe there is any assumption of hydrostatic equilibrium in these models.

DEUTSCH: Can you say anything about the scaling properties in the region where the flow is approximately adiabatic? Is the flow relatively insensitive to the temperature or to the density? Do you expect this same model to apply, let us say, to the flows at large distances from other stars?

SCARF: I would not want to make any such statement, because I think that the dependence of the asymptotic flow on surface conditions is extremely nonlinear and complex. In the problem I discussed, there are several special considerations that may not apply in another case. First, the escape velocity is less than the thermal speed, which in turn is less than the streaming speed—these conditions may not be true for another star. Secondly, because the base temperature is so high, the solar conductive energy transport is large throughout the lower corona, and this causes the sonic transition to occur; if the temperature drops very rapidly with the distance, the pressure gradients may not yield a wind at all. Furthermore, the star's density must be high enough to make this transition occur where the plasma still behaves like a fluid. If the transition occurs out in the exosphere, where collisions are negligible, then we don't have to worry about it. We have thought of trying to apply our techniques to another star, but we were always baffled because we didn't have enough data concerning surface conditions.

DEUTSCH: I fully agree with your comments about considerations closer in. But do stellar winds generally approximate adiabatic flows at greater distances?

SCARF: Yes, I think that, in general, the thermal conductivity and the viscosity must be cut off, either because of the velocity-dependent effects or because of the magnetic fields. The magnetic fields inhibit both of these coefficients, which is another reason for going to the adiabatic solution. I believe that ultimately the adiabatic solution becomes the dominant one.

LÜST: Would you further explain your last point, where you said that you were not convinced by the reasoning of Dr. Parker and others when they concluded

that there are no possible subsonic solar-wind solutions?

SCARF: I think that we have to distinguish between two possibilities here. If the star rotates and has a relatively strong magnetic field, as the Sun does, then I agree that the lowest-pressure or solar-wind solution is an inevitable final state. I think that this is basically so because it appears to be impossible to satisfy $\nabla \times \mathbf{B} = \mathbf{i}$ and $\mathbf{F} = e(\mathbf{E} + \mathbf{v} \times \mathbf{B}) = 0$ for both protons and electrons when the field is strong and wrapped up into a close, tight spiral. However, this configuration would be required in the case of subsonic flow, since v(r) would then become very small compared to Ωr in a region where the field is still capable of exerting strong forces [say $r \approx (7 \text{ to } 10) \text{ R}_s$]. On the other hand, for a hypothetical non-magnetic. non-rotating star, the only properties that distinguish the various steady-state flow patterns are those that involve the pressures and pressure gradients at large distances. It is true that even the "subsonic" solutions with a finite energy flux ultimately become supersonic, because the equivalent fluid temperature formally decreases at large distances, and in this sense a supersonic wind is still generally inevitable. However, this very distant "transition" must occur far beyond the limit of true fluid behavior, and it is not really accurate to describe such a pattern as a solar wind. Accordingly, I labeled this as a "subsonic" solution in Fig. 3, Paper 13, and the question in my mind has to do with the possibility that such a distribution may be meaningful for a hypothetical star. It is true that this is not the lowest-pressure solution, nor the most stable solution, but we have no rigorous

ideas about the time scale for the formation of a conventional wind; so I think that we cannot rule out this type of solution.

EDITORS' COMMENT: A discussion then took place among several people concerning the detailed manner in which the solar wind "chose" one of several competing solutions to the governing equations. The situation was summarized and clarified by Dr. Parker.

PARKER: If you specify the flow velocity down near the surface of the Sun by just arbitrarily pulling a number out of a hat, in general you will not find a solution that will apply from the Sun out to infinity. Solutions for a given temperature tend to terminate, and unless you pick exactly the right solution, you get stuck in some way. However, you shouldn't worry about this, because the conditions at the critical point determine the whole flow pattern. Just let the flow seek its own equilibrium and it will automatically climb onto the critical solution. As Axford said: when you turn on a jet engine you think, "Gosh, it's a fluid; are there ways for it to anticipate the solutions out in the adiabatic region?" Well, I suspect there are. Scarf has already pointed out that we were arguing about exactly the same point some years ago.

EDITORS' COMMENT: Dr. Petschek suggested that in the collisionless outer corona, microscopic plasma instabilities might be more important than the hydromagnetic instabilities discussed by Scarf. He also noted that the fluctuations do more than maintain fluid-like flow, and he suggested that it should be possible to define transport coefficients associated with these effects.

SCARF: We should really include magnetic effects at the beginning of the analysis. However, I don't know what the thermal conductivity or the viscosity would be. They would certainly not have the coefficients associated with long-range Coulomb collisions. Particles can influence each other by scattering from the field irregularities, and this scattering must certainly mean that some energy transfer (thermal transfer) is possible. But as far as I know, it is not yet possible to write equations, or transport coefficients, describing this behavior.

ZIRIN: Let me mention a point that is important to discussions of the corona. Some of you may be aware of a discrepancy that has bothered solar physicists for many years, namely: the difference between the coronal temperature as measured from Doppler line-broadening, and the coronal temperature as indicated by ionization-balance calculations.

Much to everybody's joy, Dr. Alan Burgess of London has recently pointed out¹ that the process of dielectronic recombination, under coronal conditions, has a coefficient that is larger by a factor of about 20 than the coefficient of radiative recombination. The observed ionization balance can now be said to correspond to a much higher temperature—about 1.5 million deg—which agrees with the Doppler temperature. Other calculations have been made by Jefferies in Boulder, and Trefftz in Munich, with roughly the same results.

For those of you who are not familiar with the process of dielectronic recombination, the capture of an electron by an ion may result in either the emission of a photon or the excitation of the ion to a higher state. In the latter case, the captured electron gives up some of its energy to one of the bound electrons. The resulting doubly-excited state of the next lower ion then decays by ordinary photon emission.

¹Burgess, Alan, Astrophysical Journal 139, 776 (1964)

CHAPTER XIV

EFFECTS OF DIFFUSION ON THE COMPOSITION OF THE SOLAR CORONA AND THE SOLAR WIND

J. R. JOKIPII¹

California Institute of Technology, Pasadena, California.

This report summarizes an investigation into the effects of radial diffusion in the solar corona and the solar wind. The existence of a solar wind with a flux of 3×10^8 protons/cm² sec at 1 AU has been assumed, and a kinematic description of the effects of diffusion has been obtained. The effects on the dynamics of the solar wind have not been investigated. Some aspects of the latter problem have been discussed by E. N. Parker at the Cloudcroft Symposium (Ref. 1).

This work was initially motivated by the fact that the *Mariner-2* plasma data consistently indicated a ratio of alpha particles to protons substantially less than the accepted solar value of 0.1. The present investigation indicates that radial diffusion in the corona can cause a substantial decrease in the abundance of alpha particles and other heavy ions in the solar wind. Also, these abundances may be substantially increased in the lower corona. In other words, the solar wind leaves these ions behind in the lower corona, tending to increase their coronal abundance and to decrease their solar-wind abundance.

In order to obtain a quantitative estimate of this settling out, a simple but hopefully quite general model has been developed. The corona flows outward to form the solar wind. No matter what the precise details of the flow are, it should be statistically time-independent if averaged over times that are long when compared with random coronal fluctuations. Thus for a given element, the equation of continuity reads: $nvr^2a(r) = constant$, where a(r) is a measure of the departure from spherical symmetry, and n and v are time-averaged particle density and radial velocity respectively. Dividing the continuity equation for element A by that for protons, one obtains

$$\left(\frac{n_A}{n_p}\right)_{r_0} = \left(\frac{n_A}{n_p}\right)_{r_0} \left[\frac{(v_A/v_p)_{r_0}}{(v_A/v_p)_{r_1}}\right]$$
(1)

¹National Science Foundation Predoctoral Fellow

Obviously, if the term in brackets is different from unity, we expect changes in the abundance of element A relative to protons. Note that Eq. 1 does not require the flow to be spherically symmetric.

Now, how does one compute the ratios of velocities in Eq. 1? Since the mean free paths in the corona are small, the gas dynamic diffusion equations are called for. The following discussion will be limited to alpha particles, but similar results have been obtained for heavier ions.

Assume the magnetic field to be nearly radial. The coronal gas is essentially a ternary mixture of protons, alpha particles, and electrons, and the radial component of the diffusion equation can be written in the form

$$\frac{v_{p} - v_{\alpha}}{v_{p}} = \frac{v_{D}}{v_{p}} = \frac{T^{3/2}}{n_{p}v_{p}r^{2}} \left[f(n_{\alpha}/n_{p}) - g(n_{\alpha}/n_{p}) \frac{r^{2}}{R_{S}^{2}} \frac{dT}{dr} + h(n_{\alpha}/n_{p}) \frac{r^{2}}{R_{S}^{2}} \frac{T}{1 - (v_{D}/v_{p})} \frac{d}{dr} \left(\frac{v_{D}}{v_{p}} \right) \right] \tag{2}$$

The three terms on the right correspond to pressure, thermal, and concentration diffusions; and f, g, and h are slowly varying functions of n_{α}/n_{p} . If spherical symmetry is introduced here, $n_{p}v_{p}r^{2} = constant$ and has a value that can be obtained from the *Mariner* data. The dependence of v_{D}/v_{p} on n_{α}/n_{p} , T, and dT/dr can then be determined from Eq. 2 and is shown in Fig. 1 for $n_{\alpha}/n_{p} = 0.1$. It is immediately apparent that the

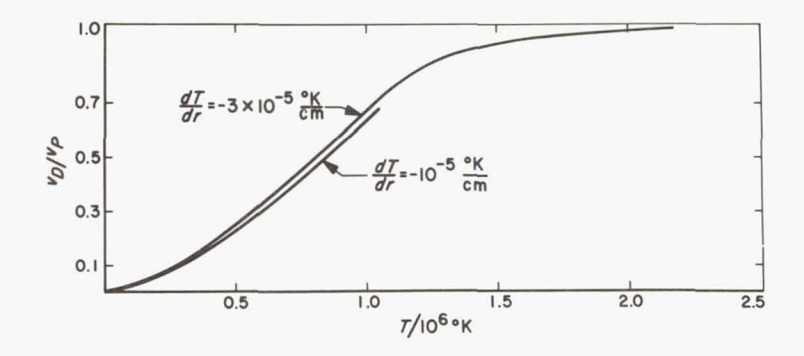


Fig. 1. Relative diffusion velocity of alpha particles and protons as a function of temperature for a solar-wind proton flux $n_{\nu}v_{\nu}=3\times10^{8}/\mathrm{cm^{2}}$ sec at 1 AU and for $n_{\nu}/n_{\nu}=0.1$

diffusion velocity v_D can be an appreciable fraction of the proton velocity in the corona. The curves also illustrate the small dependence on the coronal temperature gradient.

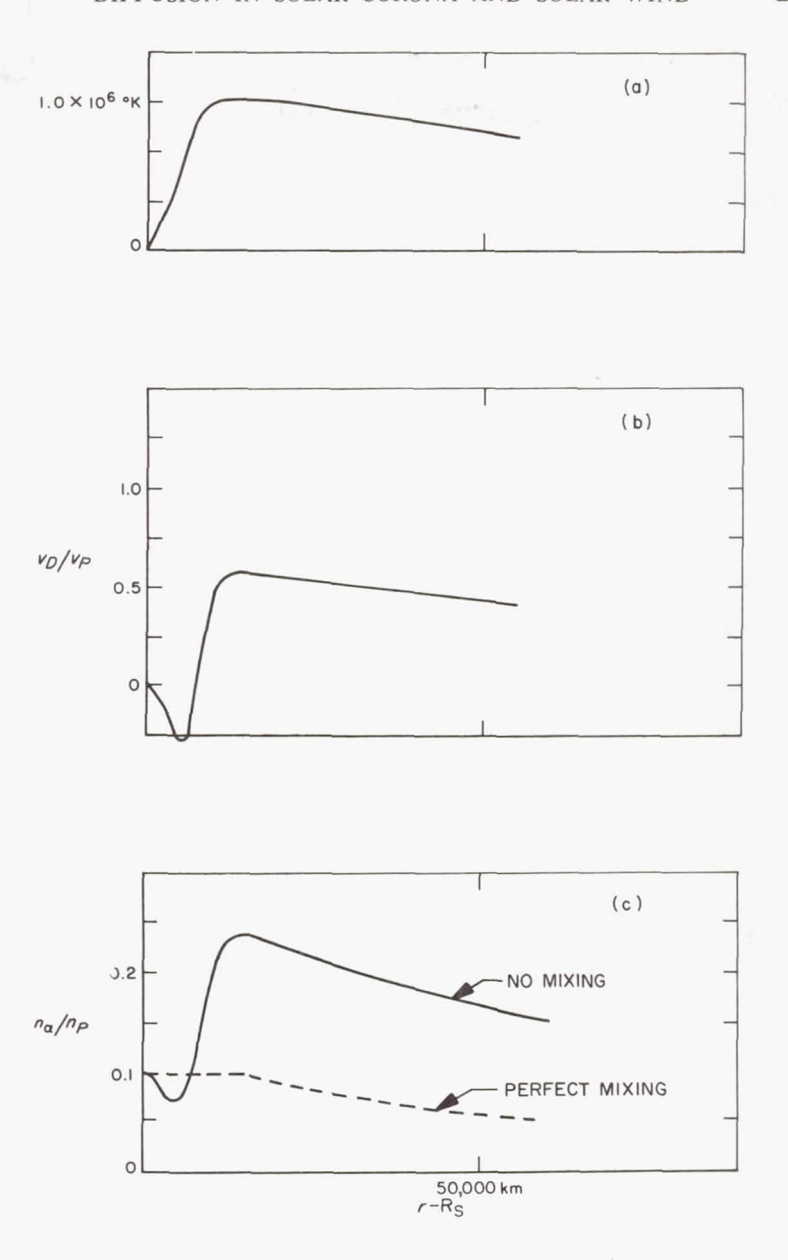


Fig. 2. (a) Radial temperature variation assumed for the calculations, (b) calculated relative diffusion velocity as a function of height above the photosphere, and (c) calculated relative alpha-particle abundance as a function of height above the photosphere

The validity of Eq. 2 in the outer solar wind is perhaps questionable. However, it seems reasonable to assume that the diffusion velocity goes to zero for large r, either because Eq. 2 is valid and the temperature falls, or because tangled magnetic fields prevent diffusion.

Equations 1 and 2 can now be used to compute n_{α}/n_{p} as a function of radius. The results for the typical temperature profile shown in Fig. 2a are sketched in Fig. 2b and 2c. Here a photospheric value of 0.1 for n_{α}/n_{p} has been assumed, although similar behavior is expected for other values. As we go outward, the large temperature gradient in the chromosphere forces v_{D}/v_{p} to be negative and decreases n_{α}/n_{p} slightly. In the corona, the temperature is very high and n_{α}/n_{p} is increased. Finally, at larger r, n_{α}/n_{p} returns to 0.1. This behavior of n_{α}/n_{p} is indicated by the solid line in Fig. 2c.

At this point, it is desirable to put more physics into the problem. The layer of large alpha-particle abundance is unstable and tends to mix with the lower regions. That is, the regions with large alpha-particle abundance tend to sink because of their higher density. This mixing tends to keep $n_{\alpha}/n_{p} \sim 0.1$ in the corona. If the mixing were perfect, the run of n_{α}/n_{p} with r would be given by the dotted line in Fig. 2c. The actual behavior of n_{α}/n_{p} probably falls somewhere between the dotted and solid curves in Fig. 2c. That is, mixing will occur, but it will probably not be sufficient to keep n_{α}/n_{p} precisely at its photospheric value. Thus we may have both an increase in the concentration of alpha particles (and hence, other heavy ions) in the solar corona, and a decrease in the solar wind.

It should be emphasized that these results are for average values only, and fluctuations in time are to be expected. The *Mariner* data apparently do indicate the presence of such fluctuations.

I am grateful to Prof. Leverett Davis, Jr., for initially drawing my attention to this problem and for many helpful discussions.

REFERENCES

1. Parker, E. N., The Solar Corona, ed. by J. W. Evans, Academic Press, New York (1963) p. 11.

DISCUSSION OF JOKIPH PAPER

ATHAY: It should be kept in mind that our main information about helium abundance in the Sun comes from the spectra of prominences which condense out of the corona and from the spectrum of the chromosphere. We get the same abundance for the chromosphere as for the corona. Another point is that other dynamic processes may be much more important than diffusion. Spicules feed matter into the lower corona at such a rate that the entire corona could be replaced in an hour's time. Similarly, the matter flowing downward in prominences could completely siphon the coronal material in about 10 hours' time.

DAVIS: I think it is very desirable to have the corona stirred by processes other than the overturning due to the separation. Such processes help provide the well-stirred lower part of the model. If, however, your stirring continues so high into the outer layers that you stir clear through the diffusion level, then you wouldn't end up with a lower density of heavy ions in the solar wind.

ZIRIN: One question which has been of great interest lately is the supposed difference between the abundance of iron in the corona and the abundance in the photosphere. The determinations of iron abundance in the corona give a much higher value than does the curve-of-growth analysis of the photospheric spectrum. JOKIPII: What I regard as a very interesting part of this calculation is that in it we have a mechanism that may be responsible for the high iron concentrations in the corona. The same mechanism may also reduce the solar-wind concentrations. GOLD: Any significant separation of ions occurring in the corona would provide a means for determining the source of gas on any one occasion. I believe it likely that the gas sometimes comes from very low in the solar atmosphere and sometimes comes from higher coronal regions. It would be nice to be able to determine the source of any single lot of gas by making measurements with a space probe. Perhaps by measuring the alpha-proton ratio, or any other ion ratio, we could establish the characteristic abundance in plasma from flare outbursts or from M regions. It is well worth looking for such a distinction in the data.

JOKIPII: I agree. This gives us, in effect, a probe of the corona. If we can measure the abundances accurately, we can get a better picture of conditions in the corona.

PARKER: There is evidence, as many people have pointed out,¹ that the ratio of the elements in the energetic solar particles, from helium on up, is remarkably constant from one event to another, suggesting very strongly that you are seeing the true solar abundance.

Fichtel, C. E. and D. E. Guss, *Physical Review Letters* **6**, 495 (1961) Biswas, S. and P. S. Freier, *Journal of Geophysical Research* **66**, 1029 (1961) Biswas, S., *Journal of Geophysical Research* **67**, 2613 (1962) Ney, E. P. and W. A. Stein, *Journal of Geophysical Research* **67**, 2087 (1962) Biswas, S., P. S. Freier, and W. A. Stein, *Journal of Geophysical Research* **67**, 13 (1962)

Page intentionally left blank

RECONNECTION AND ANNIHILATION OF MAGNETIC FIELDS

H. E. PETSCHEK

Avco-Everett Research Laboratory, Everett, Massachusetts

I SHOULD like to discuss a rather idealized plasma configuration in which two adjacent magnetic-field regions have oppositely directed field lines. The problem is to determine the velocity at which these field lines approach each other and become reconnected. This problem is obviously closely related to the question of detachment of the field lines from the solar surface. However, the details of the application of this analysis to the solar problem have not been worked out.

Parker and Sweet (Ref. 1) have made an analysis in which the approach velocity turns out to equal the Alfvén speed divided by the square root of the magnetic Reynolds number. For any reasonable solar-plasma conductivity, and for a reasonable length scale of the configuration parallel to the boundary, the magnetic Reynolds number is very large. Thus the velocity is a very small fraction of the Alfvén speed.

The present analysis, which involves plasma-wave phenomena, indicates that the velocity for approaching field lines is roughly equal to the Alfvén speed divided by the logarithm of the magnetic Reynolds number. Since logarithms rarely exceed about ten, the velocity turns out to be about one tenth of the Alfvén speed. In other words, I propose that the process for bringing the field lines together is much more rapid, and that the approach velocities are not too different from the expected fluid-flow velocities involved.

Diffusion Model

The picture suggested by Parker and Sweet is shown in Fig. 1, which also shows relevant equations. In this model, the fluid flows into the boundary between the two opposing magnetic fields at velocity u_{xo} , and then flows along the boundary at velocity v. To find the steady state, they match the rate at which the magnetic field diffuses outward through

¹For a more detailed discussion of some aspects of this analysis, see Ref. 2

the fluid to the rate at which the fluid moves into the boundary. The diffusion velocity of the field is roughly $c^2/4\pi\sigma\delta$, where 2δ is the width of the boundary region. Eliminating δ by means of the continuity equation, and noting that Bernoulli's law for this configuration implies that the fluid velocity along the boundary is roughly equal to the Alfvén speed, they come up with the result: $M_o = u_{xo}/V_A = 1/\sqrt{R_m}$.

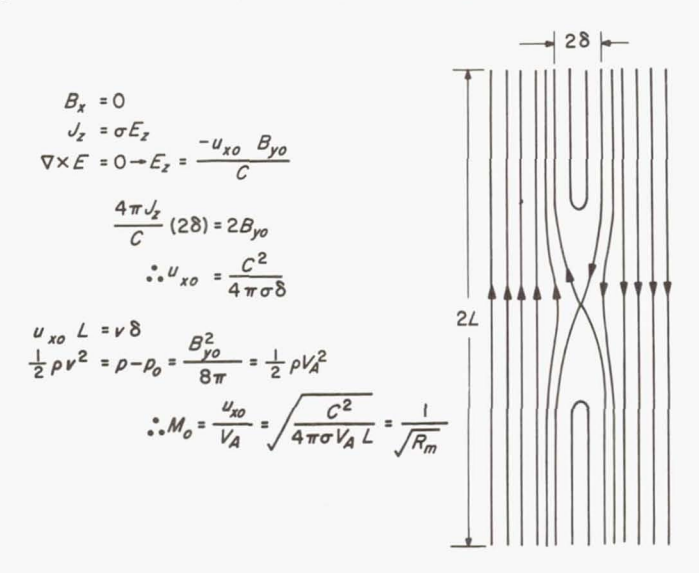


Fig. 1. Parker-Sweet model for field collapse at a neutral point

This analysis, however, overlooks the fact that there is a wave-propagation mechanism that can produce the final field configuration from the initial one. By a wave-propagation mechanism, I mean a steady-flow configuration in which there are standing waves, in the same sense that the magnetosphere's bow shock is a standing wave in the plasma flow; that is, the wave propagates relative to the fluid, but remains stationary in a coordinate system that is stationary with respect to the magnetosphere. The wave-propagation speed is independent of the electric conductivity in the medium. If the reconnection can be accomplished principally by means of waves, the reconnection rate will be significantly increased and be much less dependent on the value of the conductivity.

Plasma Waves

Let me briefly mention the wave modes that can exist in the plasma. If you write the hydromagnetic equations and ask for the linear wave propagation speeds at various angles to the magnetic field, you get the result shown in Fig. 2. The outer circle represents a "fast" wave, which is

the most familiar to us and which travels at roughly the same velocity in all directions; the velocity is of the order of either the speed of sound or the Alfvén speed, depending on the relative magnitudes of the magnetic and particle pressures. There are also intermediate waves and slow waves. (I believe the intermediate waves are really the ones that Alfvén discussed first.) You will notice that the intermediate and slow waves do

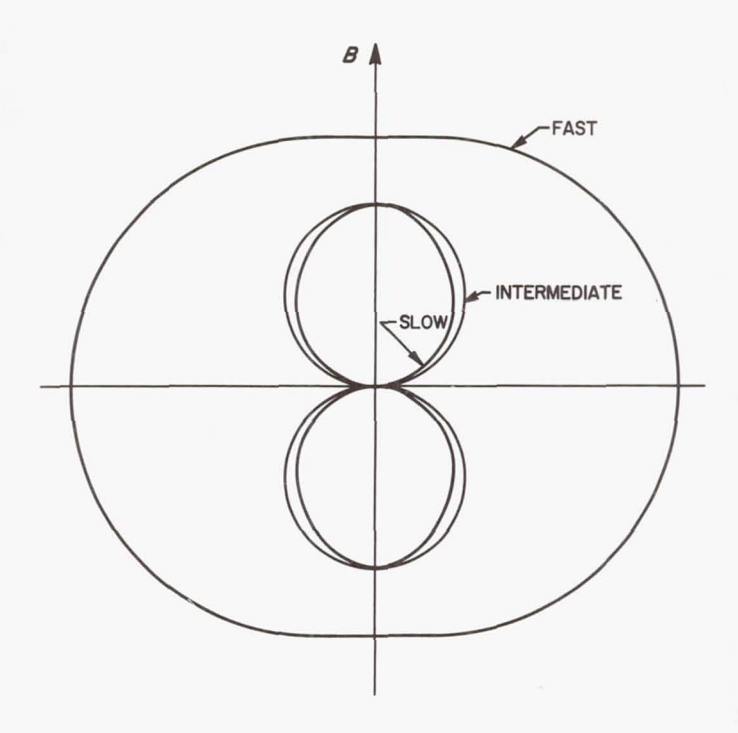


Fig. 2. Wave-propagation speeds at various angles to a magnetic field. The wave speed is proportional to the distance from the origin

not propagate at all in a direction normal to the magnetic field; that is, when the waves are precisely normal to the field, their propagation velocities go to zero. However, if we assume a small component of the magnetic field to be normal to the boundary—and such a component exists even in Parker's pictures—then these two waves will have small but finite propagation velocities.

Standing Wave Configuration

Now, let's see if we can construct a picture in which a combination of these waves leads to a change in field direction. Let's take the particular case in which the particle density is the same on both sides of the boundary. (A difference in particle densities means only that slightly different waves are required, and thus affects only the details of the picture.) A conceivable magnetic-field and wave configuration is shown in Fig. 3. We will examine this picture for self-consistency. Initially we will ignore the region in the immediate vicinity of the neutral point, where we will find later that the wave solution must be matched to a diffusion solution in order to avoid a singularity. Figure 3 shows a symmetrical picture with two waves propagating away from the boundary. At the wave fronts, there is a sharp change in field direction and a corresponding sudden change in flow velocity along the boundary; that is, the region between the waves contains fluid moving rapidly in the y direction and has a magnetic field that is only in the x direction.

If y is distance measured along the boundary, and δ is the half-thickness of the boundary layer, then the conservation-of-mass requirement leads to the relation

$$u_{ro}y = v\delta \tag{1}$$

where we have assumed that the density between the waves is the same as it is outside of them. (Compressibility does not significantly alter the rate of connection.)

The momentum equation in the y direction may be written as

$$\frac{d}{dy}(\rho v^2 \delta) = -\frac{B_{yo}B_x}{4\pi} \tag{2}$$

where B_x is the x component of the magnetic field within the boundary layer. Equation 2 has equated the rate of change of momentum flux within the boundary layer to the magnetic forces. The pressure-gradient term is omitted, since the pressure within the boundary layer is independent of y. The drop in pressure to the ambient pressure, which was considered in the previous analysis, would actually occur somewhere near the end of the boundary. Equations 1 and 2 may be combined in the form

$$M_o^2 \frac{d}{dy} \left(\frac{y^2}{\delta} \right) = -b_x \tag{3}$$

where we have introduced the notations $b_x = B_x/B_{yo}$ and $M_o = u_{xo}/V_A$. At appreciable distances from the neutral point we expect wave propagation

to be dominant. In this case, by equating the velocity of fluid flowing into the boundary layer with the wave-propagation speed, we get

$$M_o = |b_x| \tag{4}$$

It is important to remember that the wave propagation speed depends only on the normal component of the magnetic field, not on the magnitude of the field. The absolute value of b_x is required in Eq. 4, because a wave

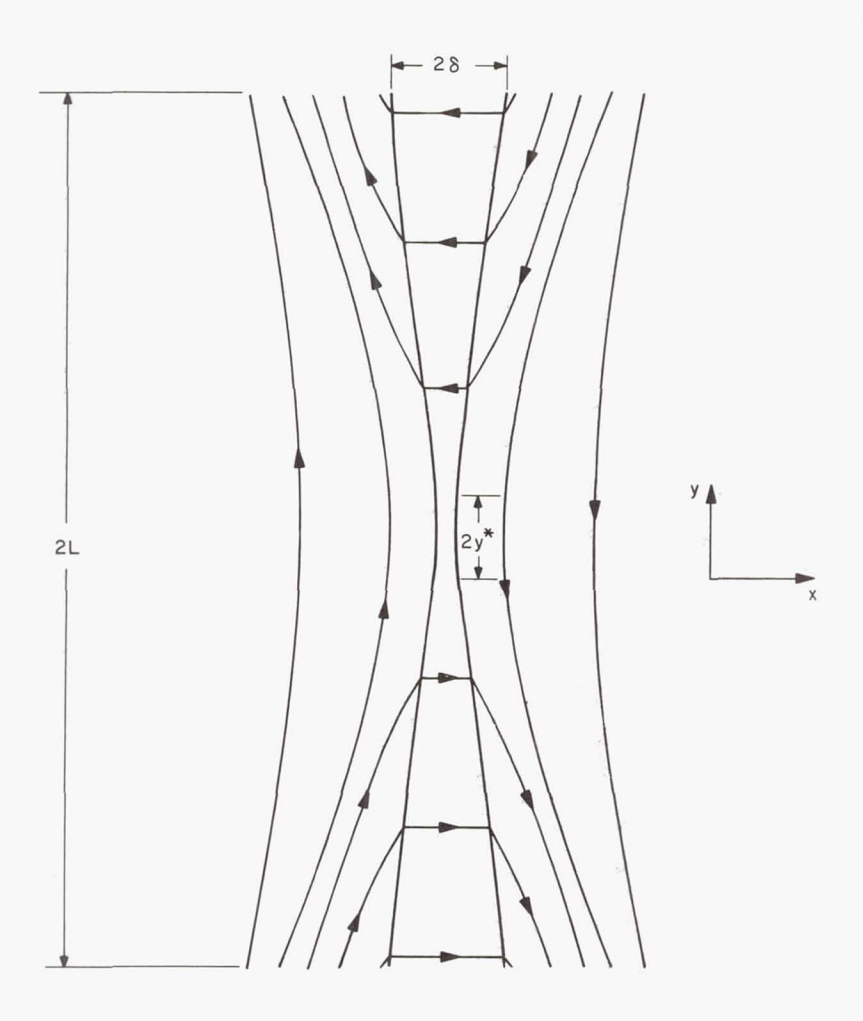


Fig. 3. Standing-wave patterns associated with flow into a neutral point

can propagate in either direction along the magnetic field. For a flow that is only slightly distorted from a uniform flow, this equation requires that $|b_x|$ be constant along the boundary layer. The combination of Eq. 3 and 4 thus gives

$$\delta = M_o|y| \tag{5}$$

which indicates that the thickness of the boundary layer increases linearly with y.

Diffusion Region

Since the X-type neutral point requires that b_x be an odd function of y, the constancy of $|b_x|$ implies a discontinuous jump of b_x at the neutral point, which is, of course, unreasonable. Thus, near the neutral point the wave picture breaks down, and diffusion must be considered.

If wave propagation is neglected entirely in the diffusion region, then Parker's analysis applies within this region. The height of the diffusion region, $2y^*$, is small, however, compared to the total length of the boundary region, 2L. If L is replaced by y^* , the bottom equation in Fig. 1 then determines a consistent value of y^* for a given approach velocity u_{xo} of the magnetic field lines. It is easy to check that, within a factor of two, the diffusion-region solution and the wave-region solution match according to two other related criteria: (a) the thicknesses of the boundary as determined by the diffusion (Fig. 1) and wave-region (Eq. 5) analyses are equal at $y = y^*$; and (b) the value of b_x rises linearly within the diffusion region, and at $y = y^*$ it reaches M_o , which is the value required by the wave-region analysis (Eq. 4).

External Flow Field

Combining the wave and diffusion regions, the picture developed thus far describes conditions in the boundary region for arbitrary values of the incoming flow velocity. Included in these conditions is the requirement for a particular variation of the normal component of the magnetic field, b_x . We must now determine whether this required b_x is consistent with a flow pattern in the region external to the boundary. Obviously, the requirement that field lines go through the boundary results in a bowing of the field lines towards the neutral point as illustrated in Fig. 3. Since there aren't any strong currents in the external region, and since we are dealing with a high-conductivity medium—neglecting joule dissipation. Furthermore, since the field lines must be bent only slightly, the external flow will be only slightly distorted from a uniform flow towards the boundary, and it may be treated as a linear perturbation on such a uniform flow. It can be easily verified that for an incompressible flow, both the flow and the mag-

netic field are solutions of Laplace's equation to first order in such an expansion. At the opposite limit of vanishing gas pressure as compared to magnetic pressure, the magnetic field is still a solution of Laplace's equation, since in this case the flow can not tolerate significant $j \times B$ forces. The appropriate solution of Laplace's equation is determined by the condition that the normal component of magnetic field is given by Eq. 4 for $|y| > y^*$ and varies linearly between $-y^*$ and y^* . The largest change in magnetic field in the external flow will occur near the neutral point, just outside the diffusion portion of the boundary. Evaluating the change in magnetic field at this point by the method indicated above, we find

$$\frac{\Delta B_y}{B_{yo}} = -\frac{2M_o \ln (R_m)}{\pi} \tag{6}$$

Limiting Flow Velocity

The above analysis defines the flow field in terms of the rate of approach of field lines, M_o , and it would appear to be valid for a range of values of M_o . This is quite reasonable, since one can imagine cases where the flow velocity is limited by external conditions to a value lower than the rate at which reconnection is allowed to occur at the neutral point. For the present discussion, we are interested in the limiting rate determined by reconnection at the neutral point in the absence of external restraints. In other words, we must ask whether there is a limiting value of M_o above which the flow cannot exist.

Equation 6, taken at face value, would imply a change in sign of B_y for sufficiently large values of M_o . We must remember, however, that in both the external flow and the boundary, we assumed that $\Delta B_y/B_{yo} \ll 1$. The analysis is therefore not valid above some value of M_o . We can determine roughly whether the nonlinear terms in this expansion tend to limit the flow. The flow rate through the diffusion region is proportional to the Alfvén speed and therefore to the magnetic-field strength just outside of the diffusion region. Since V_A decreases as M_o increases, we may expect that the process does indeed limit itself when $\Delta B_y/B_{yo}$ becomes significant. An accurate determination of the limit would require a much more sophisticated analysis. However, a reasonable approximation should be obtained if one simply estimates that the nonlinear terms become important and limit the flow when $\Delta B_y/B_{yo} = \frac{1}{2}$. Substituting this value in Eq. 6, we find for the limiting reconnection rate

$$M_o(\max) = \frac{\pi}{4 \ln(R_m)} \tag{7}$$

As indicated in the introduction, this result shows that the velocity at which field lines cross the boundary and reconnect decreases only logarithmically with increasing magnetic Reynolds number, and that

even for extreme conductivities and length scales, this velocity will therefore still be of the order of one tenth of the Alfvén speed.

REFERENCES

- PARKER, E. N., Journal of Geophysical Research 62, 509 (1957).
 PARKER, E. N., Astrophysical Journal Suppl. Series 77, 8, 177 (1963).
 SWEET, P. A., Proceedings of the IAU Symposium on Electromagnetic Phenomena in Cosmical Physics, No. 6, ed. by B. Lehnert, Cambridge University Press, New York (1958) p. 123.
- PETSCHEK, H. E., AAS-NASA Symposium on the Physics of Solar Flares, SP-50, ed. by W. N. Hess, National Aeronautics and Space Administration, Washington, D.C. (1964).

Session IV

THE SOLAR WIND AND THE MAGNETOSPHERE

Page intentionally left blank

SOLAR-WIND INTERACTION WITH THE MAGNETOSPHERE: FLUID DYNAMIC ASPECTS

W. I. AXFORD

Cornell University, Ithaca, New York

The Solar Wind as a Fluid

To discuss the flow of the solar wind past the magnetosphere as a fluid flow is quite appropriate. This might at first seem surprising, since the collision mean free path in the interplanetary medium near the Earth is of the order of 1 AU. However, the casual notion that the mean free path is the characteristic scale that determines whether or not the medium exhibits fluid behavior is rather misleading.

Let us consider two extreme cases of flow past an obstacle. First, for the case of Newtonian flow, the individual particles of the gas move quite independently, and if they happen to run into the obstacle, they bounce off. The particles individually strike the obstacle because they do not know any better; that is, they have not been warned of the presence of the obstacle in their path, so they cannot take any evasive action. In the second case, where the gas behaves as a fluid, the particles do take evasive action; most of them, in fact, manage to avoid hitting the obstacle and instead flow around it. Somehow the particles have received information concerning the presence of the obstacle and have acted upon it. A fluid may therefore be described as an educated gas. It is not necessary to refer to collisions in this discussion; rather, the key is information. The situation is somewhat analogous to traffic flow. When a stream of automobiles approaches a signal light that suddenly turns red, the first car will stop, then the next car, and so on; the information is passed from the signal to successive cars without the necessity for collisions (Ref. 1).

How is information distributed in a fluid? In effect, it is propagated by waves. Thus an obstacle in the flow attempts to generate a spectrum of waves, which is peaked at a wavelength comparable to some typical dimension of the obstacle. If most of the wave spectrum thus generated can propagate, and if the particles can receive the information carried

by the waves and act accordingly, then the particles behave as a continuous fluid: otherwise they behave in the Newtonian fashion.

Consider the case of a baseball moving through air, where the only propagating wave mode is the acoustic wave. The baseball generates a pressure field around itself. This pressure field can be regarded as a field of "virtual" phonons that impart information to the oncoming air molecules in the manner we have described, causing the air molecules to flow around the baseball without necessarily impinging on it. However, sound waves are heavily damped if their wavelength is comparable to or less than the collision mean free path; hence, the shorter wavelengths in the virtual phonon spectrum are absent. If the air is so rare that the mean free path is greater than the dimensions of the baseball, then most of the spectrum is missing and very little information concerning the presence of the baseball is imparted to the air, which therefore behaves as a Newtonian flow.

In a plasma, it is not necessary to depend on ordinary sound waves to carry information, and the mean free path no longer plays a vital role. As long as waves are available in the appropriate part of the spectrum and can propagate without being severely damped, the medium will behave as a continuous fluid. An immense variety of waves can propagate in a collision-free plasma, and it is not clear at what point the transition to the Newtonian condition takes place. One might expect some degree of fluid-like behavior to persist even when the characteristic dimension of an obstacle approaches the Debye length; it is certainly safe to assume that the plasma behaves like a fluid if the obstacle size is greater than the ion Larmor radius. In the case of the interplanetary medium near the Earth, the ion Larmor radius is at most about 10³ km and the Debye length is about 10 m. Thus, since the width of the magnetosphere is about 10⁵ km, we must consider that the flow of the solar wind past the magnetosphere corresponds to the flow of a continuous fluid.

Supersonic Flow and Shock Waves

A plasma is a dispersive medium, and as a result, the transport of information can be quite complicated. In order to decide whether a flow is to be considered supersonic or subsonic, I suggest that one compare the flow velocity with the phase velocity of the waves that carry most of the information (those with wavelengths comparable to the body size). Thus, for the case of the solar wind and the magnetosphere, where the important waves are the magnetoacoustic waves, we form an effective Mach number by taking the ratio of the solar-wind velocity v to the phase velocity of fast-mode magnetoacoustic waves. The phase velocity is given by

where V_A is the Alfvén speed and V_S is the sound speed in the interplanetary medium. Since V_S and V_A are probably comparable, and v is of the order of 5 to 10 V_A (Ref. 2), it is clear that the solar wind should be considered supersonic as far as the magnetosphere is concerned. However, the solar wind could appear to be subsonic for objects much smaller than the magnetosphere.

While the solar wind remains supersonic, the magnetosphere cannot make its presence felt upstream; and in order to make the solar wind flow around the magnetosphere, something drastic must be done. In fact, a shock wave is set up on the upstream side of the magnetosphere, thus producing a subsonic flow. The shock wave is a collision-free one, and its thickness is expected to be of the order of the proton Larmor radius (Ref. 3), which we have already noted is small compared to the size of the magnetosphere.

The characteristics of collision-free shocks are known only in a sketchy fashion, and the magnetosphere shock is the first example to be probed successfully. Various theories suggest that the shock should have a turbulent structure and that wave-wave scattering is perhaps the main cause of dissipation; furthermore, the region downstream should appear quite turbulent and irregular. Perhaps the best analogy to a collision-free shock in a plasma is a hydraulic jump or bore on the surface of water, where these features are quite clearly evident.

Wave-wave interactions in the shock can lead to the production of waves with such short wavelengths that they can propagate upstream against the solar wind; fast particles (presumably mostly electrons) produced as a result of the turbulence can also propagate upstream. Due to the escape of these fast particles and waves, information concerning the state of the fluid prior to the shock transition is lost, and this loss contributes to the irreversibility of the phenomenon. The loss of information is equivalent to an increase of entropy.

Observations to date are in excellent agreement with all of these ideas; however, since the magnetosphere shock is the best example of a collision-free shock that we have available, it is extremely important that it be examined in greater detail with regard to the spectra of both the particles and the waves. The high-frequency waves might be especially interesting, and we might expect the shocked region to be "luminous" in the sense that such waves are continually emitted and move upstream—just as luminescence occurs as a result of collisions in the gas surrounding a re-entering missile, or in an ordinary shock tube.

The observed stand-off distance of the shock from the magnetosphere boundary should be compared only cautiously with theoretical predictions; for not only do the calculated distances require a knowledge of the radii of curvature of the boundary and a knowledge of the ratio of specific heats, but they do not take into account a possible hydromagnetic effect resulting from field lines being "hung up" (draped around the front of the magnetosphere) and thus adding to the effective size of the magnetosphere. It seems sufficient to say that the observed position of the shock at a distance of typically 13 to $14~R_{\rm E}$ is a reasonable one.

The Shape of the Magnetosphere

Rather surprisingly, the magnetosphere has not changed a great deal in the last 30 years, since Chapman and Ferraro made their original model using an image dipole to distort the geomagnetic field in an appropriate manner (Ref. 4). The topology of this simple model is essentially the same as that of the currently fashionable models – in particular, the low-latitude field lines have a donut-shaped configuration completely enclosed by the high-latitude field lines, which form a "tail." The division between these two regions is determined by two neutral points on the surface of the magnetosphere, and these neutral points are linked to points on the Earth at high geomagnetic latitudes on the noon meridian. [In a sense, the neutral points act somewhat like the poles of the distorted dipole field, since cosmic rays of the lowest energy can strike the Earth in their vicinity. There is a difference from the undeformed dipole, however, in that the whole tail region is accessible to low-energy cosmic rays. Thus, if there is a little scattering in pitch angle, these low-energy cosmic rays can precipitate over the whole polar cap, as defined by the neutral points.]1 If there is some connection of field lines between the geomagnetic and interplanetary magnetic fields, as Dungey, Petschek, and others have suggested, then this description is slightly altered. In particular, the two neutral points merge into one, and a further neutral point or line appears in the tail.

A great deal of effort has been put into calculations of the shape of the magnetosphere using the Newtonian approximation. Although such calculations may be useful for the forward part of the magnetosphere, they are unlikely to help a great deal in understanding the magnetosphere as a whole; and certainly in view of the limited accuracy of the Newtonian approximation, numerical representations to several decimal places are not justified. One can estimate very easily that the geocentric distance to the forward stagnation point is typically $10~R_{\rm E}$. Furthermore, the magnetosphere must be somewhat broader in the equatorial plane at 90 deg to the Earth–Sun line than is implied by this value, since the Mach number of the external flow is greater than unity and hence the pressure is only a fraction of the stagnation pressure. A distance of 13 to 15 $R_{\rm E}$ from the Earth to the boundary seems quite appropriate. Near the neutral points, the distance to the boundary is still typically $10~R_{\rm E}$, because the geomag-

¹Added in manuscript

netic field strength decreases in this direction and so compensates for the reduction of the external pressure of the solar wind in this vicinity.

I believe that geomagnetic storms, auroras, and associated phenomena are evidence of a dissipative interaction between the solar wind and the magnetosphere. The dissipation implies the existence of transverse stresses at the magnetosphere boundary, and these stresses may have a profound influence on the magnetosphere shape, especially in the tail. Thus viscous or ohmic dissipation leads to the formation of a tail that is much more extended and contains much more magnetic flux than any tail that a nondissipative interaction could produce. The observations of *Explorers* 10 and 14 (Ref. 5 and 6) suggest strongly that the tail is as pronounced as I have suggested. However, it will be necessary to wait for the *IMP* observations before anything really definite can be said.

It is not easy to estimate the length of the tail, since the dissipative processes are not that well understood. One should expect, however, that the magnetosphere commonly reaches well beyond the orbit of the Moon—that is, to a distance of 60 $R_{\rm E}$ or more. A tail 40 $R_{\rm E}$ in diameter with an average magnetic-field strength of 30 γ (as suggested by the *Explorer-10* observations) would have to be about 200 $R_{\rm E}$ in length to contain enough energy to meet the requirements of a typical magnetic storm (about 10^{23} ergs). However, since all of the energy does not have to be contained in the tail at any one time, 200 $R_{\rm E}$ could be regarded as a possible upper limit. If field-line reconnection is the dominant process, the length of the tail implied here is the distance to the rear neutral line; just before reconnection, the field lines extend to great distances downstream, but this should perhaps be thought of as constituting a wake rather than a tail.

Using the above values of the tail diameter and of the field strength, we can estimate that the field lines leading to the neutral point(s) on the upstream side of the magnetosphere intersect the Earth at a geomagnetic latitude of approximately 72 deg. There is probably a real range of 70 to 75 deg, but this is nevertheless significantly different from the values suggested by calculations based simply on the Newtonian approximation. A number of ionospheric phenomena that could be associated with the direct penetration of solar-wind particles at the neutral points have patterns of occurrence that agree with my estimate.

The main effect of both viscous and ohmic dissipation at the boundary of the magnetosphere is to carry field lines from the front of the magnetosphere into the tail. In the case of a purely viscous interaction, the transverse stresses exerted by the solar wind move the field lines as a whole, causing them to slip smoothly around the surface (unless there is some turbulent mixing). In the case of purely ohmic dissipation, the field lines on the forward side of the magnetosphere are broken at a neutral point and become connected to the interplanetary magnetic field; the two

segments are then carried by the solar wind and are draped over the tail of the magnetosphere, where they become reconnected once again. In fact, both processes must occur, but so far it has not been possible to decide, on either theoretical or observational grounds, whether one or the other process is dominant.

Magnetospheric Interchange Motions

Let us now transfer our attention to the plasma flow inside the magnetosphere. Magnetospheric motions are of the interchange type, since $\beta = 8\pi nkT/B^2$ is generally very small (Ref. 7 and 8). That is, the lines of force are permuted in such a way that the magnetic configuration is left unchanged. Hence $\partial \mathbf{B}/\partial t = \nabla \times \mathbf{E} = 0$, and the electric field can thus be derived from a potential. Since the low-energy plasma (whistler medium) moves approximately in such a manner that $\mathbf{E} + \mathbf{v} \times \mathbf{B} = 0$, we see at once that the streamlines of the interchange motion and the lines of force of the magnetic field should be equipotentials of the electric field.

Interchange motions are possible in the magnetosphere because the lines of force pass through the insulating lower atmosphere—if the insulating atmosphere were absent, the field lines would be held rather firmly by the solid Earth, which is almost a perfect conductor in this context. The transition from the highly conducting magnetosphere to the insulating lower atmosphere is not sharp; instead there is a gradual change that takes place roughly in the altitude range 90 to 150 km, where the conductivity is such that any electric field that is not otherwise maintained is discharged in a matter of seconds. Obviously, magnetospheric motions must be mechanically driven so that the polarization charges corresponding to the associated electric field are continually replenished against the loss due to leakage across the ionosphere.

[Fortunately, the lower ionosphere has a very high Hall conductivity relative to its direct (Pedersen) conductivity; that is, most of the current flowing in the ionosphere is caused by the $\mathbf{E} \times \mathbf{B}/B^2$ drift of electrons $(\omega \tau_e >> 1$ above 90 km), with the ions being stopped by the background neutral particles ($\omega \tau_i << 1$ below 150 km). Consequently, the pattern of ionospheric currents can, to a first approximation, be interpreted immediately in terms of the motion of the feet of lines of force; it is necessary only to reverse the sense of the current pattern to obtain the pattern of magnetospheric motion at ionospheric levels. The motion at other points in the magnetosphere can be obtained by simply mapping the ionospheric motion along lines of force of the geomagnetic field.

Tidal motions in the neutral atmosphere are an important cause of magnetospheric motions, and are associated with the S_q and L ionospheric current systems. Atmospheric motions on a small scale contribute a "noisy" background to these tidal motions, all of which cause the

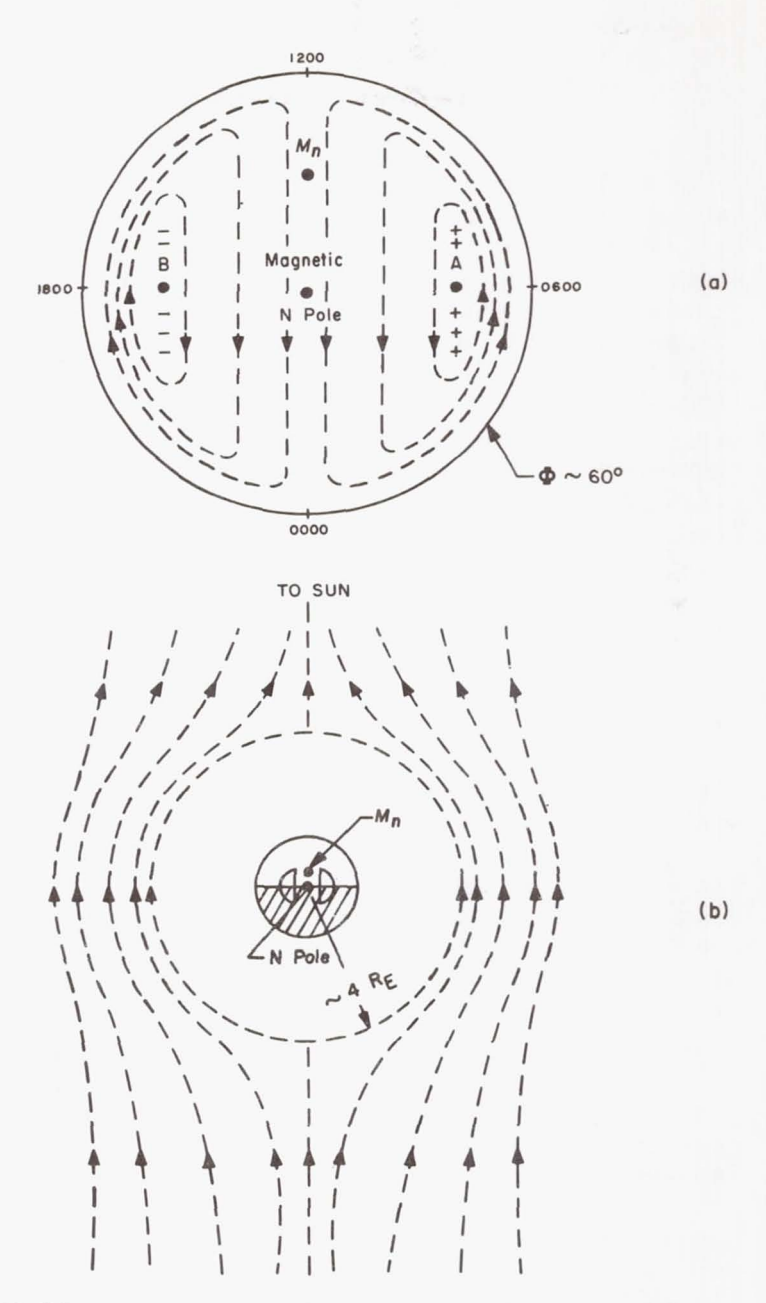


Fig. 1. (a) DS current pattern over the northern hemisphere. Electrostatic potential is suggested by charges (b) DS current and potential pattern, projected to the surface of the magnetosphere

magnetospheric plasma to be continually stirred around.]² The rotation of the Earth, also, produces a steady pattern of motion in the whole magnetosphere. The magnetospheric motions that appear to be caused by the solar wind are those associated with the DS current system during magnetic storms, and with the similar S_{qp} current system (Ref. 9) during magnetically quiet periods. An idealized sketch of the magnetospheric motion at ionospheric levels and the corresponding motion in the equatorial plane of the magnetosphere is shown in Fig. 1. The cause of this motion has been interpreted to be the dissipative component of the interaction between the solar wind and the magnetosphere, and it may be either viscous (Ref. 10 and 11) or ohmic (Ref. 12 and 13) or both. The suggested complete pattern of motion in the equatorial plane of the magnetosphere for the case of a purely viscous interaction is shown in Fig. 2. The situation for the case of ohmic dissipation is very similar, and is discussed elsewhere by Dr. Dungey and Dr. Petschek.

Since the geomagnetic field is non-uniform, interchange motions must involve changes in the volume of the magnetospheric plasma. Consequently, there are energy changes in the plasma which can be considered as being due to compression and rarefaction. However, it is perhaps more illuminating to consider these energy changes in terms of the motion of individual particles in the non-uniform magnetic and electric fields (Ref. 14), although we emphasize that cooperative phenomena may be important and that a self-consistent treatment is required.

It will be remembered that the work done in compressing a gas does not go wholly into internal energy; there is an amount—equal to kT per particle—that is effectively stored in the form of strain energy in the container. In the case of the magnetosphere, this is apparent as a deformation of the magnetic field, which we usually describe as the ring-current effect. Note that the ring current that would be produced as a result of the magnetospheric circulation sketched in Fig. 1 and 2 is essentially the same as that originally described by Alfvén (Ref. 15), except that the sense of motion is reversed. This reversal is required to produce agreement with the direction of the DS currents, which were not satisfactorily treated by Alfvén. Another difficulty of Alfvén's theory, which is absent in the dissipative-interaction theories, is that the electric field he describes would be rapidly discharged by the ionosphere so that the magnetospheric motions would not persist for any length of time.

The Electric Field and Energy Dissipation in the Magnetosphere During Magnetic Storms

It can be shown (Ref. 16) that the electric potential difference ψ_{AB} (see Fig. 1) associated with the *DS* current system during a magnetic storm is ²Added in manuscript

typically of the order of 20,000 v. The energy input rate (Φ_M) that is required to explain the observed stressing of the geomagnetic field, the dissipation occurring in the aurora, and the dissipation in ionospheric joule heating is of the order of 10^{18} to 10^{19} ergs/sec. During a storm, the

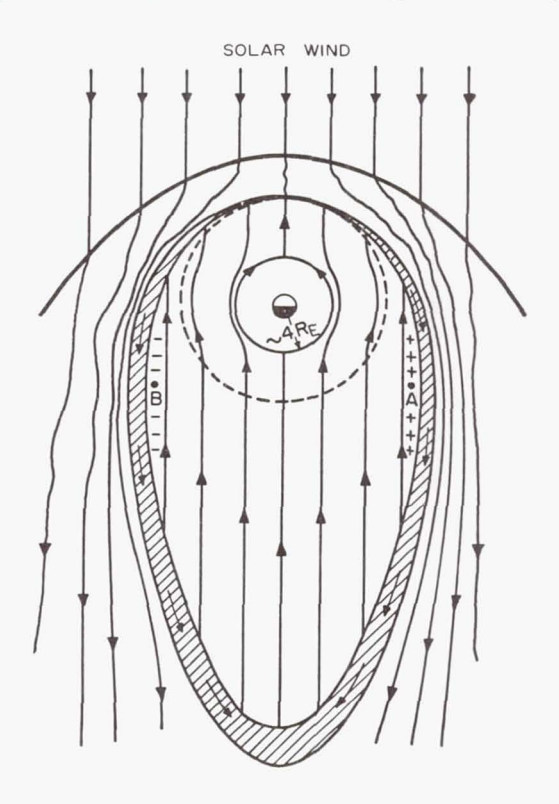


Fig. 2. Sketch of the equatorial section of the Earth's magnetosphere, looking from above the North Pole. Streamlines of the solar wind are shown on the exterior; the internal streamlines represent the circulation presumably set up by viscous interaction between the solar wind and the surface of the magnetosphere. The internal streamlines are also equipotentials of an associated electric field due to accumulations of positive and negative charges as indicated at A and B. (From Ref. 1)

solar-wind energy flux incident on the magnetosphere is two or three orders of magnitude larger than Φ_M , so the effective drag coefficient has the quite reasonable value of about 0.01.

Any magnetic-storm theory should include an explanation of the observed values of ψ_{AB} and Φ_{M} . This can now be done for the case in which ohmic dissipation at the magnetosphere boundary is the dominant cause of solar-wind drag.³ For the case of a purely viscous interaction,

³See Paper 18

we must first consider the mechanism that causes viscous stresses, since these stresses are probably not due to ordinary turbulent or molecular mixing between the solar wind and the surface layers of the magnetosphere.

As observed earlier, it is in many respects more convenient to treat the interaction of the solar wind with the magnetosphere in terms of hydromagnetic waves rather than in terms of particles; the effects of viscosity and heat conduction can be treated in a similar fashion. Hydromagnetic waves crossing the boundary of the magnetosphere transfer energy (producing the effect of heat conduction) and momentum (exerting normal and transverse stresses on the medium). [It has been estimated that the net rate of energy transfer across the magnetosphere boundary by longitudinal magnetoacoustic waves is roughly $0.2 \xi V_A \text{ ergs/cm}^2 \text{ sec}$, where ξ is the energy density of these waves in the solar wind. A transverse stress $D_W \sim 0.2 \ \xi$ is exerted on the boundary, due to the asymmetric refraction and reflection of the incident waves. Thus $D_W \sim 2 \times 10^{-10}$ dyne/cm² and the total energy input is $\Phi_W \sim 5 \times 10^{18}$ ergs/sec, where we have taken $\xi = 10^{-9} \text{ erg/cm}^3$ (Ref. 17). Arguments based on viscousboundary-layer theory lead to the result that if viscosity is the dominant dissipative component of the solar-wind-magnetosphere interaction, then $\psi_{AB} = 2 \times 10^4$ v implies that the effective kinematic viscosity must be roughly $\nu \sim 10^{13}/\text{cm}^2$ sec, the drag must be $D_{\nu} \sim 2 \times 10^{-10}$ dyne/cm², and the rate at which energy is transferred to the magnetosphere by the viscous stresses is $\Phi_v = 10^{19}$ ergs/sec. Thus there is a remarkably good agreement between Φ_{W} , Φ_{W} and Φ_{V} and between D_{W} and D_{V} .]

On this basis, we suggest that viscosity is likely to be important, and could explain the observed effects; however, we cannot at present decide whether viscous or ohmic dissipation is dominant, although both could be important. It is interesting that the *IMP* magnetic-field observations appear to show that the magnetic field just inside the boundary of the magnetosphere fluctuates considerably, implying that a substantial amount of energy is in fact entering the magnetosphere in the form of waves. On the other hand, the magnetic-field reversal often observed at the boundary of the magnetosphere (Ref. 6) seems to imply that ohmic dissipation occurs, since in a perfectly conducting fluid the sense of the magnetic field is irrelevant, and parallel field lines are not able to communicate information to each other concerning their direction.

The whole magnetic storm phenomenon appears to be plausibly explained by a suitable combination of a number of theories. Thus, the sudden commencement is presumably the result of a shock wave impinging on the magnetosphere (Ref. 18); the initial phase is due to a compression of the magnetosphere as suggested by Chapman and Ferraro

⁴Added in manuscript

(Ref. 4); the *DS* magnetic variations and the aurora are associated with magnetospheric interchange motions due to dissipation at the magnetosphere boundary as described here; finally, the ring current is also a result of the interchange motions and is produced more or less in the manner described by Alfvén (Ref. 15).

REFERENCES

- LIGHTHILL, M. J. and G. B. WHITHAM, Proceedings of the Royal Society of London, Series A, 229, 317 (1955).
- SNYDER, C. W., M. NEUGEBAUER, and U. R. RAO, Journal of Geophysical Research 68, 6361 (1963).
- 3. CAMAC, M., A. R. KANTROWITZ, M. M. LITVAK, R. M. PATRICK, and H. E. PETSCHEK, Nuclear Fusion Suppl. Pt. 2, 423 (1962).
- 4. Chapman, S. and V. C. A. Ferraro, Terrestrial Magnetism and Atmospheric Electricity (Journal of Geophysical Research) 36, 77, 171 (1931).
- HEPPNER, J. P., N. F. Ness, C. S. Scearce, and T. L. SKILLMAN, Journal of Geophysical Research 68, 1 (1963).
- 6. CAHILL, L. J. and P. G. AMAZEEN, Journal of Geophysical Research 68, 1835 (1963).
- GOLD, T., Journal of Geophysical Research 64, 1219 (1959).
 DUNGEY, J. W., Cosmic Electrodynamics, Cambridge University Press, New York, (1958).
- 9. NAGATA, T. and S. KOKUBUN, Nature 195, 555 (1962).
- 10. AXFORD, W. I. and C. O. HINES, Canadian Journal of Physics 39, 1433 (1961).
- 11. PIDDINGTON, J. H., Geophysical Journal 3, 319 (1960).
- 12. DUNGEY, J. W., Physical Review Letters 6, 47 (1961).
- LEVY, R. H., H. E. PETSCHEK, and G. L. SISCOE, Avco-Everett Research Laboratory, Research Report 170, Dec (1963).
- 14. HINES, C. O., Planetary and Space Science 10, 239 (1963).
- ALFVÉN, H., Tellus 7, 50 (1955).
 ALFVÉN, H., Tellus 10, 104 (1958).
- 16. AXFORD, W. I., Planetary and Space Science 12, 45 (1964).
- 17. SONETT, C. P. and I. J. ABRAMS, Journal of Geophysical Research 68, 1233 (1963).
- GOLD, T., Gas Dynamics of Cosmic Clouds, ed. by H. C. VAN DE HULST and J. M. BURGERS, North-Holland Publishing Co., Amsterdam (1955) p. 103.

Page intentionally left blank

CHAPTER XVII

SOLAR-WIND INTERACTION WITH THE MAGNETOSPHERE: PARTICLE ASPECTS¹

J. W. DUNGEY

Imperial College of Science and Technology, London, England

I AM going to use the "open" or "connected" model, as Axford calls it (Paper 16), without much apology, because there are a few other people in the world who believe in it and they are all here. I shall talk about the motion of individual particles, not about fluid flow. Of course, fluid flow is important, but since the problem can be divided into two parts, and since I don't understand things like turbulence, I am very happy to ignore the fluid aspects.

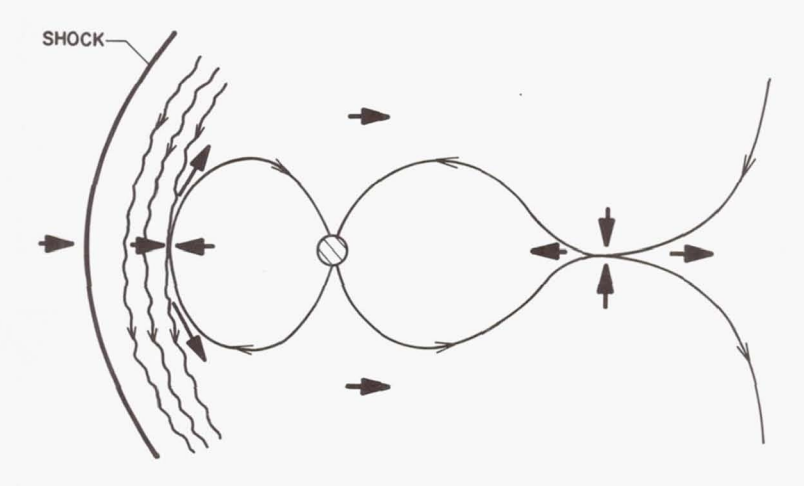


Fig. 1. "Connected" model of the magnetosphere and the interplanetary magnetic field. The light lines are lines of magnetic force; the short, heavy arrows indicate the local direction of the plasma flow

¹See Ref. 1 for an earlier treatment of this subject

The Topology of the Geomagnetic Field

Figure 1 is a model of the magnetic field in a meridian plane, with noon to the left and midnight to the right. Later I am going to argue a little with Axford about where the line through the forward neutral point intersects the Earth. I think it intersects the Earth at a higher geomagnetic latitude than he does.

I shall try to describe the topology of this field. There are only a few magnetic lines shown on this figure, and they are special ones which go through the two current sheets associated with neutral points (identified by converging/diverging plasma-wind velocity vectors). Incidentally, the right-hand current sheet should probably extend much farther back, but it was compressed to keep it on the illustration.

The topology is slightly similar to the Chapman-Ferarro one, in that lines of force from neutral points cover whole surfaces. The situation here is that there are two rather special lines of force (not in the plane of the paper) which connect these two points. Lines from one of these neutral points cover a surface that connects to one entire auroral zone, and lines from the other cover a surface that connects to the other auroral zone (Ref. 1).

The important distinction is between lines that close without going outside of the magnetosphere or very far from the Earth, and lines that come up from the poles and extend for a long distance. The exterior lines are separated from the interior lines by the surfaces just mentioned. The impression one gets from the last couple of days' discussion is that if one follows a line from the North Pole, he will eventually land in the Sun, at least on some days. When we discuss the motion of particles, we would like to know where the lines in the transition region go. There is a little uncertainty here, but I am going to say that they extend quite far from the Earth.

The Electric Field in the Magnetosphere

If one wants to talk about particles in magnetic fields, then instead of dealing explicitly with the fluid motion, he can talk about the electric field that is associated with the motion:

$$\mathbf{v} \times \mathbf{B} = -c\mathbf{E} \tag{1}$$

I will find the electric field from the DS pattern (Fig. 1, Paper 16). The electric potential is positive on the morning side and negative on the evening side (both maximum at the auroral zone). I am going to assume that the electric field is perpendicular to the magnetic field everywhere (Eq. 1) except in the neighborhood of these current sheets, which need special treatment. Alfvén likes to put in an electric field that is parallel

to the magnetic field in some parts of the magnetosphere, but I am ruling out the idea of parallel fields completely. If one assumes a steady state and a given static field, then the electrostatic potential is constant on a line of force. Knowing the potential on the polar cap, one knows the electrostatic potential on all field lines which connect to the polar cap, and thus he knows the potential and the electric field everywhere. Nearly everywhere in Fig. 1, the electric field points in a direction opposite to the orbital motion of the Earth, which is to say, out of the plane of the figure.

This electric field fits onto the electric field one would have in interplanetary space if the interplanetary magnetic field were directed southward. I am not sure of the latest observations, but in the *Explorer-12* observations there is clearly a mean southward component in the transition region (Ref. 2). We therefore expect the electric field in that region to fit onto the electric field in the magnetosphere.

The Motion of the Plasma Particles

Now that the electric and magnetic fields have been described, we can ask: What are the particle motions? One would really like to follow backward all possible particle trajectories and apply Liouville's theorem. Nearly all trajectories that we followed would go back to the solar wind. That is, if one worked a trajectory back through lots of gyrations, he would find it emerging at some point in the solar wind. Then if he found out from Dr. Snyder what the value of the velocity distribution function f was for such a particle, he would know what the value of f was everywhere, provided Liouville's theorem is true. This is the ideal calculation, and I think it helps one to think about the location of both the energetic particles and the non-energetic particles.

Now we have to consider the question of the actual trajectories, and we would like to use an adiabatic theory as much as possible. In fact, adiabatic theory can be used over a considerable portion of all the trajectories. When I say "adiabatic theory," I mean that one uses the first two adiabatic invariants—the magnetic moment μ and the longitudinal invariant I:

$$\mu = \frac{mv^2}{2B}$$

$$I = \oint v_{\parallel} \, ds \tag{2}$$

where B is the field strength, m is the mass, v_{\perp} and v_{\parallel} are velocity components relative to the field direction, and $\oint \dots ds$ is a line integral taken along a field line between mirror points for a given orbit.

I can be written as v times some function (which is an integral) of the

equatorial pitch angle α and of the particular line of force which the particle follows:

$$I = vG(\alpha, \text{field line}) \tag{3}$$

But if one knows the magnetic field, it is practicable to make some computations, so that one can find out the values of I for a large number of particles. The fact that v is outside the integral means that one does not have to repeat the computations for each different energy.

Axford has talked about adiabatic compression, and this is the kind of thing I want to discuss. The discussion can be made more precise by using μ and I.

Another way of looking at the particle motion is to consider it in terms of drifts, again obtained by the adiabatic approximation but without actually using I. There are drifts caused by electric fields, by gradients of magnetic-field strength, and by the curvature of the lines of force. If you put these all together, you can see how particles drift. If this method is valid, you can determine where a particle goes simply by computing μ and I, although you can't determine the time it takes to move.

Now, what are the interesting particles? The interesting cases occur when the drifts caused by electric fields are comparable to that caused by the non-uniformity of the magnetic field. The drift caused by non-uniformity is proportional to the particle energy. For a very-low-energy particle, the drift caused by the electric field, $\mathbf{E} = -\mathbf{v} \times \mathbf{B}/c$, dominates, and there is little change of energy. For a very energetic particle, the drift caused by non-uniformity of the magnetic field dominates, and in general there is a change in energy, but the *DS* potential (in this case about 20 kv) is not important for the high-energy particles. One expects, and indeed it turns out, that the two components of drift are comparable for particles whose energy is of the order of the electric potential difference. Therefore, we are interested in particles with energies of the order of 10 or 20 kev.

Now, as we work back along the trajectory, we may find that the particles lose energy. If they lose energy to the point where their energy is less than 1 kev, then they are moving more or less with the fluid, and it is easy for us to determine where they come from.

Now let's be a little more precise and discuss particular kinds of trajectories. Trapped particles bounce between two mirror points, one in each hemisphere. Some particles, as they drift around the Earth, may cease to be trapped on the day side, because they drift outside the region where both ends of the lines of force intersect the Earth. Others are totally trapped and drift round and round on a shell. In this latter case, one can use the parameters μ and I to see how the particles drift around the Earth and to find their shells. Close in, the shells are symmetrical in terms of longitude. Farther out, the shells may be distorted.

I would like to discuss this distortion. The shells of these trapped particles will be distorted by two different effects related to the solar wind. One effect is due to the distortion of the magnetic field, as seen in Fig. 1. It is well known that the magnetic field is pushed in on the solar side, and I think the field is pulled out on the night side. At any rate, if one computes I for fields that have been pushed in and pulled out, one finds that the shells for particles with a given energy will be closer to the Earth on the night side than on the day side (Ref. 3). This conclusion seems to fit with O'Brien's observations of the boundary of trapping for 40-kev electrons (Ref. 4).

The second effect is due to the electric field; electrons have higher energy on the morning side (positive potential) than on the evening side (negative potential). Thus an electron's trapping shell goes closer to the Earth on the morning side. For protons, the effect is the other way around. You can put these effects into the actual velocity distribution. In the range of L (shell parameter)² between 4 and 8, one expects to find a higher intensity of 40-kev electrons on the morning side than on the evening side. It is in just this range of L that McDiarmid, Burrows, and others have found a maximum of 40-kev electrons at 8 o'clock in the morning (Ref. 6). [However, the observed rate of dumping suggests that the lifetime of the electrons is much less than the time for drift round the Earth (Ref. 7). If so, the important mechanisms cannot conserve the longitudinal invariant.]³

Now what about the particles that are trapped far out on the night side? They drift across the night side but then, according to the conservation of the two adiabatic invariants, there is nowhere that they can be trapped on the day side. Presumably they go in and out of the magnetosphere from the solar wind. The effect of the magnetic-field gradient on those particles with energies of 10 kev or less is to cause the electrons to drift eastward across the night side and thus gain energy from the *DS* field. Similarly, protons drift westward across the night side and also gain energy.

What do we find if we trace back the trajectories of these particles? One possibility is that if the particles have sufficiently low energy, they will lose nearly all their energy and then simply move with the fluid. We say that these particles have come from the solar wind. Suppose, however, we take a particle with somewhat higher energy. This particle doesn't lose all its energy, but it must still cross the boundary surface of the closed lines of force. In this case, we have to give special consideration to what happens at this surface. One thing that happens is that the adiabatic

²For a discussion of the magnetic-shell parameter L, see Ref. 5

³Added in manuscript

theory breaks down. The longitudinal invariant cannot be used, because there probably is no mirror point—unless it is at the Sun. But apart from that, remember that the surfaces are covered by lines of force which come from the neutral point. Since the particles move very much faster along a line of force than they do across the field, one expects that nearly all these particles pass near, if not completely through, the night-side current sheet.

Thus it is necessary to make a special investigation of motion in the current sheet, and here too the adiabatic treatment is completely useless. A student at Penn State, Mr. Speiser, has been studying this problem. It is a nasty, self-consistent-field problem, and we do not have a good model of a current sheet. Speiser's work was started well before we knew about Petschek's model (see Papers 15 and 18), which possibly would help. Speiser has simply taken all the field components to vary linearly with the coordinates, just to make life easier for the computer, and then he has computed the particle trajectories.

Now, we are particularly interested in auroral particles. These particles are able to get into very much stronger fields (0.5 gauss) than the 50- γ fields found far out in the magnetosphere. So the most interesting particles are those that come out of the current sheet with very small pitch angles. Speiser has studied the particles coming out with zero pitch angle and has computed the trajectories back until they get into a region where the adiabatic theory is sound. He has then calculated the energy with which the particles went into the neutral sheet, and has used this energy as a negative measure of the distribution function f. A very low value for this energy suggests a high intensity; so he looked for low input energies. He has found that high intensity in the outgoing particles is restricted to thin fan beams. The overall structure is almost embarrassingly like that of auroral forms (draperies and rayed arcs), but I don't want to get too excited about it. For one thing, the computations are for protons, whereas the aurora is produced by electrons.

Let me now briefly consider what happens to the particles farther out on the exterior lines and on the transition region lines. Do these lines really go out to the Sun or very far away? I am not really very sure. One thing I would like to point out is that the field in the transition region is probably several times stronger (about 20 or 30 γ) than the general interplanetary field (about 5 γ). Consequently, particles will tend to go out into the distant field; they won't mirror back since there is no field strong enough to mirror them back. I imagine that particles in the transition zone go mainly along the lines of force for a long distance. Conversely, a lot of the particles far out on the night side have come down the lines of force from a great distance.

The day-side current sheet will accelerate some particles, and so will

the shock; so energetic particles are produced on the day side, but where do they go? A few of them surely do come down onto the day-side auroral zone, and some onto the polar cap. However, if one traced a typical trajectory back from the polar cap or the day-side auroral zone, I think one would expect it to leave the region of the Earth without going through the shock.

Time-Dependent Effects

I think the key problem in the aurora is associated with the time dependence of the fields that I have been discussing. The *DS* field is generally found as an average. Fairfield of Penn State has studied hourly averages from the IGY data, in which this *DS* pattern nearly always appears. Looking at the magnetograms for the same periods of time, he found that the disturbance appears to consist entirely of bays (Ref. 8). So the *DS* pattern really occurs in a series of pulses.

Akasofu has recently made a very nice study of the aurora during the IGY (Ref. 9). He finds a development cycle (Fig. 2) that I imagine is associated with bays. The cycle starts off in a kind of quiescent state, as shown in Fig. 2a (the day side is toward the top of the figure). When there hasn't been a disturbance for a time, there are arcs between 60 and 70 deg north latitude on the night side. (Incidentally, it looks to me as though the place where the day-side neutral point connects is near the extrapolated point of closure of the arcs, which is considerably higher than Prof. Axford's latitude of intersection). A disturbance begins with a brightening at midnight, and spreads from there on an initial time scale of 5 to 10 min and a subsequent one of 10 min to a half hour. The way in which the disturbance spreads from a highly localized area suggests that it starts from that area rather than coming from the outside. The source of the disturbance is a key question now.

Assuming that this disturbance causes the magnetic bay, one would expect the disturbance to come from the solar wind. I have a slight indication that it does. Fairfield has been correlating bays observed during the *Explorer-12* flight with the behavior of the *Explorer-12* magnetometer. He has only studied one day, which had two bays. It was rather a special day in that the boundary did not show a reversal of the field. About a quarter of an hour before each bay, the field direction at the satellite changed drastically. Although one seems to be able to reach some important conclusions about the general picture in terms of static fields, the observed time dependence must still be accounted for. In this respect, I think that the bay is a key phenomenon. I think that bays have an important effect on the outer belt.

Hess and Nakada (Ref. 10) have been analyzing some of Leo Davis' data on trapped protons (Ref. 11), which brings out this adiabatic effect

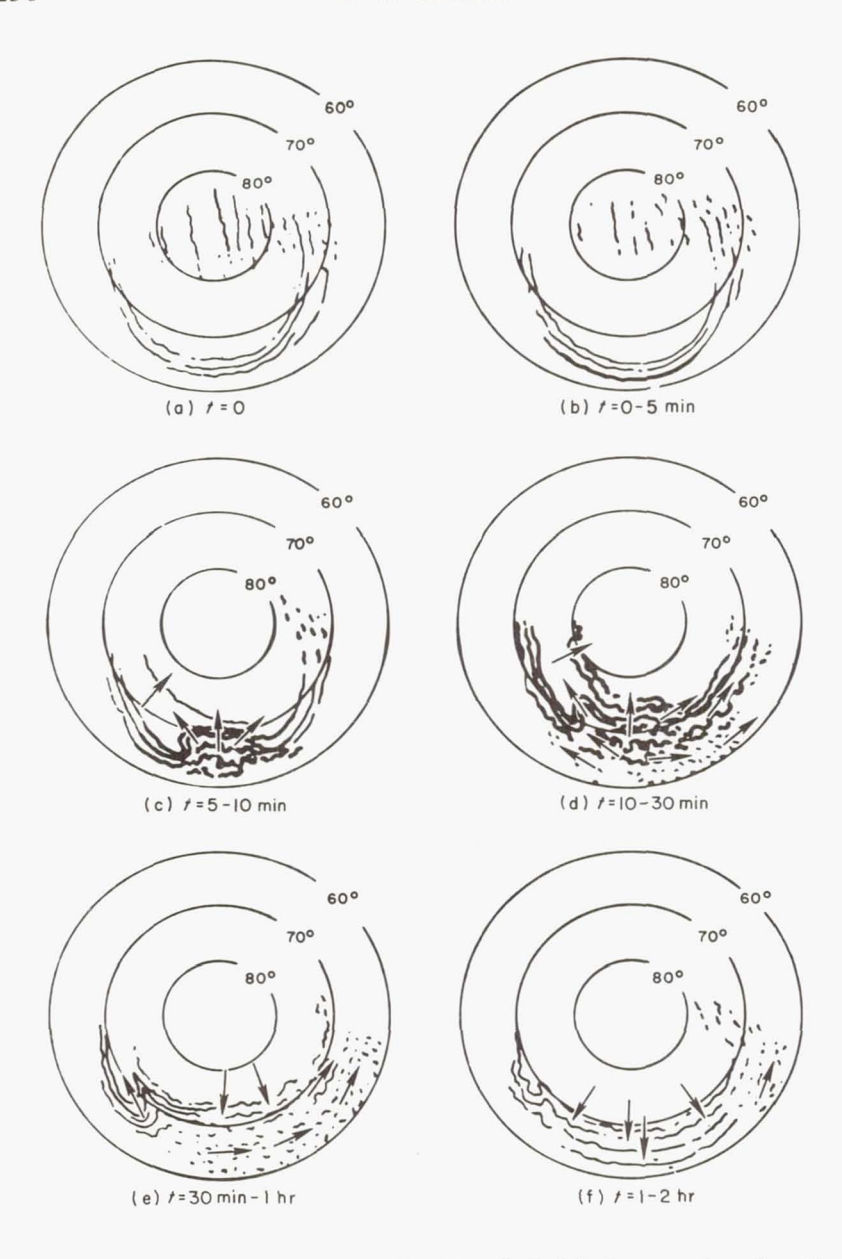


Fig. 2. Development of an aurora (after Akasofu, Ref. 9). Recovery from (f) to (a) requires 2 to 3 hr

that Prof. Axford mentioned. Davis finds an exponential spectrum, for which the parameter E_0 is a measure of the proton energy or temperature. E_0 is plotted against L in Fig. 3 (solid lines, each line representing a certain equatorial pitch angle). E_0 varies rapidly with L; it also varies slightly with

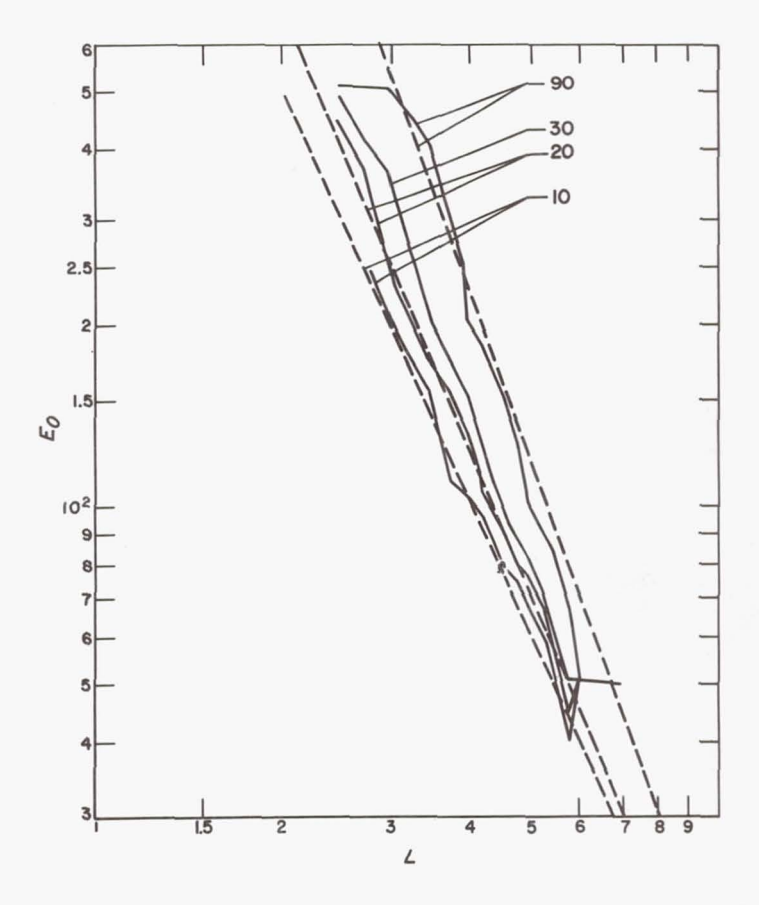


Fig. 3. Plot of the "temperature" E_0 of trapped protons vs. the magnetic shell index L. The solid curves are observations, identified by equatorial pitch angle (Ref. 11); the dashed lines are calculated (Ref. 10)

equatorial pitch angle. You can calculate how E_0 would vary with L (even allowing for the different pitch angle) for particles undergoing adiabatic motions. The dashed lines in the figure represent the calculations of Hess and Nakada. They have gone into this problem a little further. They have taken Davis' data and have calculated the velocity distribution function for fixed values of μ and I. Figure 4 shows one case, and indicates how the

distribution function for fixed μ and I varies with L. It is interesting that the distribution function always decreases inward, suggesting a source at the outside.

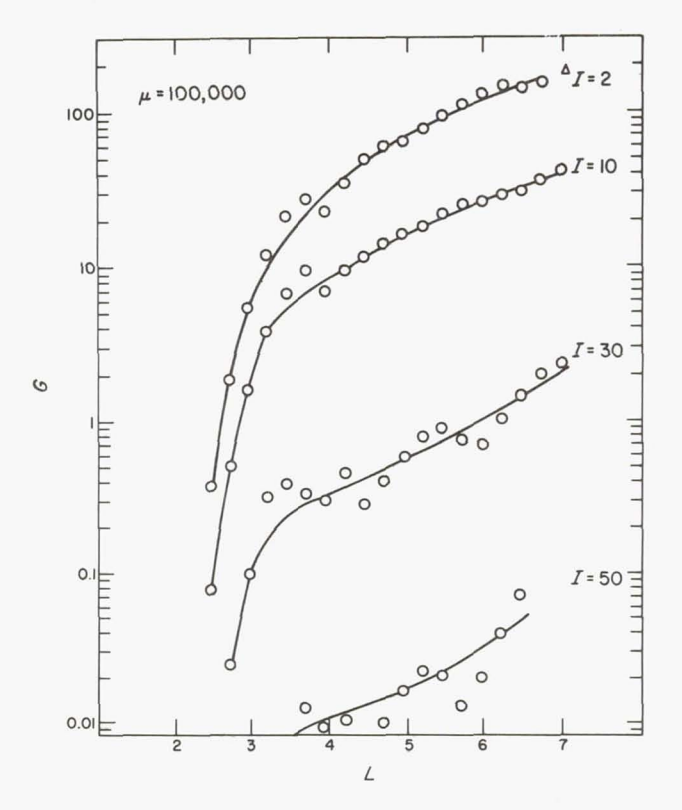


Fig. 4. Variation of the proton distribution function G with the manetic shell index L for $\mu = 10^5$ and various values of I. Data from L. R. Davis

From Fig. 3, I deduce that the source at the outside should have a temperature like 20 kev and that there is some mechanism stirring the particles in. This mechanism must be very effective from large L down to about L=3 or L=4. This inner boundary is just about where Carpenter finds a sudden drop of electron density with increasing L (Ref. 12). His findings fit my model if the DS flow takes thermal ions outward across the magnetopause faster than they can diffuse up from the upper ionosphere.

I think this diffusion process is due to bays, because bays have a time scale of something less than 1 hr, and the time it takes for these particles to drift around the Earth is several hours. If a bay occurs as a particle is

drifting around the night side, the particle will gain some energy. If the particle came around the day side while the bay was still occurring, it would lose this energy again. But since the bay is over before a particle can get from the night side to the day side, the energy is not lost. Other particles are going around the day side when the bay occurs, and they lose energy. The result is diffusion. The diffusion coefficient will be a strong function of L, diffusion being much more effective for large values of L. This model gives some idea of why Hess and Nakada's curves are similar to the experimental curves and suggests another probable effect of the solar wind on trapped particles. [Nakada and Mead have found that sudden impulses also give diffusion times of the right order and L-dependence, so there are currently two satisfactory sources for the diffusion process.]⁴

Finally, one should consider disturbances with much higher frequencies. We have considered periods of a half-hour or so, but it may well be that disturbances with periods of seconds have important effects on the trapped particles.

One important observation is by O'Brien (Ref. 13); when he saw very high intensities of particles at high latitudes, the loss cone had disappeared. This, he says, means there are fresh particles, since if the particles had been bouncing to and fro with low mirror heights, they would have shown a loss cone.

Chamberlain has recently described an interesting mechanism for producing auroras, which is rather instructive (Ref. 14). He has taken an instability studied by Krall and Rosenbluth (Ref. 15) The cause of this instability is a pressure gradient across the magnetic field. Of course, the theory of the instability assumes a uniform field. In fact, the criticisms of this theory depend on the application of the uniform field model to the dipole-field case.

In his theory, Chamberlain defines a coordinate system in which the undisturbed field $\bf B$ is in the Z direction, and the pressure gradient is in the X direction. He then considers waves that travel in the -Y (westward) direction. The waves are characterized by a magnetic disturbance $\Delta \bf B$ in the X direction, parallel to the pressure gradient. The theory does everything very correctly. But when you look at the magnetograms and make some approximations from the sizes of gyro radii, you find that the phase velocity of the wave is pretty close to the "bulk drift" of the electrons.

One gets confused by two different meanings of the word "drift." There are drifts of individual particles in the magnetosphere: electrons drift eastward and protons drift westward. What we are talking about here, however, is a pressure gradient which implies a *bulk* drift not tied to that

⁴Added in manuscript

of an individual particle. Take a small element of space, count all the particles in that space at a particular instant of time, and take their mean velocity: the result is a bulk drift. Chamberlain's pressure gradient requires a westward bulk drift of the electrons and an eastward bulk drift of the protons.

The instability grows, because those protons resonate whose individual drift happens to coincide with the wave velocity; and for some velocity distributions the wave gains energy. Individual electrons drift eastward, so that they cannot resonate in this way. But in applying this mechanism to the magnetosphere, Chamberlain says that if the actual wave frequency is very low, and if some electrons can drift eastward sufficiently fast, then the apparent frequency is equal to their bounce frequency, and another kind of resonance will result. Chamberlain suggests that the electrons gain energy as a result of this resonance.

I haven't said anything about the electric field in this wave. One has to be very careful with electric fields, because they depend on the frame of reference. If you go into the frame of the wave, which is also the frame of the bulk drift of the electrons, the wave has no electric fields at all. But in the frame of the Earth, or of electrons drifting eastward, there is an electric field in the Z direction, and the bouncing electrons which resonate with it can gain energy.

I have some reservations about Chamberlain's mechanism, however, because it is always rather surprising in a plasma to get an electric field parallel to a magnetic field. I have a feeling that there may be some disturbance he has missed. Because one has a pressure gradient to start with, the wave produces a disturbance pressure gradient in the Z direction. This, then, puts in some more electric field, and I think you can possibly reduce Chamberlain's electric field by a considerable factor. This kind of disturbance certainly needs further consideration.

I didn't say that the wave number has to be large, but short wavelengths may be important to the aurora. For short wavelengths, the current density for a given ΔB and the electric field both increase, leading to more readily observable effects.

The obvious conclusion from Chamberlain's mechanism is that one will get a rayed arc, because dumping will occur when the electric field is in a certain direction. The separation of the rays will be given by the wavelength. Also, because the wave is moving westward, the rays in the arc should be moving westward at the appropriate speed, though, of course, if the plasma as a whole is moving from *DS* motion, one has to superimpose the two motions. Perhaps this theory explains rayed arcs.

REFERENCES

- 1. DUNGEY, J. W., Geophysics, The Earth's Environment, ed. by C. DEWITT, J. HIEBLOT, and A. LEBEAU, Gordon and Breach, New York (1963) pp. 526-537.
- CAHILL, L. J. and P. G. AMAZEEN, Journal of Geophysical Research 68, 1835 (1963).
 CAHILL, L. J., Space Research III, ed. by W. PRIESTER, Interscience Publishers, a division of John Wiley and Sons, Inc., New York (1963) p. 324.
- 3. MALVILLE, J. M., Journal of Geophysical Research 65, 3008 (1960).
- 4. O'Brien, B. J., Journal of Geophysical Research (8, 989 (1963).
- 5. McIlwain, C. E., Journal of Geophysical Research 66, 3681 (1961).
- McDiarmid, I. B., J. R. Burrows, E. E. Budzinski, and Margaret D. Wilson, Canadian Journal of Physics 41, 2064 (1963).
- 7. McDiarmid, I. B. (private communication).
- 8. FAIRFIELD, D. H., Journal of Geophysical Research 68, 3589 (1963).
- 9. AKASOFU, S.-I., Planetary and Space Science 12, 273 (1964).
- 10. HESS, W. N. and M. P. NAKADA (unpublished).
- DAVIS, L. R. and J. M. WILLIAMSON, Space Research 111, ed. by W. PRIESTER, Interscience Publishers, a division of John Wiley and Sons, Inc., New York (1963) p. 365.
- 12. Carpenter, D. L., Journal of Geophysical Research 68, 1675 (1963).
- 13. O'BRIEN, B. J., Journal of Geophysical Research 69, 13 (1964).
- 14. CHAMBERLAIN, J. W., Journal of Geophysical Research 68, 5667 (1963).
- 15. KRALL, N. A. and M. N. ROSENBLUTH, The Physics of Fluids 6, 254 (1963).

Page intentionally left blank

CHAPTER XVIII

THE MECHANISM FOR RECONNECTION OF GEOMAGNETIC AND INTERPLANETARY FIELD LINES

H. E. Petschek1

Avco-Everett Research Laboratory, Everett, Massachusetts

THE question of reconnection of field lines between the Earth's dipole field and the interplanetary field was emphasized by both Dr. Axford and Dr. Dungey (Papers 16 and 17). I think this subject was initially introduced by Dr. Dungey some time ago. As far as I know, the processes that occur at the neutral point have never been examined for the purpose of arriving at a quantitative estimate of field-cutting efficiency at the magnetopause. However, the theory that I discussed yesterday (Paper 15), when applied to the magnetopause, does give a rate of field reconnection that fits the magnetosphere convection pattern.

At the end of his talk, Dr. Axford gave two criteria for producing the internal convection and the DS current system. One was that the potential difference across the polar region must be of the order of $20 \,\mathrm{kv}$; the other was that the energy input must be of the order of $10^{19} \,\mathrm{ergs/sec}$. I had been prepared to defend the former figure; I hadn't considered the latter. I did make some calculations of energy input while Dr. Dungey was talking, however, and they seem to agree with Dr. Axford's figures, so I will mention them also.

Figure 1 shows the magnetosphere boundary with the shock wave in front of it. As I mentioned yesterday, there are three types of waves in magnetohydrodynamics. The fast wave, or rather its nonlinear extension, is the shock wave in front of the magnetosphere. The boundary is then resolved into the two other waves. These are illustrated here for the case of finite density in the region between the shock and the boundary, and zero density inside the magnetosphere. The details of the waves would change somewhat if there were a finite density inside the magnetosphere, but the boundary would still resolve into the two wave modes shown.

¹Much of this work was done in collaboration with George Siscoe and Richard Levy

Although the figure shows the interplanetary field as perpendicular to the ecliptic, the conclusions will not be altered significantly for other orientations. In this particular case, there is a neutral point in the immediate subsolar region; in fact, there is actually a neutral line going all around the

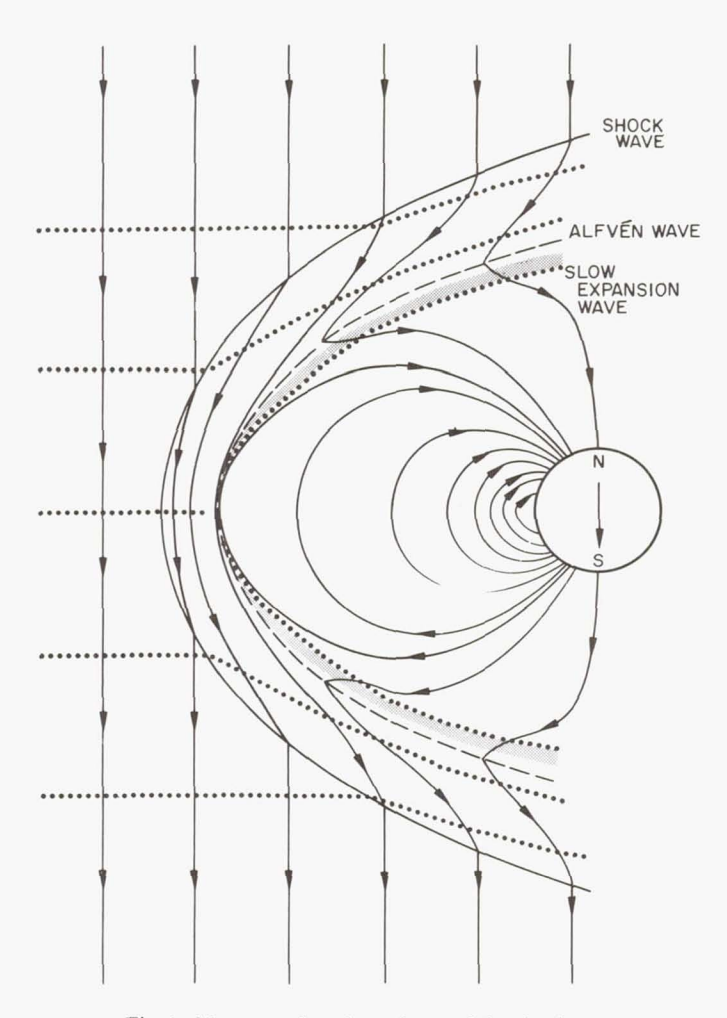


Fig. 1. Magnetosphere boundary and the shock wave

equator of the magnetosphere boundary. If the field outside the magnetosphere were tilted somewhat, you would not have a precise neutral line. There would still be a line of symmetry, but it would run across the magnetopause at some angle to the ecliptic.

Figure 2 emphasizes the region around the neutral point. Between the two fields, an Alfvén (intermediate) wave and a slow wave come together at a finite angle. This wave pattern is slightly different from the one I discussed yesterday, in which there was one wave propagating in each direction from the boundary (see Fig. 3, Paper 15). The analysis is essentially the same, however, and since these waves still propagate at a

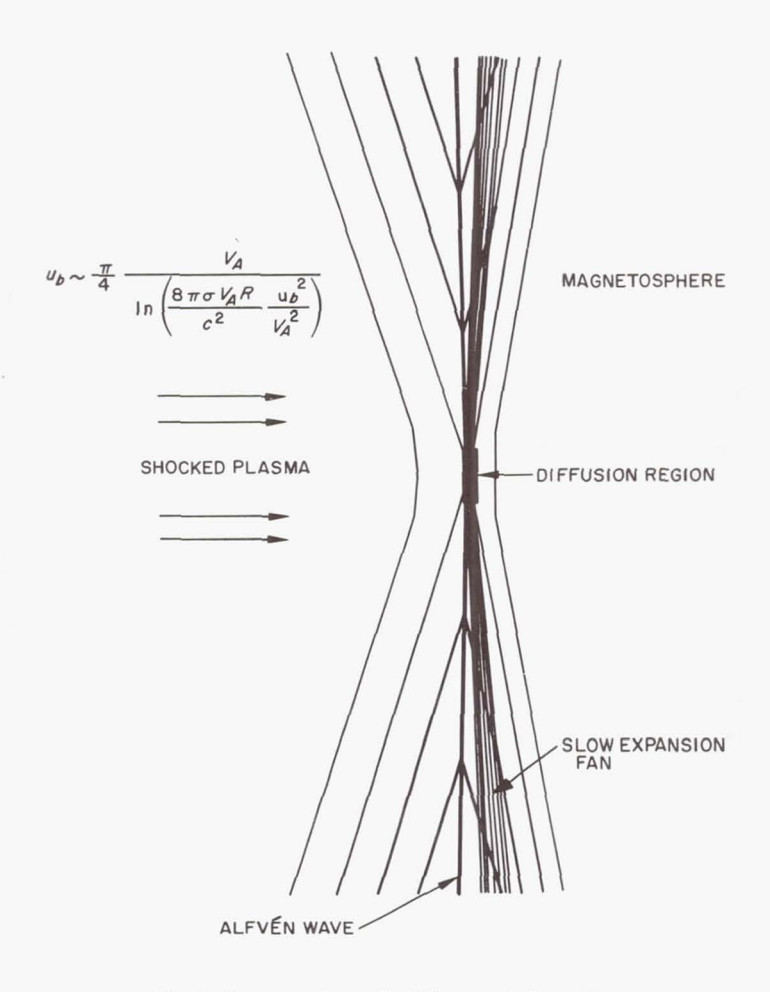


Fig. 2. Reconnection of field lines at the boundary

speed proportional to the normal component of the magnetic field, the rate at which field lines approach the boundary and reconnect is also essentially the same. The equation defining the field-line velocity, u_b , in

terms of the Alfvén speed V_A (which is based on the magnitude of the magnetic field and the density just outside the boundary), the conductivity σ , and the magnetosphere radius R, is also shown in Fig. 2.

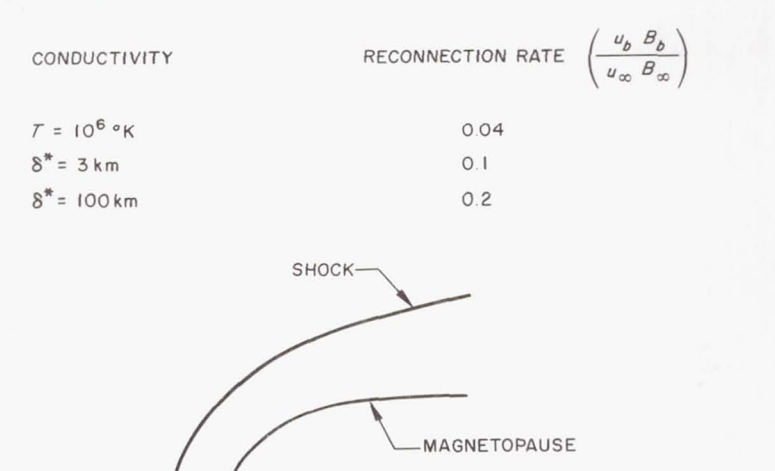
I would also like to mention some things that may be observable by instruments passing through the magnetopause. On the basis of this picture, the Alfvén wave changes the direction of the magnetic field; in this case, the component in the plane of the wave changes by 180 deg. An interplanetary magnetic field that was not perpendicular to the ecliptic would rotate through a smaller angle. Across the Alfvén wave there should be no change in field magnitude, particle pressure, or particle density. Across the slow wave, the field intensity should increase to balance the decreasing gas pressure as the density decreases. Thus the change in magnetic-field direction should occur slightly farther out than the place where magnitude changes. The angle between the Alfvén wave and the slow-wave center lines should be of the order of 0.1 rad; which means that at about $10~R_{\rm E}$ from the neutral line, there should be a separation of about $1~R_{\rm E}$ between the two waves.

Let us now return to the overall pattern and estimate the expected magnitude of the internal convection pattern. Assuming that the flow conditions in the interplanetary plasma are known, we can find the magnetic field strength, B_b , and the density immediately behind the shock wave (see Fig. 3). Using the formula in Fig. 2, we can calculate the rate $u_b B_b$ at which field lines become reconnected per unit length along the neutral line. The ratio of this reconnection rate to the rate at which field lines cross the shock wave, $u_\infty B_\infty$, determines what fraction of the field lines incident on the shock wave become reconnected to the dipole field. The remaining field lines must go around the magnetosphere in the layer between the shock and the magnetopause, as do all of the field lines in models that neglect reconnection.

This ratio is given at the top of Fig. 3 for three different values of conductivity, since the conductivity of the medium is really unknown. The first is an extreme case, which I include only to illustrate that the reconnection rate isn't very sensitive to the value of conductivity. In this case, the conductivity is the one associated with binary collisions and corresponds to a temperature of 10⁶ °K. Since the mean free path is larger than an astronomical unit, such a conductivity isn't very reason able—yet even on the basis of this value, 4% of the field lines are reconnected.

An estimate of the maximum value of the conductivity can be obtained by saying that the thickness of the diffusion region cannot be less than the electron gyro radius if the region is to carry the required current. Even if the thermal velocity of all the electrons is entirely in one direction, the magnetic-field direction can't change in less than that distance, which is about 3 km. For a diffusion region of this thickness, 10% of the field lines are reconnected.

I personally favor an estimate of about 100 km (the ion gyro radius) as the thickness of the diffusion region. This thickness gives a reconnection rate of 20%. Thus I think that at least 10%, and probably about 20%, of the field lines incident on the magnetosphere become connected to the dipole region.



Bb

Ub

U = 8 VA 00

 B_{∞}

Fig. 3. Parameters describing the connection of the dipole field to the interplanetary field

Figure 4 shows a cross-section of the magnetosphere perpendicular to the Earth-Sun line and intersecting the Earth. (The field lines do not necessarily lie entirely in this plane.) In this projection the shock wave and magnetopause are shown schematically as concentric circles. Some of the field lines (about 20%, we said) are connected and go through the boundary, while the others slide by in the intermediate region.

In order to obtain the first of Axford's numbers – namely, the potential difference across the polar region – we notice that the field strength

outside the shock boundary is about 5γ . The diameter of the magneto-pause is about 10^5 km. Since 20% of the field lines become connected, the projection of the connected region outside corresponds to a length of 2×10^4 km. We also know that the wind velocity is about 500 km/sec. Then the product of velocity, field strength, and length gives a potential difference of 50 kv. This potential difference must be the same as the one that was obtained at the polar ionosphere and that Axford estimated to be 20 kv. A slightly different estimate of the polar potential is also shown in Fig. 4. The field strength at the poles is, of course, known. The size of the region in which the field lines move in an antisolar direction

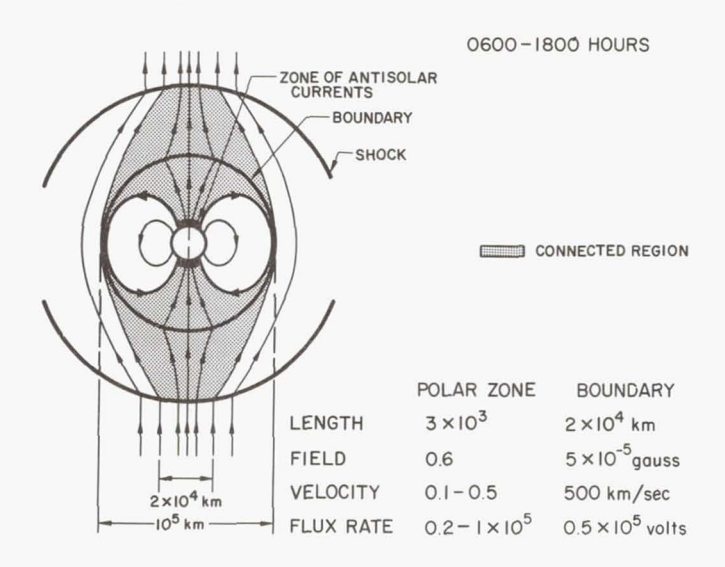


Fig. 4. Cross-section of the magnetosphere perpendicular to the Earth–Sun line, and parameters involved in estimating the *DS*-current driving potential

corresponds to the region in which the *DS* current system shows currents directed toward the Sun. The velocity used in the polar region corresponds to the observed range of visual auroral velocities. The product of these numbers gives a potential difference ranging from 20 to 100 kv. Thus the polar potential as determined by the rate of field cutting agrees substantially with both of the estimates based on polar observations.

Concerning Axford's value for the required energy input into the magnetosphere, I have just made the following estimate: ϕ , the stress on the magnetosphere boundary, is given by:

$$\phi = \frac{B_n \delta B_t}{4\pi} \tag{1}$$

where B_n is the normal component of the magnetic field, and δB_t is the change in tangential component of the magnetic field. Multiplying Eq. 1 by the surface area of the magnetosphere $(2\pi RL)$, where L is the length), and the velocity of the solar wind, we obtain for the power input

$$P = 2\pi R L v \phi \tag{2}$$

Using $B_n=1~\gamma$, which corresponds to 20% of the 5- γ interplanetary field; $B_t=10~\gamma$, which agrees more or less with the *Explorer-10* results some distance behind the Earth; $R=10^5~{\rm km}$; $L=10^6~{\rm km}$; and $v=400~{\rm km/sec}$, one obtains $P=2\times10^{19}~{\rm ergs/sec}$. This is obviously closer to the required value of 10^{19} than is justified by the nature of the calculation.

DISCUSSION OF PAPERS BY AXFORD, DUNGEY, AND PETSCHEK

The Acceleration of Trapped Particles by Violation of the Third Invariant

PARKER: I have a rather general comment on most of the ideas expressed this morning concerning the acceleration of particles by combinations of electric and gradient drifts. It strikes me that these ideas were proposed quite some time ago by Paul Kellogg¹ and have probably been forgotten.

Kellogg made the point that one can violate the third invariant of the trappedparticle motion if one has a time-dependent geomagnetic field, and that one can accelerate particles in this way because the first invariant is not violated. At the time, there was considerable interest in the mechanism. I made some calculations and convinced myself that the mechanism was legitimate and effective; and Prof. Davis, I know, has also made some calculations.

BLOCK: I am not familiar with Kellogg's work, but it seems to me that particle acceleration caused by gradient drifts along an electric field was proposed first by Alfvén in 1939, when he originally proposed his auroral theory.²

PARKER: Unfortunately, the idea was in a context that one can no longer believe. **BLOCK:** I am not going to argue about that now; I am just saying that this mechanism was inherent in his theory.

AXFORD: The diffusion of particles into the magnetosphere due to a breakdown of the third invariant appears to be a likely explanation for much of the trapped radiation. I would like to point out that the third invariant can be broken as a result of fluctuating electric fields corresponding to interchange motions in the magnetosphere, as proposed some years ago by Gold.³ This mechanism, which can be expected to be operating all the time, differs from the one discussed by Kellogg and Parker in that the magnetic field remains undistorted and the electric fields are curl-free to a first approximation.

¹Kellogg, P. J., Nature 183, 1295 (1959)

²Alfvén, H., Kungliga Svenska Vetenskapsakademiens Handlinger, Series 3, (1939)

³Gold, T., Journal of Geophysical Research **64**, 1219 (1959), Astrophysical Journal Suppl. **4**, 406 (1960)

^{.....,} Journal of the Physical Society of Japan 17, Suppl. A-1, 187 (1962)

The Direction of the Interplanetary Field and its Role in Magnetic Storms

BLOCK: I would like to make some comments on Dungey's mechanism. It seems to me that it is very similar to Alfvén's theory, with two important exceptions, namely: you have reversed the magnetic field outside the magnetosphere, and you don't allow any electric fields along the field lines. Is that correct?

DUNGEY: Yes. I should comment on this southward tendency of the interplanetary field. I don't want to claim that I predicted that the field would point to the south. We can't really have a southward component all the time. I think we have to sort out the different kinds of phenomena—such as bays—and determine what interplanetary conditions correspond to what things we see on the Earth.

The model I discussed in my paper, by the way, was first proposed to me as a

Ph.D. problem by Fred Hoyle a very long time ago.

BLOCK: I think you have the same opinion that Alfvén does, that the lower boundary of the auroral zone, toward the lower latitudes, is determined by the diamagnetic repulsion of the plasma that is moving into the magnetosphere. Is that right?

DUNGEY: Well, the diamagnetic repulsion is a way of talking about pressure,

isn't it? But this comes back to the fluid side of the picture.

BLOCK: If you consider individual particles, then the μ of the particles causes a diamagnetic repulsion which counteracts the electric-field drift.

AXFORD: Perhaps a simpler way of saying that is: we have only about 20 kv of electric potential available, which effectively limits the attainable particle energies regardless of the configuration of the electric field.

BLOCK: That amounts to exactly the same thing.

AXFORD: Alfvén's picture is included in all other theories that involve electric fields, with the modification that the sign of the field is reversed so that we get the *DS* current system in the right direction. Thus in the interior of the magnetosphere the plasma flows toward the Sun instead of away from the Sun.

BLOCK: In Stockholm we have performed some recent experiments in which the electric field across a model magnetosphere was measured when plasma was projected toward the field. The projected magnetized plasma in some cases had Alfvén's field direction and in other cases had Dungey's field direction. The experiments showed that the electric field was short-circuited with Alfvén's field direction, whereas it was measurable with Dungey's field direction. So the experiment provided strong support for Dungey's geometry. His magnetic-field geometry is probably more efficient for injection of particles into the magnetosphere. **GOLD:** I had a reason for saying, a year and a half ago, that the field in space has to have a preferred direction in which the component normal to the ecliptic is more often antiparallel than parallel to the external part of the Earth's magnetic field. Such a field direction is necessary to account for the fast particles detected from east- and west-limb flares. I concluded that, over the period during which the statistics were accumulated - essentially two years - there seemed to be a general tendency for the fields in space to have this direction more often than the other. Mariner seems to have substantiated this conclusion for the period just following the one I considered. So it may be true that the field has this configuration a large part of the time, perhaps changing with the 23-year solar cycle.

⁴Alfvén, H. and C.-G. Fälthammer, Cosmical Electro-dynamics, 2nd ed., Oxford University Press, London (1963) p. 540

⁵Gold, T., Proceedings of the Study Week on the Problem of Cosmic Rays in Interplanetary Space, Pontifical Academy of Science, Vatican City, (1963) p. 431

BLOCK: There is an additional reason to assume that the interplanetary field has this southward direction. If you place a magnet in a magnetic field, there will be a torque on the magnet that will rotate it so as to establish the configuration with the lowest magnetic energy. In this case, the Earth can't flip over. But if the solar wind contains a sort of disordered field, pointing sometimes in one direction and sometimes in the other direction, then the southward direction would most easily allow the field to hang onto the Earth's field. The other direction would more easily allow the field to slip past the Earth's field.

GOLD: But this effect has nothing to do with the predominant direction of the

interplanetary field.

DAVIS: I think that this matter of the opposite polarity between the interplanetary field and the Earth's field is very significant. I think there are two possible explanations for this configuration. (1) The interplanetary field points sometimes one way and sometimes another. However, the plasma mechanisms at work near the magnetopause (inside the shock) preferentially hold the field when it is in the direction opposite to the Earth's field. Thus, near the Earth we see this configuration more of the time. (2) The *Mariner* data indicate a tendency for the interplanetary field to be directed in the southward direction, although the major component is in the ecliptic. I think the same thing was suggested by the *IMP* data. I think neither the *Mariner* people nor probably the *IMP* people would like to make much of a point of this indication. It would be surprising if such a tendency were not connected with the general solar cycle. The direction would then presumably reverse every 11 years, and should have reversed sometime around 1960, although I forget the exact date.

Therefore, the time at which Prof. Gold obtained his statistics becomes very critical. Furthermore, if the polarity is important for the aurora, we must ask whether there is a 23-year cycle in auroral properties. If not, we had better forget the whole business.

CHAPMAN: Do I understand that the supply of auroral energy depends upon

the interplanetary field having a southward direction?

PETSCHEK: If the geomagnetic and interplanetary fields are at an angle θ to each other, then the reconnection rate should be proportional to $\sin (\theta/2)$. You can resolve the fields into two components; one in which the fields are parallel on both sides of the neutral point, and one in which the fields are antiparallel and annihilate each other. The important component is the one for which the fields are antiparallel. If the interplanetary field were in the ecliptic, the reconnection rate would be reduced by a factor of $1/\sqrt{2}$. Thus, you would expect to see some effects from the 23-year solar cycle, but they may not be very pronounced. **AXFORD**: I don't see that the direction of the interplanetary field can be very important. If the interplanetary-field lines merge onto the geomagnetic-field lines in the manner described by Dungey, Petschek, and others, the merging would seemingly have to occur in a patchy fashion all over the surface of the magnetosphere, wherever the internal and external field lines are suitably aligned. Even if the interplanetary-field component normal to the ecliptic had a tendency to be antiparallel to the geomagnetic field, it is unlikely that this antiparallelism would survive when the solar wind passes through the shock wave standing beyond the magnetosphere. The field just beyond the magnetopause is likely to be very messy, irrespective of the condition of the field outside the shock wave, and the merging mechanism should therefore be able to cope with randomly-oriented external field lines.

COLEMAN: I would like to make a comment concerning the interplanetary-field

directions. The distribution of the orientation, as observed by *Mariner*, is peaked almost in the ecliptic, generally pointing away from the Sun but with a small component, normal to the ecliptic, pointing southward. Nevertheless, for something like 40% of the time this small normal component points northward. This distribution is typical of the time (about a week) during which the spacecraft was rolling and during which we knew the spacecraft magnetic field quite accurately.

NESS: In the theoretical problems presented this morning, the interplanetary field was always taken to be normal to the ecliptic—either parallel or antiparallel to the Earth's dipole axis. I would like to know how one incorporates into this picture the interplanetary data, which indicate that the interplanetary field has a very strong tendency to be close to the ecliptic.

PETSCHEK: I commented before that the reconnection rate depends on $\sin (\theta/2)$. You are saying that θ should be 90 rather than 180 deg, which changes things by a factor of $1/\sqrt{2}$. A field in the ecliptic will also distort the picture of the field lines in Fig. 4, Paper 18.

GOLD: In the first place, even if the magnetic field has a very substantial component in the direction of flow, which it evidently has a large part of the time, the discussion is not changed very much, because the orientation gets fouled up in the vicinity of the Earth as the lines of force get tipped over. It is the small component in the nonradial directions that you are concerned with, because this small component is the one that determines how the field lines are going to be packed when they are pressed against the Earth's magnetosphere.

I wish to make another point concerning the direction of the interplanetary field. It is still not experimentally established whether the seasonal variation in the average frequency and intensity of magnetic storms is related to the periods of equinoxes, or whether it is related to the periods of maximum solar latitude of the Earth. Unfortunately, it is accidental that, at the present time in the 26,000-year period of precession, these two effects have almost the same phase. If we on the Earth had seen the effect at another time, we would not be bothered in this way.

If it were the equinox effect that enhanced the magnetic storms, then the position of the Earth's dipole—which, of course, is wobbling by 11 degrees each day but which is also inclined by 23.5 degrees—would be critical. Magnetic storms would have their greatest intensity when the Earth's dipole was most nearly perpendicular to the flow.

BRANDT: There is a very short and not well known paper in which Prof. Öpik⁶ discusses the number of flares occurring in both the northern and southern solar hemispheres. The basic information was taken from a paper by Bell,⁷ and the analysis was applied to a 23-year period. I specifically checked this time span, hoping that we wouldn't get into any solar-cycle arguments. Of these flares, 56 percent occurred in the northern hemisphere—a result which is not statistically different from 50 percent. There were terrestrial effects following 74 of the flares observed during this time; of these flares, 86.5 percent occurred in the northern hemisphere. Öpik has computed that the probability of this happening in a random sequence is 2×10^{-10} .

In other words, it is very unlikely that this lack of symmetry is an accident. There must be some physical reason that flares in the northern hemisphere pro-

⁶Öpik, E. J., Irish Astronomical Journal 6, 29 (1963)

⁷Bell, B., Smithsonian Contributions to Astrophysics 5, No. 7, 69 (1961)

duce particles that impact the Earth, whereas flares in the southern hemisphere do not. I think an explanation suggested by Prof. Öpik merits attention, although it is not really theoretically defensible. His theory is based on the fact that the Sun's velocity, with respect to the galaxy, is 20 km/sec northward. Hence, there is a local interstellar wind which pushes preferentially on one side of the solar-wind region and bends the lines of force downward. The interstellar wind doesn't have to bend the field lines very much to cause the observed asymmetry. It seems to me that this theory predicts a consistently southward magnetic field near the ecliptic, independent of the phase of the solar cycle. The problem with this theory is that it is a little hard to imagine how the interstellar gas can make itself felt this close to the Sun; but I don't think we understand this effect well enough to rule it out.

WILCOX: Although the northern solar hemisphere contributed over 50 percent of the great-storm sources in the last five solar cycles, Bell has shown that in cycles 10 through 14 (1856 to 1901), the southern solar hemisphere was predominant in this respect. In cycle 13, the southern solar hemisphere contributed 80 percent of the great-storm sources. Thus the northward motion of the solar system toward its apex in Hercules would seem to be excluded as an explanation

for the north-south asymmetry of great-storm sources.

An alternative explanation is possible. In a 23-year period (1937–1959) studied by Bell, 62 percent of the major flares occurred in the north.8 Northern spot groups, however, produced 86 percent of the major flares that were followed by a great storm. Thus, although there were a larger number of flares in the northern solar hemisphere, this fact alone is not sufficient to explain the asymmetry. The fundamental cause may be related to an asymmetry in the solar magnetic field which could result in asymmetric coronal heating and an asymmetric flux of solar-wind plasma and magnetic field. An asymmetry in the solar wind could explain why activity in the northern solar hemisphere has a greater geomagnetic effect.

A north-south asymmetry in the solar magnetic field would seem to be allowed by H. W. Babcock's theory,9 in which the magnetic flux in each hemisphere is independently amplified by the differential solar rotation. If one hemisphere had more magnetic energy, the effect might well persist for several solar cycles. The possibility that the two solar hemispheres have different magnetic conditions is observed by H. D. Babcock. 10 In 1957 the main magnetic field of the southern polar cap reversed its polarity, and after a delay of about 18 months a similar reversal occurred in the north. A more quantitative comparison of the magnetic conditions in the two solar hemispheres may become available when the solar magnetograph is used with the addition of advanced data handling techniques. 11 KERN: I have a question with regard to Dr. Petschek's calculations of the reconnection rate. For the direction of the interplanetary field parallel to the solar wind or normal to the dipole axis, there are, in principle, two places at which neutral points could develop; one behind the Earth and one in front of the Earth. If there are really only two points, very small areas are involved. Is the reconnection rate at all sensitive to the size of the region in which reconnection is possible?

⁷Bell, B., Smithsonian Contributions to Astrophysics 5, No. 7, 69 (1961)

⁸Bell, B., Smithsonian Contributions to Astrophysics 5, No. 12, 187 (1962)

Babcock, H. W., Astrophysical Journal 133, 572 (1961)

¹⁰Babcock, H. D., Astrophysical Journal 130, 364 (1959)

¹¹ Howard, R. (Private Communication)

PETSCHEK: Strictly speaking there are only two neutral points. However, the calculated reconnection rate is insensitive to the angle through which the field rotates across the boundary. Thus it occurs even when there is not a precise neutral point, that is when the angle is not 180 degrees. As a result, one would expect reconnection to occur along a line on the magnetosphere surface. For the special case of an interplanetary field directed antiparallel to the dipole field, this line is clearly defined as the equator of the boundary, since this is one case in which a neutral line exists. For a more general field orientation, one would expect the reconnection to occur along a somewhat skewed line on the surface.

KERN: I was interested in whether or not the flux calculations were based on three-dimensional models.

PETSCHEK: The flow analysis which determined the rate at which field lines approach one another was two-dimensional. However, it was applied to a three-dimensional magnetosphere by assuming that the length of the line along which reconnection occurs was equal to the magnetosphere diameter.

Instability, Development of Magnetic Storms, and the Energy Supply

KENNEL: I wish to comment about Prof. Dungey's remarks on the universal or drift-wave instability and about Chamberlain's application of the theory to auroras. First of all, the universal instability has been observed in a laboratory Q-machine¹²—a long cylindrical tube with a length of many ion Larmor radii, a radius of only a few ion Larmor radii, and a uniform magnetic field parallel to the axis. The wave stood along the axis of the cylinder. The wavelength was twice the machine length, and the wave propagated azimuthally at the velocity of the pressure drift of the electrons as predicted. The "azimuthal wavelength" was a few ion Larmor radii—indicating that the mode was localized and non-hydromagnetic.

In his discussion of the auroral universal instability, Chamberlain considered calculations for which the wave had no propagation parallel to the magnetic field. It turns out that this assumption is a poor one for waves whose propagation vector has any component at all parallel to the magnetic field. For low- β plasmas, there is an incredibly small cone of angles around the perpendicular for which the perpendicular assumption is realistic. Outside this cone, the calculations of Rudakov and Sagdeev¹⁴ are applicable. The universal instability is just the ion acoustic mode modified by spatial gradients. The wave propagates parallel to the magnetic field with a velocity a few times greater than the ion thermal velocity. This is the resonant velocity for the electrons that drive the instability, and it appears to be too low to be that of auroral electrons interacting resonantly with the waves. I do

¹²Lashinsky, H., Physical Review Letters, 12, 121 (1964)

¹³The pressure-drift velocity of the electrons is expressed as

$$\left(\frac{1}{\Omega} \frac{kT_e}{m_e} \frac{1}{p} \frac{\partial p}{\partial x}\right)$$

where

$$\Omega = \frac{e|B|}{m_e c}$$

$$p = n_e k T_e$$

¹⁴Rudakov, L. I. and R. Z. Sagdeev, Nuclear Fusion Suppl. Pt. 2, 481 (1962)

not know what would happen if mirroring particles of high energy came back in phase with the ion wave, as Chamberlain suggests; but the finite extent of laboratory machines and of the magnetosphere requires you to consider waves that are not precisely perpendicular to **B** (with the above consequences) and makes such a mirror resonance harder to visualize.

The mode has frequencies well below the ion-cyclotron frequency. At $10~R_{\rm E}$, the equatorial ion-cyclotron period is 1 second. Any universal instability phenomenon must be slower than this, and it seems impossible to account by this means for such things as the 0.1-second fluctuations in electron precipitation observed by balloons.

I wish also to remark upon the interchange mode, which is Axford's interest. A few years ago, it was discovered that for some plasmas the interchange mode was more stable than theoretically predicted, and for the magnetosphere the interchange mode is the convection mode. Subsequent calculations¹⁵ indicate that in linear theory, the interchange is stabilized by energetic ions with Larmor radii comparable to convecting tube diameters. If there is any relation at all between linear calculations and nonlinear convection, one can ask whether the convection is sensitive to and could be slowed by energetic ions.

AXFORD: I think your discussion of the stability resulting from finite-Larmorradius effects could be applicable to the inner regions of the magnetosphere and possibly to the trapped-radiation zones. Near 4 $R_{\rm E}$ it seems to be very difficult to make the interchanges occur.

BRATENAHL: I want to ask about the possible stabilization of the interchange processes by the ordinary viscosity of the insulating layer, because the atmosphere is really kind of sticky. This is something Hines, I guess, was considering. What has happened to that theory?

AXFORD: The effect of the ionosphere is similar to the immobilization of plasma by a conducting end wall that intersects the field lines. Apart from the finite-Larmor-radius effect, interchange motions are impeded by the currents flowing in such a resistive wall; as the conductivity of the wall increases, the interchange processes become more and more difficult, because the electric field involved in the interchange process tends to be short-circuited by the walls. For a given speed of interchange motion, there is a given electric field and therefore a given current in the wall. This current represents dissipation, and therefore stickiness. However, the electric field (and hence the current) is proportional to the velocity, so that the interchange motions cannot be completely suppressed—they can only be slowed down.

On the other hand, unless there is in the magnetosphere a dynamo of some sort that maintains the electric field, the conductivity of the ionosphere will discharge the field within a few seconds. The dynamo must be mechanically driven; for example, by atmospheric tides, by the rotating Earth, or by the solar wind. The electric field in Alfvén's magnetic-storm theory is not maintained in this way, and thus we expect it to be short-circuited unless some device operates to prevent a short circuit.

DUNGEY: In connection with the interchange instability, I would like to mention the work of Brian Taylor of the Culham Laboratory in England. ¹⁶ He has produced a necessary and sufficient condition for stability against interchange modes.

¹⁵Rosenbluth, M. N., N. A. Krall, and N. Rostoker, *Nuclear Fusion Suppl.* Pt. 1, 143 (1962)

¹⁶ Taylor, J. B., The Physics of Fluids 6, 1529 (1963)

It is a simple condition and is expressed in terms of a quantity similar to the sort of thing that I mentioned in connection with Hess and Nakada's work. This quantity is the derivative of the distribution function with respect to energy when the two invariants are kept constant, which, in the case of the magnetosphere, means that L is changing. A sufficient condition for stability 17 is that;

$$\left(\frac{\partial f}{\partial E}\right)_{\mu,I} < 0$$

The necessary and sufficient condition for stability is that some kind of integral, involving this derivative and taken over a flux tube, be less than zero. It is essentially a variational principle.

Figure 4, Paper 17, shows that f plotted against L, with fixed μ and I, always has the same slope. In fact, it shows that the sufficient condition (without the integral) is satisfied. You can argue, of course, that instabilities occur until the thing becomes stabilized.

GOLD: I have been very much impressed by O'Brien's observations of auroras and of the electrons responsible for most of the auroral luminosity. ¹⁸ The electrons have a nearly isotropic distribution below only certain heights on an auroral line of force. At greater heights, the flat pitches are absent, and it looks as if the electrons have just been accelerated along the lines of force. If that is really true, then one has to think of the auroral flux of electrons as being produced by an electric field along the particular lines of force. I don't say that I know how to do that, but it seems clear to me that no method of shuffling particles around from one orbit to another will suffice. I can see no way to shuffle them so that they end up with very steep pitches only. This consideration seems to me to be a very important additional constraint on the theory of the main electron flux of an aurora.

CHAPMAN: Figure 1 has a bearing on this subject. The geomagnetic storm of December 4, 1958, is shown in these records from College, Alaska, and from Honolulu. I would like to draw your attention to the particular traces labeled "H." Note that the College scale is about a third of the Honolulu scale.

At a certain instant (labeled SC), there was a quite normal sudden commencement, of a type that often leads to a magnetic storm with a ring current and many polar substorms. One may take the field jump to represent an intensification of plasma flow; but on this occasion, the fields oscillated quite a bit, and one can see that the oscillations are extremely similar on both of these traces. Many other records from other stations also repeat these variations. The plasma oscillated in intensity for several hours, and although there was no development of a substorm, the magnetosphere was alternately compressed and released over this period. This record, of course, shows that neither the intensification of the plasma nor its unsteady variation necessarily lead to further developments in auroras and polar magnetic substorms.

At the bottom of the figure are the College all-sky auroral pictures selected at the hourly intervals. During the period of the onset, no aurora was visible. The main phase began to appear about $6\frac{1}{3}$ hours after the sudden commencement. A ring current must have developed, and soon afterwards there were strong magnetic bays. Then an aurora appeared, and auroral and magnetic substorms began.

¹⁷Kruskal, M. D. and C. R. Oberman, The Physics of Fluids 1, 275 (1958)

¹⁸O'Brien, B. J., Journal of Geophysical Research 69, 13 (1964)

O'Brien, B. J. and H. Taylor, Journal of Geophysical Research 69, 45 (1964)

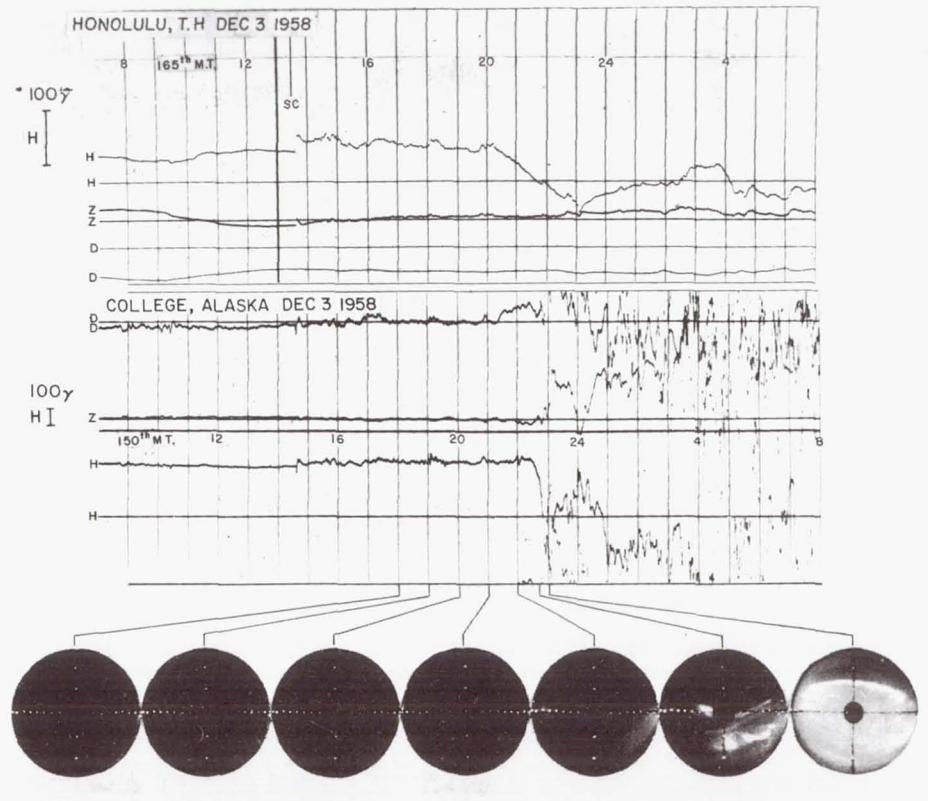


Fig. 1. Development of the magnetic storm of December 4, 1958 and the associated all-sky photographs from College, Alaska

I show this slide to demonstrate that there is no necessary development of a storm, and no necessary feeding of kinetic energy into the magnetosphere caused by the compression of the magnetic field in continuing and unsteady plasma flow. **AXFORD:** This particular storm seems to support very well, in fact, the suggestion that interchange motions play a dominant role in magnetic storms. The interchange motions build up the ring current, and without these motions (as evidenced by DS) there should be no ring current. On the other hand, it is reasonable for the ring current to be weak or absent even if DS is quite strong. since energetic particles are required to produce the ring current and these may not be available in sufficient numbers.

Furthermore, although the interchange motions may start up almost immediately following a sudden commencement, there may be a considerable delay before the ring current starts to build up, since it takes quite a long time for solar-wind particles to be carried deep into the magnetosphere and energized by the motions. When the sudden commencement occurs, the particles are introduced into the magnetosphere immediately; but possibly nothing is observable until, say, 4 hours later, when the first particles reach auroral zone latitudes. Concurrently with, or just prior to, the building up of the ring current, auroral and magnetic bay activity should be pronounced.

CHAPMAN: But sometimes the main phase starts within an hour or so of the sudden commencement.

AXFORD: I know, and that is rather interesting. If, before the storm starts, there happen to be particles already halfway into the magnetosphere, as it were, then a shorter time is required for the particles to reach the auroral zone. In a series of storms, there may well be such leftovers, and the initial phases could become quite short.

DUNGEY: I would like to offer an alternative explanation for the time difference between the initial phase and the main phase of the storm. Thinking in terms of solar wind, let us assume that a plasma stream, which is going to cause a storm, leaves the Sun. This stream has a shock in front of it, as first proposed by Gold, and I think the initial phase of the storm is caused by this shock. There is simply an increase in pressure. I think the main phase of the storm is caused by something in the high-pressure gas, and the best guess is a strong southward interplanetary field. However, this is a question still to be answered.

Newtonian Flow and the Shape of the Magnetopause

BEARD: This is kind of an interruption to the discussion, but I want to comment in a rather trivial and brief way on Prof. Axford's strictures concerning the results of the Newtonian calculation. I think many of the points that Prof. Axford made are well taken, but if we have fluid flow around a magnetopause, the primary difference from the Newtonian model-in which the particles bounce off-is a difference in pressure. Instead of being $2nmv^2 \cos^2 \psi$ (where ψ is the angle between the normal to the magnetopause and the solar-wind velocity vector), the momentum of the particles exchanged at the surface is reduced to $nmv^2 \cos^2 \psi$, because the stuff flows around instead of bouncing off. Since the $\cos^2 \psi$ factor remains the same in the two approaches, the shape on the forward side is the same as the one Prof. Axford mentioned. A little difference in pressure (aside from the factor of 2 in particle pressure) isn't going to matter much, because the surface pressure depends on the inverse sixth power of the distance from the Earth.

Since the surface in the equatorial plane is quite different from a hemisphere,

this forward pressure of the solar wind is still the dominant effect at a large angle toward the back side. You would calculate, on a Newtonian basis, that the surface at an Earth-Sun-satellite angle of 140 degrees is at about 20 R_E if the subsolar surface is at 10 R_F. This calculated shape agrees with that measured by Explorer 10.

The difference occurs between the prediction of the Newtonian theory and the prediction of the fluid theory, where the pressure of the wind on the surface is very, very small, and any interplanetary magnetic-field pressure may not be neglected. In the fluid theory, whatever happens in the transition region dominates everything and, in fact, closes the tail. In the Newtonian picture, the tail is an open cylinder, which is not observed.

The surface near the front is very well calculated by Newtonian theory. This is the site of the dominant current, from which you can calculate the distorted magnetic field. Thus, the Newtonian picture is a very good one from which to calculate the magnetic field, but the calculation has to be done precisely.

PETSCHEK: In connection with Dr. Beard's comments, I want to say that the observed shape of the magnetosphere boundary doesn't differ much from the calculated shape. However, in the Explorer-10 data, one thing that does disagree violently with the Newtonian theory is that the measured field strength was about 15 γ, whereas the dipole-field strength would have been about 2 γ. If you enclosed all the field lines in the cavity, the field strength would actually be less than 2 v. Therefore, the magnetic pressure of the measured field is greater, by a factor of nearly 100, than that of the field predicted by Newtonian theory. I think the only way of explaining such an increase in magnetic pressure is by assuming some kind of shear stress along the boundary, as Axford mentioned. I suggest that the field lines are sticking through the boundary and are being pulled back.

BEARD: Are you referring to the field in the transition layer or to the field in the magnetopause?

PETSCHEK: I am referring to the field in the magnetopause. Am I wrong on that? NESS: No. That was a very fair statement about the Explorer-10 results with regard to field strength. The point you neglected to mention is that from IMP we are getting indications of the same picture where the cavity flares out.

SLUTZ: One must allow not only for the dipole field but for the field produced by the electrical current in the magnetopause. It turns out, when you make a model calculation, that this perturbation field is comparable to the dipole field at the front face of the magnetosphere, but it is large compared to the dipole field at the back face.

Page intentionally left blank

CHAPTER XIX N 6 6. 3.8.9.6 5. ON THE OCCURRENCE OF TOPOLOGICAL CHANGES OF THE MAGNETOSPHERE

B. U. Ö. SONNERUP

Royal Institute of Technology, Stockholm, Sweden

The Topology of the Magnetosphere

In the absence of an interplanetary magnetic field, the solar-plasma flow confines the terrestrial magnetic-field lines to a closed magnetosphere, such as the well known Chapman-Ferraro cavity. Even in the presence of an interplanetary field, the closed character of the magnetosphere is, in general, preserved; because of the frozen-field condition, the solar wind sweeps back into the geomagnetic tail any terrestrial field lines reaching into interplanetary space. In the tail, field lines of opposite directions approach each other; and if there is some mechanism for reconnection, a geomagnetic tail of finite extent results. However, there is one type of open magnetosphere—that is, a configuration in which the Earth's polar field lines reach into interplanetary space—that may be maintained even in the presence of a solar wind. This configuration can be obtained if the interplanetary magnetic field in the vicinity of the magnetosphere is antiparallel to the terrestrial field in the equatorial plane. This topology is illustrated in Fig. 1, which shows the magneticfield lines obtained by superposition of a homogeneous antiparallel field upon a dipole field. This is the geometry studied by Dungey (Ref. 1), who has dicussed the general nature of the flow pattern including the reverse plasma flow in the interior of the magnetosphere. The model is topologically equivalent to the one discussed by Dr. Petschek this morning (Paper 18).

The Explorer-12 magnetometer experiment (Ref. 2) indicates that the interplanetary field just outside the magnetosphere frequently has the direction assumed in Dungey's geometry; that is, it is roughly perpendicular to the ecliptic and antiparallel to the terrestrial field. This field direction is probably a local effect caused by the interaction of the solar wind with the magnetosphere, because at large distances the interplanetary field has the geometry found by Mariner 2 (Ref. 3). However, for the purpose

of the present discussion, only the interplanetary-field direction in the immediate vicinity of the magnetosphere is important. Thus, when the interplanetary field is antiparallel to the equatorial terrestrial field, the magnetosphere may be either open, as Dungey has assumed (see Fig. 1),

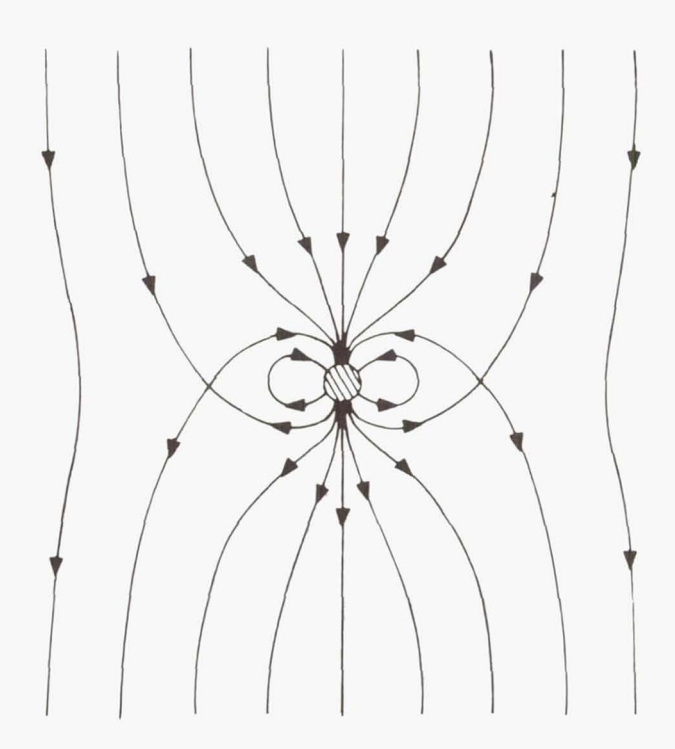


Fig. 1. Open magnetosphere model obtained by the superposition of a dipole field on a uniform antiparallel field (Dungey's magnetosphere model)

or closed, as shown in Fig. 2a. In the latter case, there is a field-reversing current layer at the surface of the magnetosphere. The question is: do both of these geometries occur in practice?

In order to shed some light on this problem, I have investigated the linear stability of the closed configuration under the assumption of a stationary interplanetary plasma (Ref. 4). In other words, I have assumed in my calculation that the solar-wind velocity is equal to zero, which is an embarrassing statement to make in a solar-wind conference. However, I will argue that my results may apply also in the case of a nonvanishing solar wind. I find that the current layer is unstable; it tends to become thinner at one of the neutral regions and thicker at the other, as shown in Fig. 2b. I predict that this instability then goes through the stages

indicated in Fig. 2c and 2d, with the final result being a configuration that is topologically equivalent to Dungey's geometry. The current layer that accumulates over one of the polar regions would, in the real case, be swept away by the solar wind.

The process at the radially expanding neutral ring may be described as a disruption and subsequent reconnection of the field lines. The

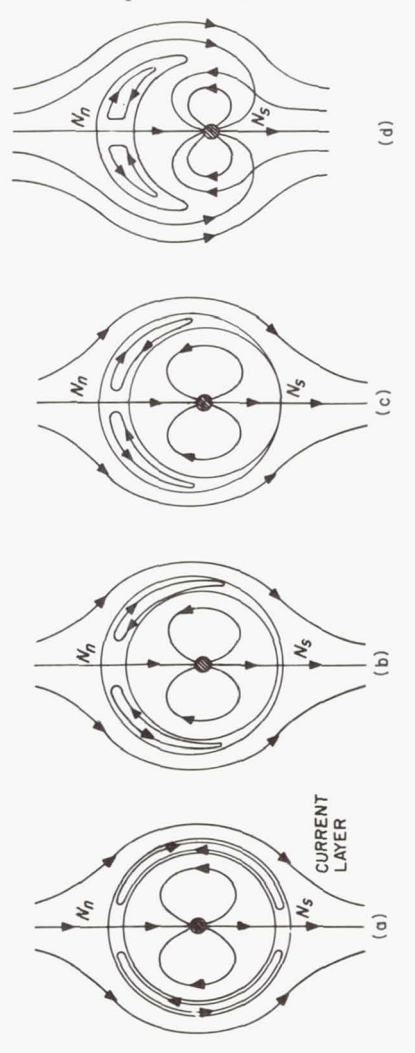


Fig. 2. Transition from a closed to an open magnetosphere. The instability changes the initial configuration shown in (a) into the one shown in (b). The further development of this instability is indicated in (c), where the current layer has become infinitely thin at $N_{\rm S}$ and in (d) where the process of opening has started

reconnection occurs in such a way that interplanetary-field lines are joined with terrestrial ones. There is also a symmetric mode of instability where field lines are cut at two neutral rings—one over each polar region.

This instability may, in principle, occur even in the presence of the solar wind, because the solar-wind plasma can flow past the magnetosphere in its intermediate (Fig. 2d) and final (Fig. 1) states in the manner described by Dungey (Ref. 1) and Petschek (Paper 18). Thus, the plasma flow need not cause a return to the closed topology. We also have some evidence from laboratory experiments (Ref. 5) in support of Dungey's flow pattern, which Dr. Block pointed out this morning (discussion of Papers 16–18). However, I must point out that the instability can occur only if the neutral points on the external surface of the current layer remain in positions just opposite to the neutral points on the internal current-layer surface. If the plasma flow moves the external neutral points to other positions, then the instability may be effectively prevented. For example, the instability could not occur in a configuration of the type shown in Fig. 3. With the *Explorer-12* magnetic measurements in mind,

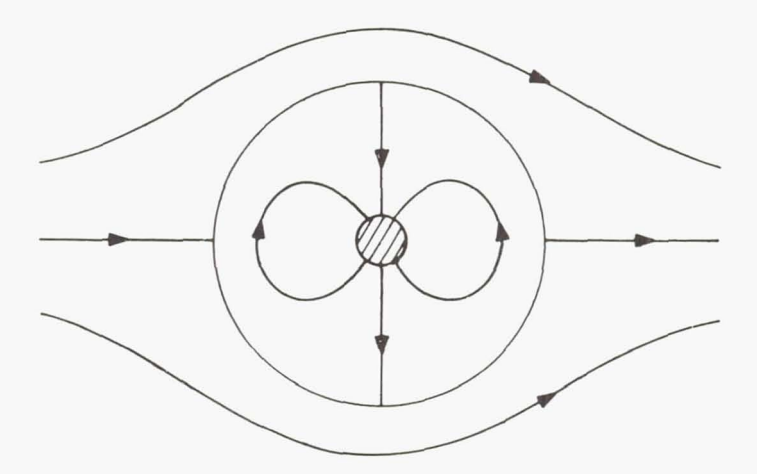


Fig. 3. Example of a magnetospheric configuration where the instability cannot take place. This configuration can be maintained only with aid of the solar wind

it appears reasonable to assume that, in the real case, conditions will occasionally be favorable for the development of the instability; so that a transition from the closed to the open state of the magnetosphere occurs.

Magnetic Storm, Main Phase

We can consider the main phase of the magnetic storm to be the result of a transition from the closed to the open magnetosphere. Such a transition should be observed on the surface of the Earth as a world-wide decrease in the horizontal component of the geomagnetic field. This decrease should be about equal to the 50-to-100- γ field induced by the current layer. The characteristic transition time should approximate the time required for an Alfvén wave to travel from one neutral region to the other along the surface of the magnetosphere. For a particle density of 30 protons/cm³, a magnetic-field strength of 40 γ , and a typical magnetosphere radius of 10 R_E , the transition time is 20 min. These results agree rather well with the magnitude and characteristic time of the well-defined decrease in the horizontal-field component at the onset of the main phase of magnetic storms, such as the one shown in Fig. 4.

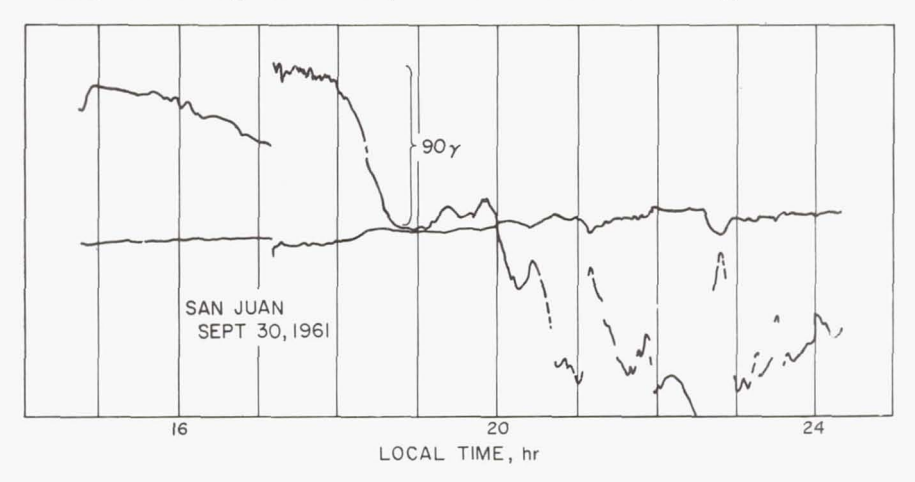


Fig. 4. Variation of the horizontal magnetic-field component at San Juan during the magnetic storm of September 30, 1961

After the transition has occurred, fresh solar plasma enters the interior of the magnetosphere in the manner described by Dungey, and the result is a further world-wide decrease in the horizontal component of the magnetic field and an enhanced DS current system. Thus, the polar substorms and the main phase develop simultaneously, which agrees with the observations (Ref. 6). Another likely effect, caused by the partial short circuit in the ionosphere and along the neutral ring, is a rather strong sweep-back of the polar field lines that extend into interplanetary space. Piddington suggested that the main phase could be caused entirely by this sweep-back effect, but he found it difficult to explain how the polar field lines are connected to a passing cloud of solar plasma (Ref. 7). The instability discussed here is a mechanism that could explain this process.

If the main phase of the storm is to be explained in terms of a change in the magnetospheric topology, it must be assumed that the magnetosphere is closed under normal conditions. The mechanism by which it returns from the open to the closed state, after a magnetic storm, is not very well understood.

The transition requires that the interplanetary fields have a particular direction and that particular conditions prevail near the neutral points. This requirement may explain why the duration of a storm's initial phase can vary within wide limits and why some storms do not have any main phase (Ref. 8). In developing theories for the magnetic storm, it is very important to keep in mind the widely different characters of individual storms. Thus, the explanation proposed here may be adequate only for storms in which the onset of the main phase is rather rapid and well defined. For storms with a slow and poorly defined transition from the initial phase to the main phase, the interplanetary plasma may leak into the magnetosphere by some other mechanism.

It should be possible to distinguish between the open and closed models of the magnetosphere by studying the nature of the field reversal at the surface of the magnetosphere. The closed geometry has an O-type neutral point inside the field-reversing current layer, while the open geometry has an X type neutral point. These points should be located near the geomagnetic equatorial plane if the interplanetary field just outside the magnetopause opposes the terrestrial field. The sense of rotation of the magnetic-field vector can be observed from a spacecraft crossing the magnetosphere boundary above or below the neutral point. From this observation it should be possible to distinguish between the X- and the O-types. A change from the O- to the X-type would indicate the occurrence of a transition of the sort discussed previously. The Explorer-12 magnetometer data published by Cahill and Amazeen (Ref. 2) appears to be compatible with an O-type neutral point, but an examination of the detailed magnetometer records is necessary before any definite conclusions can be drawn. Such a study will be undertaken in collaboration with Prof. Cahill. In particular, conditions at the magnetopause during the storm, shown in Fig. 4, will be investigated.

REFERENCES

- 1. DUNGEY, J. W., Physical Review Letters 6, 47 (1961).
- 2. Cahill, L. J. and P. G. Amazeen, Journal of Geophysical Research 68, 1835 (1963).
- COLEMAN, P. J. JR., L. DAVIS, JR., E. J. SMITH, and C. P. SONETT, Science 138, 1099 (1962).
- 4. Sonnerup, B. U. Ö., Journal of Geophysical Research (submitted for publication).
- 5. Danielsson, L. and L. Lindberg, Arkiv för Fysik (to be published).
- 6. Akasofu, S.-I. and S. Chapman, Journal of Geophysical Research 68, 3155 (1963).
- 7. PIDDINGTON, J. H., Journal of Geophysical Research 65, 93 (1960).
- 8. AKASOFU, S.-I. and S. CHAPMAN, Journal of Geophysical Research 68, 125 (1963).

THE MOTION OF PARTICLES TRAPPED IN THE MAGNETOSPHERE

E. W. Hones, Jr.

Institute for Defense Analysis, Washington, D.C.

Introduction

In order to study the motions of particles in the magnetosphere, a computer code has been written that calculates the drift of particles under four influences considered to be important: (1) magnetic-field gradient, (2) magnetic line curvature, (3) an electric rotational field; that is, the electric field that would cause co-rotation of the plasma with the Earth, and (4) an electric field across the tail of the magnetosphere, as discussed by Axford (Ref. 1). The first application of this machine code has been a study of the motions of particles assumed to be injected and initially mirroring near the magnetic neutral lines at the front of the magnetosphere. The study of these particular motions was undertaken in an attempt to understand the morning spiral patterns of magnetic activity and radio absorption, descriptions of which have been published by several people (e.g., Ref. 2). More specifically, it was an attempt to see whether these spiral patterns might signify (a) the entry of solar-wind plasma through the front of the magnetosphere and (b) the ultimate precipitation of the plasma along a path determined by the electromagnetic fields within the magnetosphere (Ref. 3). Oguti, also, has considered in some detail the possibility of auroral streams entering the magnetosphere through the neutral points (Ref. 4).

Assumed Magnetic and Electric Fields

Figure 1 is the magnetospheric model that was used for this study. Notice that the line from the neutral point intersects the Earth about 10 deg from the pole. The lines of force in the figure are labeled with the colatitude of their Earth intersections.

A uniform electric field across the tail of the magnetosphere was chosen to simulate the electric field postulated by Axford (Ref. 1). An intensity of 3 μ v/cm was chosen, which is equivalent to a potential difference of about 20 kv across the entire magnetosphere. (This field is not exactly

like Axford's, since in his model the magnetic lines of force are equipotentials.) Furthermore, the component of this field parallel to the lines of force was ignored, and only the perpendicular component was considered in calculating particle motions.

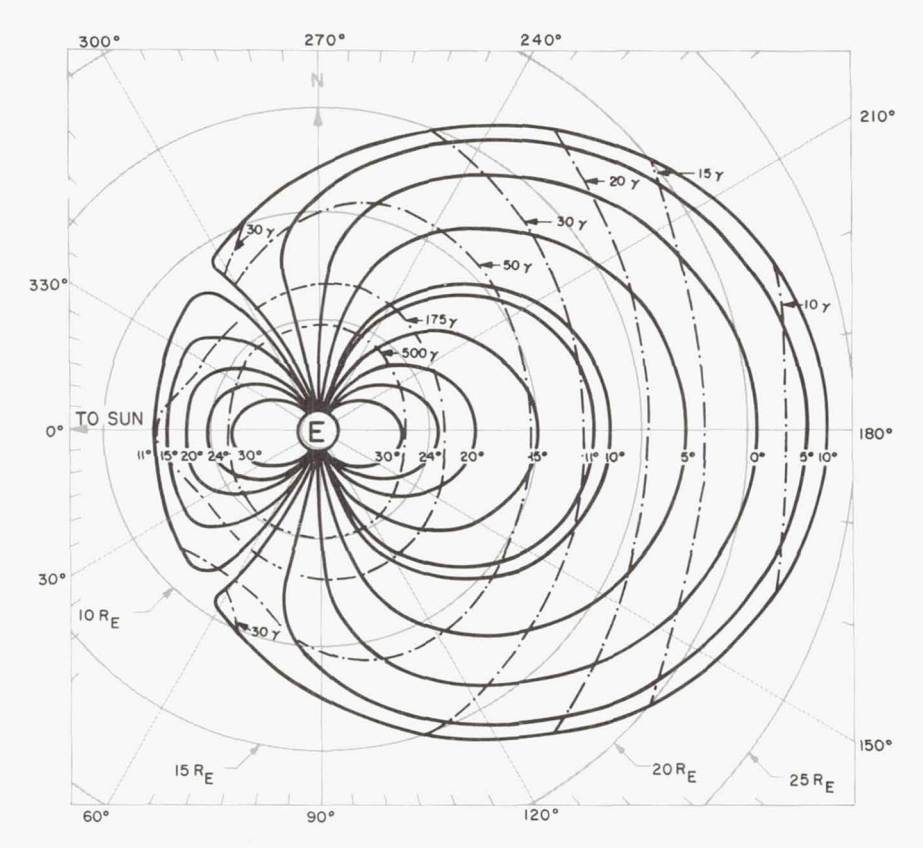


Fig. 1. Noon-midnight meridian projection of a model magnetosphere. The magnetic lines of force are labelled by the polar angle of their point of Earth-intersection. The dot-dashed lines are lines of constant field strength. (From Ref. 3)

Figure 2 illustrates a basis for the assumption of an electric field across the tail of the magnetosphere. The left half of the figure is an auroral pattern published by Akasofu (Ref. 5). It shows that the quiet auroral arcs do not lie along lines of constant magnetic latitude, but go far to the south near midnight. A projection of these structures into the equatorial plane (right half of Fig. 2) reveals a pushed-forward effect for both the curve *ab* and the arcs *cd* and *ef* that go over the polar cap. This effect supports the

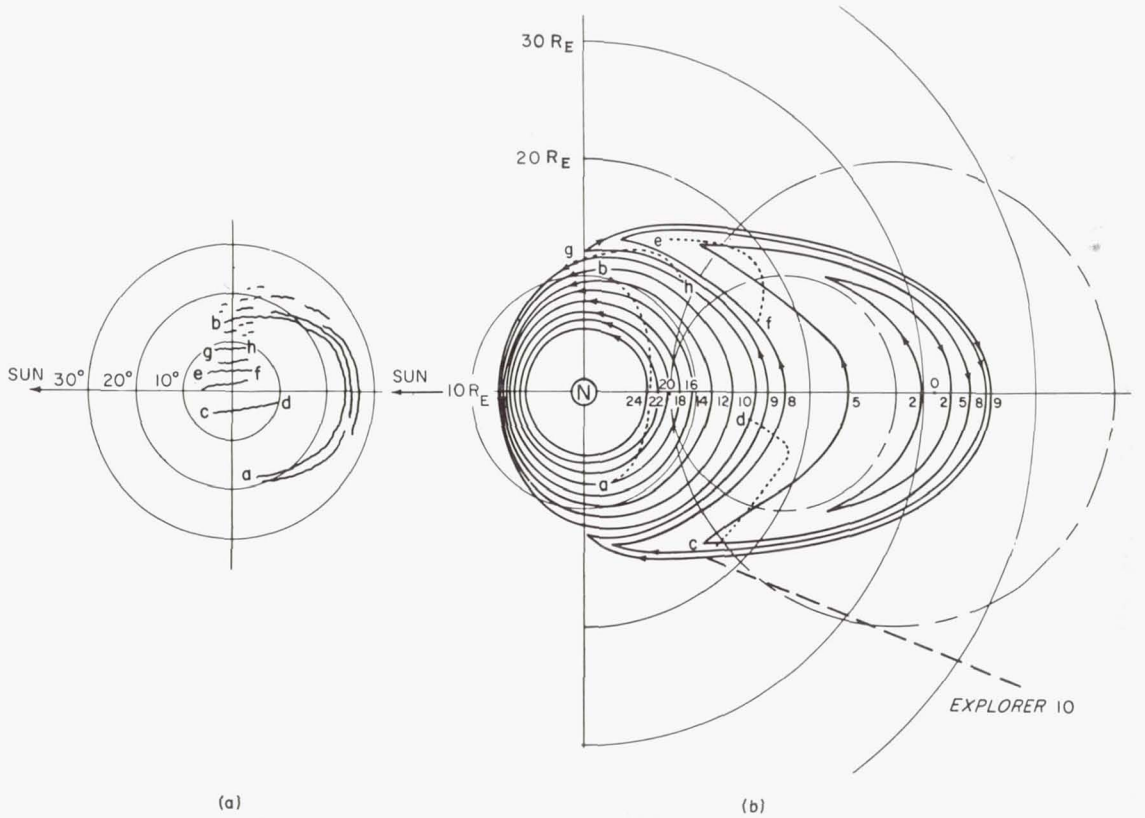


Fig. 2. (a) Auroral patterns (from Ref. 5): (b) the same patterns projected to the equatorial plane along magnetic-field lines. Corresponding patterns are identified by letters

view that there is a transverse electric field that pushes the particles forward through the tail of the magnetosphere.

Figure 3 shows the major features of Axford's model (Ref. 1). There is a positive space charge in the region around A and a negative charge in the region around B—producing a transverse electric field. The internal stream lines are equipotential surfaces of this electric field.

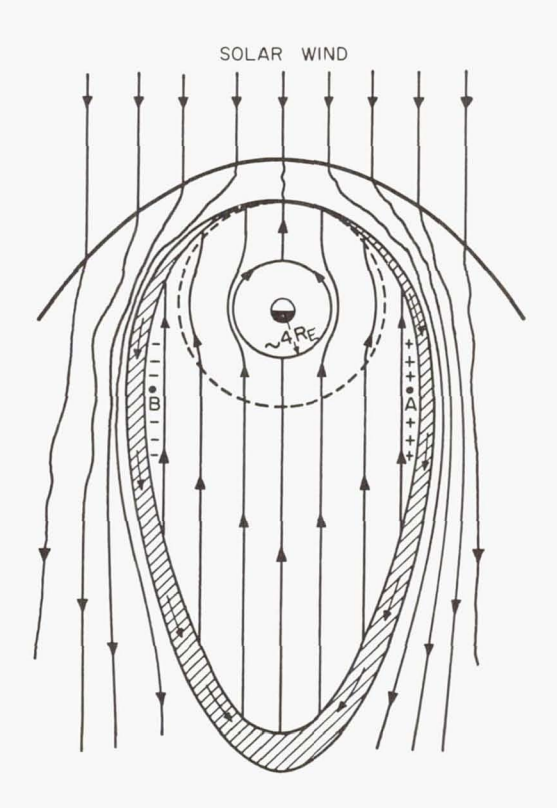


Fig. 3. Sketch of the equatorial section of the Earth's magnetosphere, looking from above the North Pole: streamlines of the solar wind are shown on the exterior; the internal streamlines represent the circulation presumably set up by viscous interaction between the solar wind and the surface of the magnetosphere. The internal streamlines are also equipotentials of an associated electric field due to accumulations of positive and negative charges as indicated at A and B. (From Ref. 1)

Auroral and Other Geophysical Observations

Figure 4 is taken from Ref. 2 and shows the Antartic polar cap. Section c represents the equinoctial period, whereas sections a and b represent summer and winter, respectively. The solid line in each case is the locus

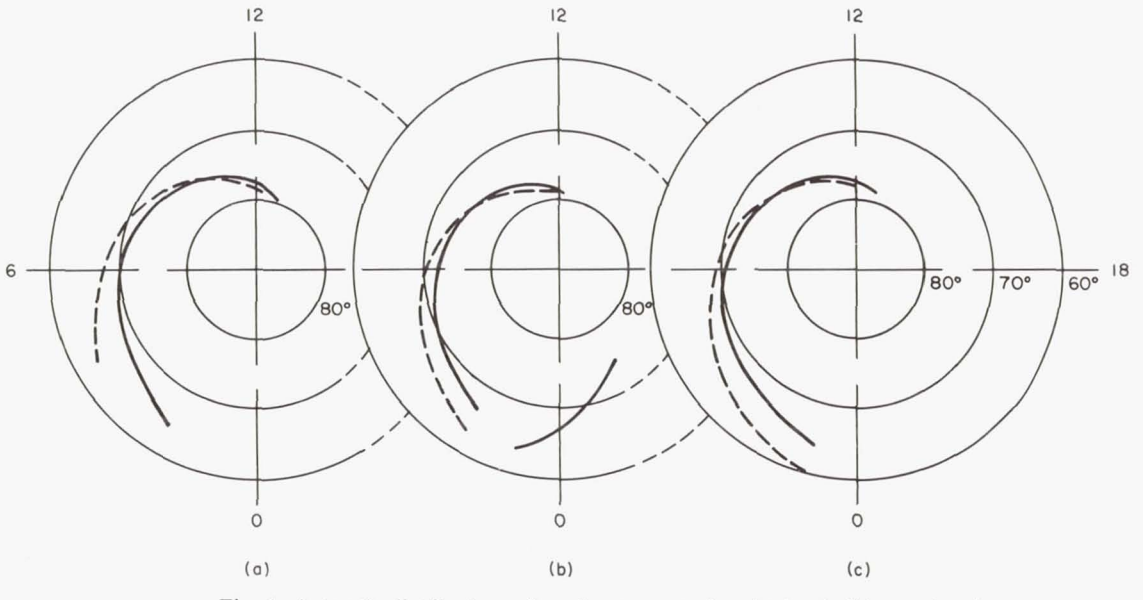


Fig. 4. Antarctic distributions of maximum magnetic agitation (solid curve) and maximum radio absorption (dashed curve). (a) Summer, (b) winter, (c) spring or fall. (From Ref. 2)

of maximum magnetic agitation, and the dashed line represents maximum radio absorption. The striking feature is that this morning spiral pattern appears to start at about 10 deg colatitude, quite near the noon meridian.

The next few figures show some observed auroral features that are of interest because they resemble certain features of the computational results that are to be described.

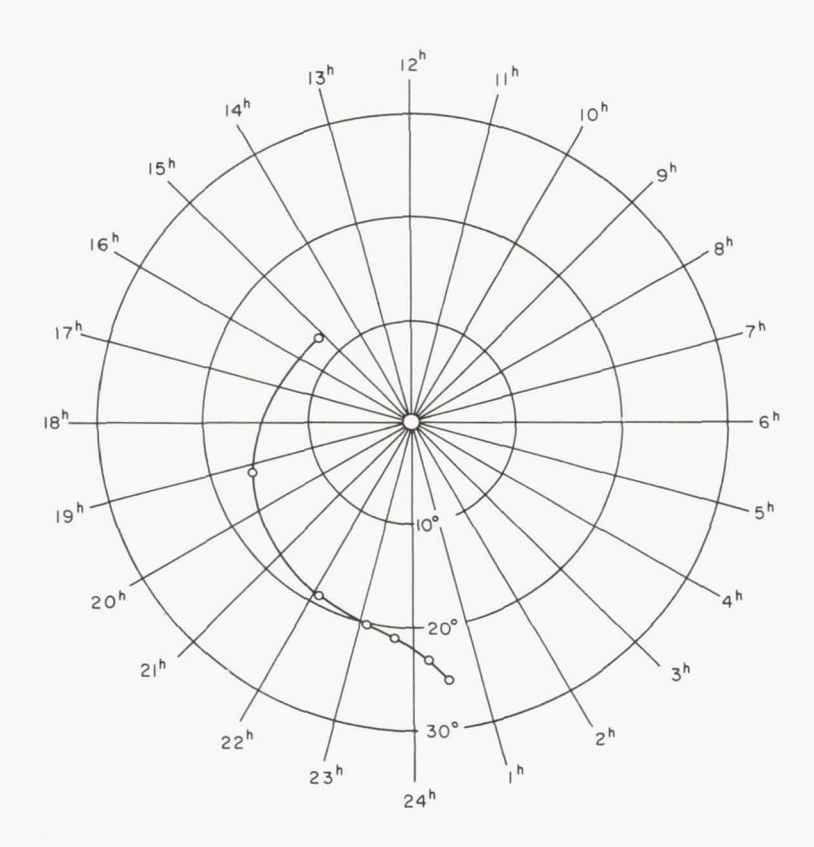


Fig. 5. Maximum probability of the occurrence of overhead auroras, with geomagnetic colatitude and approximate geomagnetic time as coordinates. (From Ref. 6)

Figure 5 shows the locus of the maximum probability for occurrence of overhead auroras plotted as a function of geomagnetic colatitude and geomagnetic time (Ref. 6). This is also a spiral pattern (an evening one), starting at high latitude near noon and descending to magnetic colatitudes of the order of 25 deg near midnight.

Figure 6 shows the variation of visible auroras in local time at Ellsworth (Ref. 6). The important feature here is the early appearance of the H α light; H α emission appears in the sky about 2 hr before the appearance of the brighter forms. It is thought that the brighter forms can be attributed entirely to the precipitation of electrons, whereas the H α

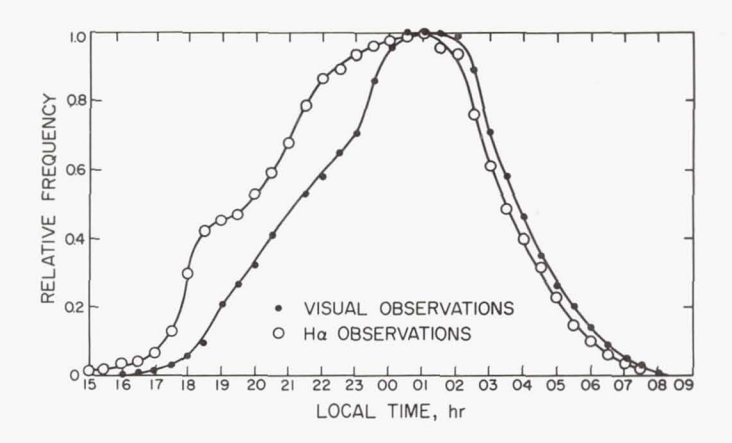


Fig. 6. Daily variation of all visible auroras at Ellsworth. (From Ref. 6)

radiation comes from energetic hydrogen atoms formed when trapped protons undergo charge-exchange collisions with neutral atmospheric constituents. The observation of a quiet, fairly broad band of $H\alpha$ emission in the evening is very typical and has been reported by a number of observers. Most observers also see bright auroral arcs; often there is actually a separation, with the bright auroral arcs being to the north of the broader $H\alpha$ emission. The situation after midnight is not quite so clear; things get very confused then, and the $H\alpha$ emission sometimes disappears. But the early appearance of $H\alpha$ in the evening is the particularly significant feature for the present discussion.

Figure 7 is taken from a paper by Neil Davis (Ref. 7) and shows auroral patterns over Alaska just before midnight. The pattern, Davis reports, is fairly characteristic: it consists of electron-precipitation arcs opening toward the west with a width of 3 or 4 deg in magnetic latitude. The patterns tend to move westward, and there appears to be a clockwise motion of forms within the arcs.

Figure 8 (from Ref. 7) gives the general pattern of alignment of auroral forms over the entire polar region. We shall be particularly concerned with the pattern within 10 deg of the pole. Auroras are seen there much less frequently, but when they are seen, they very often have a characteristic orientation along the Earth–Sun line.

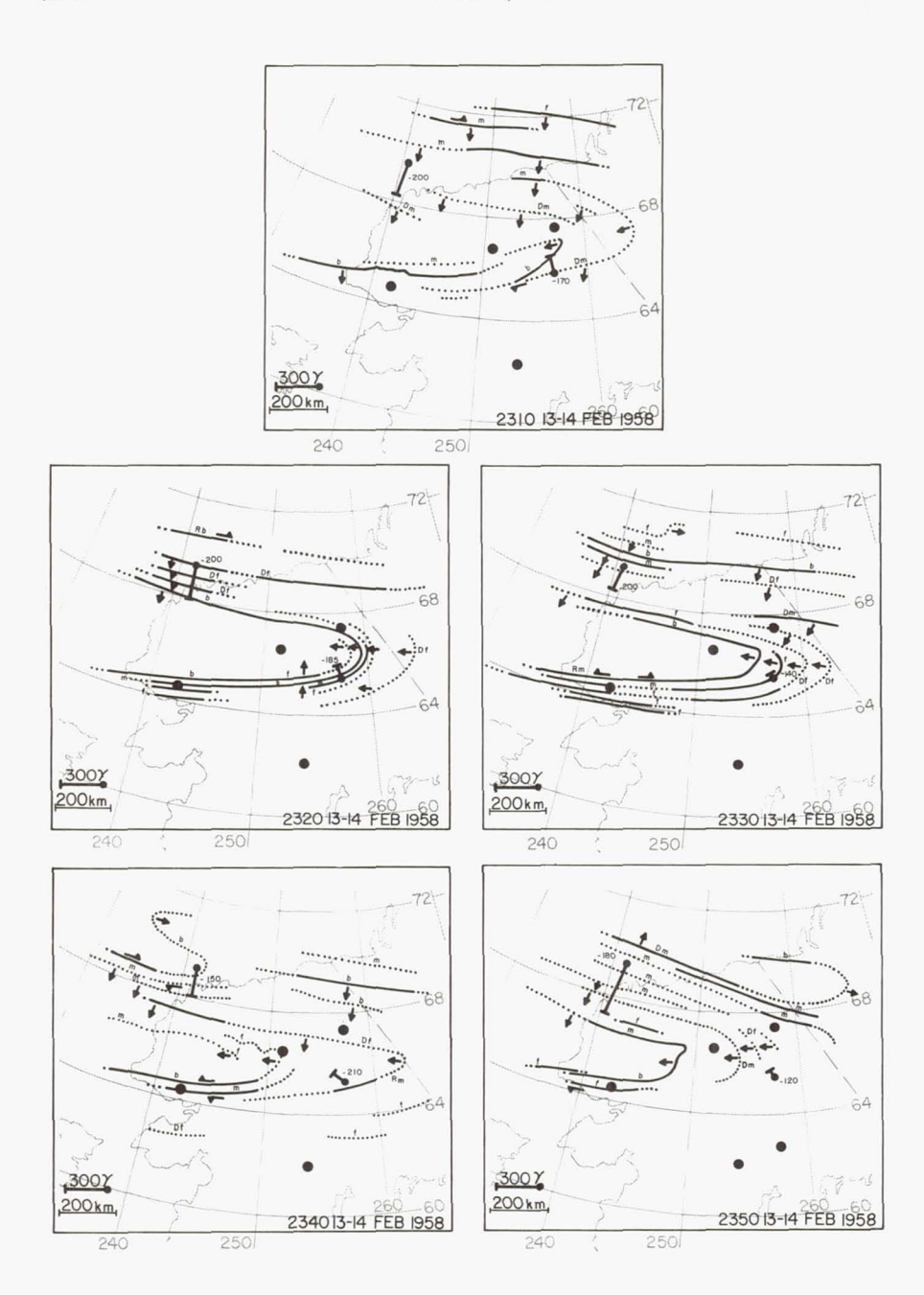


Fig. 7. Synoptic maps representing the aurora at 10-min intervals during the 23-hr (LT) display of February 13-14, 1958. (From Ref. 7)

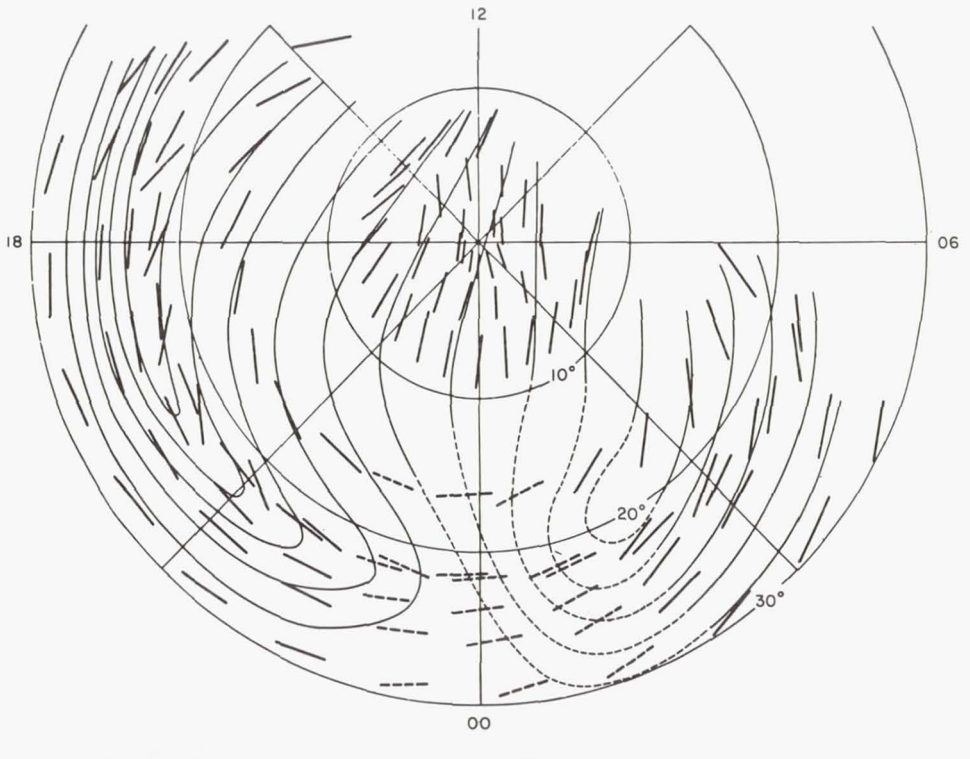


Fig. 8. The alignments of auroral forms with geomagnetic colatitude and approximate geomagnetic time as coordinates. The smooth curves show the average auroral alignment. The dashed lines represent the discontinuous post-break-up aurora. (From Ref. 7)

Results of Calculations

We shall discuss the calculated motions of protons initially mirroring at positions along the 13-deg line, which is just a little south of the neutral line (see Fig. 1), and also the motions of protons starting on the 8-deg line, which is just north of the neutral line. All trajectories will start in the noon-meridian plane.

The computer program calculates the successive mirror-point positions (altitudes labelled h and given in km), the equatorial crossing points, the bounce time, the total time since injection (t, in sec), and the kinetic energy of the particle when it mirrors (F, in ev). Also, the line of force through each mirror point is traced down to the Earth, to determine the location of its Earth-intersection.

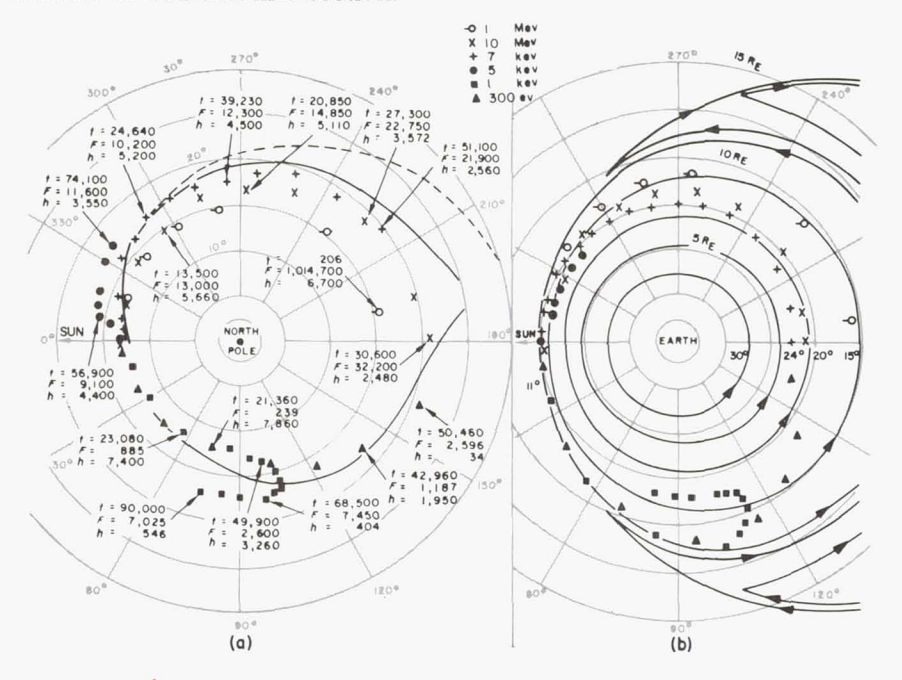


Fig. 9. Parameters of various particle orbits (a) projected along the field lines onto the north magnetic polar cap and (b) in the equatorial plane. Calculations are for protons initially mirroring on the 13-deg line at an altitude of about 6,800 km. Various energies are identified by symbols. Points are labelled: t, time from injection in sec; F, energy in ev; and h, mirroring altitude in km

Some results of the calculations are shown in Fig. 9, 10, and 11, each of which shows (a) the projections of particle trajectories along lines of force onto the north polar cap and (b) the loci of successive equatorial intersections of the particles.

Figure 9 shows calculations for protons injected on the 13-deg line at an altitude of about 1 R_E . Plots are shown for protons with energies

ranging from 300 ev to 1 Mev. Note that the 1-Mev protons take 206 sec to get around to the midnight side, gain 15 kev in getting there, and drop down slightly in altitude. A comparison of the equatorial-plane trajectory with previous (unpublished) calculations of integral-invariant shells in this same model of the magnetosphere shows, as expected, that the high-energy, low-mirroring, 1-Mev particle follows such a shell very closely.

Consider, next, the 7-kev proton. It fairly quickly descends in latitude and gains energy. Its energy has increased to 10 kev in 24,000 sec, and it has descended in altitude 1,000 km or so. After 51,000 sec, its energy is

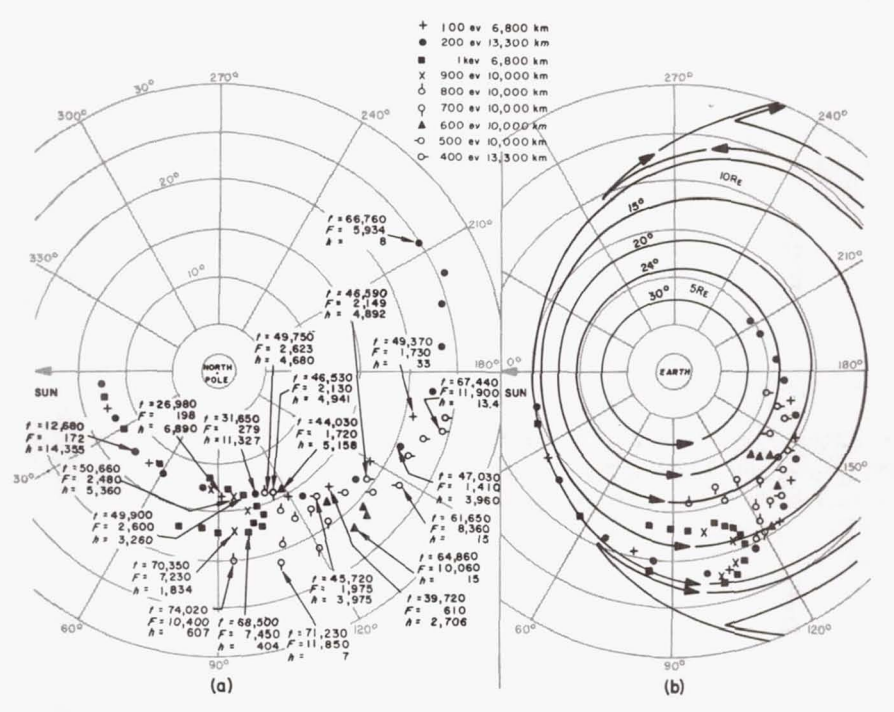


Fig. 10. Parameters of various particle orbits (a) projected along field lines onto the north magnetic polar cap and (b) in the equatorial plane. Calculations are for protons initially mirroring at various altitudes and energies on the 13-deg line. Energies are identified by symbols. Points are labelled: t, time from injection in $\sec F$, energy in ev; and h, mirroring altitude in km

22 kev and it mirrors at 2,500 km. The 5-kev proton's path, energy, and mirror altitude are even more strongly altered by the electromagnetic field. Still lower-energy protons—protons of 1 kev, for example—are carried eastward by the co-rotation electric field. When the particles reach the tail region they are energized by the transverse electric field, until finally they turn around and proceed westward, still gaining energy.

The solid and dashed lines in the left-hand part of the figure (taken from Fig. 4c) are included to illustrate the similarities between these observed morning spirals and the computed potential precipitation pattern of few-kev protons entering the front of the magnetosphere. If the observed morning spirals are indeed related to entering protons, as implied above, they give evidence of the co-rotation of the plasma, because in the calculations it is the co-rotation field that causes the initial sharp progression to lower latitudes.

Figure 10 shows, again, low-energy protons starting on the 13-deg line, but at altitudes ranging from 1 to 2 R_E . The 1-kev proton path is the same

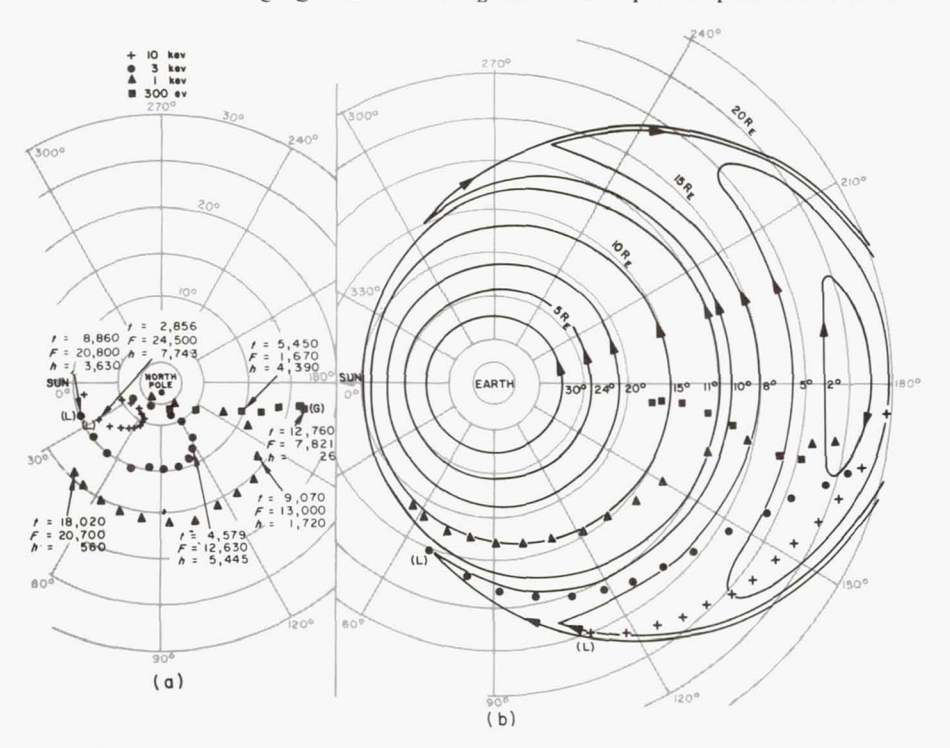


Fig. 11. Parameters of various particle orbits (a) projected along field lines onto the north magnetic polar cap and (b) in the equatorial plane. Calculations are for protons initially mirroring on the 8-deg line at an altitude of 12,500 km and with various energies. Energies are identified by symbols. Points are labelled: t, time from injection in sec; F, energy in ev; and h, mirroring altitude in km

as in the previous figure. This figure illustrates some consequences of the lower-energy (<5 kev) protons' initially being carried to the east by the co-rotation field. Eventually, when they get into the transverse electric field, they are energized and, since their magnetic drift velocity is proportional to their kinetic energy, they may ultimately turn around. The

net effect is that these particles form a broad region of potential proton precipitation. This broad region is reminiscent of the evening $H\alpha$ emission. At a station progressing into the evening, the first emissions to be seen are due to protons being forced down, neutralized, and precipated, while later in the evening the bright arcs of the electrons are seen. It may also be significant that the proton trajectories project onto the polar cap as westward-opening loops, though it is not clear what relation these may have to the westward-opening loops of electron precipitation reported by Davis.

Figure 11 shows the trajectories of particles starting with various energies at a 12,500 km altitude on the 8-deg line—that is, just north of the neutral point. The 10-kev proton follows a path that leaves the magnetosphere at the point marked (L). Lower-energy particles pass close to the pole. A very interesting fact is that there are approximately-straight-line trajectories for some of these lower-energy particles. The 300-ev protons precipitate at the point marked (G), whereas the high-energy protons come back and form a westward-pointing pattern at a very high latitude. These forms resemble those of high-latitude arcs of electron precipitation reported by Davis (Ref. 7).

Some of the results of these calculations support the view that solar-wind particles may enter the magnetosphere at the front—possibly near the neutral points, since that is the region to which the calculations apply. There is a suggestion here, also, that the magnetospheric plasma rotates even at large radial distances, and that this rotation is the reason for the broad $H\alpha$ emission observed south of the evening auroral arcs. Finally, the morning and evening precipitation patterns, spiralling as they do from high latitude near noon to low latitude near midnight, imply that particle streams move from the front of the Earth toward the back, rather than the other way, because as the particles are forced to lower latitudes, they gain energy and descend and can therefore precipitate. If the particles went from the back of the Earth toward the front, and thus from low latitudes to high latitudes, then they would lose energy, their mirror points would increase in altitude, and they would not precipitate.

REFERENCES

- 1. AXFORD, W. I., Planetary and Space Science 12, 45 (1964).
- 2. YUDOVICH, L. A., Geomagnetism and Aeronomy 3, 423 (1963).
- 3. Hones, E. W. Jr., Journal of Geophysical Research 68, 1209 (1963).
- 4. OGUTI, T., Report of Ionosphere and Space Research in Japan 16, 363 (1962).
- 5. AKASOFU, S.-I., Planetary and Space Science 12, 273 (1964).
- 6. MALVILLE, J. M., Journal of Geophysical Research 64, 1389 (1959).
- 7. Davis, T. N., Journal of Geophysical Research 67, 75 (1962).

DISCUSSION OF HONES PAPER

MEAD: I am a little confused. Are both of the first two adiabatic invariants conserved in your calculations?

HONES: I assume that μ is conserved; I don't bother with the second invariant I, although I calculate it for each bounce. I calculate the trajectory, using the guiding-center approximation. In this calculation I use some fairly rough approximations to obtain the rotational part of the electric field. Also, as you notice, the magnetic lines of force are not taken to be electric equipotentials, because I assume a uniform transverse electric field. Both of these approximations contribute to a change of I in these calculations. Thus, when the particles enter the electric field, I increases. If I ignore the electric fields, I naturally is found to remain constant.

MEAD: But you predict that *I* actually does change, even though the time for this change to occur may be shorter than the interval between mirrorings?

HONES: Prof. Dungey points out to me that if the electric field were everywhere perpendicular to the lines of force, you wouldn't expect *I* to change. As I say, my electric field only approximates a conservative field. I presume he is right.

GOLD: I should think that it is unsound to make a numerical calculation without separately accounting for quantities that are conserved to a high degree of precision. After all, you can easily carry these calculations to a point where you will infringe on the conservation of these quantities merely by an accumulation of errors. If you are treating this complicated orbit in detail, then it is quite unthinkable that you can trace it very far before you make a gross change in the quantity which you independently know to be conserved. I am sure that some of the orbits can be better approximated merely from the knowledge that the second invariant is conserved. The same principle would apply in calculating, for example, the orbit of the Earth. After a few hundred orbits around the Sun, you would have a different astronomical unit because of accumulated errors.

HONES: Some calculational checks have shown me that the numerical calculations are sufficiently convergent for the distances that I consider. For example, I find that when I calculate the trajectory of a particle without considering any electric fields, the second invariant remains constant for hundreds of bounces, while the particle drifts half-way or more around the Earth.

DUNGEY: There is one inconsistency in this model: you take a uniform electric field, and then remove the part of it parallel to the magnetic field. Since this means that the electric field now has a curl, there should be a corresponding $\delta \mathbf{B}/\delta t$. I think that this probably affects the longitudinal invariant also.

HONES: Well, I don't know. I think the only effect of using a more realistic field would be to give me a slightly different energization rate or something. Certainly I can apply the other type of electric field.

DUNGEY: It wouldn't surprise me if the longitudinal invariant varied under the field that you have.

HONES: That is right. When I turn on the electric field I can see a change in I. I won't go into detail. I am not surprised that I varies with both the nonconservative electric field in the tail and the approximate rotational field. But since I doesn't vary for the higher-energy particles, I am satisfied.

CHAPTER XXI N 6 6. 3. 8. 9. 6 7.

EXPLORER-18 PLASMA MEASUREMENTS

E. F. LYON

Massachusetts Institute of Technology, Cambridge, Massachusetts

THE general nature of the *Explorer-18* plasma-measurement experiment is, I believe, familiar to everyone. I should like, however, to describe some of the specific data obtained and to present some of the conclusions drawn from these data. The analyses presented here represent the work of Dr. Bridge, Dr. Egidi, myself, and a number of other people at both MIT and MIT Lincoln Laboratories.

Instrumentation

I shall begin by briefly describing the detector, which is shown schematically in Fig. 1. The instrument is similar to the detector flown on *Explorer 10*. The 6-in. Faraday cup has four grids and two collectors at

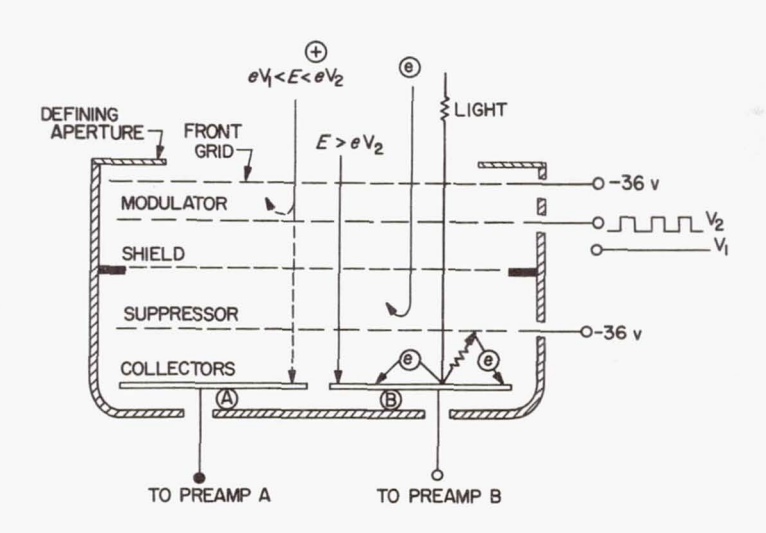


Fig. 1. Diagram of the plasma detector flown on IMP 1 (Explorer 18)

the back, which are followed by some preamplifiers, filters, processors, logarithmic compressors, and so on—all feeding the spacecraft telemetry system.

The key feature of this detector is the modulation grid, which carries a 1-kc square-wave voltage. This voltage alternates between two positive values (V₁ and V₂) for the modulation of protons, and between two negative values for the modulation of electrons. When the modulator grid is at V_1 , only those protons with energies greater than eV_1 can pass this grid and reach the collectors; when the grid is at V₂, only those protons with energies greater than eV2 can reach the collectors. Thus protons with energies between eV_1 and eV_2 are "chopped" at a frequency of 1 kc, and the ac current to the collectors should represent only the protons with energies between eV_1 and eV_2 . In principle, the high-energy electrons in the plasma and the direct and indirect photoelectrons that reach the collectors generate a direct current and produce no net signal. The front grid is at a potential of -36 v and repels all electrons with energies less than 36 ev. Theoretically, electrons with energies great enough to pass the front grid always get past the positive potential on the modulator, because they are accelerated as they approach it and then decelerated after they pass through it. However, there is a slight modulation of the electrons by the modulator grid – a spurious effect that was not in the design of the instrument. This modulation is due to two effects: (a) the positive voltage on the modulator grid shifts the trajectory toward the center of the cup, with a resultant aberration of the electron trajectory, and (b) some of the electrons actually strike the wires to give a sort of capture-transparency modulation, which depends somewhat upon the voltage. These two spurious electron effects cause ac currents of opposite polarity at the collector, so the net modulation of electrons is very slight.

Obviously, there is no modulation of electrons with energies less than 36 ev, and the modulation is also fairly ineffective for very high-energy electrons. In the laboratory, the modulation of electrons having intermediate energies seems to be three orders of magnitude less effective than the modulation of positive ions.

We mentioned this problem at the *IMP* symposium at Goddard, but I mention it here again because we now feel that electron modulation is not an important effect. We feel that what we see in the transition region are indeed very hot protons.

Concerning the physical description of the cup: the defining aperture on the front is about 11 cm in diameter, so the actual aperture is 97 cm²; the angle of acceptance is roughly conical about the axis of symmetry, with a total "half-maximum" angle of 67 deg; and the solid angle is very close to 1 sterad. The overall sensitivity of the instrument is about 6×10^6 particles/cm² sec.

Sequence and Timing of Measurements

Figure 2 shows the sequencing of the various energy windows (channels), and will give you an idea of the timing involved, which is fairly important. There are five proton channels and one electron channel. The main telemetry format of the spacecraft is divided into four sequences, with a nominal duration of 80 sec each—the exact figure is 81.9144 sec.

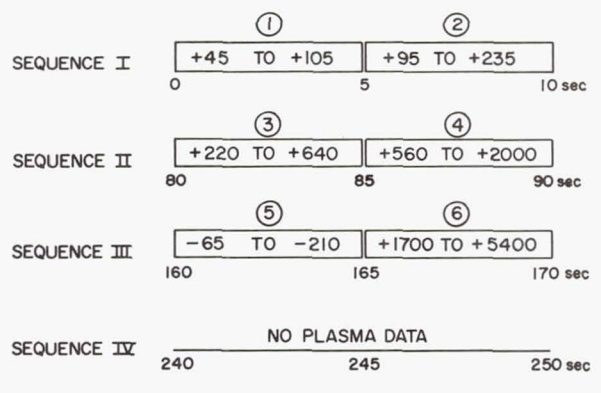


Fig. 2. Schematic of the plasma-measurement sequencing

Our six measurements are sprinkled throughout the first three sequences.

The modulation voltage in our first measurement, which we call channel 1, alternates between 45 and 105 v. This proton measurement lasts for about 5 sec. It is almost immediately followed by channel 2, another proton measurement of equal duration, in which the voltage alternates between 95 and 235 v.

In the next telemetry sequence, channels 3 and 4, the voltage ranges are from 220 to 640 v and from 560 to 2,000 v, respectively. The starts of channels 1, 3, and 5 are nominally 80 sec apart. Channel 5 is our only electron channel, and the voltages are -65 and -210 v. The voltages for channel 6, which is a high-energy proton channel, are 1,700 and 5,400 v.

Since the measurement period is 5 sec for each channel, and since one roll of the satellite takes about $2\frac{1}{2}$ sec, there is more than one roll per measurement period. The early part of each 5-sec interval is unusable because of turn-on transients, which are caused by the fact that the power supplies have been turned off. The very last part of each period is also unusable because of calibration requirements and some book-keeping functions. The usable portion of each measurement period is about 4 sec, which corresponds to about $1\frac{1}{4}$ to $1\frac{1}{2}$ satellite rolls. Sequence IV, which is devoted to the rubidium-vapor magnetometer, is not used for plasma measurements, so the total elapsed time between the start of one spectrum and the start of the next spectrum is about 5 min. The

detailed timing of the measurements that I've just outlined becomes important when you consider changes in the character of the plasma.

The measurements are further complicated by the fact that, due to power and bandwidth limitations, the actual voltage corresponding to the ac current cannot be transmitted as a function of time. It must be sampled and held for about 160 msec, which corresponds to roughly 20 deg of satellite rotation. This limitation becomes a fairly important degrading factor.

Map of the Transition Zone

Figure 3 shows the climax of all the data we wish to present today. I think the most distinctive feature of the plasma data is the evidence of the satellite's passage through the shock front and through the magnetopause. The figure summarizes the observed transitions – I will later discuss how these transitions appear in the data. The trajectories shown in the figure are not direct projections. The points at the extremities of the transition region are plotted in terms of solar-ecliptic coordinates. The horizontal displacement shown in the figure is the solar-ecliptic X component, X_{se} ; the vertical displacement is $\sqrt{Y_{se}^2 + Z_{se}^2}$. Thus each individual point in space is rotated about the Earth-Sun line into the plane of the paper.

So this map represents what Explorer 18 would see if the magneto-sphere were symmetrical about the Earth-Sun line, or if the trajectory were entirely within a plane containing the Earth-Sun line. The map takes no cognizance of geomagnetic latitude. However, we have drawn no important conclusions that require the assumed symmetry about the Earth-Sun line for their validity.

The curvature of the trajectory lines is slightly inaccurate, but the real significance of this map lies in the end points. The shock front, of course, somehow goes through the outer end points, and the magneto-pause goes through the inner end points. The question mark on Orbit 21 indicates that the data are incomplete: we don't know where the end point is yet. Two orbits that are particularly interesting are Orbit 6, in which the entire transition seems to be displaced toward the Earth, and Orbit 13, which has a somewhat anomalous behavior outside the shock front and which also seems to be displaced.

We will later discuss the implications of this figure, and will try to discuss the results in terms of *Explorer 10*, whose orbit was more or less in an antisolar direction. From the next few months of *Explorer-18* data, we hope to show that the *Explorer-10* observations are consistent with a transition through the magnetopause, rather than through the shock front.

Example of a Transition-Zone Spectrum

Figure 4 shows the signals in the six channels as a function of time. These data were obtained when the satellite was in the transition region

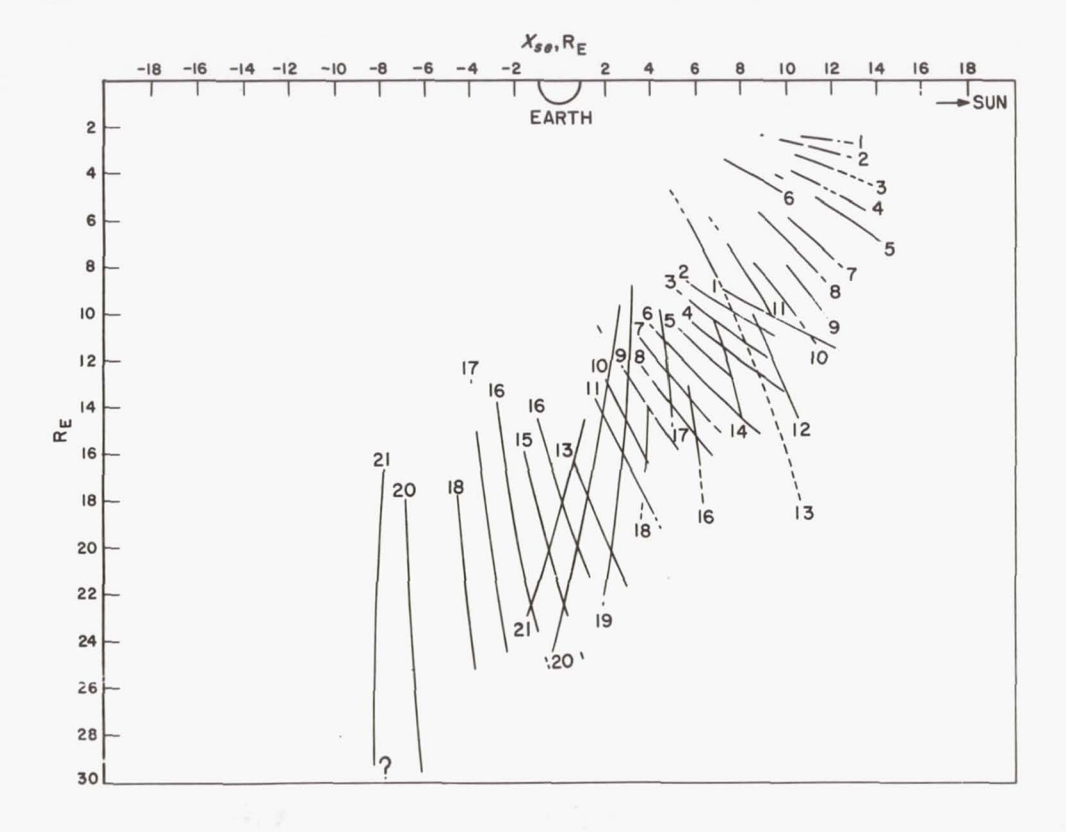


Fig. 3. Meridian section of the transition region obtained by rotating points in space around X_{se} . The numerals denote the orbit numbers

300 E. F. LYON

during the outbound pass of Orbit 2. Some of the data are missing at the beginning, and perhaps some of the data shown represent turn-on transients and probably should be erased. The arrows indicate Sun times and will give you an idea of the time required for one complete revolution.

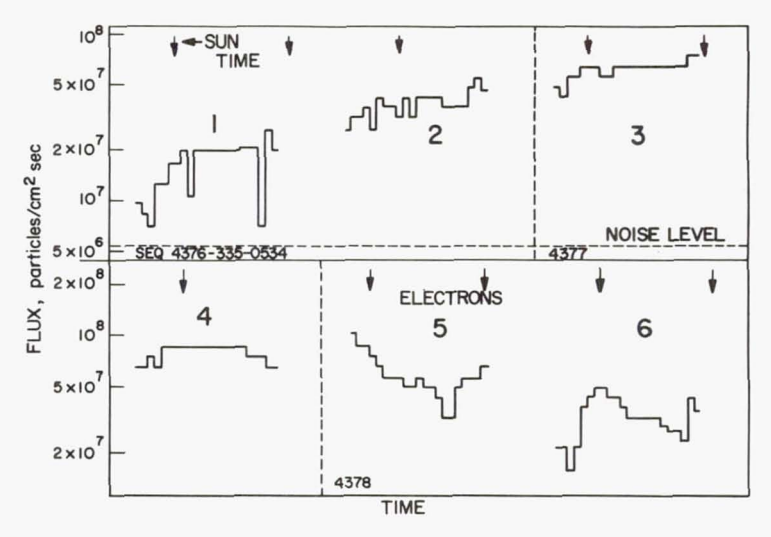


Fig. 4. Plasma detector response measured during the outbound portion of Orbit 2, in the transition region. Distance = 11.8 R_E , ecliptic longitude = 311 deg, ecliptic latitude = -26 deg, time at start = Day 335, 0534 UT

The spacing of channels 1 and 2 is accurate with respect to the time base, and the sequential Sun times shown for these two channels are also correctly spaced. There is a jump in time of 70 sec or so between channels 2 and 3, and also between channels 4 and 5. The logarithmic scale on the left represents the ac current—the sum of the currents measured in the two collectors.

You can see currents well above the noise level, and a very distinct absence of roll modulation. The detector sees an isotropic extremely hot, proton flux. This remarkable absence of roll modulation is characteristic of the transition region near the Earth–Sun line.

We originally worried about the possibility that these signals were caused by extremely hot electrons. However, on the basis of Serbu's measurement of integral electron fluxes on *IMP*, and Freeman's cadmiumsulfide detector measurements on *Explorer 12*, we no longer think that these are electrons—we think they are protons.

Typical Interplanetary Spectra

Figure 5 shows a typical spectrum outside the shock. The current is plotted on a linear scale. You will notice that there is very little signal in

channels 1 and 2, whereas channel 3 has a relatively large signal peaked very close to the Sun times, and an extremely low signal in directions away from the Sun. When we consider the response of the detector and the effect of the sampling, we find that the width of the peak is roughly consistent with a flux from the direction of the Sun. There is essentially no signal in channels 4, 5, or 6.

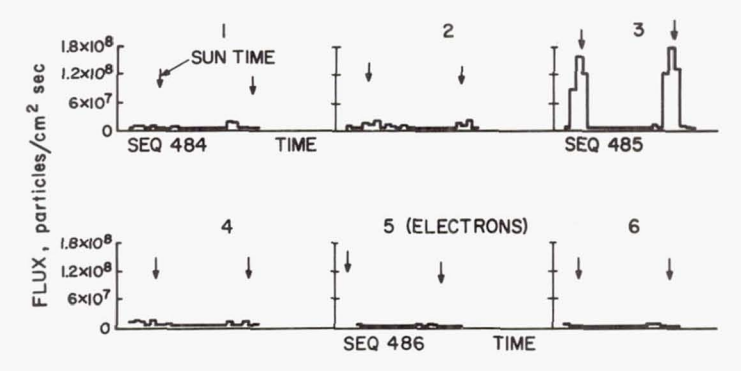


Fig. 5. Plasma detector response outside the transition region, during Orbit 1.

The time at the start of the measurements is Day 331, 1259 UT

Although I don't plan to talk much about this outer region today, I do want to give a few typical values and to note two slightly different characteristic behaviors of the plasma.

There are times when we see a fairly quiet plasma, that is, a moderately uniform, constant flux and a moderately steady plasma velocity, typically on the order of 300 km/sec. For the particular period shown in Fig. 5, the proton density was about $7\frac{1}{2}/\text{cm}^3$ and no electrons were observed. Then there are times when we see a period of moderately disturbed proton flux. It is disturbed in the sense that the flux may increase and decrease on a time scale of four or five samples, which would be a half-hour or so. Typical velocities are from 300 to 600 km/sec, with fluxes a little over $10^8/\text{cm}^2$ sec.

Dependence on Sun-Earth-Satellite Angle

Figures 4 and 5 suggest a way of detecting the transition region by either (a) looking at the maximum and minimum signals in one or more channels; or (b) using the measurements from all channels to find a flux, and then looking at the maxima and minima of that flux; or (c) looking at the maxima and minima of the electron channel.

The data in these two figures were obtained fairly close to the subsolar region, that is, early in the flight. In the transition region of extremely hot, turbulent gas near the subsolar point, we saw a very marked absence of

roll modulation. Now, as we moved about the Earth away from the subsolar point, we expected, from our *Explorer-10* results, to see an increase in roll modulation in the transition region.

A portion of Orbit 10, outbound, which was farther from the subsolar region than the earlier orbits, is shown in Fig. 6. The current scale in this

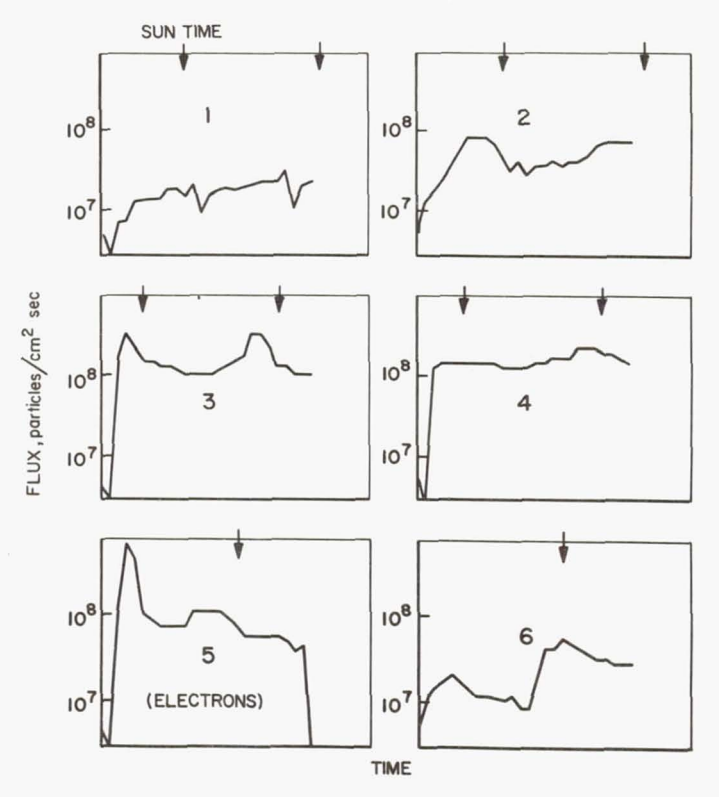


Fig. 6. Plasma detector response measured during the outbound portion of Orbit 10, in the transition region. Distance = 15.2 $R_{\rm E}$, normal–Sun angle = 36 deg, ecliptic latitude = -23 deg, ecliptic longitude = 283.2 deg, time at start = Day 1, 1033 UT

figure is again logarithmic. The big spike in the electron channel (channel 5) is a turn-on transient. It is particularly noticeable because we get the electron voltage by first turning on a dc supply and then shifting the dc voltage to a negative potential. These events don't happen simultaneously, and as we go through ground, we get a very big spike. In fact, the first three or four points shown for channel 5 should be thrown away.

The satellite was in the transition region for the period of time shown in the figure. You can notice a little roll modulation, although its phase with respect to the Sun may be questionable. Most of the signal occurs

in channels 3 and 4. There is an extremely large, isotropic signal in the electron channel, which serves as a good indicator for the transition region.

Figure 7 again shows Orbit 10, outbound, but with the satellite at a distance of about 18 $R_{\rm E}$ and outside the shock. The flux values have not

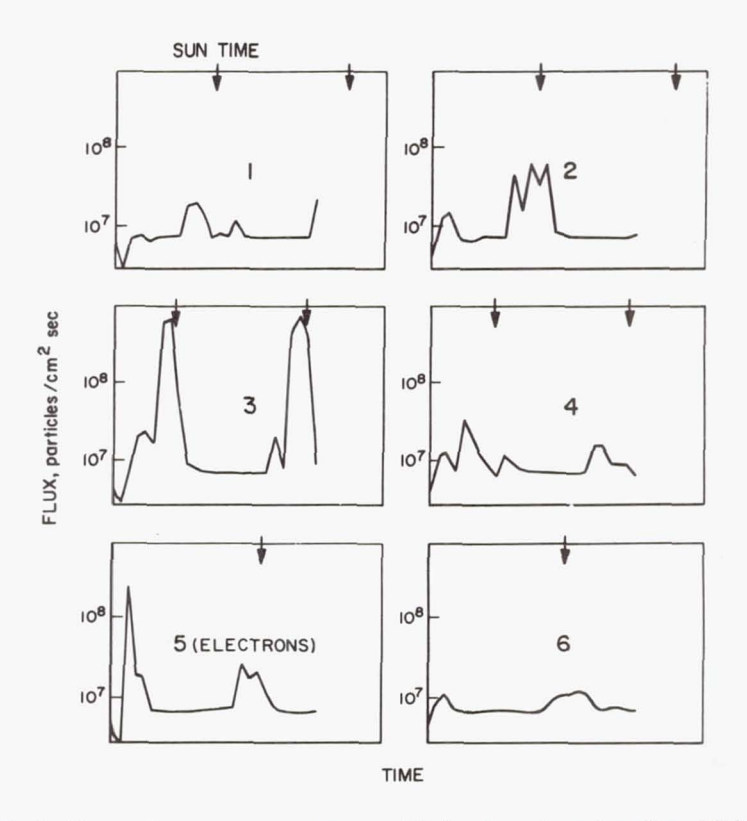


Fig. 7. Plasma detector response measured during the outbound portion of Orbit 10, outside the transition region. Distance = 17.8 $R_{\rm E}$, normal–Sun angle = 36 deg, ecliptic latitude = -20.8 deg, ecliptic longitude = 286.3 deg, time at start = Day 1, 1306 UT

been corrected for the response of the detector—in particular, they have not been corrected for the effect of the angle (~ 36 deg) between the normal to the cup and the satellite—Sun line. The satellite was approaching the point where the measured values of a flux from the solar direction began to decrease significantly due to the cup response function. This effect was very noticeable a little later in the flight. However, in Fig. 7 you can still see a high degree of roll modulation. In this case the flux is seen almost entirely in channel 3, except for a small amount seen in channel 2.

304 E. F. LYON

Figures 8 and 9 show data obtained in the transition region and outside the shock, respectively, during Orbit 20, outbound. The satellite was at an angle of slightly more than 90 deg to the Earth–Sun line, and was at a distance of about 30 $R_{\rm E}$, which is quite near apogee. The currents were significantly affected during this orbit by the large angle between the cup

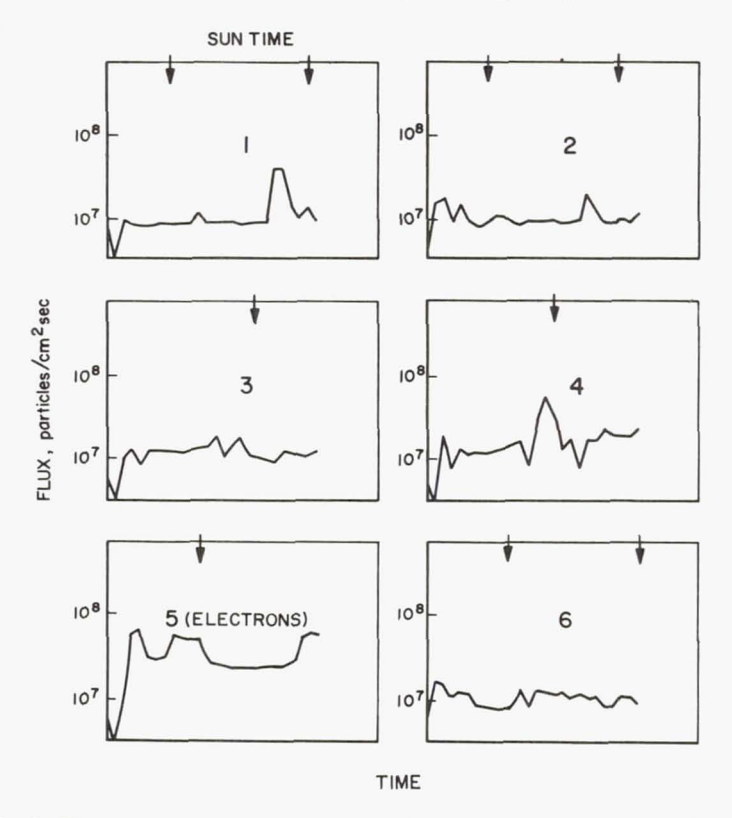


Fig. 8. Plasma detector response measured during the outbound portion of Orbit 20, in the transition region. Distance = 29.9 R_E, ecliptic latitude = -10 deg, ecliptic longitude = 257.7 deg, time at start = Day 41, 0807 UT

normal and the Sun line, so that for a flow directed radially outward from the Sun, the signals were quite weak. Thus the flux *appeared* to be considerably lower than it had been during earlier orbits, but this was not necessarily the case.

Figure 8 shows a peak in channel 4. Because the satellite was at such a large angle to the Earth-Sun line, there was roll modulation; but there were also signals above the noise level during the times that the detector was pointing away from the Sun. There is also a significant signal in the electron channel, in marked contrast to the electron measurement out-

side the shock (Fig. 9), where the main electron current was really the turn-on transient. From this point on, we generally identify the transition region on the basis of the electron channel rather than on the basis of the proton behavior.

Comparison with Explorer 10

Figure 10 illustrates the orbit of *Explorer 10*. There were a number of times when *Explorer 10* seemed to observe a high degree of roll modulation, which was interpreted as a moderately cold bulk flow of a local solar

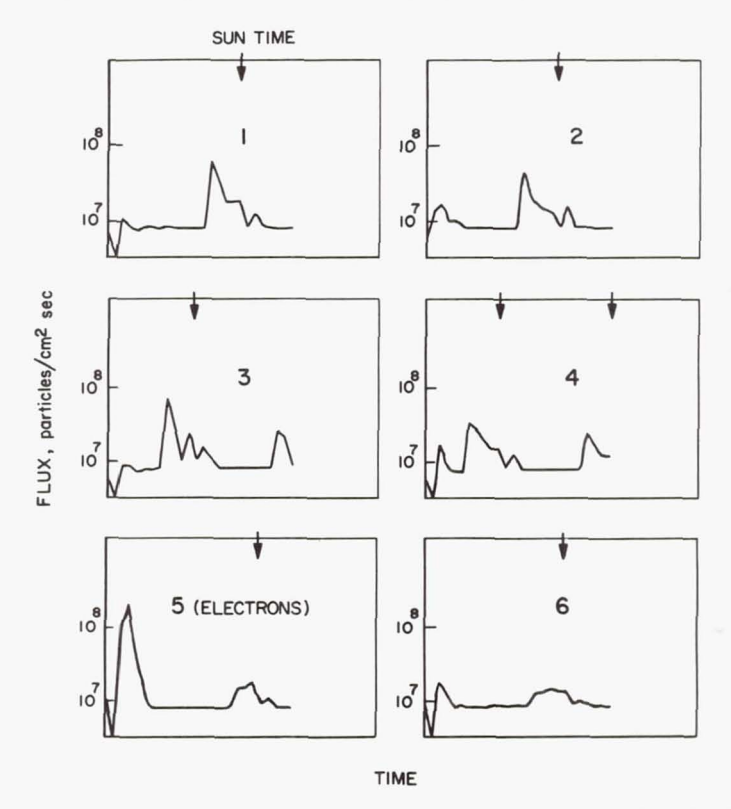


Fig. 9. Plasma detector response measured during the outbound portion of Orbit 20, outside the transition region. Distance = $30.6~R_E$, ecliptic latitude = -3 deg, ecliptic longitude = 258 deg, angle between normal (equatorial plane of satellite) and satellite–Sun vector = 37.8 deg, time at start = Day 41, 1129 UT

wind (Ref. 1). Some raw *Explorer-10* data are shown in Fig. 11. The modulation voltages (corresponding to V_2 , with $V_1 = 0$) are given at the bottom of the figure. The instrument had integral channels, so that any flux measured in one channel automatically appeared in all higher channels as well. The signal seemed characteristically to be down at the noise

level, with the exception of the peak signal close to the Sun. There was no indication of any isotropic flux.

From the geometry of the orbit, I think we have to interpret the *Explorer-10* data as indicating that the spacecraft passed through the magnetopause into the transition region rather than through the shock front into interplanetary space; but we then have to explain why *Explorer*

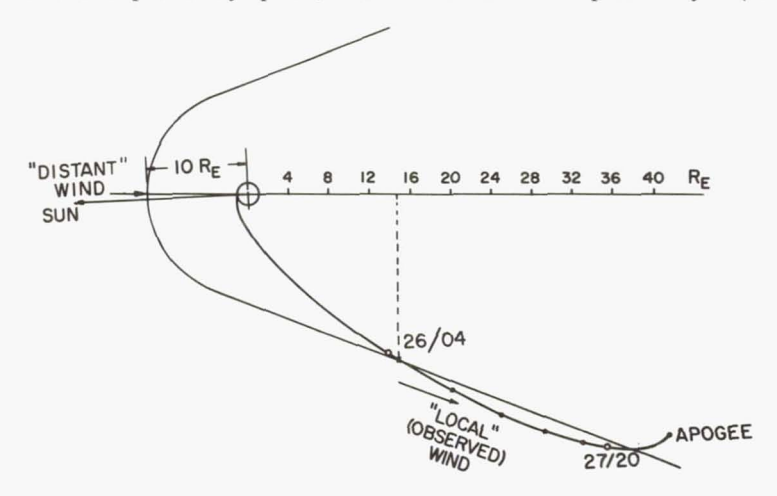


Fig. 10. Explorer-10 orbit and the supposed location of the magnetopause

10 saw no indication of an isotropic flux. From the *IMP* data obtained during Orbits 1 and 2 (Fig. 4 and 5), Orbit 10 (Fig. 6 and 7), and Orbit 20 (Fig. 8 and 9), we saw that as the satellite moved away from the subsolar point, the plasma had a decreasingly isotropic nature and an increasing degree of roll modulation. Thus we expected to see a highly directional flow at the sides of the magnetosphere, and we feel that our observations on *Explorer 18* were quite consistent with those of *Explorer 10*. The principal differences in the two sets of data may be explained by the facts that (a) *Explorer 18* hasn't yet gone as far around the Earth as *Explorer 10* did, and (b) the angle between the cup-normal and the solar directions was about 20 deg on *Explorer 10* and about 35 deg on *Explorer 18*.

Summary Plots Through the Transition Zone

Figure 12 is a summary plot, in which the points represent spectra taken 5 min apart. Since a proton spectrum requires readings from all five proton channels, each proton parameter plotted is sort of an average over 3 min—the time to go from channel 1 to channel 6.

Curves b and c show the sum of the signals in all five proton channels as a measure of the total proton flux. The logarithmic scale goes from

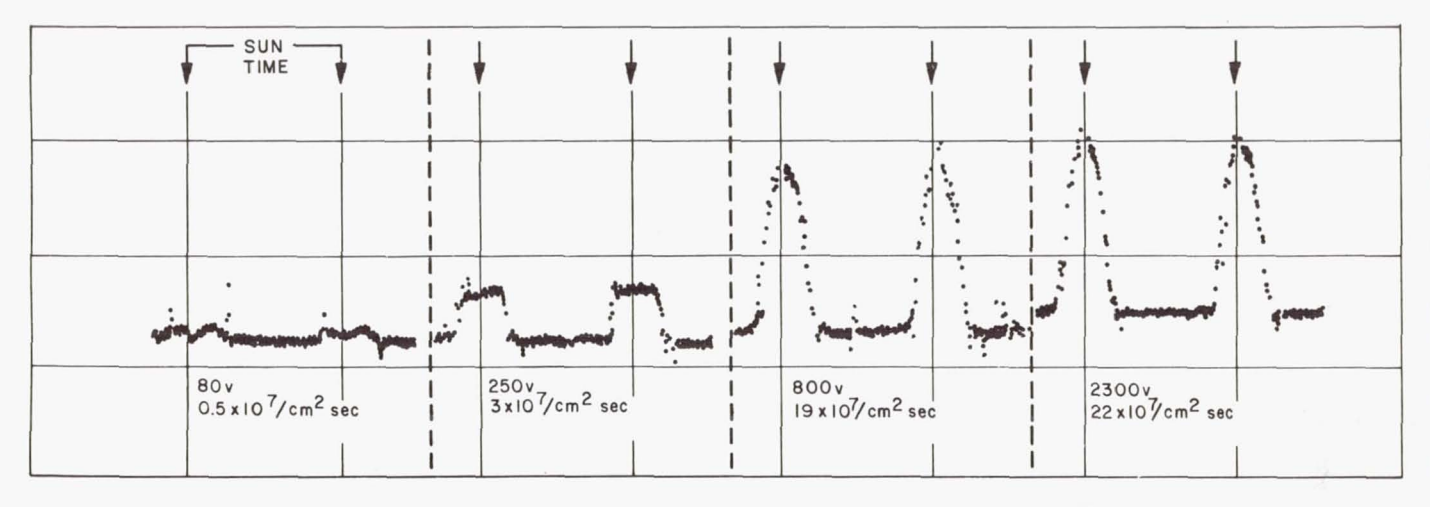


Fig. 11. Explorer-10 plasma detector response, starting on March 26, 1212 UT. The modulation voltages are given below the data as well as the calculated proton fluxes

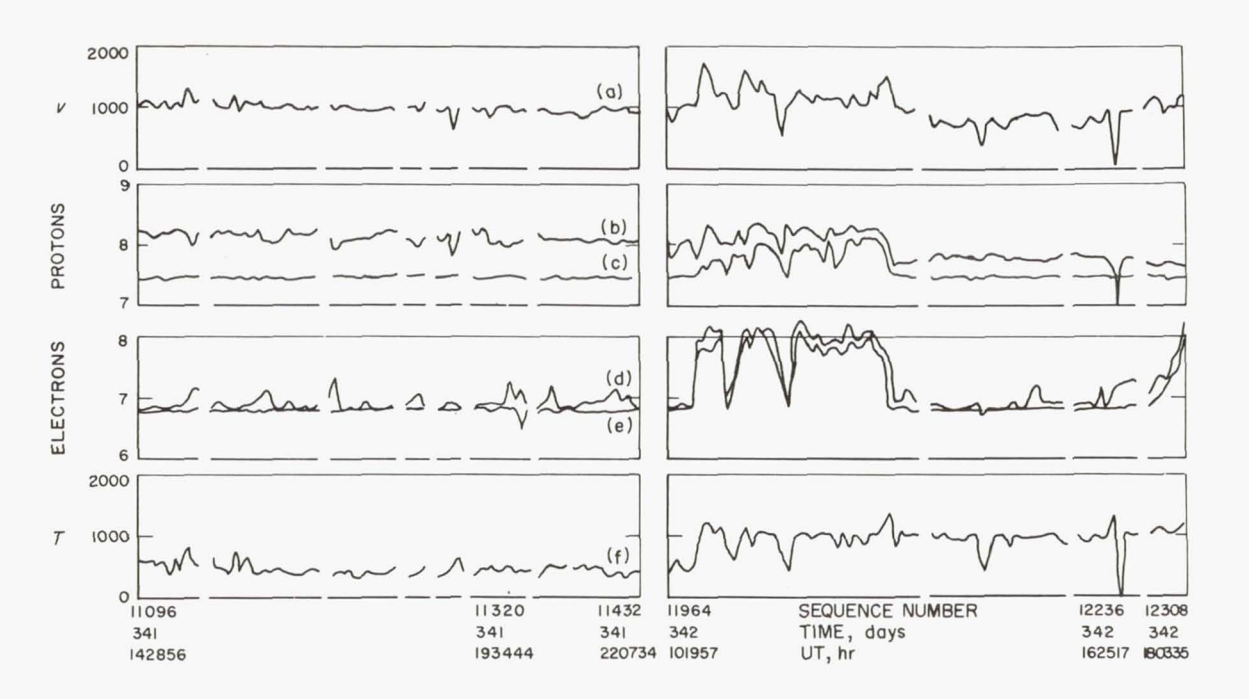


Fig. 12. Summary data for the transition region on Day 342. Time series of:
(a) average proton energy; (b) maximum or solar-directed proton flux; (c) minimum or non-solar-directed proton flux; (d) maximum or solar-directed electron flux;
(e) minimum or non-solar-directed electron flux; (f) second moment of proton energy distribution

10⁷ to 10⁹ particles/cm² sec. Curve b represents the flux observed in the solar direction, while curve c represents the minimum flux observed over all possible angles of rotation. The same is true of the two electron flux curves, d and e, for which the scale is also logarithmic.

Curve a is the average energy of the proton distribution; that is, it is the sum of the flux in each channel times the geometric mean voltage of that channel divided by the sum of the fluxes. It is an average value or first moment of the distribution.

Curve f is the second moment of the distribution, which is defined as:

$$T = \left[\frac{\Sigma F_j(V_j - V)^2}{\Sigma F_j}\right]^{\frac{1}{2}}$$

where F_j and V_j are the flux and voltage in channel j and V is the average voltage as plotted in curve a. So curve f represents an rms voltage, if you like, or the second moment of the distribution, or a crude measure of the temperature (although it cannot be associated numerically with the actual temperature of the plasma).

The curves on the left-hand side of Fig. 12 correspond to the time when the spacecraft was outside the shock, where the temperature is low. There is then a break in time (center of figure), and the axis is redrawn. As the satellite entered the transition region, the breadth of the electron distribution—or the electron temperature—increased. Within the transition region, we saw also an increase in the minimum proton flux and an increase in both the minimum and maximum electron fluxes. Sometimes, as the satellite went through the boundary, we saw a distinct line of demarcation—but sometimes we didn't.

The proton flux and the average energy were both relatively constant or stable outside the shock. Sometimes, however, there were fluctuations in this region. Such a fluctuation once occurred when IMP was a couple of $R_{\rm E}$ outside the shock. We suddenly saw a rather large spike in the proton channel and a change in average proton energy. The average energy in that case had been about 1,000 ev. Suddenly the energy jumped to 1,700 ev, stayed there for 10 min, and then dropped back down to 1,000 ev. At the same time the maximum proton flux decreased slightly and the minimum proton flux increased considerably. The most distinctive character was in the electron flux, which jumped from essentially nothing to about $2 \times 10^9/\text{cm}^2$ sec, both maximum and minimum. I think Dr. Ness will have a little more to say about this later (Paper 22).

Occasionally the conditions within the transition region appeared to be similar to those outside the shock. The time scale of these variations was probably shorter than the 5-min sample, because the variations tended to be washed out in the proton channels. In a particular proton spectrum,

some channels may have had fluxes characteristic of the transition region, while other channels may have had fluxes characteristic of interplanetary space. In such a case, the calculated average parameters tend to wash out the sharp character of the transitions through the boundary, although the sharp transitions were still present and you can still see them in Fig. 12. The far right side of the figure represents the time when the spacecraft was inside the magnetosphere.

Another transition, observed during Orbit 2, outbound, is shown in Fig. 13 by a plot of the maximum and minimum flux in one of the energy channels—rather than by a plot of the total proton or electron flux as in the previous figure. The flux is given for channel 3, which runs from 220 to 640 v.

The far left side of the figure represents the time when the satellite was inside the magnetosphere; during this time we saw essentially no flux. As the satellite passed through the magnetopause, we saw an increase in both the flux from the solar direction and the minimum flux. Then as the satellite left the transition region, we saw quite a lot of structure that correlated nicely with the magnetometer data. Outside the transition region, we saw a moderately strong, steady proton flux from the solar direction. The distances given in Fig. 3 for this orbit were about 10 $R_{\rm E}$ for the magnetopause and 15 $R_{\rm E}$ for the shock front.

Low-Altitude Electron Flux

Figure 14 is a plot of the electron signal observed near perigee. It corresponds quite nicely to the data given by Gringauz (Ref. 2) on the electron density increase as you approach the Earth.

As *IMP* approached perigee, we saw a rise in both the maximum and the minimum electron flux. There are data missing because of the data-recovery problem as the satellite moved close to the Earth and swept around it very rapidly. There appears to be asymmetry about the Earth–Sun line.

A Transition-Zone Anomaly

There is another interesting phenomenon, about which there is still, I think, some controversy. On the bottom of Fig. 15 I have plotted the 3-hr values of Kp for the period January 13 through January 20, 1964. Kp was comparatively low for a couple of days and then, although there was no storm, it showed a marked, moderately rapid increase up to about 5 or 5—. The proton flux, averaged over a tenth of a day for this same period, is plotted above Kp. There is a considerable amount of data missing, for a reason which will later be obvious. The proton flux had been running along fairly steadily at a little over $10^8/\text{cm}^2$ sec. It seemed to decrease slightly, and then increased by an amount just over an order of magnitude. This increase, in turn, was followed by another decrease.

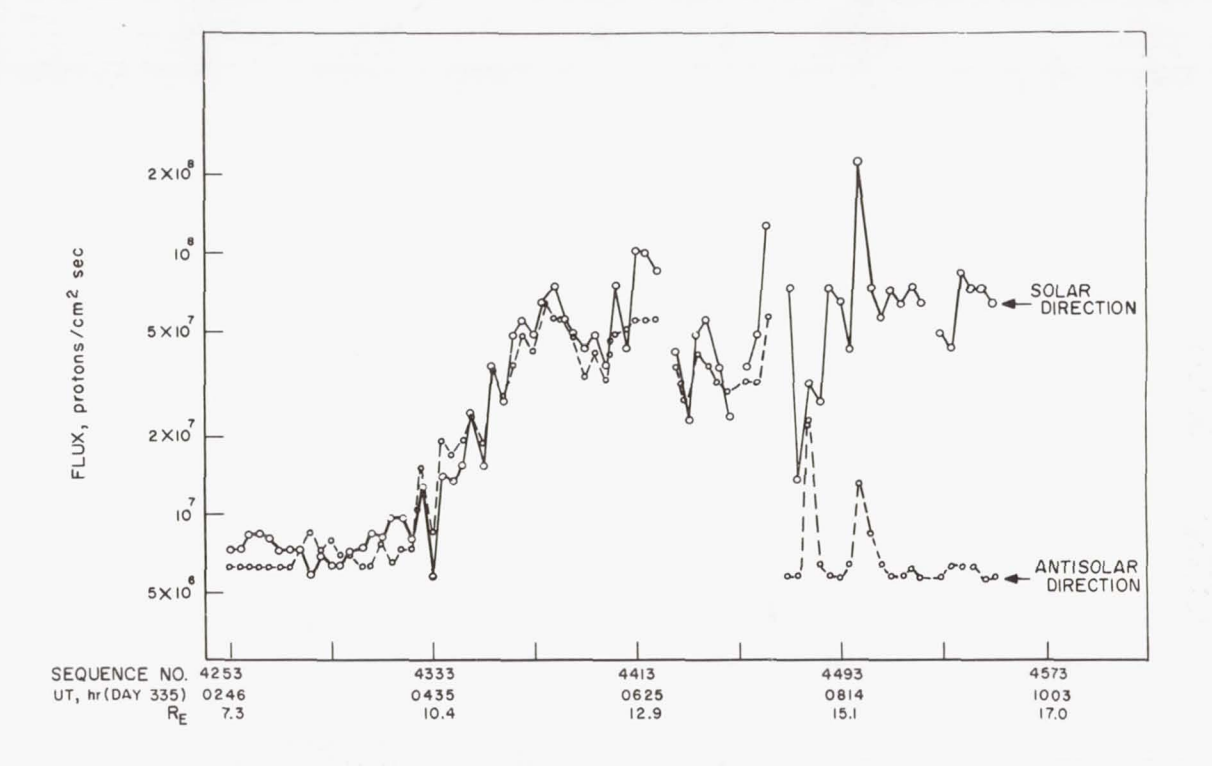


Fig. 13. Proton flux in energy window 3 (220 to 640 v) for Orbit 2, outbound, starting at 0246 UT, Day 335

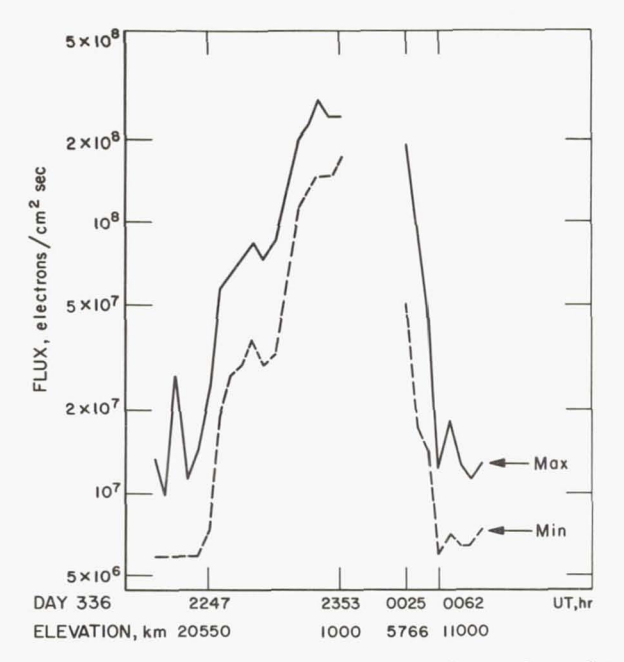


Fig. 14. Maximum and minimum electron flux near first perigee, plotted as a function of time and altitude

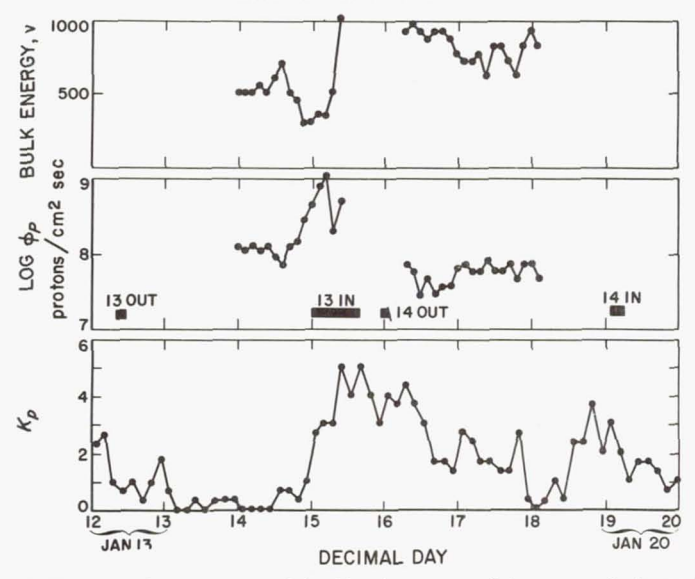


Fig. 15. Top: 0.1-day averages of the kinetic energy of the proton bulk motion; center: logarithmic plot of the 0.1-day averages of the proton flux; bottom: 3-hr average of the geomagnetic index Kp, all plotted vs. time for January 13 through 20, 1964. The bars in the center indicate passage through the transition region

At the same time the bulk energy, which had been moderately stable, increased, then decreased, then increased again, and then perhaps gradually drifted down.

There is obviously a good deal of structure that may be rather hard to explain at this point. However, this phenomenon may provide an explanation for the anomalous behavior shown in Fig. 3 during Orbit 13, inbound. The transition region apparently extended both quite far out and quite far in. The little solid blocks in Fig. 15 represent the periods of time during which we saw the isotropic plasma in the transition region. Passage through the transition region usually took about 0.1 to 0.2 days. But Orbit 13, inbound, which occurred simultaneously with the increases in Kp, proton flux, and proton energy, had an extremely long transition-region passage time and an extremely peculiar nature.

When we look at the summary data for Orbit 13, we see a high degree of roll modulation with the minimum proton flux close to the noise level (corresponding to plasma flowing away from the Sun) interspersed with data in which the minimum flux is quite high. The plasma seemed to hesitate in deciding what region it wanted to be in. This back and forth behavior continued from the initial observation near the numeral 13 in Fig. 3, all the way in to the point at which we started to draw a solid line—where there was a definite return to solidly isotropic signals. Then, still closer to the Earth, the nature of the plasma again seemed to be quite variable.

It is somewhat tempting to associate this behavior tentatively with a condition in which a moderately low solar-wind velocity begins to increase and thus to compress the boundary, coincident with the satellite passing through the transition region. Of course, the satellite is not traveling in a direction exactly normal to the boundary surface, so the velocity of the outer boundary of the transition region may be somewhat less than the satellite's velocity.

Let us make a crude attempt to put some numbers into this model. From the smoothed values of the observed flux and energy increases we calculate that the plasma pressure increased by a factor of 10, or maybe 12. Now let

$$\frac{nmv^2}{n_0mv_0^2} = \frac{B^2}{B_0^2} = \frac{r_0^6}{r^6}$$

which is the appropriate set of relations for describing a balance between the plasma pressure and the magnetic pressure of a dipole field. If we say the field was compressed by a factor of 2, then $r_0/r = 2$, and $(r_0/r)^6 = 64$. Thus the observed plasma-pressure change was probably not sufficient to account for the field compression, based on this simple model.

We also tried this same sort of calculation on the magnetopause, or inner boundary. We estimated the undisplaced position of the magnetopause from the adjacent end points in Fig. 3, and we took the inner end of the solid portion of Orbit 13 to be the disturbed position of the magnetopause. In this case, the change in plasma pressure was apparently too great to fit the model.

Thus the model is extremely speculative. However, I think it is obvious that we do see both the inner and outer boundaries of the transition region move somewhat from one orbit to the next. I should also mention that this particular orbit coincided with the second passage of the Moon's wake. Perhaps the displacement of the boundary and the increase in Kp have something to do with the satellite passing through this wake.¹

REFERENCES

- Bonetti, A., H. S. Bridge, A. J. Lazarus, B. Rossi, and F. Scherb, Journal of Geophysical Research 68, 4017 (1963).
- GRINGAUZ, K. L., Artificial Earth Satellites 12, 114 (1963).
 Space Research II, ed. by H. C. VAN DE HULST, C. DE JAGER, and A. F. MOORE, Interscience Publishers, Inc., New York (1961) p. 574.

¹From a study of the magnetometer and trajectory data, N. F. Ness has concluded that the Moon's wake was *not* detected on Orbit 13 (see Paper 28)

CHAPTER XXII

OBSERVATIONS OF THE MAGNETIC FIELD AT THE MAGNETOPAUSE AND INTERACTION REGION BY IMP-1

N. F. NESS

Goddard Space Flight Center, NASA, Greenbelt, Maryland

Introduction

I have already had an opportunity to describe the *IMP-1* satellite (Paper 6) and to discuss the accuracy of the magnetic measurements. The accuracy, you will recall, is $\pm \frac{1}{4} \gamma$ — which is important, because the first data on the magnetopause and the interaction region were obtained from *Explorer 12* (Ref. 1), whose magnetic measurements had an accuracy of only $\pm 12 \gamma$. However, a great deal of information was gained from the *Explorer-12* satellite, in spite of the relatively poor accuracy. On the basis of what had been learned from *Explorer 10* (Ref. 2), it was strongly suggested that any "boundary" detected was the magnetopause.

I have previously discussed the orientation of the satellite orbit in space. I should like to remind you that a satellite's orbit is fixed only in inertial space while the Earth moves around the Sun; hence the orbit changes in relation to the Sun on an annual basis. The abscissa in Fig. 1 represents the lifetime of *IMP* measured in days from launch, and the solid line represents the angle between the Earth-apogee and the Earth-Sun vectors; this angle was initially 25.6 deg. As time progressed, the satellite apogee moved away from the Earth-Sun line at a rate of about 1 deg/day.

The data to be discussed include the first 19 orbits of the satellite. The orbital period is about 4 days, so that the apogee–Sun angle ranges from 25 deg to about 93 deg. After 90 days in orbit, the apogee of the satellite is always inside the shock wave associated with the interaction of the solar wind with the geomagnetic field. We anticipate that the satellite will continue to function at least until it reaches the maximum apogee–Sun angle; although, due to the Earth's shadow, there is some doubt as to whether the satellite will survive longer. Thus we hope to map the night-side magnetosphere for at least 60 to 90 days, which should give us precise information on the topology of the magnetic field in this region. There have been pertinent measurements made in this region by *Explorer*

14 (Ref. 3), but the *Explorer-14* apogee (15.5 R_E) was considerably lower than the *IMP* apogee (31.7 R_E).

The particular coordinate system chosen is shown in Fig. 6, Paper 6. This coordinate system was convenient for discussing interplanetary-

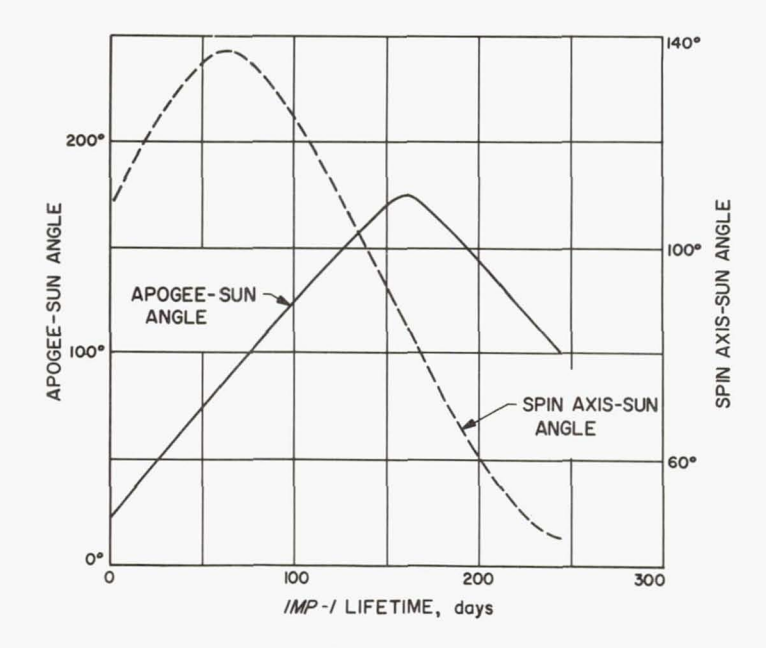


Fig. 1. Angle between the Earth-apogee vector and the Earth-Sun vector (solid curve, scale at left), and the angle between the satellite spin axis and the Earth-Sun vector (dashed curve, scale at right) vs. days since launch

field measurements, and is equally appropriate for discussing the magnetosphere and the transition region. Hence we shall be discussing the magnetic-field results in terms of a magnitude F and two angles: θ , which measures latitude above and below the ecliptic, and ϕ , which measures the azimuth relative to the solar direction. The initial apogee of the IMP satellite was in the +X, -Y quadrant in the solar-ecliptic coordinate system.

Examples of the Magnetic-Field Data at the Extremity of the Geomagnetic Field

Figure 2 shows the data obtained on January 5, during the outbound pass of Orbit 11. In Paper 6 we saw the interplanetary magnetic-field data for the following 24-hr period, and this presentation is in the same format, except that here the magnitude scale has been extended. The fields

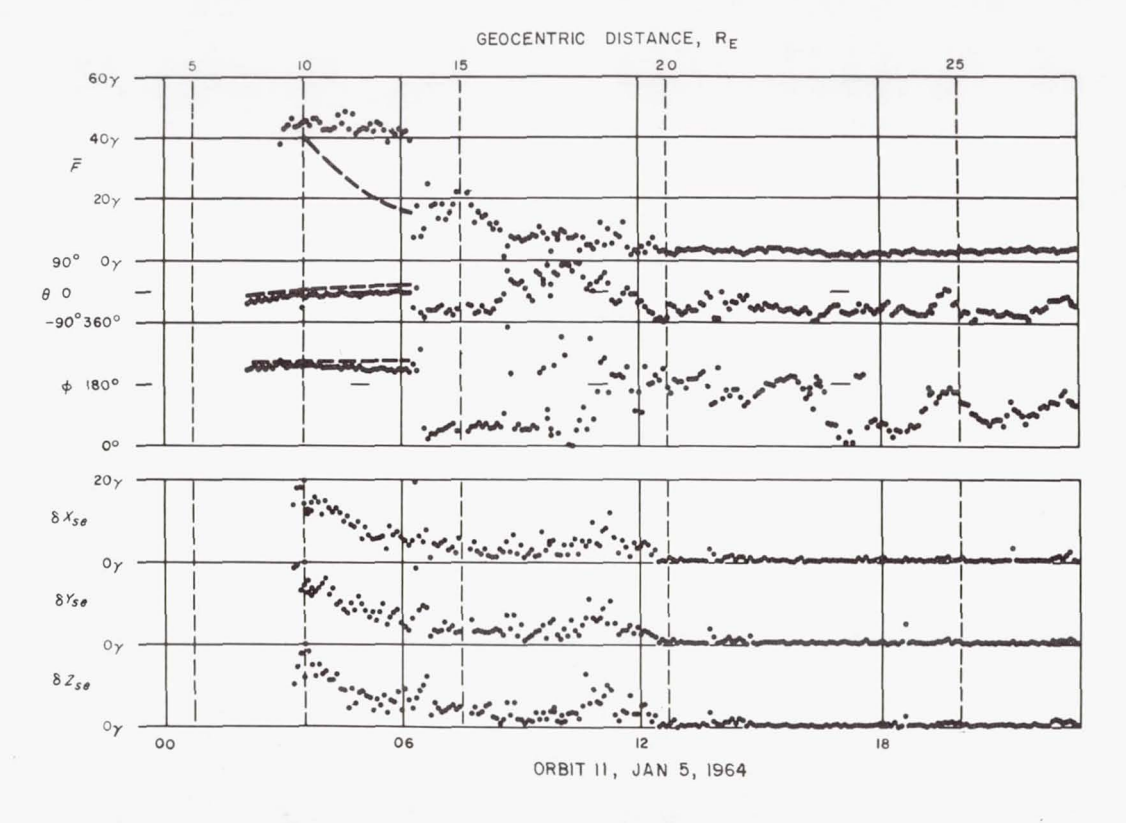


Fig. 2. Magnetic-field data from Orbit 11, outbound pass. Each point is a 5-min average. The dashed lines represent the undistorted, theoretical, geomagnetic field

318 N. F. NESS

measured were much larger than those encountered in interplanetary space; indeed, they exceeded 40 γ . Although it was possible to measure stronger fields with the fluxgate magnetometers for certain field orientations (with respect to the spacecraft), I am not confident of the values above 40 γ when such values are provided by fluxgate-magnetometer data only. We have not yet folded in the rubidium-vapor magnetometer data, which will give us valid field strengths up to several hundred γ .

The dashed lines in the figure represent the theoretical values of F, θ , and ϕ as determined by the Finch and Leaton coefficients. At the distances being discussed, the theoretical values do not differ greatly from a centered-dipole approximation, because the only important term in the spherical harmonic expansion is that corresponding to the dipole term. As the satellite progressed outward from the Earth, the two angles agreed roughly with the theory, although θ appeared to be slightly more negative than anticipated.

We are going to identify as the magnetosphere that region of space traversed by the satellite up to 0620 UT. My comment this morning was meant to point out that frequently the Earth's field lines at the magnetopause are not normal to the ecliptic. The observed orientation is associated with the fact that the Earth is beyond the solstice and is approaching vernal equinox; in other words, it depends on the tilt of the Earth's rotation axis with respect to the ecliptic, together with the tilt of the dipole axis with respect to the rotation axis.

The angle ϕ was not as large as it should have been theoretically. The magnitude at 10 R_E was approximately equal to the theoretical model; it finally reached a value more than twice as large as the theoretical magnitude. Then at approximately 0620 UT, when the satellite was at a geocentric distance of 13.6 R_E, there was an abrupt change in the magnitude and in the two angles defining the vector field. Indeed, the component that had been pointing away from the Sun suddenly pointed back toward the Sun. But notice that although ϕ changed by 180 deg, which is exactly what certain theories require, the angle θ also changed by about 60 deg. Therefore, the field change was not simply one of inversion: the field was also being rotated.

Now, as the satellite progressed in its orbit, the field orientation remained approximately the same, while the field strength varied from 7 γ to as high as 20 γ . Occasionally the field strength decreased to zero. It continued to fluctuate quite a bit until *IMP 1* reached the interplanetary region of cislunar space.

Dessler has argued that the magnetopause boundary, which we have identified as being located at a distance of 13.6 R_E , must be a stable surface (Ref. 4 and 5). The continuity of the variance across the boundary,

¹See discussion of Papers 16-18



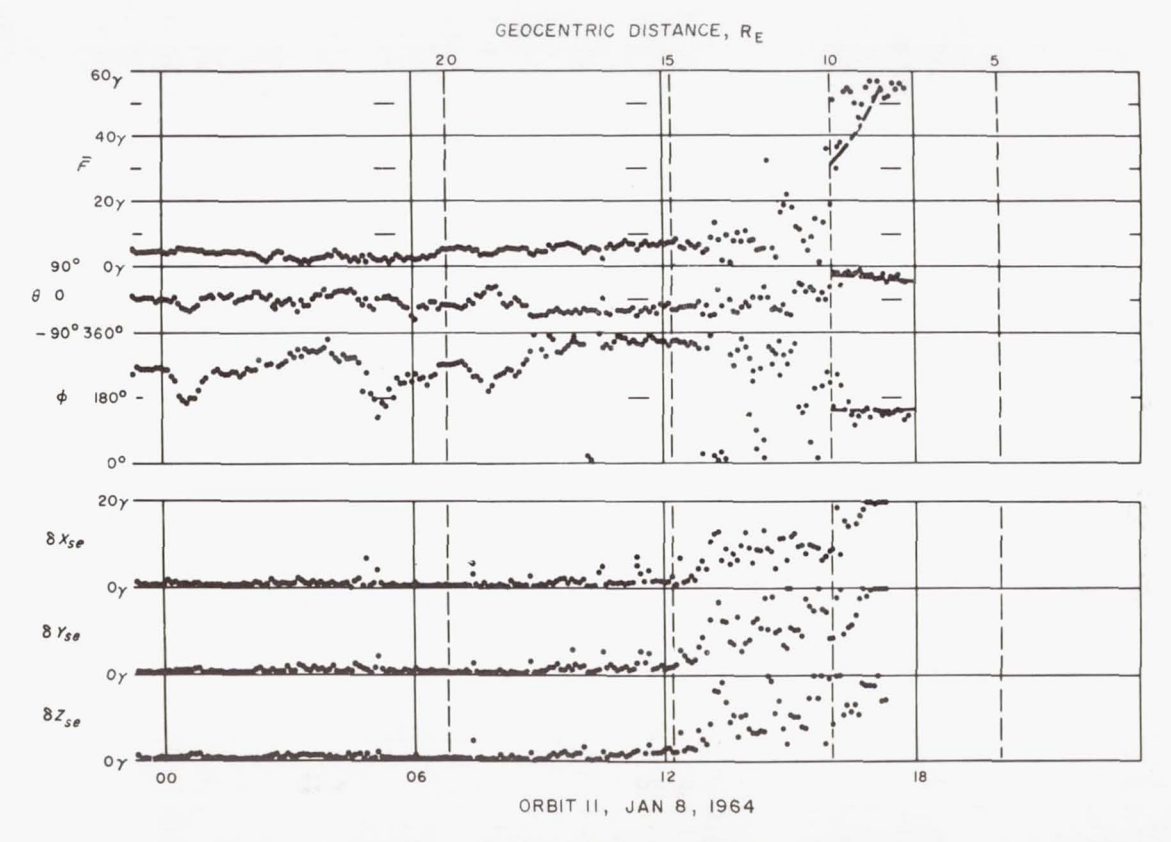


Fig. 3. Magnetic-field data from Orbit 11, inbound pass

320 N. F. NESS

however, indicates that energy is propagated across the boundary in the form of disturbances associated with the transition region, in contrast to a "stable" boundary.

There is one other point about the data shown in Fig. 2, in which the shock wave was located at a distance of 19.7 R_E. Our identification of the shock-wave position is based on the appearance of an abrupt change from a very stable field configuration to a highly unstable one as shown by the variance data. In some cases the identification was straightforward; but in others it was not so easy, possibly because we do not know what the proper physical bases are for making such an identification. In addition, we do not understand the processes that lead to the brief increases that occur in the variance when the satellite is several R_E beyond the shock wave. A rather broad increase occurred, for example, at about 1350 UT in Fig. 2, and other examples can be given in which the increase is more temporally limited. The phenomenon appears to be spatially associated with the shock surface rather than with the undisturbed interplanetary medium.

Figure 3 presents the data obtained on the inbound pass of Orbit 11; as before, time progresses to the right. By now I think you can identify the boundaries by yourselves; we have identified the magnetopause boundary at a distance of 9.7 $R_{\rm E}$. Although it was less well defined than on the outbound pass, the magnetopause still showed the characteristic abrupt change in the angle ϕ . In this case the field was more nearly normal to the ecliptic than it was in Fig. 2, although the change in magnitude is not as clearly defined. For this particular orbit, the shock wave is identified at 16 $R_{\rm E}$. There was no abrupt increase in the field, only a steady increase together with a very localized increase in the variance. You may argue, with some justification, about our particular identification of the boundaries. However, the bases upon which we identified our boundary crossings were constant; they didn't change as we went from one orbit to another. Future detailed reviews of the correlated plasma and magnetic-field data may require such a change, however.

Figure 4 shows the data for the outbound pass of Orbit 15, which was some 16 deg farther away from the Earth–Sun line. This orbit was a classic; it produced the kind of data one likes to include in a review paper, because nobody is going to quibble about boundary positions. In this case the geomagnetic field was mapped over a much greater interval of time and over a much greater distance. Again the internal field was almost in the ecliptic, and the theoretical value of ϕ was larger than the observed value. The field was distorted backward in an antisolar direction, which indicates that on the dark side the field lines tend to become parallel to the magnetopause surface. This situation is similar to the one found by Explorer 10 (Ref. 2).



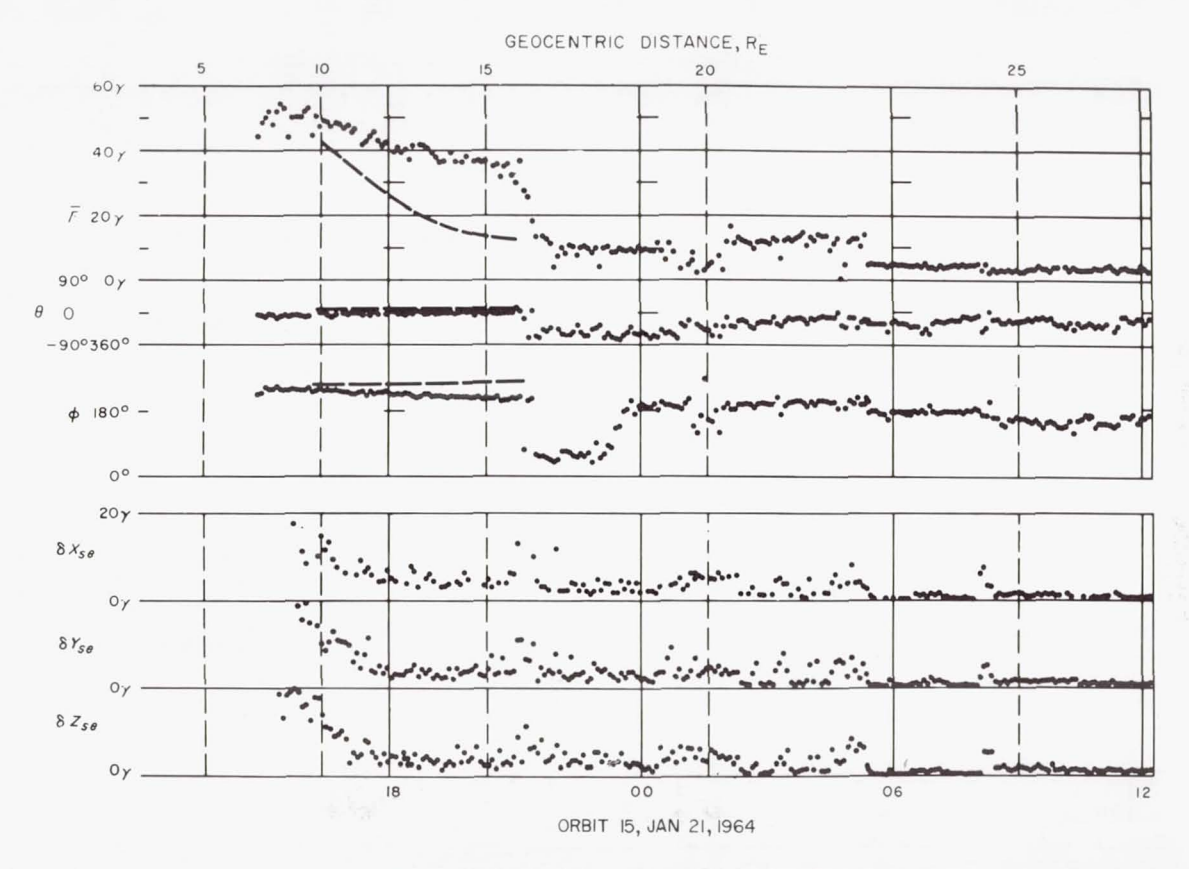


Fig. 4. Magnetic-field data from Orbit 15, outbound pass



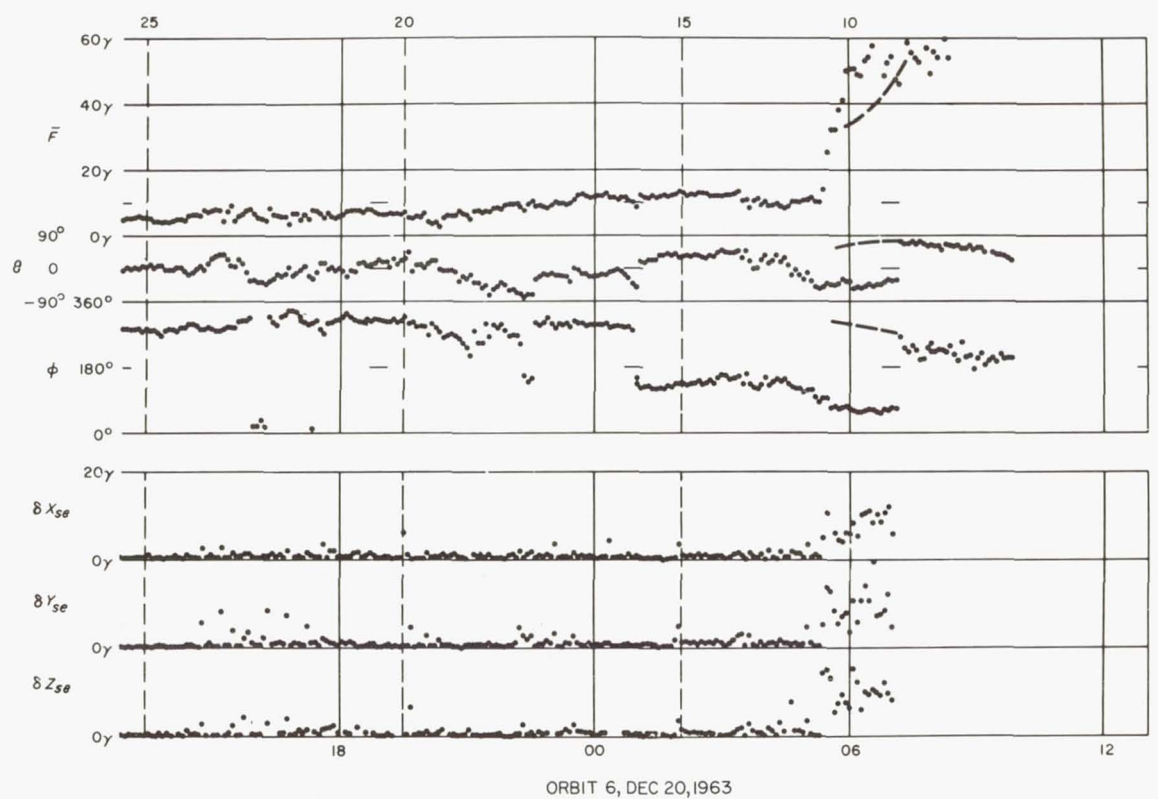


Fig. 5. Magnetic-field data from Orbit 6, inbound pass

The boundary of the magnetosphere is clearly indicated by the changes in both magnitude and angle: ϕ again changed by about 180 deg, and again there was a change in θ . As the satellite crossed into the transition region, the field was pointing toward the Sun and about 60 deg below the ecliptic. Then as the satellite continued to move away from the Earth, the field suddenly returned to its previous direction while still within the transition region.

Beyond the chosen shock-wave boundary, a very localized increase in the variance of the magnetic field appeared in all three components at about 0800 UT. I do not believe that these variance increases were associated with the interplanetary phenomena that we have identified as neutral sheets (see Paper 6). We have inspected these particular variance increases in detail, and the field did not really go to zero. As I pointed out previously, this phenomenon appears to have been spatially associated with the shock-wave surface.

Figure 5 illustrates the inbound pass of Orbit 6, which has previously been referred to as an anomalous orbit by the MIT experimenters on the basis of their inspection of the plasma data (Paper 21). It also appeared to be anomalous in the magnetic-field data. As the satellite returned from apogee, an abrupt 180-deg change occurred in the angle ϕ ; at the same time, the field, which had been pointing below the ecliptic, changed and pointed just slightly above the ecliptic. There was a simultaneous small increase in the magnitude, followed by a decrease, and then another rapid increase. However, the later angular changes did not coincide with the second magnitude increase. In general, the variance was small until approximately 0500 UT, when the satellite was well inside the region where the first-observed field changes occurred. It is very difficult to identify a magnetopause or a shock-wave boundary using the definitions previously given. We have tentatively placed the shock-wave at approximately 0500 UT and the magnetopause at about 0710 UT.

Determination of the Positions and Shapes of the Boundaries

The distances to the magnetopause and shock-wave boundary crossings, in units of R_E , are plotted in Fig. 6 through 9; consecutive boundary crossings are connected by straight lines. These figures also contain the Fredericksburg K index and the angle χ_{ss} , which is the geomagnetic latitude of the subsolar point. This angle reaches -36 deg at the solstice; the average value of χ_{ss} increases with time as vernal equinox is approached.

The first two magnetopause and shock-wave boundary points shown in Fig. 6 were measured during the outbound and inbound passes of the first orbit. Their geocentric distances were slightly different for the two passes. As the orbit progressed from the Earth-Sun line to the night side, the discrepancy between the positions of the boundaries determined

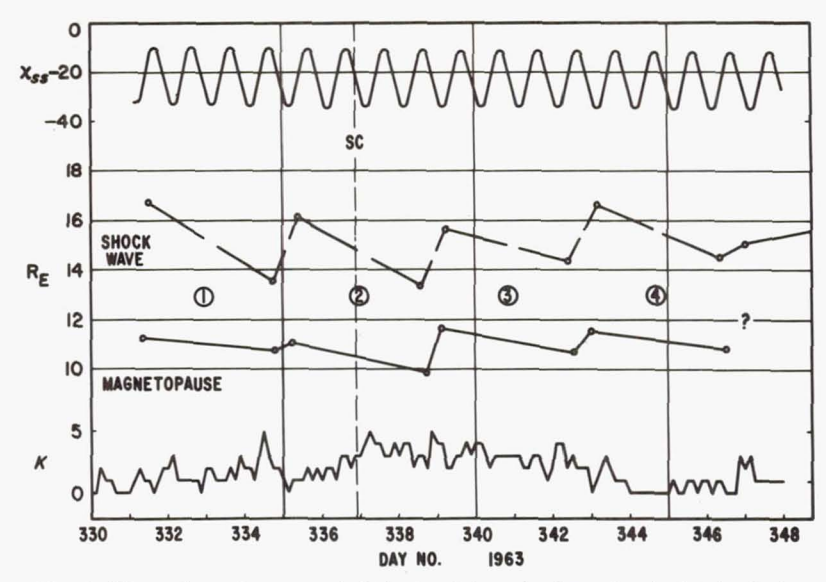


Fig. 6. Plots of χ_{ss} , the magnetic latitude of the subsolar point, in deg (top), the positions of the shock wave and magnetopause in units of R_E (center), and the Fredericksburg 3-hr geomagnetic index K (bottom) vs. time for Days 330 through 348, 1963

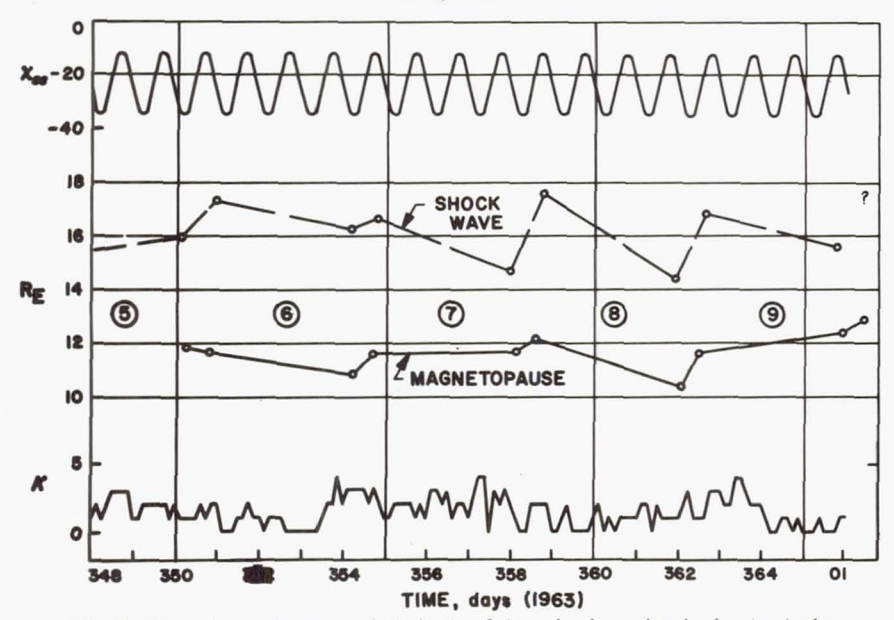


Fig. 7. Plots of χ_{ss} , the magnetic latitude of the subsolar point, in deg (top), the positions of the shock wave and magnetopause in units of $R_{\rm E}$ (center), and the Fredericksburg 3-hr geomagnetic index K (bottom) vs. time for Day 348, 1963, through Day 1, 1964

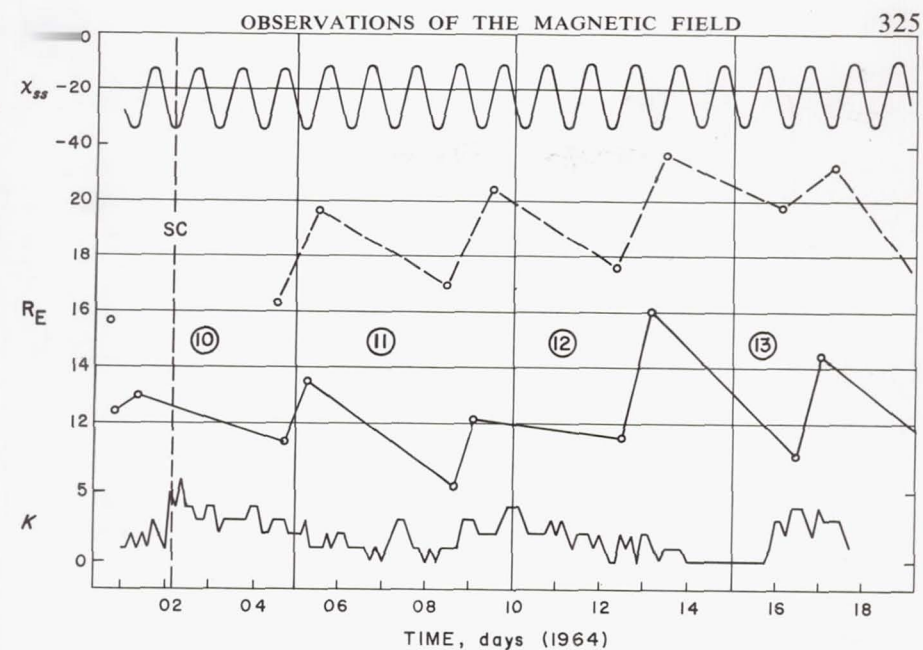


Fig. 8. Plots of χ_{ss} , the magnetic latitude of the subsolar point, in deg (top), the positions of the shock wave and magnetopause in units of $R_{\rm E}$ (center), and the Fredericksburg 3-hr geomagnetic index K (bottom) vs. time for Days 1 through

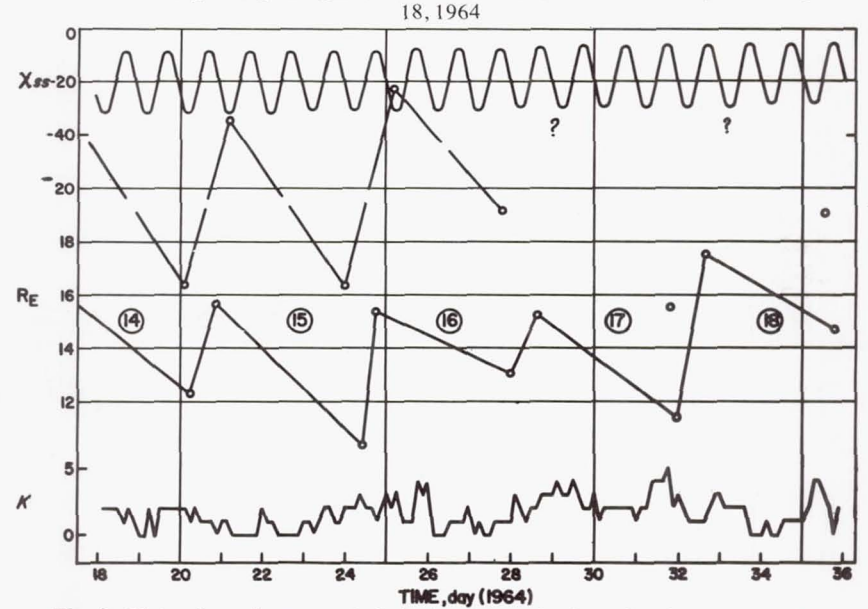


Fig. 9. Plots of χ_{ss} , the magnetic latitude of the subsolar point, in deg (top), the positions of the shock wave and magnetopause in units of R_E (center), and the Fredericksburg 3-hr geomagnetic index K (bottom) vs. time for Days 18 through 35, 1964

during the outbound and inbound pass of each orbit became much larger. Also, the distances to both the magnetopause and the shock wave became larger. At the same time, we have to consider certain transient phenomena as well as the variation of χ_{ss} . The maximum correction that will be made to the position of a boundary crossing to account for the effect of χ_{ss} is

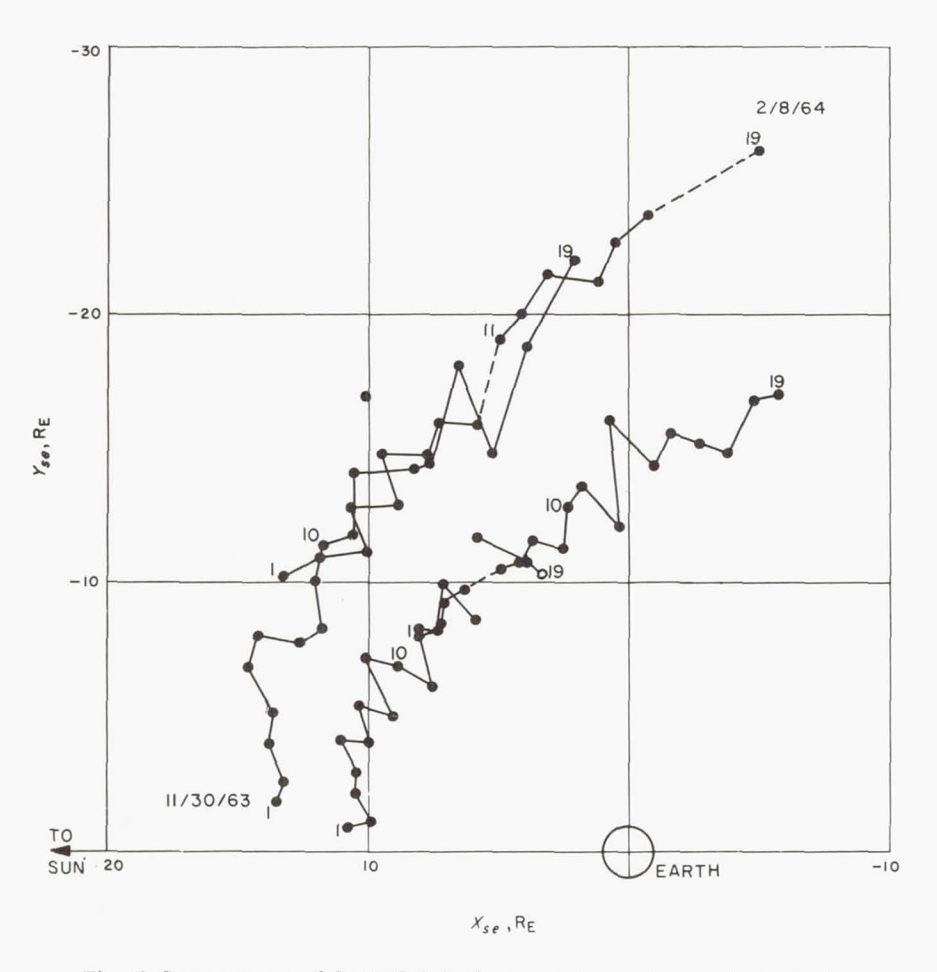


Fig. 10. Summary map of the IMP-I shock-wave and magnetopause transversals, as determined by the magnetometer experiment through the 19th orbit. Distances are given in units of $R_{\rm E}$

12%, which, although small, is about the same as the maximum observed variation of the boundary position. We feel that the correction for χ_{ss} is physically significant; it is a first-order correction for the variable angle of attack of the solar wind on the geomagnetic field. The residual

variations in boundary distances indicated the variability of the solar-wind pressure. The geomagnetic event of December 2 is indicated in Fig. 6; it compressed the magnetosphere with respect to its size on the previous inbound pass, but the boundary recovered by the time of the Orbit-3 outbound pass. The question marks in Fig. 9 indicate passes for which it was difficult to identify the boundary crossings according to our tentative rules; rather than prejudice ourselves, we have omitted these boundaries altogether.

Figure 10 is a summary presentation of the boundary crossings as determined thus far. The inbound passes of Orbits 1 through 19 are connected by straight-line segments; the outbound passes of Orbits 1 through 19 are similarly connected. The dashed lines indicate either that data for a boundary crossing are missing or that we are doubtful that the boundary crossing was properly identified. For example, we have put a dashed line for Orbit 13, which has been discussed previously as a rather anomalous type of boundary crossing according to the plasma data (see Paper 21).

Comparison of Observed and Theoretical Boundaries

Figure 11 illustrates the dependence of the magnetopause expansion factor K on χ_{ss} for a simple dipole field. The observed distance of each

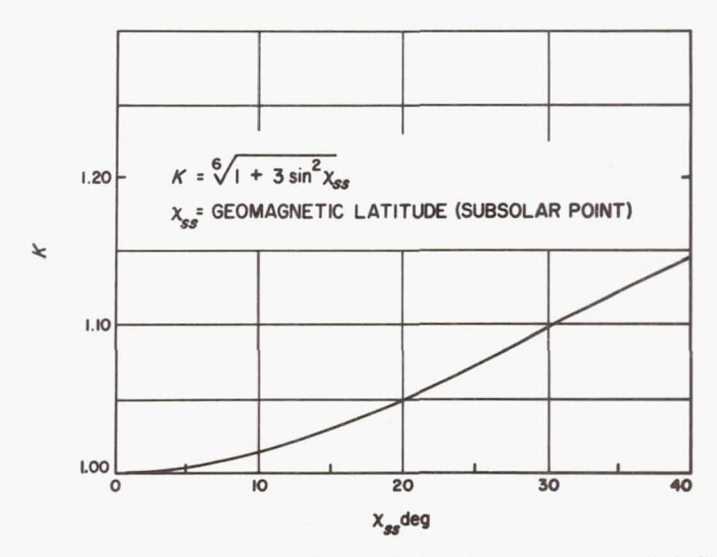


Fig. 11. Magnetopause expansion factor, K, plotted vs. the geomagnetic latitude of the subsolar point, χ_{ss}

boundary crossing is divided by the value of K appropriate to the value of χ_{∞} at the time of the crossing.

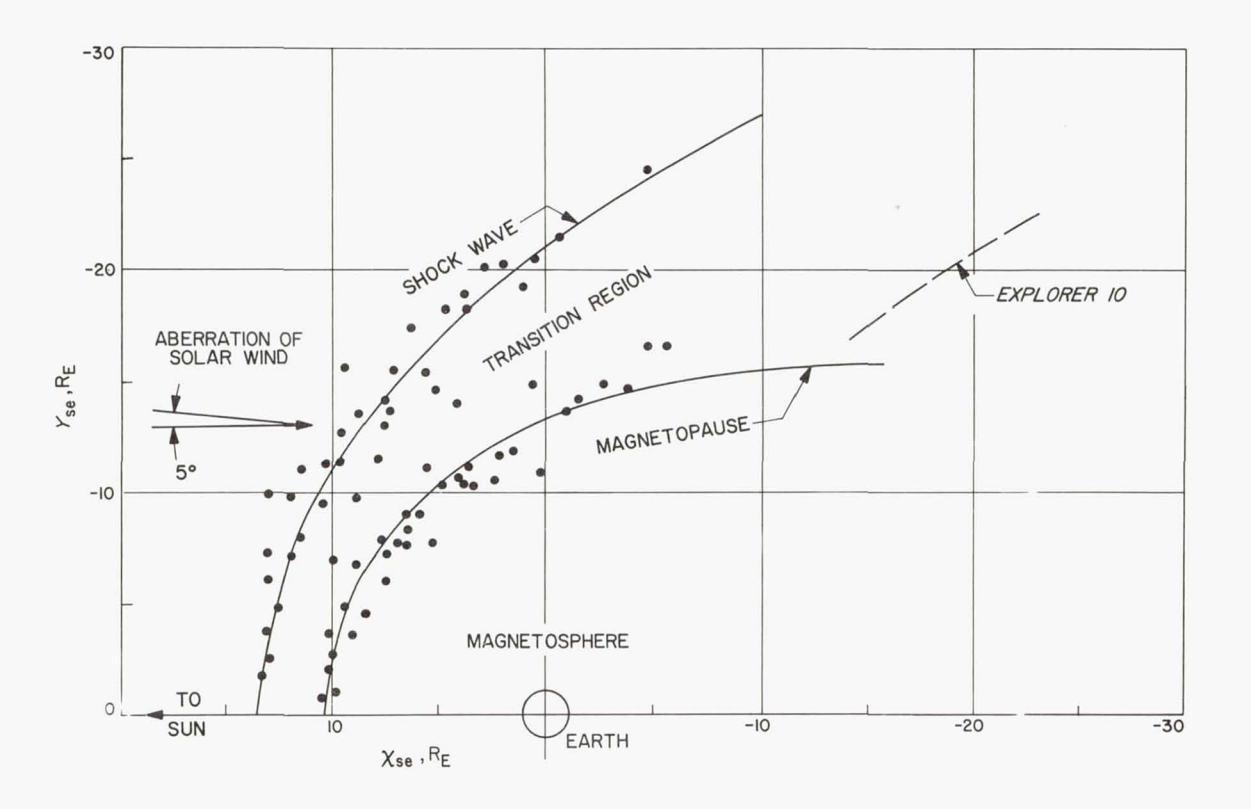


Fig. 12. Summary map of the shock wave and magnetopause, showing the rectified *IMP-1* boundary crossings (points) and the theoretical shapes (curves). The magnetopause geometry as determined by *Explorer 10* is also shown

Figure 12 shows the resulting corrected boundary positions as well as the theoretical position. The shock-wave boundary was calculated by Spreiter and Jones (Ref. 6), using blunt-body aerodynamics. To obtain the excellent agreement shown here, we had to rotate the direction of the pressure source by 5 deg, due to the aberration of the solar wind; a 5-deg aberration corresponds to a velocity of 360 km/sec. The curves were fitted to the data visually rather than by the least-squares method. It will be interesting to see whether the agreement between the observed and the theoretical positions holds on the dark side of the Earth.

The values chosen for the geocentric distances to the magneto-pause and to the shock wave (on the Earth–Sun line) are 10.25 and 13.4 R_E, respectively. The ratio of these two distances agrees well with the values predicted by authors who considered this problem from an aero-dynamic viewpoint (Ref. 6 and 7).

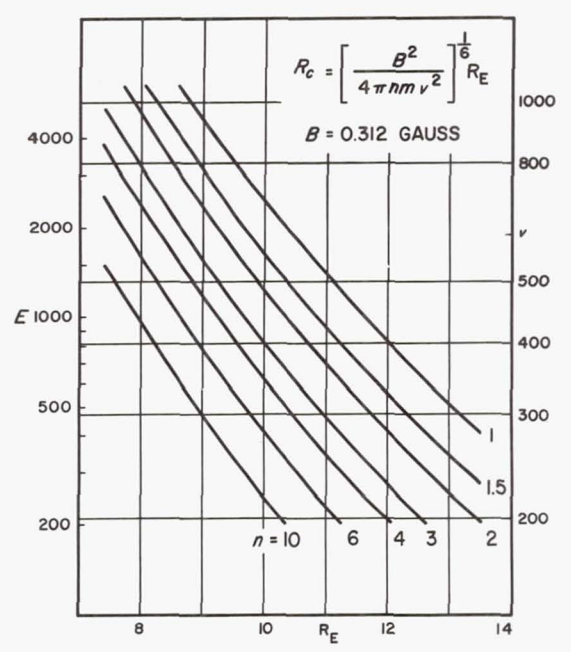


Fig. 13. Calculated proton energy (E, in ev) or velocity (v, in km/sec) vs. the distance of the magnetopause at the subsolar point (in units of R_E) for several values of proton density $(n, \text{ in cm}^{-3})$

Figure 13 summarizes what was described this morning as the Newtonian approximation of the solar-wind interaction with the geomagnetic field. The figure shows the expected relation between proton density, the position of the magnetopause, and the proton energy or velocity.

The pressure behind a shock wave is related to the pressure in front

330 N. F. NESS

of the shock wave. Now, if the effective pressure on the magnetopause is something like a half to one times the pressure in the undisturbed solar wind, then we can estimate the particle density necessary to contain the geomagnetic field, because we know the approximate velocity of the undisturbed solar wind from the MIT plasma detector. For a velocity of 400 km/sec, the density must be about 3 protons/cm³; or 6 protons/cm³ if the net directed pressure in the transition region is half the pressure outside. The theoretical distance to the magnetopause at the subsolar point, R_c , is given by

$$\frac{R_c}{R_E} = \left[\frac{B^2}{4\pi nmv^2}\right]^{1/6}$$

where B = 0.312 gauss, so that

$$\frac{\delta R_c}{R_c} = \frac{1}{6} \frac{\delta (nmv^2)}{(nmv^2)}$$

For a variation in the position of the magnetopause corresponding to $\delta R_c/R_c \leq 0.1$, as indicated by our data, the pressure of the solar wind can have varied by no more than 60% over the first 19 *IMP* orbits. Based on our consideration of the magnetic-field data, together with a reason-

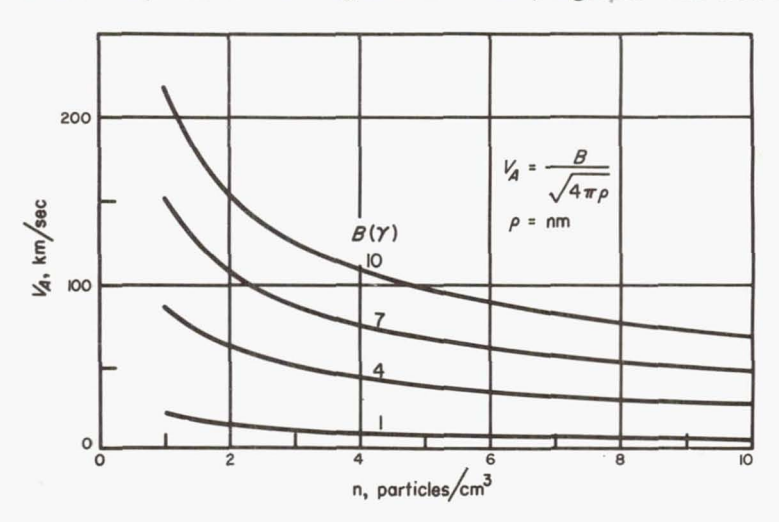


Fig. 14. Alfvén velocity V_A plotted vs. proton density n for several values of magnetic-field strength B

ably proper use of Newtonian and aerodynamic flow theories, estimated plasma properties are quite consistent with the actual plasma data obtained by the MIT experiment.

Figure 14 is a plot of the Alfvén velocity V_A as a function of particle density and magnetic-field strength. If we assume that it is the Alfvén velocity alone that is appropriate for the calculation of the Mach number of the flow, then we can compare the stand-off distances observed by the *IMP* satellite with theoretical stand-off distances computed from available aerodynamic models of high-speed or super-Alfvénic flow around a blunt body. I have previously pointed out (Paper 6) that the interplanetary field generally lies between 4 and 7 γ , with excursions to values as low as 1 γ and as high as 10 γ (except for the one case where we probably detected the wake of the Moon—see Paper 28). We have also indicated that the particle density is probably about 4 to 6 protons/cm³. For these values of particle density and magnetic field, the corresponding range of Alfvén velocities is between about 40 km/sec and about 75 km/sec. For a 400-km/sec solar wind, the corresponding Alfvén Mach numbers range between 7 and 10.

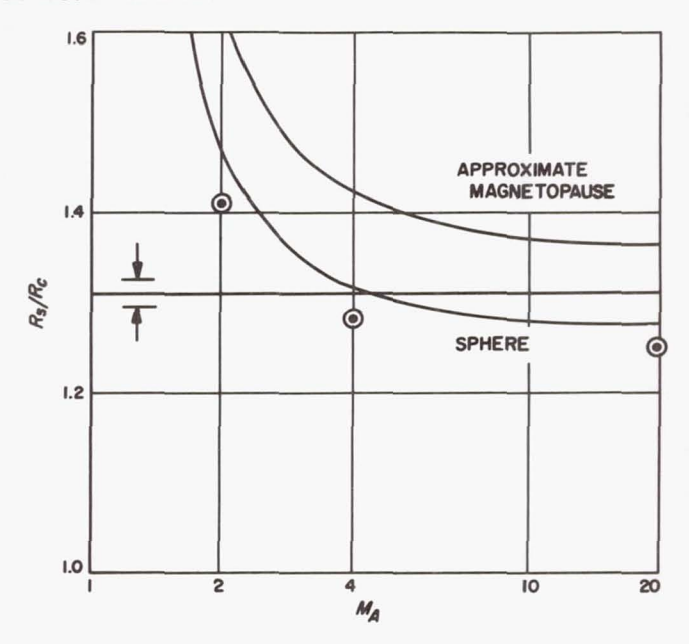


Fig. 15. Plots of the ratio R_s/R_c vs. Mach number M_A calculated for a sphere and a body with approximately the same shape as the magnetosphere, for $\gamma = 2$. R_s is the distance of the shock front, while R_c is the distance of the magnetopause from the center of the Earth, both at the stagnation point. The solid curves are from Ref. 3, and the circled points are from Ref. 4

Figure 15 shows the theoretical ratio of the shock-wave stand-off distance to the magnetosphere boundary distance as a function of Mach

332 N. F. NESS

number. The upper line in this figure corresponds to a blunt-body aerodynamic flow model for a specific-heat ratio of 2.0 (Ref. 6). The stand-off ratio for a spherical body is shown for comparison. The arrows bracket the stand-off ratio found from the magnetic-field data, which is 1.31 ± 0.01 . The observed ratio is thus substantially below the approximate magnetosphere curve. We know what happens in the case of a sphere when the specific-heat ratio is changed from 2 to 5/3, and thus I believe our results indicate that a value of 2.0 is too high, and that a value closer to 5/3 is probably more appropriate.

Figure 16 summarizes our interpretation of the conditions surrounding the Earth. This interpretation, of course, is based on the magnetic-field data described above. In this schematic drawing, a slight aberration is shown for the solar wind, and the interplanetary field is illustrated at

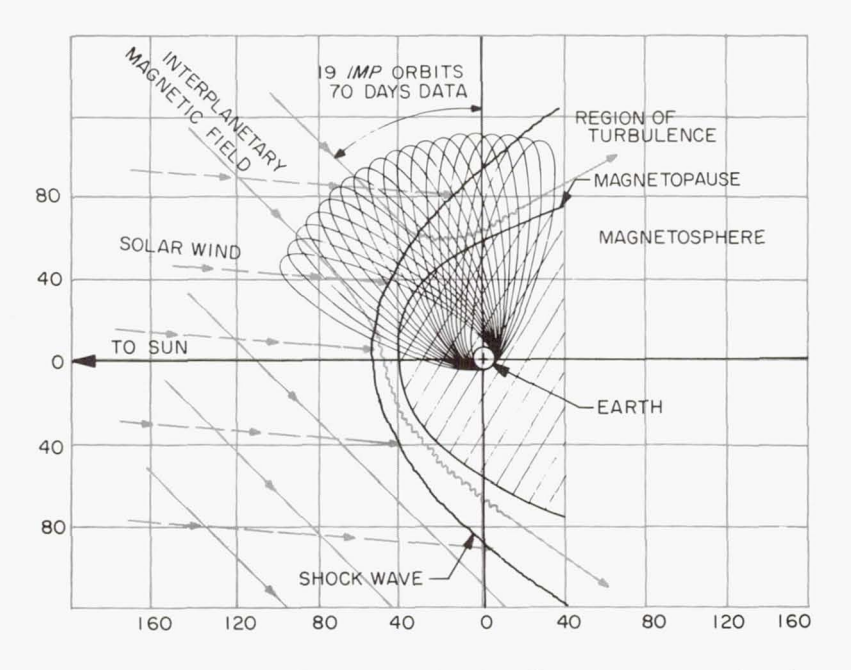


Fig. 16. Summary map of the near-Earth region of interplanetary space, based on the interpretation of the *IMP* magnetic-field data. The drawing is in the ecliptic; distances are given in thousands of miles

the streaming angle. When the orbit of *Explorer 10* is rotated around the Earth–Sun line to the ecliptic, it is seen that the boundary locations determined by *Explorer 10* agree fairly well with those determined by *IMP*.

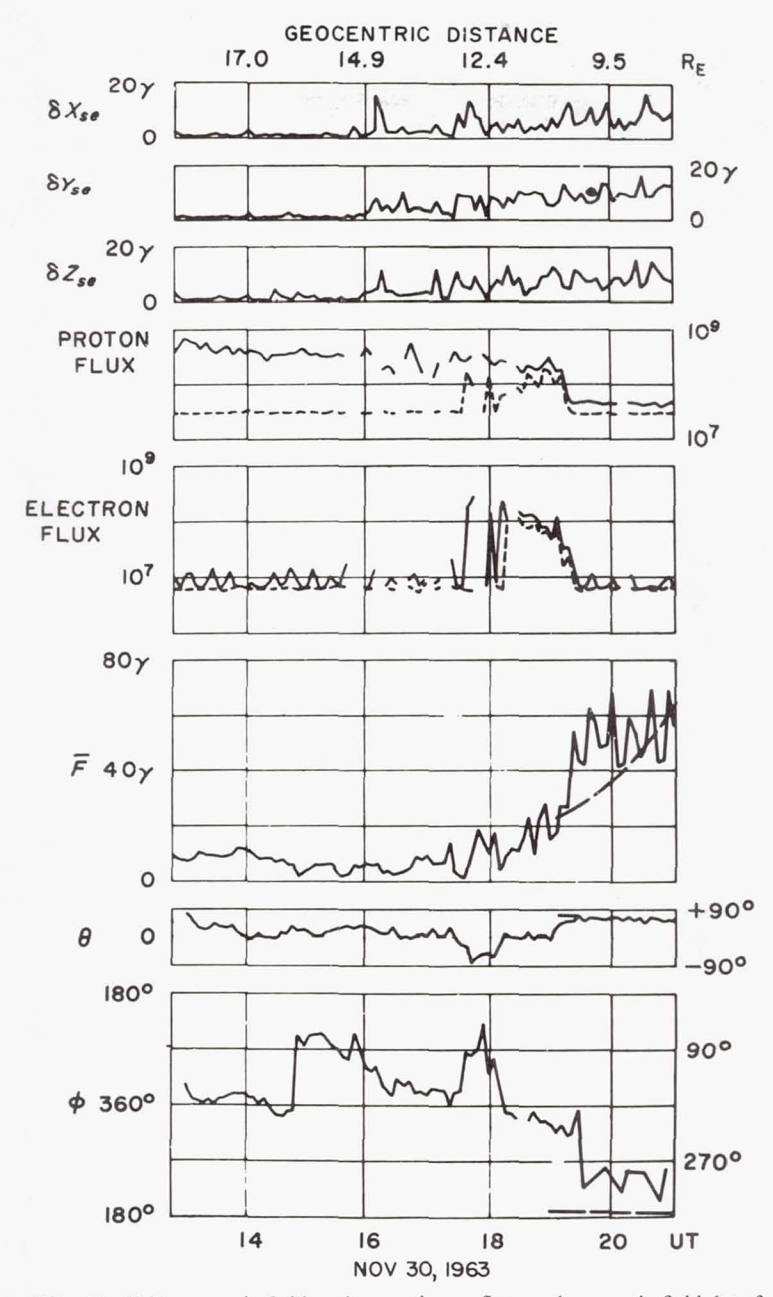


Fig. 17. *IMP* magnetic-field variance, plasma flux, and magnetic-field data from Orbit 1, inbound pass. Proton and electron flux are given in units of particles/cm² sec. The solid lines are fluxes from the Sun, the dashed lines are minimum fluxes

334 N. F. NESS

[Explorer 12 observed the magnetopause at 8 or 9 $R_{\rm E}$ near the stagnation point. This apparent discrepancy may be due to the probable decrease in solar-wind pressure during the time interval between the two satellite observations.]²

Correlation of Plasma and Magnetic-Field Data

Figure 17 illustrates a correlation of the magnetic-field data with the plasma data; this correlation represents a joint effort with the MIT experimenters. The data were obtained on the inbound pass of Orbit 1, very close to the Earth–Sun line. The magnetopause was detected at about 1920 UT, when the field suddenly increased and the angle ϕ changed abruptly. During this particular orbit, the geomagnetic field was almost normal to the ecliptic. Both the electron flux and the proton flux abruptly dropped to zero as *IMP* crossed the boundary at 10.8 R_E.

On the basis of magnetic-field data, we placed the shock wave at 13.6 $R_{\rm E}.$ This choice of boundary, however, doesn't fit the plasma data well: exactly what the plasma characteristics are in this region is hard to say, except that they are still variable. On the basis of the isotropy of the plasma flux, 13.0 $R_{\rm E}$ would be selected as the shock-wave distance. On the other hand, if we had based our choice of the shock-wave position on the magnetic-field variances alone, we might have placed it close to 14.7 $R_{\rm E}\,(\sim\!1610$ UT), outside of which the plasma also appears to have been quite uniform and steady.

Another interesting feature, which was not seen more than once or twice, occurred at about 1450 UT: the magnetic field changed by about 90 deg in the ecliptic, while at the same time the magnitude became very small. However, we don't see any corresponding variations either in the plasma properties or in the magnetic variance.

Summary

We conclude that there is a shock wave associated with the solar plasma flow around the Earth and its magnetic field, and this shock wave can be understood on the basis of an aerodynamic analogy. But, in addition, our detection of something beyond that shock wave indicates that the flow around the Earth has the properties of a plasma flow, and that we may have seen a transitory, but nonetheless spatially coherent, indication of the particle nature of the plasma. Another possibility is that the phenomenon resulted from the inherent instabilities associated with the plasma. We must continue to study correlations with other particle detectors on board the same satellite. More detailed correlations between the plasma and magnetic-field data will be forthcoming.

²Added in manuscript

REFERENCÉS

- 1. Cahill, L. J. and P. G. Amazeen, Journal of Geophysical Research 68, 1835 (1963).
- HEPPNER, J. P., N. F. NESS, C. S. SCEARCE, and T. L. SKILLMAN, Journal of Geophysical Research 68, 1 (1963).
- CAHILL, L. J. JR., IG Bulletin 79, Transactions, American Geophysical Union 45, 231 (1964).
- 4. Dessler, A. J., Journal of Geophysical Research 66, 3587 (1961).
- 5. Dessler, A. J., Journal of Geophysical Research 67, 4892 (1962).
- 6. SPRIETER, J. R. and W. P. Jones, Journal of Geophysical Research 68, 3555 (1963).
- 7. Kellogg, P. J., Journal of Geophysical Research 67, 3805 (1962).

Page intentionally left blank

THE SHAPE OF THE MAGNETOSPHERE AND THE DISTORTION OF THE GEOMAGNETIC FIELD

GILBERT D. MEAD

Goddard Space Flight Center, NASA, Greenbelt, Maryland

Basic Assumptions

The emphasis so far today has been on a fluid-dynamic approach to the study of the magnetosphere problem. I should like at this point, however, to review certain aspects of the Newtonian approach. Rather than admit that the Chapman–Ferraro approach is no longer very appropriate, I would like to defend it on the basis of a couple of significant points.

First of all, the Newtonian approach has been the only one, so far, that has been able to give some rather detailed results on both the shape of the magnetosphere and the strength and direction of the magnetic fields inside it. Quantitative predictions have been obtained that can be compared in detail with the data. Secondly, I don't feel that the assumptions based on the Newtonian approach have been invalidated, even though the shock wave predicted by the fluid approach must be taken into consideration. And finally, I think that, in a number of very significant areas, the results of Newtonian theory are supported by the *Explorer-12* and *IMP* data; and this fact indicates that the approach cannot be too far wrong.

So I would like, first, to review the assumptions upon which the Newtonian theory is based, and second, to try to determine the validity of the results based on these assumptions. Some of the results that I shall be discussing have already been published (Ref. 1 and 2).

First, we assume that the magnetosphere is closed; in other words, that the interconnection of field lines between the Earth and interplanetary space (the subject that we heard about this morning—Papers 17, 18, and 19) is not an important process, at least for the problems we are considering. According to the figures we heard this morning, perhaps 10% of the field lines are interconnected (Paper 18). I am not sure what that means—I wish those who make these assumptions about field-line interconnection could describe the effect in more detail. Since I don't know

precisely how to make such a calculation, our assumption is that the magnetosphere is closed.

Secondly, we assume that the magnetopause (not the shock wave) is determined by a balance between the magnetic pressure inside the boundary and a plasma pressure outside. I don't think that the pressure-balance equation is significantly affected by the presence of a shock wave or by fluid behavior outside the magnetospause.

The pressure inside the magnetopause is simply $B^2/8\pi$, but one must be careful in choosing the value of B. The value that we use is the self-consistent one: we take high-order approximations from an iterative procedure. In this way we avoid the original problem in which one had to know the shape of the magnetosphere in order to determine B, and vice versa.

The outside pressure is $2nmv^2\cos^2\psi$, where ψ is the angle between the velocity vector of the solar wind and the normal to the surface. This should probably be reduced by a factor of 2 because of the thermalization that occurs as the plasma passes through the shock wave. This will affect the scale, but not the shape, of the magnetopause. The factor of $\cos^2\psi$ may not be exact, either. However, the exponent of $\cos\psi$ must be close to 2 or 1.5-I don't think the exact value has a very important effect on the results.

Thus, although our formulas are based on the Newtonian approach, I believe that the fluid approach would give rather similar boundary conditions.

Up to now, we have assumed that the solar-wind velocity vector is perpendicular to the dipole vector, which means that our results are valid only during the spring and fall solstices. During the winter and summer, the results must be somewhat modified.

The Shape of the Magnetosphere

Figure 1 shows the magnetosphere shape as determined by applying the pressure balance condition at 5-deg intervals on the surface; the pressures are balanced at each point to within a small fraction of 1%. The results are described in an Earth-centered coordinate system in which the Earth-Sun line is the Z axis. θ is the polar angle and ϕ is the azimuth angle, with the equatorial plane corresponding to $\phi = 0$ deg. Distance is expressed in units of r_0 , which is equal to $(M^2/4\pi nmv^2)^{1/6}$, where M is the magnetic moment of the Earth's dipole field, and $2nmv^2$ is the pressure exerted by the solar wind at the subsolar point. The top curve in the figure is the boundary in the equatorial plane: the bottom curve is the boundary in the noon meridian. On the day side, the surface is nearly a hemisphere, as previously pointed out by Beard (Ref. 3). The point marked N is the position of a null point in the magnetic field.

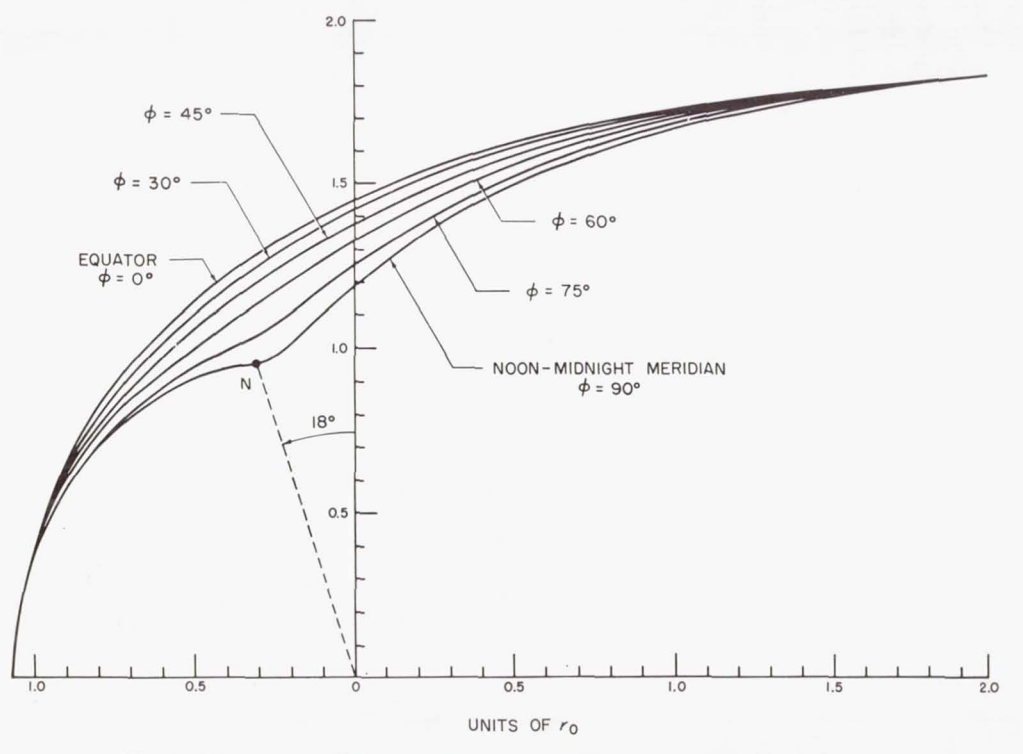


Fig. 1. Intersection of the calculated boundary of the geomagnetic field with planes of constant ϕ . The $\phi=15$ deg boundary is not shown because it is practically indistinguishable from the $\phi=0$ deg boundary. The Sun is at the left

Notice that all the lines seem to merge at the right. This feature means that, at great distances on the dark side, the surface becomes essentially cylindrical, with no closure of the cavity. Unfortunately, this shape does not agree very well with the *Explorer-10* data, which indicate that the surface may flare out at a fairly large angle in this region. The discrepancy could be caused by a number of effects. For instance, there may be some additional internal magnetic or plasma pressures that we haven't included, or conversely, the outside pressure may really be much smaller or may decrease at a much more rapid rate than it does in our theory. I suspect that this basic disagreement, if it really exists, results from the fact that there may be significant internal sources of pressure which we haven't considered. *IMP* hasn't yet passed through this region of space—I am very anxious to see what the *IMP* data will show during the next couple of months.

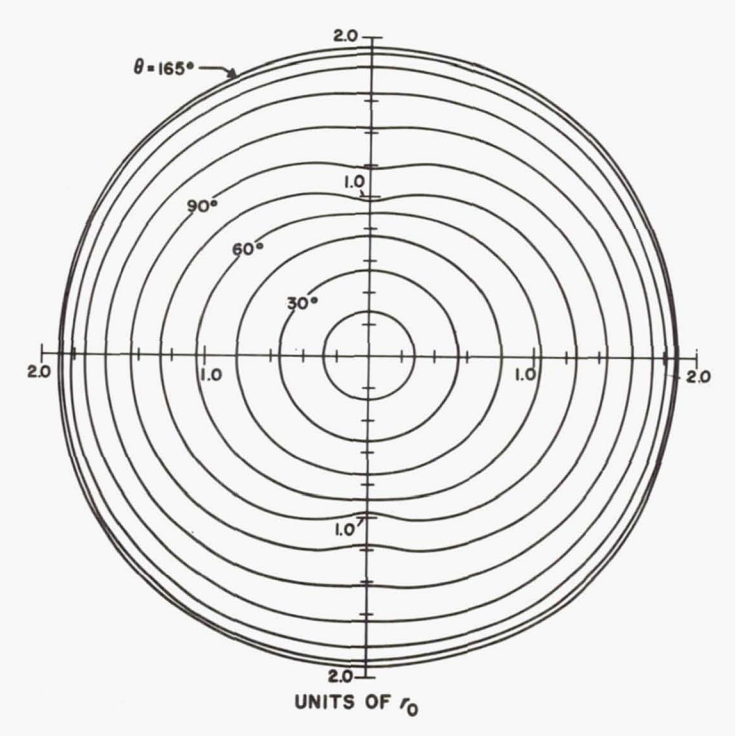


Fig. 2. View of the magnetopause as seen from the Sun. Each curve is the cross-section of the surface for a fixed value of θ (the angle with the Earth–Sun line)

Figure 2 is a view from the Sun of our calculated magnetopause. Notice the dimples at the null points. At large angles to the Earth–Sun line, the magnetopause has a cylindrical shape, as shown by the outer circle in the figure.

The Effect of Solar-Wind Temperature

In order to eliminate the assumption of zero temperature, I have examined a model in which the solar plasma has both a streaming velocity and a kinetic temperature. The plasma produces some transverse pressure on the boundary and thus tends to close it. Figure 3 shows how the boundary closes for various assumed values of kinetic temperature. A model like this one, of course, is subject to several reservations. The

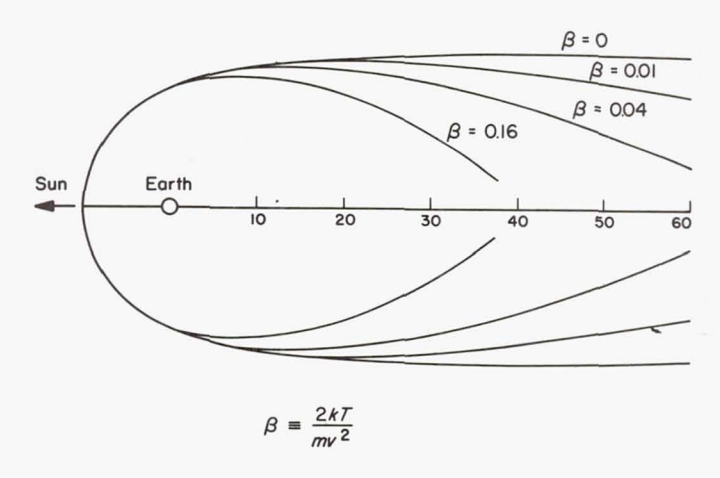


Fig. 3. Shape of the magnetopause for several values of β , the ratio of the thermal energy to the streaming energy of the plasma. Distance is in units of R_E

parameter β is the same as Marcia Neugebauer's θ (Paper 1); it is the ratio of the thermal kinetic energy to the streaming energy. Her results show that this ratio is usually about 0.01 and very rarely greater than 0.02. If the subsolar point of the boundary is at 10 R_E , and if $\beta=0.01$, then the boundary just begins to close off at 60 R_E , which is the distance to the Moon. Thus I believe that, at the distance of the Moon, the magnetosphere still exerts an effect.

The Field Within the Magnetosphere

The calculation of the magnetic field inside the magnetopause is based on another set of assumptions, most of which, I think, are fairly well justified. The main assumption is that the curl of the magnetic field is zero inside the boundary. In other words, the magnetic field is caused by currents at the boundary, but there are no currents inside the boundary where we are trying to determine the distorted magnetic field. If there were large currents near the Earth, then this assumption, and consequently our results, would be invalid.

This allows us to express the distorted magnetic field as the negative

gradient of a scalar potential, which can be expanded in a series of spherical harmonics. We assume that the solar wind is perpendicular to the dipole field and parallel to the Earth–Sun line, in which case the magnetic field has two planes of symmetry—the equatorial plane and the noon-meridian plane. These symmetries decrease the number of non-zero coefficients in the expansion, so that we can describe the field inside the magnetosphere rather simply, with only a few terms.

In a different spherical coordinate system in which θ is now colatitude and ϕ is now the local time measured from the midnight meridian, the dominant terms of the field components are:

$$\begin{split} B_r &= -\frac{0.62 \cos \theta}{r^3} - g_1^0 \cos \theta - 2\sqrt{3} \ g_2^1 r \sin \theta \cos \theta \cos \phi \\ \\ B_\theta &= -\frac{0.31 \sin \theta}{r^3} + g_1^0 \sin \theta - \sqrt{3} \ g_2^1 r (2 \cos^2 \theta - 1) \cos \phi \\ \\ B_\phi &= \sqrt{3} \ g_2^1 r \cos \theta \sin \phi \end{split}$$

where r is expressed in units of R_E .

The terms containing g_1^0 give a constant field in the northward direction everywhere inside the magnetosphere; this field must be northward because of the north-south and east-west symmetries. The terms containing g_2^1 give a field gradient that is stronger in the solar direction. Because of these latter terms, the field is not azimuthally symmetric.

The coefficients g_1^0 and g_2^1 depend on the solar-wind intensity through the parameter r_b , which is the distance to the boundary at the subsolar point:

$$g_1^0 = -0.2515/r_b^3$$
 gauss $g_2^1 = 0.1215/r_b^4$ gauss

With $r_b = 10 \text{ R}_{\text{E}}$, g_1^0 is 25 γ , which means that the surface current produces a 25- γ field near the Earth.

Figure 4 shows the distorted field in the equatorial plane. In the solar direction, the magnitude of the field just inside the boundary is somewhat more than twice the magnitude of the undistorted geomagnetic field. Away from the Earth–Sun line, the ratio is still about 2.

The fields at 30 deg north latitude are shown in Fig. 5, along with the angles δ and ϵ . These angles determine the field's direction and are the same as the solar-ecliptic angles θ and ϕ given by Heppner and others (Ref. 4) and by Ness (Papers 6 and 22). The angle δ is the angle that the field makes with the ecliptic, while ϵ is the azimuthal angle between the

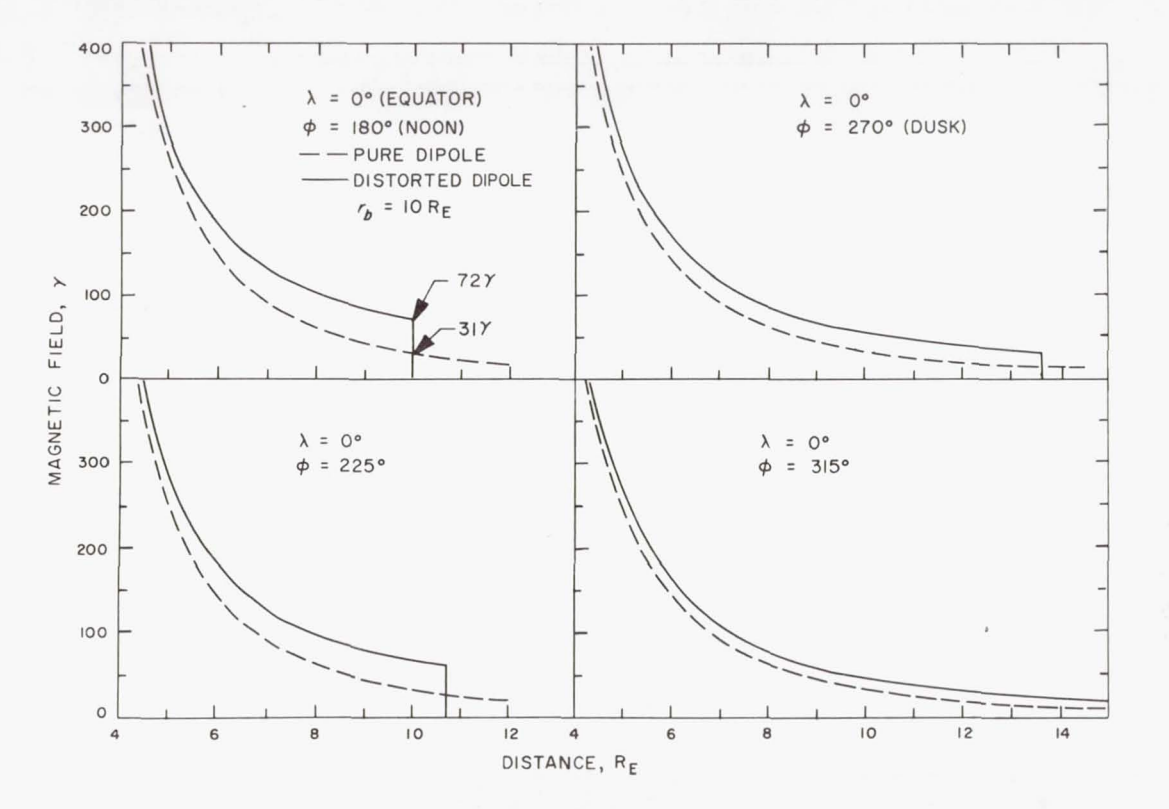


Fig. 4. Magnitude of the distorted field (solid line) as compared with the undisturbed dipole field (dashed line) in the equatorial plane ($\lambda = 0$). The direction is perpendicular to the equatorial plane

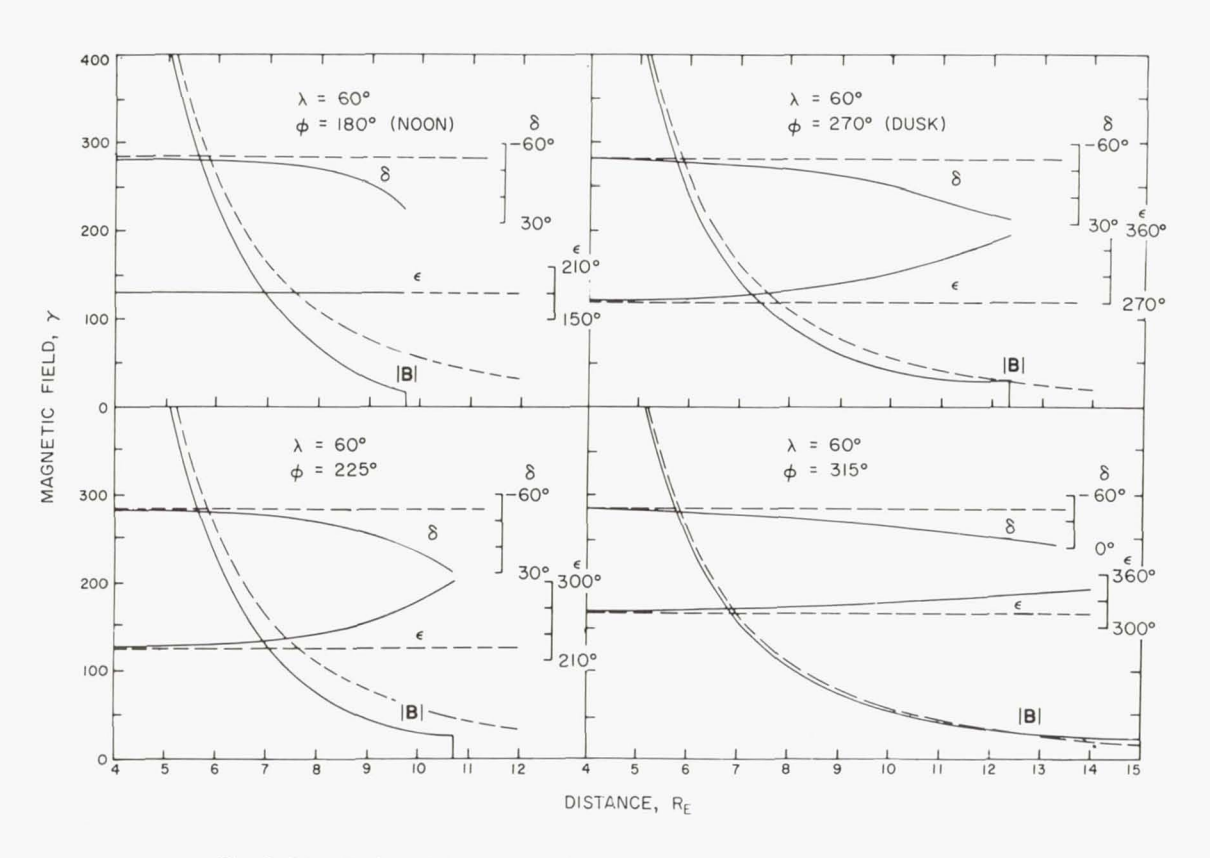


Fig. 5. Magnitude and direction of the distorted field (solid line) compared with the undisturbed dipole field (dashed line) at a latitude λ of 30 deg north

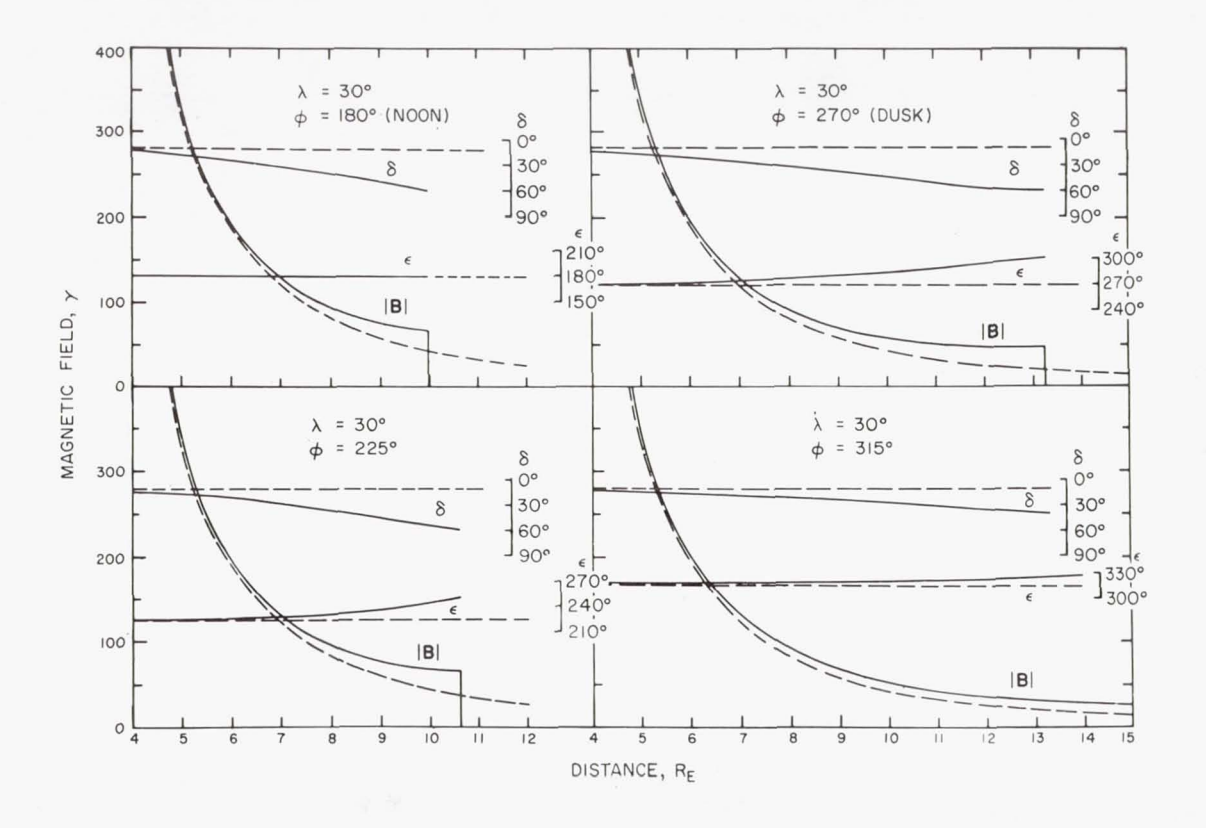


Fig. 6. Magnitude and direction of the distorted field (solid line) compared with the undisturbed dipole field (dashed line) at a latitude λ of 60 deg north

Earth–Sun line and the field component in the ecliptic. This figure demonstrates that both the magnitude and the direction of the total field depart considerably from those of the dipole field alone. Figure 6 presents similar plots for a latitude of 60 deg.

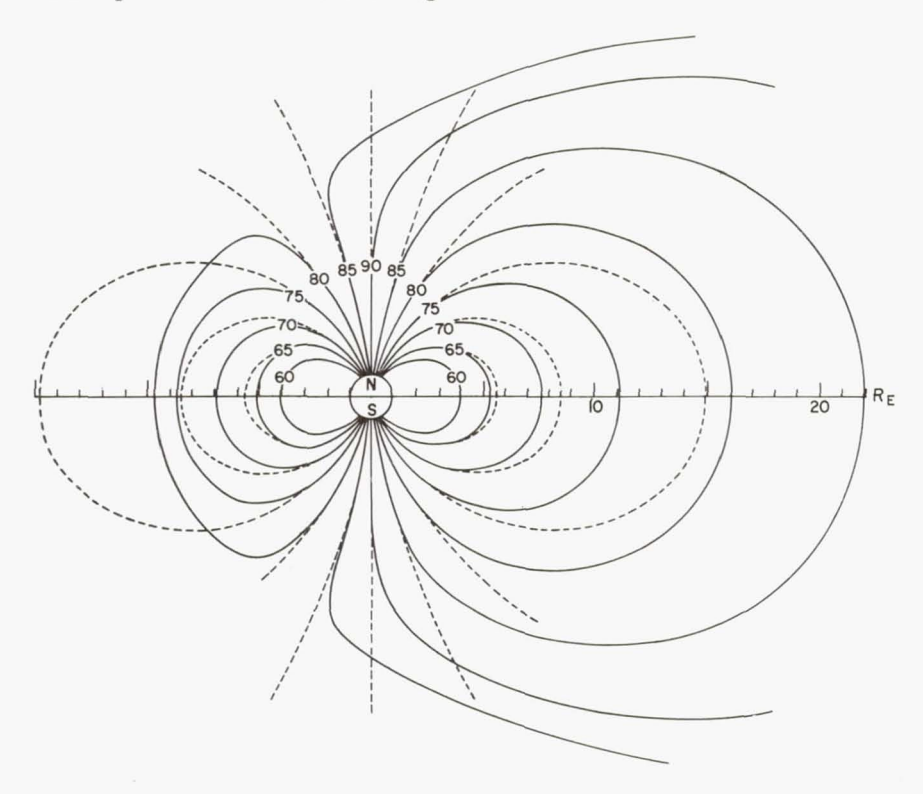


Fig. 7. Configuration of the distorted field (solid line) compared with the undisturbed dipole field (dashed line) in the plane of the noon meridian

Figure 7 shows the pattern of field lines based on our calculations. It shows the field compressed on both the solar and antisolar sides, so that I would disagree with Prof. Dungey's comment (Paper 17) that the lines of force are compressed on the day side and drawn out on the night side.

Thus we see that the Newtonian approach permits quite specific calculations of the distortion of the field. I feel that, in order to understand the trapped-particle data, it is important to understand where the field lines go. For this reason I am searching for a way to modify these calculations by including some of the non-Newtonian concepts, and I would be happy if anyone could help.

REFERENCES

- 1. MEAD, G. D. and D. B. BEARD, Journal of Geophysical Research 69, 1169 (1964).
- 2. MEAD, G. D., Journal of Geophysical Research 69, 1181 (1964).
- 3. BEARD, D. B., Journal of Geophysical Research 65, 3559 (1960).
- 4. HEPPNER, J. P., N. F. NESS, C. S. SCEARCE, and T. L. SKILLMAN, *Journal of Geophysical Research* 68, 1 (1963).

DISCUSSION OF PAPERS BY LYON, NESS, AND MEAD

Variability of the Transition Region

SCARF: The comparison of plasma-probe with magnetometer data for the first inbound pass of *Explorer 18* (Fig. 17, Paper 22) shows that the transition region can be remarkably broad and complex. I would like to return to Dr. Axford's very nice explanation of the meaning of supersonic flow, and to comment briefly on the possible origin of these complications.

In order to justify the use of continuum flow for a collisionless plasma-field interaction, one examines the waves which can be produced in the transition region. If v_0 (the wind speed) is greater than any reasonable wave speed, then the flow is "supersonic." Since v_0 is considerably greater than the local Alfvén speed, it has become customary to associate the highly super-Alfvénic flow with a distinct shock front. As Dr. Axford pointed out, however, other kinds of waves can be generated in the interface; one type that has not been discussed here is a longitudinal ion acoustic wave. The speed of this wave is $\sqrt{\gamma kT_e/m_p}$; where kT_e is the electron thermal energy, m_p is the ion mass, and $\gamma \ge 1$ depends on the shape of the electron distribution. For $\gamma = 1$, $T_e = T_i$, the ion-wave speed is somewhat less than the Alfvén speed, and the incident flow is supersonic in terms of sound waves as well as in terms of Alfvén waves. Actually, the ion waves are heavily damped for $T_e = T_i$, so that they need not be considered in this case.

However, if nonlinear effects—such as those associated with charge-separation electric fields—locally increase T_e/T_i , then damping is unimportant, and only a very small current or electron—proton drift speed is needed to generate instability. In the outer transition region, the MIT plasma probe shows that the electrons do, in fact, undergo greater thermalization than do the ions. From equipartition arguments we find that the maximum possible value of kT_e is $m_p v_0^2/4$, with a consequent reduction of the local ion-drift speed to $\sim v_0/\sqrt{2}$. Following this thermalization, the ion-wave velocity is $\sqrt{\gamma} v_0/2$, and the wave speed thus approaches or exceeds the local ion speed, $v_0/\sqrt{2}$.

I want to suggest that the ion-wave instability is relevant to the explanation of the broadening and variability of the transition region, the appearance of upstream precursors, superthermal electron peaks, and the occasional disappearance of any distinct outer boundary. Since the ion-wave frequencies overlap the local electron gyro frequency—

$$\nu_{max} = \frac{\sqrt{kT_e/m_p}}{\lambda_D}$$

¹Bernstein, W., R. W. Fredricks, and F. L. Scarf, *Journal of Geophysical Research* 69, 1201 (1964)

where λ_D is the Debye length—the wave–particle interaction can distort the electron-velocity distribution at low energies (0.5 to 3 kev) and can produce a small non-Maxwellian tail ($E \gtrsim 30$ kev). (In some experiments at Oak Ridge,² 100-kev electrons were easily produced by a related beam-plasma instability; Stix³ showed that in this case the electron plasma waves interact via the electron cyclotron resonance.) This distortion produces high-energy peaks, particularly in regions where the local magnetic disorder is small; and it tends to raise γ and broaden the ion-wave source region by the fast-diffusion process. The incident wind becomes less supersonic, and small fluctuations allow isolated precursors to travel upstream and dump ion-wave energy in isolated electron spikes. When the distortion of the velocity distribution is high enough, the incident wind becomes subsonic with respect to ion acoustic waves, and the entire sheath relaxes until the next solar-wind enhancement initiates a new transient.

GOLD: I want to comment about Orbit 13, which Mr. Lyon was discussing. I wonder whether it is quite fair to think of the dynamic pressure as having to change by a factor as big as the one he assumed. The stand-off distance depends, after all, on what occurs behind the shock front and, in particular, on what materials have been deposited there. Could we not have a great variation in this material occurring at the time of Orbit 13? For example, if an extremely crinkly field had been in existence outside at that time, its crinkliness would have tended to become greatly amplified as it passed through the shock, and the field would then perhaps have been in a medium which had far less pressure for a given compression. A very contorted field will possibly give way much farther than will a field whose lines are more or less parallel. In other words, γ is nothing like 5/3, but is whatever the chance geometry of the field imposes. Maybe the field at the time of Orbit 13 was very wobbly, which made the stand-off distance much smaller.

LEES: The value of γ may approach 1 in places where there are many degrees of freedom.

NESS: Magnetic-field data were shown for Orbit 6; however, I haven't plotted the data for Orbit 13. The conditions during Orbit 13 may not have been the same, but the data for Orbit 6, during which we saw a very strange set of conditions, indicated that the field outside was very stable. Clearly, we have to do some additional work to find out what the field conditions were during Orbit 13, in order to determine whether the variance was particularly high. I don't recall that it was.

FREEMAN: I would like to make a brief comment about the variability of the boundary position. I think this comment may place the *IMP* data in the proper context with respect to the changing solar cycle.

During the 112-day lifetime of Explorer 12, which took place some $2\frac{1}{2}$ years earlier in the solar cycle, there were three magnetic storms with main-phase excursions in excess of 100 γ . The average magnetospheric boundary position

²Alexeff, I., R. V. Neidigh, W. F. Peed, E. D. Shipley, and E. G. Harris, *Physical Review Letters* 10, 273 (1963)

See also

Kharchenko, I. F., Ya. B. Fainberg, R. M. Nikolayev, E. A. Kornilov, E. I. Lutsenko, and N. S. Pedenko, *Nuclear Fusion Suppl.* Pt. 3, 1101 (1962)

Smullin, L. D. and W. D. Getty, Physical Review Letters 9, No. 2, 3, (1962)

³Stix, T. H., Princeton University Plasma Physics Laboratory MATT-239, Princeton University (1964)

during the first $2\frac{1}{2}$ months of data from *Explorer 12* was at approximately $10~R_E$ (66,000 km, to be precise). However, the closest observed boundary position was at about 8.5 R_E , while the farthest observed position was beyond the satellite apogee, which was at $13~R_E$. Both of these extremes were observed on several occasions. These observations indicate that *Explorer 12* saw a much more variable magnetospheric boundary position than *IMP* did, which would be expected on the basis of the enhanced magnetic activity at that time.

NESS: Your statement that the average distance of the magnetopause was about $10 R_E$, which I hadn't realized before, makes the long term constancy of the solar wind even more impressive. If the average pressure of the solar wind is roughly constant through $2\frac{1}{2}$ years of the solar cycle, we can conclude that there is something basic about the physics on the surface of the Sun, even though the variability

is much higher in other solar-cycle phenomena.

SLUTZ: Isn't the constancy of the magnetopause's position perhaps more a testimony to the insensitivity of the sixth root, since theoretically the distance from the Earth's center is proportional to (pressure) $^{-1/6}$? The figures that were quoted -8 and 13 R_E – correspond to a change in the solar-wind pressure by a factor of 18.

Dr. Mead has, I think, very appropriately and ably commented on the difficulties of studying the flow about the magnetosphere. Insofar as this flow affects the shape of the back portion of the magnetosphere, one could have a very wide range of pressure functions from the head pressure to the back pressure and still get very nearly the same shape, which testifies again to the glories of the sixth root. However, an interesting feature is that it takes very, very little back pressure to hold the back end of the magnetosphere in to only 25 or 35 $R_{\rm E}$.

WILKERSON: I want to ask Mr. Lyon about Dr. Ness' last slide, which compared the magnetic and plasma data. Outside the magnetic boundary, there appeared to be a fairly regular oscillation of the electron flux. There were perhaps about six oscillations in a 2-hour period, which looked like, say, a millicycle phenomenon. These oscillations perhaps arose from structure in the solar wind, or perhaps originated at the Sun itself.

LYON: I can only say that sometimes we do see such behavior and sometimes

we don't. The effect is probably real.

AXFORD: With regard to the observation of fluctuations in a collision-free shock, it should be realized that such a shock is very much like a hydraulic jump. If one looks at the hydraulic jump formed when a river comes up against a bridge piling, it will be seen that the jump is quite sharp, but it dithers all over the place and there is considerable fluctuation on a small scale. We should expect to see a similar messy and confused structure in the collision-free shock.

SMITH: I have a question for Dr. Ness. You had an opportunity to observe reasonably-high-frequency fluctuations during the fluxgate sampling periods, and Dr. Scarf indicated that high-frequency fluctuations may be important. Have you

had an opportunity to look at this aspect of the data?

NESS: No, but it is an obvious thing to investigate. In anticipation of this work, I should like to point out the limitations in our sampling and analysis procedures, and the spectral bands we are going to be able to investigate. We sample for about 5 seconds once every 20 seconds, and sampling every 20 seconds leads to a

⁴These magnetospheric boundary positions were determined by the State University of Iowa energetic-particle detectors carried on *Explorer 12*. See Freeman, J. W. Jr., *Journal of Geophysical Research* **69**, 1691 (1964)

folding frequency of 0.025 cps. Since we are doing some smoothing which will help solve the aliasing problem, we can expect that the spectrum we eventually get will be free of any strobe effect.

SMITH: One other thing: *Explorer 12* observed some very large fields on certain passes. The oscillations were 50 γ or so, peak-to-peak, with relatively long periods. I wonder if you have seen anything of comparable magnitude. If not, we may have another indication of changing solar conditions.

NESS: If I recall the work of Cahill to which you are referring, *Explorer 12* was considerably inside the magnetosphere relative to the positions I have been discussing.

SMITH: The observations I was thinking of were in the transition region, outside the characteristic change in field direction that indicates the termination of the magnetosphere. Also, there were very large changes on *Pioneer I* – 50 or 100 γ , peak-to-peak. It is difficult to determine from your variances and from your averaged data whether you see such large fluctuations.

NESS: No, we do not.

SMITH: Can you estimate what the largest magnitude may be?

NESS: Near the Earth–Sun line we probably see a maximum average of around 10 to 20 γ , and a maximum variance of 5 to 15 γ .

PETSCHEK: I should like to ask Dr. Ness whether he has had a chance to look for any correlation between the direction of the magnetic field ahead of the shock and the appearance of both the shock transition and the precursor. The reason for this question is that waves and particles can propagate much more freely along field lines; therefore, you might expect a broader shock and more of a precursor if the magnetic field were normal to the shock.

NESS: Not as yet.

BEARD: If you follow the individual particle trajectories, then it is easy to show that as you move from the weak interplanetary field into the transition region—in which the magnetic field is greater by a factor of 2 or 3—there will be an electric field at the boundary, and all of the forward motion of the protons will be given to the electrons that go through this boundary. Thus in the transition layer, electrons will have an energy of the order of 1 keV, which is akin to what Prof. Axford has said.

In this connection, I am very worried about the *IMP* plasma measurements. A satellite in a medium in which there are a great many electrons having an energy of the order of 1 kev will become negatively charged to about 1 kv, and all the protons detected by the satellite will have fallen through this potential and will thus have a very high energy. Although secondary electrons and, to a much lesser extent, photoelectrons, can reduce this potential, I doubt that a complete reduction is possible for most satellite surface materials.

NESS: It is unfortunate that Dr. Serbu isn't here to answer this very critical question about the possibility of satellite charging. I think his *IMP* ion-trap experiment indicates no spacecraft charging, except to perhaps a volt or two negative.

BLOCK: I wonder if it is possible to measure the charge of the satellite. Someone should think seriously about it.

BRIDGE: I don't know how to do it. Some instrumentation has been developed to provide information on the charge of satellites in the ionosphere, but I am not sure that any of these techniques can be extended for use in deep space. I think it would be nice if some more theoretical work were done.

As for the influence of 1-key electrons, it is quite obvious that for such electrons

impinging on metal surfaces, the secondary-electron production rate is great enough to nullify the incoming current and to hold the spacecraft potential near zero.

LÜST: I have a question for Prof. Axford. Sometimes you consider the important parameter to be the Debye length, while at other times you use the gyration

radius. Would you comment on this?

AXFORD: When I say that the minimum thickness of a collisionless shock is the gyration radius, I am trying to be conservative. However, one might expect some degree of fluid-like behavior, even when the dimensions of a body in the flow approach a few Debye lengths.

GOLD: The size of a body must be equivalent to many Debye lengths for the streaming instability to develop.

Open vs. Closed Magnetosphere

DAVIS: This is a slight change in subject, but we heard considerable discussion this morning about whether the field lines connect across the magnetopause. In the *IMP* data, we see discontinuous changes in the field as we go across the boundary. If the change in the field is discontinuous, and if the field lines do not cross the boundary, then the plane of the boundary can be determined from the field lines on the two sides. Based on this assumption, do the *IMP* data indicate a sensible boundary?

NESS: We haven't yet taken the cross product necessary to determine the surface shape. We could possibly get a considerable amount of scatter if the surface is not perfectly smooth or if it changes with time. Such scatter could degrade our sensitivity to this very critical measurement of connectivity.

SMITH: I have a question for Mr. Lyon. Did you see any plasma inside the

magnetosphere?

LYON: No protons, just electrons.

The Back of the Magnetosphere

SLUTZ: I would like to mention a calculation that agrees very well with Dr. Mead's calculation for the front face of the magnetosphere, but gives a very different picture for the back.

I have carried through a self-consistent solution in which the pressure is taken to be $A+B\cos^2\psi$, and I have obtained a complete solution, including both the front and back faces. The constant A can be interpreted as a thermal pressure, while the constant B is the mass-motion pressure. My solution very definitely shows a rather broad and flat back face of the magnetosphere. If we take $A=10^{-2}\,B$, as indicated by the data from *Mariner 2*, the back face will extend to about 25 R_E; if we take $A=10^{-3}\,B$, it will extend to 35 R_E; and if we take $A=10^{-4}\,B$, which is unreasonable, it will extend to only 40 or 50 R_E.

Now this raises an interesting question. Certainly the flow of solar wind does not close around such a short, fat boundary. Consequently, I propose that—analogous to the aerodynamic flow around a relatively blunt object—there is a second region in back in which the fluid separates from the boundary and closes, perhaps at a very large distance. This second region is a "backwater" of solar-wind turbulence, and the pressure here can be very small and still limit the back boundary of the magnetosphere to 25 or 35 R_E. Experiments in real fluids indicate that the pressure in such a region is 2 or 3 times the static pressure in the flowing fluid.

If you take two such boundaries for the case $A=10^{-3}\,B$, and if you set the front face at the distance indicated by Cahill's *Explorer-12* data,⁵ then the position of the back boundaries agree with the positions of the boundaries observed by *Explorer 10.*⁶ Of course, we are approaching the moment of truth with the observations about to come from *IMP*, and it will be very interesting to see what develops.

AXFORD: If only the pressure of the solar wind were involved, then the field lines on the back side of the magnetosphere would be curved, as in a dipole field. However, the evidence indicates that the field is dragged out, which requires a shear stress in addition to the normal stresses that are usually taken into account. **BRIDGE:** It was mentioned earlier today that the magnetic-field fall-off observed on *Explorer 10* was much slower than that expected for the dipole field. Do any other results show the radial variation of the field behind the Earth?

NESS: Yes. It does increase as you come around the back side.

BRIDGE: I should think that the radial variation would considerably affect some of the pictures that have been drawn of the magnetic-field configuration.

⁵Cahill, L. J. and P. G. Amazeen, *Journal of Geophysical Research* **68**, 1835 (1963) ⁶Heppner, J. P., N. F. Ness, C. S. Scearce, and T. L. Skillman, *Journal of Geophysical Research* **68**, 1 (1963)

Session V

SOLAR-WIND INTERACTION WITH COMETS AND WITH THE MOON

Page intentionally left blank

CHAPTER XXIV

THE INTERACTION OF THE SOLAR WIND 9. 7 0. WITH COMETS (NATURAL AND ARTIFICIAL)

LUDWIG BIERMANN AND REIMAR LÜST

Max-Planck-Institut für Physik und Astrophysik, Munich, Germany (Presented by Reimar Lüst)

Introduction

Despite the fact that we will get better and better results from spacecraft in the coming years, important observational evidence concerning the solar wind will continue to be obtained from comets as well as from radio-wave scattering, zodiacal light, and cosmic rays. In fact, if we understand properly the interaction of the solar wind with comets, we may hope to obtain further detailed information about the solar wind that cannot be obtained in the near future from space probes. One reason is that comets occur in any latitude, while it will remain difficult to orbit space vehicles at large angles to the ecliptic.

We will discuss four points: (1) the evidence that we have for the solarwind interaction with comets; (2) the different types of interaction that may occur between the solar wind and comets; (3) some of the theoretical aspects that may be important in this connection (this topic will be discussed further by Prof. Biermann in Paper 25); and (4) some preliminary ion-cloud experiments that may help us in understanding the physics of comets and their interaction with the solar wind.

Properties of Comets

By way of background information, let us briefly describe the properties of comets. There are three types of comet tails, according to the classifications given by Bredikhin. Type-I tails consist of CO+, N₂+ CO₂+, and other ions, and this type is of especial interest to our discussion today. Type-II and Type-III tails are composed mainly of dust particles or nonionized molecules. The differences between Type II and Type III are not relevant here.

It is believed that a comet has a solid nucleus with a diameter of about 10 to 20 km. This nucleus probably consists of dust and frozen molecules composed of C, N, O, and H. According to a model proposed by Whipple (Ref. 1 and 2), the molecules form a sort of icy block, with the dust particles frozen into the block.

If a comet approaches the Sun to within a few astronomical units, it develops a coma consisting of non-ionized gas molecules like CN, C_2 , C_3 , CH, NH, and OH. It will have, in addition, one or two tails. The long, straight tail is a Type-I tail and points in a direction almost radially away from the Sun; the other tails, Types 11 and 111, are often curved. The coma has a diameter of very roughly 10^5 km; the tails have a diameter of about 10^5 km and are up to 10^6 or 10^7 km long.

Figure 1 shows Comet Mrkos 1957d on four different days. The picture was taken at Mt. Palomar with the 48-in. Schmidt telescope. You can see very clearly that there are two different types of tails. One is curved and has no structure, while the other is the straight, ionized tail, which we will discuss here. You can see certain changes occuring in the 4-day interval.

Accelerations in Ionized Comet Tails

The question now is: what is the evidence that the solar wind is interacting with these Type-I comet tails, as was first proposed by one of the authors (Ref. 3)? The most striking observational evidence for such an interaction is the acceleration observed in the comet tails. The Type-I tails normally have high accelerations, of the order of 10^2 or 10^3 times solar gravity, while the dust tails have accelerations of the order of solar gravity (which is equal to 0.6 cm/sec² at 1 AU). The accelerations in dust tails can be explained by the pressure of sunlight. However, the accelerations in ionized tails are far too high to be explained by this mechanism. This leads us to believe that these high accelerations have something to do with the interaction of the charged particles with the solar wind.

Correlation Between Geomagnetic and Cometary Disturbances

The second and more direct evidence of such an interaction is the correlation between the geomagnetic and cometary disturbances. Of course, only a few cases of such a correlation have been found, because the comet has to be in the right position. Specifically, the comet has to be in the lower heliographic latitudes, otherwise it will not be hit by the enhanced corpuscular stream. Also, the difference in longitude between the Earth and the comet must not be too great, otherwise the corpuscular stream will have changed its intensity. However, two very striking evidences for such a correlation between the geomagnetic perturbation and the activity of the comet have been found (Ref. 3): Comets Halley 1901 II, and Whipple–Fedtke–Tevzadze 1962g. Rhea Lüst also found a very good correlation for Comet 1899 I, which appeared during a period of low solar activity when only one strong persistent source of corpuscular radiation was present on the Sun.



Fig. 1. Four views of Comet Mrkos 1957d, photographed with the 48-in. Schmidt telescope. Photograph from the Mt. Wilson and Palomar observatories

But of course these cases are connected with only the enhanced geomagnetic activity. The next question is whether the existence of an ionized comet tail depends on the presence of enhanced corpuscular radiation. It has been statistically determined that the presence of a plasma tail does not noticeably depend on the general level of solar activity. A very good demonstration of this fact is that several comets with normal tail activity have appeared during extended periods of low geomagnetic activity.

Aberration Angle

There is one very striking piece of evidence of the interaction of a Type-I comet tail with the normal, undisturbed solar wind. This evidence was found by Hoffmeister and explained by Biermann. The direction of an ionized tail is not quite in the radial direction; it lags behind the radius vector with respect to the orbital motion of the comet. The angle between the tail and the radius vector is on the order of 3 to 6 deg, and can be explained as a kind of aberration caused by the component of the comet's orbital velocity perpendicular to the radius vector. This velocity is about 30 to 50 km/sec. If we assume the simplest case of a mechanical momentum transfer, then from the observed aberration angle we calculate a solar-wind velocity of a few hundred km/sec.

Since the aberration angle apparently reflects the orbital motion of the comet, which is on the order of 30 to 50 km/sec, and since we obtain the right order of magnitude for the solar-wind velocity, it is clear that the solar-wind velocity component perpendicular to the radius vector cannot be large: it cannot be more than 50 km/sec and is probably even less than 30 km/sec. If the solar wind at 1 AU were co-rotating with the Sun, it would have a velocity on the order of 450 km/sec perpendicular to the radius vector, which certainly does not show up in the comet tails. This is very strong evidence that the solar wind at 1 AU is not co-rotating with the Sun. Statistical investigation shows also that there is no difference in aberration angle between comets with direct orbits and comets with retrograde orbits. Therefore, this kind of observation provides very strong additional evidence that the solar wind does not co-rotate with the Sun out to 1 AU.

Types of Interaction

The next question is: what types of interaction can we expect? I will discuss different types, and then will try to draw some theoretical conclusions.

1. Mass Flow

Of course, the first type of interaction is simply by means of the mass flow, since the mass of the solar wind flows past the comet. From the observations of comets, and particularly from the interpretation of the observations of the O I line (Ref. 4) and the origin of the CO⁺ ions, Biermann and Trefftz conclude that about 10^{31} molecules/sec are lost from a rather bright comet (Ref. 5). With an average molecular weight of 20, this rate corresponds to a mass loss of the order of 3×10^8 gm/sec. The mass flow of the solar wind through a coma with a radius of 10^5 km would be about two orders of magnitude smaller than the mass loss of the comet. Therefore a sphere somewhat larger than 10^6 km is necessary to make the two mass flows comparable.

2. Charge Transfer

The next interaction mechanism that should be discussed is the so-called charge transfer between the solar wind and the cometary material. This means that a solar proton encountering a neutral CO or N_2 molecule may produce an ion of the molecule by picking up an electron to form a neutral hydrogen atom. Now, the cross-section for this kind of interaction depends strongly on the nature and the energy of the particles. In the case of CO, particularly, this cross-section is very large (about 3×10^{-15} cm²) at velocities of 200 to 2,000 km/sec. If one assumes that the solar wind has a flux of 10^8 ions/cm² sec, then one can obtain a time scale for charge transfer of about 35 days. For a comet, this is a rather long time scale. A time scale on the order of one day, or even shorter, is required to explain the changes observed in the features of the comet tails. Therefore, this mechanism cannot be solely responsible for the ionization of the cometary material. Nevertheless, charge transfer may play a very important role in the physics of comets.

3. Transfer of Momentum and Energy

It should be mentioned, of course, that there is a transfer of momentum and energy from the solar wind to the cometary material. The observed large accelerations in the cometary plasma tails, as derived from the displacements of clouds, filaments, or other structures of the plasma, are now commonly ascribed to the transfer of momentum from the solar to the cometary plasma. We know that in the quiet solar wind there is a momentum flux on the order of 10⁻⁸ dyne/cm² and an energy flux of about 10⁻¹ erg/cm² sec. But the crucial question is: how much of this momentum or energy flux can be transferred to the comets and their tails? Table 1 lists some of the important parameters to be considered in discussing this question. The values shown in the table represent order-of-magnitude calculations.

a. Long-Range Coulomb Collisions

Now, let us consider how we may explain the necessary momentum transfer (Ref. 3). One interaction mechanism between the solar wind

and the cometary material is, of course, long-range Coulomb collisions. Direct interaction between the solar protons and the ionized molecules

TABLE 1. Important parameters for study of the momentum transfer process

Assumed parameter	S
electron density	1 to 10/cm ³
electron thermal velocity	108 cm/sec
magnetic field	10^{-5} gauss
Calculated paramete	rs
Debye length	$10^3 \mathrm{cm}$
plasma frequency	105 rad/sec
proton cyclotron frequency	10 ^{−1} rad/sec
electron cyclotron frequency	102 rad/sec
proton radius of gyration	
(thermal velocity, 104 °K)	160 km
(solar-wind velocity)	$10^4 \mathrm{km}$
electron radius of gyration	
(thermal velocity, 104 °K)	4 km

is relatively small, and the electrons therefore play a vital coupling role for this mechanism. The ionized molecules are accelerated by collisions with solar electrons, and the electron momentum, in turn, is replenished by the momentum of the solar protons.

The acceleration a that one may attain by this process is given by:

$$a = \frac{e^2 nv}{M_c \sigma}$$

where e is the charge of the electron, n the number density of the solar plasma, M_c the mass of cometary ions, σ the electric conductivity (esu), and v the stream velocity of the solar wind. If one now introduces the numbers that have been observed so far, let's say $v=3\times10^7$ cm/sec, $n=10/\text{cm}^3$, $M_c=28$ amu, and $\sigma=10^{13}/2$ cgs (for a temperature of 10^4 °K), then the acceleration is somewhat less than unity—in contrast to the observed values, which are of the order of 10^2 cm/sec² for normal cases. The exceptional accelerations of 10^3 cm/sec² might be the result of either higher density or higher velocity in the solar stream.

Therefore, one must conclude that this mechanism is not sufficient. However, it should also be mentioned that direct collisions could still be important very near to the nucleus—out to a distance of, say, 10^5 km.

b. Plasma Instabilities

Another mechanism that could be more efficient for the transfer of momentum depends on the so-called plasma instabilities. There are many types of plasma instability that could perhaps enhance the interaction of the solar plasma with the cometary plasma. Since a stream of one gas (the solar particles) encounters another gas (the cometary particles), one thinks of the so-called "two-stream" instability. This case has been treated by Hoyle and Harwit (Ref. 6), who conclude that this type of instability can grow for a brief period if the solar electrons are cool enough—say, cooler than about 10^3 °K for reasonable values of the temperature of the cometary electrons. However, this type of instability will have only a transient effect; as soon as the electrons lose their translational velocity, their temperature becomes high enough to restore plasma stability even for succeeding generations of inflowing electrons.

For the moment, it does not seem possible to transfer sufficient momentum by the two-stream instability. However, we don't yet know that all relevant types of instability have been investigated. Thus some type of plasma instability may be an important factor in the transfer of momentum from the solar wind to the cometary ions.

c. Magnetic Fields

Nevertheless, it is worthwhile to study other mechanisms for the transfer of momentum. Since 1951, the coupling by magnetic fields has been discussed by Biermann, by Alfvén, and by Harwit and Hoyle (Ref. 3, 7, and 8).

It has already been stated that the solar wind has a momentum flux of the order of 10^{-8} dyne/cm². The amount of momentum flux necessary to explain the accelerations in the plasma tails is of the order of 10^{-9} dyne/cm², and corresponds to a mass loss of 10^{28} CO⁺ ions/sec with a velocity of 10^7 cm/sec over a cross-section of about 10^{21} cm². Such a momentum flux requires a magnetic field of the order of 10^{-4} gauss. For a field of this strength, the radii of gyration are small compared to the dimensions of the comets, and the gyration period of the ions (~ 1 sec) is short compared to the time scale of events that occur in the tails. The magnetic coupling of the two different-velocity plasmas becomes effective on a time scale having the same order of magnitude as the gyration period of the ions in question. These investigations will be reported in more detail by Prof. Biermann (Paper 25).

Comets as Probes of the Solar Wind

1. Natural Comets

If the proposed picture is correct—and we feel, from the many arguments given here, that it is—then the comets with ionized tails may be used as natural probes for the investigation of the solar wind. We can hope to obtain information about the direction, the velocity, and other kinematic properties of the solar wind. These natural probes would be, of course, particularly important for investigating those regions that cannot

yet be reached by space vehicles, namely: regions far out of the ecliptic or generally far away from the Earth's orbit. The natural probes can also be used when there are no space vehicles in orbit. However, we can use these natural probes in the most efficient way only if we understand the physics of the cometary plasma and its interaction with the solar wind. As we have pointed out, the comets have not yet been calibrated very precisely.

2. Artificial Ion Clouds

A calibration of the natural comets could be obtained by observing the interaction of the solar wind with an artificial ion cloud of known properties. We have started, in Munich, with preparations for ejecting such a cloud from a space probe, or from a satellite with a highly eccentric orbit.

a. Description of the Experiment

The cloud will be observed from the ground. In order for us to detect and measure structures in the cloud, its surface brightness must be at least comparable to the surface brightness of the night sky in the relevant spectral region. This condition determines the minimum mass to be ejected, taking into account the diffusion of the cloud after the ejection, and at first assuming no use of filters. Furthermore, the time t_{min} during which the cloud is observable must be sufficiently long to enable measurements of displacements and accelerations and to permit observations of the structure as a function of time.

Due to weight limitations, it is planned, at present, to eject the gas in a non-ionized state; the gas should become ionized by photo-ionization. Charge exchange with the protons of the solar corpuscular radiation takes place so slowly that it is not an important process.

The most suitable elements for such experiments are the heavier alkaline-earth metals and some of the rare earths. At present, we are planning to use barium or rare earths, because the ions of these elements have very strong resonance lines in the visible spectral region and because the probability for photo-ionization by sunlight seems to be quite high. Although the photo-ionization rate is not very well known at present, a reasonable estimate gives a minimum mass for barium of the order of 1 kg. This estimate is based on an observation time of about 10³ sec and a temperature of about 2,000 °K for the ejected gas.

Finally, it should be mentioned that the assumed observation time can be considerably lengthened, and the minimum mass considerably lowered, by using spectral filters for the observing instruments. In this way the brightness of the night sky would be strongly reduced. Spectral filters will certainly be used, but for a first experiment we would like to keep the mass of barium around 1 kg. The evaporation of the barium will be done chemically.

b. The Interaction of the Solar Wind With the Ion Cloud

In discussing the interaction of the solar wind with the ion cloud, one has to consider whether the cloud will stay together, or whether the individual ionized particles will just be blown away by the solar wind due to the electric field $E = -v \times B/c$ and the magnetic field B. It can be shown that the individual-particle picture does not apply, and that the cloud should stay together for the required observation time of 10³ sec.

According to our present knowledge of the ionization time for barium. it will take about 104 sec for the mass density of the cloud to equal, as a result of diffusion, the density of the surrounding interplanetary plasma. This time may be even longer if one considers the effect of magnetic fields. Another consideration is whether the electric current that can be carried by the cloud will be sufficient to shield the cloud against an outside magnetic field. An estimate shows that such shielding will be possible during the observation period of 10³ sec, even if the magnetic field changes abruptly over a radius of gyration.

c. Preliminary Experiments

We have performed some preliminary experiments in the ionosphere, mainly for testing purposes. At the same time, though, we tried to carry out useful measurements in the ionosphere. These experiments were carried out in the French Sahara in connection with a French group headed by Prof. Blamont. So far, we have had four launchings that created such artificial clouds. I will not discuss these experiments in detail, since it would mean referring to the ionosphere. I will mention only that we have measured the diffusion or the change of radius of the clouds with time, and in this way tried to determine the diffusion coefficient. It turned out that the observed diffusion could not be explained as solely thermal diffusion, and that turbulent diffusion must still be present at altitudes of 100 to 200 km.

REFERENCES

- 1. WHIPPLE, F. L., Astrophysical Journal 111, 375 (1950). 2. WHIPPLE, F. L., Astrophysical Journal 113, 464 (1951).
- 3. BIERMANN, L., Zeitschrift für Astrophysik 29, 274 (1951) Memoires in-8° de la Société Royale des Sciences de Liège, Series 4, 13, 291 (1953).
- 4. SWINGS, P. and J. L. GREENSTEIN, Comptes Rendus Hebdomadaires des Séances de l'Académie des Sciences 246, 511 (1958).
- 5. BIERMANN, L. and E. TREFFTZ, Zeitschrift für Astrophysik 59, 1 (1964).
- 6. HOYLE, F. and M. HARWIT, Astrophysical Journal 135, 867 (1962).
- 7. ALFVÉN, H., Tellus 9, 92 (1957).
- 8. HARWIT, M. and F. HOYLE, Astrophysical Journal 135, 875 (1962).

Page intentionally left blank

MAGNETOHYDRODYNAMIC ASPECTS OF THE INTERACTION OF THE SOLAR WIND WITH COMETS

LUDWIG BIERMANN

Max-Planck-Institut für Physik und Astrophysik, Munich, Germany

I WOULD like to discuss, in a little more detail, the interaction between comets and the solar wind from the point of view of magnetohydrodynamics and fluid dynamics.

First, it should be said that the figure of 1031 molecules/sec given in Paper 24 refers to the loss rate from a fairly bright comet quite easily seen with the naked eye. Furthermore, this figure is an approximation in the following sense. The selection of molecules and ions that we can observe from the ground (CN, C2, CO+, and a few others) is determined by spectroscopic circumstances. Many of the molecules that, from general considerations, we think should be present have no resonance bands in the spectral range above 3,000 Å. Therefore, because of the great dilution of solar light over the distances in question, we do not expect to detect these molecules. Swings' detailed analysis of the mechanism of excitation has shown that this model is substantially correct (Ref. 1). Hence we are certainly entitled to assume that there are many more molecules than those we see in the ordinary spectral range. Eleonore Trefftz and myself have recently made a quantitative estimate on the basis of the observations of the forbidden lines of oxygen (Ref. 2). These lines were first identified in a number of objects by Swings and Greenstein (Ref. 3), but their presence has perhaps not yet been established beyond doubt for a large number of comets. The loss rate must be established with greater accuracy in the future. Spectral observations in the far ultraviolet, using spacecraft or rockets, should make this possible. We plan to make such observations ourselves in a few years.

To the list of relevant numerical data given by Dr. Lüst, I would like to add the time scale of ionization. In addition to the mechanism of charge transfer, we have, of course, photo-ionization by solar ultraviolet light. Using recent results on the solar far ultraviolet and the particle fluxes, we find that these two fluxes give rather similar ionization rates of about

10^{-6.5} to possibly 10⁻⁷/sec, depending on the molecule in question. These figures lead to the difficulty Dr. Lüst mentioned earlier, namely: that the observed time scales of the origin of and variations in cometary structures do not agree with the ionization time scale. This problem has been considered and perhaps resolved (Ref. 2); I will not discuss it further because it has no direct connection with the subject of interactions.

The molecular loss rate of $10^{31}/\text{sec}$ can be used, together with the observed outflow velocity, to derive a stationary density for non-ionized molecules of $(10^{25}/r^2)/\text{cm}^3$, where r is the distance in cm from the nucleus. Even at a distance of 10^5 km, the overall density of non-ionized particles would, on this model, still be $10^5/\text{cm}^3$. This density should of course be on the high side for many comets. We can similarly derive the stationary density of ions around the nucleus from the photo-ionization rate of $10^{-6.5}$ to $10^{-7}/\text{sec}$. On this model the ion density depends on the inverse first power of this distance. One can use these data to obtain further insight into, for instance, chemical reactions.

Since the radius of gyration is smaller than the size of the visible structures, we see that the interplanetary magnetic fields may couple the cometary plasma with the solar plasma, if the cometary molecules are ionized in one of the ways discussed above. However, we must consider the time scale for coupling to be sure it is shorter than the time in which structural changes are observed.

To discuss this further, we can use the equations of magnetohydrodynamics; specifically, the three-fluid equations for a mixture of electrons and two kinds of ions. As initial conditions, we can assume that the two ion species have different mass velocities and that the electrons move with the average velocity of the plasma ions, so that the net electric current is zero. Then we can immediately see from the equations that the mass velocities of the two kinds of ions tend to become equal on a time scale given by the gyration periods of the ions in question. Thus the range of the coupling time scale is between a fraction of a second and about 10 sec, while the changes that we see in comets occur within 10 to 20 min or from hour to hour or from night to night. Consequently, we conclude that the magnetic coupling is likely to be effective.

We can use the equations of magneto-fluid dynamics to study some more details of the comet–solar-wind interaction. I will write down the equations expressing the usual conservation laws for the plane-parallel case, to show how they differ from those ordinarily used in magneto-fluid dynamics. First we have an equation for the number density n of ions (and electrons):

$$\frac{\partial n}{\partial t} + \frac{\partial (nv)}{\partial x} = n_o \nu_i \tag{1}$$

where $n_o =$ number density of neutral molecules, $v_i =$ ionization rate, and v = mass velocity of the plasma. Normally, the right-hand side of Eq. 1 would be zero, but in the case under consideration we have to take into account the production of ions by photo-ionization. The interaction cross-section of non-ionized molecules being relatively small, we can, as a rough approximation, assume that the molecules streaming out from the comet do not interact with the plasma until they become ionized. After they are ionized, they are affected by the magnetic field and by the long-range forces associated with the other ions and the electrons. The right-hand term represents a local addition to the number of charged particles.

Next we have a similar equation for the mass:

$$\frac{\partial}{\partial t}(n\bar{m}) + \frac{\partial}{\partial x}(n\bar{m}v) = n_o \nu_i (M + m_e) + n_o n_p w_{po} Q_{po} (M - m_p)$$
 (2)

where \bar{m} is the mean molecular weight, Q_{po} is the cross-section for charge transfer, w_{po} is the relative velocity of the interacting particles (the subscripts p and o refer to the solar protons and the neutral particles respectively), and $(M-m_p)$ is the difference in ionic mass produced by the process. Of course, we again get a term representing the addition of particles to the plasma by photo-ionization. M is the mass of the ions so produced, which is generally larger than m_p , the mass of the ions in the solar plasma. The last term on the right is the change in mass resulting from the charge-transfer process. This process does not change the number of charged particles, but is of great consequence for the average mass. Assume, for instance, that only 1% of the protons transfer their charge to molecular ions such as CO or N_2 : the result is something like a 20% or 30% increase in the average mass.

The equation for the transfer of momentum reads:

$$\frac{\partial}{\partial t}(n\bar{m}v) + \frac{\partial}{\partial x}\left(n\bar{m}v^2 + p + \frac{B^2}{8\pi}\right) = -n_o n_p w_{po} Q_{po} m_p v \tag{3}$$

In addition to the usual terms, we have the transfer connected with the magnetic field. On the right-hand side, we have to consider terms connected with photo-ionization and charge transfer. There is no *addition* to the momentum, because the velocity of the cometary molecules is initially quite small and does not increase substantially in the processes of charge transfer or photo-ionization. This conclusion has been questioned as far

as charge transfer is concerned, but Trefftz and I have shown that the gain of momentum in this process is actually quite small (Ref. 4). Therefore, only a loss of momentum appears on the right-hand side of Eq. 3.

Then we have the equation for the energy:

$$\frac{\partial}{\partial t} \left(\frac{n \overline{m} v^2}{2} + p + \frac{B^2}{8\pi} \right) + \frac{\partial}{\partial x} \left[\frac{n \overline{m} v^3}{2} + 2 \left(p + \frac{B^2}{8\pi} \right) v \right]$$
 (4)

$$= \frac{-n_0 n_p w_{po} Q_{po} m_p w_{po}^2}{2}$$

The left-hand side shows the terms found in discussions of magnetohydrodynamic shock waves. There is a question about how many degrees of freedom we are to use. We have used two degrees of freedom instead of the three that we have heard proposed at this conference (see Paper 22). On the right-hand side of Eq. 4, we have a loss of energy that occurs because solar protons disappear, taking their energy with them (the energy gain from photo-ionization is relatively small).

Finally, there are equations for the conservation of magnetic flux and for the conservation of the mean magnetic moment of the proton's gyration:

$$\frac{\partial}{\partial t}B + \frac{\partial}{\partial x}(Bv) = 0$$

$$\frac{\partial}{\partial t}\left(\frac{w^2_{po} - v^2}{B}\right) + v\frac{\partial}{\partial x}\left(\frac{w^2_{po} - v^2}{B}\right) = 0$$
(5)

One result that we have been able to obtain from this set of equations refers to the solar-wind interaction with the rarefied cometary gas at large distances (toward the Sun) from the comet. The regime of interest here is one in which there is still a small fractional loss of solar particles but an appreciable relative increase in the mean molecular weight \bar{m} . For a charge transfer cross-section of 3×10^{-15} cm², this would correspond to a sheet of gas with a surface density of the order of 10^{13} molecules/cm². Treating this as a quasi-steady-state problem, we have been able to show that the mass velocity of the plasma is initially proportional to $\bar{m}^{-3/2}$ (Ref. 5). In other words, the product $\bar{m}v$ is not constant: it decreases toward the comet whenever this process takes place. This is a point of some interest, because in zero-order approximation one might expect this product to be constant (Ref. 6).

The point I would like to stress again is that we seem to have a problem of magneto-fluid dynamics, the velocity of the solar wind being supersonic in free interplanetary space. The comet is a source of charged particles that somehow arrange themselves with the solar stream—a situation which, in some respects, resembles the solar wind flowing around the Earth. It can be shown (Ref. 5) that there is, at least in the plane-parallel case, no stationary solution for which the mean molecular mass increases by a factor of more than 4/3. In reality, of course, the mass change can be much higher. The conclusion is that we cannot have a stationary solution without shock waves, and that the three-dimensional character of the problem must on no account be neglected.

So we would expect to find, around a comet, some analogue of the Earth's magnetopause and a shock front in the direction of the Sun. Furthermore, we would expect the mass velocity to have some observable gradient around the comet. In the pictures that Dr. Lüst has shown you, some streamers could be seen outside the main Type-I comet tail. Such streamers are quite often seen, and are observed to be displaced in the course of time—in a few hours or so—toward the main tail. If the displacement of these streamers is taken as indicating the flow of plasma, most of which is invisible—as smoke or clouds indicate the flow pattern of our atmosphere—we can obtain an impression as to the nature of the mass flow and can link this information to theoretical models derived from our equations.

REFERENCES

1. SWINGS, P., Lick Observatory Bulletin 19, No. 508, 131 (1941).

2. BIERMANN, L. and E. TREFFTZ, Zietschrift für Astrophysik 59, 1 (1964).

3. SWINGS, P. and J. L. GREENSTEIN, Comptes Rendus Hebdomadaires des Séances de l'Académie des Sciences 246, 511 (1958).

4. BIERMANN, L. and E. TREFFTZ, Zeitschrift für Astrophysik 49, 111 (1960).

5. BIERMANN, L., F. B. BROSOWSKI, and H.-U. SCHMIDT, Sitzungsberichte der Bayerische Akademie der Wissenschaften (1962).

6. HARWIT, M. and F. HOYLE, Astrophysical Journal 135, 875 (1962).

DISCUSSION OF LÜST AND BIERMANN PAPERS

GOLD: How close to the Sun is there evidence about the absence of co-rotation? BIERMANN: The comet observations ordinarily extend to 0.5 AU. Many comets come much nearer to the Sun, but if they come too near you can't see them. Hoffmeister studied this problem in 1942. We have since looked at 10 or 20 cometary orbits both perpendicular to the ecliptic and with retrograde and direct motions near the ecliptic; we didn't see any evidence of co-rotation in the behavior of the tails of these comets.

GOLD: So you feel confident that there is no co-rotation even at half an astronomical unit?

BIERMANN: Yes.

AXFORD: I would like to point out the possible importance of electrons in

¹Hoffmeister, C., Zeitschrift für Astrophysik 22, 265 (1943)

processes other than charge transfer. Even in the undisturbed solar wind, one might expect the electron temperature to be comparable to the ion temperature, which is about 10^5 °K. So the electrons have energies of at least 10 ev, which is quite substantial, and they could play an important part in the excitation of certain lines, particularly the forbidden oxygen lines. Furthermore, it is possible that there is a shock that causes energy to be transferred to the electrons from the protons, producing a large flux of kev electrons. It seems to me we should find a good deal of ionization resulting from these fast electrons.

BIERMANN: If you make an estimate of the time scale, you see that the excitation process is slow because the cross-section for this type of reaction is fairly small. Even if you assume an electron velocity of 10^9 cm/sec and an electron density of $10/\text{cm}^3$, then the flux is only $10^{10}/\text{cm}^2$ sec. With a cross-section of 10^{-17} cm², the excitation rate is $10^{-7}/\text{sec}$. Although this rate is probably too slow to be of major significance for the excitation of the O I lines, one should not entirely

forget about it.

AXFORD: {Beard suggested that a higher cross-section is likely; however, I feel I should leave this to the decision of the experts. Electrons have an advantage in that they can make many ionizing collisions, whereas charge transfer produces only one ion for each solar-wind proton.]² Furthermore, it is difficult to understand how a ray could be formed from cold molecules, unless you put the molecules in a line and ionized them all at once. It is more likely that the ionization takes place near the nucleus and that the ions spread out along a magnetic-field line. One is dealing with very heavy ions with no initial energy (charge transfer cannot give the ions much energy), but in order to make a ray within a reasonable length of time—that is, within a few hours—the particle has to move out quickly. The electrons can produce this effect, since they run along the lines of force and drag the ions out with them, thereby enhancing the diffusion of initially slow ions along the lines of force.

BIERMANN: Of course, the electrons get a great deal of energy because the ionizing quanta are in the 20- to 30-ev range. The subsequent development is a very complicated matter, and until we have done quite a lot of thinking about it, I probably should not go into it more here.³

BRATENAHL: Has anyone thought about detecting radio noise from electron processes in comets? Such noise would be expected, but may be orders of magnitude too small to be observed. But if it could be observed, I should think the

results would be quite useful.

BIERMANN: This has been tried, but the results were, as far as I know, inconclusive. I agree that we should at times expect radio noise, but it is difficult to estimate how much intensity we should expect and at what frequencies. We would be happy if observers with radio telescopes would direct their attention to low-frequency emission from comets. We should expect to find something at a very low frequency, if anywhere, and of course low frequencies are difficult to work with.

ANDERSON: Dr. Lüst, did I understand you to say that there is a correlation between the production of comet tails and heliographic latitude, and that there is no correlation between the production of tails and the general level of solar activity?

LÜST: There is no correlation between the formation of Type-I tails and the

²Added in manuscript. See Paper 26

³Biermann, L. and E. Trefftz, Zeitschrift für Astrophysik 59, 1 (1964)

level of solar activity. Stumpff has found that the percentage of comets showing Type-I tail activity is greater at the lower heliographic latitudes, but the effect is not strong.⁴

GOLD: One surely expects some correlation between the acceleration of the heavy ions and the level of solar activity. The amount of gas in the tail should depend on solar heating and shouldn't have any correlation with solar activity, but the speed at which the gas is swept away surely should change with the level of the solar-wind intensity.

BIERMANN: Antrack, Rhea Lüst, and I have recently investigated about 100 comets—essentially the brighter comets of the last 60 years or so. We have divided them according to solar-cycle phase and have examined the frequency of tails having visible plasma materials. We do not find that this frequency depends on solar activity, although there may be a variation of the order of 20 percent.

As to your other point, it is obvious that the cases of strong acceleration do correlate with solar activity. All of the individual cases that we have investigated depend in some measure on solar activity as determined by the magnetic character figures, which are correlated with the sunspot number.

With regard to the latitude effect, we have looked at the latitude of the comet's perihelion, reasoning that the most conspicuous things will take place there. We have tried to verify Stumpff's results without success, but the picture is a very complicated one.

VOGT: How far from the Sun can the direction of the solar wind be determined from the observation of comet tails?

BIERMANN: The greatest distance at which a Type-I comet tail has been observed is 5 AU (Comet Humason 1962/64, observed at about the orbit of Jupiter).

Page intentionally left blank

A THEORY OF TYPE-I COMET TAILS

DAVID B. BEARD

University of California. Davis, California

THE ROLE of the solar wind in accounting for the behavior of Type-I comet tails was pointed out some time ago by Biermann (Ref. 1). Alfvén (Ref. 2) later emphasized the importance of the interplanetary magnetic field in the coupling between cometary ions and the protons in the solar wind. By examining some of the dynamics of tail formation, Harwit and Hoyle (Ref. 3) quantitatively extended both Alfvén's work and the work of Biermann and Trefftz on charge exchange (Ref. 4). The previous speakers have presented an excellent review of this work and of subsequent developments.

Although charge exchange certainly occurs, and probably accounts for the start of the tail-formation process, it cannot account for the high ion densities observed in comet tails. Furthermore, neither charge exchange nor solar-wind pressure can account for the high velocity of mass motion required for the rapid growth of the tail rays. As discussed by Harwit and Hoyle and modified by Prof. Biermann (Paper 25), the interplanetary magnetic-field lines initially move with the velocity of the solar-wind protons, but they are slowed drastically when charge exchange occurs between the protons and the stationary, massive, cometary gas molecules. A hemisphere of slowly moving field lines, frozen in the plasma of ionized cometary molecules, forms an obstacle to the rapidly moving interplanetary-field lines. These interplanetary-field lines pile up on the surface of the hemisphere and slip around its edge, as illustrated in Fig. 1, 2, and 3.

The protons in the solar wind penetrate more deeply into the relatively stationary compressed field than do the electrons, which have less momentum. The resultant charge separation produces an electric field at the outer edge of the compressed-field region. On entering the compressed-field region, the protons and electrons traverse this electric field, which causes the electrons to acquire energy from the protons until their momen-

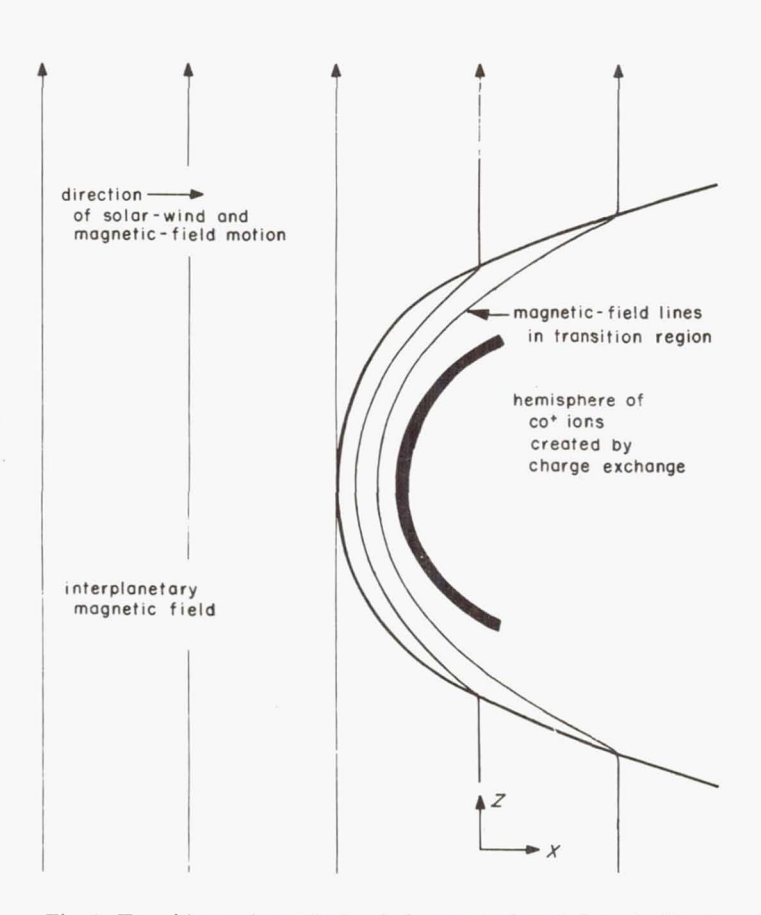


Fig. 1. Transition region at the head of a comet, viewed along the Y axis

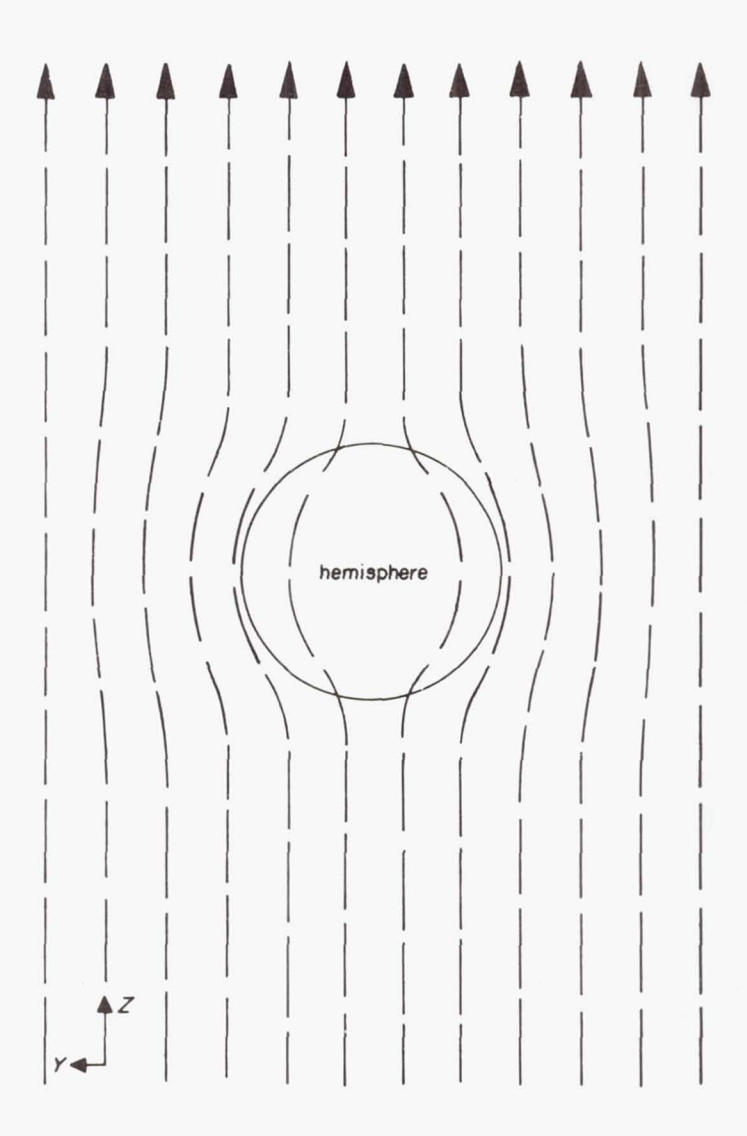


Fig. 2. Transition region at the head of a comet, viewed from the Sun (along the X axis)

tum is equal to the proton momentum. No further charge separation then takes place, and the protons and electrons move on through the transition region. The orbits are illustrated in Fig. 4 and 5.

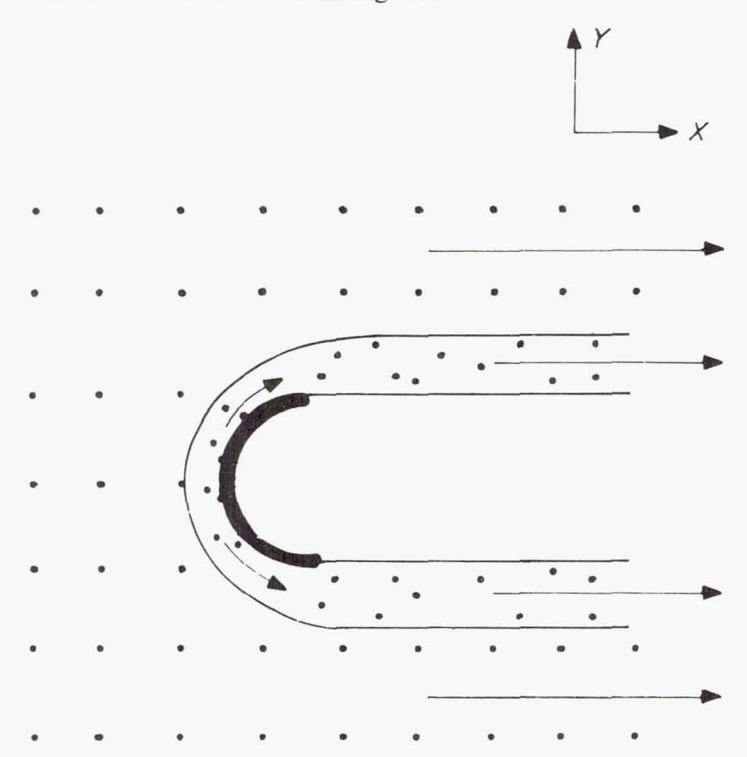


Fig. 3. Transition region at the head of a comet, viewed along the Z axis. The arrows denote the velocity of the field lines

The theory of particles bouncing off a stationary magnetic field (Ref. 5 to 8) is slightly changed when the magnetic field is moving with a velocity \mathbf{v}_{ℓ} . In the reference frame of the moving field, the particles have an ordinary cyclotron motion; but in the stationary coordinate system in which the boundary is at rest, an effective electric field $-\mathbf{v}_{\ell} \times \mathbf{B}$ appears. This electric field is caused by the velocity of the magnetic-field lines which are trapped with the particles that are moving into the transition region. Taking the X axis normal to the boundary and the Z axis parallel to the magnetic field (see Fig. 1), we have the following equations for the case of normally incident particles:

$$\ddot{y} = -(e/mc) B(\dot{x} - v_{\ell}) \tag{1}$$

$$\ddot{x} = (e/m) E(x) + (e/mc) B\dot{y}$$
 (2)

Integrating once over time, we obtain

$$v_{y} = -(e/mc) \int_{-\infty}^{x} B dx' + (e/mc) \int B v_{\ell} dt$$
 (3)

$$v_{x}^{2} = v_{0}^{2} + 2(e/m) \int_{-\infty}^{x} E dx' - (e/mc)^{2} \left[\int_{-\infty}^{x} B dx' \right]^{2}$$

$$+ 2(e/mc)^{2} \int_{-\infty}^{x} B \int (Bv_{\ell} dt'') dx'$$
(4)

Since the particle density is proportional to $1/v_x$, and since significant charge separation may not occur, the x components of the electron and ion velocities are approximately equal. Hence

$$\int_{-\infty}^{x} E(x')dx' = -(e/2m_ec^2) \left[\int_{-\infty}^{x} Bdx' \right]^2$$

$$+(e/m_cc^2) \int_{-\infty}^{x} B \int (Bv_\ell dt'') dx'$$
(5)

The second term is small, but it reduces the electric field in the charge-separation layer as expected, because the kinetic energy of the protons in the frame of the moving field lines is reduced. The $\Delta B/B$ drift is in the direction of the $\mathbf{v}_{\ell} \times \mathbf{B}$ field, and produces a particle energy loss that is negligible—less than 60 ev for the electrons and less than 1 ev for the protons.

The electron energy in the transition layer is the original ion kinetic energy, $m_i v_0^2/2$, and the ion energy is now $m_e v_0^2/2$. Since the momentum is $v_0 \sqrt{m_i m_e}$ for both electrons and protons, no further charge separations can occur. The energy per electron-proton pair is unchanged by the magnetic and electric forces. However, the momentum per electron-proton pair has been reduced by a large factor, thus confining the region of higher field strength to a sharply defined volume. For the stationary case, the magnetic-field strength in the charge-separation region depends on x approximately as e^{x/x_0} , where

$$x_0^2 = m_e c^2 / 8\pi n_0 e^2$$

For the present problem, we must replace x_0 by $x_0' = \frac{x_0}{1 - v_\ell/v_0}$ to account for the reduction in the boundary current. This reduction arises because v_{ey} is decreased by the $\mathbf{v}_{\ell} \times \mathbf{B}$ field.

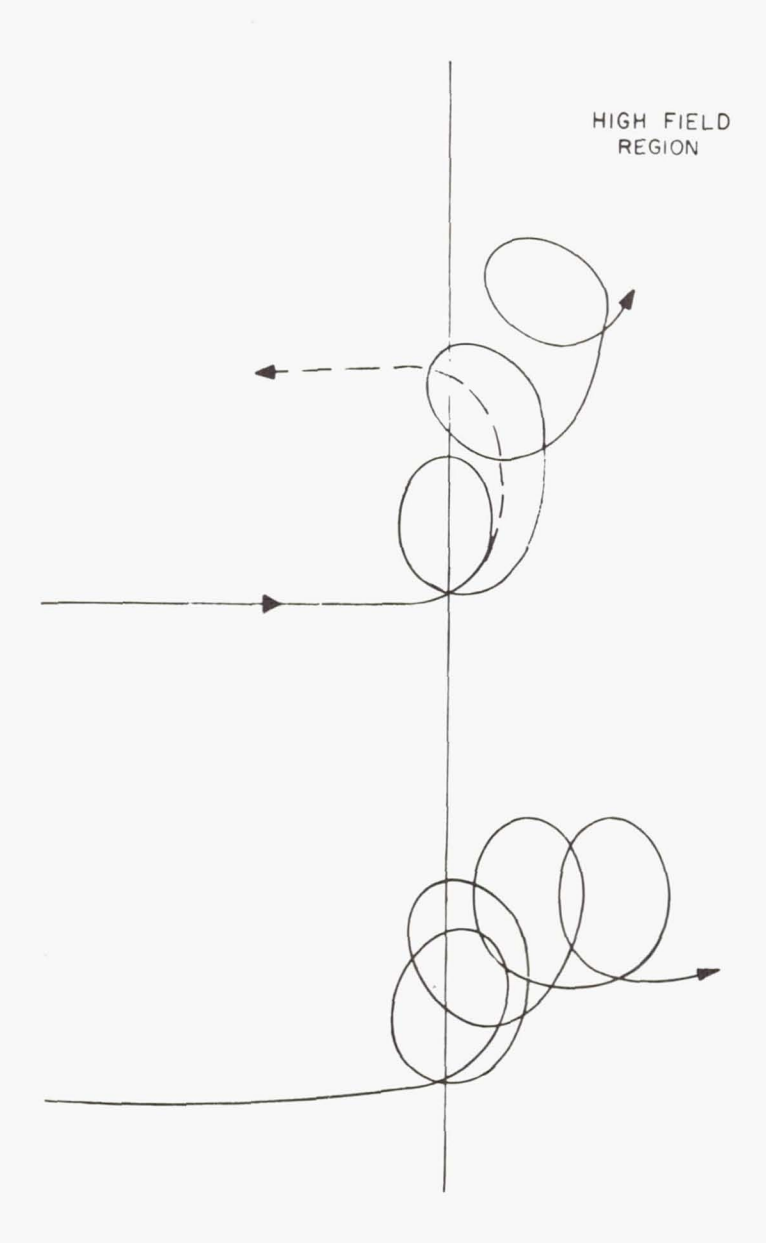


Fig. 4. Trajectories of a charged particle entering a region of high-strength magnetic field. The dotted line denotes the particle trajectory for a stationary magnetic field; the solid line is for a moving magnetic field. The direction of the field is perpendicular to the page

Thus all of the electrons in the transition region have kinetic energies of about 1 kev and velocities that are two orders of magnitude higher than the proton velocities. Consequently, the cometary gases will be much more readily ionized by electron impact than by charge exchange

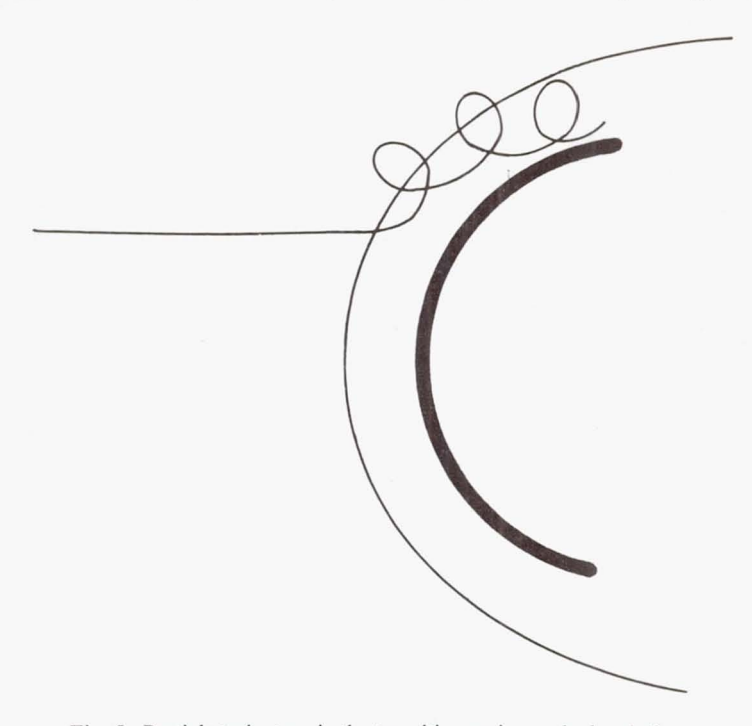


Fig. 5. Particle trajectory in the transition region at the head of a comet

with protons. Moreover, since the electrons are circling the field lines, the number of cometary ionizations per unit length of magnetic-field line is not limited by the original charge density as it is in charge transfer. The cross-section for ionization by electron impact remains high (1 to $3 \times 10^{-16} \text{cm}^2$), even for electron energies as low as a few tens of ev. Several hundred cometary ions/cm³ can be produced.

Aside from producing the observed large ion densities, energetic electrons can also account for the observed rapid formation of the tail rays. As Prof. Axford remarked (discussion of Papers 24 and 25), the electrons will diffuse rapidly away from the comet head along the magnetic-field lines. This diffusion will cause charge separation, which creates an electric field parallel to the magnetic field and accelerates the cometary ions up to the electron energies. The time to form a tail ray 10^{10} cm long is about 5,000 sec.

As the ionization by electron impact in the transition region proceeds, the velocity of the magnetic-field lines in the transition region is reduced, and a new transition layer is created at a greater distance from the comet nucleus. Eventually, the density of neutral molecules in the transition region becomes too low to sustain any significant further ionization. The process then stops until the tail ray is pushed into the comet head far enough for a new ray to be formed.

The acceleration of each unit length of tail ray varies inversely with its mass and directly with the pressure (nmv^2) of the solar wind. For an isotropic electron velocity, it can be shown that the acceleration depends linearly on the distance from the comet head. Therefore, the tail rays should theoretically remain straight, as they are folded, like the spokes of a fan, onto the axis of the tail structure. As Dr. Lüst mentioned, the axis of the tail structure is essentially parallel to the radius vector from the Sun.

The point I wish to make is that tail rays are formed by energetic electrons in the transition layer that is located on the outer surface of "slowed" interplanetary magnetic-field lines. The thickness of the slowed-field-line region must be at least 10³ km in order for the thickness of the transition region (as estimated by magnetic-flux considerations) to be greater than a proton gyro radius. Otherwise, the charge-separation electric field will not be created.

REFERENCES

- 1. BIERMANN, L., Zeitschrift für Astrophysik 29, 274 (1951).
- 2. ALFVÉN, H., Tellus 9, 92 (1957).
- 3. HARWIT, M. and F. HOYLE, Astrophysical Journal 135, 875 (1962).
- 4. BIERMANN, L. and E. TREFFTZ, Zeitschrift für Astrophysik 49, 111 (1960).
- 5. Ferraro, V. C. A., Journal of Geophysical Research 57, 15 (1952).
- DUNGEY, J. W., Cosmic Electrodynamics, Cambridge University Press, New York (1958).
- ROSENBLUTH, M. N., Magnetohydrodynamics, ed. by R. K. M. LANDSHOFF, Stanford University Press, Stanford, Calif. (1957) p. 57.
- 8. BEARD, D. B., Journal of Geophysical Research 65, 3359 (1960).

CHAPTER XXVII N 6 6. 3. 8. 9. 7 3. THE MAGNETOSPHERE OF THE MOON

T. GOLD

Cornell University, Ithaca, New York

LIKE a comet, the Moon is an obstacle in the path of the solar wind. In many ways, the analysis of the Moon-solar-wind interaction is very much simpler than the analysis of a comet-solar-wind interaction. I think we can develop a fairly extensive theory, and make a sound prediction as to what will be observed in the vicinity of the Moon as a consequence of this interaction.

All this is true only if the Moon has no inherent magnetic field. If it has, then of course its magnitude will affect the issue greatly. But on the assumption that the Moon is just a lump of rock, possessing no more than the very minute remnants of magnetic fields that a rock would have, we can calculate what would happen if it were magnetized only by its interaction with the solar wind.

The Field Around a Stationary Moon

The magnetic time constant for the Moon is $L^2\mu\sigma$, where L is a length (the diameter, say), μ is the permeability, and σ is the conductivity. The time constant will be between 1 month and a hundred years (or maybe even more), on the basis that the Moon is made of rock like the Earth's crust but is probably not terribly hot inside. Most likely it will be a few years. At any rate, the important thing about this magnetic time constant is that it is almost certainly long compared to the lunar day, and the Moon will therefore rotate many times during the natural decay time of the magnetic field.

Let us start with the assumption that the Moon has no magnetic field at all (Fig. 1), and that the solar wind is hitting the Moon's surface. The conductivity of the plasma is interrupted, because the plasma ions that hit the Moon's surface are de-ionized and can no longer act as conductors. The body of the Moon must take over the conduction from the ions and electrons of the solar wind.

382 T. GOLD

Now, although we started with an unmagnetized Moon, in a short time the magnetic lines of force brought by the solar wind are pushed into the front surface of the Moon (Fig. 2). Unless the time constant is so short that the magnetic lines of force can go through the Moon at the

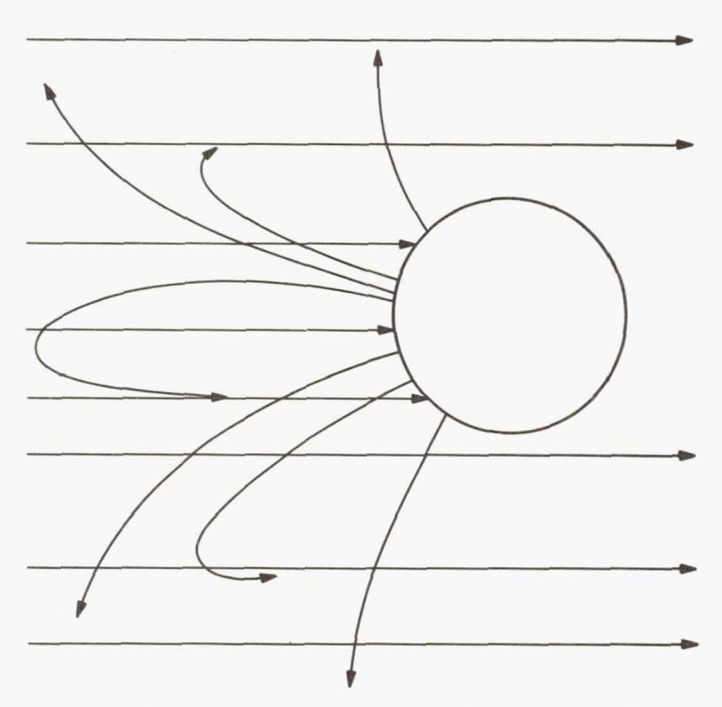


Fig. 1. Trajectories of solar wind particles (1- to 10-kev protons and low-energy electrons) striking an unmagnetized Moon. Only neutral particles are thermally re-emitted

speed of the solar wind—that is, in a few seconds—the lines of force will be hung up on the front side. The time constant is certainly longer than a few seconds.

Additional lines of force continue to move toward the Moon at a speed of a few hundred km/sec, so that suitable electric fields must be generated to distort them. Since it only takes a few seconds for the solar wind to cross the Moon, it is clear that there will be a long field-free tube behind the Moon and field lines accumulated on the front side.

How long will this process go on? The lines will be rammed into the front surface until no further lines can be pushed in by the stagnation pressure of the wind. The field strength that will be built up on the front surface of the Moon will equal the stagnation-field strength (Fig. 3). For a normal solar wind as we now know it, say 4 particles/cm³ moving at 300 km/sec, the stagnation field is 30γ .

The gas has to be compressed by only a factor of about 10 for the field to go from its ambient strength to the stagnation-field strength. It thus takes only a few seconds for the stagnation-field to be built up. The enhanced field will be quite close to the front surface, because a few seconds corresponds to only a few kilometers of field-penetration thickness. So, we have a thin magnetic skin on the front.

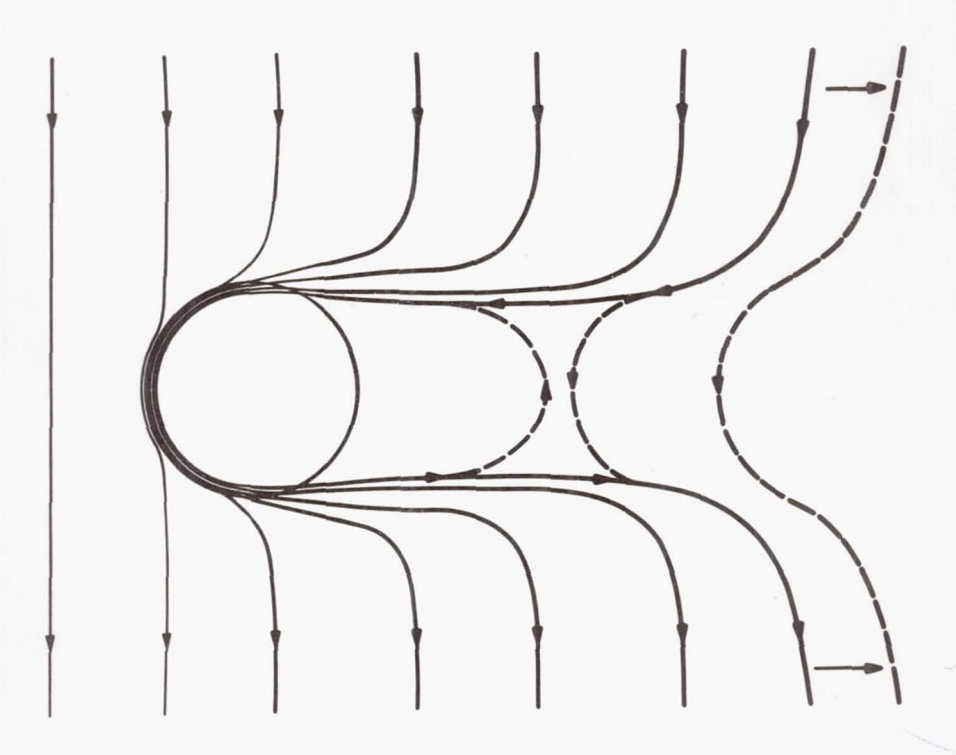


Fig. 2. Development of a magnetic cavity as magnetic-field lines imbedded in the solar wind accumulate on the front surface of the Moon

Behind the Moon, the usual situation for dissipation is set up. Opposing lines of force will become adjacent in the drawn-out wake, and at a low density this situation will give rise to rapid dissipative processes that will reconnect the field and decrease the field energy. A closed magnetic bag will then result, as shown in Fig. 3.

We now understand that as soon as the field strength on the front side has reached a value such that the gas can no longer strike the Moon directly, there will be a shock wave standing in front of the Moon just as there is in front of the Earth. This shock wave will form, provided that its thickness is much less than the Moon's radius.

384 T. GOLD

Of course, the shock will be close to the body of the Moon in this case, and any variation in the stagnation pressure will cause a big change in the position of the shock. This is quite unlike the case of the Earth, where the position of the shock wave is so wonderfully stabilized by the inherent

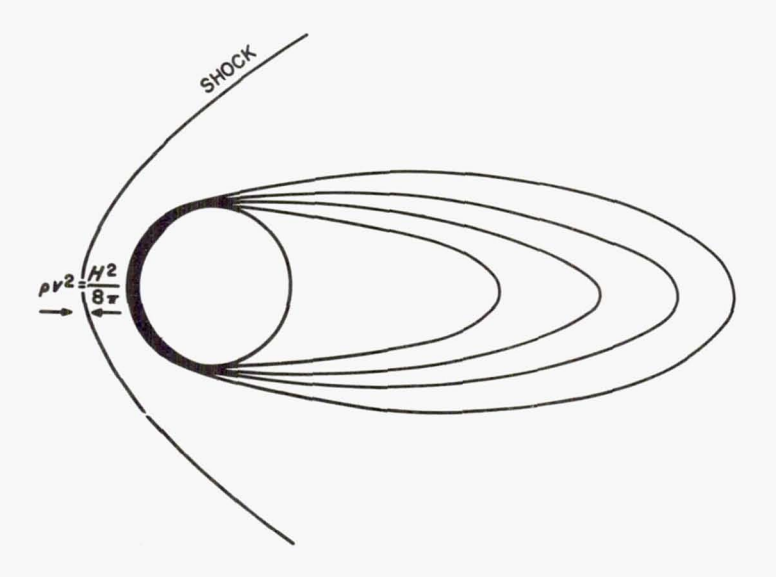


Fig. 3. Final development stage of the Moon's magnetosphere, after dissipation has closed up the lines of force in the wake

magnetic field of the Earth. Near the Moon, we have only those fields that get plastered in, and the configuration doesn't have the stabilizing influence of an inverse sixth-power law, which an inherent dipole field provides.

Figure 4 is an end-on view of the lunar magnetosphere and demonstrates that once the stagnation pressure is achieved, the field will cleave and slide around the body of the Moon in the dimension transverse to the field.

To summarize, then, the front side of the Moon has the stagnation field built upon it. If the stagnation pressure increases a little, then the flow will ram a little more field into the Moon on a time scale of seconds. If the stagnation pressure drops a little, there will be a shock wave standing in front, and the magnetopause will be essentially outside the body of the Moon. As soon as the pressure drops, the plasma flow cleaves and goes around the Moon; the only time that the Moon itself is hit by gas is when the stagnation pressure increases.

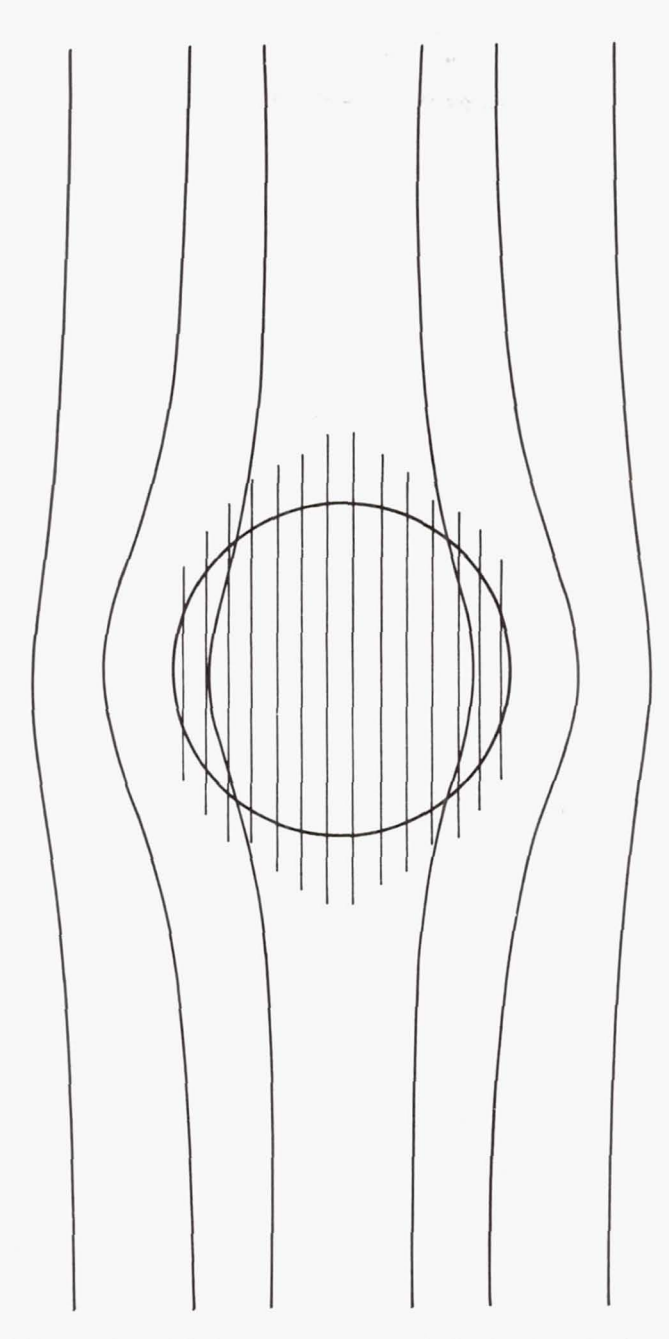


Fig. 4 End-on view of the lunar magnetosphere, indicating the deflection of field lines in the solar-plasma flow pattern.

386 T. GOLD

You can see that the strength of the field brought in by the solar wind is unimportant from this point of view. It wouldn't matter, for example, if the solar wind had a field strength of only 10^{-7} gauss. Such a weak field wouldn't alter the above description at all, except that it would take a few seconds longer to press the stagnation field into the front face of the Moon.

The Effect of Rotation

In a rotating body being magnetized from one side, the field component that is consistently built up is the component in the polar direction. The component in the equatorial direction is destroyed by the rotation, because a field that is in one direction when it is pushed into the front side is in the opposite direction when it has been carried around to the back. Since the component in the polar direction is not reversed by the rotation, it is preserved except for a gradual decay. Calculations have been made for a sphere that is magnetized while rotating about an axis perpendicular to the field direction. The case is a well known one, because the sphere behaves like a diamagnet. When you spin a conducting sphere about an axis that is perpendicular to a magnetic field, the field does not penetrate the sphere. A neutral point always develops in the middle, and the field collapses.

DAVIS: Does this calculation require the external field to be applied on both sides of the sphere or only on the one side?

GOLD: Just on the one side. If you apply the field on one side, then when it has moved around to the other side it is doubled over on itself. It is a difficult problem, and I don't know all the answers to that part of it. But it is well known that a sphere rotating in this direction is, in fact, a diamagnet and excludes the field.

In view of these considerations, the solar-wind field component that points in the direction of the Moon's axial rotation can be expected, in the course of time, to build up a poloidal field along the axis of the Moon. Now, the strength of this poloidal field depends upon how many times, statistically, the solar-wind field is in one direction and how many times it is in the other, together with the time constant for decay. Therefore, shells of opposite poloidal components will build up and decay.

Although it is too complicated to determine the situation in a multipolarity case, it is interesting to consider the situation for one sign. Suppose, just for simplicity, that we expose the Moon forever to one field direction along the axis of rotation, and then suppose that we have, just in front of the Moon on the solar side, a certain value of magnetic field—specifically, the stagnation field. Then the stagnation field would penetrate, to some given extent, the front face of the Moon, and there would be almost no field on the back of the Moon. If the Moon is spinning very fast compared to the magnetic time constant, then on the front side there

would be just a thin layer in which the field has the value of the stagnation field, and on the back there would be a thin layer in which the field drops off sharply to zero. Between these two layers, the field would have a uniform strength of about half the stagnation field.

You can see that the diffusion of the axial magnetic-field component in a conductor and the conduction of heat are both described by the same equation. I have the same problem that I would have if I were to take a spinning sphere and apply a heat source to one side of it, letting the other side cool. The whole sphere will be heated to a uniform temperature, except that, at any one instant, a thin layer at the front will be hotter and a thin layer at the back will be colder. If the sphere spins more slowly, so that the rotation period approaches the diffusion time constant, then the temperature distribution degenerates into a more gradual curve. Hence, there is a possibility that the magnetization curves in the Moon will give information about the internal conductivity.

Of course, all this is complicated by the fact that the interplanetary field is not always in the same direction, so that the magnetic field on the Moon might have nodes in it. If you went over the surface of the Moon with a magnetometer, you could find the multipole field that had resulted from previous periods of opposite magnetization. You might actually find a few cycles of opposite-polarity field lines sticking out. If, in fact, the time constant of the Moon turns out to be very long, like a hundred years, then a few of these nodes could very likely be preserved.

A Suggested Experiment

A close orbiter would enable us to determine, independently of the nodes problem, the time history of the sense of the magnetic-field component normal to the ecliptic, as well as the time history of the solar-wind stagnation pressure. A polar orbit would be preferable to an equatorial one, and it would be desirable to have instruments capable of finding harmonics higher than the lowest harmonics in the Moon's poloidal field. Under these circumstances, we could certainly deduce the time constant of the Moon and determine how strong the fields have been in the past. We could thus recognize, for example, the effects of the solar cycle. We assume that there is a poloidal field along the axis of rotation, with a strength equal to the average strength of the solar-wind stagnation pressure over a period roughly determined by the time constant. By mapping this field, we could learn more about the time history of the solar wind.

Energetic Electrons and X-rays

I would like to refer again to the point that the Moon may have a shock wave some of the time. It can certainly have that shock wave if the shock interaction occurs in a layer thin enough compared to the size of the Moon.

388 T. GOLD

Then we might expect that, as in the case of the Earth, the shock will tend to produce energetic electrons, that is, the shock will tend to transfer very rapidly some of the energy of the protons to electrons. This process seems to be observed in the IMP data (Paper 21). If the shock wave does produce energetic electrons, then we might worry about what happens to these electrons, because the electron fluxes are quite high $-10^9/\mathrm{cm}^2$ sec or even more. Well, a large part of the time the electrons will be striking the Moon's surface, and a large part of the time they will be escaping from it. The shock wave will easily move right into the Moon's surface, and with it will move all the energetic electrons that are generated. Therefore, we can imagine that a very time-variable X-ray source will be produced by this process.

Let me give you the approximate X-ray intensities that should then prevail during magnetic storms, since it is only at such times that the phenomenon is significant. If a solar wind of 10 particles/cm³ at 1,000 km/sec gives up its energy to electrons, which then strike the Moon, there will be about 10 ergs/cm² sec on the Moon. Then, if the efficiency for X-ray production by these electrons is 10^{-4} or 10^{-3} (and we believe that this is typical for kev electrons), X-ray energy will be generated at a rate of 10^{-3} or 10^{-2} erg/cm² sec. For the whole Moon, the rate will be 2×10^{14} to 2×10^{15} ergs/sec, or 20 to 200 megawatts. In terms of the number of 5-kev X-rays (at the lower efficiency), this rate corresponds to 10^{22} quanta at the Moon or $1/\text{cm}^2$ sec at the Earth. I think a quantity like this is hard, but not impossible, to detect.

In using these figures, I have assumed a not-very-violent magnetic storm. One would imagine that 10 particles/cm³ with a velocity of 10³ km/sec would be produced quite often at solar maximum. Since the efficiency will vary greatly with the velocity, the X-ray source will be very unsteady, even during a magnetic storm.

One must not think that he would see X-rays during an entire magnetic storm. He would see them only on the occasions of increasing pressure and never on the occasions of decreasing pressure. He would see the time derivative of the storm, as it were.

These lunar X-rays may present quite a deplorable situation for astronauts. The X-ray fluxes are not small, and though 5-kev X-rays are not too hard to shield against, I am not sure that a thin space suit is enough shielding. Then, too, the X-ray energies go up to more than 5 kev on occasions, and the hazard will depend very critically on how much more. Of course, the X-rays would also have a very important effect on all photographic instruments.

While X-rays can be detected much more readily from an orbiter, they can also be detected from the Earth. Measurements of the X-ray fluxes should indicate, in the first place, whether the basic hypothesis discussed

here is correct, namely: that we should see great increases in the X-ray flux depending on the variation in the stagnation pressure. Such measurements would also show whether a shock wave is indeed built up and whether, like the shock wave in front of the Earth, it can almost miraculously produce hot electrons so quickly.

In conclusion, it seems to me that the Moon is remarkably well suited to assist one in the investigation of both the magnetohydrodynamic flow of the solar wind and the time-history of this flow.

DISCUSSION OF GOLD PAPER

PETSCHEK: Am I right in concluding that the total flux over the Moon should be less than about 15 γ (which is half of the stagnation-field strength) times the area of the Moon's disk, and maybe less because of reversals?

GOLD: That is right.

COLBURN: I would like to know whether the flow of magnetic-field lines around the Moon affects the accumulation of an atmosphere, since the small amount of heavy elements in the solar wind is deflected around the Moon instead of accumulated.

GOLD: Yes. The situation there, of course, is like the situation for comets. If any gas comes out of the Moon, then the moment it is ionized (and the longest estimate for the ionization time is not much more than a week) it is stuck in the solar wind. These ions will then pick up the speed of the solar wind in a fraction of a second. Most of the ions formed will then miss the Moon and be lost from the lunar atmosphere. Under these circumstances, it is quite inconceivable that any kind of an atmosphere is built up on the Moon by the slow exhalation of gas from its interior. There is no use in discussing xenon and krypton and other very heavy molecules just because they are gravitationally bound: gravity has virtually no effect on the *ionized* gas.

MACKIN: Would your conclusions be affected appreciably by the assumption of

an insulating surface layer?

GOLD: If you covered the Moon entirely with a high-quality dielectric that could withstand kilovolts, then the conclusions would be affected. But such a dielectric would have to be such a good insulator that the magnetic time constant would be of the order of seconds. For rock, that seems impossible.

BIERMANN: Wouldn't you expect the thickness of the transition zone in front of the lunar surface to be a few Larmor radii? An orbiter would have to be within

such a distance from the Moon to be able to detect the field easily.

GOLD: Yes. However, a long tunnel with a low field strength in its interior will be strung out behind the Moon. We understand that such a tunnel will grow to a certain length, but will not become infinitely long. It will close itself off by the dissipation mechanism we have been laboring with, that is, dissipation resulting from the proximity of opposing lines of force. It will therefore construct a sort of solar-wind bag that hangs on the back of the Moon.

BEARD: That is very interesting. You would expect a comet tail to extend even

farther, because the ions in the comet tail are so much more massive.

GOLD: The question is: how far does this bag really drag itself out? It seems perfectly possible for it to extend even as far as the Earth. At any rate, a substantial fraction of the distance to the Earth seems plausible.

390 T. GOLD

SNYDER: I agree that this bag may very well extend a large fraction of the distance to the Earth, but I find it inconceivable that it would reach the Earth. If it did, would it not have effects on the Earth's magnetosphere every month?

GOLD: There is nothing in my considerations that tells us whether it should extend halfway or the whole way to the Earth. If it regularly goes across the Earth, we would expect to see effects on the magnetosphere. We haven't seen any such effects.

JOKIPII: There does appear to be some correlation between magnetic storms and the position of the Moon. There is evidence of a 29-day effect that is different from the 27-day effect caused by the rotation on the Sun.¹

GOLD: This is one of those nasty coincidences, like the fact that the Moon subtends a half-degree and the Sun subtends a half-degree. And the Moon rotates once around the Earth in about the time that the Sun rotates once on its axis. These coincidences, like the one mentioned yesterday about the fact that the equinox corresponds to maximum solar latitude, cause trouble with statistics. A 27-day recurrence is hard to distinguish from a 28-day recurrence, isn't it, particularly if it only occurs a few times? One might well be confused.

SLUTZ: But if the field inside the front face of this bag were about 20γ , and if the bag did extend as far as the Earth, then the field near the back face would be distinctly less than 1γ . This would lead you to wonder whether you would see any effect even if the bag were long enough to reach the Earth. The change in pressure on the magnetosphere of the Earth would be very small compared to the pressure from the solar wind.

DAVIS: However, the bag might cause a kind of vacuum in the wind.

GOLD: There should be a change in the flow of the wind, and this change should be large enough to determine whether the bag passes over the Earth's magnetosphere regularly. But of course a near-eclipse configuration may be necessary. Maybe you have to look for an effect only at the time of a solar eclipse.

DUNGEY: Dr. J. Tauer of Prague, Czechoslovakia, has found an effect on micropulsations at the time of eclipses. I think this effect is more likely to be detected at the ground than are the slowly varying disturbances.

DAVIS: There should be some aberration; you needn't have an optical eclipse.

GOLD: The Moon has to be in the right plane for an optical eclipse, but the bag will not hit the Earth at the same time as the eclipse occurs.

LEES: In "ordinary" fluid mechanics, one finds that the turbulent wake shed by a blunt body moving at hypersonic speeds extends for thousands of body diameters behind the body. For example, at a distance of 1,000 body diameters, the wake breadth is about 10 body diameters and the temperature on the axis is still about 7 times ambient, for a flight speed of 20 times ambient sound speed. The level of temperature fluctuations inside the wake is correspondingly high. Therefore, if one takes the big jump of making some sort of analogy, one can expect that appreciable disturbances will be detected by an Earth satellite that happens to pass across the wake of the Moon in the solar-wind plasma.

GOLD: The size of the bag depends particularly on the speed of annihilation of opposing field lines.

LEES: Petschek has calculated a pretty rapid speed of reconnection.2

²Petschek, H. E., AAS-NASA Symposium on the Physics of Solar Flares, SP-50, ed. by W. N. Hess, National Aeronautics and Space Administration, Washington, D.C. (1964)

GOLD: Certainly, in response to your story, in the future I will draw the bag with a wake of eddies extending behind it for a long distance.

PETSCHEK: The wakes that you are used to in aerodynamics, I think, are detected at great distances because of the sensitive detection methods used. I don't think that you can expect to detect a very long wake containing magnetic fluctua-

tions of the same order of magnitude as the magnetic field itself.

GOLD: I forgot one other point. During those times when the field on the Moon is replenished, you have a momentary configuration in which the ions are slamming into the surface, but the electrons cannot do so because of their much smaller momentum. Thus, at these moments, the potential of the Moon rises to a large fraction of the protons' potential (about 5 kv) in order to draw the electrons along with the protons. It seems to me that, since the wind sometimes hits the Moon and sometimes does not, the Moon will often be at a substantial electrostatic potential. This suggestion could be in error only if there is enough conduction to discharge the potential along the neutral plane in the direction transverse to both the field and the solar wind, and I don't know whether there is or not.

DAVIS: In Fig. 3, Paper 27, there is rather substantial magnetic flux between the surface of the Moon and the shock wave. Now, suppose we triple the momentum flux of the solar wind. Everything will certainly be pushed in, but by the time the transition layer has been compressed to one third its original thickness, we have tripled the magnetic strength and increased the magnetic pressure by a factor of nine. Won't that stop everything before any gas really reaches the Moon?

GOLD: The compression may stop before the shock wave reaches the Moon, but it will certainly drive some of the gas that is behind the shock into the Moon. This gas will still be flowing, after all.

DAVIS: But now it will flow fairly slowly. After going through the shock, it will slow down.

GOLD: Yes. But some gas has to be hitting the Moon's surface in order to push new field lines into the Moon.

DAVIS: The gas pushes on the old field lines outside.

GOLD: They are imbedded in the gas and will not move into the Moon's surface except with the gas that is being pushed in. If you don't allow me any gas to shove into the Moon at all, I can prove to you that the Moon's field will decay completely. Hung-up lines of force always depend for their existence on the fact that some gas has hit the Moon, though not necessarily at the initial speed.

BIERMANN: I recall having discussions with Hinteregger some years ago concerning the possibility of detecting X-rays created by the impact of solar particles on the Moon. I have a vague recollection that he mentioned some of the observational evidence, which I think was negative. But there are many people here who may know. So let me ask you if there have been attempts to measure X-rays from the Moon.

GOLD: Even on the quite favorable assumptions that I have made, it isn't too easy to detect lunar X-rays from the Earth. No past experiments would have had the sensitivity to detect them. Thus, there is no evidence contradicting the production of lunar X-rays, but the detection efficiencies required are not far beyond those we hope soon to achieve.

SNYDER: These X-rays would be detected in bursts of a few seconds?

GOLD: Yes.

Page intentionally left blank

N 6 6.

3.8.9.74

A PROBABLE OBSERVATION OF THE WAKE OF THE MOON

N. F. NESS

Goddard Space Flight Center, NASA, Greenbelt, Maryland

Introduction

The most obvious interaction between the Moon and the Earth is a gravitational interaction in which the pull of the Moon on the Earth leads to a daily variation in the terrestrial force of gravity. This variation is on a scale of tens of microgals, where 1 gal = 1 cm/sec² acceleration. We understand this interaction quite well; we suspect that gravitational variations also affect the atmosphere, and that there are lunar tides in the atmosphere just as there are lunar tides in both the fluid and the solid Earth. The daily variations of the geomagnetic field have been indirectly related to the Moon's gravitational effect on the Earth's atmosphere.

Any 29.5-day periodic geomagnetic effect may be associated with a lunar magnetic field or a lunar magnetosphere wake, since we now know that the solar wind will greatly disturb any lunar field, regardless of the field's origin (Paper 27). There are a variety of publications on the subject of geomagnetic effects with 29.5-day periodicity, and depending on which particular paper you read, you can either prove or disprove the existence of such an effect (Ref. 1, 2, and 3).

We suggest that the *IMP* data give the first conclusive evidence of the existence of the Moon's wake. The data from the first four orbits of *IMP* show that the field in the interplanetary medium was very steady and quite low in magnitude (Paper 6). Both a magnetopause and a shock-wave boundary were readily discernible. However, on December 14, 1963, during the fifth orbit, the variance and magnitude of the field exceeded those that had been nominally measured at a position well outside the Earth's shock wave. This condition persisted for some time, and then the field and variance returned to the normal low levels. The satellite then passed back through the Earth's shock wave on the inbound portion of the orbit.

Today I am going to discuss mainly the relative positions of the Moon,

394 N. F. NESS

the satellite, and the Earth. In the future we will investigate the data more thoroughly to better understand the details of the observed phenomena.

Satellite and Lunar Positions for Detection of the Wake

Figure 1 is a plot, in the ecliptic, of the relative positions of the Moon and the satellite during the fifth orbit of *IMP*. The numbers 12 through 16 designate the dates in December, 1963. The positions of the shock wave and the magnetopause have been included.

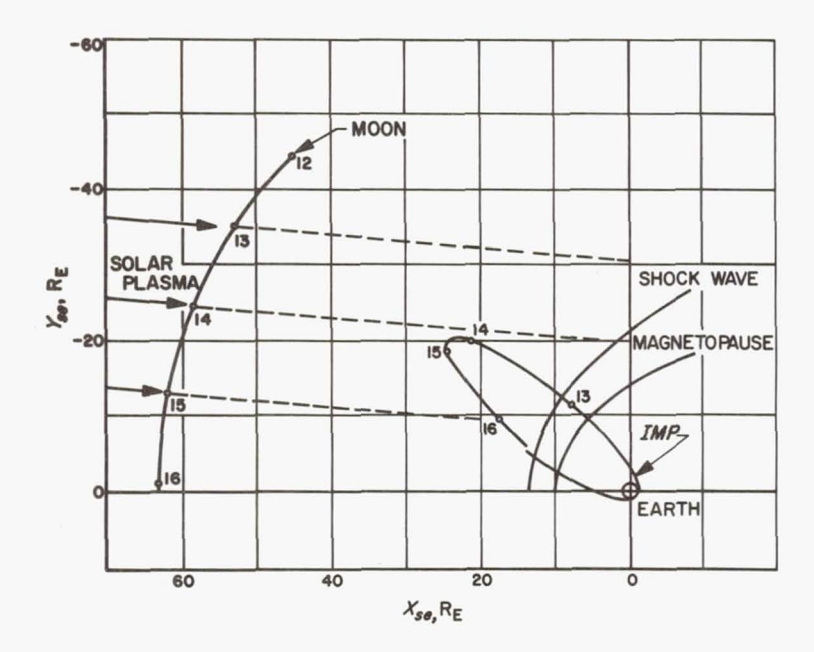


Fig. 1. Projection of Moon and *IMP* positions on the ecliptic, December, 1963 (Orbit 5)

On December 13, *IMP* was in the transition region. If we assume a 5-deg aberration of the solar wind, and if the Moon does have a wake that trails behind it, indicative of the direction of the wind, we see that the wake would have been far away from the satellite. On December 14, however, the relative positions of the Moon and the satellite were favorable for detecting the Moon's wake. On December 15, the Moon had gone past the satellite, while on December 16 the satellite moved back inside the shock wave. Figure 2 shows a projection of the Moon and satellite positions on a plane normal to the Earth–Sun line. The numbers 13 through 16 again designate the days of the month.

In an attempt to summarize the relative locations of the satellite and the

Moon, I have defined a number of specific parameters. D_{SM} is the distance between the satellite and the Moon, while D_{YZ} is the projection of D_{SM} on the YZ plane. λ_{YZ} (Fig. 2) is essentially the zenith angle of the vector D_{YZ} on the YZ plane. Looking down on the ecliptic, we define a similar angle, λ_{XY} . Figure 3 is a plot of these parameters for the critical period in December, 1963; distances are given in R_E .

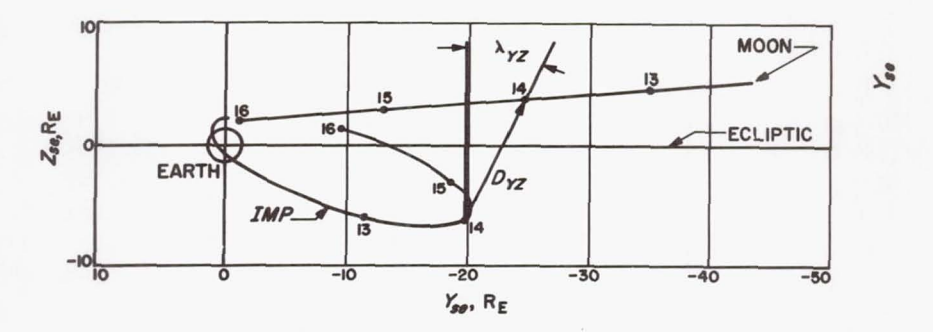


Fig. 2. Projection of Moon and *IMP* positions onto a plane perpendicular to the Earth–Sun line, December, 1963 (Orbit 5)

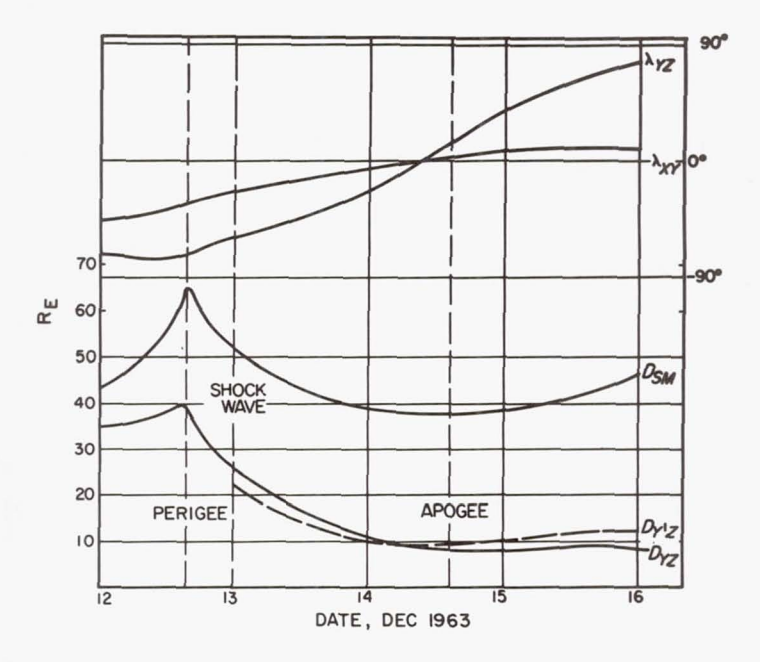


Fig. 3. Plots of the angles λ_{YZ} and λ_{XY} , and the distances D_{SM} , D_{YZ} , and $D_{Y'Z}$ vs. time for the period December 12 – 16, 1963 (Orbit 5)

396 N. F. NESS

At the point where λ_{YZ} and λ_{XY} cross, the Sun was almost eclipsed by the Moon; the satellite was about 9 R_E – or 33 lunar radii (R_M) – below the Sun–Moon line, while the total distance between the satellite and the Moon was about 38 R_E or 140 R_M.

The aberration of the solar wind shifts λ_{XY} by an amount equal to the aberration angle—about 5 deg. $D_{Y'Z}$ is the projection of D_{SM} on the YZ plane as the plane is rotated 5 deg from the normal to the Earth–Sun line. You can see that there is some difference between D_{YZ} and $D_{Y'Z}$, primarily at the time of closest approach to the "apparent Sun"–Moon line.

Early on December 13, IMP passed through the shock wave into interplanetary space, where the data were similar to the type of interplanetary data obtained from Orbits 1 through 4, and 6 through 9. From about noon on December 13 to noon on December 15, the characteristics of the magnetic-field data changed considerably: the field became turbulent, reaching a maximum turbulence during the middle of December 14, before IMP reached apogee. The maximum field strength, which lasted for about 3 hr on December 14, was 14.6 γ .

At the time the data were received, we thought that possibly the instrument had failed; it was only on subsequent orbits that we confirmed the operation of the instrument. We were then forced to reconsider the explanation of the variations in the magnetic field. Investigation of solar

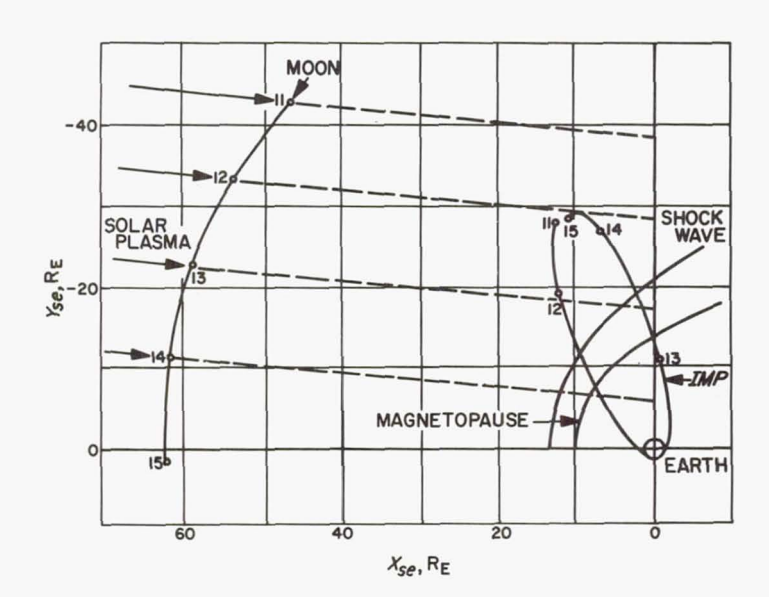


Fig. 4. Projection of Moon and *IMP* positions on the ecliptic, January, 1964 (Orbit 13)

conditions, Kp indices, and magnetograms in the polar region showed nothing abnormal relative to quiet conditions. As a result, we suggest that the data represent evidence for a magnetohydrodynamic wake of the Moon as it interacts with the solar wind.



The January and February Interceptions

Figure 4 shows the position of the satellite in the ecliptic during the month of January, 1964. On January 11 (Orbit 13), *IMP* was near apogee and was moving toward perigee; on January 13, as the Moon passed by,

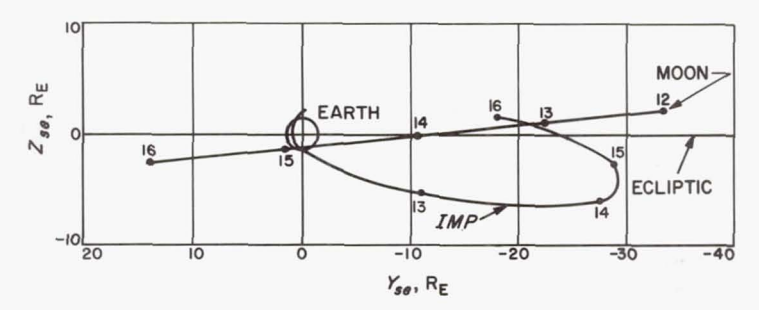


Fig. 5. Projection of Moon and *IMP* positions onto a plane perpendicular to the Earth–Sun line, January, 1964 (Orbit 13)

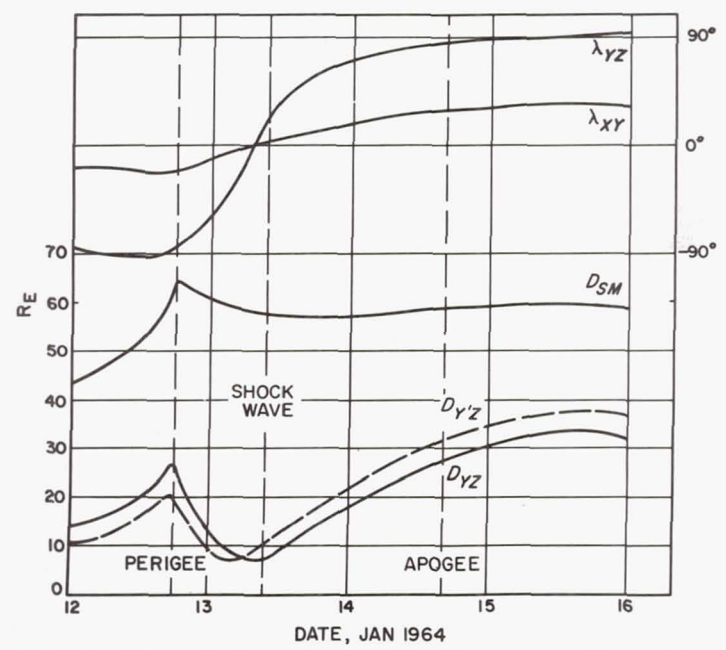


Fig. 6. Plots of the angles λ_{YZ} and λ_{XY} , and the distances D_{SM} , D_{YZ} , and $D_{Y'Z}$ vs. time for the period January 12 – 16, 1964 (Orbit 13)

398 N. F. NESS

the satellite was within the magnetosphere. Thus there was no possibility of directly detecting the wake of the Moon at this time—although during Orbit 13, inbound, the shock wave appeared somewhat anomalous (see Paper 21). The projections of the satellite and Moon positions onto the YZ plane are shown in Fig. 5. The relevant distances and angles are plotted in Fig. 6, and show that the angular position for detecting the wake was favorable when the satellite was between perigee and the shock wave.

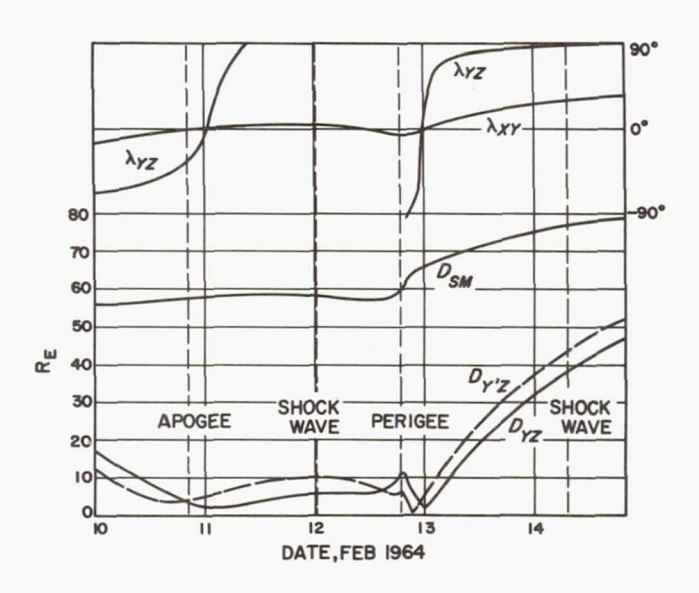


Fig. 7. Plots of the angles λ_{YZ} and λ_{XY} , and the distances D_{SM} , D_{YZ} , and $D_{Y'Z}$ vs. time for the period February 10–14, 1964 (Orbits 20 and 21)

Similar plots for the February interception are given in Fig. 7: portions of Orbits 20 and 21 are shown. In this case, the satellite was near apogee when the Moon went by; and if the wake extended for a distance of $58~R_{\rm E}$ (or $194~R_{\rm M}$), we should have been able to see it. In our first analysis of the data from Orbit 20,however,we find no indication of the wake similar to that observed in December, which suggests that the satellite was beyond the lunar wake.

Flow Pattern Considerations

Figure 8 is a schematic diagram that represents our concept of the wake and shows a length consistent with our data. In Paper 22 we concluded that the flow of the solar wind about the magnetosphere had a Mach number between 7 and 10. We see from Fig. 9 that this range of Mach

numbers corresponds to Mach angles between $5\frac{1}{2}$ and 8 deg. During the December intercept, the wake was detected when the satellite was about 8 R_E from the Sun–Moon line and 40 R_E from the Moon. Thus the observed angle of less than 11.3 deg is consistent with the suggestion that we have identified the Moon's wake.

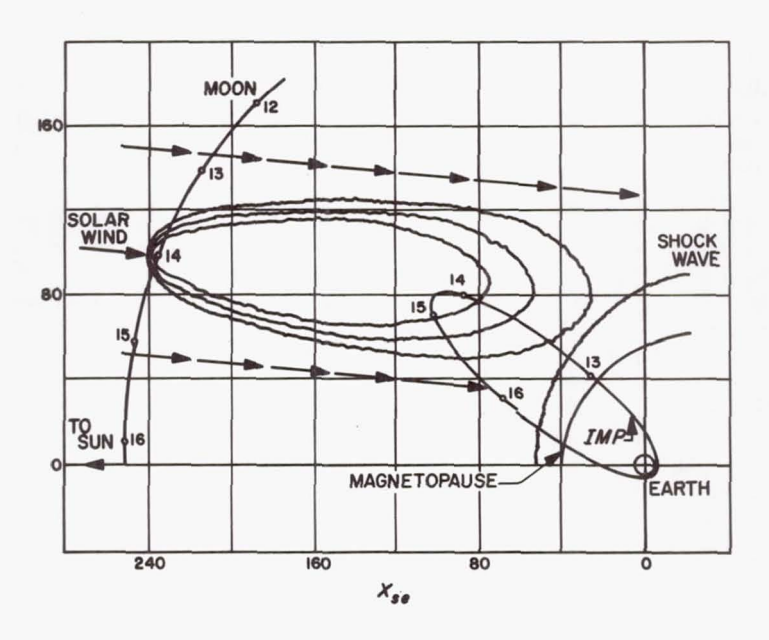


Fig. 8. Sketch of the Moon's wake, superimposed on the ecliptic view of Fig. 1.

Distances are in units of 1,000 miles

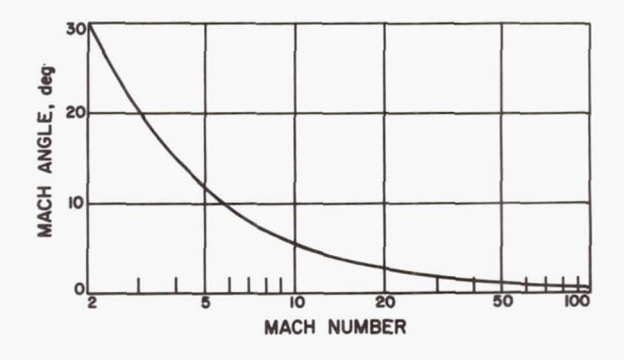


Fig. 9. Mach angle as a function of Mach number for supersonic flow around a body

REFERENCES

- 1. BIGG, E. K., Journal of Geophysical Research 69, 4099 (1964).
- 2. MICHEL, F. C., A. J. DESSLER, and G. K. WALTERS, Journal of Geophysical Research 69, 4177 (1964).
- 3. Stolov, H. L. and A. G. W. Cameron, *Journal of Geophysical Research* (submitted for publication).

DISCUSSION OF NESS PAPER

BEARD: I have a question to ask, since this is a Jet Propulsion Laboratory conference. Was anything like this ever hinted at in the data from the *Mariner* flight past Venus?

SNYDER: No: *Mariner* passed on the sunlit side of Venus. It was never anywhere near the tail.

DEUTSCH: The weather has also been mentioned in connection with lunar-related phenomena. E. G. Bowen and others¹ have pointed out a correlation between rainfall figures and the longitude of the Moon.

NESS: Yes, I tried to point out that there are lunar-associated phenomena in a wide variety of areas. However, I think that some investigators may have made false interpretations of statistical correlations that show high coherency but have no direct physical relationship.

AXFORD: A study of the correlation between Kp and the Moon has recently been carried out by Michel, Dessler, and Walters.² They found no relationship whatever between lunar period and Kp.

NESS: However, one should not attach too much significance to correlations with Kp, since it is probably not even subject to the normal laws of algebra, like addition and subtraction, so necessary in computing correlation coefficients.

¹Adderley, E. E. and E. G. Bowen, *Science* **137**, 749 (1962); Bigg, E. K., *Nature* **197**, 172 (1963); Bradley, D. A., M. A. Woodbury, and G. W. Brier, *Science* **137**, 748 (1962).

²Michel, F. C., A. J. Dessler, and G. K. Walters, *Journal of Geophysical Research* **69**, 4177 (1964).

NAME INDEX

Abrams, I. J., 241 Briggs, B. R., 173 Adderley, E. E., 400 Brusowski, F. B., 369 Adlam, J. H., 173 Bruce, C. E. R., xxiii-xxiv Akasofu, S. I., xx, xxi, xxiii, xxviii, 249, Brüche, E., xvii 250, 255, 280, 282, 293 Bryant, D. A., V (1), 80, 141 Alexeff, I., 348 Budzinski, E. E., 247, 255 Alfvén, H., xvi, xviii, xix, xx, xxi, xxvi, 223, Burgers, J. M., 212 238, 241, 244, 263, 264, 269, 361, 363, Burgess, A., 214 373, 380 Burrows, J. R., 247, 255 Allen, J. E., 173 Amazeen, P. G., 141, 241, 255, 280, 335, Cahill, L. J., 141, 241, 255, 280, 335, 350, 352 352 Anderson, H. R., IV, 56, 65-67, 69, 71, Camac, M., 241 194-196, 370 Cameron, A. G. W., 400 Antrack, 371 Carmichael, H., 136, 141, 192 Appleton, E.V., xxii Carpenter, D. L., 252, 255 Carr, T. D., 212 Athay, R. G., xvii, 33, 160, 212, 213, 218 Auer, P. L., 173 Chambre, P. L., 212 Axford, W. I., XVI, xxi, xxvii, 80, 123, Chamberlain, J. W., xvi, 118-120, 196, 200, 203, 212, 253-255, 268, 269 140-142, 157, 190, 192-195, 212, 214, 241, 243, 244, 246, 249, 251, 257, 261-Chandrasekhar, S., 113, 120 265, 269, 272, 273, 281, 282, 284, 293, Chapman, S., Fwd, xviii, xix, xx, xxi, xxii, 347, 349-352, 369, 370, 379, 400 xxvii, xxviii, 23, 119, 120, 200, 203, 212, 234, 240, 241, 244, 265, 270, 272, 275, Babcock, H. D., 267 280, 337 Babcock, H. W., 150, 157, 159, 163, 164, Chatterton, N. E., 212 Chree, C., xvi 267 Cline, T. L., V, 67, 80, 81, 103, 138, 141-Bartels, J., xv, xvi, xxvii Beard, D. B., XXVI, xix, 272, 273, 338, 143, 194, 195 347, 350, 370, 380, 389, 400 Colburn, D. S., X, 46, 173-175, 389 Bell, B., 266, 267 Coleman, P. J., Jr., III, 50, 103, 141, 173, Bennett, W. H., xvii 184, 192-194, 265, 266, 280 Bercovitch, M., 192 Bernstein, W., 347 Danielsson, L., 280 Biermann, L., XXIV, XXV, xvi, 21, 66, Davis, L., Jr., III, IX, 22, 32, 50-52, 106, 67, 103, 121, 155, 163-164, 173, 193, 121, 141, 142, 157-164, 173-175, 177, 194, 199, 212, 355, 358, 359, 361, 363, 184, 192, 195, 218, 219, 263, 265, 280, 369-371, 373, 380, 389, 391 351, 386, 390, 391 Bigg, E. K., xxvii, 390, 400 Davis, L. R., 249, 251, 252, 255 Birkeland, K., xvii Davis, T. N., 287, 293 Biswas, S., 219 de Bergerac, C., 105 Blackwell, D. E., 206, 208, 212 de Hoffman, F., 210 Blamont, J. E., 363 de Jager, C., 203, 212 Desai, U. D., V (1), 80, 141 Block, L. P., xxi, 33, 263-265, 278, 350 Bollhagen, H., 212 Dessler, A. J., 156, 157, 123, 140, 183, 212, 318, 335, 400 Bonetti, A., 141, 192, 314 Bowen, E. G., 400 Deutsch, A., 22, 33, 120, 159, 161, 162, Bradley, D. A., 400 213, 400 Brandt, J. C., 32, 206, 266, 267 Dungey, J. W., XVII, xix, 103, 159, 173, Bratenahl, A., 122, 159-160, 163, 196, 269, 234, 238, 241, 255, 257, 264, 265, 268-272, 275-280, 294, 346, 380 370 Bredikhin, 355 Egidi, A., 295 Bridge, H. S., VIII, 22, 67, 71, 81, 105, Erickson, W. C., 208, 212 106, 141, 142, 192, 295, 314, 350-352 Evershed, J., xvii Brier, G. W., 400

Fainberg, Ya. B., 348
Fairfield, D. H., 249, 255
Fälthammer, C.-G., 264
Fan, C. Y., 80
Fejer, J. A., 156, 157
Ferraro, V. C. A., xviii, xix, xx, xxviii, 234, 240, 241, 244, 275, 337, 380
Fichtel, C. E., 219
Finch, H. F., 318
Frank, L. A., 53, 65, 66, 140, 141
Fredricks, R. W., 347
Freeman, J. W., 300, 348-349
Freier, P. S., 219

Getty, W. D., 348 Gloeckler, G., 80 Gold, T., XXVII, xvi, xvii, xviii, xix, xx, xxi, 46, 52, 102, 104-107, 121-122, 136, 142-143, 153, 157-164, 173 183, 219, 241, 263-266, 270, 272, 294, 348, 351, 369, 371, 389-391 Gorgolewski, S., 111, 114, 120 Gottlieb, B., 123, 140, 212 Greenstein, J. L., 363, 365, 369 Gringauz, K. I., 140, 141, 310, 314 Guss, D. E., 219

Harris, E. G., 348
Harwit, M., 361, 363, 369, 373, 380
Heppner, J. P., 241, 335, 342, 347, 352
Hess, W. N., 105, 122, 249, 251, 253, 255, 270
Hewish, A., 109, 110, 111, 114, 120
Hills, H. K., 66
Hines, C. O., xxvii, 241, 269
Hinteregger, H. E., 391
Hoffmeister, C., 358, 369
Högbom, J. A., 111, 114, 120
Hones, E. W., Jr., XX, 293, 294
Howard, R. F., 51-52, 267
Hoyle, F., 264, 361, 363, 369, 373, 380
Hurley, J. D., xix
Hurwitz, H., 173

Ingham, M. F., 119, 120

Jacchia, L. G., *xxii*Jefferies, J. T., 214
Johnson, F. S., *xix*Jokipii, J. R., XIV, 23, 219, 390
Jones, W. P., *xix*, 329, 335
Judge, D. L., 140, 141

Kahn, F. D., *xxii*, *xxiii* Kantrowitz, A. R., 241 Kellogg, P. J., *xix*, *xxi*, 263, 335 Kelso, J. M., 140 Kennel, C., 268, 269 Kern, J. W., 267, 268 Kharchenko, I. F., 348 Kilb, R. W., 173 Kokubun, S., 241 Kornilov, E. A., 347 Krall, N. A., 253, 255, 269 Kruskal, M. D., 270

Langmuir, I., xviii Lashinsky, H., 268 Lazarus, A. J., 141, 192, 314 Leaton, B. R., 318 Lees, L., 348, 390 Leighton, R. B., XI, xvii, 71, 182-184, 194 Levy, R. H., 241, 257 Lighthill, M. J., 241 Lincoln, J. V., 32 Lindberg, L., 280 Lindemann, F. A., xviii, xxii Litvak, M. M., 241 Ludwig, G. H., V (2) Lüst, R., XXIV, xxvi, 22, 106, 120, 122, 157, 164, 173, 194, 212, 213, 351, 365, 366, 369-371, 380 Lüst, Rh., 356, 371 Lutsenko, E. I., 348 Lyon, E. F., XXIII, 134, 348, 349, 351

Macagno, E., 141 Mackin, R. J. Jr., 389 Malville, J. M., 255, 293 Martyn, D. F., xix Maunder, E. W., xvi McCracken, K. G., 136, 141, 192, 212 McDiarmid, I. B., 247, 255 McDonald, F. B., V, 80, 141 McIlwain, C. E., xxi, 255 Mead, G. D., XXIII, 81, 103, 162, 253, 294, 347, 349, 351 Meyer, P., xvi, 192, 195, 212 Michel, F. C., 400 Milne, E. A., xxiii Morrison, P., xvi, 188, 192 Mustel', E. R., 33

Nakada, M. P., 249, 251, 253, 255, 270
Neher, H. V., 54, 56, 62, 65, 66
Neidigh, R. V., 348
Nerurkar, N., 57, 66
Ness, N. F., VI, XXII, XXVIII, 22, 43-44, 50, 103-106, 121, 160, 174, 175, 183, 241, 266, 273, 309, 314, 335, 342, 347, 349-352, 400
Neugebauer, M., I, II, 3, 21-23, 33, 34, 66, 105, 106, 134, 141, 155, 156, 158, 165, 173, 175, 192, 241, 341
Ney, E. P., 219
Nikolayev, R. M., 348
Noble, L. M., 151, 157, 203, 212

Nagata, T., 241

Dayashi, T., *xxvii*Derman, C. R., 270
O'Brien, B. J., 247, 253, 255, 270
Oguti, T., 281, 293
Olbert, S., 173, 175
Öpik, E. J., 266, 267

Parker, E. N., XII, xvi, xvii, xx, xxi, xxiii, xxv, 21-23, 33, 34, 66, 94, 102, 103, 105, 106, 118-121, 123, 135, 142, 153, 155, 157, 160, 161, 173, 183, 192-196, 199-203, 209-215, 218, 219, 221-223, 226, 228, 263
Patrick, R. M., 241
Peed, W. F., 348
Pendenko, N. S., 348
Petschek, H. E., XV, XVIII, 22, 120, 160-161, 175, 214, 228, 234, 238, 241, 248, 265-268, 273, 275, 278, 350, 389-391

Rao, U. R., 3, 21, 66, 192, 241 Richter, N., 212 Romishevskii, E. A., *xix* Rosenbluth, M. N., 253, 255, 269, 380 Rossi, B., 141, 192, 314 Rostoker, N., 269 Rudakov, L. I., 268 Runcorn, S. K., *xxvi*

Piddington, J. H., 183, 241, 279, 280

Sagdeev, R. Z., 268 Sarabhai, V., 189, 192 Scarf, F. L., XIII, xx, 151, 157, 203, 212-214, 347-349 Scearce, C. S., 83, 241, 335, 347, 352 Schaaf, S. A., 212 Scherb, F., 141, 192, 314 Schlüter, A. S., xxvi, 173 Schmidt, A., xx Schmidt, H.-U., 369 Schuster, A., xviii Seek, J. B., 83 Serbu, G. P., 300, 350 Shipley, E. D., 348 Simpson, J. A., 80, 189, 192, 212 Sims, A. R., 140 Siscoe, G. L., 241, 257 Six, N. F., 212 Skillman, T. L., 241, 335, 347, 352 Slee, O. B., 109, 115, 120 Slutz, R. J., xix, 34, 195, 273, 349, 351-352, 390 Smith, A. G., 212 Smith, E. J., III, 22, 50, 66-67, 104, 106, 107, 140, 141, 147, 164, 170, 173-175,

182, 183, 192, 280, 349-351

Smullin, L. D., 348 Snyder, C. W., I, II, 3, 21, 22, 32-34, 46, 66, 81, 140, 141, 154-159, 165, 173, 175, 192, 194, 241, 245, 390, 391, 400 Sonett, C. P., III, 50, 140, 141, 173, 192, 241, 280 Sonnerup, B. U. Ö., XIX, 280 Speiser, T. W., 248 Spreiter, J. R., xix, 173, 329, 335 Stein, W. A., 219 Steljes, J. F., 136, 141, 192 Stix, T. H., 348 Stolov, H. L., 400 Stoney, J., xvi Störmer, C., xvii, xx Stumpff, P., 371 Sturrock, P. A., 173 Sweet, P. A., xxiv, 221, 222, 228 Swings, P., 363, 365, 369

Tauer, J., 390
Taylor, H., 270
Taylor, J. B., 269
Teller, E., 210
Thompson, W. B., 173
Trefftz, E., 214, 359, 363, 365, 368-370, 373, 380

Van Allen, J. A., 29, 53, 65, 66, 140, 141 van de Hulst, H. C., 204 Venkatesan, D., 192 Vestine, E. H., xxvii Vogt, R. E., 67, 80, 195, 371

Walters, G. K., 400 Webber, W. R., 57, 66 Whipple, F. L., 355, 363 Whitham, G. B., 241 Wilcox, J. M., 43, 46, 51, 155, 183-184, 267 Wilkerson, T., 33, 122, 134, 162, 174, 349 Williamson, J. M., 255 Wilson, M. D., 247, 255 Winckler, J. R., 70 Wolfe, J. H., 168 Woodbury, M. A., 400 Wyndham, J. D., VII, 109, 114, 120-122

Yudovich, L. A., 293

Zhigulev, V. N., *xix* Zirin, H., *xiii*, *xvii*, 34, 51, 120, 200, 212-214, 219

SUBJECT INDEX

Acceleration of charged particles see also	time variation (Ellsworth), 287
Magnetosphere, particle motions	Auroral particles see also Aurora, theory
in bow shock, 370, 388	of
drifts as cause, 246, 291-292	electrons
interchange motions as cause, 238	in brighter forms, 287
by interplanetary electric field, 164	observations of, 270
by interplanetary magnetic field, 72,	hydrogen atoms, 287
164, 195	origin, 249
ion-acoustic-wave instability as cause,	trajectories, 248
347. 348	Auroral zone
neutral points, 248-249	connection to neutral point, 244
trapped particles, 238, 263	lower boundary and diamagnetic effects,
by violation of adiabatic invariants, 263	264
Adiabatic invariants	Blast wave (interplanetary)
in determining shells of trapped parti-	effects on galactic cosmic rays, 187, 188
cles, 246-247, 251-252	magnetic-field distortion, 187
expressions for, 245-246	trigger mechanism for solar wind, 211
in particle motion calculations, 245-246,	Bow shock
294	acceleration of particles in
violation of, 263	electron observations (IMP), 302-
	303, 388
Atmosphere, Earth's	
heating by neutral hydrogen, xxii	neutral point model, 248-249
tidal motions in, 236, 393	change in specific-heat ratio, 348
Aurora see also Auroral particles; Auroral	comets see Comets, bow shock
zone	disappearance, interpretation of, 347,
arcs	348
alignment of, 287	dissipation in, 233
electron precipitation in, 287	electric fields in, 350
geomagnetic latitude of, 282	example of collision-free shock, 233
particle motion calculations, 293	existence consistent with space-probe
separation from $H\alpha$ emission regions,	observations, 129, 131
287, 293	information loss, 233
theoretical prediction of, 254	location and shape
electric fields associated with, 254, 270	correction for latitude of subsolar
energy input rate, 239	point, 326, 327
forms of	magnetic and plasma observations
all-sky photographs, Dec. 4, 1958, 270	compared, 334
development during storm, 249	magnetic observations (IMP), 318-
theoretical prediction, 254	323, 328, 334
$H\alpha$ emission, 287, 293	plasma observations (IMP), 128, 131,
solar-activity dependence, 196	298, 310, 313, 314, 334
spiral patterns (of probability maxi-	theoretical, 233, 234, 329, 330-332,
mum), 286	348
substorms, xxvii, xxviii	theory and observations compared,
theory of see also Auroral particles	329, 331-332, 348-349
electric fields, 254	variation in, 313, 314, 327, 348-349
particle motions, 281	magnetic-field changes at
rayed arcs, 254	amplification of irregularities, 348
universal (pressure-gradient)	disordering, 265
instability	IMP observations, 317-320
compared with observations, 269	magnetohydrodynamic wave, nonlinear
importance of wave direction, 268-	extension of, 257
269	Moon see under Lunar magnetosphere
resonances associated with, 253-	precursors see subhead upstream dis-
254	turbance

ow shock (continued)	Comet tails, ionized (Type I)
result of supersonic flow, 233	aberration angle, 358
stabilizing influence of geomagnetic	accelerations in
field, 384	correlation with solar activity, 371
standing wave in plasma flow, 222	magnetohydrodynamic equations,
standoff distance see subhead location	366-368
and shape	magnitude of, 356
studies of (historical), xix	mechanisms for coupling to solar
thickness of	wind, 358-361, 373
estimated, 233	method of determination, 359
relation to magnetic-field direction,	composition of, 355
350, 351	correlation with geomagnetic activity.
turbulent structure of, 233, 349	356-358 see also subhead solar-
upstream disturbance	activity dependence
interpretation, 334, 347, 348	distance from Sun at which observed
magnetic observations (IMP), 320-	(limits), 369, 371
323, 334	electrons, importance of
plasma observations (IMP), 309	energies expected, 370, 373, 377
relation to magnetic-field direction,	
350	ionizing efficiency, 370
	ray formation, 370, 379-380
Charge exchange	spectral-line excitation, 370
auroral H α emission, 287	formation of, 373-377 see also subheads
in comets, 359, 365, 367-368, 373	rays, rapid growth of; electrons,
cross-section (H+ – CO), 359	importance of; see also Comets,
in ionosphere, xxi-xxii	ionization of
momentum transfer in, 367-368	ion density
ring-current and main-phase develop-	distribution, 366
ment, xxi	electron collisions as cause, 379
role in solar-wind termination, 210	insufficiency of charge exchange, 373
Comets	rays, rapid growth of
artificial see Ion clouds, artificial	energetic electrons as cause, 370, 379-
bow shock	380
electron acceleration in, 370	insufficiency of charge exchange, 373
existence predicted, 369	insufficiency of solar-wind pressure,
charge exchange see Charge exchange	373
coma, 356	successive-ray-formation mechanism,
density distribution, 366	380
ionization of, 359, 365-366, 373	solar-activity dependence of, 356-358,
magnetohydrodynamic equations, 366-	370-371
368	solar-latitude dependence of, 370-371
mass flow	solar-wind interaction with, 199, 356-
loss rate, 359, 361, 365	358
structure, 369	streamers, 121, 369
velocity at head of comet, 368	time variations in, 356, 359, 365-366
nucleus, 355-356	Conductivity, electrical
radio noise from, 370	effect on reconnection rate, 260, 261
specific	in ionosphere, Hall vs direct, 236
1899 I, 356	at magnetopause, 260, 261
Halley 1910 II, 356	Conductivity, thermal
Mrkos 1957d, 356, 357	coefficient in hydrogen plasma, 200
Whipple-Fedtke-Tevzadze 1942g, 356	definition of coefficient, 199
tails see also Comet tails, ionized (Type	magnetic-field effect on, 214
I)	role in corona, 203
accelerations in, 356	Coordinate systems (for magnetic data)
classification of, 355-356	IMP, 86, 90, 148, 149, 316
composition of, 355	Mariner 2, 36, 47, 148, 149
dimensions of, 356	Corpuscular streams see Solar wind, high-
sunlight pressure on, 356	velocity streams
use in study of solar wind, 361-362	Correlation coefficient, definition of, 61

(

	the second secon
Cosmic-ray instrumentation, 53, 73, 74	plasma ion observations
Cosmic rays see also Galactic cosmic rays;	intermittent flux, 129
Solar cosmic rays; Solar protons	magnetopause location and shape,
electrons	298
acceleration in solar wind, 195	in transition region
flare, July 1961, 195	angular distribution, 305-306
flare, March 1964, 195	flux, 127-131
flux observed, 77, 78	spectrum, 305
galactic vs solar origin, 77, 78	velocity, 127
IMP observations, 75-78, 80	plasma spectrometer, 295
comparison with proton variations,	trajectory, 127, 128, 305, 306
75, 79	Explorer 12
correlation with solar activity, 78, 80	cadmium-sulfide detector observations,
time variations, 75, 76, 78, 79	300
28-day periodicity, 75, 78	energetic-particle observations at mag-
flux in interplanetary space (Mariner 2),	netopause, 348-349
54-56	lifetime, 348
galactic see Galactic cosmic rays	magnetic-field observations
ionization (chamber) rate	correlation with bays, 249
in interplanetary space (Mariner 2),	
	large fluctuations, 350
54-62	magnetopause, 280, 334
over Thule, 56-57	magnetosphere, 337
neutron-monitor data, 54-60	transition region
nomenclature, xxv	oscillations, 350
solar see Solar cosmic rays; Solar	southward tendency, 245, 275
protons	magnetometer accuracy, 315
spatial correlation (Mariner 2), 62	solar protons
studies of (historical), xxiv-xxv	decay time, 71, 72
variation with distance from Sun	diffusion through interplanetary
Mariner-2 observations, 62	fields, 81, 138
spatial vs temporal variations (Mari-	dispersionless oscillations, 69-71
ner 2), 54	energy spectrum, 69, 72, 80
Debye length, 232, 351	M-region effects, 71
Drifts of charged particles	production time scale, 72, 80, 141-142
adiabatic invariants in analysis of, 246,	recurrence due to solar rotation, 71-
294	73, 80, 81, 138, 139
distinction from bulk drift, 253, 254	trapped with flare plasma, 72, 81
electron drift in ionosphere, 236	trajectory, 69, 71, 127, 128, 131
energy changes produced by, 246, 290-	Explorer 14
292	magnetic observations in tail, 235, 315-
energy dependence of, 246	316
in magnetosphere, 290-293	plasma observations of shock front, 168,
types of, 246, 281	169, 174
Electric charge on spacecraft	trajectory, 127, 128, 131
	Explorer 18 see Interplanetary Monitoring
effects of, 17, 350	Platform (IMP)
IMP measurement of, 350	
method of determination, 350	Flow, types of
value in transition region, 350-351	fluid application to collisionless plasma,
Electrostatic spectrometers see Plasma	
spectrometers	232
Experiments, suggested	definition of, 231
at magnetopause, 260	dependence on size of obstacle, 351
solar wind, 123-125	role of information in, 231, 232
Explorer 10	Newtonian
magnetic observations	application to magnetosphere
magnetopause location, 273, 332	defense of, 337
in tail	shortcomings, 234, 235
field direction, 320	definition of, 231
field strength, 235, 263, 273, 352	supersonic, definition of, 232, 347

uid flow see Flow, types of correlation with cometary disturbances, Forbush decrease see under Galactic cos-356, 358 mic ravs Kp index Galactic cosmic rays correlation coefficients involving, 400 deceleration in interplanetary fields see correlation with atmospheric heating, subheads energy of; Forbush decrease; penetration into solar correlation with interplanetary field fluctuations, 49-50 system density correlation with Moon's position, 400 dependence on distance from Sun. correlation with solar-wind energy 185, 188, 189, 193 density, 14, 15, 16 interstellar vs near-Earth, 191, 193 correlation with solar-wind velocity, diffusion see subhead penetration into 3, 13, 34, 196 solar system relation to neutral-hydrogen wind, electrons, 195 see also Cosmic rays, electrons tool for studying sources of highenergy of velocity plasma, 34 in interstellar space, 194 lag behind sunspot cycle, 196 near Earth, 191 morning spiral pattern of, 281, 284 relation to DS-current pattern, 249 energy density in interstellar space Geomagnetic field see also Magnetosphere comparison with near-Earth, 191boundary of see Magnetopause connection to interplanetary magnetic effect on solar-wind termination, field see Magnetopause, magnetic reconnection at energy available from hydrogen dipole approximation, 318 burning, 194 effects of Moon on, 393 estimate of, 191-194 Finch and Leaton coefficients, 318 implications for galactic containinclination to ecliptic, 318, 320 ment, 193 latitude of subsolar point, 323-326 near Earth, 53 magnetosphere tail, 351-352 Forbush decrease Newtonian theory of solar-wind intereffect of successive blast waves, 193, action assumptions, 341-342 energy spectrum of, 187, 188 expression for, 342 Mariner-2 observations, 58 field-line pattern, 346 theory of magnitude of field, 342-345 Gold model, 136 self-consistent field, 338 Parker model, 186-188 observed vs theoretical penetration into solar system Explorer-10 observations, 352 diffusion analysis, 188, 189 IMP observations, 317-321 electron-proton comparison, 195 termination of see Magnetopause energy loss during, 191 Geomagnetic storms impedance produced by field distor-Dec. 4, 1958, 270-272 tions, 186, 187 Dec. 2, 1963 periodic variations IMP location, 98 diurnal, 190-193 IMP magnetic observations, 99-103, 11-year, 123, 188, 189 324, 327 27-day, 189, 190 magnetograms, 99 streaming in solar system, 190, 191 magnetosphere compression (IMP time spent in solar system, 191 data) 324, 327 time variations see also subheads perineutral surface observed, 102 odic variations; Forbush decrease onset time, 99, 102 correlations between Mariner 2 and propagation velocity, 102 Earth, 66 DS-current system see under Iono-IMP observations, 75 sphere; see also Magnetosphere, Galactic magnetic field, 193 interchange motions Gamma rays, secondary (IMP), 74-77 Geomagnetic activity effects of neutral hydrogen, xxi

Geomagnetic storms (continued) energy dissipation mechanisms, 239,	ionization in ionosphere, xxi-xxii relation to atmospheric heating, xxii
energy input, 235, 239, 240, 262-263 interplanetary magnetic fields during	relation to ring current, xxi IMP see Interpanetary Monitoring Plat- form (IMP)
(Mariner 2), 105	Injun-3 observations, 270
initial phase	Instability see Plasma instabilities
compression phenomenon, 240	Instrumentation see entries for individual
duration of, 270, 272, 280	instruments
magnetic bays	Interplanetary magnetic field
diffusion caused by, 252, 253	acceleration of charged particles by, 72,
effects on radiation belt, 249, 251,	164, 195
252	Archimedes spiral
relation to DS-current system, 249	absence of electromagnetic force, 201
time scale, 252	angle to ecliptic, 149
magnetosphere compression, 240, 270,	assumptions underlying, 185
324, 327	connection of lines to Sun, 142-143,
main phase see also subhead ring current	157, 163-164
differences between storms, xx, xxi	effect of solar-wind velocity, 25, 26,
magnetosphere topology change, 278-	96, 104, 105, 185, 186
280	far from Sun, 123, 183, 186
time for establishment of, 279	IMP observations, 92-96, 105
M-region storms	Mariner-2 observations, 36, 39, 40,
correlation with active regions (Mari-	47-50, 105-107, 147-149
ner 2), 33	polarity see subhead direction
correlation with high-velocity streams	radial dependence of field compo-
(Mariner 2), 28	nents, 185, 186
IMP observations, 103	refraction at oblique shock, 157
October 7, 1962	studies of (historical), xvi
Explorer-14 location, 168, 174	subsonic flow, self-consistency prob-
Explorer-14 plasma observations, 168, 169	lem, 211 conditions during solar cosmic-ray
Mariner-2 location, 165, 169	events (Mariner 2), 66, 67
Mariner-2 observations see Shock	connection of lines to Sun, 139, 142,
front (October 7, 1962)	157, 163, 193 see also subhead
magnetograms, 167	disconnection of lines from Sun
magnetosphere compression, 169	Davis model, 153-156
ring current	direction
absence of, 272	IMP observations, 92-96, 99-102,
Alfvén model, 238	104, 160
delay, 272	Mariner-2 observations, 36, 40, 43,
magnetospheric motions as cause,	46-49, 51, 107, 147-149, 164,
238, 272	266
neutral hydrogen as cause, xxi	nonradial components, importance
storm of December 4, 1958, 270	for magnetosphere reconnection,
studies of (historical), xx, xxi	266
seasonal variation, 266	polarity (along spiral), 43, 51, 52,
sequence of events in, xx, 272	107, 147, 164 see also subhead
studies of (historical), xx	filamentary structure
sudden commencement theory of, xx ,	relation to auroral energy, 265
27-day periodicity, 142 see also subhead	southward component see subhead southward tendency of
M-region storms	during sudden commencement, 99-
Helium abundance see under Solar co-	102
rona; Solar wind; Sun	disconnection of lines from Sun, 105,
Hydrogen, neutral (solar)	106, 160-161
eclipses, xxi-xxii	distortion by blast wave, 187
ejection from Sun, xxiii	distortion by Moon, 382 see also Lunar
ionization in transit from Sun, xxii	magnetosphere

mterplanetary magnetic field (continued) Mariner-2 observations, 49, 107 effects on cosmic rays see Galactic cos-Parker model mic rays Archimedes spiral in, 185, 186 energy density compared with comparison with Davis model, 155, cosmic-ray energy density, 53 magnetic-field-fluctuation energy dencomparison with Gold model, 105, sity (Mariner 2), 22 106, 153, 183 plasma thermal-motion energy relation to solar magnetic field, 46, 105, density 106, 183 Mariner-2 observations, 18 role in coupling cometary plasma to theory, 105, 106 solar wind, 366 filamentary structure see also under solar-cycle variations, 104 Solar corona southward tendency of Gold and Parker models, 105, 106 cosmic-ray observations, 264 IMP observations, 94-96, 103, 104, disappearance in bow shock, 265 121 IMP observations, 104, 148, 149 fluctuations interpretation of, 265, 267 comparison of IMP, Mariner-2, and magnetic-storm main phase, 272 Pioneer-5 observations, 103, 104 Mariner-2 observations, 46, 148, 149, correlation with Kp index (Mariner 264, 265 2), 49-50 near magnetopause, 245, 265, 275 correlation with solar-cosmic rays spiral pattern see subhead Archimedes (Mariner 2), 66, 67 spiral correlation with solar-wind velocity storage of protons in, 72, 135, 138-139 (Mariner 2), 19-21, 49-50 storm fronts see Geomagnetic storms; heating of plasma by, 19-21 Shock front (October 7, 1962); IMP observations, 92-96, 99, 210, 334 Shock fronts Mariner-2 observations, 22, 39, 40, structure 43, 45, 46, 48-50, 210 distortion due to plasma motion, 104, relative changes of magnitude and 105, 150-152 direction, 92, 94, 105, 106 effects of stirring on, 150-152 source of, 154, 155 relation to coronal fields, 104, 105, transport coefficients associated with, 150-152 214 termination disordered fields at, 210, 211, 213 Gold model Archimedes spiral in, 142-143, 153 processes involved, 123 theories see subheads Davis model; comparison with Parker model, 105, Gold model; Parker model 106, 153, 183 following flare, 136 27-day periodicity (Mariner 2), 43, 45, 106, 147 see also subhead longlimitations of, 106 history implied by lunar field distribulived configurations tion, 387 Interplanetary Monitoring Platform (IMP) irregularities see subheads fluctuations; cosmic-ray observations, 74-80, 195 description of, 83-85 filamentary structure; structure electric potential of, 350 long-lived configurations, 72, 73, 141, energetic proton observations, 75 142 see also subhead 27-day expected lifetime of, 315 ion-trap observations, 300, 350 periodicity magnetic observations see also Bow magnitude shock; Geomagnetic field; Geo-IMP observations, 92-96, 99-102 magnetic storms; Interplanetary Mariner-2 observations, 48, 49 magnetic field; Lunar magnetoneutral surfaces accelerating effects of, 195 sphere; Magnetopause; Magnetassociated with storm front (IMP), osphere; Transition region method of data analysis, 86, 87 102 purposes of, 84 Gold model, 105 magnetometer, rubidium-vapor IMP observations, 96, 102 bias fields for vector information, 85-IMP observations, 94-96, 103

Interplanetary Monitoring Platform (IMP)	polarity, 244, 264
(continued)	electric potential associated with, 23
data example, 89	239, 261, 262, 264 energy input rate, 239
description, 85, 87 dynamic range, 87, 318	as evidence of interchange motion,
	272
magnetometers, fluxgate accuracy, 315	necessary conditions for, 257
	pattern for viscous solar-wind inter-
configuration on satellite, 85 description, 85	action, 238, 239
dynamic range, 318	relation to magnetic bays, 249
frequency resolution, 349	studies of (historical), xxvii
zero shifts, 87, 89, 90	time dependence of, 249
plasma observations see subhead ion-	electric field in
trap observations; see also Bow	associated with DS-current system,
shock; Lunar magnetosphere;	239, 244, 245, 261, 262, 264
Magnetopause; Magnetosphere;	mechanical origin, 269
Shock fronts; Solar wind; Tran-	electrical conductivity, 236
sition region	electron drifts in, 236
plasma spectrometer	ionization by neutral hydrogen, xxi-xxii
description, 295-298, 302	motions in, mapped through magneto-
energy resolution, 297	sphere, 236-238
spurious modulation of electrons,	radio absorption, spiral pattern, 281,
296, 300	284-286
time resolution, 297, 298, 306 view direction, 131	Ion traps see also Plasma spectrometers
scintillation-counter telescope	IMP, 300, 350
data analysis method, 75-77	Lunik 2, 126-129
description of, 74	Lunik 3, 127-129 Venus probe (Soviet), 127, 128, 130,
observations, 74-80, 195	131
time resolution, 74	Kp index see under Geomagnetic activity
spacecraft magnetic field, 83, 85, 88	Laval nozzle and coronal streaming, 154,
spin rate, 87	155, 200
Sun-Earth-probe angle, 83, 84, 91, 92,	Liouville's theorem, application to mag-
127, 128, 315	netosphere, 245
telemetry format, 87	Lunar magnetosphere
trajectory	bow shock
apogee, 83, 127, 128, 315, 316	conditions required for, 383, 387
in ecliptic coordinate system, 91, 92,	electron acceleration in, 388
316, 394, 397, 398	motion of, 384
period, 83 relative to Moon, 394-399	stand-off distance of, 389
Interplanetary plasma see Solar wind;	compression of, 391
Solar corona	development of, 382, 391
Interstellar medium, density and tempera-	effect of insulating surface layer, 389
ture, 210	electric potential of Moon, 391
Interstellar wind, result of Sun's velocity,	energetic electrons in, 388
267	Mach angle, 399
Ion clouds, artificial, 362, 363	magnetic field
Ionosphere	closure, 383
artificial ion-cloud observations, 363	effect of interplanetary field strength
current systems, 236, 238 see also sub-	on, 386
head DS-current system	nodes, 387 relation to solar-wind history, 387
diffusion in, 363	rotation effects, 386, 387
DS-current system	strength of, 382
electric field associated with	time to develop, 383
description, 244, 245	total flux, 389
effects on particle energies, 246, 247, 264	rotation effect, 386, 387
247, 204	. Sunton succes, a so, a so,

ar magnetosphere (continued) location and shape correction for latitude of subsolar development of, 383 point, 323, 326, 327 geomagnetic effects, 390, 393 effect of solar-wind pressure, 272, IMP location relative to, 394-398 330, 349 IMP magnetic observations of, 393, effect of thermal pressure, 341, 351-352 IMP plasma observations of 314 from energetic-particle observations, length of, 389-391 (Explorer 12), 348-349 magnetic-field strength in, 390 from magnetic observations, 318, theory 320, 323-328, 332 assumptions, 381, 382 neutral points, 234, 235 description of, 382, 383 from plasma observations, 128, 131, summary, 384 298, 310 X-ray production, 388 stagnation point, 234 Lunik 2, 126-129 of tail, 235, 349, 351-352 Lunik 3, 127-129 theory of Mach number, definition for plasma, 232, Chapman-Ferraro model, 234 233 Newtonian model, 234, 329, 337-Magnetic bays see under Geomagnetic storms Newtonian vs fluid approxima-Magnetic-field reconnection see also Intertions, 272 planetary magnetic field, disobservations vs Newtonian theory, connection of lines from Sun; 273, 329 Magnetopause, magnetic recontime variations of, 313, 314, 327, 348, nection at; Magnetosphere, mag-349 netic-field lines width, 232, 234 diffusion model, 163, 221, 222 magnetic field at rate of connection of lines across, 351 see dependence on magnetic-field angle, also subhead magnetic reconnec-265, 266, 268 tion at in diffusion model, 163, 221, 222 direction, 318, 320, 323, 334 laboratory experiments, 163 magnitude (IMP), 318, 320, 323, 334 in wave model, 160, 221-228, 259, Newtonian theory, 342-346 260 magnetic reconnection at see also subwave model head neutral points; see also diffusion region in, 226 Magnetic-field reconnection equations for, 224-226 associated with instability, 278 external flow field, 226, 227 distributed nature of, 265 limit of validity, 227 effective area of, 267, 268 limiting flow velocity, 227 efficiency of (neutral point analysis), Magnetic fields, spacecraft 260, 261 equation for rate of, 259, 260 effect on determination of fields in space, 35, 174 illustration of, 257, 258, 261, 262 neutral-point analysis of, 257 IMP, 83, 85, 88 Mariner 2, 36, 40-42, 46, 50, 51, 173, relation to interplanetary-field direc-174 tion, 265, 266, 268 Magnetic Reynolds number, 160, 221, relation to magnetosphere convection 222, 227 pattern, 257 Magnetic storms see Geomagnetic storms waves (MHD) associated with, 257 Magnetohydrodynamic equations, 366neutral points on see also subhead magnetic reconnection at; see also 369 Magnetometers see Explorer 12; Inter-Magnetic-field reconnection planetary Monitoring Platform description, 259, 260 relation to interplanetary-field direc-(IMP); Mariner 2 Magnetopause see also Solar wind, intertion, 258 action with magnetosphere topology (open vs closed), 280 dissipation at, 235, 238-241 plasma pressure on, 338 electric currents in, 273 shape see subhead location and shape

Magnetopause (continued)	neutral points
stability, 318-320	acceleration at, 248, 249
stresses at, 235, 239, 240, 262, 263, 272, 352	connection of field lines to Earth 235, 244, 249
tail see subhead location and shape; see also Magnetosphere, tail	connection of field lines to surfaces 244
Magnetosphere	current sheets associated with, 244
Chapman-Ferraro model, 234	as poles of distorted dipole field, 234
compression of during geomagnetic	reconnection site, 235
storms, 240, 270, 327	particle motions see also subheads in
connected model see subhead topology	terchange motions; trapped par-
convection in see subhead interchange	ticles; see also Adiabatic invari
motions	ants; Drifts of charged particles
electric fields in	
	acceleration of trapped particles, 263 264, 290-292
Alfvén model, 238	The state of the s
associated with co-rotation, 281, 291	adiabatic invariants, 245-247, 294
associated with DS-current system, 237	application of Liouville Theorem 245
associated with fluid motions, 244	departure from magnetosphere, 293
during geomagnetic storms, 238, 239	diffusion, 252, 253, 263
effect on particle motions, 247, 290-	drifts, 246, 253, 254
293	electric-field effects on, 247, 290-293
equations, 236	influences on, 281
model experiments, 264	injection from solar wind, xviii-xix
potential difference across polar cap,	xxi, 235, 245, 247, 248, 281, 293
261, 262	night-side behavior, 247
relation to interplanetary electric	resonant effects, 254
field, 245	special treatment near current sheet
electric potential across, 264	248
electrons in see subhead plasma	spiral patterns, 281, 292, 293
energy input rate, 239	trajectory calculations, 245, 246, 290
field-line reconnection see subheads	294
magnetic-field lines; neutral	trapped vs untrapped particles, 246
points; see also Magnetopause,	plasma
magnetic field at; Magnetopause,	beta of, 236
magnetic reconnection at	evidence for co-rotation, 292, 293 motions of, 236-239
injection of solar particles, xviii-xix, xxi, 235, 245, 247, 248, 281, 293	observations of low-energy electrons
interchange motions	IMP, 310
acceleration effects of, 238	Luniks, 126-129, 310
damped by energetic ions, 269	whistlers, 252
definition of, 236	ring current see under Geomagnetic
DS current as evidence for, 272	storms
effects of in ionosphere, 236	shape see Magnetopause, location and
insulating atmosphere necessary, 236	shape see Magnetopause, location and
mechanical origin of, 236, 238	solar-wind interaction with see subhead.
reconnection rate consistent with,	magnetic-field lines; distortion by
257, 260	solar wind; see also Magneto
role in geomagnetic storms, 272	pause; Solar wind, interaction
solar wind as cause, 238	with magnetosphere
magnetic field see Geomagnetic field	studies of (historical), xviii-xix
magnetic-field lines	tail see also Magnetopause, location and
connection to Earth, from neutral	shape
points, 235, 244, 249	accessibility to cosmic rays, 234
connection to interplanetary fields,	effect of stresses on shape of, 235
234, 235	energy stored in, 235
distortion by solar wind, 247, 342-346	length of, 235
"exterior" vs "interior", 244	magnetic field in, 351-352
model experiments, 264	origin of, 235, 236
model emperation, ac.	

netosphere (continued)	magnetic time constant, 381, 387
lopology	removal of atmosphere by solar wind,
Chapman-Ferarro model, 234, 244	389
closed, 276-278, 280	X-rays produced at surface, 387-389,
closed-to-open transition, 278-280	391
open, 244, 275, 280	Navier-Stokes equations for solar corona
trapped particles in see also subhead	choice of solutions (supersonic vs sub-
particle motions	sonic), 200-202, 204-206, 210-
absence of loss cone, 253	214
asymmetric distribution, 247	inviscid approximation, 203, 207
boundary of trapping zone, 247	limit of validity, 207, 208
shells of, 246, 247	viscous corrections, 206
spectrum, 251	Neutral points see also under Magneto-
wake see subhead tail	pause; Solar magnetic-field lines;
Mariner 2	see also Magnetic-field reconnec-
cosmic-ray observations see Cosmic	tion
rays; Solar cosmic rays	diffusion region thickness, 260, 261
Geiger counters, 29, 53	flow analysis, 224-226
ionization chamber, 53, 65	standing waves, 223, 224, 259
magnetic-field observations see Geo-	Newtonian flow see under Flow, types of
magnetic storms; Interplanetary	Pioneer 1, 126-128, 350
magnetic field; Shock front (Oc-	Pioneer 4, 127, 128
tober 7, 1962)	Pioneer 5, 103, 126-128
magnetometer, 22, 35, 43	Plasma
orientation in space, 35, 36	definition of beta, 236
plasma observations see Solar wind	effective Mach number, 232, 233
plasma spectrometer	instabilities see Plasma instabilities
angular resolution, 3	
description, 3	pressure drift, 268
energy resolution, 3	thermal conductivity coefficient, 200
method of calculating density, 8	viscosity coefficient, 200
method of calculating alpha-proton	waves see Waves
ratio, 16-18	Plasma instabilities
method of calculating velocity and	associated with interchange motions see
temperature, 5-8	also Magnetosphere, interchange
sensitivity to direction-of-incidence, 8	motions
time resolution, 3, 22	mechanical driving force, 269
spacecraft magnetic field see Magnetic	role in magnetic storms, 272
fields, spacecraft	stability conditions, 269, 270
trajectory	ion-acoustic-wave, 347, 348
distance from Earth, 54, 60	see also subhead universal
distance from Sun, 29, 54, 60	magnetohydrodynamic (in corona),
position during shock-front observa-	209, 214
tion, 165, 169	microscopic (in corona), 214
relative to Archimedes spiral, 66	two-stream
relative to Venus, 400	acceleration of electrons by, 347-348
solar latitude, 46	dependence on size of obstacle, 351
Meteorological phenomena, extraterres-	role in comet—solar-wind interaction,
trial influences on, xxvii, 400	
M regions see Geomagnetic storms; Sun	361
Moon	universal, 268, 269
bow shock see under Lunar magneto-	Plasma spectrometers see also Ion traps
sphere	IMP see under Interplanetary Monitor-
electric potential of, 391	ing Platform (IMP)
electrons incident on surface, 388	Mariner 2 see under Mariner 2
geophysical effects of, xxvii, 393, 400	Prandtl number, 200
magnetic-field studies (historical), xxvi	Protons, energetic see Galactic cosmic
magnetosphere see Lunar magneto-	rays; Solar cosmic rays; Solar
sphere	protons

Q-machine, 268	brightness distribution, 212
Radio astronomy see Solar corona, radio	composition of see also subhead hellul
observations Parking Hyggrid agustians (interplane	abundance in
Rankine-Hugoniot equations (interplane- tary shock front), 170-173	diffusion model, 215-219 iron abundance, 219
Ring current see under Geomagnetic	co-rotation with Sun, xxvi
storms	see also under Solar wind
Shock front (October 7, 1962)	density of, see also under Solar wind
compression of magnetosphere, 169	latitude dependence (electrons), 113
Explorer-14 observations, 168, 169, 174	limits set by radio observations (elec
Mariner-2 observations, 8, 12, 165-167,	trons), 120
170, 171	radial dependence, 120, 151, 203
magnetic field, 167, 171	206, 212
magnetograms, 167, 168	dielectronic recombination, 214
method of analysis, 169-171, 173	diffusion equation, 216
orientation of shock plane, 169	emission, correlation with solar-wind
periodic structure, 167 plasma density, 8, 12, 169-171	velocity, 32 filamentary structure
plasma temperature, 8, 12, 171, 174,	direction of, 111
175	further observations required, 122
plasma velocity, 8, 12, 171	method of observation, 111
Rankine-Hugoniot equations, 170-173	nature of, xvii, 111, 120, 121
specific-heat ratio changes, 171, 172,	relation to plasma motion, 121
174, 175	relation to visible structures, 116-117
thickness, 167	size of, 116, 117, 121, 122
velocity, 169, 171, 173	fluid equations
Shock fronts see also Shock front (Octo-	dynamic balance, 203
ber 7, 1962)	hydrostatic, 200 Navier-Stokes, 206
energy partition, 175 fluctuations in structure, 349	region of validity, 199, 208
geomagnetic storms, initial phase, 272	viscous effects, 206, 207
hydraulic jump analogy, 349	heating, 159, 203, 267
information loss in, 233	helium abundance in see also subhead
solar-wind termination, 196, 210	composition of; see also under
specific-heat ratio changes, 171, 172,	Solar wind
174, 175	mixing effects, 217-219
thickness, 67, 167	radial dependence, 217-218
transit time, 136	temperature-gradient effect, 218 magnetic effects in, 32, 33, 51, 195, 211
velocity relative to positive-ion velocity, 140, 170, 171	214
Solar-activity cycle effects	magnetic field see Solar magnetic fields
auroral phenomena, 265	Solar magnetic-field lines; Inter
comet tails, 356, 358, 370, 371	planetary magnetic field
cosmic rays, 123, 188, 189	mean free path in, 199, 208, 216
geomagnetic activity, 196	models of see subhead theory of
interplanetary magnetic field, 104, 159,	radio observations of
264	current status, 109, 115-116, 122
magnetopause location, 348, 349	instrumentation, 109
radio observations of solar corona, 113 solar magnetic-field reversal, phase lag,	radio sources, relative to Sun, 109
267	refraction vs scattering, 121
solar wind, 191, 196	scattered distribution
Solar breeze, 200	anisotropy, 111
Solar corona	definition, 109
adiabatic flow region, 208, 213	dependence on wavelength, 110
asymmetry of	116, 122
heat input, 267	latitude dependence, 113
radio observations, 117-119	radial dependence, 110
temperature, 194-195	smallest observed, 115-116

corona (continued) November 10, 1961, 71 solar-activity dependence, 113 December 1, 1961, 71 theory, 113-115 October 23, 1962, 62-65 March 16, 1964, 195 structures, visible, 158-162 scale height, 199-209 specific ionization of (Mariner 2), 62 scaling properties, 213 trapping and disordered fields, 210 Solar magnetic fields see also Solar magslip flow, 208 sonic transition in, 200, 203, 212-214 netic-field lines streaming velocity, radial dependence asymmetry of of, 208, 209 azimuthal (Mariner 2), 43 north-south, 183-184, 267 temperature of asymmetry at solar minimum, 195 Babcock model see under Solar magnetic-field lines electron-ion discrepancy, 214 radial dependence, 208, 209, 217 bipolar regions, 159, 160, 177 theory of, see also under Solar wind correlation with chromospheric emisbased on radio observations, 117-120 sion, 177, 179 Chamberlain model, 200, 203 dipole moment, 158, 161, 182 Chapman model, 200 effects on solar-wind flow, 32, 33, 51, common assumptions, 200 195, 211-214 Parker model, 199-201 flux convected outward, 149 thin-shell conductive-heating model, magnetic nozzles, 154, 155, 158-160, 203-206 162 magnetic structures, 154, 158, 159, 161, viscosity effects on electron density, 207, 208 162 see also subhead magnetic effects on streaming velocity, 207 nozzles; see also Solar wind, importance of, 199, 207, 208, 212 localized sources of maps, 111, 122, 178, 179, 181 Navier-Stokes equations, 206 radial limit of effects, 208, 213 near disk filaments, 179 stabilizing effect of, 212 near plage regions, 179 Solar corpuscular radiation see also Solar near quiescent prominences, 180 near sunspot groups, 177, 181 wind electric neutrality, xviii polarity at given latitude, 183, 184 interaction with geomagnetic field (hispolar regions, 149, 182 torical), xviii unipolar regions Solar corpuscular streams see Solar wind, description of, 182 during Mariner-2 flight, 51-52 high-velocity streams Solar cosmic rays see also Solar protons Solar magnetic-field lines see also Solar magnetic fields composition of, 219 across disk filaments, 179, 182 correlation, Earth vs Mariner 2, 66 Babcock model, 150, 159, 163 decay time (Mariner 2), 62 bipolar regions, 159-160, 182 dispersionless oscillations of concentration in channels, 182 during decay phase (Mariner 2), 65 connections of, 153, 157, 158-159, 161-Explorer 12 vs Mariner 2, 71 during rise phase (Mariner 2), 62-65 164, 182-183 see also subhead reconnection rise time (Mariner 2), 62 cutting-off see subhead reconnection electrons, 195 divergence of, 157, 182 energy spectrum (Mariner 2), 65 effects of plasma motion on, 155 see flux (Mariner 2), 62 also Solar corona, magnetic efionization rate (Mariner 2), 62 fects in relation to interplanetary magnetic field near sunspot groups, 181 (Mariner 2), 66, 67 necking-off see subhead reconnection specific events November 10-12, 1960, 136 neutral points, 160, 163 radio observations, 111, 113, 122 July, 1961, 195 reconnection see also subheads Bab-September 10, 1961, 69-71, 143 cock model; neutral points September 28, September 30, and in corona, 150, 163-164 October 27, 1961, 71-73, 80, 81, 138, 141, 143 electric field produced by, 164

```
Solar magnetic-field lines (continued)
                                                 cyclotron frequencies in, 360
     moving location of, 160-161, 164
                                                  Debve length in, 232, 360
     necessity for, 160, 161
                                                  density of see also under Solar corona
     rate of, 158, 160, 162-164
                                                    calculated from magnetopause posi-
     reverse solar wind implied, 160, 162,
                                                         tion, 329, 330
                                                    dependence on distance from Sun, 12,
  unipolar regions, 182
                                                         13, 151
Solar protons see also Solar cosmic rays
                                                    IMP observations, 301, 330
  decay time (Explorer 12), 71
                                                    Mariner-2 observations, 8, 12, 13
  energy spectrum, 69, 72, 80
                                                  direction of motion see also subheads
  Explorer-12 observations, 69-73, 138
                                                         co-rotation with Sun; reversed-
  geomagnetic storms, 71, 135, 136, 141
                                                         flow region
   M-region effects, (Explorer 12), 71
                                                    comet-tail aberration angles, 358
  oscillations of
                                                    IMP observations, 132, 301
     balloon observations, 70
                                                    limits set by Mariner-2, 34
     Explorer-12 observations, 69-71, 80
                                                    nonradial departure from active re-
  production of
                                                         gions, 33, 154
                                                    refraction in oblique shock, 157, 162
     coincident with H\alpha flare brightening,
                                                    size of nonradial component, 34,
          135-136
     time scale (Explorer 12), 72, 80, 141
                                                          162-163
   propagation from Sun
                                                  distribution function see also subheads
     diffusion through interplanetary field,
                                                         spectra; temperature; velocity
          81, 135, 136, 138
                                                    IMP observations, 134, 309
   direct propagation mode, 135
                                                     Mariner-2 observations, 17
     recurrent events, 71-73, 80, 81, 135,
                                                  electrons in (IMP), 134, 301, 309, 349
          138, 139
                                                  energy flux, 359
     summary of propagation modes, 135-
                                                  energy of positive ions (IMP), 134, 309
          140
                                                         see also subhead velocity of
     trapped with flare plasma, 135, 136
                                                  energy partition
   recurrent events (Explorer 12), 71-73,
                                                    ion vs electron, 175
          80, 81, 138, 139
                                                     proton vs alpha, 16, 17, 175
   relation to interplanetary magnetic
                                                     thermal vs magnetic-field, 18, 105,
                                                         106, 210
          field, 72, 136, 142
                                                  escape vs ejected flows, xv-xvi
   rise times
     for diffusion through interplanetary
                                                  flux observations (positive ions)
          field, 135
                                                     dependence on distance from Sun
     for direct propagation, 135
                                                          (Mariner 2), 13
   time variations, 72, 80
                                                     IMP, 127, 132-134, 301, 306, 308,
   transit time for direct propagation, 72,
                                                          309
                                                     Lunik-2, 126-129
   trapped by interplanetary field, time
                                                     Lunik-3, 127, 128
          scale, 72, 142
                                                     Venus-probe (Soviet), 127, 128, 130,
Solar wind
   acceleration of particles in, 164, 195
                                                  helium abundance in see also under
   adiabatic flow region, 208, 213
                                                          Solar corona
   asymmetry of
                                                     comparison with solar composition,
     north-south, 51, 267
     polar vs equatorial outflows, 194, 195
                                                     correlation with solar rotation, 33
     radio observations, 119
                                                     diffusion calculations, 215-217, 219
                                                     Mariner-2 observations, 16-18, 215
   blast wave as triggering mechanism, 211
   continuous presence, 34, 134, 157, 158
                                                     as probe of coronal conditions, 219
                                                     singly ionized, 22-23
   co-rotation with Sun see also subhead
           direction of motion; see also
                                                     time variations, 23
                                                  high-velocity streams
           under Solar corona
                                                     Mariner-2 observations, 8, 106, 147
     domination of magnetic stresses, 152,
                                                     source of, 157, 158
           155
                                                          see also Sun, M regions
      radial limit of, 155, 358, 369
                                                     studies of (historical), xvi
      theory of, near Sun, 155
```

specific-heat ratio in, 171, 174, 175, velocity increase rate (Mariner 2), 331, 332 106 spectra (energy/charge), positive ions interaction with comet tails see Comet see also subhead distribution function tails, ionized (Type I) IMP observations, 300-304 interaction with magnetosphere see also Magnetopause; Magneto-Mariner-2 observations, 3-5 stability of flow, 211, 212 sphere, solar-wind interaction stream interactions analysis of, 156, 157 energy and momentum transfer rates. as cause of field fluctuations, 154, 157 240 field configuration resulting from, energy incident during magnetic 156, 157 storm, 239 Mariner-2 magnetic-field observaevidence for dissipation, 235 tions, 50 ohmic dissipation, 235, 236, 238-240 Mariner-2 plasma observations, 8, 21 relation to tail formation, 235 studies of (historical), xv-xvi, xviii studies of (historical), xviii temperature transverse stresses, 235, 239, 240 of alpha particles (Mariner 2), 16-17 turbulent backwater, 351-352 comparison with adiabatic expansion, viscous dissipation, 235, 237-240 jets see subhead high-velocity streams dependence on distance from Sun, 13, Larmor radius in, 232, 360 208, 209 localized sources of see also Sun, IMP observations of, 309 M regions Mariner-2 observations of, 5-8, 12, Davis model, 158-159 175 difficulty in identification, 160 shock-wave heating, 21 identification of altitude by helium termination ratio, 219 collisionless shock at, 196, 210 plages, 27, 29-32, 159 distance from Sun, 183, 196, 210 time variations, 158 effect of cosmic-ray pressure, 193 mean free path in, 231 pressure balance at, 193, 196, 210, models see subhead theory of 211 momentum flux processes involved in, 123, 193, 196 estimate of, 359 theory of see also under Solar corona, history implied by lunar field, 387 theory of Mariner-2 observations, 14, 15, 16 adiabatic expansion, 33, 208, 213 variations, 14, 15, 16, 330 Chamberlain model motion in strong-field region, 155 see comparison with radio observaalso subheads co-rotation with tions, 118, 119 Sun, direction of motion solar breeze, 200 neutral hydrogen see Hydrogen, neutral common assumptions, 200 observations see also subheads refer-Davis model, 153-156 ring to parameters observed magnetic considerations, 153-155 comparison of methods, 355, 361, Parker model 362 coronal heating, 202, 203 ideal, 123, 125 comparison with radio observaorigin of see subhead localized sources tions, 118, 119 of; theory of; see also Solar independent variables, 155, 156 corona, theory of magnetic considerations, 153 overtaking streams see subhead stream minimum pressure principle, 211, interactions plasma frequency, 360 predictions, 200, 201 plasma shells, xvii stability, 211, 212 pressure see subhead momentum flux transit time from Sun, 33 reversed-flow region, 160, 163 turbulence in shock-wave heating, 21 distinction from temperature (Marsolar-cycle variations, 191, 196 iner 2), 21, 22

r wind (continued)

Solar wind (continued)	folly of attempting, 160
produced by magnetic-reconnection,	plages, 159
164	studies of (historical), xvi
velocity of	oscillations on surface, relation to in
consistent with coronal density, 203,	terplanetary field, 67
206	outbursts
correlation with coronal emission, 32	origin of high-velocity plasma, 158
correlation with Kp index, 3, 13, 34,	161-162
196	role in magnetic-field transport, 158
dependence on critical-point condi-	161, 163
tions, 200-201, 214	surge phenomena, 161-162
dependence on distance from Sun	photosphere
Mariner-2 observations, 13	extension of granules into corona
Parker theory, 123	117
Scarf theory, 208, 209	magnetic fields in see Solar magnetic
dependence on pressure far from	fields; Solar magnetic-field lines
Sun, 210, 211, 213	plages
IMP observations, 127, 134, 196, 301	activity level variation, 34
Mach number, 162, 331	association with high-velocity streams
Mariner-2 observations, 5-8, 12, 196	27, 29-32, 159
relation to comet-tail aberration	magnetic field associated with, 179
angles, 358 27-day periodicity	properties of, 159 role in coronal heating, 159
	prominences, 159-160, 180, 218
Mariner-2 observations, 8, 140	
studies of (historical), xvi Stellar winds, 211, 213	radio emission (Type IV) and sola
	cosmic rays, 66-67
Sun see also Solar	spicules, injection of matter into cor
active regions, 33	ona, 218 sunspot groups, magnetic field associ
asymmetry (active hemisphere), 51-52	ated with, 177, 182
chromosphere emission correlated with magnetic	velocity in galaxy, 267
field, 177, 179	Transition region (between bow shock
extension of spicules into corona,	and magnetopause)
117	brief changes to interplanetary condi
origin of high-velocity plasma, 158,	tions (IMP), 309, 310, 313
160, 161	complexity, interpretation of, 347-348
spectrum and composition, 218	determination of boundaries, 301-304
corona see Solar corona	318-323, 326, 327, 334
disk filament, 179, 180, 182	electric field, 245
flares see also subhead outbursts	ion acoustic waves in, 347-348
cause, xxiii-xxiv	magnetic field in
electrical-discharge theory, xxviii-	Explorer 12, 245, 350
xxiv	IMP, 318, 320-323, 334, 349, 350
height, 161	oscillations, 349, 350
observations, 161-162	Pioneer 1, 126-128, 350
	Pioneer 5, 126-128
plasma emission, xvii	
sequence of events, 135	southward component, 245
terrestrial effects, statistics, 264, 266,	particle trajectories in, 248, 249
267	plasma in
velocities in, 161-162	angular distribution, 300-306, 313
helium abundance	electrons
flare-particle data, 219	energy, 347, 350
methods of determination, 218	IMP observations, 134, 302-304
numerical value of, 215	309
M regions, association with visible fea-	temperature, 347
tures see also Solar wind, local-	velocity distribution, 347
ized sources of	energy, positive ions (IMP), 132
active regions, 33	134, 313
active regions, so	

Explorer-10 observations, 127-129, 305, 306
flux, positive ions, 127, 128, 132, 306, 309
IMP observations, 132-134, 298-313, 334
specific-heat ratio, 332
spectra, positive ion, 298-310
velocity, positive ions (Explorer 10), 127
studies of (historical), xix
thickness
anomalous behavior, 313, 314, 323
consistency of observations, 131

Van Alle

Transport coefficients see Conductivity, electrical; Conductivity, thermal; Viscosity

normal, 313, 323-327

Van Allen belts see Magnetosphere, trapped particles Vehicle charge see Electric charge on spacecraft Venus plobe (Soviet), 127, 128, 130, 131 coefficient of, 199, 200, 208 magnetic effects on, 214 in Navier-Stokes equations, 206 energy transport into magnetosphere by, 240, 318-320 ion-acoustic, longitudinal, 347-348 magnetoacoustic, 232, 233 magnetohydrodynamic, 222, 223, 257 role in information transmission, 231, 232 spectra of, 231, 232 wavelength, limiting values of, 231, 232

Zodiacal light, 212